

ISSN: 2349-6495(P) | 2456-1908 (O)



International Journal of Advanced Engineering Research and Science

(IJAERS)

An Open Access International Journal



Journal DOI: [10.22161/ijaers](https://doi.org/10.22161/ijaers)

Issue DOI: [10.22161/ijaers.4.5](https://doi.org/10.22161/ijaers.4.5)

AI PUBLICATIONS

Vol.- 4 | Issue - 5 | May, 2017

editor@ijaers.com | <http://www.ijaers.com/>

FOREWORD

I am pleased to put into the hands of readers Volume-4; Issue-5:2017 of “**International Journal of Advanced Engineering Research and Science (IJAERS)** (ISSN: 2349-6495(P)| 2456-1908(O)” , an international journal which publishes peer reviewed quality research papers on a wide variety of topics related to Science, Technology, Management and Humanities. Looking to the keen interest shown by the authors and readers, the editorial board has decided to release print issue also, but this decision the journal issue will be available in various library also in print and online version. This will motivate authors for quick publication of their research papers. Even with these changes our objective remains the same, that is, to encourage young researchers and academicians to think innovatively and share their research findings with others for the betterment of mankind. This journal has DOI (Digital Object Identifier) also, this will improve citation of research papers.

I thank all the authors of the research papers for contributing their scholarly articles. Despite many challenges, the entire editorial board has worked tirelessly and helped me to bring out this issue of the journal well in time. They all deserve my heartfelt thanks.

Finally, I hope the readers will make good use of this valuable research material and continue to contribute their research finding for publication in this journal. Constructive comments and suggestions from our readers are welcome for further improvement of the quality and usefulness of the journal.

With warm regards.

Dr. Swapnesh Taterh

Editor-in-Chief

Date: Jun, 2017

Editorial Board

Dr. C.M. Singh

*BE., MS(USA), PhD(USA), Post-Doctoral fellow at NASA (USA)
Professor, Department of Electrical & Electronics Engineering, INDIA*

Dr. Ram Karan Singh

*BE.(Civil Engineering), M.Tech.(Hydraulics Engineering), PhD(Hydraulics & Water Resources Engineering),BITS- Pilani
Professor, Department of Civil Engineering, King Khalid University, Saudi Arabia.*

Dr.Asheesh Kumar Shah

*IIM Calcutta, Wharton School of Business, DAVV INDORE, SGSITS, Indore
Country Head at CrafsOL Technology Pvt.Ltd, Country Coordinator at French Embassy, Project Coordinator at IIT Delhi, INDIA*

Dr.Swapnesh Taterh

*Ph.d with Specialization in Information System Security
Associate Professor, Department of Computer Science Engineering
Amity University, INDIA*

Dr.Ebrahim Nohani

Ph.D.(hydraulic Structures), Department of hydraulic Structures, Islamic Azad University, Dezful, IRAN.

Dr.Dinh Tran Ngoc Huy

*Specialization Banking and Finance, Professor, Department Banking and Finance
Viet Nam*

Dr.Sameh El-Sayed Mohamed Yehia

*Assistant Professor, Civil Engineering(Structural), Higher Institute of Engineering -El-Shorouk Academy,
Cairo, Egypt*

Dr.Ahmadad Nabih Zaki Rashed

*Specialization Optical Communication System, Professor, Department of Electronic Engineering,
Menoufia University*

Dr. Alok Kumar Bharadwaj

BE(AMU), ME(IIT, Roorkee), Ph.D (AMU), Professor, Department of Electrical Engineering, INDIA

Dr. M. Kannan

*Specialization in Software Engineering and Data mining
Ph.D, Professor, Computer Science, SCSVMV University, Kanchipuram, India*

Dr.Sambit Kumar Mishra

*Specialization Database Management Systems
BE, ME, Ph.D, Professor, Computer Science Engineering
Gandhi Institute for Education and Technology, Baniatangi, Khordha, India*

Dr. M. VenkataRamana

*Specialization in Nano Crystal Technology
Ph.D,Professor, Physics,Andhara Pradesh, INDIA*

DR. C. M. Velu

Prof. & HOD, CSE, Datta Kala Group of Institutions, Pune, India

Dr.RabindraKayastha

*Associate Professor, Department of Natural Sciences
School of Science, Kathmandu University, Nepal*

Dr. P. Suresh

Specialization in Grid Computing and Networking, Associate Professor, Department of Information Technology, Engineering College, Erode,Tamil Nadu ,INDIA

Dr. Uma Choudhary

Specialization in Software Engineering Associate Professor, Department of Computer Science Mody University, Lakshmangarh, India

Dr.Varun Gupta

Network Engineer,National Informatics Center , Delhi ,India

Dr. Hanuman Prasad Agrawal

Specialization in Power Systems Engineering Department of Electrical Engineering, JK Lakshmipat University, Jaipur, India

Dr.Hou, Cheng-I

Specialization in Software Engineering, Artificial Intelligence, Wisdom Tourism, Leisure Agriculture and Farm Planning, Associate Professor, Department of Tourism and MICE, Chung Hua University, Hsinchu Taiwan

Dr. Anil TrimbakraoGaikwad

Associate Professor at BharatiVidyapeeth University, Institute of Management , Kolhapur, India

Dr. Ahmed Kadhim Hussein

Department of Mechanical Engineering, College of Engineering, University of Babylon, Republic of Iraq

Dr.GamalAbd El-Nasser Ahmed Mohamed Said

Computer Lecturer, Department of Computer and Information Technology, Port Training Institute (PTI), Arab Academy For Science, Technology and Maritime Transport, Egypt









Mr. T. Rajkiran Reddy










*Specialization in Networking and Telecom
Research Database Specialist, Quantile Analytics, India*










M. HadiAmini










Carnegie Mellon University, USA



Vol-4, Issue-5, May 2017

Sr No.	Detail
1	<p><u>Factors Affecting Project Performance in Kurdistan Region of Iraq</u> Author: SevarNeamat  DOI: 10.22161/ijaers.4.5.1</p> <p style="text-align: right;"><i>Page No: 001-005</i></p>
2	<p><u>Experimental Study of Cement Mortar Incorporating Pond Ash with Elevated Temperature Exposure</u> Author: D. S. Lal  DOI: 10.22161/ijaers.4.5.2</p> <p style="text-align: right;"><i>Page No: 006-009</i></p>
3	<p><u>Mitigating Instability in Electric Drive Vehicles Due to Time Varying Delays with Optimised Controller</u> Author: Niresh J, Dr.Neelakrishanan, Muthu C, Sabareesh G, Saravanan P, TharanVikram S  DOI: 10.22161/ijaers.4.5.3</p> <p style="text-align: right;"><i>Page No: 010-017</i></p>
4	<p><u>Central Bank of Syria and its Role in the Syrian Economy</u> Author: Dr.Ghassan Farouk Ghandour  DOI: 10.22161/ijaers.4.5.4</p> <p style="text-align: right;"><i>Page No: 018-023</i></p>
5	<p><u>Environment Impact Assessment from Mining & Associated Industrial Activities on Environmental Quality of Ballari Region</u> Author: T. H. Patel, Dr. V. Venkateshwara Reddy, Dr. S.R. Mise  DOI: 10.22161/ijaers.4.5.5</p> <p style="text-align: right;"><i>Page No: 024-027</i></p>
6	<p><u>Autonomous Mobile Vehicle based on RFID Technology using an ARM7 Microcontroller</u> Author: Mr. Ravi Chandra Bathula, Mr.Sharath Chandra Inguva  DOI: 10.22161/ijaers.4.5.6</p> <p style="text-align: right;"><i>Page No: 028-031</i></p>
7	<p><u>Numerical Investigation of a Naca Air Intake for a Canard Type Aircraft</u> Author: B.H. da Silveira, P.R.C. Souza, O. Almeida  DOI: 10.22161/ijaers.4.5.7</p> <p style="text-align: right;"><i>Page No: 032-040</i></p>
8	<p><u>Combination between Cobit 5 and ITIL V3 2011</u> Author: El Baz Mourad, Motii Malik, Armand Collins Anong, BelaissaouiMustappha  DOI: 10.22161/ijaers.4.5.8</p> <p style="text-align: right;"><i>Page No: 041-047</i></p>
9	<p><u>Equilibrium Isotherm, Kinetic and Thermodynamic Studies of the Adsorption of Erythrosine Dye onto Activated Carbon from Coconut Fibre</u> Author: Ikhazuangbe P.M.O., Kamen F.L., Opebiyi S.O., Nwakaudu M.S., Onyelucheya O.E.</p>

	 DOI: 10.22161/ijaers.4.5.9	<i>Page No: 048-054</i>
10	<p><u>Heartbeat and Temperature Monitoring System for Remote Patients using Arduino</u> Author: Vikramsingh R. Parihar, Akesh Y. Tonge, Pooja D. Ganorkar</p>  DOI: 10.22161/ijaers.4.5.10	<i>Page No: 055-058</i>
11	<p><u>Explosions, Abnormal Loads on Structures</u> Author: Hajdar E. Sadiku, Esat Gash, MisinMisini</p>  DOI: 10.22161/ijaers.4.5.11	<i>Page No: 059-064</i>
12	<p><u>MHD Free Convective Radiative and Chemically Reactive Flow Over a Vertical Porous Surface in the Presence of Diffusion-Thermo Effect</u> Author: G. Sreenivasulu Reddy, S.Geethan Kumar, S. Karunakar Reddy, P. Durga Prasad, S.Vijayakumar Varma</p>  DOI: 10.22161/ijaers.4.5.12	<i>Page No: 065-078</i>
13	<p><u>Segmentation of Unstructured Newspaper Documents</u> Author: Santosh Naik, R. Dinesh, Prabhanjan S.</p>  DOI: 10.22161/ijaers.4.5.13	<i>Page No: 079-083</i>
14	<p><u>A Design of Crown Square Fractal Antenna Using Transmission Line Feed</u> Author: Jyoti Dadwal, Arushi Bhardwaj, Dr.YogeshBhomia</p>  DOI: 10.22161/ijaers.4.5.14	<i>Page No: 084-088</i>
15	<p><u>Heat Transfer Enhancement for Tube in Tube Heat Exchanger Using Twisted Tape Inserts</u> Author: A. H. Dhumal , G. M. Kerkal , K.T. Pawale</p>  DOI: 10.22161/ijaers.4.5.15	<i>Page No: 089-092</i>
16	<p><u>Assessment of Heavy Metals in Fodder Crops Leaves Being Raised with Hudiaara Drain Water (Punjab-Pakistan)</u> Author: Arif Malik, SaimaJadoon, Muhammad Imran Latif , MawishArooj</p>  DOI: 10.22161/ijaers.4.5.16	<i>Page No: 093-102</i>
17	<p><u>Design of a Pipeline Leakage Detection System</u> Author: Maidala. A Y, Odujoko A.O., Sadjere E.G., Ariavie G.O</p>  DOI: 10.22161/ijaers.4.5.17	<i>Page No: 103-110</i>
18	<p><u>Numerical and Experimental Study of Natural Convection Air Flow in a Solar Tower Dryer</u> Author: Germain W. P. Ouedraogo, SieKam, Moussa Sougoti, OusmaneMoctar, Dieudonne</p>	

	Joseph Bathiebo  DOI: 10.22161/ijaers.4.5.18	<i>Page No: 111-118</i>
19	<u>A Queuing Model to Optimize the Performance of Surgical Units</u> Author: M.G.R.U.K. Ferdinandes, G.H.J. Lanel, M.A.S.C. Samrarakoon  DOI: 10.22161/ijaers.4.5.19	<i>Page No: 119-123</i>
20	<u>A Genetic Algorithm Based Feature Selection for Classification of Brain MRI Scan Images Using Random Forest Classifier</u> Author: Dr. S. Mary Joans, J. Sandhiya  DOI: 10.22161/ijaers.4.5.20	<i>Page No: 124-130</i>
21	<u>Six Sigma Methodology for Improving Manufacturing Process in a Foundry Industry</u> Author: Sachin S., Dileplal J.  DOI: 10.22161/ijaers.4.5.21	<i>Page No: 131-136</i>
22	<u>Modeling an Academic Test by Practicing Google Drive Cloud Computing</u> Author: WaseemSaadNsaif, LaithRtalib Rasheed, Saja Salim Mohammed, Mohamed Hakem Mohamed  DOI: 10.22161/ijaers.4.5.22	<i>Page No: 137-146</i>
23	<u>Greener One-pot Synthesis of ChromenoOxazin and OxazinQuinoline Derivatives and their Antibacterial Activity</u> Author: V.Sruthi, M.Visalakshi, T.Rambabu, Ch.V.V.Srinivas, Y. Vamsi Kumar, M.Sunitha, S. Paul Douglas  DOI: 10.22161/ijaers.4.5.23	<i>Page No: 147-151</i>
24	<u>An Experimental Investigation and Modal Analysis of an Engine Supporting Bracket</u> Author: A.S. Adkine, Prof.G.P.Overikar, Prof. S .S. Surwase  DOI: 10.22161/ijaers.4.5.24	<i>Page No: 152-160</i>
25	<u>Crack Calculation of Beams from Self-Compacted Concrete</u> Author: Hajdar E. Sadiku, EsatGashi, MisinMisini  DOI: 10.22161/ijaers.4.5.25	<i>Page No: 161-166</i>
26	<u>Literature Review on Design and Working of 3 Way Pilot Operated Diaphragm Controlled Hydraulic Control Valve</u> Author: KunalMehra  DOI: 10.22161/ijaers.4.5.26	<i>Page No: 167-169</i>
27	<u>Segmentation of Optic Disc in Fundus Images using Convolutional Neural Networks for</u>	

	<p><u>Detection of Glaucoma</u> Author: R. Priyanka, Prof. S. J. Grace Shoba, Dr. A. Brintha Therese  DOI: 10.22161/ijaers.4.5.27</p>	<i>Page No: 170-179</i>
28	<p><u>A Review on Advancements in Optical Communication System</u> Author: AparnaTomar, Dr.Vandana Vikas Thakare  DOI: 10.22161/ijaers.4.5.28</p>	<i>Page No: 180-183</i>
29	<p><u>Problem Solving Approach</u> Author: Arkeya Pal, Er. Faruk Bin Poyen  DOI: 10.22161/ijaers.4.5.29</p>	<i>Page No: 184-189</i>
30	<p><u>Study of Broadside Linear Array Antenna with Different Spacing and Number of Elements</u> Author: Kailash Pati Dutta  DOI: 10.22161/ijaers.4.5.30</p>	<i>Page No: 190-194</i>
31	<p><u>A Review of Aggregate and Asphalt mixture Specific Gravity measurements and their Impacts on Asphalt Mix Design Properties and Mix Acceptance</u> Author: EsatGashi, HajdarSadiku, MisinMisini  DOI: 10.22161/ijaers.4.5.31</p>	<i>Page No: 195-201</i>
32	<p><u>Super complete-antimagicness of Amalgamation of any Graph</u> Author: R.M Prihandini,IkaHesti Agustin, Dafik, RidhoAlfarisi  DOI: 10.22161/ijaers.4.5.32</p>	<i>Page No: 202-206</i>
33	<p><u>Charge Discreteness as Model in Charge Migration in a Chain of DNA Molecules under Radiation</u> Author: Hector Torres-Silva , Erik Santos  DOI: 10.22161/ijaers.4.5.33</p>	<i>Page No: 207-211</i>
34	<p><u>Employees' Emotional Intelligence Determinants in Handling Dengue Fever (Case Study: Jember Regency, East Java Province, Indonesia)</u> Author: A.T. Hendrawijaya, T.A. Gumanti, Sasongko, Dan Z.Puspitaningtyas  DOI: 10.22161/ijaers.4.5.34</p>	<i>Page No: 212-219</i>
35	<p><u>Cloud Computing Security with Identity-Based Authentication Using Heritage-Based Technique</u> Author: Rishi Kumar Sharma, Dr.R.K.Kapoor  DOI: 10.22161/ijaers.4.5.35</p>	<i>Page No: 220-227</i>

36	<p><u>Effective Handover Technique in Cluster Based MANET Using Cooperative Communication</u></p> <p>Author: Suryakumar.V, Dr. V. Latha</p> <p> DOI: <u>10.22161/ijaers.4.5.36</u></p> <p style="text-align: right;"><i>Page No: 228-236</i></p>
37	<p><u>Efficient Routing Scheme for Mobile Wireless Sensor Networks using Hybrid multi-hop LEACH</u></p> <p>Author: Mr Mallikarjun Mugli, Dr A. M. Bhavikatti</p> <p> DOI: <u>10.22161/ijaers.4.5.37</u></p> <p style="text-align: right;"><i>Page No: 237-243</i></p>

Factors Affecting Project Performance in Kurdistan Region of Iraq

Sevar Neamat

Department of Mechanics Engineering, University of Zakho, Zakho, Kurdistan - Iraq

Abstract— Construction industry consists of many parts which result in a complexity in its nature. In Kurdistan Region (KR) of Iraq, construction projects have a lot of drawbacks in measuring their time of the product, cost, and safety of the work. The research below is to recognize and estimate the issues impacting the product performance in KR. The results that we got from the previous studies participated in preparing this research. A study is investigated for 63 factors of consultants and constructors viewpoints. The total questionnaire was 120. 83 answers are (69%) resulted from the participants: 16 (64%) to owners, 22 (63%) to consultants and 45 (75%) to contractors. Significant issues decided were: The delay in execution of projects due to shortage and closure of materials; the labors' availability in their work according to project duration; managing of projects and providing the skills of leadership; Alteration in prices of materials; highly qualified and expert persons need; Using of good materials and equipment.

Constructing organizations should reach their strong purpose in their production. Perfect methods and approaches must be recognized for controlling the impact of political and economic conditions. Additionally, a training program should be provided to progress the innovators in the construction industry construction projects. Organizations in the KR should assess the sharing of the market earlier than implementing projects. The reason is going to the difficult economic situation in the KR. This will help the administrations to accomplish works positively.

Keywords— Construction firms, construction management, factors affect the performance, project performance, Kurdistan region construction projects.

I. INTRODUCTION

Working in construction has a chief part in the enlargement and attainment the targets of public. It considers is one of the major businesses and gives to about 10% of (GNP) in developed nations. The economic condition has a noticeable effect on construction industry [1]. Project performance is affected by many indicators such as time, cost, and quality. The Kurdistan Region (KR) construction project performance affects by many

problems and complex subjects as in [2]. There are numerous causes like terminations, alteration of sketches and alteration of the plans. Moreover, we have extra various causes impacting KR projects like an underprivileged management and leadership.

In this study, the features moving the performance in the KR construction manufacturing have been planned. However, the investigation aimed to categorize the subjects and characteristics which touch the performance of construction projects.

II. STATEMENT OF THE PROBLEM

The research study in [3] has shown an unsuccessfulness in plans is mostly linked to the dissatisfaction in the product work of the company. Furthermore, various explanations and features which point to such this problem. In the KR, some works got effectiveness in performance. Additionally, the system used for performance may not be able to solve this point. Construction projects performance problem looks via different guidelines. At the end of 2015, a lot of plans ended bad projects. There were many causes: problems by customers, infrastructures ending, modification of the projects plan, extra jobs. There are other pointers of performance in the KR, the organization behavior among members, checking, and feedback and leadership expertise. Though, many significant subjects connected in a fruitless performance in the KR such economic factors and political.

III. OBJECTIVES

A study is prepared for examining impacts touching the constructing performance in the KR. The main target of an investigation can be seen in the following points:

1. Recognizing the issues impacting the performance of construction projects
2. Defining owner's opinions together with consultants and contractors to identify relation significance in the KR construction projects

IV. RESEARCH METHODOLOGY

This study presented the chief factors influencing the construction projects performance in the KR. From a

literature review, various methods and approaches had been investigated to attain the necessary goals. There are many preceding types of research concentrated on issues touching the performance in projects. Some of the researches concentrated on construction projects performance measurement. Others, concentrated on various features connected to performance such as the development of information technology.

A variation in the targeted topics as presented in the past, requested variance methods. The chief methods are achieved during researches such as surveying questionnaire and doing interviews.

V. RELATED WORKS

Researchers of [4] investigated 42 public sector cover some projects in Nigeria to assess the performance especially related to duration and cost. Key Performance Indicators (KPIs) are established for a real purpose using in industry project work. Brown and Adams settled a novel method for measuring the impact of managing a project building on the quality, timing and cost in performance [5]. Authors of [6] examined time and cost relations in community subdivisions in Malaysia by using the analysis regression to clarify cost and timing performance relation. Iyer and Jha in [7] investigated the issues influencing the cost performance by making an allowance for a questionnaire study. Academics in [8] observed the relationship between time and cost by means of 161 construction plans projects which finished in the different Australian States. Ugwu and Haupt in [9] investigated a KPI by in a country like South Africa. A study was directed by linking of the practical interviews with companies, specialists and obtainable administration rules of ecological influence valuations and maintainable. For multi-criteria decision, the analytical hierarchical process (AHP) revised a comprehensive model in order to integrate all necessary possession built on timing together with cost in performance [10]. The second measurement of the agenda is related to the concentrating on the measurement. It explains at which organizational level the measurement may use.

The research [11] depended on the literature review and suggested a performance measurement system as a model. Additionally, the system contains constructing work viewpoint counting the innovation and learning, processes. Moreover, it has been projected a survey containing pointers touching the performance of projects. Authors of [12] got an outlining software to display and monitor the project performance. Furthermore, a questionnaire is recognized to include the project performance factors in the Project Performance Monitoring System (PPMS). The observing procedure is computerized by the use of WWW and database or by

suggesting the technologies used in [13] and [14]. Also, Data collection and distribution are equally distributed. After that it is changed to require the Project Performance International (PPI) magnitude using algorithms. Investigators of [2] and [15] talked about a performance of construction industry project as a factor which affects the competitiveness level in the KR construction industry in order to have a product at the same level of the high competitive country together with an innovative system for managing the construction projects.

VI. RESEARCH METHODOLOGY

The research debates the main issues touching the performance by including the construction organizations in the KR. The simple method which is deliberated to gain the objective of this research by categorizing the issues touching constructing project performance. The performance subject had been studied in many types of research and papers for understanding main local issues impacting the construction project performance in the KR. Additionally, many other factors added automatically as it is suggested by the limited specialists such as project. Also, 63 factors those are affecting the constructing performance are nominated. The features are gathered and divided into 10 collections. The groups can explain an understandable text of the chief key performance pointers. Finally, the features had been mentioned are grouped due to studies and also provided as suggested by local specialists.

5.1. DATA MEASUREMENT

To have the ability to choose the suitable approach for analyzing, we should have a better idea about the level of measurement. Every measurement type has the special method for it not for others. In our research, a Likert scale is normally used to level the data according to their level of importance which are usually integer numbers. The Likert (1, 2, 3, 4, and 5) are used to indicate the ascending and descending in an interval between scales not indicating absolute quantities, where scale 5 goes to the very high important and 1 indicates the very low important.

5.2. GROUP ONE: COST FACTORS:

In the first position, we have increase in the escalation of material prices, those are ranked be owners and contractors. Nevertheless, this factor comes in the second position by the consultants. From the results, it is clear that escalation of material prices is less significant in consultant answers than owners and contractors. The reason is because of the effect of the factor on the liquidity of owners and the contractor's profit as we can see in the **Table.1**.

Table.1: RII and rank of cost factors

Factors	Owner		Consultant		Contractor	
	RII	Rank	RII	Rank	RII	Rank
(1) Cost factors						
Escalation of material prices	0.85	1	0.823	2	0.9	1
Differentiation of coin prices	0.8	4	0.82	3	0.86	2
Cash flow of project	0.822	2	0.79	4	0.85	3
Material and equipment cost	0.822	2	0.76	5	0.811	5
Liquidity of organization	0.727	5	0.85	1	0.842	4

In the fourth position by the owner, we have differentiation of coins prices. Consultants leveled it in third class and the contractors gave the second level to it. It is normal to see the up and down in the prices of a coin is significant with contractors work due to its effect on cost and profit of contractors.

A second position project cash flow is leveled by owners. By the consultants' answers, it comes in the fourth level. According to contractors, answers got the third level. For owners together with contractors, cash flow is more significant than for consultants. Since it measures the performance cost in every level of constructing work. Some authors commented in using of cash flow which is important scale to measure the construction projects' cost performance. The material and cost equipment comes in the second position by the owners, but it leveled in the fifth level by the consultants and the contractors. Additionally, it illustrated that the subject is more significant with owners more than others.

The cost of material and equipment is considered as project mechanisms that touch the owners' liquidness together with project financial plan. They commented that cost of material and cost of equipment infrequently impact the performance cost in research of Indians' and South Africans' building projects. Liquidity of organization is leveled in the sixth position by the owners. Also, it leveled in the first level by the consultants and by the contractor's answers in the fourth position. This feature is measured as a very significant one among the cost performance. It mainly depends on liquidness of association [9]. The result is agreed with [11] as liquidity is significant in assessing of cost and budget performance. The reason comes due to various economic and political situation.

5.3. GROUP TWO: TIME FACTORS:

The Average delay because of closures and materials shortage is considered a very significant factor. Also ranked as a first position among all features for contractors together with consultant and owner. Building projects in the KR are suffering many drawbacks in

constructing due to closures and materials shortage. This considered a problem for evaluating the time performance of projects as we can see in the **Table.2**.

Table.2: RII and rank of time factors

Factors	Owner		Consultant		Contractor	
	RII	Rank	RII	Rank	RII	Rank
(2) Time factors						
Site preparation time	0.679	7	0.661	9	0.591	9
Planned time for project construction	0.75	4	0.759	5	0.761	5
Percentage of orders delivered late	0.692	6	0.763	4	0.77	4
Time needed to implement variation orders	0.699	5	0.7	7	0.69	7
Time needed to rectify defects	0.654	8	0.67	8	0.635	8
Average delay in claim approval	0.59	9	0.725	6	0.761	5
Average delay in payment from owner to contractor	0.822	3	0.771	3	0.832	3
Availability of resources as planned through project duration	0.869	2	0.855	2	0.9	2
Average delay because of closures and materials shortage	0.889	1	0.891	1	0.94	1

Availability of resources as planned through project duration comes in the second position in owners answers. The consultants and contractors graded the factor in the second level. Moreover, if incomes are unobtainable as calculated for the duration of the project, the project may have many problems in the time performance. Also, the average delay in the payment is leveled in the third level by contractor, owner, and consultants.

Additionally, the feature gets the similar line for both contractor and consultant considered more significant for them. Since it can be connected to prescribed relations among them. Also, the contractors unable to develop the level of the project if it is not ordering by consultants.

5.4. GROUP THREE: QUALITY FACTORS:

In the fourth position, the participation of managerial levels with decision-making are decided by the owners, consultants and contractors answers. Furthermore, the feature catches a similar degree for in all parts due to an involvement of administrative levels with decision making results in the best implementation and measuring the work performance as we can see in the **Table.3**.

Table.3: RII and rank of quality factors

Factors	Owner		Consultant		Contractor	
	RII	Rank	RII	Rank	RII	Rank
Participation of managerial levels with decision-making	0.81	4	0.781	4	0.79	4
Availability of personals with high experience and qualification	0.86	2	0.842	1	0.861	1
Conformance to specification materials in project	0.88	1	0.811	3	0.819	3
Quality of equipment and raw materials in project	0.831	3	0.839	2	0.859	2

Having high and expert people comes in the first level by consultants and contractors answers and are classified by in the second level by owners. Though, a feature is in a high order of significance to high and expert people and help them in implementing a project in a profession and success way. Conformance to specification materials in project, the factor graded in the first level by owners and classified in the third level for others.

The raw materials quality together with equipment quality is classified by the consultants and contractors answers in the second level, but in the third level by owners. Also, a feature is very significant for consultant and contractor more than for owner.

VII. CONCLUSION

By considering the construction sector very essential department in the world, since it helps in achieving and getting the goals of society. There are many factors affecting its performance. The reason about this study is to go back to discuss the main features affect the Kurdistan Region (KR) constructing Industry. A questionnaire style of study is established in order to recognize the necessary tools affecting the KR industry sector. In this research, we studied the attitude of contractors, consultants, owners towards the factors affecting the performance. A pilot study of the questionnaire consisted of 30 questionnaires. From the literature review, we find sixty-three factors by dividing them into 10 groups.

The research study has investigated many factors that have been discussed and examined such as time, quality, productivity, client satisfaction, regular and community satisfaction, people, health and safety, innovation and learning, and environment. Factors are divided into owners, contractors, and consultants. The total number of questionnaires were 120. They are distributed as 25 to owners, 35 to consultants and 60 to contractors. The answers that we received were 83 questionnaires out of 120, which gave us the rate of 73.33%. The good experiences are helped to discover the attitude of the virtual importance of project performance. At the end, the

relative importance index method (RII) is calculated in order to determine owners, consultants and contractors attitudes in the Kurdistan Region construction projects.

REFERENCES

- [1] R. Navon, "Automated project performance control of construction projects," *Autom. Constr.*, vol. 14, no. 4, pp. 467–476, 2005.
- [2] S. D. Salahaddin, "Factors Affecting the Competitiveness and Innovation in Northern Iraq Construction Industry," 2016.
- [3] K. Karim and M. Marosszeky, "Process monitoring for process re-engineering-using key performance indicators," presented at the International conference on construction process reengineering, CPR, 1999, vol. 99.
- [4] T. Wegelius-Lehtonen, "Performance measurement in construction logistics," *Int. J. Prod. Econ.*, vol. 69, no. 1, pp. 107–116, 2001.
- [5] A. Brown and J. Adams, "Measuring the effect of project management on construction outputs: a new approach," *Int. J. Proj. Manag.*, vol. 18, no. 5, pp. 327–335, 2000.
- [6] A. P. Chan, "Time–cost relationship of public sector projects in Malaysia," *Int. J. Proj. Manag.*, vol. 19, no. 4, pp. 223–229, 2001.
- [7] K. Iyer and K. Jha, "Factors affecting cost performance: evidence from Indian construction projects," *Int. J. Proj. Manag.*, vol. 23, no. 4, pp. 283–295, 2005.
- [8] P. E. Love, Y. Raymond, and D. J. Edwards, "Time–cost relationships in Australian building construction projects," *J. Constr. Eng. Manag.*, 2005.
- [9] O. Ugwu and T. Haupt, "Key performance indicators and assessment methods for infrastructure sustainability—a South African construction industry perspective," *BUILD. Environ.*, vol. 42, no. 2, pp. 665–680, 2007.
- [10] S. M. Dissanayaka and M. M. Kumaraswamy, "Comparing contributors to time and cost performance in building projects," *BUILD. Environ.*, vol. 34, no. 1, pp. 31–42, 1998.
- [11] M. Samson and N. Lema, "Development of construction contractors performance measurement framework," presented at the 1st International Conference of Creating a Sustainable, 2002.
- [12] S. O. Cheung, H. C. Suen, and K. K. Cheung, "PPMS: a web-based construction project performance monitoring system," *Autom. Constr.*, vol. 13, no. 3, pp. 361–376, 2004.
- [13] K. Jacksi, N. Dimililer, and S. R. Zeebaree, "State of the Art Exploration Systems for Linked Data: A

- Review,” *Int. J. Adv. Comput. Sci. Appl. IJACSA*, vol. 7, no. 11, pp. 155–164, 2016.
- [14] K. Jacksi and S. Badiozamani, “General method for data indexing using clustering methods,” *Int. J. Sci. Eng. Res.*, vol. 6, no. 3, 2015.
- [15] S. Neamat and I. Yitmen, “Factors Affecting the Innovation and Competitiveness in Kurdistan Region of Iraq Construction Industry,” *Int. J. Adv. Eng. Res. Sci. IJAERS*, vol. 4, no. 2, pp. 157–162, 2017.

Experimental Study of Cement Mortar Incorporating Pond Ash with Elevated Temperature Exposure

D. S. Lal

Department of Civil Engineering, R.C.Patel Institute of Technology, Shirpur, Dist. Dhule, Maharashtra, India

Abstract— Pond ash is to be investigated for its use as a partial replacement for sand in cement mortar (1:4). The effort is to be made for the utilization of Pond Ash as sand replacement material in mortar which may introduces many benefits from economical, technical and environmental points of view. The project will present the results of the cement mortar of mix proportion 1:4 in which sand will partially replace with Pond Ash as 0%, 10%, 30%, 40% and 50% by weight of sand. It is proposed to prepare two set of mixture proportions. First will be a control mix (without Pond Ash with regional fine aggregate (sand) and the other mixing will contain Pond Ash obtained from Thermal Power plant industry. The compressive strength test is to be conducted with partial replacement of Pond Ash with sand. The strength property of mortar with Pond Ash for strength at 28 days as partial replacement with the cement in the cement mortar 1:4 is to be determined. Similarly the other set of cement mortar incorporating Pond Ash is to be kept in elevated temperature up to 1100° C and tested for its compressive strength. The results for controlled cement mortar and Pond Ash mortar for compressive strength at normal temperature and elevated temperature is to be compare.

Keywords— Pond Ash, Cement Mortar, Elevated Temperature, Compressive Strength.

I. INTRODUCTION

In the present study, Pond Ash samples were collected from disposal sites of Bhusawal- Thermal power plant. The effort made was to study the effect of high temperature on mortar in two sets incorporating pond ash. First cement mortar containing Pond Ash replaced with fine aggregate (0-100percentage) at normal temperature and second set containing cement mortar containing Pond ash replaced with fine aggregate (0-100 percentage) at elevated temperature. In recent years, the research and development by domestic and foreign experts have made available high-performance concrete (HPC) with high strength and high workability. The addition of fly ash and Pond Ash in order to improve workability, enhance

durability, minimize environmental pollution and CO2 emission, reduce production cost and utilize resources efficiently nonetheless, research on the effect of high temperature on properties of concrete with fly ash added has been scarce but merits further study. A proper amount of fly ash would give a better and stronger concrete mixture under high temperature and pressure. Concrete containing fly ash is of a denser structure and has better fire resistance compared with that without fly ash added. This study examines the impact of pond ash addition on properties of mortar mixed at different replacement percentages and at high temperature. It is hoped tha the high-temperature properties of pond ash mortar can contribute to a better understanding of the resource recovery of pond ash and its degradation under high temperature.

Occasionally, cement concrete structures are subjected to high temperatures (reactor vessels, thermal shock, fire, coal gasification vessels, some industrial applications, etc.). In most cases, such elevated temperatures result in considerable damage to cement concrete structures and masonry walls. Recently, high-strength concrete and high strength mortar are widely used in different parts of civil engineering structures. As they become more commonly used, the risk of being exposed to high temperatures also increases. Thus, better understanding of the behavior of high-strength mortar at high temperatures gains importance for predicting the mortar properties.

As per Ash Report shown below in table 01 for the year 2013-14 for 210 MW Units following statistical data was collected:

Table.1: Amount of Coal Consumption, FA, PA Generated

Total coal consumption (MT)	Ash generated (MT)	Fly Ash generated (MT)	Pond Ash generated (MT)
2058420	867624	694099	173525



Fig.1: Ash Generation in Thermal Power Plant-Bhusawal

Figure 01 above shows ash produced after combustion of coal in thermal power plant.

II. LITERATURE REVIEW

Several researches have been done by researchers on different material about the effect of high temperature. Some are discussed herein:

According to the study conducted by M. S. Morsy et al. (2010) the influence of elevated temperatures on the mechanical properties, phase composition and microstructure of silica flour concrete. The hardened concrete was thermally treated at 100, 200, 400, 600 and 800° C for 2 hours. The results showed that the addition of silica flour to OPC improves the performance of the produced blended concrete when exposed to elevated temperatures up to 400° C.[1]

Md. Akhtar Hossain et al. presents their research on fire resistance of cement mortar containing high volume fly ash. Terrorist attack, accidental fire breakout and different type of explosions produce a rapid change of temperature for a short period. In such a situation, the material properties play an important role in minimizing the potential damage due to high rise of temperature. The test results indicate that the mortar containing 50% fly ash as a replacement of cement exhibits greater resistance to high temperature. Also, compressive and bond strengths of mortar containing different percentage of fly ash initially increase with the increase of temperature but after 200° C they decrease with the further increase of temperature.[2]

K. Sobolev et al. conducted their research on the development of high-strength mortars with improved thermal and acid resistance. As granulated blast furnace slag (GBFS) cement, containing up to 60% slag, is sometimes used in repair materials applied at intermediate temperatures of 150–300° C. It was found that the enhancement of GBFS–Portland cement-based materials can be achieved with the help of silica fume (SF) and a super plasticizer (SP). The effect of different SPs on the compressive and flexural strength of SF–blast furnace slag Portland cement mortars was investigated. These

mortars, in addition to high strength, demonstrate high thermal and acid resistance.[3]

The effects of high temperature on the mechanical properties of cement based mortars containing pumice and fly ash were investigated by Serdar Aydın et al. Four different mortar mixtures with varying amounts of fly ash were exposed to high temperatures of 300, 600, and 900 °C for 3 h. The residual strength of these specimens was determined after cooling by water soaking or by air cooling. Also, microstructure formations were investigated by X-ray and SEM analyses. Test results showed that the pumice mortar incorporating 60% fly ash revealed the best performance particularly at 900 °C.[4]

Daniel L.Y. Kong et al. studied the effect of elevated temperature on geo polymer paste, mortar and concrete made using fly ash as a precursor. The geo polymer was synthesized with sodium silicate and potassium hydroxide solutions. Various experimental parameters have been examined such as specimen sizing, aggregate sizing, aggregate type and super plasticizer type. The study identifies specimen size and aggregate size as the two main factors that govern geo polymer behavior at elevated temperatures (800 °C). Strength loss in geo polymer concrete at elevated temperatures is attributed to the thermal mismatch between the geo polymer matrix and the aggregates.[5]

A comparative study was conducted by Ahmad A.H. et al. on concrete mixes, reference mix without an additive and that with an admixture. Concrete was exposed to three levels of high temperatures (200,400,600) °C, for a duration of one hour, without any imposed load during the heating. Five types of admixtures were used, super plasticizer, plasticizer, retarder and water reducing admixture, an accelerator and an air entraining admixture. Mechanical properties of concrete were studied at different high temperatures, including: compressive strength, splitting tensile strength, modulus of elasticity and ultimate strain. Test results showed a reduction in the studied properties by different rates for different additives and for each temperature, the decrease was very limited at temperature up to (200°C) but was clear at (400, 600)° C.[6]

III. METHODOLOGY

3.1 Material Used:

Ordinary Portland cement conforming to BIS: 8112 [7] and ASTM C-150 [8] was used throughout the research work. Sand conforms to BIS: 383(1970) [9] and IS:2116-1980 [10]. The sand was properly graded and of medium sized with a fineness modulus of 2.0 to 2.2. Pond ash as per IS:3812:2003 [11], the generic name of the waste product due to burning of coal or lignite in the boiler of a

thermal power plant is pulverized fuel ash (PFA) [11,12]. PFA can be fly ash, bottom ash, pond ash or mound ash. Fly ash is the pulverized fuel ash extracted from the flue gases by any suitable process like cyclone separation or electrostatic precipitation. PFA collected from the bottom of boilers by any suitable process is termed as bottom ash. The terminology pond ash is used when fly ash or bottom ash or both mixed in any proportion is conveyed in the form of water slurry is deposited in pond or lagoon. ASTM C 618-03 categorizes fly ash into two classes; class F and class C, which are equivalent to SFA and CFA, respectively of IS 3812: 2003. Bureau of Indian Standards (BIS) has published the specifications of pulverized fuel ash, IS 3812: 2003 in two parts, Part-I for use as pozzolana in cement, cement mortar and concrete and Part-II for use as admixture in cement mortar and concrete. Both the parts of the code define fly ash as a special class of PFA. This code can be adopted for characterization depending on its use as pozzolana or mineral admixture.

3.2 Test Methods:

All laboratory experiments were conducted in general accordance with the applicable procedures outlined by the IS:4031 (part 1)-1996 ,(part 4)-1988,(part 5)-1988, IS:516-1959. To evaluate the possibility of reducing the cement content of rendering and plastering mortars with pond ash, four tests, compressive strength test, fineness modulus, settling time and consistency were performed. The reference mortar was a cement and sand mortar without addition of pond ash.

3.3 Mix Proportions:

In the present study, total of 2 mixes in 1:4 fractions were prepared. In the first series of mixes one part of cement and 4 parts of sand & pond ash is taken with pond ash replacement in sand varying from 0 to 100%. In the second series of mixes one part of cement & pond ash (PA) and 4 parts of sand is taken with pond ash replacement in cement varying from 0 to 100%. All mixes are prepared at room temperature and elevated temperature.

IV. RESULT AND DISCUSSION

The Experimental work consists of conduction of compressive strength test for all proportions of cement mortar cubes of 7.07 mm x 7.07 mm size shown in figure 01 below. There were two sets of sample series tested (Series-I-Pond Ash Replaced with Sand & Series –II-Pond Ash Replaced with Cement). The result showed considerable gain in the strength when pond ash is replaced with sand up to 40-50 %. Further with increase in percentage the strength goes down. It is observed in Series –II that the gain in strength is limited only up to 10-20 % replacement.



Fig.1: Mortar cubes prepared during experimental work for curing and compressive testing in the

Table.2: Compressive Strength at Normal Temperature

Sr No	% Replacement Proportion	Compressive Strength (MPa) Sand Replacement	Compressive Strength (MPa) Cement Replacement
1	0%	13.4	13.4
2	10%	10.8	14.13
3	20%	6.7	10.67
4	30%	6.5	5.63
5	40%	5.95	3.56
6	50%	4.68	1.97
7	60%	2.53	0.8
8	70%	1.15	0
9	80%	1.36	0
10	90%	1.16	0
11	100 %	1	0

Table 03: Compressive Strength at Elevated Temperature

Sr No	% Replacement Proportion	Compressive Strength (MPa) Sand Replacement	Compressive Strength (MPa) Cement Replacement
1	0%	2.97	2.97
2	10%	2.43	2.467
3	20%	2.27	2.99
4	30%	2.73	1.46
5	40%		1
6	50%	3.06	0.33
7	60%	2.53	---
8	70%	2.06	---
9	80%	1.48	---
10	90%	0.87	---
11	100 %	1.42	--

It is observed from table 02 and 03 that the values of compressive strength taken after burning that the cement replacement mortar sustained to elevated temperature as compared to sand replacement mortar. The graph below in figure 02 and 03 shows considerable drop in the compressive strength when exposed to elevated temperature.

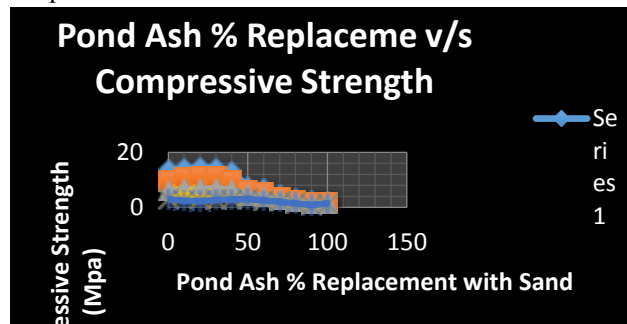


Fig.2: Drop in the strength of cement mortar incorporating pond ash with sand

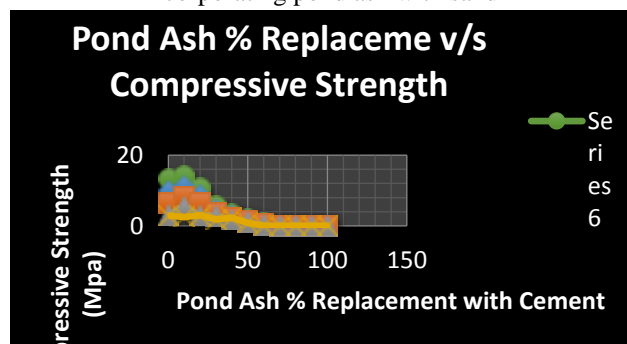


Fig.3: Drop in the strength of cement mortar incorporating pond ash with cement

V. CONCLUSION

The compressive strength test was done in two sets – sand replacement with pond ash and cement replacement with pond ash (0%-100%). Four cubes of each percent were made, two for atmospheric temperature and two for elevated temperature and observing the difference between them. For sand replacement, compressive strength of 0%-40% at normal temperature was about 13-14 MPa and after 50% strength was decreasing. At 200oc-400oc strength was optimum but after 400oc cubes give negative results i.e. they melt. But the compressive strength of cement replacement was optimum up to 20% replacement only. Above 20%, it gives very low strength values.

REFERENCES

[1] M. Morsy, S. Alsayed and M. Aqel, “Effect of Elevated Temperature on Mechanical Properties and Microstructure of Silica Flour Concrete,” International Journal of Civil & Environmental Engineering, vol. 10, No. 01, pp. 01–06, 2010.

[2] Akhtar Hossain, Mohammad Nurul Islam and Md. Rajibul Karim, “Fire Resistance Of Cement Mortar Containing High Volume Fly Ash”, 31st Conference on Our World In Concrete & Structures: 16 - 17 August 2006, Singapore.

[3] K. Sobolev, and A.Yeginobali, “The Development Of High-Strength Mortars With Improved Thermal And Acid Resistance”, Journal of Cement and Concrete Research, Elsevier Ltd., Vol 35, 2005, pp. 578-583.

[4] Serdar Aydin and Bulent Baradan, “Effect of high temperature on the mechanical properties of cement based mortars containing pumice and fly ash”, Journal of Cement and Concrete Research, Elsevier Ltd., Vol 37, 2007, pp. 988-995.

[5] Daniel L.Y. Kong et al. “The effect of elevated temperature on geo polymer paste, mortar and concrete made using fly ash as a precursor”, Journal of Cement and Concrete Research, Elsevier Ltd., 2010, pp. 334-339.

[6] Ahmed A. H., “Effect of High Temperature on Mechanical Properties of Concrete Containing Admixtures”, Journal of Al-Rafidain Engineering Vol.18 No.4 August 2010, pp.43-54.

[7] BIS 8112 (2005) Specification for 53 grade Ordinary Portland Cement, Manak Bhavan New Delhi.

[8] ASTM (C) 150-86, Standard Specification for Portland cement, Annual Book of ASTM Standards, 1988, (Vol. 4.01-Cements, Lime, Gypsum), Easton, USA.

[9] BIS 383 (1970), Specification for Coarse and Fine Aggregate from natural Sources for Concrete (Second Revision), Bureau of Indian Standards, New Delhi, India.

[10] BIS 2116 (1980) Specification for Sand for masonry mortars (1st revision), Manak Bhavan New Delhi, India.

[11] BIS-3812 (Part-1):2003 Pulverized fuel ash-specification for use as pozzolana in cement, cement mortar and concrete, Bureau of Indian Standards, New Delhi, India.

Mitigating Instability in Electric Drive Vehicles Due to Time Varying Delays with Optimised Controller

Niresh J¹, Dr.Neelakrishanan¹, Muthu C, Sabareesh G, Saravanan P, Tharan Vikram S²

¹Department of Automobile Engineering, PSG College of Technology, Coimbatore, Tamil Nadu, India

Abstract--The instability in the Electric vehicle would reduce the performance and even severely damage the system. This instability is mainly due to the random time-varying delays occurring in CAN network and the improper efficiency of controllers. This uncertainty and error occurrence makes it difficult to design the electric vehicles considering the advantages of Electric Vehicles being, the future to reduce harmful emissions due to fossil fuels, the instability can be mitigated by using optimized H_∞ controller. The results of Simulations through MATLAB demonstrate the Effectiveness of the improved controller by comparing with the normal PI controller. The results of comparison illustrate the strength of explicitly.

Keywords: CAN-Control Area Network, H_∞ Controller, LQR Controller (Linear Quadratic Regulator), MATLAB-Matrix Laboratory, Optimization.

I. INTRODUCTION

Owing to the emerging vehicular pollution to the environment and the deterioration of fossil fuels that increase the effect of global warming, the development of alternate energy source vehicles has been in fast pace. Nowadays there is great demand for vehicle driving safety, manoeuvrability, and driving comfort. Meanwhile the electric vehicle is at rapidly growing phase due to its simpler transmission, electronic initiative chassis and regenerative braking system of each wheel.

Rapid improvement in electric motor, battery, and control technologies makes the four-wheel-independent drive electric vehicle (4WID-EV) as an emerging configuration of EV. Quick dynamics of vehicle control, faster energy propulsions, good energy optimisation and structural flexibility makes the electric vehicles with in-wheel motors more preferable. There have been researches and works going in a way to develop a integrated control system to control the uncontrolled motion of steering and yaw rate.

Vehicle's lateral stability mainly depends on the steering controls and yaw moment controls.

Yu and Moskwa designed a four-wheel steering and independent wheel torque control system to enhance vehicle maneuverability and safety [1].

Bedner *et al.* proposed a supervisory control approach to manage both braking and four-wheel steering systems for vehicle stability control [2]. A coordinated and reconfigurable vehicle dynamics control system that can coordinate the steering and braking actions of each wheel individually was designed in [3]. There are also some works focusing on combining active front-wheel steering (AFS) and DYC systems. An integrated front-wheel steering and individual wheel torque controller was proposed to govern the vehicle lateral position using frequency weighted coordination [4]. Nagai also proposed an integrated control system of AFS and DYC to control the vehicle yaw rate and the sideslip angle using a model-matching controller [5]. A vehicle yaw stability control approach coordinating steering and individual wheel braking actuations was developed in [6]. A coordinated controller of AFS and DYC based on an optimal guaranteed cost method was designed in [7]. Mokhiamar and Abe compared different combinations of DYC with AFS, active rear-wheel steering (ARS), and AFS + ARS in simulation in [8].

Heinzl *et al.* also compared three different control strategies, namely, AFS, AFS plus unilateral braking, and ARS plus unilateral braking for vehicle dynamics control in a severe cornering and braking maneuver situation in simulation [9].

Among all the solutions coordinating the steering-based system and the DYC control system, the combination of AFS and DYC shows the best compromise between control performance and system complexity. With in-wheel motors, each wheel of the 4WID-EV can generate not only individual braking torque but individual driving torque as well, are able to yield greater direct yaw-moment than the conventional vehicles. In addition, the 4WID-EV dynamics control capability can be further enhanced by the integration of an AFS. Li *et al.* proposed

an integrated model predictive control algorithm of AFS and DYC to improve the control performance of 4WID-EVs with in-wheel motors [10]. However, all of these aforementioned control methods for combined AFS and DYC assumed that the controllers, sensors, and actuators were directly connected by wires. In other words, the 4WID-EV was considered as a centralized control system. Rather, with the development and appearance of in-vehicle networks and x-by-wire technologies, the control signals from the controllers and the measurements from some sensors are exchanged using a communication network in modern vehicles [11], i.e., Controller Area Network (CAN). Thus, a 4WID-EV is a networked control system rather than a centralized control system, which imposes the effects of network-induced delays into the control loop. The unknown and time-varying delays of the network communication between different controllers could degrade the control performance of the entire system or even make the system unstable. For example, according to the research of Caruntu *et al.*, time varying delays of the CAN can lead to driveline oscillations in the control of a vehicle drive train [11]. However, the instability in electric vehicle makes it difficult to be designed and used in normal road conditions. The instability is due to three main reasons

1. Driver action
2. Road disturbances
3. Network induced delays

1.1 Driver action:

The electric vehicle usually follows Drive-by-wire mechanism and even a small error can cause severe damage to the entire network and controller. For instance, if a driver had to make a right turn at 50kmph, in normal vehicles differential will take of this by rotating the outer wheel in a faster rate than the inner wheel. In case of electric vehicles with in-wheel motor, the controller will take the responsibility of the differential and it should code in such way, it should avoid under steer or over steer.

1.2 Road Disturbances:

The road obstacles also play a crucial role in designing the electric vehicles, cause a small bump in the road can a deviation in the yaw rate and it may lead to yawing moment of vehicles. It also includes the wind disturbances that will cause the vehicle to be unstable. Hence the road disturbances will also be the reason for electric vehicle instability.

1.3 Network induced delays:

Generally in most of the vehicles, both mechanical and electric vehicles have the usage of CAN bus network in order to reduce the use of wires which may add extra weight to the vehicle. The CAN Bus interconnects each system and provides a common platform for information to be transferred. In CAN bus network, there are three types of delays

- Process delay
- Transmission delay
- Packet-queue delay

1.3.1 Process delay:

In network, process delay is the time it takes routers to process the packet header. Processing delay is a key component in network delay. In the past, the processing delay has been ignored as insignificant compared to the other forms of network delay. However, in some systems, the processing delay can be quite large especially where routers are performing complex encryption algorithms or modifying packet content.

1.3.2 Transmission delay:

In a network, transmission delay is the amount of time required to push all the packet's bits into the wire. In other words, this is the delay caused by data-rate of the link.

1.3.3 Packet-queue delay:

In network, the queuing delay is the time a job waits in a queue until it can be executed. It is the key component of network delay and it contributes maximum out of these three delays.

For vehicle lateral stability control, steering-based systems and direct yaw-moment control (DYC), systems are most effective, and there have been various research studies on the combination of two systems. With in-wheel motors, each wheel of the 4WID-EV can generate not only individual braking torque but also individual driving torque, and can able achieve better yaw moment control than other systems.

However, all these aforementioned control methods for Combined AFS and DYC were assumed that the controllers, sensors and actuators were directly connected by wires. In other words the 4WID-EV was considered to be a centralized control system.

With the development of in-vehicle network, the control signals from the controllers and the sensors are exchanged through a communication network, i.e., Controller Area Network(CAN). Thus a 4WID-EV is a networked control system rather than centralized control system, which imposes the effects of network-induced delays into the control loop. The unknown and time-varying delays of the network communication between different controllers can degrade the control performance of the entire system or even make the EV unstable a time-varying CAN lead

to driveline oscillations in the control of a vehicle drive train.

II. METHODOLOGY

In an AFS system, the front-wheel steering angle is determined as a sum of two contributions. One is directly determined by the driver from her/his steering wheel angle input, and the other is decided by the steer-by-wire controller. One input is from the steering wheel of the driver, whereas the other is from the servo motor controlled by the electronic controller of the AFS system, which is connected to the in-vehicle network via the CAN bus.

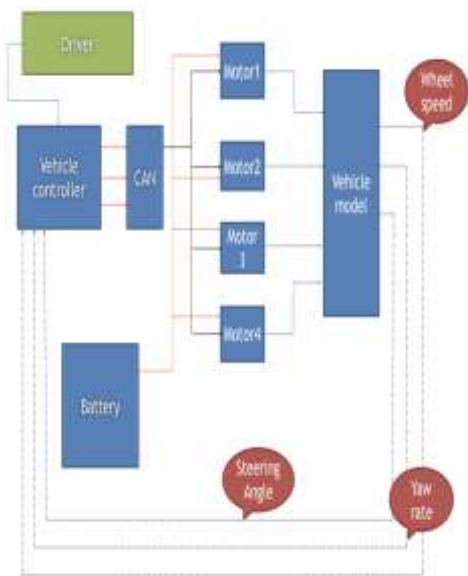


Fig.1: Schematic of the Project

The upper-level controller decides the steering angle to be superposed to the front wheels and the direct yaw moment to be imposed to the vehicle, whereas the lower-level controller distributes the total direct yaw-moment to the torque commands of the four in-wheel motors. This paper only studies the upper-level controller, which has the direct responsibility on the system robustness against time-varying network delays. In most vehicle motion control systems, the yaw rate sensor and the longitudinal/lateral acceleration sensor are usually directly connected with the vehicle controller, from which the vehicle yaw rate and the sideslip angle can be measured or estimated by the upper-level controller directly without going through the in-vehicle network.

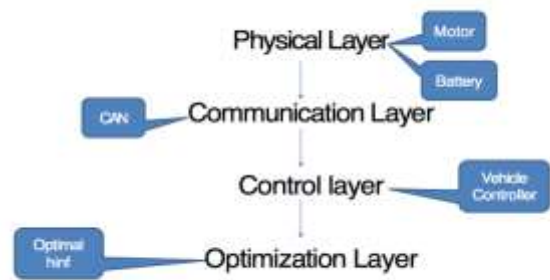


Fig.2: Layers of project

There are four layers in the project

2.1 Physical Layer:

It consists of motor, and its components and battery. It's the layer that we can feel and touch in the model.

2.2 Communication layer:

It consists of the CAN bus network.

2.3 Control layer:

It has the controller system used in the electric vehicles. The controller used here is PI controller as the basic controller and errors are rectified using the LQR controller, further enhanced by the combination of both.

2.4 Optimization layer:

The future work will be the optimization of the model done through LQR method, which is done by Hinf method.

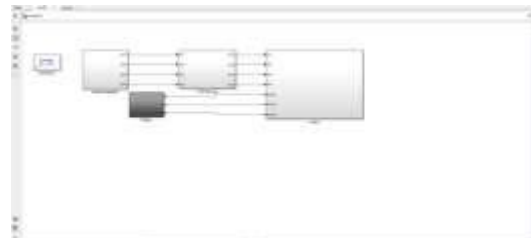


Fig.3: Model Outline

III. WORKING METHOD

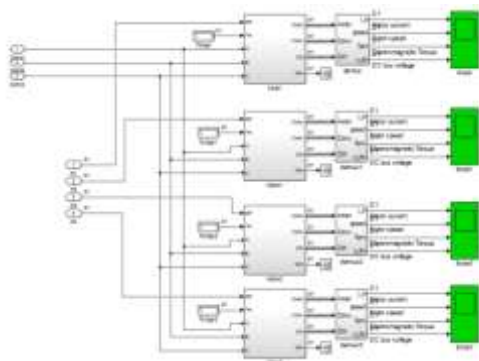
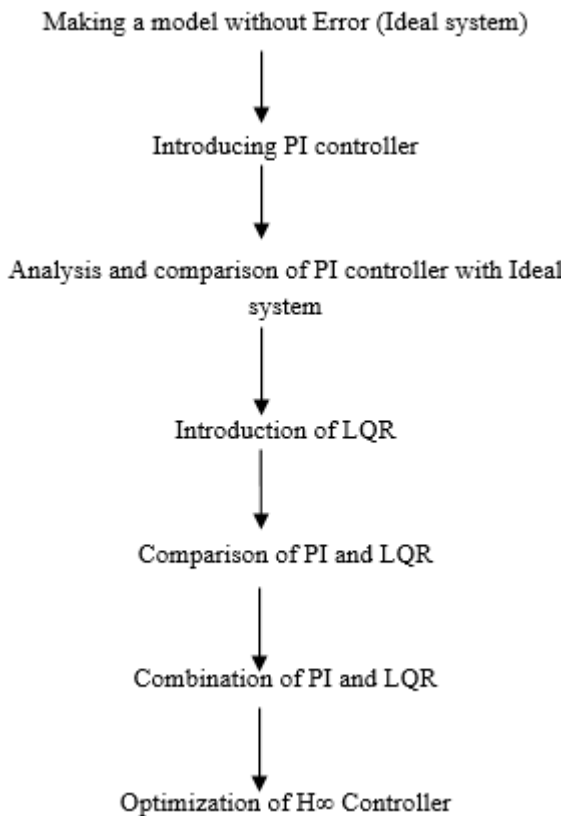


Fig.4: Complete model without delay

The above model Fig.4 has been done as a reference model to compare the results with the output from this. This system is said to be ideal since it has no error, all the input is converted into output. The model with errors Fig.5 has the same PI Controller used in the ideal system, both uses the same controller, the only difference is, here the instability due the road disturbance, driver action and controller delay will be considered.

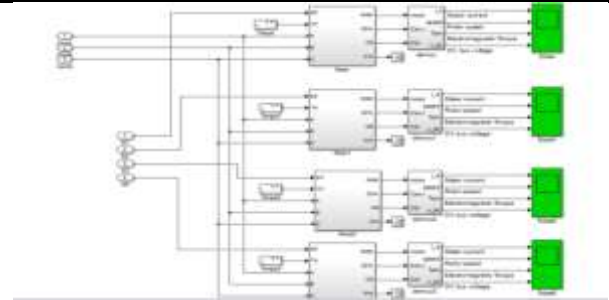


Fig.5: Complete model with delays

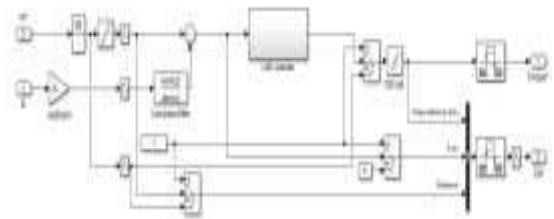


Fig.6: LQR Controller

The third model Fig.6 has the LQR controller that will reduce and minimize the instabilities caused by various disturbances. Comparison the results of controllers has been discussed below.

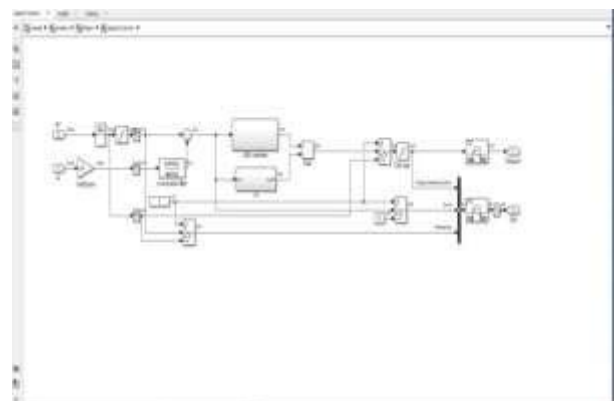


Fig.7: Combination of PI and LQR Controller

PI and LQR Controllers are combined to see the combined efficiency of both the models. The combination is actually over shades the disadvantages of the PI Controller. The LQR Controller takes full responsibility and it makes the system a little advantageous than the normal PI Controller.

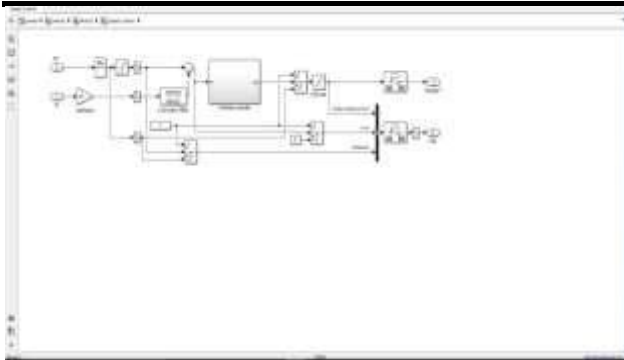


Fig.8: H_{∞} Controller

Finally after analyzing the PI, LQR and Combined PI and LQR Controllers, the next step is optimizing the H_{∞} Controller so as to get the output that over shadows all the above used controllers.

IV. RESULTS AND DISCUSSION

The models are performed using SIMULINK. The LQRD controller is designed and simulations are conducted in SIMULINK. The parameter values are given for the in-wheel motor. First the PI controller with no delays called as ideal system is simulated and results are taken. Then the PI controller with delays is been simulated in SIMULINK and the results are taken. After comparing these two models, a LQRD controller is introduced in order to reduce the delays further. The CAN-induced delays are assumed to be time varying delays and uniformly distributed in interval of $[0, 1.7T_s]$, where $T_s=10\text{ms}$ is considered to be the sampling period of closed loop system. The Matrix used in the conventional LQR are

$$Q_c = \begin{bmatrix} 2000 & 0 \\ 0 & 100000 \end{bmatrix}$$

$$R_c = \begin{bmatrix} 8000 & 0 \\ 0 & 0.00001 \end{bmatrix}$$

$$J = \sum_{i=0}^{\infty} (e_i^T Q e_i + u_i^T R u_i)$$

Then use the `lqr` command in MATLAB, and hence the control gain matrix of LQRD is

$$K_c = \begin{bmatrix} 0.099 & 0.945 \\ 1716.6 & 44485 \end{bmatrix}$$

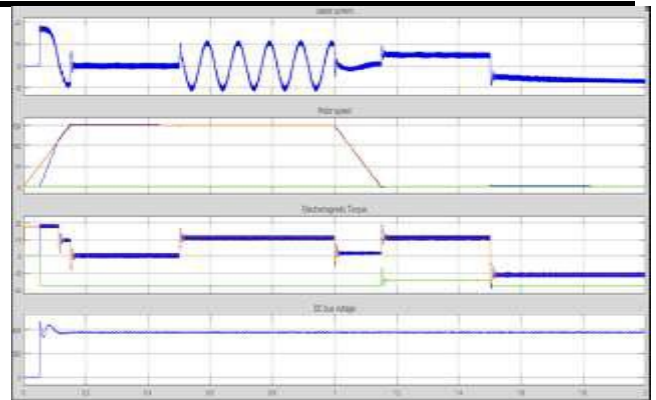


Fig.9: PI controller without delays

Fig.6 shows a PI controller without delays .This is an ideal system where there are no errors. All the input is converted into output.

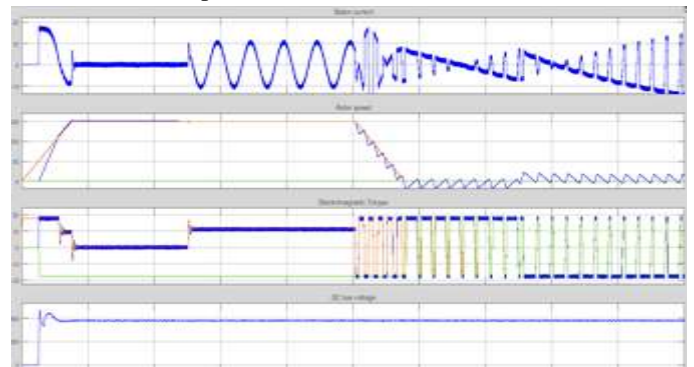


Fig.10: PI controller with delays

Fig.7 shows the PI controller with delays. Here the speed, current, torque and voltage varies with time which causes instability of electric vehicles. The blue color represents reference value and other color represents actual value. The wiggles are more here.

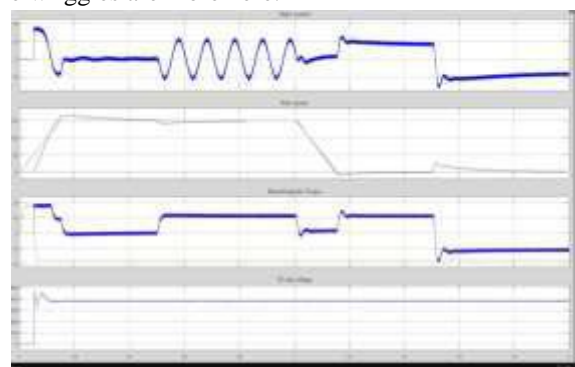
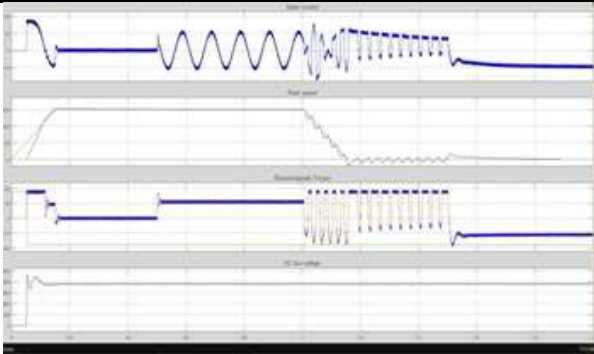


Fig.11: LQRD Controller

Fig.11 represents LQRD controller where the delays are reduced by optimizing it. Comparing with PI controller the delays are very much reduced in LQRD controller. The wiggles are reduced here. There is no big variation in output.



• Fig.12:..Output obtained as a result of combining LQR and PI Controller

- The output obtained by the combination of LQR and PI controllers has an efficiency less than that of LQR Alone and greater than the PI controller.
- Hence it wont be good to have the combination of PI and LQR to have a great working condition.
- LQR controller alone will suffice according the output, for this kind of environmental condition.
- Further Hinf controller may have a better output when compared with the others.

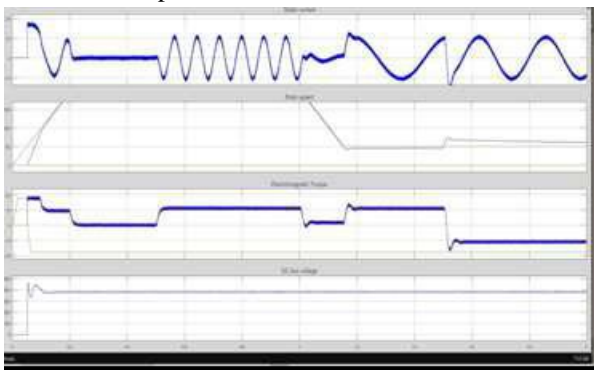


Fig.13:..Output of H_{∞} Controller

The output obtained from the H_{∞} Controller has a much better rotor speed characteristics and torque characteristics when compared with the other controllers. It has an unbelievable efficiency of 3.45% in comparison with the rotor speed.

V. COMPARISON OF COMBINED PI AND LQR WITH H_{∞} CONTROLLER

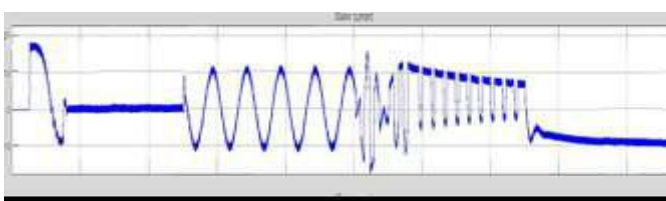


Fig.14: Comparison of Stator current between Combined LQR and PI with H_{∞}

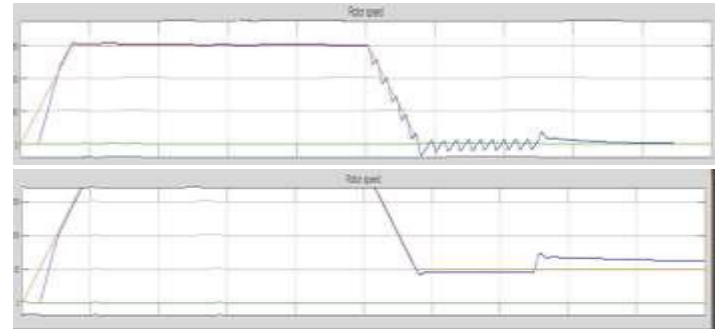


Fig.15: Comparison of Rotor speed between Combined LQR and PI with H_{∞}

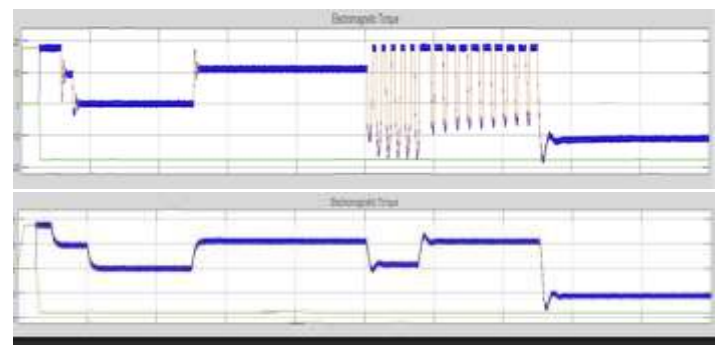


Fig.16: Comparison of Electromagnetic Torque between Combined LQR and PI with H_{∞}

VI. COMPARISON OF LQR AND H_{∞} CONTROLLER

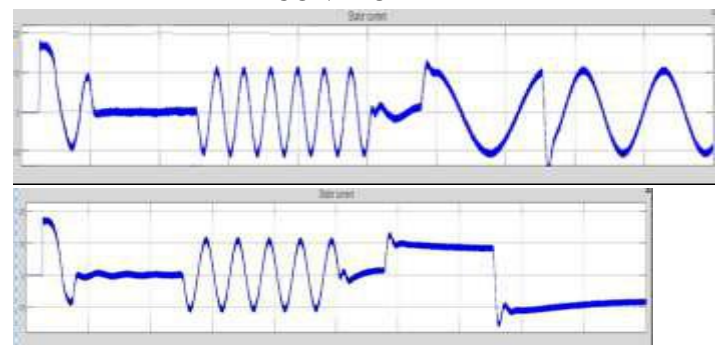


Fig .17: .Comparison of Stator current between LQR and H_{∞}

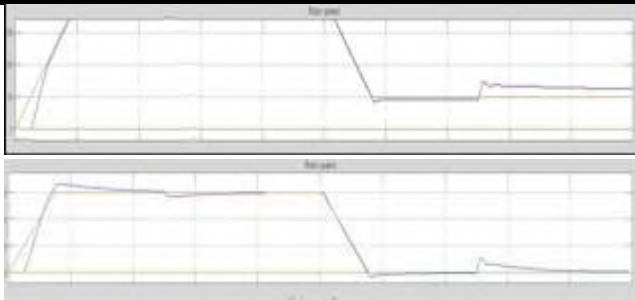


Fig.18: Comparison of Rotor speed between LQR and H_{∞}

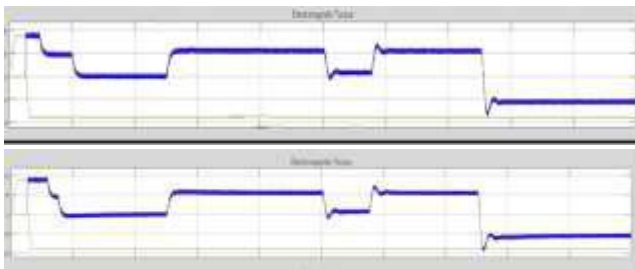


Fig.19: Comparison of Torque between LQR and H_{∞}

VII. CONCLUSION

In this paper we have reduced the time varying delays in the CAN network by using a LQRD controller. This is been incorporated for lateral motion and stability control of 4-Wheel Independent Drive EVs. The PI controller with delays produces ripples and fluctuations in the electromagnetic torque. So LQRD is used to reduce the time varying delays and fluctuations in electromagnetic torque. The comparison between the results ensures the robustness and performance of the vehicle due to reduce in the time varying delays in the closed loop system. This paper indicates the time varying delays in networked control systems would cause the system performance. So with this LQRD controller the robustness of the system is increased.

REFERENCES

- [1] S. Yu and J. J. Moskwa, "A global approach to vehicle control: Coordination of four wheel steering and wheel torques," *J. Dyn. Syst. Meas. Control*, vol. 116, no. 4, pp. 659–667, Dec. 1994.
- [2] E. J. Bedner, Jr. and H. H. Chen, "A supervisory control to manage brake and four-wheel-steer systems," presented at the Soc. Automotive Eng. Conf., Detroit, MI, USA, 2004, Paper 2004-01-1059.
- [3] J. Wang, "Coordinated and reconfigurable vehicle dynamics control," Ph.D. dissertation, Dept. Mech. Eng., Univ. Texas, Austin, TX, USA, 2007.
- [4] S. Brennan and A. Alleyne, "Integrated vehicle control via coordinated steering and wheel torque

inputs," in *Proc. Amer. Control Conf.*, 2001, pp. 7–12.

- [5] M. Nagai, M. Shino, and F. Gao, "Study on integrated control of active front steer angle and direct yaw moment," *JSAE Rev.*, vol. 23, no. 3, pp. 309–315, Jul. 2002.
- [6] B. A. Guvenc, T. Acarman, and L. Guvenc, "Coordination of steering and individual wheel braking actuated vehicle yaw stability control," in *Proc. IEEE Intell. Veh. Symp.*, 2003, pp. 288–293.
- [7] X. Yang, Z. Wang, and W. Peng, "Coordinated control of AFS and DYC for vehicle handling and stability based on optimal guaranteed cost theory," *Veh. Syst. Dyn., Int. J. Veh. Mech. Mobility*, vol. 47, no. 1, pp. 57–79, 2009.
- [8] O. Mokhiamar and M. Abe, "Effects of model response on model following type of combined lateral force and yaw moment control performance for active vehicle handling safety," *JSAE Rev.*, vol. 23, no. 4, pp. 473–480, Oct. 2002.
- [9] P. Heinzl, P. Lugner, and M. Plochl, "Stability control of a passenger car by combined additional steering and unilateral braking," *Veh. Syst. Dyn. Suppl.*, vol. 37, pp. 221–233, 2002.
- [10] G. Li, W. Hong, and H. Liang, "Four-wheel independently driven in-wheel motors electric vehicle AFS and DYC integrated control," presented at the Soc. Automotive Eng. Conf., Detroit, MI, USA, 2012, Paper 2012-01-0258.
- [11] C. F. Caruntu, M. Lazar, R. H. Gielen, P. P. J. van den Bosch, and S. D. Cairano, "Lyapunov based predictive control of vehicle drivetrains over CAN," *Control Eng. Pract.*, vol. 21, no. 12, pp. 1884–1898, Dec. 2012.
- [12] Y. Chen and J. Wang, "Design and evaluation on electric differentials for over-actuated electric ground vehicles with four independent in-wheel motors," *IEEE Trans. Veh. Technol.*, vol. 61, no. 4, pp. 1534–1542, May 2012.
- [13] J. Wang and R. G. Longoria, "Coordinated and reconfigurable vehicle dynamics control," *IEEE Trans. Control Syst. Technol.*, vol. 17, no. 3, pp. 723–732, May 2009.
- [14] D. Piyabongkarn, R. Rajamani, J. A. Grogg, and J. Y. Lew, "Development and experimental evaluation of a slip angle estimator for vehicle stability control," *IEEE Trans. Control Syst. Technol.*, vol. 17, no. 1, pp. 78–88, Jan. 2009.
- [15] K. Nam, S. Oh, H. Fujimoto, and Y. Hori, "Estimation of sideslip and roll angles of electric vehicles using lateral tire force sensors through RLS

- and Kalman filter approaches,” *IEEE Trans. Ind. Electron.*, vol. 60, no. 3, pp. 988–1000, Mar. 2013.
- [16] H. Kim and J. Ryu, “Sideslip angle estimation considering short duration longitudinal velocity variation,” *Int. J. Autom. Technol.*, vol. 12, no. 4, pp. 545–553, Aug. 2011.
- [17] H. Zhao, Z. Liu, and H. Chen, “Design of a nonlinear observer for vehicle velocity estimation and experiments,” *IEEE Trans. Control Syst. Technol.*, vol. 19, no. 3, pp. 664–672, May 2011.
- [18] S. You, J. Hahn, and H. Lee, “New adaptive approaches to real-time estimation of vehicle sideslip angle,” *Control Eng. Practice*, vol. 17, no. 12, pp. 1367–1379, Dec. 2009.
- [19] L. Imsland, T. A. Johansen, T. I. Fossen, H. F. Grip, J. C. Kalkkuhl, and A. Suissab, “Vehicle velocity estimation using nonlinear observers,” *Automatica*, vol. 42, no. 12, pp. 2091–2103, Dec. 2006

Central Bank of Syria and its Role in the Syrian Economy

Dr. Ghassan Farouk Ghandour

College of Financial & Administration-Department of Accounting & IT, Cihan University/ Sulaiymani, Kurdistan Region Government/Iraq.

Abstract— Syria as a developing country suffered from backwardness of monetary policy and dependence of central bank to government, so monetary authority couldn't attain final aims of monetary policy and on the other hand couldn't stimulate Syrian economy to attain real growth.

But in the recent years Syrian government tends to reform the monetary policy and give some independence to central bank of Syria through modernizing current laws and regulations.

Keywords— monetary policy, economy, inflation, currency.

I. INTRODUCTION

Monetary policy considers important part of general economic policy it can effect and move all economic indexes and variables like (general level of prices (inflation), level of employment and investment, growth rate of GDP (gross domestic product) and national income and distribution of them between individuals and sectors. Central banks in the world consider the monetary authorities that use implementations of monetary policy to attain the final aims of monetary policy (stability the general level of prices and stability the exchange rate of national currency).

Research hypotheses

In order to address the problem of this research and to facilitate the answer to the questions posed, we can develop a number of hypotheses based on the collected information, so we assume the following:

- 1- Monetary policy is one of the most important means of economic policy to influence economic activity
- 2- Monetary policy performance can be effective and efficient only if a set of standards and controls are available

Research importance

This research derives its importance from the position of monetary policy from the perspective of economic schools, its role in addressing economic imbalances, its position in the economic reform programs supported by the international financial institutions, and the transition

to a market economy, which is more important than the position it enjoys This policy aims at achieving economic stability and driving growth as the most important parts or items of economic policy.

Research objectives

This research aims at reaching several points, the most important of which are:

- 1- Highlighting the theme of monetary policy in all its aspects to show its importance and role in economic activity as well as uncover mechanisms and methods of work and everything related to them
- 2- Attempt to evaluate the performance of the controls or criteria on which monetary policy is based in the national economy in light of the economic reforms adopted

Research Methodology

A combination of the descriptive curriculum and the analytical approach will be used as the descriptive approach relates to the review of school ideas and the presentation of the structure of the Syrian economy. The analytical approach was based on trying to understand the elements of monetary policy and reform programs, using the foundations and relations based on them, and diagnosing the problems that were raised, as well as trying to put a quantitative expression of the various stages experienced by the Syrian economy.

First: establishment The Central Bank of Syria:

The Central Bank of Syria was established by Legislative Decree No. (87) dated 28/3/1953 which included the Basic Monetary System of Syria (and that modified by the law No. (23) dated 17/3/2002) . The Bank started its operations on the first of August 1956, with its headquarters in the city of Damascus , and 11 branches located in the governorates of Syria(1)

Second: The Management of the Central Bank of Syria

The bank is managed by the Governor who heads the Administration Committee. The Committee includes one Deputy Governor and three Executive Directors. The Governors insure the compliance with the laws and basic rules and regulations of the Bank

Third: The Structure of the Central Bank of Syria:

- ❖ The Central Bank of Syria is an independent public sector establishment operating under the guarantee of the state, and within the guidelines issued to it by the Council of Ministers. The Capital of the bank is fully subscribed by the state (3)
- ❖ The Central Bank coordinates the activities of money and credit establishments within its authorities and general guidelines issued to it by the Council of Ministers in a way that realizes the objectives of fiscal , monetary and banking policies of the state.
- ❖ The Central Bank of Syria is solely empowered to issue, for the account of the state , the paper currency , in the amounts needed to meet the requirements of national economic development and sustained growth , and to facilitate the developmental process in various economic and social sectors . The monopoly of issuing the national currency given to the Central Bank makes it the sole financial institution capable of managing monetary circulation.
- ❖ The bank exercises control over the banking system, and ensures the proper implementation of the provisions of the Basic Monetary Law, and related rules and regulations, and monetary and banking criteria.

Fourth: independence of the central bank of Syria:

Central Bank of Syria is subordinate to council of ministers and works within guidelines issued by government.

Arabian monetary fund's has issued book under address(monetary policies in Arabian countries) discusses through it the independence of monetary authorities in Arabian countries in accordance with many indexes that appear independence of Arabian central banks ranged between 0.603 in Lebanon and 0.339 in Mauritania, and Syria occupied before last rank with 0.364(2)

Table.1: independence of Arabian central banks

The country	Independence rank
Lebanon	0.603
Saudi	0.502

Egypt	0.500
Algeria	0.497
Libya	0.452
Tunis	0.430
Jordan	0.426
UAE	0.393
Morocco	0.375
Syria	0.364
Mauritania	0.339

Recourse: Arabian monetary funds

Fifth: Main Functions of the Central Bank of Syria

The main functions performed by the Bank are:

1- Issuing the national currency:

The issuing of national currency is a monopoly of the state (4), and exercised solely on behalf of the state by the Central Bank of Syria. The Syrian Pound is the basic unit of the Syrian currency. The Basic Monetary Law has defined the denominations in which the Syrian banknotes may be issued, as well as, the coins and their withdrawal from circulation and exchange. The basic unit of the Syrian currency is the “Syrian Pound” which is divided into 100 Syrian Piastres. The denominations of Syrian banknotes in circulation are SP 1000, SP 500, SP 200, SP 100, SP 50, SP 25, SP 10, SP 5 and SP 1

Table.2: currency issued by central bank of Syria, Numbers in billion of Syrian pounds

year	2006	2007	2008	2009	2010	2011
Notes Issued	209	235	265	292	341	404
Coins Issued	1.9	2.1	2.4	2.4	3.0	3.4
Currency Issued	211	237	267	294	344	407

Recourse: central bank of Syria report 2011

We can notice that currency issued by central bank of Syria increase from 211 billion Syrian pounds issued in 2007 to 407 billion Syrian pounds issued in 2011.

The main reason to issue the currency isn't to finance GDP (gross domestic product) but to finance the deficit of budget that emergent because of badness of fiscal policy follows up in Syria. So growth rate of money supply always is more than growth rate of GDP.

Table.3: Relationship between growth rate of M2 and GDP and budget deficit

Number: in billion Syrian pounds (without the rates)

Year	2006	2007	2008	2009	2010	2011
Money supply M2	586	730	865	939	1059	1188
Growth rate of M2	20%	25%	18%	9%	13%	12%
GDP (market price)	904	974	1017	1067	1251	1390
Growth rate of GDP	10%	8%	4%	5%	17%	11%
Deficit of budget	91.6	92.7	106.8	125.3	143.5	103.5

Deficit /GDP	10.1%	9.9%	10.5%	11.7%	11.9%	8.4%
GDP/M2	1.5%	1.3%	1.2%	1.1%	1.2%	1.2%

Resource: central bank of Syria report 2011

-We can notice from table no. (3) That medial annual growth rate of money supply was 16.1% and in the same period (2006-2011) medial annual growth rate of GDP was 9.2% that caused a high inflation arrived to 10% in 2010

- Deficit budget increased from 91.6 billion S.P in 2006 to 143.5 billion S.P in 2010 after that, it declined to 103.5 in 2011.

2- The Central Bank is the Bank of Banks (5)

The Central Bank is regarded by the Basic Monetary Law as the Bank of Banks as it rediscounts purchases, reassigns drafts and commercial promissory notes, and

grants loans and advances to finance the activities of various economic sectors, all in its capacity as lender of last resort. These operations are performed through the banks as it is prohibited to deal directly with individuals. The Central Bank, in its capacity as a bank of banks, can monitor and control the implementation of credit policy and assess its appropriateness to requirements of the national economy.

Central bank of Syria defines interest rates through definition of rediscount rate that specified to every bank alone

Table.4: Rediscount rates for specialist Syrian banks

	Loans and Advances			Rediscount
	Long-Term	Medium Term	Short-Term	
Commercial Bank of Syria				
Commercial Transactions Bills				5.00
Industrial Transactions Bills				4.25
Agricultural Transactions Bills				3.25
Financing of Export			3.25	
Financing of Storage & Export of Agricultural Products			3.25	
Financing of Public Sector Commercial Goods Storage			4.75	
Financing of Storage & Export of Wheat and Barley			3.25	
Other Loans and Advances			5.75	
Industrial Bank				
Commercial Transactions Bills			4.25	3.50
Industrial Transactions Bills				2.75
Advances		3.00	2.75	
Agricultural Cooperative Bank				
Public and Mixed Sectors and Individuals	3.00	2.50	2.50	2.75
Cooperatives	2.50	2.00	1.75	2.00
Real Estate Bank				
Housing Institutions and Municipalities	4.00			
Housing Cooperatives	4.00			
Individual Housing	4.50			
Hospitals, Schools and Tourism	6.00			
Vacationing Residence (Individuals and Investors)	6.00			
Popular Credit Bank				
Small Industries Transactions Bills (300 days)				2.50
Small Industries Financing Bills (300 days)				2.75
Small Tradesmen Transactions Bills (120 days)				3.25
Small Tradesmen Financing Bills (120 days)				3.50
Financing of Small Industries		3.00	2.75	
Financing of Small Tradesmen		3.75	3.50	

Recourse: central bank of Syria report 2011

3- Issuing national public debt instruments and participating in international financial negotiations

The Central Bank of Syria issues national public debt instruments for various terms (through Basic Monetary System) , performs all related reissue and refund operations, and, in general, all financial operations related to loans issued or guaranteed by the state. Also it participates in negotiating international payments , foreign exchange , and clearing agreements. Moreover , it enters into all related arrangements required for the implementation of such agreements.

Furthermore, the Bank participates in the negotiations of external loans entered into for the account of the state, and it represents the state in negotiations in the areas of international monetary cooperation .

4- Banks required reserves

The Central Bank of Syria may require the banks to invest their required reserves , and their special reserves in securities issued by the state or guaranteed by it, or to invest a fraction of its surplus funds and a part of their deposits in government securities .

5- Acting as the government bank, and its financial agent.

The Central Bank is empowered by the basic monetary law to act as the state bank, its cashier and financial agent inside and outside the Syrian territories in all banking , cashier, and credit transactions of the state .

6-Managing the Foreign Exchange Bureau for the account of the state .

Syrian Pound is pegged to the United States Dollar, and the Syrian Pound exchange rate with other currencies is derived by reference to their exchange rates expressed in US Dollars in International Financial markets and the pegged rate of the Syrian Pound to the US Dollar.

But in the last months monetary authority tended to peg Syrian pound to other currency as Euro and Yen (6)

- Foreign exchange regulations in effect now allow the unlimited importation of Syrian and other currencies. They also allow exportation of the Syrian currency with resident travellers to Jordan and Lebanon only, with a maximum amount of SP 5000 per person.
- Syrian nationals and residents, leaving to Arab and foreign countries (excluding Jordan & Lebanon) are allowed to carry with them a maximum of US Dollar 2000, or its equivalent in other foreign currencies, per person and each time, without being asked about the source of these funds. The maximum amount is reduced by one half for a child traveller less than 15 years old on the date of the travel.

- Non-resident Arabs and foreign nationals are allowed to export upon departure what they brought with them in foreign currency and other means of payment subject to a limit of US Dollar 5000 or its equivalent in other foreign currencies. For larger amounts, the non resident traveller must show evidence of importing these amounts in the form of a customs declaration.
- The Central Bank of Syria also performs the following:.
- All special operations in foreign exchange, management of international reserves with a view to safeguarding them and ensuring the stability of foreign exchange rates .

There are three exchange rates of Syrian pounds:

- ❖ Official Exchange Rate
- ❖ Neighboring Countries Exchange Rate
- ❖ Non-Commercial Transactions Exchange Rate
- ❖ Export Proceeds:

The Foreign Exchange Regulations allowed the private sector exporters to withhold 75% of their export proceeds in foreign currencies for the purpose of financing their imports or for selling to other importers. The remaining 25% have to be surrendered to the Commercial Bank of Syria.

Exporters of fruits, vegetables and medicines of all public, private, and joint sectors are allowed to withhold 100% of their export proceeds to finance imports.

7- Payment for Imports:

Foreign exchange needed to pay for imports of foreign trade public sector establishments is provided through the annual foreign exchange budget. These establishments may obtain their import licenses upon presenting the documents needed for their imports. Foreign exchange needed for imports of the private sector is secured from the sector's own resources as follows :

- Resulting from 100% and 75% of export proceeds in foreign exchange.
- Foreign currency accounts of non - resident Syrian nationals with Commercial Bank of Syria fed with funds resulting from activities abroad.
- Credit facilities from abroad for 180 days.
- Direct payment in foreign currencies to the Commercial Bank of Syria of the value of imports to cover open documentary credits or bills for collection.
- -Foreign currencies bought by importers from private sector exporters, or from joint projects through Commercial Bank of Syria , and at the exchange rates contained in the "neighboring market rate bulletin".
- Acquires capital of financial institutions subject to special legal provisions

- All operations of facilitating the transport of establishment and management of clearing rooms. currency. Also it may establish or participate in the

Table.5: exchange rates of Syrian pounds

	2011	2010	2009
	December	December	December
Period Average			
Exchange Rates (LS per \$)			
Official Exchange Rate	11.2	11.2	11.2
Neighboring Countries Exchange Rate	46.3
	49.9	48.6	...
Non-Commercial Transactions Exchange Rate	...	52.2	51.6
	53.4		
Non-Commercial Transactions Exchange Rate			
Euro	66.8	67.6	58.6
Sterling Pound	97.3	100.2	83.2
Japanese Yen	48.7	49.1	43.7
Saudi Riyal	14.3	13.8	13.7
Jordanian Dinar	75.9	73.3	72.3
Lebanese Pound	0.036	0.035	0.036
Egyptian Pound	8.2	7.7	8.1
Turkish Pound	39.760	0.037	0.052
Irakian Dinar
End of Period			
Exchange Rates (LS per \$)			
Official Exchange Rate	11.2	11.2	11.2
Neighboring Countries Exchange Rate	46.3
	49.9	48.6	...
Non-Commercial Transactions Exchange Rate	...	52.2	51.6
	54.9		
Non-Commercial Transactions Exchange Rate			
Euro	65.0	71.0	63.4
Sterling Pound	94.4	100.6	89.4
Japanese Yen	46.5	49.5	46.8
Saudi Riyal	14.7	13.8	13.7
Jordanian Dinar	77.6	73.3	72.3
Lebanese Pound	0.037	0.034	0.034
Egyptian Pound	8.2	9.0	7.6
Turkish Pound	40.660	0.039	0.037
Irakian Dinar

Resources: statistics of central bank of Syria 2011

Sixth: Supervision and Control

Supervision over the functions of the Central Bank is exercised by the council of Ministers ,in accordance with the relevant provisions of the Basic Monetary Law while

financial control over the Bank's accounts and expenditures is vested in the Central Bureau for Financial Control .

Seventh: Current Developmental Projects in the Bank

During the last several years the Syrian economy has witnessed important structural development as a result of economic adjustment policies which all still being pursued. These policies have affected various economic social financial and monetary activities in the country.

The Central Bank of Syria, mindful of the need to monitor and facilitates this important and far reaching economic and social developments has embarked on implementing a new strategy that comprises of several new developmental plans aimed at updating the bank laws and regulations, modernizing current operating methods, by introducing advanced technologies, and utilizing the best computer systems in all bank functions and activities.

II. CONCLUSIONS AND RECOMMENDATIONS

As we seen within the previous pages monetary policy in Syria suffers from various problems, and if we want to refer it, we have to verbalize the role of central bank of Syria to realizes the objectives of monetary policy and through grants central bank of Syria the independence that needed by it to control the monetary policy tools to attain the general economic objectives.

23 laws (basic monetary law) consider important law to refresh central bank of Syria and monetary policy that began to move interest rates since 2003 and control with money supply in harmony with other indexes.

REFERENCES

- [1] www.mas.gov.sg .
- [2] Abdul-Zamil, Khalid: The Role of Monetary Policy in the Design of Economic Policy, PhD 3- 3- Thesis, University of Damascus, 2005.
- [3] Jomah, Muhammad Saleh: Monetary Policy in Syria, Dar al-Redha, Damascus, 2005.
- [4] www.araboo.com/dir/syria-central-bank
- [5] www.cafe-syria.com/Finance.htm - 16k
- [6] strategis.ic.gc.ca/epic/internet/inimr-ri.nsf/en/gr110367e.html - 15k
- [7] www.banquecentrale.gov.sy/ - 4k
- [8] Arabian monetary funds monetary policies in Arabian countries 1996, UAE, Abo dubai, P89-10
- [9] law dated 17/2/203 (basic monetary law)
- [10] strategis.ic.gc.ca/epic/internet/inimr

Environment Impact Assessment from Mining & Associated Industrial Activities on Environmental Quality of Ballari Region

T. H. Patel¹, Dr. V. Venkateshwara Reddy², Dr. S.R. Mise³

¹Department of Civil Engg., R.Y.M.E.C. Ballari, India

²Department of Civil Engg, JNTUH Hyderabad, India

³Department of Civil Engg, PDACE, Kalburgi, India

Abstract— Bellary district is known for Iron ore deposits and many Iron and Steel plants and sponge Iron plant are established in this region.(6)

The impact from mining and industrial activities may have impact on Environment if Environmental protection measures are not implemented.

In this paper efforts have been made to assess impact on the Air quality, Water quality and noise environment. Also an attempt has been made to suggest mitigative measures to attenuate environmental impacts on environment.

Keywords— EIA, AAQ, NAAQ, Mitigative measures, CPCB, KSPCB.

I. INTRODUCTION

Mining and steel Industrial activities contribute towards national development, Implementation of sustainable development concepts in these activities will ensure no significant environmental impacts and industrial development. The Mining activities caters the need of iron and steel plants, sponge iron plant and also other consumers. Steel is essential commodity for common man and for national development.(6)

Bellary region is considered as one of the major hot spot of the Karnataka State due to problems arising out of mining and other associated industries. Accordingly environmental impact assessment(EIA) of Bellary region has been under taken considering Air, Water and Noise components of Environment

II. OBJECTIVE

To assess the environment impact from the mining and associated industry and environmental quality of Bellary region. Environmental impact on environment include Air, Water, Noise quality within 10 KMS radius of Bellary have been studied to assess the impact.

III. MATERIALS & METHODS

- Description of study areato assess the impact of mining and other associated industry baseline environmental quality with 10 K.M Radius of Bellary studied.
- Environmental quality parameters The environmental component include air quality, and noise level materialized data Bellary considered for study.

METEOROLOGICAL DATA

Meteorological Data to assess wind direction and speed, temperature, humidity, generated during study period at Bellary used for this study.

AMBIENT AIR QAULITY

Ambient air quality data generated from 2013 to 2016 for the parameter PM-10, PM - 2.5, SO 2 and NO x with in 10 Kms. Radius at 6 AAQM Stations.

WATER QUALITY

Surface water samples collected at 1 locations to assess impact on water environmental

NOISE LEVEL

Day time and night time noise in Db(A) collected at 1 locations to access impact of noise

IV. RESULTS & DISCUSSIONS

The Meteorological and environmental data collected in Bellary region during the study period

METEOROLOGICAL DATA:

The Meteorological data during2016 which includes wind speed,Wind Direction, and ambient temperature, relative humidity are collected and summarized in table-I.

Table.1: Meterological data

Sl.No	Parameters	Maximum	Minimum
1	Temperature o C	43.5	13.7
2	Relative humidity %	97	17.0
3	Wind Speed in m/s	0.8	8.3
4	Predominant direction	WSW/WNW/SE	

AMBIENT AIR QUALITY DATA

The results of Ambient Air quality data monitored in study area for PM-10, PM 2.5 SO 2 and NO x with in 10 Kms. Radius at 8.00 AAQM Stations are given in Table.

Table.2: Summary of Ambient Air Quality Data

SL. No.	AAQM LOCATION	PM 10			PM 2.5			SO 2			NO x		
		Min	Max.	Avg.	Min	Max.	Avg.	Min	Max.	Avg.	Min	Max.	Avg.
1.	Bellary Municipal Corporation	29.4	136.0	88.9	20.2	43.4	31.6	5.3	10.4	9.3	8.2	17.1	14.2
2.	Regional Office KSPCB Bellary	30.1	102.4	71.6	22.2	48.7	35.6	7.3	9.2	7.8	10.2	14.2	11.6
3.	Halkundi Village	24.0	43.0	32.6	8.6	26.2	16.8	2.1	4.9	3.1	4.9	11.2	8.2
4.	Belgal village	26.0	55.0	31.8	13.6	29.6	16.1	3.0	11.1	6.8	4.9	33.1	8.9
5.	VeniVerapura	28.6	143.6	92.1	14.9	72.8	46.8	5.2	14.4	8.8	11.6	46.2	26.5
6.	Janikunte	24.2	89.6	37.8	16	45.6	18.9	3.6	8.2	2.1	3.8	11.8	4.9

All units are in ug/m³

Air Quality Impacts: AERMOD was developed by AMS/EPA Regulatory Model Improvement Committee (AERMIC). To assess the Air Quality Impacts AERMOD version 8.8 used. Meteorological data for winter season is used.

To Predict the Air quality impact AERMOD 8.8 model run to assess the contribution in Ground level Concentration from point sources.

The Baseline Air Quality and Contribution to Ground Level Concentration is given in the Table

Table.3: Summary of Ambient Air Quality Impact

SL. No.	AAQM LOCATION	PM 10			PM 2.5			SO 2			NO x		
		Base line	GLC Pred	%	Base line	GLC Pred	%	Base line	GLC Pred	%	Base line	GLC Pred	%
1.	Bellary Municipal Corporation	88.9	12.6	14.1	31.6	4.1	12.9	9.3	2.7	29.1	14.2	5.1	35.9
2.	Regional Office KSPCB Bellary	71.6	8.1	11.3	35.6	3.8	10.6	7.8	2.2	28.2	11.6	4.1	35.3
3.	Halkundi Village	32.6	7.2	22.0	16.8	3.2	19.1	3.1	1.1	35.4	8.2	2.6	31.7
4.	Belgal village	31.8	9.3	29.2	16.1	4.3	26.7	6.8	2.5	36.7	8.9	3.1	34.3
5.	VeniVerapura	92.1	24.6	26.7	46.8	9.5	20.2	8.8	2.9	32.9	26.5	8.3	31.3
6.	Janikunte	37.8	9.7	25.6	18.9	4.7	24.8	2.1	0.5	23.8	4.9	1.4	28.5

All units are in ug/m³

WATER QUALITY DATA

The results of water quality data monitored during study period are given in the table 3

Table.4: Water Quality of – Surface Water T. B. Dam Water

Sl.No.	Parameter	Values
1.	Ph	8.5
2.	Conductivity (umhos/cm)	236
3.	TDS (mg/l)	160
4.	Turbidity NTU	18
5.	T.Hardness as Caco3 (mg/l)	78
6.	Calcium as Ca (mg/l)	19.2
7.	Magnesium as Mg (mg/l)	7.3
8.	Chlorides as cl(mg/l)	22
9.	Sulphates as So4 (mg/l)	27.2
10.	Nitrates as No3 (mg/l)	0.13
11.	Fluoride as F	0.2
12.	BOD	2.7
13.	Alkalinity as CaCo3 (mg/l)	70
14.	Total Iron as Fe	0.79

NOISE LEVEL

The results of noise level monitored during study area are given in Table 4

Table.5: Noise Levels
 Locations Gandhinagar, Bellary

Time	CPCB NORM	MIN. dB(A)	Max. dB(A)	Average dB(A)
Day Time	75	35.8	63.6	57.6
Night time	70	33.9	56.4	46.2

The PM 10 Levels are exceeding the NAAQ limits of 100 ug/m3. It was envisaged that the major contribution is from Transportation of Vehicles in unpaved roads and contribution from industries and other sources.

From Water quality monitoring results it was observed that the surface water meets the CPCB stipulated limit of surface water quality Part –C.

For ground water most of the parameters meets the standard of IS10500.

The Ambient noise level meets the norms of CPCB limits during day and night time.

V. CONCLUSION

The present study indicates that the Ambient Air quality for PM 10 exceeding limits of NAAQM limits of 100 ug/m3. As this is attributed namely due to transportation of vehicles.

The following mitigatives measures has to be ensured.

- The unpaved roads has be paved

- By pass roads adjacent habitation is to be provided

- Preventing over load and spillages on the Road

With this measures and ensuring emission level within the limits from associated industries PM 10 Levels can brought within the limits.

To sustain water quality industries and Municipalities has treat the effluents/sewerage within the limits and maximizing recycle/reuse.

REFERENCES

[1] APHA (2006). Standard methods for examination of water and wastewater, 21st Edition, American Public Health Association; Washington.
 [2] Air (prevention and Control of pollution) Act, 1981, and notifications issued there under, “**The Environmental Protection and pollution control Manual**”, (2000), Karnataka Law Journal Publications, Bangalore.

- [3] Beer Tom (2001), “**Air Quality as a Meteorological Hazard**”, Journal of Natural Hazards, No.23, pp 157-169.
- [4] Bhanarkar.A.D, Gajghate.D.G and Hassan.M.Z (2001), “**Air quality management in iron and steel industry**”,Journal of Environmental Pollution control, No.5, pp 17-26.
- [5] Hand Book on Environmental Legislation & Technology, Karnataka State pollution Control Board, Bangalore 2000,pp 181,185,187,286,296.
- [6] Indian Council of Forest Research & education, Dehradun, ‘Macro level Environment Impact assessment Study report of Bellary District, Karnataka, Vol I, Nov 2011, pp 18-22,36-39,60-69,103-112.
- [7] Mackenzie L. Davis, David A. Cornwell (1998), “**Introduction to Environmental Engineering**”, McGraw- Hill Book Co, Singapore.
- [8] M. Mahadeva Swamy, M.G.Yathish (1994) “**Air quality modeling for a single point source**”, Indian Journal of Environment, Vol 36, No.4, pp 36-43.
- [9] Rao.M.N, Rao.H.V.N (1989), “**Air Pollution**”, Tata McGraw-Hill Publishing Company Limited, New Delhi.
- [10] **Survey of India, Toposheet no. 52 A/12**, First edition (1973), Govt of India, New Delhi.
- [11] The Environment (Protection) Rules, 1986 and notifications issued there under, “**The Environment Protection and Pollution Control Manual**” (2000). pp 109-110, 136-140, Karnataka Law Journal Publications, Bangalore.
- [12] Wark Kenneth, Warner F. Cecil (1981), “**Air pollution, Its Origin and Control**”, II edition, Harper and Row publishers, New York, USA.
- [13] Website: *www.epa.gov* (2005), “**Air pollution dispersion models**”, United States Environment Protection Agency, USA.

Autonomous Mobile Vehicle based on RFID Technology using an ARM7 Microcontroller

Mr. Ravi Chandra Bathula, Mr. Sharath Chandra Inguva

Assistant Professor, Dept. of ECE, Guru Nanak Institute of Technology, Hyderabad, Telangana, India.

Abstract— Radio Frequency Identification (RFID) system is looked upon as one of the top ten important technologies in the 20th century. Industrial automation application is one of the key issues in developing RFID. Therefore, this paper designs and implements a RFID-based autonomous mobile vehicle for more extensively application of RFID systems. The microcontroller LPC2148 is used to control the autonomous mobile vehicle and to communicate with RFID reader. By storing the moving control commands such as turn right, turn left, speed up and speed down etc. into the RFID tags beforehand and sticking the tags on the tracks, the autonomous mobile vehicle can then read the moving control commands from the tags and accomplish the proper actions. Due to the convenience and non-contact characteristic of RFID systems, the proposed mobile vehicle has great potential to be used for industrial automation, goods transportation, data transmission, and unmanned medical nursing etc. in the future. Experimental results demonstrate the validity of the proposed mobile vehicle.

Keywords— Radio Frequency Identification, RFID Reader, RFID Tag, Industrial Automation, ARM 7 MCU.

I. INTRODUCTION

The project aims at making the robot to move in a particular Defined direction, connected at the Controller, specified by the user at the RFID Tag. The project uses the RFID technology and Embedded Systems to design this application. The main objective of this project is to design a system that continuously checks for the RFID and changes the direction of the ROBOT accordingly.

This project is a device that collects data from the RFID section, codes the data into a format that can be understood by the controlling section. This receiving section controls the direction of the robot as per the command received from the RFID section. The objective of the project is to develop a microcontroller based control system. It consists of a RF Reader and Tag, microcontroller and the robotic arrangement.

The software application and the hardware implementation help the microcontroller read the data From RFID Tag and accordingly change the direction of the robot. The measure of efficiency is based on how fast the microcontroller can read the data, detect the signal received and change the direction of the robot. The system is totally designed using RFID and embedded systems technology. The performance of the design is maintained by controlling unit.

II. HARDWARE ARCHITECTURE

Fig. 1 shows the hardware architecture of the proposed autonomous mobile vehicle. The proposed vehicle can be divided into four parts.

- 1) The RFID tags stuck on the tracks;
- 2) The RFID reader used to communicate with RFID tags and transmit the moving control commands to Micro Controllable Unit, (MCU) module;
- 3) The MCU module used to receive the moving control commands from RFID reader and control the mobile vehicle; and
- 4) The mobile vehicle.

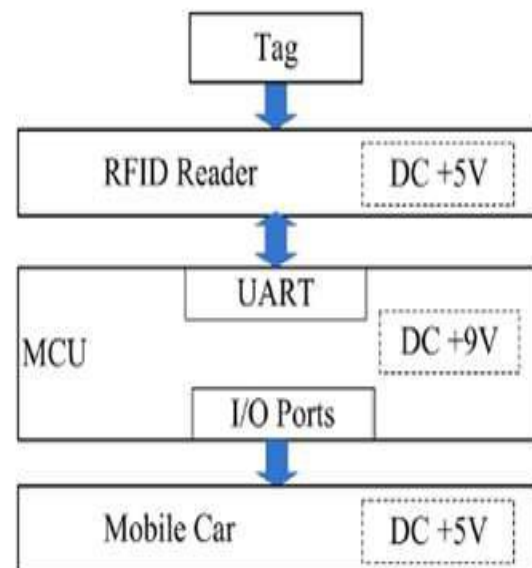


Fig.1. Hardware Architecture for the proposed Vehicle

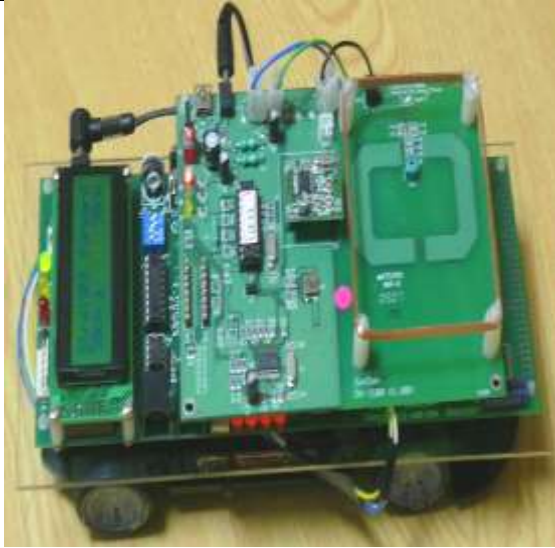


Fig.2. Physical Architecture of the proposed Vehicle

Firm Ware for the Proposed Vehicle:

Due to limited budget, a simple and cheap motor is used in the proposed autonomous mobile vehicle. Of course, a high precise motor can also be integrated into the proposed vehicle to achieve more advanced and accurate control without modifying the architecture represented in this paper. Two motors are used in the proposed vehicle for direction and speed controls, respectively. Fig. 2 shows the driving circuit used in the motor control of the proposed autonomous mobile vehicle. From Fig. 2, it can be seen that two control signal generated by MCU are used to control one motor. For direction control, the control signals 1 and 2 are used to control the vehicle to turn left and turn right, respectively. For speed control, the control signals 3 and 4 (not shown in Fig. 2) are used to control the vehicle to move forward or speed up and move backward or speed down, respectively.

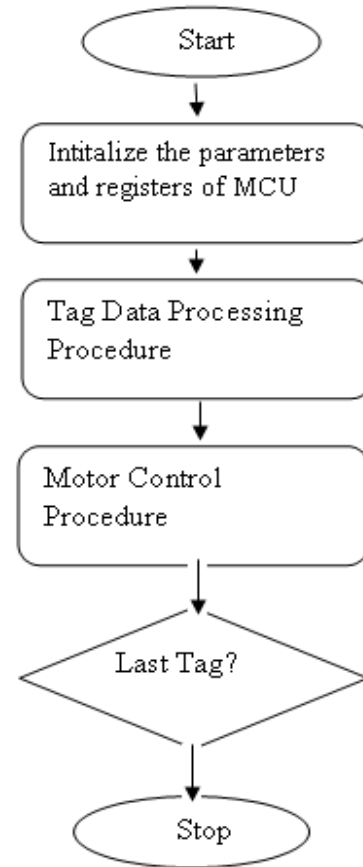


Fig.3. Flowchart for the programming of the proposed vehicle

The firmware programmed in LPC2148 is designed to communicate with RFID tags and control the motors according the commands received from the tags. Therefore, the main firmware programmed as shown in Fig. 3 can be divided into two parts; tag data processing procedure and motor control procedure. The flowchart of tag data processing procedure is shown in Fig. 4. From Fig. 4, it can be clearly observed that MCU will transmit the request command to tags and then received control commands from tags periodically. The control commands should include the moving forward/backward, direction and speed etc. If the commands have been received completely, the commands will be further transmitted from RFID reader to MCU.

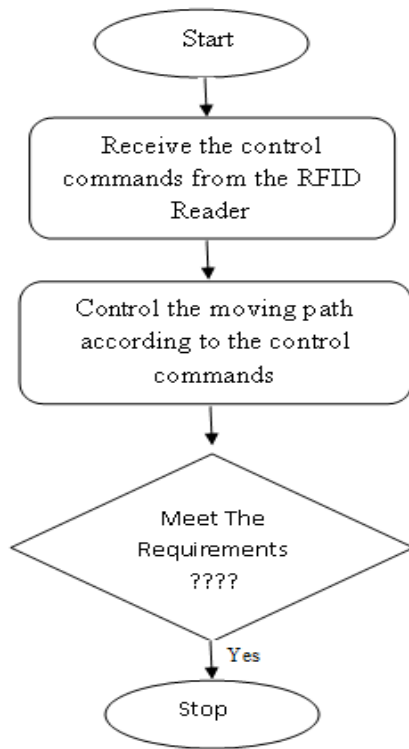


Fig.4. Flowchart of Tag data Processing Procedure

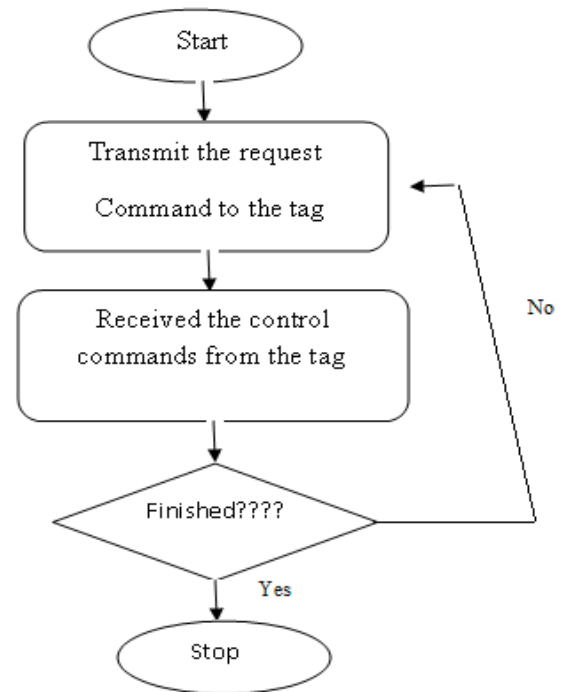


Fig.5. Flowchart of Motor Control Procedure

Fig. 5 shows the flowchart of motor control procedure. From Fig. 5, it can be seen that after the MCU received the control commands from RFID reader, the MCU will calculate and then send the PWM signals through the control signals 1-4 to motors; and therefore, the vehicle will move according to the signals. A PI-based feedback control method is used in this paper to make sure that the required moving path can be achieved.

The RFID tags in use possess use possess (64 pages x 4 bytes) memory capacity. The tag used only employs 3 bytes to control moving path of one vehicle. . Of course, more accurate control commands can also be planned; for example, more divisions for direction and speed control such as turn 10 deg. left with speed 10 cm/s etc. can be planned and stored in tags to control the vehicle.

III. EXPERIMENTAL RESULTS

A RFID-based autonomous mobile vehicle was designed and implemented in this paper. Several moving paths can be planned as said earlier and can be tested; however, only four cases are taken into consideration while testing originally. Four tags are used to control the vehicle with respect to the three cases, respectively. All test cases showed that the proposed vehicle can move according to the control commands received from the tags. Therefore the validity of the proposed system can be demonstrated.

IV. CONCLUSION

A RFID-based autonomous mobile vehicle was successfully designed and implemented in this paper. By writing the moving control commands into the RFID tags beforehand and sticking the tags on the tracks, the autonomous mobile vehicle can then read the moving commands from tags and accomplish the proper actions. Experimental results demonstrated the validity of the proposed system. Some more comprehensive and advanced control methods and their corresponding control commands can also be designed and stored in tags and then used to control the vehicle accurately, the research will be investigated in the future.

REFERENCES

- [1] Landt, J.; "The history of RFID," IEEE Potentials, Volume 24, Issue 4, Oct.-Nov. 2005, pp. 8 - 11
- [2] Weinstein, R.; "RFID: a technical overview and its application to the enterprise," IT Professional, Volume 7, Issue 3, May-June 2005, pp. 27 – 33
- [3] Bansal, R.; "Coming soon to a Wal-Mart near you," IEEE Antennas and Propagation Magazine, Volume 45, Issue 6, Dec. 2003, pp. 105 – 106
- [4] Perakslis, C.; Wolk, R.; "Social acceptance of RFID as a biometric security method," IEEE Technology and Society Magazine, Vol. 25, Issue 3, 2006, pp. 34 – 42
- [5] "Special issue on RFID systems" IEEE Transactions on Automation Science and Engineering, Vol. 4, Issue 1, Jan. 2007
- [6] Jabbar, H.; Taikyeong Jeong; Jun Hwang; Gyungleen Park; "Viewer identification and authentication in IPTV using RFID technique," IEEE Transactions on Consumer Electronics, Vol. 54, Issue 1, February 2008, pp. 105 – 109
- [7] Roussos, G.; "Enabling RFID in retail," Computer, Volume 39, Issue 3, March 2006 pp. 25 - 30
- [8] Dianmin Yue; Xiaodan Wu; Junbo Bai; "RFID application framework for pharmaceutical supply chain," IEEE International Conference on Service Operations and Logistics, and Informatics, Vol. 1, Oct. 2008, pp. 1125 – 1130
- [9] Rajparthiban, R.; Aravind, C.V.; Kannan; "Development of an active RFID communicator for automatic control applications," 5th International Colloquium on Signal Processing & Its Applications, March 2009, pp. 276 - 277
- [10] Gandino, F.; Montrucchio, B.; Rebaudengo, M.; Sanchez, E.R.; "On improving automation by integrating RFID in the traceability management of the Agri-food sector," IEEE Transactions on Industrial Electronics, Vol. 56, Issue 7, July 2009, pp. 2357 – 2365
- [11] Floerkemeier, C.; Fleisch, E.; "RFID applications: interfacing with readers," IEEE Software, Vol. 25, Issue 3, May-June 2008, pp. 67 – 70
- [12] Shun-Yu Chan, Shang-Wen Luan, Jen-Hao Teng, Ming-Chang Tsai, "Design and implementation of a RFID-based power meter and outage recording system," IEEE International Conference on Sustainable Energy Technologies, Singapore, 2008
- [13] Roh, S.-g.; Choi, H.R.; "3-D tag-based RFID system for recognition of object," IEEE Transactions on Automation Science and Engineering, Vol. 6, Issue 1, Jan. 2009, pp. 55 – 65
- [14] Sheng, Q.Z.; Xue Li; Zeadally, S.; "Enabling next-generation RFID applications: solutions and challenges," Computer, Vol. 41, Issue 9, Sept. 2008, pp. 21 – 28
- [15] Myungsik Kim; Nak Young Chong; "Direction sensing RFID reader for mobile robot navigation," IEEE Transactions on Automation Science and Engineering, Vol. 6, Issue 1, Jan. 2009, pp. 44 - 54

Numerical Investigation of a Naca Air Intake for a Canard Type Aircraft

B.H. da Silveira, P.R.C. Souza, O. Almeida

Experimental Aerodynamics Research Center, Federal University of Uberlandia, Uberlandia, Brazil

Abstract—The present work aims to investigate the implementation of a new air intake on a canard type aircraft, through efficiency and drag calculations using a commercial CFD code. Preliminary semi-empirical studies proved that the NACA air inlet was the best option available since it reduces aerodynamic drag. Later, a set of numerical studies were performed with the air intake mounted on a flat plate (theory check) and in the aircraft's fuselage, in order to check the effect of the incoming flow disturbed by the fuselage. These simulations were performed using Reynolds-averaged Navier-Stokes (RANS) and turbulence modeling. Data analyses were based on the air inlets efficiency, drag, velocity profiles and the effect of the fuselage's curvature. The results confirmed that the NACA air intake has satisfactory performance, especially in reducing drag, and led to further considerations about the design of the aircraft in terms of sizing the air intakes. Also, the approach applied in this work was considered to be a methodology for new design implementation and/or selection. The CFD results have been corroborated by an empirical approach from the ESDU (Engineering Science Database Unit). This study was part of collaboration between the Brazilian Aircraft Factory (FABE) and the Federal University of Uberlândia (UFU).

Keywords—Air inlet, Aerodynamic drag, Efficiency, CFD, Naca.

I. INTRODUCTION

For the operation of several systems on an aircraft, as air conditioning, auxiliary turbines, ventilation and engine, it is necessary acquisition of outside air. This capture is only possible through the existence of air inlets. When discussing the construction of a gas turbine engine, understanding the function of the inlet is rather important since it has a great impact on engine performance, improving the entire aircraft. It is also possible to see other applications for refrigeration and other cooling systems, for instance. For aeronautical application, it may be identified at least two types of air intakes: NACA and scoop.

The NACA duct, have no external projections, as shown in Fig. 1, resulting in low aerodynamic drag and do not require specific structural reinforcements, causing no

impact on the weight of aircraft. However, this type of air intake is generally less efficient than a scoop inlet because most of the incoming flow is from the boundary layer which develops upstream of the inlet. Its operation is based on the deviation of the air flow into the throat of the air inlet, this deviation caused by the diverging slope and by the generation of vortices in their side walls.



Fig.1: NACA air inlet – J-HangarSpace, 2015.

Whereas the scoop air inlets, which appear in Fig. 2, are external projections designed to capture air outside the boundary layer, thereby recovering higher dynamic pressure and leading to a higher efficiency. The major disadvantage of this type of installation in relation to NACA intakes is the amount of aerodynamic drag, which causes weight gain and affects the aerodynamic performance of aircraft flight. Another disadvantage is the ingestion of liquids (water), foreign objects and the formation of ice.



Fig.2: Scoop air inlet – Kerbal Space Program, 2013.

The majority of the recent studies use CFD techniques for analysis and experimentation of air inlets for different types of application (Taskinoglu, et. al, 2002), both in conditions of supersonic and subsonic flow. For the type of air inlet concerned, there are several techniques to

improve performance and efficiency. It can be cited, pulsating jets, vortex generators, flow deflectors and optimization of geometrical parameters (Rodriguez, 2000).

Traditionally in order to evaluate the performance of the air inlets features three parameters. The first is mass flow of air which enters the air intake or more precisely, the ratio between this mass flow and the theoretical mass flow that would enter under conditions of undisturbed flow. The second is the dynamic pressure recovery efficiency of the entry, which is defined as the ratio between the dynamic pressure in the throat of the inlet and dynamic pressure in the undisturbed flow. The last one is the drag coefficient at the entrance.

Currently, one of the resources for which it has sought to increase the efficiency of air inlet type NACA is the use of vortex generators (de Faria and Oliveira, 2002). In particular, some Boeing 737's have this kind of inlet for feeding the Auxiliary Power Unit (APU) located in the tail. However, very little, information is available in the open literature about the influence of the main geometric parameters which determine efficiency and drag curves of these types of air inlets.

What is accessible related to conventional air inlets is published in Engineering Sciences Data Unit, ESDU (item n° 86002, 1986). This database possess several studies which conclude that dynamic pressure recovery efficiency is strongly influenced by variations in mass flow, increasing thickness of the boundary layer results in low efficiency and a uniform and continuous flow at the entrance of the throat.

The focus of this paper is to analyze the variation of the NACA inlet efficiency, using Computational Fluid Dynamics (CFD) for obtaining the results to a canard type aircraft. A set of numerical studies were performed with the air intakes mounted on a flat plate (theory check) and in the aircraft's fuselage. These simulations were performed using Reynolds-averaged Navier-Stokes (RANS) simulations conducted by the well-known CFD ++ commercial code from MetacompInc®. An analysis based on the air inlets efficiency, drag, velocity profiles and the effect of the fuselage's curvature are detailed in the following sections in order to evaluate the implementation feasibility of this component for a canard-type aircraft.

II. CASE STUDY – CANARD TYPE AIRCRAFT

The actual application or namely a case study is a general aviation aircraft classified in the experimental category called Bumerangue EX-27. The Bumerangue EX-27 Crosscountry is a quadriplace aircraft, monoplane, single

engine installed in the pusher configuration, namely a canard configuration, with retractable landing gear and closed cabin with two access doors in the front. The fuselage is built with composite (fiberglass) with epoxy resin laminated through vacuum process as usually employed in aeronautical construction. All fixation points are constituted by stainless steel 304 according to the imposed strength limits. The rudders and canard are also made by fiberglass. The powerplant system is composed by a Continental TSIO 360 EB Turbo – air refrigerated developing 210HP at 2700 rpm and equipped with a MT propeller with stainless steel protection and fiberglass. The whole wing is one piece of fiberglass and all fixation parts also received chemical treatment against corrosion and electrostatic paint.

Fig. 3 provides an overview about the Bumerangue EX-27 Crosscountry aircraft. As this aircraft is powered in a pusher configuration, the engine is installed at the back of the aircraft and requires special attention in terms of cooling (air ventilation). In order to guarantee the right air flow through the engine compartment additional air inlets must be placed at the rear end of the aircraft. The options are scoops and NACA air inlets which have been addressed in this work. As mentioned before, the approach is to select an air intake that could supply the air requirement for the engine compartment with a minimum penalty on drag for the whole aircraft. Thus, the main goal is to see if the NACA intake could comply with such requirements.



Fig.3: Bumerangue EX-27 Cross-Country airplane (courtesy from FABE LTD.).

III. EMPIRICAL METHOD

Previous calculations for sizing a NACA air intake for the airplane have been performed with the use of a well-known semi-empirical method, namely, ESDU (Engineering Science Database Unit) – ESDU (1986). To predict and calculate the parameters from the flush inlet (NACA) – Fig. 4 – this semi-empirical method utilizes a catalogued database to compute the drag and pressure recovery of small auxiliary air inlets totally or partially immersed in the boundary layer. This approach is suitable at subsonic speeds. Essentially, the theory of two-

dimensional boundary-layer calculation is used as reference and modified in the light of the available experimental data.

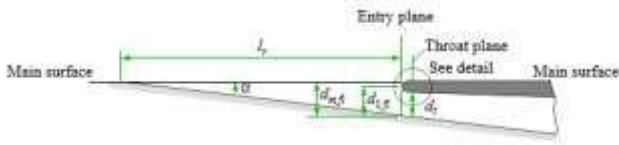


Fig. 4: Scheme and parameters of the inlet designed - ESDU, 1986.

The aircraft in question is being analyzed at the operational condition described in Table 1. Two different flight conditions were specified at this atmospheric condition: a) cruise condition at 2° AOA (Angle of attack); b) critical condition at 15° AOA, emulating a take-off flightpath.

Table.1: Design condition.

Parameters	Operational Condition
Speed	120 knots (61.73 m/s)
Angle of attack (AOA)	15°
Altitude	3000 ft (914.4 m)
Temperature	25°C
Density	1.121 kg/m ³
Pressure	90812 Pa

Using the ESDU with the objective of corroborating the CFD calculation, it is given the following variables with their respective values in Table 2, which are the mass flow, the boundary-layer thickness and the boundary-layer momentum thickness. Also, considering the throat aspect ratio and a ramp angle as depicted on Table 2. This NACA parameters leads to what was considered to be the minimum size of the flush inlet to provide air to the engine.

Table.2: Flush inlet design parameters.

ESDU parameters	Units
\dot{m}	0.016 slug/s
δ_h	0.1 ft
θ_0	0.01 ft
α_{ramp}	7°
w/dt	4

For a curved-divergent ramp inlet operating at maximum efficiency – Fig. 4, once given initial conditions to the problem it is calculated the mass flow parameter by equation (1):

$$\frac{\dot{m}}{\rho_0 V_0 \theta_0^2} = \frac{0,2330}{1,121 \times 61,73 \times (0,003048)^2} = 363,209 \quad (1)$$

Knowing the throat aspect ratio, w/dt = 4, now by using the Fig. 20 (From ESDU 1986) for sizing a flush inlet to operate at maximum ram pressure efficiency, it was found:

$$\frac{\theta}{dt} = 0.075 \quad (2)$$

Now, it is known the value of the boundary layer momentum thickness, $\theta = 0.003048$. Then, it is possible to define dt = 0.0464m.

Further, having the value of dt, it is possible to get the width, from the throat aspect ratio:

$$w = dt \times 4 = 0.16256 \text{ m}$$

The lip is calculated assuming to be elliptically rounded with the lip length and thickness in the throat plane both equal to a quarter of the throat diameter in equation (2):

$$l = t = 0.25 \times dt \quad (3)$$

$$t = 0.25 \times (0.0464 \text{ m})$$

Thus,

$$t = 0.01016 \text{ m}$$

The maximum external height of the inlet, d_{mf} and the lip highlight height, d_{1fl} , determined in the inlet plane relative to the ramp floor, are calculated by equations (4) and (5):

$$d_{mf} = dt + t - l_1 \tan \alpha = 0,04955 \quad (4)$$

$$d_{1fl} = dt + 0,5t - l_1 \tan \alpha = 0,044472 \quad (5)$$

The inlet capture area A1 is given through equation (6):

$$A1 = w \times d_{1fl} \quad (6)$$

$$A1 = 0.0072294 \text{ m}^2$$

From Fig. 17 (ESDU, 1986) the maximum ram pressure efficiency, for a ramp angle equal to 7 and a throat aspect ratio of 4 is function of $\frac{\theta}{dt}$ which gives an efficiency of 0.82. Furthermore, the modified mass flow ratio at this value of efficiency is obtained interpolating on Figure 18 (ESDU, 1986) as $Mm = 0.425$, using equation (7) it can be found the following ratio:

$$\frac{\dot{m}}{\dot{m}_0} = 0,475 \frac{dt}{d_{1fl}} = 0,475 \frac{0,04064}{0,044472} = 0,4341 \quad (7)$$

In order to evaluate the total drag of this air-intake it was followed the diagram from Fig. 5. Then, the total inlet

drag coefficient is given by Equation (8) and is divided in three components: ram drag, spillage drag and incremental drag correction.

$$C_{Dfl} = 2K_{fl} \frac{\dot{m}}{\dot{m}_0} + k_{\alpha} k_M k_{spfl} C'_{Dfl} + \Delta C_D \quad (8)$$

For the first component, the value of K_{fl} is calculated from equation (9) and according to the characteristics of the case, from Fig. 10a (ESDU), $k_{\psi} = 1$:

$$K_{fl} = k_{\psi} \left(\frac{\Psi_T}{\Psi_0} \right) \quad (9)$$

The Fig. 2 (ESDU) gives the momentum flow ratio with the respective values of δ/d_{1fl} and M . Finally, it is possible to achieve the ram drag component:

$$2k_{\psi} \left(\frac{\Psi_T}{\Psi_0} \right) \frac{\dot{m}}{\dot{m}_0} = 0,7336$$

Now, for the spillage drag component which is the second term from equation (8), the factor k_{α} , k_M and k_{spfl} is obtained from Fig. 12, 13 and 14 (ESDU):

$$\begin{aligned} k_{\alpha} &= 1 \\ k_M &= 1 \\ k_{spfl} &= 0,1793 \end{aligned}$$

The last term of the spillage drag coefficient is given by Fig. 11 (ESDU) for a curved-divergent ramp and as a function of $(d_{mfl} - d_{1fl})/l_1$. Acquiring these results the second component is obtained as it follows:

$$k_{\alpha} k_M k_{spfl} C'_{Dfl} = 0,0287$$

The incremental drag correction, third and last term from the inlet drag is calculated as a function of mass flow ratio from Fig. 15 (ESDU):

$$\Delta C_D = 0,0017$$

Then, knowing the values from each term of equation (8), the inlet drag is:

$$C_{Dfl} = 0.764$$

Therefore, using this simple semi-empirical approach it was possible to obtain the parameters for a design estimate for the flush inlet (NACA), which are specified in Fig. 6. A diagram showing the calculation steps is given in Fig. 7.

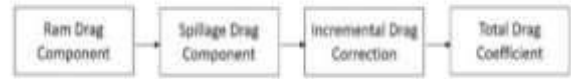


Fig. 5: Drag calculation diagram.

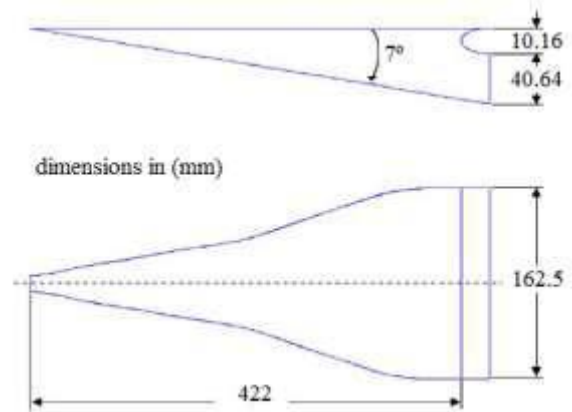


Fig. 6: NACA air inlet sizing.

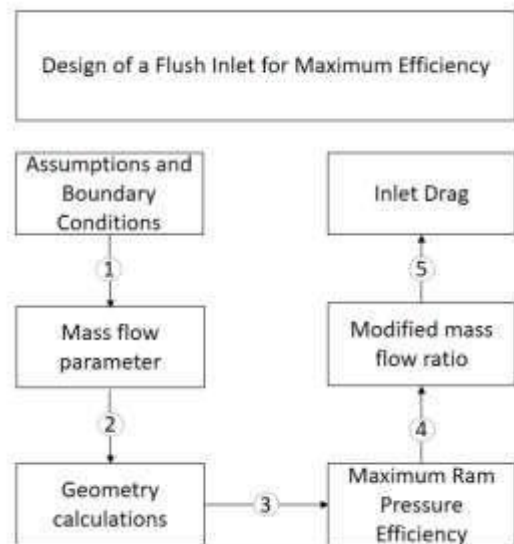


Fig. 7: Calculation diagram – summary of calculation procedure from ESDU, 1986.

Additional details for this semi-empirical method can be found in the ESDU document Item No. 86002 (ESDU, 1986).

IV. NUMERICAL METHOD

A Reynolds Averaged Navier-Stokes (RANS) approach was used in this work as a design tool and selection. The incompressible steady-state equations of motion were solved for different three dimensional domains with a NACA air inlet installed on it. The governing equations were solved with a second order accuracy through a Finite Volume formulation employed in the CFD++ software®. The final result was obtained by running 2000 iterations,

or when the residuals dropped 5 orders of magnitude. For the turbulence modeling, the $k\omega$ -SST (Shear Stress Transport, Menter (1993)) turbulence model was applied, based on experiences acquired in the past works with RANS equations applied to external flows with boundary layer detachment. The $k\omega$ -SST model is a turbulence closure comprising a transport equation for the turbulent kinetic energy (k) and specific turbulence dissipation rate (ω). This model seems to provide reasonable results for external aerodynamics analysis and have been well documented in literature – Menter (1993), Menter (1994). The CFD simulations were split in four parts:

- An initial check and/or validation of the semi-empirical approach used to size the NACA air intake. In this case, the air inlet was mounted in a flat plate, with the imposition of an incoming uniform flow;
- An incoming uniform flow based on the operating conditions of the aircraft, according to Table 1, was used to simulate only the flow over the aircraft's fuselage. The main purpose was to evaluate the velocity profile upon the air intake in the actual position along the aircraft's fuselage. This velocity profile will be used to adjust the flow simulation on step (a) of this approach;
- An improvement of step (a) is performed by using the velocity profile evaluated in step (b) and imposing it on the NACA air inlet mounted in the flat plate;
- Finally, the last step was to simulate the complete aircraft's fuselage with the NACA air inlet assembled on it, in its actual position and under the operational conditions of the airplane.

For brevity, only a summary of the computational domains and meshes for the flat plate and whole aircraft configuration will be not shown herein, in the next subsection.

4.1 Computational Domain

The initial validation was performed with the air inlet mounted in a flat plate. The computational domain for this configuration is shown in Fig. 8. The NACA air inlet was placed in the middle of the domain ($50 L_n$). A duct extension is inserted in this simulation in order to allow the flow to be completely developed inside the air intake, avoiding effect of the imposed boundary conditions. Details of the computational mesh are given in Fig. 9.

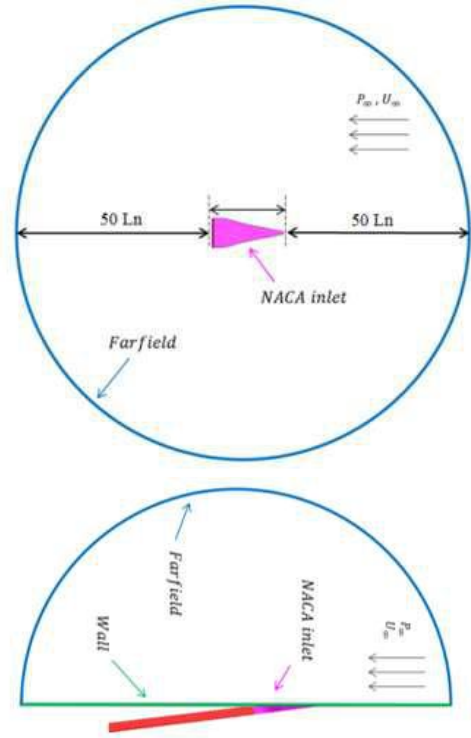


Fig. 8: Computational domain based on the length (L_n) of the NACA air inlet.

For the complete simulation, including the NACA assembled into the aircraft's fuselage, the computational domain is illustrated in Fig. 9. The size of the domains in x , y and z coordinates was selected based on previous studies (de Faria and Oliveira, 2002). The values shown below are considered suitable for such simulations and are used consistently through this whole work.

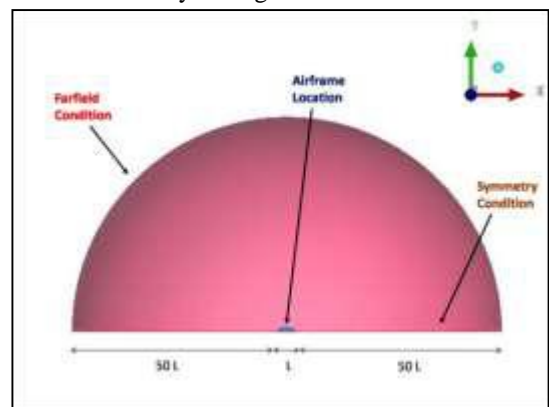


Fig. 9: Computational domain based on the Airframe's length (L).

4.2 Computational Meshes

The commercial software Ansys® IcemCFD was used to generate the unstructured meshes used in the simulations, Fig. 10 and 11 illustrate them. The discretization for the complete configuration consisted of an unstructured mesh with approximately 9 Million elements, with some refinements (density grids) on the desired regions of the

flow. For the initial validation a mesh of approximately 4 Million elements was applied. As a control parameter the surface and volumetric mesh sizing around the air intake was kept approximately constant for both domains.

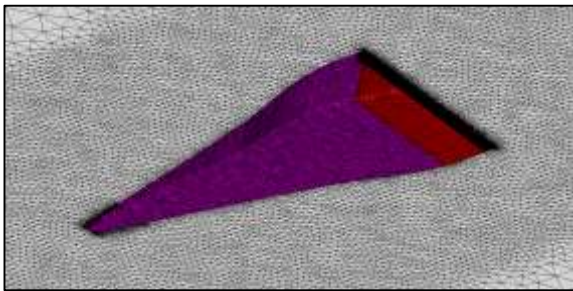


Fig.10: Mesh detail close to the NACA air intake – flat plate simulation.

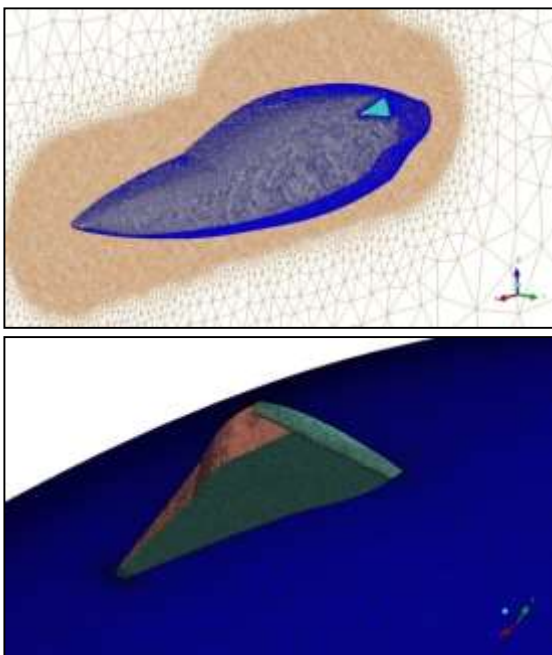


Fig. 11: Mesh details in different views – full simulation (NACA in the fuselage).

4.3 Boundary Conditions

Ambient atmospheric conditions were applied in both simulations with pressure and temperature set to 90812 Pa and 298.15 K, respectively. Walls were set to Non-slip and adiabatic boundaries. Since the outer boundary was placed far away from the body, farfield condition is assumed with minimum possibility of disturbing the internal domain solution. These set of boundary conditions are also illustrated on Fig. 7 and 8. For improving the incoming flow conditions in the flat plate simulation, a velocity profile was taken from the flow over the aircraft's fuselage and imposed in the farfield condition.

V. RESULTS AND DISCUSSION

The NACA efficiency is given by the relationship between the dynamic pressure at the throat and the dynamic pressure at infinity, according to Eq.(11):

$$\eta_{th} = \frac{P_{t_{th}} - P_{s_{inf}}}{P_{t_{inf}} - P_{s_{inf}}} \quad (11)$$

For the selected design, according to ESDU document Item No. 86002, the flush air inlet (NACA) throat area is 0.0072294 m². From the set of simulations performed in this work the achieved results for the inlet efficiencies are illustrated on Fig. 12, through the contours of dynamic pressure in the NACA's throat region. The global efficiency at the throat is calculated by summing the local (η_{th}) in each node at that location.

Fig.12(a) shows the result for the air inlet on a flat plate with a uniform flow condition. In this case, the efficiency is around 52%, showing a symmetric flow at the throat with the presence of a pair of vortices formed at the entry plane of the NACA. Despite the fact that these vortices may help the flow to go inside the air intake, in this case, the strength of them is reducing the efficiency. Moreover, the boundary layer flow is not the one developed at flight condition, since the imposition of a constant velocity is not really true. The effect of the flow profile already considering the real flight conditions of the airplane is then showed on Fig. 12(b). It can be noticed by the results the difference on hypothetical flow to a real one, efficiency fairly changes, without effects of attack angle. A great discrepancy is seen in the flow with a reduction in the strength of the vortices imposed at the NACA entry. In this case, the efficiency increased to nearly 83%. This relatively simple analysis allowed identifying the sensitiveness of this design to inlet flow conditions, especially in terms of the boundary layer's effect into the whole calculation. This interesting result showed that there is no option unless the complete simulation of the flow around the aircraft's fuselage with the NACA air intake installed on it.

Therefore, the efficiencies for the case of the air intake on the aircraft's fuselage are illustrated in Fig. 12(c) and (d). It can be seen all the effects of curvature that influence the flow stream to the air intake at the end portion of the fuselage. Two complete simulations were performed by analyzing the cruise condition at AOA around 2°(degrees) and the other in the critical condition with a 15° angle of attack (AOA). It may be noticed that in the cruise condition – Fig.12(c), there is little loss, the air inlet works very well in the recovery of pressure to the inside duct, due to the geometry of the aircraft which aids in the flow stream to the inlet air. Nevertheless, in critical condition due to influences of the high angle of attack the

NACA air intake is seeing a disturbance into the flow resulting in a decrease in the value of efficiency. At cruise condition the efficiency is around 93% against nearly 63% at the critical condition – 15° AOA.

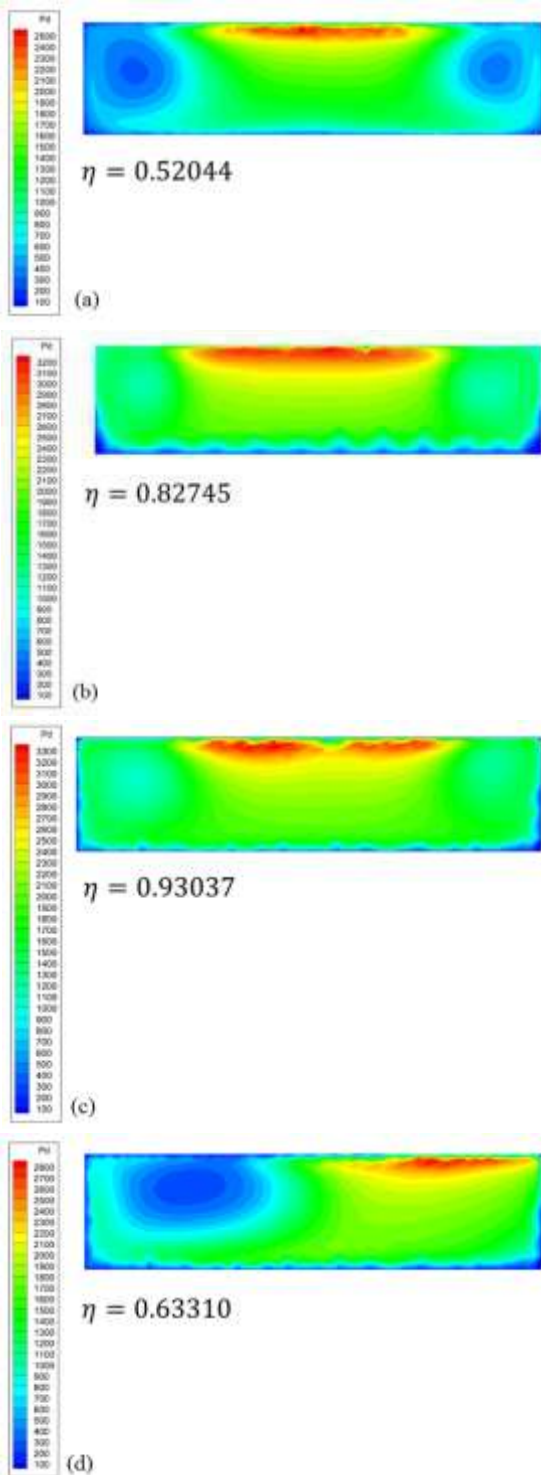


Fig. 12: Contours of dynamic pressure in the NACA's throat region: (a) NACA in the flat plate (uniform profile); (b) NACA in the flat plate (profile imposition); (c) NACA in cruise flight (0° AOA); (d) NACA in design operation (15° AOA).

It is also important to observe the flow pattern in the throat region for these two conditions. Again, in the cruise condition there is the appearance of the pair of vortices with low strength when compared with the flat plate simulations. The higher the intensity of strength of these vortices the low the efficiency is, as corroborated by Fig. 12(a), (b) and (c). At critical AOA condition, it is possible to see the asymmetry in the incoming flow at the inlet entry plane. In Fig. 6(d) it is possible to see only one vortex being formed and passing by the throat, although with higher strength. In this case, the efficiency decreased to 63%.

Fig. 13(a) and (b) allow a better understanding of the flow pattern around the aircraft's fuselage. At cruising condition, as seen on Fig.13 (a), the streamlines are rounding the fuselage of the entire aircraft and in the upper region of the aircraft; the flow is picked up with a little flow disturbance and interference. This led to a high efficiency for the NACA air intake around 83%. On the other hand, in Fig. 13 (b), representing the critical condition (AOA 15°), the streamlines are conform to the geometry of the fuselage only in the front part of the fuselage, featuring a more disordered and disturbed flow in the back portion, reducing the efficiency and pressure recovery via the air inlet located at that position.

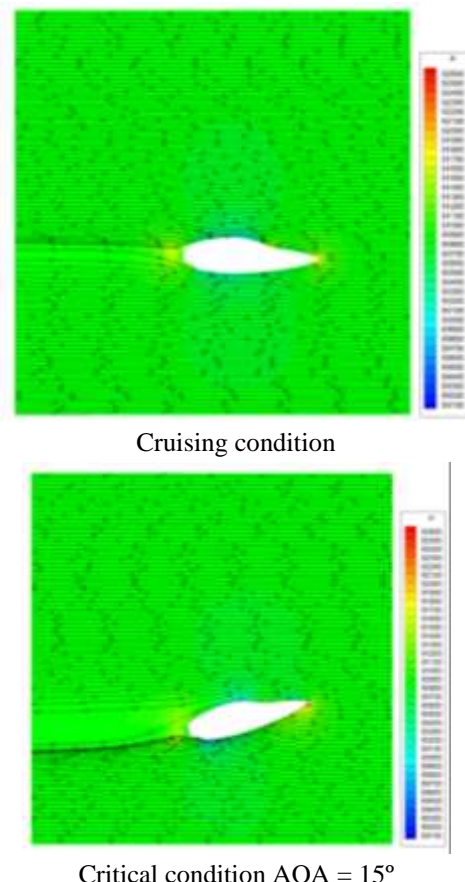


Fig. 13: Streamlines for the flow around the aircraft's fuselage.

By inspecting the Fig. 14, it is possible to see the pathlines, for the flow at cruise condition, entering the NACA air-intake. Part of the incoming flow is leaving the air-intake and becoming what is called “spillage” drag. The higher the spillage of the flow in the NACA air inlet the larger is the aerodynamic drag and lesser the air-intake efficiency.

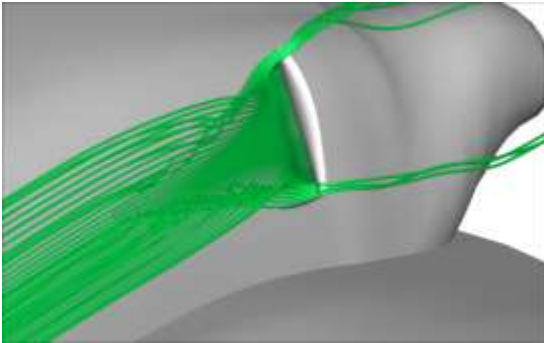


Fig. 14: Streamlines for the flow entering the NACA air-intake – cruise condition.

A closer look at the flow pattern incoming the NACA air inlet is provided in Fig. 15 (a) and (b).

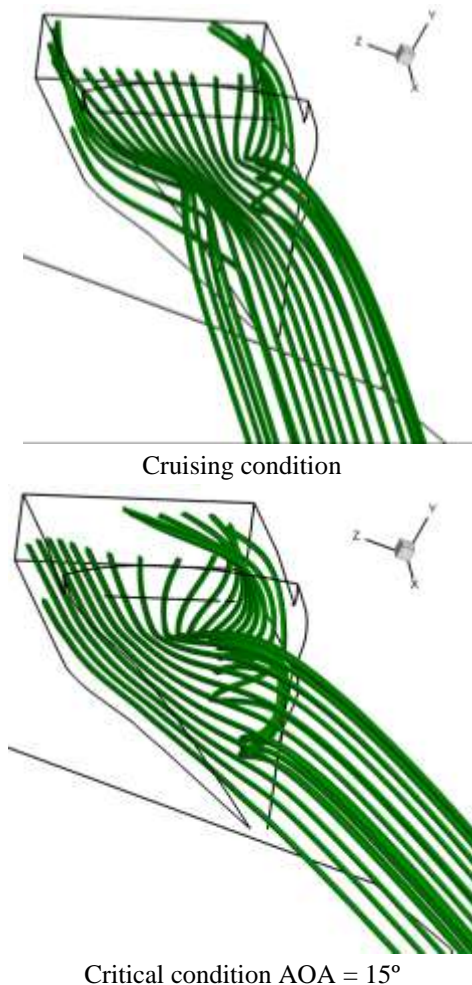


Fig. 15: Streamlines incoming the Naca air inlet.

By analyzing the flow’s pathlines, it is possible to see how the airflow behaves when captured by NACA. In the two conditions analyzed, the flow is much more orderly and permanent during the cruise, being possible to realize symmetry in the flow, while in critical condition, it is already asymmetric and totally disturbed.

Finally, by analyzing the data it is possible to affirm that the tested NACA air-intake gives reasonable efficiency in the flight conditions. The estimated drag for the component itself is given by the ESDU calculation and is around 0.764. It is important to emphasize that due to its flush geometry; the CFD drag prediction was not reasonable and it was not considered in this analysis.

The main concern in this design is to offer all mass flow rate inside the engine compartment, in order to cool it down. Based on the engine data and manufacturer’s specification, additional semi-empirical and CFD simulations may be necessary to evaluate these quantities. The approach taken herein is quite acceptable in order to check new designs for the air-intake to be implemented in this aircraft. A further step will be the inclusion of different shapes of air inlets, such as scoops. In this case, a more refined analysis should take place in order to capture with more precision the drag force.

VI. CONCLUSION

A numerical investigation of the flow inside a NACA air intake was carried out for implementing a new configuration in a canard type aircraft. In such aircraft design the need for engine cooling is a very important aspect since the engine is placed at the back portion of the fuselage. This work described a semi-empirical approach coupled with CFD simulations procedures to design and select this NACA air inlet at different flight conditions. A set of numerical studies were performed with the air intakes mounted on a flat plate (theory check) and in the aircraft’s fuselage. From the numerical computations, conducted using CFD++ with $k\omega$ -SST turbulence model, it was concluded that the air inlet efficiency is highly dependent on the incoming flow and the boundary layer profile upstream the NACA air entry plane. In addition, the location of the NACA air intake in this aircraft’s fuselage leads to efficiency of nearly 83% at cruise condition and around 63% in the critical condition at AOA approximately 15 degrees. Such conditions are restrictive in terms of mass flow rate through the engine compartment and a further study may apply to increase the size of the NACA air inlet or changing it to a SCOOP, at the price of increasing the aerodynamic drag of the whole aircraft. This study also indicates that the procedure used in this work is acceptable as an engineering tool, with relatively low cost, for design

selection and indicative of design trends. Further work may also apply to improve the aircraft's configuration.

ACKNOWLEDGEMENTS

The authors acknowledge with gratitude the support of CPAERO – Experimental Aerodynamics Research Center at Federal University of Uberlândia for carrying out this work. The first author would like to thank Eng^o Pedro Ricardo Correa Souza for helping at the mesh and CFD simulations. Finally, we would like to thank the collaboration with the Brazilian Aircraft Factory (FABE).

REFERENCES

- [1] DPW Drag Prediction Workshop, 2001. Applied aerodynamics conference, AIAA, Anaheim, CA, USA.
- [2] ESDU, 1968, The compressible two-dimensional turbulent boundary layer, both with and without heat transfer, on a smooth flat plate, with application to wedges, cylinders and cones, Item No. 68020 with amendment C, March 1988, Engineering Sciences Data Unit, London.
- [3] ESDU, 1986, Drag and pressure recovery characteristics of auxiliary air inlets at subsonic speeds, Item No. 86002 with amendments A and B, July 1996, Engineering Sciences Data Unit, London.
- [4] Hime, L. Estudo Numérico de Entradas de Ar para Aeronaves. Relatório PIBIC-CNPq, Departamento de Engenharia Mecânica, PUC-Rio, Rio de Janeiro, Julho 2004.
- [5] [http://forum.kerbalspaceprogram.com/threads/24551-Firespitter-propeller-plane-and-helicopter-parts-v7-1-\(May-5th\)-for-KSP-1-0/page38](http://forum.kerbalspaceprogram.com/threads/24551-Firespitter-propeller-plane-and-helicopter-parts-v7-1-(May-5th)-for-KSP-1-0/page38), Accessed on 01/06 at 17:20h.
- [6] <http://www.j-hangarspace.jp/>, Accessed on 01/06 at 17:15h.
- [7] Menter, F. R. (1993), "Zonal Two Equation $k-\omega$ Turbulence Models for Aerodynamic Flows", AIAA Paper 93-2906.
- [8] Menter, F. R. (1994), "Two-Equation Eddy-Viscosity Turbulence Models for Engineering Applications", AIAA Journal, vol. 32, no 8. pp. 1598-1605.
- [9] Nogueira de Faria, W.; Oliveira, G. L. Analise de Entradas de Ar Tipo NACA com Gerador de Vórtices. In 9th Brazilian Congress of Thermal Engineering and Sciences, ENCIT 2002, Caxambu-MG, Outubro, 2002.
- [10] Rodriguez, D. L. A Multidisciplinary Optimization Method for Designing Inlets Using Complex Variables. In: 8th AIAA/USAF/NASA/ISSMO Symposium on Multidisciplinary Analysis and Optimization, September 2000.
- [11] Taskinoglu, Ezgi S.; Knight, Doyle. Numerical Analysis of Submerged Inlets. In 20th AIAA Applied Aerodynamics Conference, St. Louis – Missouri, June 2002.

Combination between Cobit 5 and ITIL V3 2011

El Baz Mourad¹, Motii Malik², Armand Collins Anong³, Belaiassaoui Mustapha⁴

¹Department of Mathematics and Computer Science, University Dakar Bourguiba, Senegal

²Department of Mathematics and Computer Science, University Hassan 1, Morocco

³Department of Mathematics and Computer Science, University Dakar Bourguiba, Senegal

⁴Department of Mathematics and Computer Science, University Hassan 1, Morocco

Abstract— *IT organizations are under increasing pressure to meet the business goals of their companies. This challenge can be particularly daunting because it involves complying with regulations, such as the SarbanesOxley Act (Sarbox) and Basel II. Compliance requires strong corporate governance capabilities that are demonstrable to outside auditors. Because IT plays such a major role in business processes, the IT organization not only creates complexity for the business, but at the same time, provides the means to demonstrate this compliance. Organizations rely on guidelines such as the IT Infrastructure Library (ITIL®) and Control Objectives for Information and related Technology (COBIT) to help understand and address these challenges.*

Keywords— *Good practices, ITIL, process, COBIT, IT Governance, IT Strategy.*

I. INTRODUCTION

COBIT and ITIL have been used by information technology professionals in the IT service management (ITSM) space for many years. Used together, COBIT and ITIL provide guidance for the governance and management of IT-related services by enterprises, whether those services are provided in-house or obtained from third parties such as service providers or business partners.

Enterprises need to govern and manage their information and related technology assets and resources, and those arrangements customarily include both internal and external services to satisfy specific stakeholder needs. COBIT 5 aims primarily to guide enterprises on the implementation, operation and, where required, improvement of their overall arrangements relating to governance and management of enterprise IT (GEIT). ITIL provides guidance and good practice for IT service providers for the execution of IT service management from the perspective of enabling business value.

COBIT 5 describes the principles and enablers that support an enterprise in meeting stakeholder needs,

specifically those related to the use of IT assets and resources across the whole enterprise. ITIL describes in more detail those parts of enterprise IT that are the service management enablers (process activities, organizational structures, etc.).

COBIT is broader than ITIL in its scope of coverage (GEIT). It is based on five principles (meeting stakeholder needs; covering the enterprise end to end; applying a single, integrated framework; enabling a holistic approach; and separating governance from management) and seven enablers (principles, policies and frameworks; processes; organizational structures; culture, ethics and behavior; information; services, infrastructure and applications; people, skills and competencies).

ITIL focuses on ITSM and provides much more in - depth guidance in this area, addressing five stages of the service life cycle: service strategy, service design, service transition, service operation and continual service improvement.

In addition, COBIT and ITIL are well aligned in their approach to ITSM. The COBIT 5 Process Reference Model, as documented in COBIT 5: Enabling Processes, maps closely to the ITIL v3 2011 stages.

The distinction between the two is sometimes Described as “COBIT provides the ‘why’; ITIL provides the ‘how.’” While catchy, that view is simplistic and seems to force a false “one or the other” choice. It is more accurate to state that enterprises and IT professionals who need to address business needs in the ITSM area would be well served to consider using both COBIT and ITIL guidance. Leveraging the strengths of both frameworks, and adapting them for their use as appropriate, will aid in solving business problems and supporting business goals achievement.

Many references reflect the best practices developed over the years. The reality is that each of them focuses on a specific matter: safety, quality, customer services, auditing, project development, etc...

ITIL (Information Technology Infrastructure Library) is a set of good practice structured as multiple processes communicating with each other. Each has its own role so that, at the end, they can both respond to the two issues, which are the continuous improvement and customer satisfaction.

COBIT Is a reference of information systems; the perimeter of COBIT governance (created by ISACA Information Systems Audit and Control Association) exceeds the one vested in the management of information systems to all stakeholders encompass in the company. Malthus, According To COBIT, "governance of information systems Is The reference of leaders and the Board of Directors, it Consists of structures, command and operation processes leading the IT of the enterprise to support its strategies and business objectives, and allow them to expand."

This article helps to highlight the completeness and pooling possible between these two references based on the perspective of developing a version of COBIT that includes the most used processes of ITIL.

II. UNDERSTANDING ITIL

To define ITIL, you must be in a context of continuous improvement and customer orientation needs.

ITIL is a set of good practice structured as multiple processes communicating with each other. Each has its own role so that, at the end, both can respond to the two issues which are: the continuous improvement and customer satisfaction.

ITIL is not a standard because it does not provide criteria or a requirement-set defined internationally and certifying the organizations.

ITIL is not a methodology or method. It provides and uses methods to better explore the good practice.

The good practices provide organizations a structure, approved by years of experience in large companies globally recognized for their professionalism and thoroughness, to formalize their processes and manage their information. These good practices are used primarily as guidelines to companies serving businesses wishing to improve their quality of service.

However, to take advantage of the power of all good practices proposed by ITIL, and following the worldwide recognition of the robustness of its processes, a standard was created in 2006 based on these good practices. This standard called ISO20000 international came out to meet the needs of companies wishing to demonstrate their alignment with the good practices recommended by ITIL.

III. WHY ITIL?

ITIL provides a pragmatic approach to deal with the situations in which CIOs are faced, namely, among others:

- The IT sector is receiving more and more investment budget. It represents important expenses especially for companies to whom; the main business isn't focused on computing.
- Information systems are becoming more complex. As long as the IT workers are trying to meet the requirements and demands of their internal customers, they find themselves facing an infrastructure and a large arsenal application that must be managed and maintained while trying to be responsive.
- With the advent of new technologies of information and communication (social medias ...), users have become up - to - date with all high - tech news. Especially since the editors have popularized their software's (advent of open source) and telecommunications Infrastructure (mobile phone).
- As long as companies have spent enormous sums of money for the IT infrastructure (hardware and software), the leaders expect a return on investment and begin to tighten the budgets. Thus, the difficult situations the CIOs have to face.
- Globalization has played its part too. It introduced the practices of service between recharges its subsidiaries. This new situation has opened the eyes of CIOs who want to bill their services to their internal customers.
- All this was said, made the ambiguous role of the CIO. With the mode of outsourcing, the user begins to ask questions about the added value of CIOs as external suppliers support their claims with contracts and a better reactivity.
- For companies specialized in IT, being certified or certifying their staff improve their reputation and trust of their internal or external customers. This certification is a label that the CIO can show to proof their professionalism with standards recognized worldwide.

Client axis :

For this axis, ITIL will respond to the:

- Lack of mechanism structured for delivery and service support.
- Lack of confidence in the management of IT services.

Management axis:

- Mismanagement of resources and means.
- Failure of service in a frequent way.
- Irregularity in meeting the deadlines of requests and Claims of customers.
- Changes or modifications not coordinated or analyzed.

Decision Axis:

- Decisions are made without any pragmatic basis.

IV. THE BASIC CONCEPTS OF ITIL

Mainly, ITIL is based on five pillars:

- Customer focus.
- The life cycle of service.
- The concept of process.
- Continuous improvement.
- Communication.

Customer focus

This concept is crucial for managing IT services. It makes the customer needs the main concern of the IT specialist. Thus, what's important is not focusing on new technologies and the power of servers and telecommunications but rather meeting the functional need of the customer in the most faithful and most optimal way.

Taking into consideration the business needs of the customer and make them the main concern of the IT management is the reason to be of the IT services.

It is then necessary to fully understand the customer needs, follow up their development and establish an organization that supports them expressing and monitoring these needs.

The life cycle of service

Before describing the life cycle of the service, we must first explain its concept. In general, the service can be defined depending on the context.

In a restaurant we can evaluate the service: smiles, atmosphere, responsiveness,...

In a tennis match, the service is a trigger of play

In an organization, a service is an entity having a function and a task performed by a group of staff.

In the IT field, a service is defined as a benefit, help or assistance a user can expect from a supplier.

In daily life of IT projects, and after the post-production of projects, CIOs find themselves faced with two situations:

- Whether the operations team was not involved in the project since its design, creating a frustration having to deal with tasks from which they don't understand the point in the business.
- Or the project team, as it masters the issue, continue the project in the operational phase. This generates organizational failures and conflicts of responsibility.

To avoid this kind of anomaly, ITIL provides the solution and advocates considering the management of services from the needs study of the IT projects. Thus, the overlapping roles of the project team and operations team are avoided and the operating team is aware of the stakes

of the project and its services as well as the benefits.

This makes sure that the resources and expertise required for the operation of services after their releases are available. This involves taking into consideration the impact of performance, availability and budget since the start of the project.

The process concept

The concept of life cycle brings all necessary elements for successful projects from the specification of needs by customers until the go-live of services.

The concept of process has demonstrated its robustness when quality is the matter. ITIL has adopted this approach to structure the philosophy of its good practices as multiple processes interacting between each other.

This concept of process provides answers to the sequence of activities while undergoing examinations and performance indicators measuring the achievement of results for which the process was designed.

The process owner is responsible for the design of the process and ensures that it meets the need defined. He reports to company executives.

The process manager is responsible for implementation of the process as it was defined by process owner to which he reports.

The quality of service

This concept is the *raison d'être* of the good practices. Quality service is defined as it has the ability to respond to customer needs exactly as they were defined. The client judges their supplier, not based on their how-to-methods but rather based on their appreciation of the result within the deadline expected, while respecting the specifications defined.

In that sense, ITIL seeks to improve service in a perpetual manner based on the philosophy of Deming wheel: Plan, Do, Act, Check.

Communication

One of the contributions of ITIL is the good Communication. It harmonizes the language between customers and suppliers. This language removes any ambiguity when the IT specialists talk about the SLA agreement, incident, problem, change, ...

The good communication is an important component of the service quality. Business Directions must understand the issues of IT, their constraints and commitments. The communication also facilitates the negotiation of budgets, as projects come directly from business requirements.

The communication also reflects the transparent aspect of the CIO. This is to convey a clear picture to users, a picture illustrating the negative aspects and most of all the

positive ones of the IT management and the efforts of IT resources.

V. COBIT DEFINITION

COBIT (Control Objectives for Information and related Technology) is a unifying tool that allows managers to bridge the gap between control requirements, technical issues and business risks. Since its first version released in 1996 COBIT has evolved, version 4.1 appeared in 2007. COBIT provides a framework for structured control IT operation with 34 processes divided into four areas:

- Plan and organize (PO)
- Acquire and implement (AI)
- Deliver and support (DS)
- Monitor and evaluate (ME)

The four fields of CobiT include coherent sets of processes. PO represents the field of strategic dimension of IT governance. The AI field gathers all processes that impact resources, from acquisition to implementation. The DS field is devoted to services offered to clients of the CIO. Finally, the SE field covers largely the controlling, audit and monitoring of everything.

COBIT processes

For each of the 34 process, COBIT describes the scope and purposes and then list and develop:

- Control objectives for IT auditors, which are detailed in other publications;
- A management guide written in a logic of governance SI;
- A maturity model for each process.

Processes plan and organize (PO):

The processes described in this chapter discuss the strategy and tactics to optimize the contribution of IS to achieve the business objectives of the company.

The processes of this field are the following:

- PO1: Defining a strategic IT plan
- PO2: Defining the information architecture
- PO3: Determining technological orientation
- PO4: Defining the processes, organization and labor relations
- PO5: Managing IT investments
- PO6: Communicate the goals and management guidelines
- PO7: Managing IT human resources
- PO8: Managing Quality
- PO9: Assessing and managing risks
- PO10: Managing projects

The PO field describes the 10 strategic information

systems governance process. It concerns both huge CIOs as well as CIOs which have outsourced most of their projects or their operations.

We can couple COBIT with other references, but the PO field will remain Essential.

Processes acquire and implement (AI):

The processes described in this chapter concerns the identification, development or acquisition of IT solutions, their implementation and integration with business processes, modification and maintenance of existan systems systems.

The processes of this area are the following:

- AI2: Purchase applications and maintain them
- AI3: Purchase a technical infrastructure and maintain it
- AI4: Facilitate the operation and use
- AI5: Purchase IT resources
- AI6: Manage change
- AI7: Install and validate changes and solutions

Projection of the AI process to ITIL

The AI field covers all of the applications and infrastructure projects as well as all patches and any kind of change in the scope of information systems. It is similar to the chapter Transition Service of ITIL V3.

Some will find that the piloting the project itself is not there. It is true that the AI2 process, which covers both the development and maintenance of applications, should be more explained. It is on this level that we must link the project management methods that exist elsewhere. However, this field has the advantage of describing Processes that are often ignored, such as the AI4 process (Facilitate the operation and use), or Neglected, Such as AI1 process (decision making or not) and AI6 / 7 (change management, testing and production).

Processes Deliver and Support (DS)

This area covers the implementation of services: computer operations, security management, continuity management service, user support, data management and equipment.

The processes of this area are the following:•

- DS1: Define and manage service levels
- DS2: Manage third – party services
- DS3: Manage performance and capacity
- DS4: Ensure continuous service
- DS5: Ensure security of systems
- DS6: Identify and allocate costs
- DS7: Educate and train users
- DS8: Manage support to clients and incidents

- DS9: Manage configuration
- DS10: Manage problems
- DS11: Manage data
- DS12: Manage the physical environment
- DS13: Manage operations

Projection of DS processes to ITIL

The DS field describes completely the conditions of IT services supply. It first described the relationship with the trades (DS1) and with third parties (DS2). This preamble allows all contractual services.

Essentially, this field is the closest to the related ITIL processes. Only DS7 seems not to be described in ITIL.

Processes monitor and evaluate (ME):

The processes described in this chapter deal with the performance management, monitoring of internal control, compliance with regulatory standards and governance.

- The processes of this field are the following:
- ME1: Monitor and evaluate the performance of IS
- ME2: Monitor and evaluate internal control
- ME3: Ensure compliance with external obligations
- ME4: Implement a governance of IS

Projection of ME processes to ITIL

The process of ME domain describe four levels of monitoring and evaluation of the whole system (PO, AI and DS). Where the process is SE1 the main role as it controls it fully. It should be the starting point for all deployed processes' improvement (a little bit like the "continuous improvement" in ITIL V3).

ME2 process is more difficult to identify because it is made to monitor the well –functioning of the above process. This requires an independent responsible, preferably in internal audit, should be designed.

ME3 process has the advantage of isolating the monitoring over compliance. Finally, ME4 provides a way to audit the implementation of the governance of IS.

VI. TOWARDS A POOLING OF COBIT AND ITIL.

ITIL structures its approach of the services' management around the relationship with stakeholders: daily IT service users and project managers for controlling (businessmanagers, etc).. COBIT, in the same way, has systematically put beforehand the finality of IT services, including meeting the needs of business and the desire to align supply with demand. Both approaches share the same values regarding the

management of IT services.

The figure below lists the COBIT processes that are closest

to the ITIL processes. Note that the names of the process are often the same, reflecting the growing awareness of ITIL with COBIT designers over the versions.



Why pooling?

The steps ITIL and COBIT are often conducted separately. ITIL was a response to better structure the service centers which are, for the same reason, the only function to be represented as the heart of the process. The procedures of the service center concerning the incident management (structuring levels, climbing, registration tickets call, enrichment databases resolution, etc.) had to industrialize to meet the demands at lower cost.

Simultaneously, a growing number of organizations are outsourcing the support functions, which were not necessarily in their core business and seem complicated to manage and optimize in-house. As for tools, editors have offered more accomplished ones, able to handle all procedures and linking them to a database of resources in the broad sense (call tickets, configuration objects, but also job descriptions, etc).. All this "arsenal" was built with the ITIL framework.

The key points to consider in order of pooling the two approaches are as follows.

• Reconcile two cultures

ITIL culture is pragmatic, constantly confronted with the daily issues and geared more towards the service (service continuity, performance). it often manages data objects in a level of detail that only applies to players in the support, maintenance or operation. COBIT, however, may be perceived as too theoretical, not often useful nor concrete enough to be deployed easily and effectively.

• Structuring the whole repository

Avoid duplication of processes, which inevitably occurs if one does not describe a mapping process to ensure overall consistency.

• Make the link with the studies and developments

ITIL has trouble spread to the teams of studies and development. It is recognized neither in the management of projects at the elementary level or in the overall management of portfolios and investments.

COBIT has the advantage of giving a comprehensive framework that provides a process of transition, PO10 between ITIL and studies.

• Gradually build the data of the ISD model

ITIL gains are interesting but the risk of falling into the details is big. We must rely on the CMDB to create the data model of the CIO, ensuring distance themselves and define the granularity of the data relevant for control.

VII. TOTAL MAPPING BETWEEN ITIL AND COBIT

Below reconciliation between the phases and processes of the two repositories, ITIL correspondence is in italics.

Reconciliation of phases

- Planning and Organizing (PO) => Service strategy
- Acquiring And Implementing (AI) => Service conception
- Delivering and Supporting (DS) => Transition and operation of service
- Monitoring and evaluating (ME) => Continuous improvement of service

Reconciliation of processes

- PO1: Define a strategic IT plan => Set service strategy (Strategy service)
- PO2: Define the information architecture
- PO3: Determine technological direction
- PO4: Define the processes, organization and labor relations
- PO5: Manage IT investment => financial Management of service (strategy of service)
- PO6: Communicate the goals and management guidelines
- PO7: Managing IT human resources
- PO8: Managing Quality

- PO9: Assess and manage risk
- PO10: Manage projects

- AI1: Find IT solutions => Management and deployment into production (Phase transition of service)
- AI2: Purchase applications and maintain them
- AI3: Purchase a technical infrastructure and maintain it
- AI4: Facilitate the operation and use
- AI5: Purchase IT resources
- AI6: Manage change => Change Management (Phase transition of service)
- AI7: Install and validate changes and solutions => Management and deployment into production (Phase transition of service)

- DS1: Define and manage service levels => Service Level Management (Design Phase)
- DS2: Manage third – party services => Supplier Management (Design Phase)
- DS3: Manage performance and capacity => Capacity Management (Design Phase)
- DS4: Ensure continuous service => Continuity Management (Design Phase)
- DS5: Ensure security of systems => Security Management (Design Phase)
- DS6: Identify and allocate costs => Financial Management Service (Strategy service)
- DS7: Educate and train users => Management and deployment into production (Phase transition of service)
- DS8: Manage support to clients and incidents => Incident Management (Operation Phase)
- DS9: Manage configuration => Asset management and configuration (phase transition)
- DS10: Manage problems => Problem Management (Operation Phase)
- DS11: Manage data
- DS12: Manage the physical environment
- DS13: Manage operations => (This is a phase according to ITIL)

- ME1: Monitor and evaluate the performance of IS => Phase of continuous improvement of service
- ME2: Monitor and evaluate internal control => Phase of continuous improvement of service
- ME3: Ensure compliance with external obligations
- ME4: Implement a governance of IS => Portfolio Management Service (Phase service strategy)

VIII. RECOMMENDATION FOR A SUCCESSFUL APPROACH FOR POOLING

When used together, COBIT and ITIL provide a top-down approach for the IT governance and for the management of services. The COBIT management guide provides a comprehensive approach to manage objectives and priorities for IT activities.

When used together, the power of both approaches is amplified, with a greater likelihood of management support and direction, and a more efficient use of resources for implementation.

Structuring the process

The organization needs an effective action plan that suits their particular circumstances and the needs, but some recommendations are common to all businesses:

- Ensure that the project of setting up standards of governance is in terms of senior management and will be sponsor of this project.
- Deficiencies and ensure that IT issues are identified and listed
- Work with management in ensuring alignment of initiatives with positive impacts on business activities of the company.
- Developing dashboards to measure the performance of IT services

Planning

Establish an organizational framework (ideally as part of a global initiative of IT governance) with clear responsibilities and objectives.

Ensure the participation of all stakeholders.

- Identify project risks
- Develop strategies for improvement, and decide of the highest priority projects that will improve management and governance.
- Consider supporting COBIT control objectives using the most detailed ITIL guidelines.
- Measure results, establish a dashboard mechanism to measure current performance and monitor the results of further improvements.

Pitfalls to avoid

There are also some obvious rules, but pragmatic, that management should follow to avoid the pitfalls:

- Treat the initiative to implement a project activity with a series of phase.
- The implementation involves cultural change and new processes. Therefore, a key success factor is the

activation and motivation for change.

- Make sure there is a clear understanding of objectives.
- Manage wait times. In most companies, achieving success takes time and requires continuous improvement.
- Focus first on where it is easier to make changes and improvements and build from there, one step at a time.

IX. CONCLUSIONS

The reference of good practices was designed to meet a need of structuring the service of processes management, it responds to this need with more details and efficiency and also, ITIL remains the most deployed reference in the management of IT infrastructure and service.

On the other hand, COBIT gives a more strategically view of IT management for a better alignment of IT with the enterprise strategy.

Thus, managers of information systems are faced to two interesting references. Yet each one has a terminology, its processes and methodology of implementation. This article has put the focus on processes and common objectives of these references and the fields of possible pooling, One of the perspective of this paper is to design a version of COBIT that fully integrates common ITIL processes.

REFERENCES

- [1] Abdelaali Himi & Samir Bahsani <http://www.ijcsi.org/articles/The-IT-Service-Management-according-to-the-ITIL-framework-applied-to-the-enterprise-value-chain.php>
- [2] ITIL pour un service informatique optimal- Christian du mont Edition Eyrolles
- [3] Pour une meilleure gouvernance des systèmes d'information - Dominique Moisand; Fabrice Garnier de Labareyre Edition Eyrolles 2009
- [4] Mapping of ITIL v3 With COBIT® 4.1 IT Governance Institute www.itgi.org
- [5] C. Dumont. – ITIL pour un service informatique optimal (2e édition).
- [6] C. Dumont. – Mémento ITIL.
- [7] E. Besluau. – Management de la continuité d'activité.

Equilibrium Isotherm, Kinetic and Thermodynamic Studies of the Adsorption of Erythrosine Dye onto Activated Carbon from Coconut Fibre

Ikhazuangbe P.M.O., Kamen F.L., Opebiyi S.O., Nwakaudu M.S., Onyelucheya O.E.

Department of Chemical engineering, Federal University of Technology, Owerri, Nigeria

Abstract – Equilibrium isotherm, kinetic and thermodynamic studies of the adsorption of erythrosine dye onto activation carbon from coconut fire was carried out. The coconut fibre obtain from Elele, Rivers State Nigeria, was washed, dried, carbonized at 400°C, crushed, sieved and activated at 800°C, before it was washed and dried at 110°C. Variable influencing factors, such as contact time, temperature and initial concentration were studied through single-factor experiment, while other factors are kept constant (at 30min, 30°C and 50mg/L) in each adsorption experiment. The Freundlich isotherm fits adsorption compare to others used, the adsorption kinetic followed pseudo-second order reaction, while the thermodynamic parameters, (ΔH) = 28.73KJ/mol, (ΔG) = 94.45J/mol.K and (ΔS) = -0.10, -0.27, -0.82, -1.05, -1.77, -2.49KJ/mol. From the results obtained, activated carbon from coconut fibre, will be an excellent low-cost adsorbent for the removal of Erythrosine from industrial waste water.

Keywords— Adsorption, Coconut fibre, Erythrosine, Kinetic, Thermodynamic.

I. INTRODUCTION

Erythrosine or Acid Red is a water soluble synthetic dye that is often used as a food colorant. Beside application in drugs and cosmetics, erythrosine is applied for dyeing many food stuffs including biscuits, chocolate, luncheon meat, sweets, and chewing gums [5]. When excessively consumed, it can cause sensitivity to light, affecting thyroid hormone levels and lead to hyperthyroidism in some cases [1]. The maximum allowed level of erythrosine is 200 mg/kg in some food stuffs [5]. Monitoring and eliminating erythrosine is a necessary job due to its potential toxicity and pathogenicity. The high toxicity of erythrosine was behind many environmental studies to remove this dye from water. Photochemical degradation using TiO₂ particles, biochemical degradation, and adsorption by activated

carbon/natural adsorbents, were the most applicable procedures. Dyes removal by adsorption technique is often recommended due to the low running costs and no harmful by-products are generated as the case in other destructive procedures. In fact, most food dyes are often present at trace levels (usually in µg or ng levels) in water streams which may retard their direct quantification by most instruments [6].

In this study, the ability of coconut fibre carbon to remove erythrosine by adsorption is been studied. The adsorption capacity of dye will also be examined using the adsorption isotherm technique. The Langmuir, Freundlich Redlich-Peterson isotherms will used to fit the equilibrium data. Pseudo-first order, pseudo-second order models, activation energy and the thermodynamic equations will also be used to fit the experimental data [4].

II. MATERIALS AND METHODS

2.1 Preparation of adsorbents

Sample of coconut fibre was picked from the environment in Elele, Rivers State, Nigeria. The coconut fibre was washed with tap several times to remove the dust and other water- soluble materials. The process continued until the washing water was colorless. They were respectively dried in the open air. The dried coconut fibre was carbonized in a furnace (SX-5-12) at 400°C for 3 hours and the charred coconut fibre was allowed to cool to room temperature. It was chemically activated by weighing 100gram of the ground carbonized coconut fibre in 300 ml of 0.1M HCl solution, thoroughly mixed and heated until it formed slurry. The slurry was transferred to a crucible and heated in a furnace (SX-5-12) at 800°C for 3 hours and allowed to cool to room temperature and washed with de-ionized water, dried in an oven (MINO/75/F/DIG) at 110°C for 2 hours [3].

2.2 Preparation of adsorbate

The Erythrosine used is of laboratory grade (KEM LIGHT, India). The solution was prepared in de-ionized water from Ion-exchange (Indian) Ltd, Eleme, Port Harcourt, Nigeria. An accurately weighed quantity of the dye was dissolved in de-ionized water to prepare the standard solution. Experimental solutions of the desired concentrations were obtained by successive dilutions with de-ionized water.

2.3 Adsorption experiment

1000mg of the activated carbon of coconut fibre was mixed with 50ml of Erythrosine solution of the desired concentrations (25, 50, 75, 100, 125 and 150mg/L) at 30°C in a temperature controlled water bath with constant shaking. The samples were withdrawn after 30 minutes and dye solutions were separated from the adsorbent using Whatmann filter paper. The concentration of the filtrate was measured with a UV spectrophotometer (2OD) at 524nm. The experiment was repeated using 1000mg of the activated carbon with 50ml of 50mg/L concentration of erythrosine solution at 30, 40 and 50°C in a temperature controlled water bath with constant shaking. The samples were withdrawn after 30, 60, 90, 120, 150 and 180minutes respectively and filtered using Whatmann filter paper. The concentration of the filtrate was measured with a UV spectrophotometer (2OD) at 524nm. Again 1000mg of the activated carbon was mixed with 50ml of 50mg/L concentration of erythrosine solution at 30, 35, 40, 45, 50 and 55°C in a temperature controlled water bath (DK – 420) with constant shaking was also carried out. The samples were withdrawn after 30minutes respectively filtered and the concentration measured.

The adsorption amount of erythrosine dye adsorbed onto the coconut fibre adsorbent at equilibrium was calculated with the following equation:

$$q_e = \frac{(C_0 - C_e)V}{X} \quad (1)$$

Where C_0 (mg/L) and C_e (mg/L) are the initial and equilibrium concentration of the dye, V (L) is the volume of solution, X (g) is the weight of adsorbent in one container.

2.4 Theory

2.4.1 Adsorption isotherms

Adsorption isotherms of Erythrosine were measured using concentration-variation method at constant temperature, time and volume [7].

2.4.2 Adsorption Isotherm Langmuir adsorption isotherm (model)

The model represents one of the first theoretical treatments of non-linear adsorption and suggests that uptake occurs on a homogenous surface by monolayer adsorption without interaction between adsorbed molecules. The rate change of concentration due to adsorption should be equal to the rate

of concentration due to desorption. As a result, the Langmuir isotherm is as expressed in equation 3

$$q_e = \frac{a b C_e}{1 + a C_e} \quad (2)$$

$$\frac{C_e}{q_e} = \frac{1}{b Q_0} + \frac{C_e}{Q_0} \quad (3)$$

Where Q_0 and b are Langmuir constants, q_e is amount of solute removed or adsorbed at equilibrium. C_e is equilibrium concentration of mixtures. Thus Q_0 , b and the squared of the regression coefficient (R^2), are adsorption parameters estimated by Langmuir model.

2.4.3 Freundlich adsorption isotherm (model)

The Freundlich isotherm is an empirical relationship which often gives a more satisfactory model of experimental data. The Freundlich model can be applied onto heterogeneous surface involving multilayer adsorption. It can be expressed as follows:

$$K_f C_e^{1/n} \quad (4)$$

However, the linearized Freundlich adsorption isotherm can be expressed in the form;

$$\text{Log } q_e = \text{Log } (K_f) + \frac{1}{n} \text{Log } C_e \quad (5)$$

Where C_e and q_e are equilibrium concentration and adsorption capacity at equilibrium stage, while K_f and n are Freundlich constants which incorporates all factors affecting the adsorption process (adsorption capacity and intensity). Values of K_f and n can be obtained from the intercept and slope of a plot of adsorption capacity, q_e against equilibrium concentration C_e . Both parameters K_f and n affect the adsorption isotherm. The larger the K_f and n values, the higher the adsorption capacity. Furthermore, the magnitude of the exponent n gives an indication of the favorability of the adsorption process.

2.4.4 Redlich-Peterson isotherm (model)

The Redlich-Peterson (R-P) isotherm model can be represented as

$$q_e = \frac{K_R C_e}{1 + a_R C_R^\beta} \quad (6)$$

Where K_R is the R-P isotherm constant (1/mg), a_R is also a constant $(\frac{1}{mg})^\beta$ and β is the exponent which lies between 0 and 1.

2.5 Adsorption kinetics

The pseudo first order and second order kinetic models need to be tested at different concentrations in this study to determine which model is in good agreement with experiment q_e (adsorption capacity) value, thus suggesting which model the adsorption system follows.

2.5.1 Pseudo-first order equation

The Lagergren model assumes a first order adsorption kinetics and can be represented by the equation.

$$\frac{dq_t}{dt} = K_1(q_e - q_t) \quad (7)$$

$$\text{Log}(q_e - q_t) = \text{Log}(q_e) - \frac{K_1}{2.303} t \quad (8)$$

The values of $\text{Log}(q_e - q_t)$ were linearly correlated with t . The plot of $\text{Log}(q_e - q_t)$ versus t should give a linear relationship from which K_1 and q_e can be determined from the slope and intercept of the plot, respectively.

2.5.2 Pseudo-second order equation

The pseudo-second-order adsorption kinetic rates equation is expressed as

$$\frac{dq_t}{dt} = K_2(q_e - q_t)^2 \quad (9)$$

$$\frac{t}{q_t} = \frac{1}{K_2 q_e^2} + \frac{1}{q_e} t \quad (10)$$

The plot of (t/q_t) and t of equation 10 should give a linear relationship from which q_e and K_2 can be determined from the slope and intercept of the plot, respectively.

2.6 Kinetic parameters of activation

From the Van't Hoff equation, for isobaric and isochoric conditions, Arrhenius developed another equation called the rate constant K of a chemical reaction on the temperature.

$$\frac{d \ln K}{dT} = \frac{\Delta H}{RT^2} \quad (11)$$

For the adsorption process, upon integration and evaluation, the logarithm of the rate constant (K) could be represented as a straight line function of $1/T$

$$\ln K = -\frac{E_a}{RT} + \ln A \quad (12)$$

Where K is the rate constant, A is a frequency factor, R is the universal gas constant ($8.314 \text{ J.K}^{-1}.\text{mol}^{-1}$) and T is the absolute temperature. The value of E_a is calculated from the slope of plotting $\ln k$ versus $1/T$, and A (min^{-1}) is determined from the intercept.

2.7 Thermodynamic studies

The determination of the basic thermodynamic parameters: enthalpy of adsorption (ΔH), Gibb's free energy of adsorption (ΔG) and entropy of adsorption (ΔS), is important as it allows to estimate if the process is favorable or not from thermodynamic point of view, to assess the spontaneity of the system and to ascertain the exothermic or endothermic nature of the process. An adsorption process is generally considered as physical if $\Delta H^\circ < 84 \text{ kJ mol}^{-1}$ and as chemical when ΔH° lies between 84 and 420 kJ mol^{-1} [8].

The thermodynamic parameters of the adsorption process were determined from the experimental data obtained at various temperatures using equations 13 to 15

$$\Delta G = -RT \ln K_d \quad (13)$$

$$K_d = \frac{q_e}{C_e} \quad (14)$$

$$\ln K_d = \frac{\Delta S}{R} - \frac{\Delta H}{RT} \quad (15)$$

where K_d is the distribution coefficient for the adsorption, q_e is the amount of dye (mg) adsorbed on the adsorbent per L of solution at equilibrium, C_e is the equilibrium concentration (mg/L) of the dye in solution, T is the absolute temperature, R is gas constant, ΔG° , ΔH° , and ΔS° are Gibbs free energy change, enthalpy change and entropy change, respectively. The values of enthalpy change (ΔH°) and entropy change (ΔS°) are obtained from the slope and intercept of $\ln K_d$ versus $1/T$ plots [2].

III. RESULTS AND DISCUSSION

The results of the adsorption experiment are presented graphically in the figures below.

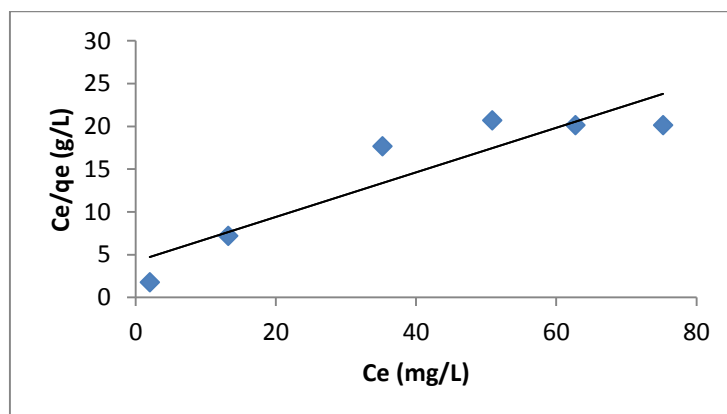


Fig.1: Langmuir model of Erythrosine

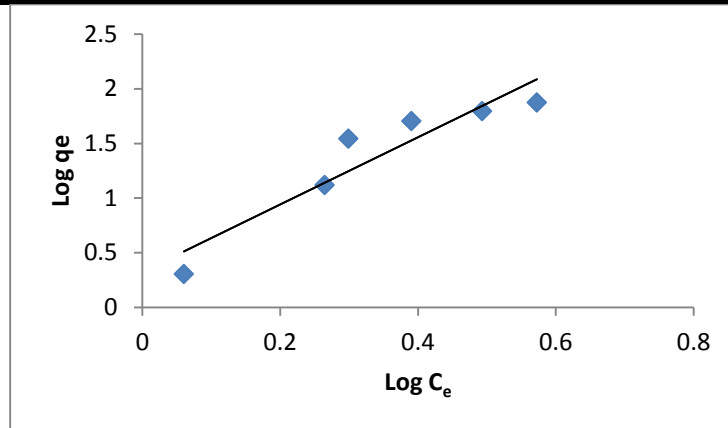


Fig.2: Freundlich model of erythrosine

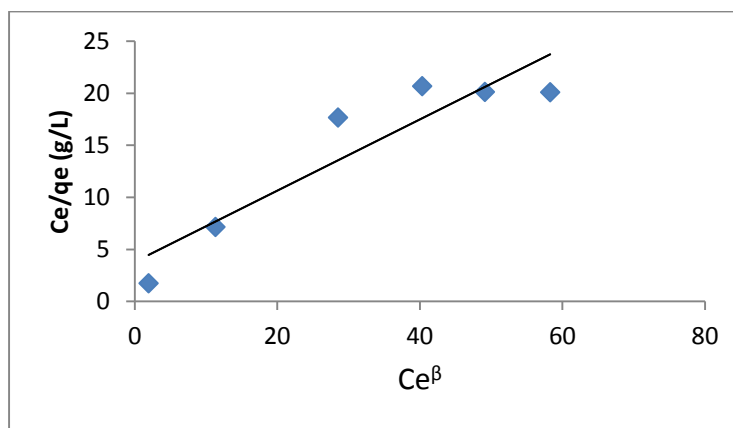


Fig. 3: Redlich-Peterson model for erythrosine

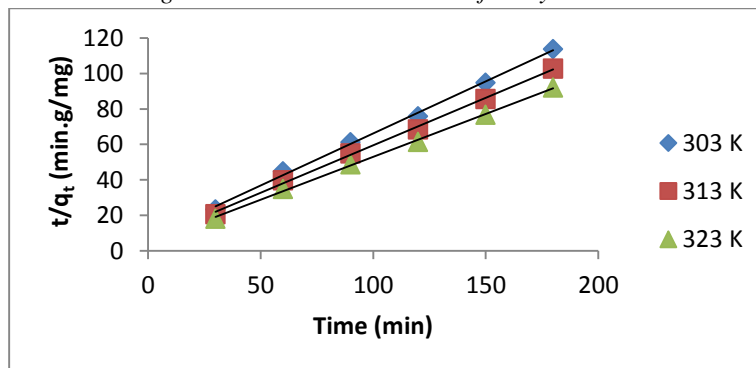


Fig. 4: Pseudo-second order reaction

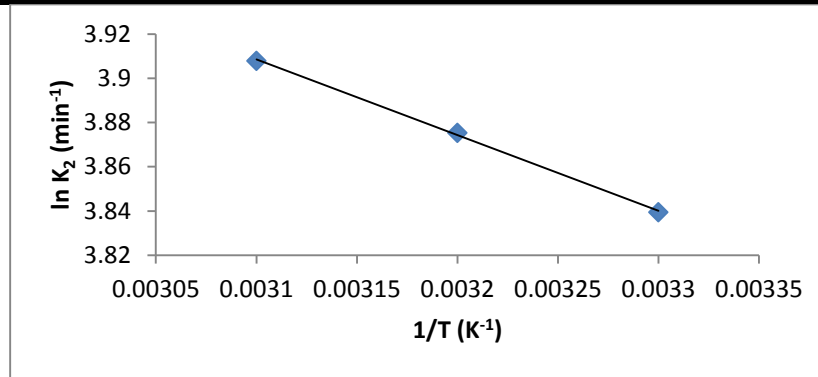


Fig. 5: Temperature dependency of reaction rate

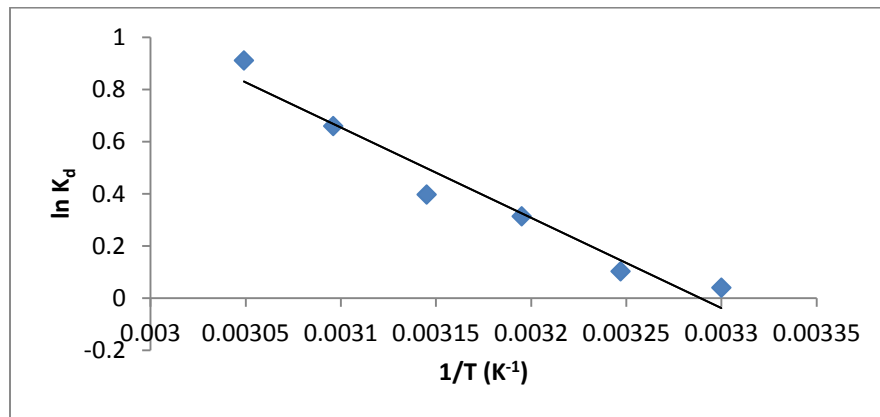


Fig. 6: Effect of temperature on erythrosine adsorption

3.1 Adsorption isotherm

The Freundlich isotherm plotted in Fig. 2 has correlation coefficient value higher than both Langmuir and Redlich-Peterson values while Redlich-Peterson is higher than Langmuir. Therefore, the Freundlich equation represents a better fit of the experiment. The parameters are presented in Table 1.

Table.1: Adsorption Isotherm constants for coconut fibre activated carbon

Langmuir			Freundlich			Redlich-Peterson		
$Q_0(\frac{mg}{g})$	$b(\frac{L}{mg})$	R^2	$K_f(\frac{mg}{g})$	$1/n(\frac{g}{L})$	R^2	$K_R(\frac{L}{mg})$	$a_R(\frac{L}{mg})$	R^2
3.8462	0.0619	0.8420	0.8872	0.2860	0.8800	0.2638	0.0902	0.855

Table.2: Thermodynamic parameters for the adsorption

Temp(K)	ΔG (KJ/mol)	ΔH (KJ/mol)	ΔS (J/mol.K)
303	-0.10	28.73	94.45
308	-0.27		
313	-0.82		
318	-1.05		
323	-1.77		
328	-2.49		

3.2 Adsorption kinetic

The plot of t/q_t versus t gives a straight line for the erythrosine adsorption as shown in Fig. 5, while the plots of $\text{Log}(q_e - q_t)$ versus t does not show good result for the

entire adsorption period, confirming the applicability of the pseudo second-order equation. Fig. 5 shows the dependency of the rate constant on temperature at 303, 313 and 323K, while values of the activation energy and frequency factor

were obtained from the plot using equation 12. The parameters are presented in Table 2.

3.3 Thermodynamic studies

The plot of $\ln K_d$ versus $1/T$ is shown in Fig 6. The values of ΔH and ΔS of erythrosine adsorption were calculated by

fitting the experimental data to equation 15. The values of ΔG were obtained by using equation 13. The standard enthalpy change (ΔH) for the adsorption is positive, indicating that the process is endothermic in nature. The parameters are presented in Table 3.

Table.3: Kinetic and Activation energy parameters

2 nd order	
30°C	
K_2 (g/mg.min)	0.0465
q_e (mg/g)	1.7036
R^2	0.997
40°C	
K_2 (g/mg.min)	0.0482
q_e (mg/g)	1.8692
R^2	0.998
50°C	
K_2 (g/mg.min)	0.0498
q_e (mg/g)	2.0704
R^2	0.997
Energy parameter	
E(KJ/mol)	2.85
C (min^{-1})	1.60

IV. CONCLUSION

Erythrosine adsorption onto coconut fibre activated carbon investigated in this research work; show that the pseudo-second order kinetic model provided the best correlation of the experimental data. The temperature variation values were used to evaluate the values of ΔH , ΔS and ΔG . The positive value of ΔH indicates that the adsorption of Erythrosine onto coconut fibre is an endothermic and the value falls in the range of physical adsorption process. The positive value of ΔS shows the existence of some structural changes at the solid-liquid interface. The results and parameters obtained, shows that coconut fibre will be an excellent low-cost adsorbent for the removal of Erythrosine dye from industrial wastewater.

V. ACKNOWLEDGEMENTS

The authors sincerely acknowledge the following people: Mr. Ikhazuangbe Benson T, NNPC-PPMC, Aviele pump station, for his financial assistance. Mr. Osibanjo Oluwakemi O, NAPIMS-NNPC, Lagos, for his financial assistance. Mr. Adeleke Kolapo and Mr. Adegbelemi Jacob, of Pharmacognosy and Pharmaceutical technology department respectively, Madonna University, Elele, for their technical support. Mr. Daramola Abayomi, of Ion-

exchange (Indian) Ltd, Eleme, Port Harcourt, for his material assistance.

REFERENCES

- [1] R. Bernstein, H.F. Haugen, and H. Frey, Thyroid function during erythrosine ingestion in doses encountered in therapy with conventional antibiotics, *Scand. J. Clin. Lab. Invest.* Vol. 35, pp. 49–52, 1975.
- [2] B. Emrah, O. Mahmut, and I.S. Ayahan, Adsorption of malachite green onto kinetic studies and process design. *Microporous and Mesoporous material*, Vol. 115, pp.234 – 246, 2008
- [3] R.H. Gumus and I. Okpeku, Production of Activated Carbon and Characterization from Snail Shell Waste (*Helix Pomatia*), *Advances in Chemical Engineering and Science*, Vol. 5, pp.51 – 61, 2015.
- [4] D. Hakan, D. Ilkanur and K. Belgin, Adsorption of Textile Dye onto Activated Carbon Prepared from Industrial Waste by ZnCl_2 Activation, *J. int. Environmental application and Science*, Vol. 3, pp.381 – 389, 2008.
- [5] A. Mittal, J. Mittal, L. Kurup and A.K. Singh, Process development for the removal and recovery of hazardous dye erythrosine from wastewater by waste materials—bottom ash and de-oiled soya as

- adsorbents, *J. Hazard. Mater.*, Vol. 138, pp. 95–105, 2006.
- [6] J. Riu, I. Schönsee, D. Barceló and C. Ràfols, Determination of sulphonated azo dyes in water and wastewater, *TrAC Trends Anal. Chem.*, Vol, 16, pp. 405–419, 1997.
- [7] S.A. Yahya, A. Rajab and S.A. Samer, Analyzing adsorption data of erythrosine dye using principal component analysis, *Chemical Engineering Journal*, Vol. 34, pp.123– 126, 2012.
- [8] Z. Zhang, Z., Moghaddam, L., O’Hara, I.M.O. and Doherty, W.O.S. Congo red adsorption by ball-milled sugarcane bagasse. *Chem. Eng. J.*, Vol. 178, pp.122–128, 2011.

Heartbeat and Temperature Monitoring System for Remote Patients using Arduino

Vikramsingh R. Parihar¹, Akesch Y. Tonge², Pooja D. Ganorkar³

Department of Electrical and Electronics Engineering, Prof Ram Meghe College of Engineering and Management, Amravati, India

Abstract— This paper describes the working of a wireless heartbeat and temperature monitoring system based on a microcontroller ATmega328 (arduino uno). Most monitoring systems that are in use in today's world works in offline mode but our system is designed such that a patient can be monitored remotely in real time. The proposed approach consists of sensors which measures heartbeat and body temperature of a patient which is controlled by the microcontroller. Both the readings are displayed in LCD monitor. Wireless system is used to transmit the measured data from the remote location. The heartbeat sensor counts the heartbeat for specific interval of time and estimates Beats per Minute while the temperature sensor measures the temperature and both the data are sent to the microcontroller for transmission to receiving end. Finally, the data are displayed at the receiving end. This system could be made available at a reasonable cost with great effect.

Keywords— *Arduino, Heartbeat Sensors, Health Monitoring System, Temperature Sensors.*

I. INTRODUCTION

In today's world, the maximum use of resource is always complimented. So, the use of wireless technology is enhanced to meet the need of remote control and monitoring. Remote patient monitoring (RPM) is a technology that helps us to monitor patient even when the patient is not in the clinic or hospital. It may increase access to health services and facilities while decreasing cost. Remote Patient Monitoring saves time of both patient and doctor, hence increasing efficiency and reliability of health services.

Heartbeat and body temperature are the major signs that are routinely measured by physicians after the arrival of a patient. Heart rate refers to how many times a heart contracts and relaxes in a unit of time (usually per minute). Heart rate varies for different age groups. For a human adult of age 18 or more years, a normal resting heart rate is around 72 beats per minute (bpm). The functioning of heart can be called as efficient if it is having lower heart rate when the patient is at rest. Babies have a much higher rate than adults around 120 bpm and older children have heart rate around 90 bpm.

If the heart rate is lower than the normal heart rate, it is an indication of a condition known as bradycardia and if the heart rate is higher than the normal heart rate, it is an indication of a condition known as tachycardia.

Like heart rate, normal body temperature also varies from person to person and changes throughout the day. The body temperature is lowest in the early morning and highest in the early evening. The normal body temperature is about 37° C or 98.6 ° F. However, it can be as low as 36.1° C (97°F) in the early morning and as high as 37.2° C (99° F) and still be considered normal. Thus, the normal range for body temperature is 97 to 100 degrees Fahrenheit or 36.1 to 37.8 degrees Celsius. Temperature can be measured by using different types of sensors. These sensors come in different forms such as thermocouples, thermistors, resistance temperature detectors (RTD), and integrated circuit (IC) sensors.

The temperature sensor produces analog output voltage which is proportional to the temperature. The temperature sensor requires analog to digital (A/D) converter so that the analog output voltage can be converted to digital form. The output of the temperature sensor is connected to the Port A of AT MEGA328R-PU arduino uno. The arduino uno processes this data and displays it in LCD as well as sends it to the receiving end for displaying at the remote place. This paper describes the design of a very low-cost remote patient monitoring system which measures heart rate and body temperature of a patient and sends the data to a remote end where the data will be displayed and physician or doctor will be able to examine him/her. This device will be much needed during emergency period or for saving time of both patient and doctor.

II. LITERAURE REVIEW

- With emerging wireless techniques like Bluetooth and Zigbee technology wearable sensors are used for patient monitoring due to the advantages like mobility and low power consumption by the system.
- The advantages are treatment can be given to the patient in priority to the disease they have when comparing with other patients, when in critical situation they can be hospitalized.

- These types of communication will only work for shorter distance and duration. A study was done to determine the types of vital signs that are routinely measured for a patient by doctor.
- The vital signs are body temperature, pulse rate and detection of fall. Body tissues mass-weighted average temperature and skin temperature are measured.
- Direct temperature measurement of peripheral tissue is more complex than core temperature measurement. Vital signals of patient health can be monitored by biomedical system using zigbee.
- The system is two tiered, used for gathering and processing biomedical signals.
- First the device with number of biosensors has to be placed on the body and second is processing by a local base station using the raw data transmitted on request by the mobile device.
- Smart wearable remote health monitoring systems are increased in usage for good quality in health services and low cost, by avoiding unnecessary hospitalizations and to ensure urgent care.
- System contributes to the enhancement of disease prevention with cost effective telemedicine platform. For physiological parameters measurement the network is approached to deal with monitoring and analysis of patient health.
- Data from sensors are acquired and transmitted to server by the network. Physiological parameters can be processed and automated by system and displayed on the monitor.

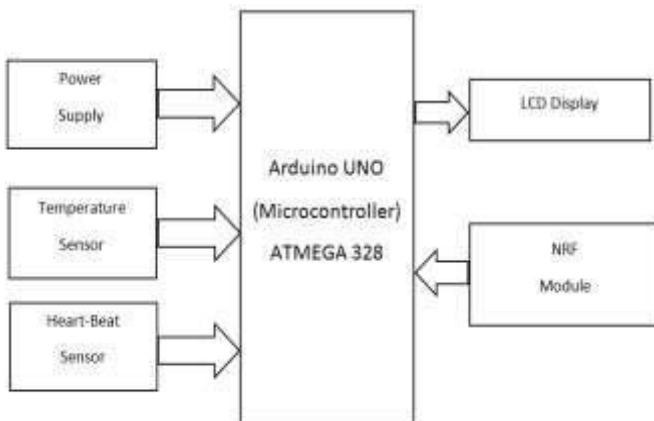


Fig. 2.1: Block diagram of transmitter section

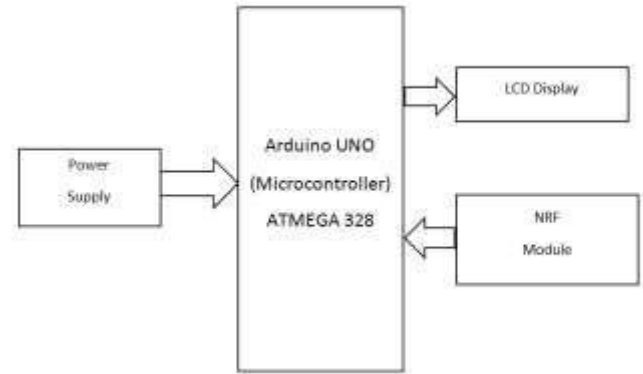


Fig. 2.2: Block diagram of Receiver section

III. PLATFORM INTRODUCTION

A Remote Health Monitoring System consists of three main components such as data sensing module, data processing module and data communication module. The data sensing module consists of temperature sensor and heart beat sensor which senses the changes in the respective physiological parameters. The information is then conveyed to the PIC microcontroller of data processing module. The data processing module analyzes the input signals. The noise signals are filtered and if the processed value exceeds than normal value, medicine which is to be given as a first aid for patient is displayed on the personal computer using GUI. The communication module is used to transfer data between person and equipment. This has basic components such as the message, the sender, the receiver, the medium and the protocol by which the message is sent to the doctor through mobile phones by information gateway for the treatment to be taken.

IV. WORKING OF SUGGESTED APPROACH COMPONENTS USED

- Arduino ATmega328
- Temperature Sensor LM35
- Heart Beat Sensor (LM358)
- nRF24L01 Module
- LCD
- Potentiometer
- Power supply

WORKING

The aim of this proposed approach is to design an automatic wireless health monitoring system. The objective is to monitor the temperature and heartbeat of the patient's body which should be displayed to the doctor using NRF technology. In hospitals, the monitoring of the patients' health is done by the staff members of the hospital. The temperature and heart rate of the patient's body is checked constantly and a record of it is kept. The required components used in this system include a power supply, ATmega328 microcontroller, a temperature

sensor, an RF TX, an RX module and an LCD display. The ATmega328 microcontroller is used as a CPU for monitoring the temperature of the patient's body. The working of this proposed health monitoring system can be explained with the help of a block diagram. This block diagram includes a power supply block that supply power to the whole circuit, and a temperature sensor is used to sense the temperature and heartbeat of a patient's body.

The circuit diagram of the automatic wireless health monitoring system mainly includes transmitter section and receiver section. In the TX section, the temperature and heart beat sensor is used to detect the temperature and heartbeat of the patient's body and the data which are sensed by the sensor is sent to ATmega328.

The transmitted information can be encoded into serial data over the air through nRF module and the temperature of the patient's body values is displayed on the LCD display using an antenna arranged at the end of a transmitter and the data from the transmitter is transmitted to the receiver end.

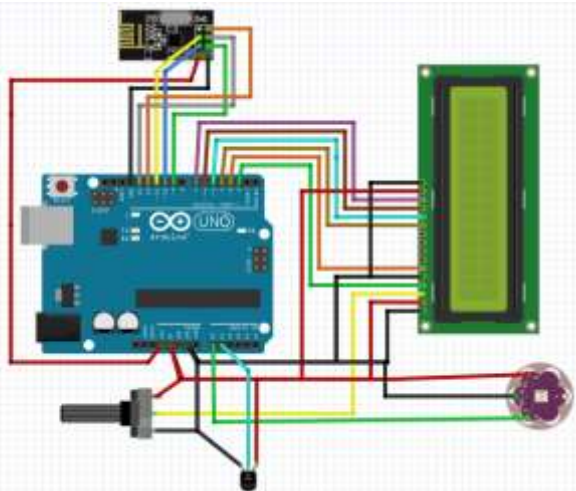


Fig. 4.1: Circuit Diagram of Transmitter section

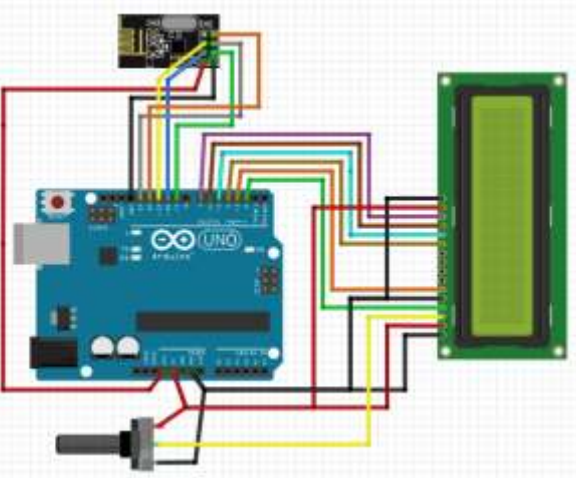


Fig. 4.2: Circuit Diagram of Receiver Section

V. DESIGN FEATURES

Health Monitoring System is done with modules of data sensing, data processing and data communication as shown in Fig. Three sensors are contained in data sensing module such as temperature sensor, heart rate sensor. Temperature sensor is used to measure the body temperature. Heartbeat sensor is used to measure the function of heart by blood flow through Finger. The output of each sensor is interfaced with Analog to Digital circuit (ADC) pins of microcontroller. Data processing module consists of ATmega328, 28-pin 8-Bit microcontroller of Harvard architecture which is a high-performance nRF circuit used to solve problems in conversion of RS232 signal voltage to TTL voltage and needed to communicate the receiver and sending SMS through information gateway, LCD is used as a display unit in connection with microcontroller for displaying the current details of physiological parameters. Patient monitoring is applicable in different situations when a patient is in the following conditions:

- In unstable physiological regulatory systems – for instance, in the case of overdose of anesthesia.
- In a life threatening condition – for instance, when there is an indication of heart attack in a patient.
- In a critical physiological state.

5.1 Single parameter monitoring system: This system is used for measuring the blood pressure of a human body, monitoring ECG, monitoring SPO2 (oxygen saturation in blood), and so on.

5.2 Multi parameter monitoring system: This system is used for monitoring multiple critical physiological signs of patients by transmitting the vital information like ECG, respiration rate and blood pressure, etc. Due to these reasons, multi parameter patient monitoring systems play a significant role in the field of medical devices.

VI. RESULTS

6.1 Temperature Measurement

When the power is turned on, all the LEDs on PCBs starts glowing, indicating that circuit is working properly. Here there is a use of the industrial temperature sensor i.e. LM 35 which gives us room temperature in °C. That temperature is displayed on the LCD.

6.2 Heartbeat Measurement

There is a cavity for measurement of the heartbeat, which consist of an arrangement of LED and LDR. Patients' finger in placed between LED and LDR, and the heart pulses are detected. The analog voltages are further processed with an operational amplifier LM 358, and this chip has two built in OPAMPs. Result is displayed on the LCD. This collected data is transmitted using nRF24L01 module. This data is received at the receiver section using

same nRF24L01 module.

VII. CONCLUSION

We have analyzed the wireless patient health monitoring system of temperature and heartbeat of humans using nRF24L01. The heartbeat was measured with the help of photodiode and bright LED while the temperature was measured by using precision integrated temperature sensor LM35. Both the data were processed in the arduino uno and sent to the remote end wirelessly by using nRF transmitter and received at the remote end by using nRF receiver. The received data was processed in the arduino uno and the data measured was displayed successfully with the help of LCD at the remote end. The wireless communication was preferred because it gives greater mobility to the sensor equipment and reduces the cost wherein there are multi-transmitting sections.

VIII. FUTURE APPLICATIONS AND DEVELOPMENTS

- The device can be connected to PC by using serial output so that measured heartbeat and temperature can be sent to PC for further online or offline analysis.
- Warning for abnormalities of health condition can be displayed.
- Sound can be added to the device so that the device makes a sound each time a pulse is received and alarm is started for abnormal health condition.
- The output can be sent to mobile phones by using GSM module or Bluetooth module for further analysis.
- More parameters (like blood pressure) can be added to the device.
- In addition to the system can also provide more than one numbers so that more than one user can receive emergency message.
- According to availability of sensors or development in biomedical trend more parameter can be sense and monitor which will drastically improve the efficiency of the wireless monitoring system in biomedical field.

REFERENCES

- [1] Manisha Shelar, Jaykaran Singh, Mukesh Tiwari, "Wireless Patient Health Monitoring System", *International Journal of Computer Applications* (0975 – 8887) Volume 62– No.6, January 2013.
- [2] Rajalakhshmi.S S.Nikilla, "Real Time Health Monitoring System using Arduino", *South Asian Journal of Engineering and Technology* Vol.2, No.18 (2016) 52–60 ISSN No: 2454-9614
- [3] C. K. Das, M. W. Alam and M. I. Hoque, "A Wireless Heartbeat And Temperature Monitoring System For Remote Patients", *ICMERE2013-PI-197*

- [4] Media Aminian1 and Hamid Reza Naji2, "A Hospital Healthcare Monitoring System Using Wireless Sensor Networks", *Aminian and Naji, J Health Med Inform* 2013, 4:2
- [5] Md. Asaduzzaman Miah, Mir Hussain Kabir, Md. Siddiqur Rahman Tanveer and M. A. H. Akhand, "Continuous Heart Rate and Body Temperature Monitoring System using Arduino UNO and Android Device". *International Conference on Electrical Information and Communication Technology* Volume 10.1109/EICT.2015.7391943.
- [6] Harshavardhan B.Patil, Prof.V.M.Umale, "Arduino Based Wireless Biomedical Parameter Monitoring System Using Zigbee", *International Journal of Engineering Trends and Technology (IJETT) – Volume 28 Number 7 - October 2015* ISSN: 2231-5381.
- [7] Prof. Y. R. Risodkar. Prof. M. K. Sangole. Amruta. R. Vankhede. Ravi. S. Medhe. Jayashri. K. Shirsat, "Web Based Health Monitoring System", *International Journal of Advanced Research in Electronics and Communication Engineering (IJARECE)* Volume 4, Issue 1, January 2015, ISSN: 2278 – 909X.

Explosions, Abnormal Loads on Structures

Hajdar E. Sadiku, Esat Gash, Misin Misini

Civil Engineering and Architectural Faculty University of Prishtina, Kosovo.

Abstract— In Kosovo as well as in many countries of the world have occurred explosions in objects, so this research have addressed the ways and possibilities of protecting the buildings by using their position as construction and design elements' after you load resisted by explosions.

This paper presents basic information on the approaches for the evaluation of the blast effects on the structures.

Motivation for the present study is recent events happening in the World where more and more structures are being destroyed by unexpected explosions in the urban areas.

Intension of this investigation is to present basic information on what will happen when an explosive device is detonated. Some of the methods to calculate blast loads are presented.

At the end it is presented simple method of designing a reinforced concrete wall barrier subject to a blast load caused by vehicle bomb. Calculation has been carried based on the kinetic energy that is delivered on the surface of the wall and that energy dissipation by the wall to resist such impulse load.

Keywords—Blast resistant design, blast waves, explosive effects.

I. INTRODUCTION

1.1. Need for Protection

In the last couple of years we are all witnessing that there are more often cases of unexpected explosions, bomb attacks, vehicle bombs, that are striking urban areas. Circumstances, time, actors and reasons for those explosions are unpredictable.

With these events there are more and more people asking questions like:

- If there is need for protection?
- Can we protect our-self and structures?
- Do we need to design structures to resist explosions, etc?

Well, the answer in all these questions definitely will be, yes. From us engineers, it will be required to design and construct special buildings, such as government buildings, embassies, military facilities, bunkers, bridges, silos, industrial facilities, etc. As we can see there is a wide range of buildings that would require to be designed taking in to consideration blast loads as one of the possible load in the load combination.

Constructing structures to resist blast effects is very expensive and often conflicts with architectural solutions and harms the activities for which the structure is designed. For these reasons in most cases it not feasible to construct structures to resist any potential incident.

1.2. Some of the Possible Threats

Of significant importance when designing buildings, in the process of protective design, is assessment of the potential threats.

Some of the primer threats to which structures may be subject are:

- Nuclear device;
- Gas and vapor cloud (Military munitions produce a detonable mixture generating blast loading over a large target area;
- Artillery shells (Fragmenting munitions delivered by heavy artillery which, depending on fusing could penetrate concrete, soil, etc. before detonation.);
- Package bomb (Common device easy infiltrated inside the structures which intension is to create high level of destruction), etc;

In order to withstand the transient loads generated by any of these threats, the elements of the structure need to be both massive and able to absorb large amount of energy. For this reason nearly all purpose-built protective structures are constructed of reinforced concrete.

1.3. What Happens When Explosion Occurs?

When an explosive device is initiated, the explosion reaction generates hot gases which can be at pressure from 100 kilo bars (10000 MPa) up to 300 kilo bars (30000 MPa) at temperatures of about 3000-4000 °C and have traveling speed of up 7400 m/s. A violent expansion of these explosive gases then occurs and the surrounding air is forced out of the volume it occupies. As a consequence a layer of compressed air-blast wave- forms in front these gases containing most of the energy released by the explosion. (Bulson, Philip. :Explosive Loading Of Engineering Structures, University of Southampton, 1997)

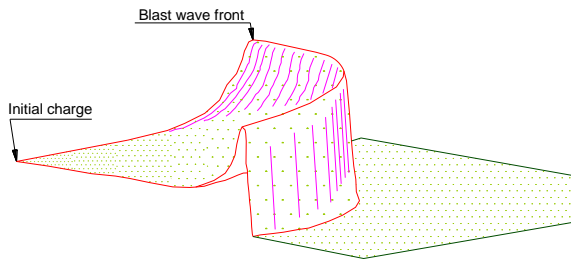


Fig. 1: Blast Wave

The violent release of energy from a detonation in a gaseous medium gives rise to a sudden pressure increase in that medium. The pressure disturbance, termed as the blast wave, is characterized by an instantaneous rise from the ambient pressure, P_o , to peak incident pressure P_{so} . At a point away from the blast, the pressure wave has almost a triangular shape as shown in Fig.2. The shock front arrives and after the rise to the peak value the incident pressure decays to an ambient value in the time, t_d , described as the positive phase duration. This is followed by a negative phase, t_{ng} , and characterized by a pressure below the pre-shot ambient pressure and a reversal of the particle flow. The negative phase is usually less important in a design than the positive phase. [2]

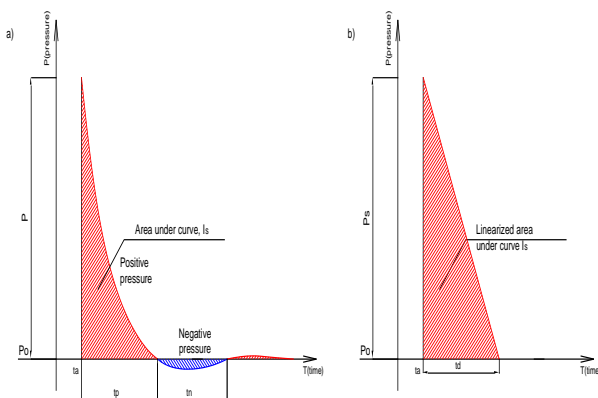


Fig. 2: Typical and Linearized Blast Pressure Wave

The equations of motion that describe a blast wave are very complex. Initially numerically these were solved by Brode and experimentally verified by Kingery. A good knowledge of the gas dynamics is needed for more comprehensive treatment

II. EQUATIONS TO DETERMINE BLAST PRESSURE

Extensive research has been conducted to predict the peak pressure values, impulse velocities and other parameters of blast waves. Most of the theoretical models and graphs were done by military research centers, in which they correlate between a scaled distance Z and the predicted peak pressures.

R- Radial standoff distance from the center of the explosive to a particular location on a structure, meters

W- Charge weight of TNT, kilograms. [1], [2]

As TNT is as considered as reference type of explosion, all other explosives need to be converted in to TNT equivalent. Table below shows conversion factors for some types of explosives:

Table.1: Conversion factors for explosives

Explosive	Specific energy Q_x (kJ/kg)*	TNT Equivalent Q_x/Q_{TNT}
Mixture B (60% RDX, 40% TNT)	5190	1.148
RDX (Cyclonite)	5360	1.185
HMX	5680	1.256
Nitroglycerine (liquid)	6700	1.481
TNT	4520	1.000
Pentolit	6012	1.330
60% Nitroglycerine dynamite	2710	0.600
Semtex	5660	1.250

The scaled distance parameter in fact presents law on blast estimating. This law says: Similar blast waves are produced at incidental scaled distance when two explosive charges of similar geometry and of the same explosive type, but of different sizes, are detonated in the same atmosphere.

Various equations by different authors are given to determine blast pressure. An empirical equation is presented by Charles N. Kingery and Gerald Bulmash with reflected pressure coefficients, are listed in the US Army technical manual TM5-855-1. This equation computed air blast environment created by the detonation of a hemispherical TNT explosive source at sea level. Information on this model is classified and therefore is not for public use.

Another empirical equation presented by the Defense Atomic Support Agency, DASA report # 1860 (1966). This equation correlates between the peak pressure with the weight and standoff distance as shown in equation:

$$P_s = 1033.5 * W * (5/R)^3 \quad (2)$$

P_s: Peak pressure at given charge weight and standoff distance in [kPa]

W: Charge weight of TNT, kilograms [kg]

R- Radial standoff distance from the center of the explosive to a particular location on a structure, meters

$$P_s = 45956 * W * R^{-2.5} \quad (3)$$

The incident impulse associated with the blast wave is the integrated area under the pressure time curve and is denoted as I_{so} . To simplify the blast resistant design

procedure, the generalized blast wave profile shown in fig.3a is usually linearized as illustrated in fig.3b.

Value of the impulse can be calculated as the area of the triangle under the linearized blast curve:

$$I_{so} = (P_{so} \cdot t_d) / 2 \quad (4)$$

Equation given by author Friedlander calculates blast pressure taking in to the consideration time factor

$$p(t) = p_s \left[1 - \frac{t}{T_s} \right] \exp \left\{ -\frac{bt}{T_s} \right\} \quad (5)$$

Of course, these days in the market there are several applicative software's that easily calculate blast pressure and other parameters, including structural analysis. Some of them are: At-Blast, Nonlin CONWEP, ABACUS, Pronto3D, etc.[1]

2.1 Blast Effects on the Structures

Figure 3 present what happens to a frame structure when a vehicle bomb explodes in front.

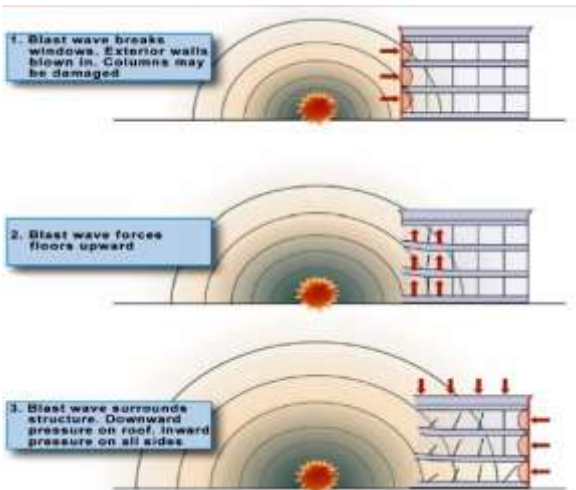


Fig. 3:Explosion in Front of the Structure

As far as the nuclear explosions are concerned, there is only one well known event, which happened during the



Fig. 4 a) Khobar Towers, US Marines HQ, Saudi Arabia, 1996 Explosive, 9 ton TNT equivalent, standoff, 25m 19 victims, 450 injured,



Fig. 4 b) Federal building A.P Murrah, Oklahoma City, USA 1995 Explosive, 1.8 ton TNT equivalent, standoff 4.5 m 168 victims, 500 injured

Second World War when two bombs were thrown in the towns of Hiroshima and Nagasaki in Japan.

Number of explosions caused by vehicle bombs or packed bombs if much bigger. [3], [4].

Table below presents average quantities that can be carried by different means of transportations. This table is important as it can be used as a good start point to predict and calculate possible blast pressure.[1]

Table.2: Conversion factors for explosives

Type of transportation	Capacity (TNT equivalent)
Pipe bomb	up to 2.5 kg
Suitcase bomb	up to 25 kg
Vehicle bomb-small vehicle	up to 250 kg
Vehicle bomb-sedan	up to 450 kg
Vehicle bomb-van	up to 2000 kg
Truck	up to 4500 kg
Truck-tanker	up to 14000 kg
Truck-lorry	up to 30000 kg

On this study will present two of the many cases, just for the comparison and presentation of the scale of the devastation that can be caused by vehicle bomb blast Fig. 4.

Loads to be protected from explosions important is the way the building is built, it is noticed by explosions that have destroyed Mail in Pristina object in relation to objects around fig. 5.



Fig. 5: Destruction of buildings with poor material compared with those of reinforced concrete

Serious injuries and fatalities in humans, cause the equipment and artillery, it can be seen from the recent war in Prekaz – Kosovo, fig 6.



Fig.6: Damaged facilities in Kosovo (Prekaz) during the Kosovo war

III. COMPARISONS OF SEISMIC AND BLAST LOADING

In general similarities between seismic and blast loading includes the following:

- Dynamic loads and dynamic structural response;
- Involve inelastic structural response;
- Focus on life safety as opposed to preventing structural damage;
- Nonstructural damage and hazards;
- Similar: performance based design; life safety issues; progressive collapse; structural integrity; ductility, continuity and redundancy; balanced design.

Differences between these two types of loading include (fig. 5):

- Blast loading is due to a propagating pressure wave as opposed to ground shaking;
- Blast results in direct pressure loading to structure; pressure is in all directions, whereas a seismic event is dominated by lateral load effects;
- Blast loading is of higher amplitude and very short duration compared with a seismic event;

- Magnitude of blast loading is difficult to predict and not based on geographical location;
- Blast effects are confined to structures in the immediate vicinity of event because pressure decays rapidly with distance; local versus regional event;
- Progressive collapse is the most serious consequence of blast loading;
- Slab failure is typical in blasts due to large surface area an upward pressure not considered in gravity design;
- Small database on blast effects on structures;
- Seismic-resistant design is mature compared with blast-resistant design.

In summary, while the effect of blast loading is localized compared with an earthquake, the ability to sustain local damage without total collapse (structural integrity) is a key similarity between seismic-resistant and blast-resistant design.

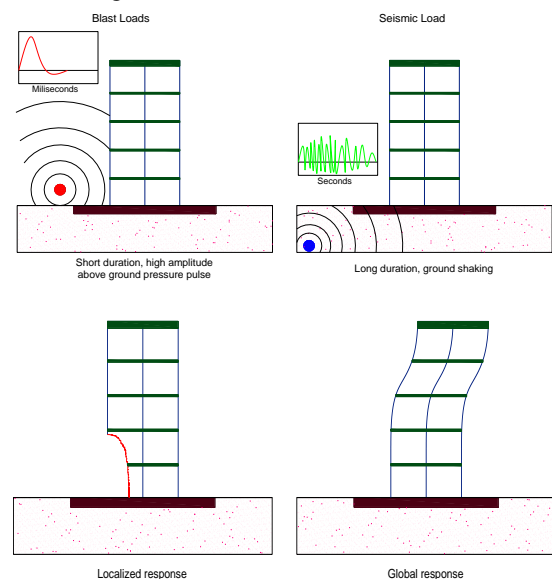


Fig. 5: Comparison of blast and seismic loading (top) and the structural response (bottom)

IV. SOME OF THE COMMON DESIGN REQUIREMENTS - TECHNICAL DESIGN MANUALS FOR BLAST-RESISTANT DESIGN

4.1 In General

American Standards, Unified Facilities Criteria, UFC 4-010-01 requires that all new and existing buildings of three stories or more be designed to avoid progressive collapse. Progressive collapse is defined in the commentary of the ASCE (American Society of Civil Engineers) 7-02 as “the spread of an initial local failure from element to element, eventually resulting in the collapse of an entire structure or a disproportionately large part of it.

4.2. Design Approaches

ASCE 7-02 defines two general approaches for reducing the possibility of progressive collapse: Direct Design and Indirect Design.

Direct design approach

Direct Design approaches include "explicit consideration of resistance to progressive collapse during the design process..." These include:

- Alternate Path (AP)
- Specific Local Resistance (SLR)

Indirect design approach

With Indirect Design, resistance to progressive collapse is considered implicitly "through the provision of minimum levels of strength, continuity and ductility". ASCE 7-02 presents general design guidelines and suggestions for improving structural integrity. These include:

od plan layout, integrated system of ties, returns on walls, changing span directions of floor slabs, load-bearing interior partitions, catenaries action of the floor slab, beam action of the walls, redundant structural systems, ductile detailing, compartmentalized construction.

However, no quantitative requirements for either direct or indirect design to resist progressive collapse are provided in ASCE 7-02.

The British Standards employ three design approaches for resisting progressive collapse:

- Tie Forces (TF), Alternate Path (AP), Specific Local Resistance (SLR).

The provisions specified that progressive collapse potential is limited if the damaged area is smaller of the following: 5% of the area of the story or 70 m²



Fig.7: Progressive Collapse Ronan Point, UK, 1968[3]

4.3. Some of the Common Design Requirements - TECHNICAL DESIGN MANUALS FOR BLAST-RESISTANT DESIGN

This section summarizes applicable military design manuals and computational approaches to predicting blast loads and the responses of structural systems. Although the majority of these design guidelines were focused on military applications these knowledge are relevant for civil design practice. [5]

A Manual for the Prediction of Blast and Fragment Loadings on Structures, DOE/TIC- 11268 (U.S. Department of Energy, 1992). This manual provides guidance to the designers of facilities subject to accidental explosions and aids in the assessment of the explosion-resistant capabilities of existing buildings.[5]

The Design and Analysis of Hardened Structures to Conventional Weapons Effects (DAHS CWE, 1998). This new Joint Services manual, written by a team of more than 200 experts in conventional weapons and protective structures engineering, supersedes U.S. Department of the Army TM 5- 855-1, Fundamentals of Protective Design for Conventional Weapons (1986), and Air Force Engineering and Services Centre ESL-TR-87-57, Protective Construction Design Manual (1989)[5] Columns and Walls - For all levels of protection, all multistory vertical load-carrying elements must be capable of supporting the vertical load after the loss of lateral support at any floor level (i.e., a laterally unsupported length equal to two stories must be used in the design or analysis

- **Upward Loads on Floors and Slabs-** In each bay and at all floors and the roof, the slab/floor system must be able to withstand a net upward load of the following magnitude:

$$1.0 D + 0.5 L \quad (6)$$

D- Dead load based on self-weight only (kN/m²) ,

L- Live load (kN/m²)

This load is applied to each bay, one at a time, i.e., the uplift loads are not applied concurrently to all bays. Floor systems in each bay and its connections to the beams, girders, columns, capitals, etc, shall be designed to carry this load. A load path from the slab to the foundation for this upward load does not need to be defined).[5]

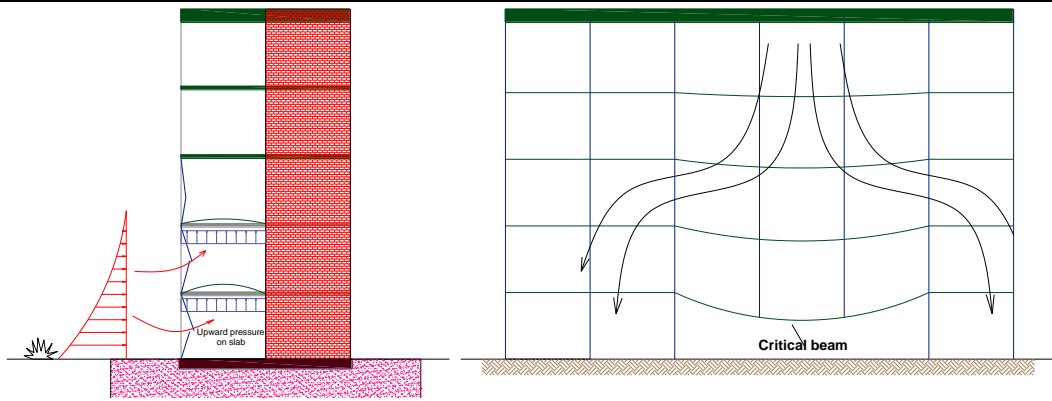


Fig.8: Uplift Loads for Slabs on the Structures Subject to Blast Loads

V. CONCLUSION

Even though all that has been presented in this document presents a small part on evaluation of the structures under the blast loads, still there are some conclusions that can be made:

- Explosions cause extreme loads on structures;
- Blast loads have nature of impulsive loads, high intensity and load duration is shorter compare to seismic loads;
- Keeping the standoff distance is the best way to mitigate effects of the blast loads;
- Progressive collapse is the worst effect on the structures that can be generated by blast loads;
- During the Kosovo war the impact of material objects in tackling explosions;
- With better protection from explosions is respect and love between people regardless of religion and race.

REFERENCES

- [1] **Bulson, Philip.** : Explosive Loading Of Engineering Structures, University of Southampton, 1997.
- [2] **K.Domiaty, J. Myers, A. Belarbi.** : Blast Resistance of Un-reinforced Masonry Walls Retrofitted with Fiber Reinforced Polymers, University of Missouri, 2002
- [3] **P.D. Smith & J.G. Hetherington.** : Blast and Ballistic Loading of Structures, Cranfield University, Royal Military College of Science, UK, 2003.
- [4] **UFC.** : Design Of Buildings To Resist Progressive Collapse, January 2005
- [5] **Gupta & J. Ramsay The University of Melbourne, Australia** : Blast Loading and Blast Effects on Structures – An Overview T. Ngo, P. Mendis, A. EJSE Special Issue: Loading on Structures (2007)

MHD Free Convective Radiative and Chemically Reactive Flow Over a Vertical Porous Surface in the Presence of Diffusion-Thermo Effect

G. Sreenivasulu Reddy¹, S.Geethan Kumar², S. Karunakar Reddy³, P. Durga Prasad^{4*},
S.Vijayakumar Varma⁵

¹Reader in Mathematics, Govt. Degree College, Pakala, Chittoor, A.P, India

³Department of Mathematics, JNTU Hyderabad, Telangana, India

^{2,4,5} Department of Mathematics, S.V.University, Tirupati, India

Abstract—The main purpose of this work is to investigate the porous medium and diffusion thermo effects on unsteady combined convection magneto hydrodynamics boundary layer flow of viscous electrically conducting fluid over a vertical porous surface in the presence of first order chemical reaction and thermal radiation. The slip boundary condition is applied at the porous surface. A uniform Magnetic field is applied normal to the direction of the fluid flow. The non-linear coupled partial differential equation are solved by perturbation method and obtained the expressions for concentration, temperature and velocity fields. The rate of mass transfer in terms of Sherwood number h , the rate of heat transfer in terms of Nusselt number Nu and the Skin friction coefficient Cf are also derived. The Profiles of fluid flow and derived quantities for various values of physical parameters are presented and analyzed.

Keywords—Diffusion-thermo effect, Thermal radiation, Chemical reaction, Magnetic field, Absorption of Radiation.

Nomenclature

A Suction velocity parameter
 B_0 Magnetic field of uniform strength
 C Species concentration
 C^* Dimensional concentration
 C_p Specific heat at constant pressure
 C_s Concentration susceptibility
 C_w Species concentration at plate
 C_∞ Species concentration far away from the plate
 Cf Skin friction coefficient
 D Molecular diffusivity
 $e_{b\lambda}$ Planck's function
 g Acceleration due to gravity

Gm Solutal Grashof number
 Gr Thermal Grashoff number
 D_m Coefficient of mass diffusivity
 K_T Thermal diffusion ratio
 $K_{\lambda w}$ Absorption coefficient at the wall
 M Magnetic field parameter
 F Radiation parameter
 Nu Nusselt number
 n^* Constant
 P^* Pressure
 Pr Prandtl number
 Q Heat source/sink parameter
 Q^* Sink strength
 Q_0 Dimensional heat absorption coefficient
 Q_1 Absorption of radiation parameter
 Q_1^* Coefficient of proportionality for the absorption
 q_r^* Radiative heat flux
 Sc Schmidt number
 Sh Sherwood number
 T Fluid Temperature
 T^* Temperature of the fluid near the plate
 T_w Temperature at the wall
 T_∞ Temperature far away from the plate
 u^*, v^* Components of dimensional velocities
 u^* Velocity of the fluid along x^*
 U_∞^* Free stream dimensional velocity
 U_p Wall dimensional velocity
 v^* Velocity of the fluid along y^*
 U_0 Scale of free stream velocity
 V_0 Section velocity
 C_p Specific heat at a constant pressure
 C_v Specific heat at a constant volume
 x^*, y^* Dimensional the distances along and perpendicular to the plate

Re_x Local Reynolds number**Greek Symbols** μ Fluid dynamic viscosity α Fluid thermal diffusivity ν Coefficient of kinematic viscosity β Coefficient of Volumetric expansion for the heat transfer β^* Coefficient of Volumetric expansion for the fluid β_0 Magnetic field coefficient β_T, β_c Thermal and concentration expansion coefficients ρ Density of the fluid σ Electrically conductivity of the fluid η Dimensionless normal distance

Fluid currents formed in a fluid-saturated porous medium during convective heat transfer have many important applications, such as oil and gas production, central grain storage, porous insulation, and geothermal energy. The study of natural convection through porous medium also throws some light on the influence of environment such as temperature and pressure on the germination of seeds. In many situations, the heat and mass transfer on the hydromagnetic flow near the vertical plate is encountered e.g., the cooling of nuclear reactor with electrically conducting coolants such as liquid sodium and mercury, studied by Rath and Parida [1]. Raptis [2], Jha and Prasad [3] have studied the steady free-convection flow and mass transfer through a porous medium bounded by an infinite vertical plate for the flow near plate by using the model of Yamamoto and Iwamura [4]. Gebhart and Pera [5] have studied the laminar flows which arise in fluids due to the interaction of the force of gravity and density differences caused by the simultaneous diffusion of thermal energy and of chemical species.

As stated by Pal and Talukdar [6], convection in porous media has gained significant attention in recent years because of its importance in engineering applications such as solid matrix heat exchangers, geothermal systems, thermal insulations, oil extraction and store of nuclear waste materials. Convection in porous media also is applied to underground coal gasification, ground water hydrology, iron blast furnaces, wall cooled catalytic reactors, solar power collectors, energy efficient drying processes, cooling of electronic equipment's and natural convection in earth's crust. Reviews of the applications associated to convective flows in porous media can be found in Nield and Bejan [7]. The fundamental problems of flow through and past porous media has been studied extensively over the years both theoretically and experimentally by Cheng [8] and Rudraiah [9]. The effect of Beavers-Joseph slip velocity and transverse magnetic

 ϕ Heat source parameter ϕ_1 Slip parameter κ Thermal conductivity**Superscripts**' Differentiation with respect to y

* Dimensional properties

Subscripts

p Plate

w Wall condition

 ∞ Free stream condition**I. INTRODUCTION**

field on an electrically conducting viscous fluid in a horizontal channel bounded on both sides porous substrates of finite thickness was studied Rudraiah et al. [10], which is equivalent to the problem of forced convection where the momentum equation is independent of concentration distribution and the diffusion equation is coupled with the velocity distribution using Beavers-Joseph slip condition at the porous interface.

In many chemical engineering processes, the chemical reaction occurs between a foreign mass and the fluid in which the plate is moving. These processes take place in numerous industrial applications e.g., manufacturing of ceramics or glassware, polymer production, and food processing. Chemical reactions can be codified as either homogeneous or heterogeneous processes. This depends on whether these occur at an interface or as a single phase volume reaction. Many transport processes exist in a nature and mass transfer as a result of combined buoyancy effects of thermal diffusion and diffusion of chemical species. Apelblat [11] studied analytical solution for mass transfer with a chemical reaction of the first order. Das et al. [12] have analyzed the effects of homogeneous first order chemical reaction on the flow past an impulsively started infinite vertical plate with uniform heat flux and mass transfer. Chambre and Young [13] have analyzed a first order chemical reaction in the neighborhood of a horizontal plate.

Radiative convective flows are encountered in various ways in the environment e.g., heating and cooling chambers, evaporation from large open water reservoirs, fossil fuel combustion energy processes, solar power technology, astrophysical flows, and space vehicle re-entry. Radiative heat and mass transfer play an important role in manufacturing industries for the design of reliable equipment. Nuclear power plants, gas turbines, and various propulsion devices for satellites, missiles, aircraft and various space vehicles are examples of such

engineering applications. If the temperature of the surrounding fluid is rather high, radiation effects play an important role and this situation does exist in space technology. In such cases, one has to take into account the effect of thermal radiation and mass diffusion.

The thermal radiation effects of an optically thin gray gas bounded by a stationary vertical plate was studied by England and Emery [14]. The radiative natural convective flow of an optically thin gray-gas past a semi-infinite vertical plate was considered by Soundalgekar and Takhar [15]. In all above studies, the stationary vertical plate is considered. The effects of the thermal radiation and free convection flow past a moving vertical plate studied by Raptis and Perdakis [16]. Ibrahim et al. [18] have recently reported computational solutions for transient reactive magneto hydrodynamic heat transfer with heat source and wall flux effects. They have also analyzed the effects of the chemical reaction and radiation absorption on the unsteady MHD free convection flow past a semi-infinite vertical permeable moving plate with heat source and suction. Due to the importance of Soret (thermal-diffusion) and Dufour (diffusion thermo) effects for the fluids with very light molecular weight as well as medium molecular weight many investigators have studied and reported results for these flows of whom the names are Dursunkaya and Worek [19], Anghel *et al.* [20], Postelnicu [21] are worth mentioning.

Chamkha [24] investigated unsteady convective heat and mass transfer past a semi-infinite porous moving plate with heat absorption. Chamkha [25] studied the MHD flow of a numerical of uniformly stretched vertical permeable surface in the presence of heat generation/absorption and a chemical reaction. Mohamed [26] has discussed double diffusive convection radiation interaction on unsteady MHD flow over a vertical moving porous plate with heat generation and Soret effects. Muthucumaraswamy and Janakiraman [27] studied MHD and radiation effects on moving isothermal vertical plate with variable mass diffusion. Rajesh and Varma [28] studied thermal diffusion and radiation effects on MHD flow past a vertical plate with variable temperature. Kumar and Varma [29] investigated thermal radiation and mass transfer effects on MHD flow past an impulsively started exponentially accelerated vertical plate with variable temperature and mass diffusion. Raptis et al. [30] studied the hydromagnetic free convection flow of an optically thin gray gas taking into account the induced magnetic field in the presence of radiation and the analytical solutions were obtained by perturbation technique. Orhan and Ahmad [31] examined MHD mixed convective heat

transfer along a permeable vertical infinite plate in the presence of radiation and solutions are derived using Kellar box scheme and accurate finite-difference scheme. Ahmed [32] investigated the study of influence of thermal radiation and magnetic Prandtl number on the steady MHD heat and mass transfer mixed convection flow of a viscous, incompressible, electrically-conducting Newtonian fluid over a vertical porous plate with induced magnetic field.

When heat and mass transfer occur simultaneously in moving fluid, the relations between the fluxes and the driving potentials are of a more intricate nature. It has been observed that an energy flux can be generated not only by temperature gradients but also by concentration gradients. The energy flux caused by a concentration gradient is termed the diffusion-thermo (Dufour) effect. In most of the studies related to heat and mass transfer process, Soret and Dufour effects are neglected on the basis that they are of a smaller order of magnitude than the effects described by Fourier's and Fick's laws. But these effects are considered as second order phenomena and may become significant in areas such as hydrology, petrology, geosciences, etc. For fluids with medium molecular weight (H_2 , air), Dufour and Soret effects should not be neglected as indicated by Eckert and Drake [17]. Prakash et al. [33] analyzed Diffusion-Thermo and Radiation Effects on Unsteady MHD Flow through Porous Medium Past an Impulsively Started Infinite Vertical Plate with Variable Temperature and Mass Diffusion. To our best knowledge, the interaction between the diffusion-thermo and chemical reaction in the presence of porous medium, heat absorption/generation, thermal radiation, radiation absorption effects has received little attention. Hence, an attempt is made to study the diffusion-thermo effects on an unsteady MHD free convective heat and mass transfer flow of a viscous incompressible electrically conducting fluid through porous medium from a vertical porous plate with varying suction velocity in slip flow regime.

To the best of our knowledge, the interaction between the diffusion-thermo and chemical reaction in the presence of porous medium, heat absorption/generation, thermal radiation, radiation absorption effects has received little attention. Hence, an attempt is made to study the diffusion-thermo effects on an unsteady MHD free convective heat and mass transfer flow of a viscous incompressible electrically conducting fluid through porous medium from a vertical porous plate with varying suction velocity in slip flow regime.

II. MATHEMATICAL FORMULATION

Consider an unsteady two dimensional flow of an incompressible viscous, electrically conducting and heat-absorbing fluid past a semi-infinite vertical permeable plate embedded in a uniform porous medium and subjected to a uniform transverse magnetic field in the presence of thermal and concentration buoyancy effects. The applied magnetic field is also taken as being weak so that Hall and ion slip effects may be neglected. We assume that the Dufour effects may be described by a second-order concentration derivative with respect to the transverse coordinate in the energy equation. Further to

$$\frac{\partial v^*}{\partial y^*} = 0 \quad (1)$$

$$\frac{\partial u^*}{\partial t^*} + v^* \frac{\partial u^*}{\partial y^*} = -\frac{1}{\rho} \frac{\partial p^*}{\partial x^*} + v \frac{\partial^2 u^*}{\partial y^{*2}} - \frac{\sigma B_0^2}{\rho} u^* + g\beta_T(T^* - T_\infty) + g\beta_c(C^* - C_\infty) \quad (2)$$

$$\frac{\partial T^*}{\partial t^*} + v^* \frac{\partial T^*}{\partial y^*} = \frac{K}{\rho C_p} \frac{\partial^2 T^*}{\partial y^{*2}} - \frac{1}{\rho C_p} \frac{\partial q_r^*}{\partial y^*} - \frac{Q_0}{\rho C_p} (T^* - T_\infty) + \frac{Q_1^*}{\rho C_p} (C^* - C_\infty) + \frac{D_m K_T}{C_s \rho C_p} \frac{\partial^2 C^*}{\partial y^{*2}} \quad (3)$$

$$\frac{\partial C^*}{\partial t^*} + v^* \frac{\partial C^*}{\partial y^*} = D \frac{\partial^2 C^*}{\partial y^{*2}} - R(C^* - C_\infty) \quad (4)$$

where x^* , y^* and t^* are the dimensional distances along x^* and y^* directions and dimensional time respectively, u^* and v^* are the components of dimensional velocities along x^* and y^* directions respectively, T^* is the dimensional temperature, C^* is the dimensional concentration, T_w and C_w are the temperature and concentration at the wall, C_∞ and T_∞ are the free stream dimensional concentration and temperature, ρ is the density, ν is kinematic viscosity, C_p is the specific heat at constant pressure, σ is the fluid electrical conductivity, B_0 is the magnetic induction, K^* is the permeability of the porous medium, q_r^* is radiative heat flux, Q_0 is the dimensional heat absorption coefficient, Q_1^* is the coefficient of proportionality for the absorption, R is the chemical reaction, β_T and β_c are the thermal and concentration expansion coefficients, D is the molecular diffusivity, D_m is the coefficient of mass diffusivity, K_T is the thermal diffusion ratio,

$Q_0(T^* - T_\infty)$ is assumed to be the amount of heat generated or absorbed per unit volume and Q_0 is a constant.

The radiative heat flux is considered, which is given by Cogley et al. [22], Pal and Talukdar [6] as

$$\frac{\partial q_r^*}{\partial y^*} = 4(T^* - T_\infty)I' \quad (5)$$

where $I' = \int_0^\infty K_{\lambda w} \frac{\partial e_{b\lambda}}{\partial T^*} d\lambda$, $K_{\lambda w}$ the coefficient of absorption near the wall and $e_{b\lambda}$ is Planck's function.

Under the above stated assumption, the initial and boundary conditions for the velocity distribution involving slip flow, temperature and concentration distributions are defined as:

$$u^* = u_{slip}^* = \frac{\sqrt{k} \partial u^*}{\alpha \partial y^*}, T^* = T_w + \epsilon(T_w - T_\infty)e^{n^* t^*}, \text{ at } y^* = 0 \quad (6)$$

$$C^* = C_w + \epsilon(C_w - C_\infty)e^{n^* t^*}, \text{ at } y^* = 0 \quad (7)$$

$$u^* = U_\infty^* = U_0(1 + \epsilon e^{n^* t^*}), T^* \rightarrow T_\infty,$$

$$C^* \rightarrow C_\infty, \text{ as } y^* \rightarrow \infty \quad (8)$$

From Eq. (1) it is clear that the suction velocity at the plate surface is either constant or a function of time only. Hence, it is assumed that

$$\vartheta^* = -V_0(1 + \epsilon A e^{n^* t^*}) \quad (9)$$

where V_0 is the mean suction velocity and $\epsilon A \ll 1$. The negative sign indicated that the suction velocity is directed towards the plate.

In the free stream Eq.(2) gives

$$-\frac{1}{\rho} \frac{dp^*}{dx^*} = \frac{dU_\infty^*}{dt^*} + \frac{\sigma}{\rho} B_0^2 U_\infty^* \quad (10)$$

On introducing the non-dimensional quantities

$$u = \frac{u^*}{U_0} \vartheta = \frac{\vartheta^*}{V_0}, y = \frac{v_0 y^*}{v}, U_\infty = \frac{U_\infty^*}{U_0},$$

our assumption that there is no applied voltage which implies the absence of an electric field. The plate is maintained at constant temperature T_w and concentration C_w , higher than the ambient temperature T_∞ and concentration C_∞ respectively. The chemical reactions are taking place in the flow and all thermo physical properties are assumed to be constant. Due to the semi-infinite plane surface assumption, the flow variables are functions of y^* and time t^* only. Under the usual boundary layer approximations the governing equations are governed by the following equations.

$$t = \frac{V_0^2 t^*}{v}, \theta = \frac{T^* - T_\infty}{T_w - T_\infty}, C = \frac{C^* - C_\infty}{C_w - C_\infty},$$

$$n = \frac{n^* v}{V_0^2}, Gr = \frac{\rho g v (T_w - T_\infty) \beta_T}{U_0 V_0^2},$$

$$Gm = \frac{\rho g v (C_w - C_\infty) \beta_C}{U_0 V_0^2}, M = \frac{\sigma v B_0^2}{\rho V_0^2},$$

$$Pr = \frac{v C_p}{K}, \phi = \frac{Q_0 v}{\rho V_0^2 C_p}, Q_1 = \frac{Q_1^* v (C_w - C_\infty)}{V_0^2 (T_w - T_\infty)},$$

$$F = \frac{4vI'}{V_0^2 \rho C_p}, Sc = \frac{v}{D}, \gamma = \frac{Rv}{V_0^2},$$

$$Du = \frac{Dm^* k_T (C_w - C_\infty)}{C_s K (T_w - T_\infty)} \quad (11)$$

In view of the above dimensionless variables, the basic field of Eqs. (2) to (4) can be expressed in dimensionless form as

$$\frac{\partial u}{\partial t} - (1 + \epsilon Ae^{nt}) \frac{\partial u}{\partial y} = \frac{dU_\infty}{dt} + M(U_\infty - U) + \frac{\partial^2 u}{\partial y^2} + Gr\theta + GmC, \quad (12)$$

$$\frac{\partial \theta}{\partial t} - (1 + \epsilon Ae^{nt}) \frac{\partial \theta}{\partial y} = \frac{1}{Pr} \frac{\partial^2 \theta}{\partial y^2} - F\theta + Q_1 C - \phi\theta + \frac{Du}{Pr} \left(\frac{\partial^2 C}{\partial y^2} \right) \quad (13)$$

$$\frac{\partial C}{\partial t} - (1 + \epsilon Ae^{nt}) \frac{\partial C}{\partial y} = \frac{1}{Sc} \frac{\partial^2 C}{\partial y^2} - \gamma C \quad (14)$$

The corresponding initial and boundary conditions in equations (6)-(8) in non-dimensional form are given below

$$u = u_{slip} = \phi_1 \frac{\partial u}{\partial y}, \theta = 1 + \epsilon e^{nt},$$

$$C = 1 + \epsilon e^{nt} \text{ at } y = 0 \quad (15)$$

$$U \rightarrow U_\infty = (1 + \epsilon e^{nt}), \theta \rightarrow 0, C \rightarrow 0$$

$$as y \rightarrow \infty \quad (16)$$

III. METHOD OF SOLUTION

The equations (12) to (14) are coupled non-linear partial differential equations whose solutions in closed-form are difficult to obtain. To solve these coupled non-linear partial differential equations, we assume that the unsteady flow is superimposed on the mean steady flow, so that in the neighbourhood of the plate, we have

$$u = f_0(y) + \epsilon e^{nt} f_1(y) + O(\epsilon^2) \quad (17)$$

$$\theta = g_0(y) + \epsilon e^{nt} g_1(y) + O(\epsilon^2) \quad (18)$$

$$C = h_0(y) + \epsilon e^{nt} h_1(y) + O(\epsilon^2) \quad (19)$$

By substituting the set of Eqs. (17)-(19) into Eqs.(12)-(14) and equating the harmonic and non-harmonic terms, and neglecting the higher order terms in ϵ , we obtain

$$f_0'' + f_0' - M_1 f_0 = -M_1 - Gr g_0 - Gm h_0 \quad (20)$$

$$f_1'' + f_1' - M f_1 = -(M + n) - A f_0' - Gr g_1 - Gm h_1 \quad (21)$$

$$g_0'' + Pr g_0' - Pr(F + \phi) g_0 = -Pr Q_1 h_0 - Duh_0'' \quad (22)$$

$$g_1'' + Pr g_1' - Pr(F + \phi + n) g_1 = -Pr Q_1 h_1 - Duh_1'' - Pr A g_0' \quad (23)$$

$$h_0'' + Sch_0' - Sc \gamma h_0 = 0 \quad (24)$$

$$h_1'' + Sch_1' - Sc(\gamma + n) h_1 = -ASch_0' \quad (25)$$

where the prime denotes the differentiation with respect to y . Now the corresponding boundary conditions are

$$f_0 = \phi_1 f_0', f_1 = \phi_1 f_1', g_0 = 1,$$

$$g_1 = 1, h_0 = 1, h_1 = 1 \quad \text{at } y = 0 \quad (26)$$

$$f_0 = 1, f_1 = 1, g_0 \rightarrow 0, g_1 \rightarrow 0, h_0 \rightarrow 0,$$

$$h_1 \rightarrow 0, \text{ as } y \rightarrow \infty \quad (27)$$

By solving the set of Eqs.(20)- (25) with the help of boundary conditions (26)-(27), the following set of solutions are obtained

$$f_0 = 1 + B_4 e^{-m_4 y} - A_3 e^{-m_2 y} - A_2 e^{-P_1 y} \quad (28)$$

$$f_1 = 1 + B_5 e^{-m_3 y} + A_4 e^{-m_6 y} - A_{10} e^{-m_2 y} - B_1 e^{-P_1 y} - B_2 e^{-m_5 y} - B_3 e^{-m_4 y} \quad (29)$$

$$g_0 = (1 - A_1) e^{-m_2 y} + A_1 e^{-P_1 y} \quad (30)$$

$$g_1 = A_9 e^{-m_5 y} + A_6 e^{-P_1 y} + A_7 e^{-m_2 y} + A_8 e^{-m_4 y} \quad (31)$$

$$h_0 = e^{-P_1 y} \quad (32)$$

$$h_1 = (1 - A_5) e^{-m_4 y} + A_5 e^{-P_1 y} \quad (33)$$

$$u(y, t) = 1 + B_4 e^{-m_6 y} - A_3 e^{-m_2 y} - A_2 e^{-P_1 y} + \epsilon e^{nt} (1 + B_5 e^{-m_3 y} + A_4 e^{-m_6 y} - A_{10} e^{-m_2 y} - B_1 e^{-P_1 y} - B_2 e^{-m_5 y} - B_3 e^{-m_4 y}) \quad (34)$$

$$\theta(y, t) = (1 - A_1) e^{-m_2 y} + A_1 e^{-P_1 y} + \epsilon e^{nt} (A_9 e^{-m_5 y} + A_6 e^{-P_1 y} + A_7 e^{-m_2 y} + A_8 e^{-m_4 y}) \quad (35)$$

$$C(y, t) = e^{-P_1 y} + \epsilon e^{nt} ((1 - A_5) e^{-m_4 y} + A_5 e^{-P_1 y}) \quad (36)$$

The coefficient of Skin-friction, the rate of heat transfer in terms of Nusselt number and the rate of mass transfer are the important physical parameters for this kind of boundary layer flow. Hence these quantities are defined and derived as follows:

$$C_{fx} = \frac{\tau_w}{\rho u_0 v_0} = \left(\frac{\partial u}{\partial y} \right)_{at y=0} = -B_4 m_6 + A_3 m_2 + A_2 P_1 + \epsilon e^{nt} (-B_5 m_3 - A_4 m_6 + A_{10} m_2 + B_1 P_1 + B_2 m_5 + B_3 m_4) \quad (37)$$

$$Nu_x = x \frac{\left(\frac{\partial T}{\partial y^*} \right)_{at y=0}}{(T_w - T_\infty)} \Rightarrow Nu_x / Re_x = \left(\frac{\partial \theta}{\partial y} \right)_{at y=0} = (-m_2 (1 - A_1) - A_1 P_1) + \epsilon e^{nt} (-m_5 A_9 - P_1 A_6 - m_2 A_7 - m_4 A_8) \quad (38)$$

$$Sh_x = x \frac{\left(\frac{\partial C}{\partial y^*} \right)_{at y=0}}{(C_w - C_\infty)},$$

$$Sh_x / Re_x = \left(\frac{\partial C}{\partial y} \right)_{at y=0}$$

$$= -P_1 + \epsilon e^{nt} (-m_4 (1 - A_5) - A_5 P_1) \quad (39)$$

Where $Re_x = \frac{V_0 x}{\nu}$ is the local Reynolds number.

IV. RESULTS AND DISCUSSION

The analytical solutions are performed for concentration, temperature and velocity for various values of fluid flow parameters such as Schmidt number Sc , chemical reaction parameter γ , Dufour number Du Magnetic field parameter M , Heat absorption parameter ϕ , Radiation

absorption parameter Q_1 , Radiation parameter F , Porous permeability parameter ϕ_1 , Solutal Grashof number Gr , mass Grashof num Gm are presented in figures 1-15. Throughout the calculations the parametric values are chosen as $Pr = 0.71, A = 0.5, \epsilon = 0.02, n = 0.1, t = 1$.

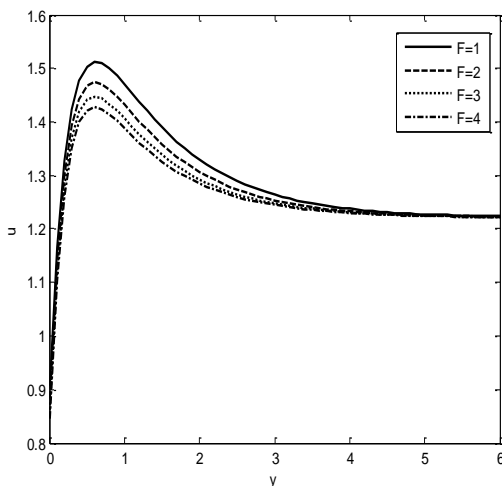


Fig.1: Velocity Profiles for various values of F

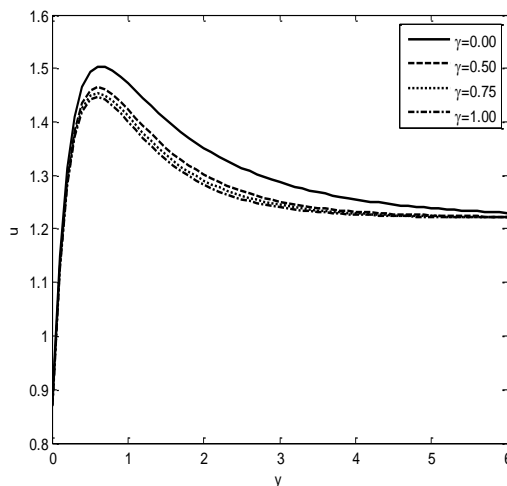


Fig.2: $Sc = 0.6, Gr = 4.0, Gm = 2.0, Q_1 = 2.0, \phi =$

with, $Gr = 4.0, Sc = 0.6, Gm = 2.0, Q_1 = 2.0, \phi = 1, M = 2.0, Du = 0.5, \phi_1 = 0.3, \gamma = 0.5.$

$1, M = 2.0, Du = 0.3, \phi_1 = 0.3, F = 2.0.$

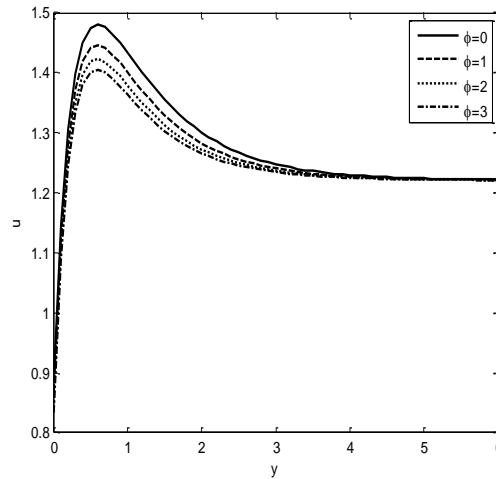
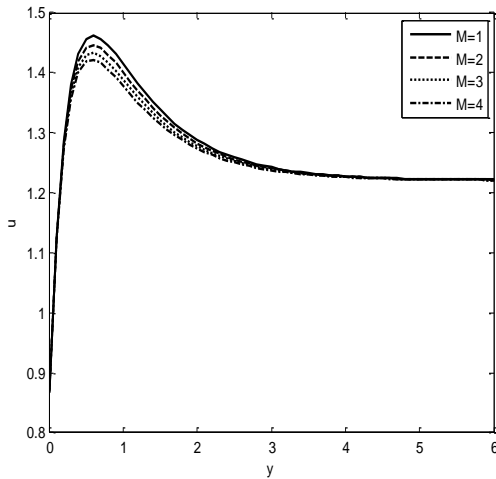


Fig.3: .Velocity profiles for various values of M with, $Sc = 0.6, Gr = 4.0, Gm = 2.0, Q_1 = 2.0, \phi = 1.0, Du = 0.3, \phi_1 = 0.3, F = 2.0, \gamma = 1.$

Fig.4: Velocity profiles for various values of ϕ with $Sc = 0.6, Gr = 4.0, Gm = 2.0, Q_1 = 2.0, Du = 0.3, \phi_1 = 0.3, F = 2.0, \gamma = 1, M = 2.$

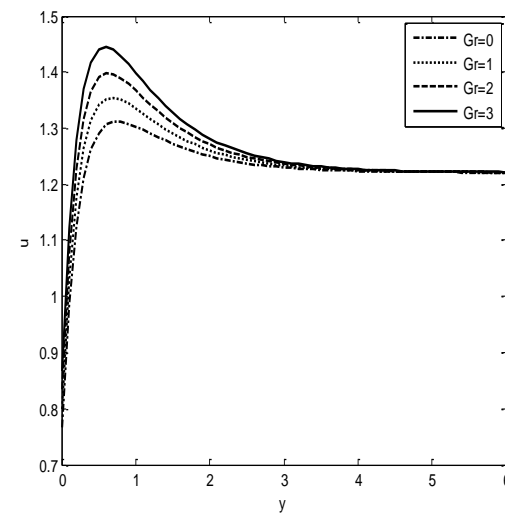
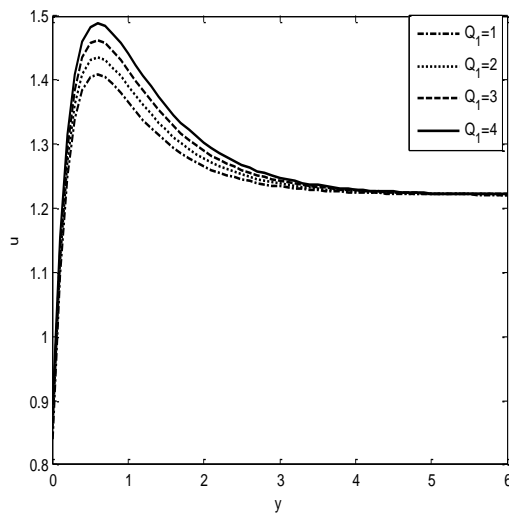


Fig.5: Velocity profiles for various values of Q_1 with $Sc = 0.6, Gr = 4.0, Gm = 2.0, M = 2.0, Du = 0.1, \phi_1 = 0.3, F = 2.0, \gamma = 1, \phi = 1.0.$

Fig.6: Velocity profiles for various values of Gr with $Sc = 0.6, Gm = 3.0, M = 2.0, Q_1 = 2.0, Du = 0.3, \phi_1 = 0.3, F = 2.0, \gamma = 1, \phi = 1.0$

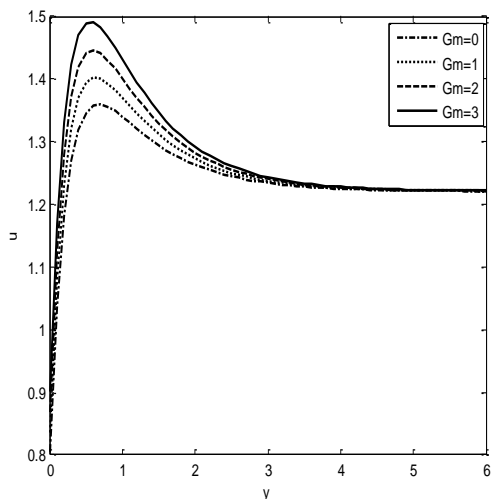


Fig.7: Velocity profiles for various values of Gm with $Sc = 0.6$, $Gr = 4.0$, $M = 2.0$, $Q_1 = 2.0$, $Du = 0.3$, $\phi_1 = 0.3$, $F = 2.0$, $\gamma = 1$, $\phi = 1.0$.

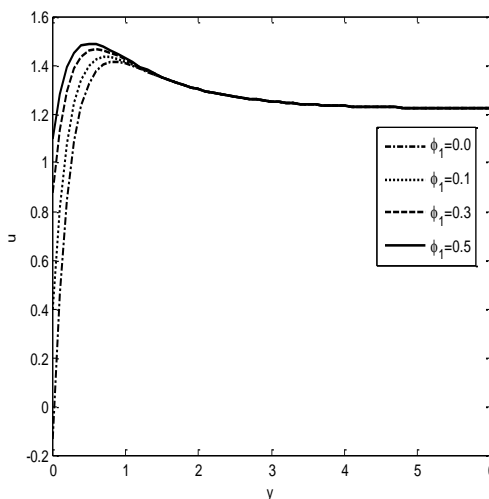


Fig.8: Velocity profiles for various values of ϕ_1 with $Sc = 0.6$, $Gr = 4.0$, $Gm = 3.0$, $M = 2.0$, $Q_1 = 2.0$, $Du = 0.3$, $F = 2.0$, $\gamma = 0.5$, $\phi = 1.0$.

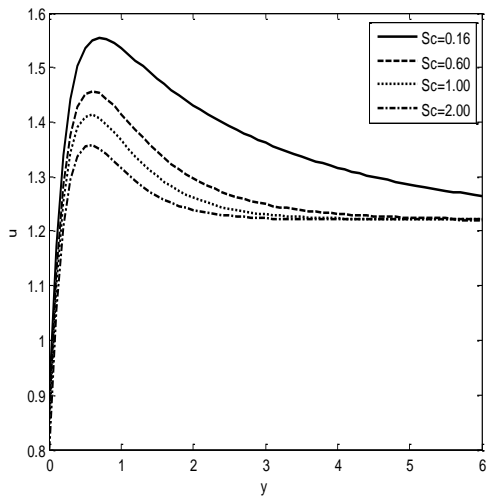


Fig.9: Velocity profiles for various values of Sc with $Gr = 2.0$, $Gm = 2.0$, $M = 2.0$, $Q_1 = 2.0$, $Du = 0.1$, $\phi_1 = 0.3$, $F = 2.0$, $\gamma = 0.5$, $\phi = 1.0$.

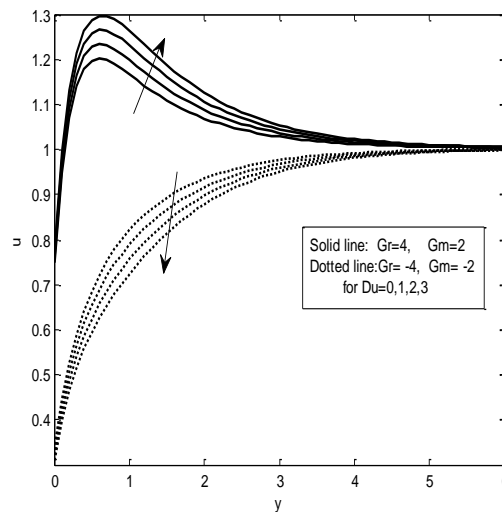


Fig.10: Velocity profiles for various values Du with $Sc = 0.6$, $Q_1 = 2.0$, $Du = 0.5$, $\phi_1 = 0.3$, $F = 2.0$, $\phi = 1.0$, $\gamma = 0.5$, $M = 2.0$.

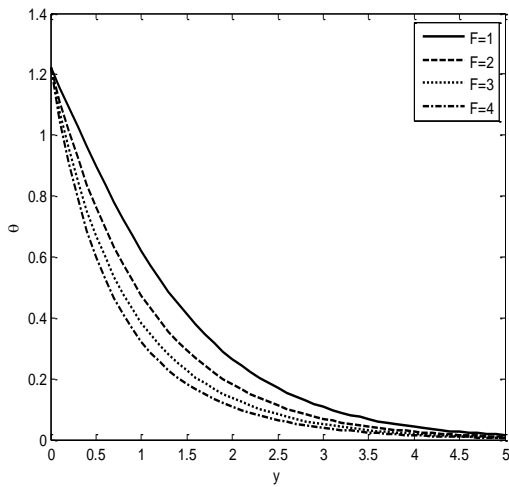


Fig.11: Temperature profiles for various values of F with $Sc = 0.6, Gr = 4.0, Gm = 3.0, M = 2.0, Q_1 = 2.0, Du = 0.5, \phi_1 = 0.3, \phi = 1.0$.

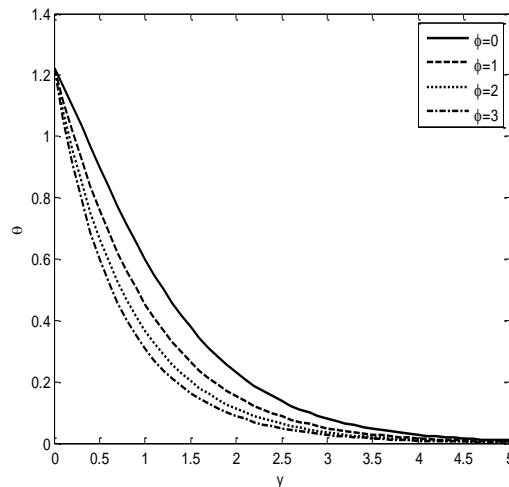


Fig.12: Temperature profiles for various values of ϕ with $Sc = 0.6, Gr = 4.0, Gm = 3.0, M = 2.0, Q_1 = 2.0, Du = 0.5, \phi_1 = 0.3, F = 2.0, \gamma = 1.0$.

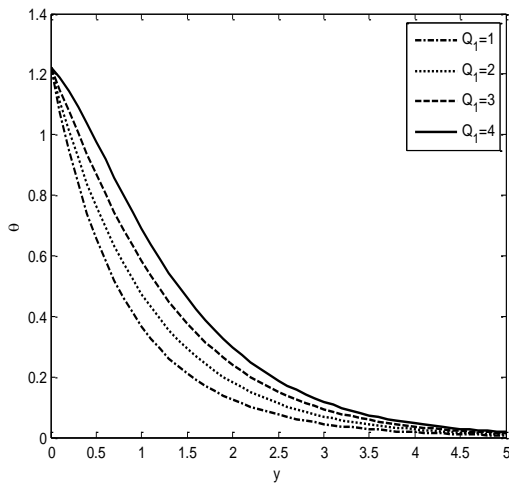


Fig.13: Temperature profiles for various values of Q_1 with $Sc = 0.6, Gr = 4.0, Gm = 3.0, M = 2.0, Du = 0.5, F = 2.0, \phi = 1.0, \gamma = 0.5$.

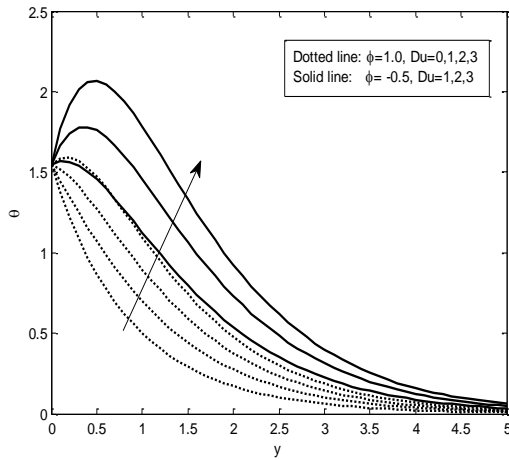


Fig. 14: Temperature profiles for various Du with $Sc = 0.6, Q_1 = 2.0, F = 2.0, \gamma = 0.5$.

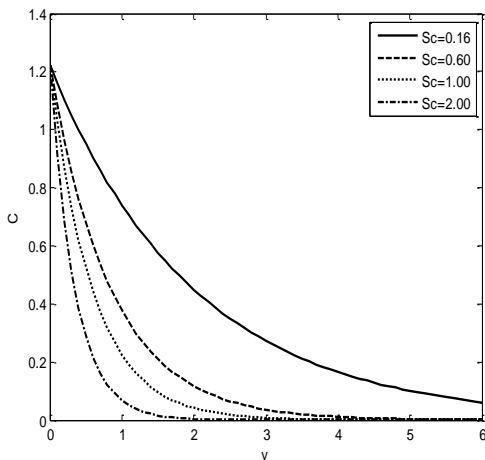


Fig.15: Concentration profiles for various values of Sc with $\gamma = 0.5$.

Table.1: Comparison of present results with those of Kim [23] & Pal and Talukdar [6] with different values of C_{fx} ,

$$Nu_x/Re_x$$

Kim[23] ($G = 2, K = \infty, U_p = 0$)	Pal and Talukdar [6] ($Gr = 2, \phi = 0, \phi_1 = 0, F = 0,$ $Q_1 = 0, Gm = 0$)	Present Results $Gr = 2, \phi = 0, \phi_1 = 0,$ $F = 0, Q_1 = 0, Gm = 0, Du = 0$
$M \quad C_{fx} \quad Nu_x/Re_x$	$M \quad C_{fx} \quad Nu_x/Re_x$	$M \quad C_{fx} \quad Nu_x/Re_x$
0 4.5383 -0.9430	0 4.5383 -0.9430	0 4.5383 -0.9430
2 3.9234 -0.9430	2 3.9234 -0.9430	2 3.9234 -0.9430
5 4.4457 -0.9430	5 4.4457 -0.9430	5 4.4457 -0.9430
10 5.2976 -0.9430	10 5.2976 -0.9430	10 5.2976 -0.9430

Table: 2: Comparison of present results with those of Pal and Talukdar [6] with different values of C_{fx} , Nu_x/Re_x ($F =$

$\gamma \quad C_{fx} \quad Nu_x/Re_x \quad Sh_x/Re_x$ (Pal and Talukdar [6])	$C_{fx} \quad Nu_x/Re_x \quad Sh_x/Re_x$ (Present results)
---	---

$2, \phi = 1, M = 2, Q_1 = 2, Gr = 4, Gm = 2, Sc = 0.6, \phi_1 = 0.3, Du = 0.0$)

0.0	4.0441	-1.3400	-0.8098	4.0442	-1.3400	-0.8098
0.50	3.7512	-1.4825	-1.1864	3.7513	-1.4825	-1.1864
0.75	3.6744	-1.5226	-1.3178	3.6744	-1.5227	-1.3178
1.00	3.6149	-1.5546	-1.4325	3.6149	-1.5546	-1.4326

Table.3: Effects of ϕ_1 ($F = 2$) and F ($\phi_1 = 0.3$) for fixed values of $Gr = 4, Gm = 2, Sc = 0.6, M = 2, \phi = 1, Q_1 = 2, \gamma = 0.1, Du = 0.5$

$\phi_1 C_{fx}$	$F C_{fx} Nu_x / Re_x$
0.0	6.2727
0.1	4.9698
0.3	3.5111
0.5	2.7143
1.0	3.6557
2.0	3.5111
3.0	3.4129
4.0	3.3400

The effect of radiation parameter F is shown in fig.1. It is observed in this figure that velocity profiles decrease with an increase in the radiation parameter F . It is clear that, the increase of the radiation parameter leads to decrease the momentum boundary layer thickness and reduces the heat transfer rate in the presence of thermal and solutal buoyancy forces. Fig.2 illustrates the effect of chemical reaction parameter γ . It is clear that at first the velocity increases and later on decreases uniformly with the increasing values of γ . It is interesting to observe that the peak values of the velocity profiles attain near the porous boundary surface. The velocity profiles for different values of magnetic parameter M are depicted in fig.3. From this figure it is clear that as the magnetic field parameter increases, the Lorentz force, which opposes the fluid flow also increases and leads to an enhance deceleration of the flow. This result qualitatively agrees with the expectations since the magnetic field exerts retarding force on the free convection flow. Fig.4 represents the fluid velocity decreases as the heat absorption parameter ϕ increases and hence momentum boundary layer thickness decrease. Figs. 5 and 13 display the effects of the radiation absorption parameter Q_1 on velocity and temperature fields. It is obvious from the figures that an increase in the absorption radiation parameter Q_1 results an increase in the velocity and temperature profiles within the boundary layer as well as an increase in the momentum and thermal thickness. This is because the large values of Q_1

correspond to an increased domination of conduction over absorption radiation, thereby increasing buoyancy force and thickness of the thermal and momentum boundary layer. From fig.5, it is clear that the velocity starts from minimum value of zero at the surface and increases till attains the peak value. For different values of the thermal buoyancy force parameter Gr and solutal buoyancy force parameter Gm are plotted in figs. 6 and 7. As seen from figures that maximum peak value is attained and minimum peak value is observed in the absence of buoyancy force. This is due to fact that buoyancy force enhances fluid velocity and increases the layer thickness with increase in the value of Gr or Gm . Fig.8 illustrates the variation of velocity distribution across the boundary layer for various values of the slip parameter ϕ_1 . It is observed that the velocity increases near the source and reaches the free stream condition. The permeability ϕ_1 is directly proportional to square root of the actual permeability K . Hence, an increase in ϕ_1 will decrease the resistance of the porous medium which will tend to accelerate the flow and increase the velocity.

The influence of Schmidt number Sc on the velocity profiles are shown in fig.9. We observe in fig.9 that at very low values of Schmidt number (e.g., $Sc = 0.16$), there is an increase in the peak velocity near the plate ($y \approx 1$). Whereas for higher values of Schmidt number, the peak shifts closer to the plate. Further it is

observed that the momentum boundary layer decreases with an increase in the value of Sc .

The temperature profiles for different values of the radiation parameter F are shown in fig.11. It is observed that an increase in the radiation parameter F results a decrease of the thermal boundary layer thickness. Further it is observed from that, the temperature is very high at the porous boundary and asymptotically decreases to zero as $y \rightarrow \infty$. Fig.12 depicts the variations in temperature profile against spanwise co-ordinate y for different values of heat absorption parameter ϕ . From this figure, it is clearly understood that heat absorption parameter condenses the thickness of the temperature boundary layer because when heat is absorbed, the buoyancy force decreases the temperature. The effect of Schmidt number Sc on the species concentration profiles is shown in fig.15. It is clear that the concentration decreases exponentially and attains free stream condition. Also it is noticed that the concentration boundary layer thickness decreases with Sc .

The temperature profiles for different values of Dufour number in heat absorption ($\phi > 0$) and heat generation ($\phi < 0$) cases are shown in fig.14. It can be seen that the fluid temperature increases with Dufour number in both the cases. Thermal boundary layer thickness is higher in the case of heat absorption than that in the case of heat generation. Physically, the Dufour term that appears in the temperature equation measures the contribution of concentration gradient to thermal energy flux in the flow domain. It has a vital role in enhancing the flow velocity and the ability to increase the thermal energy in the boundary layer. As a result, the temperature profile at all time stages increases with the increase in Du .

Fig.10 displays the velocity profiles for various values Dufour number in the cases of cooling and heating of the plate. The velocity increases with Dufour number in the case of heating of the plate and opposite trend is observed in the case of cooling of the plate.

From Table.1 and Table.2, it is observed that the skin friction at the plate decreases with increasing chemical reaction parameter γ or Magnetic parameter M . It is also noticed that the Nusselt number and Sherwood number decreases with increase in γ .

The influence of slip parameter ϕ_1 on skin-friction, and radiation parameter F on skin-friction and Nusselt number

are presented in Table. 3. It is observed that the skin friction at the plate decreases with increasing ϕ_1 or F . As the radiation parameter increases the heat is transferred from the plate to the fluid.

V. COMPARISON OF RESULTS

In order to examine the accuracy of the results of the present study, it is considered that the analytical solutions obtained by Kim [23], Pal and Talukdar [6] who computed the numerical results

for skin friction coefficient and Nusselt number. These computed and compared results are presented in Table.1. From this table it is interesting to observe that the present results in the absence of Diffusion-thermo effect and Porous medium are in good agreement with the corresponding results obtained from Pal and Talukdar [6]. It is also observed that the present results are in good agreement with those of Kim [23] when $G = 2, u_p = 0, Du = 0, Gm = 0$. Also from Table. 2, it is clear that the present results for skin-friction, Nusselt number and Sherwood number for different values of chemical reaction in the absence of porous medium and diffusion thermo effect are in good agreement with the corresponding results of Pal and Talukdar [6], which clearly shows the correctness of our present analytical solutions and computed results.

VI. CONCLUSIONS

In this paper we have studied the Dufour effect on an unsteady MHD convective heat and mass transfer flow through a high porous medium over a vertical porous plate. From the present study the following conclusions can be drawn.

1. The diffusion-thermo parameter increases the thermal and momentum boundary layer thickness.
2. The fluid velocity increases with an increasing values of slip parameter ϕ_1 .
3. The skin friction at the plate increases with an increasing values of Du .
4. The rate of heat transfer coefficient at the plate (Nu_x) increase with Dufour number while it is decreases as chemical reaction parameter (γ) or Radiation parameter (F) increases.

Appendix

$$P_1 = \frac{Sc + \sqrt{(Sc^2 + 4Sc\gamma)}}{2}, \quad m_2 = \frac{Pr + \sqrt{Pr^2 + 4(F + \phi)Pr}}{2}, \quad m_3 = \frac{1 + \sqrt{4(M_1 + n)}}{2},$$

$$m_4 = \frac{Sc + \sqrt{Sc^2 + 4Sc(\gamma + n)}}{2}, m_5 = \frac{Pr + \sqrt{Pr^2 + 4Pr(F + \phi + n)}}{2}, m_6 = \frac{1 + \sqrt{1 + 4M_1}}{2}, A_1 = \frac{(-PrQ_1 - DuP_1^2)}{(P_1^2 - PrP_1 - (F + \phi)Pr)}$$

$$A_2 = \frac{(GrA_1 + Gm)}{(P_1^2 - P_1 - M_1)}, A_3 = \frac{Gr(1 - A_1)}{(m_2^2 - m_2 - M_1)}, A_4 = \frac{Am_6B_4}{(m_6^2 - m_6 - (M_1 + n))}, A_5 = \frac{AScP_1}{(P_1^2 - P_1Sc - Sc(\gamma + n))}$$

$$A_6 = \frac{(-PrQ_1A_5 - DuA_5P_1^2 + PrP_1AA_1)}{(P_1^2 - PrP_1 - Pr(F + \phi + n))}, A_7 = \frac{(PrAm_2 - PrAA_1m_2)}{(m_2^2 - m_2Pr - Pr(F + \phi + n))}, A_8 = \frac{(-PrQ_1 + PrA_5Q_1 - Dum_4^2 + DuA_5m_4^2)}{(m_4^2 - m_4Pr - Pr(F + \phi + n))}$$

$$A_9 = 1 - (A_6 + A_7 + A_8), A_{10} = \frac{AA_3m_2 + GrA_7}{(m_2^2 - m_2 - (M_1 + n))}, B_1 = \frac{AA_2P_1 + GrA_6 + GmA_5}{P_1^2 - P_1 - (M_1 + n)}, B_2 = \frac{GrA_9}{m_5^2 - m_5 - (M_1 + n)}$$

$$B_3 = \frac{GrA_8 + Gm(1 - A_5)}{m_4^2 - m_4 - (M_1 + n)}, B_4 = \frac{(-1 + A_2 + A_3 + A_2\phi_1P_1 + A_3\phi_1m_2)}{(1 + \phi_1m_6)}, B_5 = \frac{-(1 + A_4 - A_{10} - B_1 - B_2 - B_3)}{(1 + \phi_1m_3)} + b_1,$$

$$b_1 = \frac{\phi_1(-A_4m_6 + A_{10}m_2 + B_1P_1 + B_2m_5 + B_3m_4)}{(1 + \phi_1m_3)}$$

REFERENCES

- [1] R.S.Rath, and D.N.Parida, "Magnetohydrodynamic free convection in the boundary layer due to oscillation in the wall temperature", *Wear*, Vol.78, No.1, pp.305-314, (1982).
- [2] A.Raptis, G.Tzivanidis, and N.Kafusias, "Free convection and mass transfer flow through a porous medium bounded by an infinite vertical limiting surface with constant suction", *Letters in Heat and Mass Transfer*, Vol.8, No.1, pp.417-424, (1981).
- [3] B. K.Jha, and R.Prasad, "MHD free-convection and mass transfer flow through a porous medium with heat source", *Astrophysics and Space Science*, Vol.18, No.1, pp.117-123, (1991).
- [4] K.Yamamoto, and N.Iwamura, "Flow with convective acceleration through a porous Medium", *J.Eng.Math*, Vol.10, No.1, pp.41-54, (1976).
- [5] B. Gebhart, and L. Pera, "The nature of vertical natural convection flows resulting from the combined buoyancy effects of thermal and mass diffusion", *Int. J. Heat and Mass Transfer*, Vol.14, No.12, pp.2025-2050, (1971).
- [6] D. Paland B. Talukdar, "Perturbation Analysis of unsteady magnetohydrodynamic convective heat and mass transfer in a boundary layer slip flow past a vertical permeable plate with thermal radiation and chemical reaction", *Commun Nonlinear Sci Number Simulant*, Vol.15, No.7, pp.1813-1830, (2010).
- [7] D.Nield and A. Bejan, "Convection in porous media", 2nd edition Springer, Wiley, New York, pp.62-75, (1995).
- [8] P. Cheng, "Heat transfer in geothermal system", *Adv Heat Transfer*, Vol.4, No.1, pp.1-105, (1978).
- [9] N. Rudraiah, "Flow through and past porous media", *Encyclopedia of Fluid Mechanics*, Gulf Publ. Vol.5, pp.567-647, (1986).
- [10] N.Rudraiah, D.Pal, and I.N.Shivakumara, "Effect of slip and magnetic field on composite systems", *Fluid Dyn. Res.*, Vol.4, No.4, pp.255-270, (1988).
- [11] A. Apelblat, "Mass transfer with a chemical reaction of the first order: Analytical Solutions", *The Chemical Engineering Journal* Vol.19, No.1, pp.19-37, (1980).
- [12] U.N.Das, R.K.Deka and V.M.Soundalgekar, "Effects of Mass transfer on flow past an impulsively started infinite vertical plate with constant heat flux and chemical reaction", *Forschung im Ingenieurwesen*, Vol.60, No.10, pp.284-287, (1994).
- [13] P.L.Chambre and J. D. Young, "On the diffusion of a chemically reactive species in a laminar boundary layer flow", *The Physics of Fluids*, Vol.1, pp.48-54, (1958).
- [14] W.G. England, and A.F. Emery, "Thermal radiation effects on the laminar free convection boundary layer of an absorbing gas", *Journal of Heat Trans*, Vol.91, No.1, pp.37-44, (1969).
- [15] V.M.Soundalgekar, and H.S. Takhar, "Radiation effects on free convection flow past a semi-vertical plate", *Modeling Measurement and Control*, Vol.51, pp.31-40, (1993).
- [16] A. Raptis, and C.Peridikis, "Radiation and free convection flow past a moving plate", *International Journal of Applied*

- Mechanics and Engineering*, Vol.4, No.4, pp.817-821, (1999).
- [17] E.R.G. Eckert, and R.M. Drake, "Analysis of Heat and Mass Transfer", *M.C. Graw-Hill*, New-York, (1972).
- [18] F.S. Ibrahim, A.M. Elaiw and A.A. Bakr, "Effects of the chemical reaction and radiation absorption on the unsteady MHD free convection flow past a semi-infinite vertical permeable moving plate with heat source and suction", *Communications in Nonlinear Science and Numerical Simulation*, Vol. 13, No. 6, pp.1056-1066, (2008).
- [19] Z. Dursunkaya, and W.M. Worek, "Diffusion-thermo and thermal-diffusion effects in transient and steady natural convection from vertical surface", *International Journal of Heat and Mass Transfer*, Vol.35, No.8, pp.2060-2065, (1992).
- [20] M. Anghel, H.S. Takhar and I. Pop, "Dufour and Soret effects on free convection boundary layer over a vertical surface embedded in a porous medium", *Studia Universitatis Babeş-Bolyai, Mathematica* Vol.45, No.4, pp.11-21, (2000).
- [21] A. Postelnicu, "Influence of a magnetic field on heat and mass transfer by natural convection from vertical surfaces in porous media considering Soret and Dufour effects", *International Journal of Heat and Mass Transfer*, Vol.47, No.6, pp.1467-1472, (2004).
- [22] A.C. Cogley, W.G. Vincent and S. E. Giles, "Differential approximation to radiative heat transfer in a non-grey gas near equilibrium", *American Institute of Aeronautics and Astronautics*, Vol.6, No.3, pp.551-553, (1968).
- [23] Y.J. Kim, "Unsteady MHD convective heat transfer past a semi-infinite vertical moving plate with variable suction", *International Journal of Engineering Sciences*, Vol.38, No.8, pp.833-845, (2000).
- [24] A.J. Chamkha, "Unsteady MHD convective heat and mass transfer past a semi-infinite vertical permeable moving plate with heat absorption", *International Journal of Engineering Sciences*, Vol.42, No.2, pp.217-230, (2004).
- [25] A.J. Chamkha, "MHD flow of a uniformly stretched vertical permeable surface in the presence of heat generation/absorption and a chemical reaction", *Int. Comm. Heat Mass Transfer*, Vol.30, No.3, pp.413-422, (2003).
- [26] R.A. Mohamed, "Double-diffusive convection radiation interaction on unsteady MHD flow over a vertical moving porous plate with heat generation and Soret effects", *Appl. Math. Sci.*, Vol.3, No.13, pp.629-651, (2009).
- [27] R. Muthucumaraswamy and B. Janakiraman, "MHD and radiation effects on moving isothermal vertical plate with variable mass diffusion", *Theo. Appl. Mech.*, Vol.33, No.1, pp.17-29, (2006).
- [28] V. Rajesh and S.V.K. Varma, "Thermal diffusion and radiation effects on MHD flow past an impulsively started infinite vertical plate with variable temperature and mass diffusion", *JP J. Heat and Mass Transfer*, Vol.3, No.1, pp.17-39, (2009).
- [29] A. G. Vijaya Kumar and S.V.K. Varma, "Thermal radiation and mass transfer effect on MHD flow past an impulsively started exponentially accelerated vertical plate with variable temperature and mass diffusion", *Far East J. Appl. Math.*, Vol.55, No.2, pp.93-115, (2011).
- [30] R.A. Raptis, C. Perdikis and A. Leontitsis, "Effects of radiation in an optically thin gray gas flowing past a vertical infinite plate in the presence of magnetic field", *Heat and Mass Transfer*, Vol.39, pp.771-773, (2003).
- [31] A. Orhan and K. Ahmad, "Radiation effect on MHD mixed convection flow about a permeable vertical plate", *Heat and Mass Transfer*, Vol.45, No.2, pp.239-246, (2008).
- [32] S. Ahmad, "Inclined magnetic field with radiating fluid over a porous vertical plate: Analytical study", *Journal Naval Arch. Marine Engineering*, Vol.7, No.2, pp.61-72, (2010).
- [33] J. Prakash, D. Bhanumathi, A.G. Vijaya Kumar "Radiation effects on unsteady MHD flow through porous medium past an impulsively started infinite vertical plate with variable temperature and mass diffusion", *Trans. Porous Med.* Vol.96, No.1, pp.135-151, (2013).

Segmentation of Unstructured Newspaper Documents

Santosh Naik¹, R. Dinesh², Prabhanjan S.³

¹Research Scholar, Department of Computer Science and Engineering, School of Engineering and Technology, Jain University, Bangalore, India

²Research Supervisor, Department of Computer Science and Engineering School of Engineering and Technology, Jain University, Bangalore, India

³Research Scholar, Department of Computer Science and Engineering, School of Engineering and Technology, Jain University, Bangalore, India

Abstract— Document layout analysis is one of the important steps in automated document recognition systems. In Document layout analysis, meaningful information is retrieved from document images by identifying, categorizing and labeling the semantics of text blocks from the document images. In this paper, we present simple top-down approach for document page segmentation. We have tested the proposed method on unstructured documents like newspaper which is having complex structures having no fixed structure. Newspaper also has multiple titles and multiple columns. In the proposed method, white gap area which separates titles, columns of text, line of text and words in lines have been identified to separate document into various segments. The proposed algorithm has been successfully implemented and applied over a large number of Indian newspapers and the results have been evaluated by number of blocks detected and taking their correct ordering information into account.

Keywords— Document Layout Analysis, data extraction, document page segmentation, unstructured document.

I. INTRODUCTION

Document image segmentation is an important step in a document understanding system. The main aim of a page segmentation process is to separate a document image into its regions such as text, tables, images, drawings and headings. There are three different methods for page segmentation and layout analysis viz., a) Top-down, b) Bottom-up and c) Hybrid methods [11]. Top-down method start by detecting the highest level of structures such as columns and graphics, and proceed by successive splitting until they reach the bottom layer for small scale features like individual characters. In top-down methods, a priori knowledge about the page layout is necessary. Bottom-up

methods start with the smallest elements such as pixels, merging them recursively in connected components or regions of characters and words, and then in larger structures such as columns. They are more flexible but errors are accumulated in every iteration. It makes use of methods like connected component analysis [12], run-length smoothing [13], region-growing methods [14], and neural networks [15]. Most of these methods are computationally expensive. Many other methods are there that do not fit into top-down and bottom-up categories and therefore are called hybrid methods. Among these methods are texture-based [16] and Gabor filter [17]. Some work has done based on pyramid segmentation.

II. LITERATURE REVIEW

In the method [2] for segmentation and classification of digital documents using run length smearing approach. A linear adaptive classification scheme used to discriminates text regions from others. [3] proposed X-Y cut page segmentation approach based on top down approach. In this method entire document is considered as root and respective decomposed rectangular regions as leaf nodes. Horizontal and vertical projection profiles of foreground pixels are used for decomposition. [4] Proposed a method for segmentation of document using white space analysis method. In [4] segmentation technique is independent of any threshold values in proposed method. In these method white spaces runs greater than one fifth of the page are identified in both horizontal and vertical directions. Thinning algorithm is used for thinning of lines. In this way a mesh is formed by combining lines in both horizontal and vertical directions. [5, 6] proposed bottom-up approaches for page segmentation and block identification. The method [7] uses edge information to extract textual blocks

from gray scale document images. The method detects only textual regions on heavy noise infected newspaper images and separate them from graphical regions. [8] Developed a new approach for page segmentation and classification based on white tiles. In this method, white tiles of each region have been collected together and their total area is estimated, and regions are classified as text or images. The method in [9] starts from pixel level information and finds k-nearest neighborhood pixels and start converging them. In this method, Document Image Segmented using dynamic thresholds and identification of thresholds are based on properties of distance and angle of each connected components with k-nearest neighbors. [10] proposed X-Y tree method which segments a document in multiple steps into a tree structure consisting nested rectangular blocks. In this method document is segmented into big blocks through horizontal or vertical cuts and then the same process proceeds in each one of the sub-blocks. The characteristic of the method is that its tree structure that suggests a logical order of the document. To reduce the computing cost modified methods were proposed.

From the above discussion, it is evident that there are many methods proposed in the literature to address the problem of document layout analysis. However, very few methods can be found in the literature for the analysis and segmentation of unstructured document images. Hence, in this paper, we propose a new method of segmenting unstructured document image. The proposed method, segment images occurring in a document and then we separate the headings in the document. After this we separate the columns and finally divide the text into paragraphs, lines and then words. Rest of the paper is organized as follows: Section 3 presents the proposed method. In section 4, we present the results of the proposed method and finally, conclusions are drawn in section 5.

III. PROPOSED METHOD

In this section, we present the details of the proposed method which address the problem of segmenting the unstructured document image. The method follows the top-down approach, by initially considering the complete document and trying to recursively extract text blocks from it in hierarchical way.

Our method can be categorized into the following categories

- Binarization of input image.
- Headline Segmentation.
- separating the columns

- separating the images and lines from the columns.
- Finally separating the words from the paragraphs

We discuss the above steps in detail in the following sections.

3.1 Binarization:

Scanned news paper document may be colored or grayscale image that needs to be converted to binary image to reduce the computational cost and helps to utilize simplified analysis methods. During thresholding logical and semantic content of the document need to be preserved for better understanding of the document image. Documents considered in our experiments are even colored paper, hence global thresholding algorithm Otsu[18] was used for binarization. An example of binarization is shown in figure 1 (a)



Fig 1(a): Original Document

3.2 Headline Segmentation:

In news paper documents, text blocks in heading and text blocks in columns are characterized by thick of white pixels separated by block of black pixels as



(b) Binarized Image

shown in the fig 2. Height of the headings and columns of document can be found from the horizontal projection profile as shown in the fig 3. Using the height headings and columns of text from the document can be separated as shown Fig 4. Words in the heading are segmented based on the block of black pixels represented by white strip show in the Fig 5. Using vertical projection profiles width of the word can be found as show in Fig 6. Based on the project

profile data, words are separated from the headings as shown in fig 7.



Fig 2 Heading and column text separated by white pixels

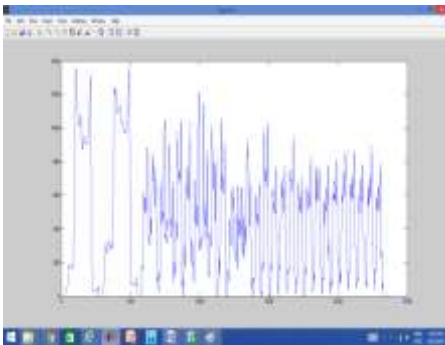
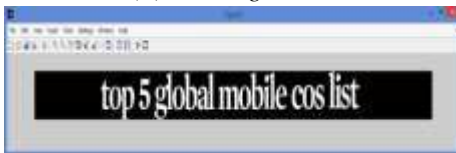


Fig. 3 Horizontal projection profile



(a) Heading block



(b) Heading 2 block

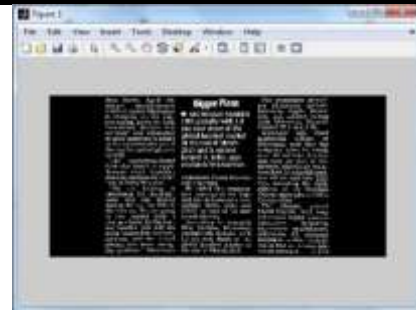
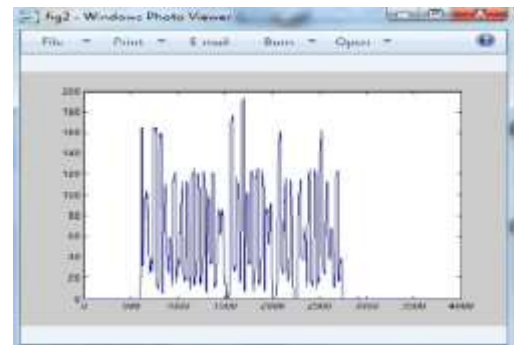


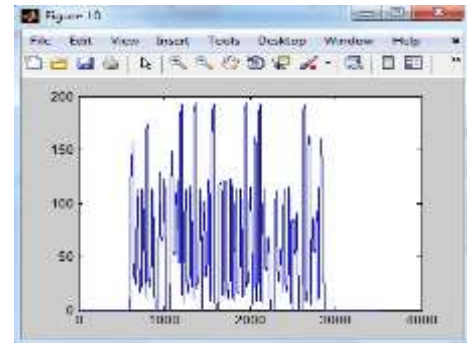
Fig 4 (c) Column Block



Fig 5: words in the heading seprted by block of black pixels represented by white strip



(a)



(b)

Fig.6(a): Vertical projection profile of the heading1(b) Heading2



Fig.7: segmented words from heading 1

3.3 Separating Columns from the Document: After the headers get separated from the images. The columns are separated, for this we use the width of the maximum occurring black run which separates the columns as shown

in the Fig 8. It can be understood that the columns can occur only in those areas where the black spaces occur in large vertical blocks. We find the width of the black run using vertical projection profile as shown in the Fig 9.

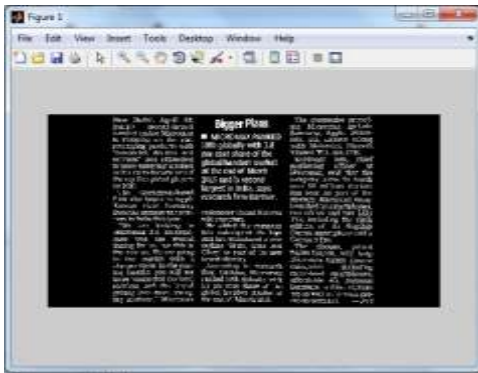


Fig 8: Columns seperated by black run

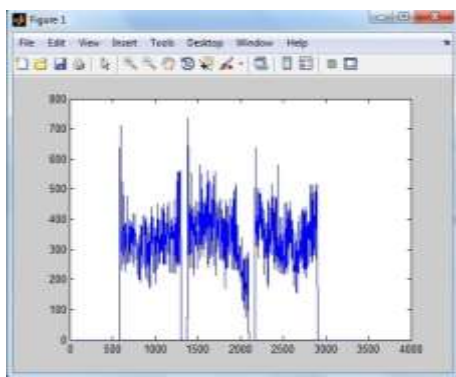


Fig. 9: Vertical projection profile of the columns

3.4 Separating images and paragraphs from the column:

In this step, we differentiate between text and images present in images. We retain only those runs of black pixels of the input image where the width of the black run is greater than or equal to twice the maximum occurring black run which is found empirically. We then use the connected component algorithm to find the height and width of these components. The components whose height is greater than a fixed threshold of 300 pixels can be said to be an image and hence removed from the document. We also consider the fact that if height is greater than a components width we call it an image and hence eliminate it from the document. We scan horizontally from each of the vertical lines to find continuous black pixel rows. We only consider those rows of black pixels where it can go horizontally till to end of the column using horizontal projection profile of the column as show in Fig 11; this is the threshold for segmenting lines from the columns as shown in the Fig 10.

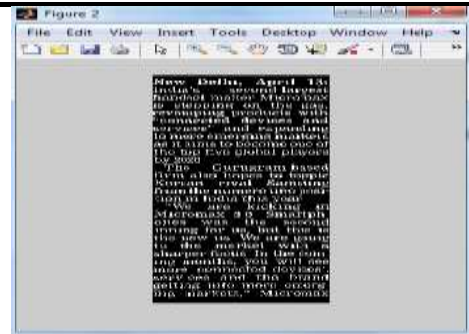


Fig 10: Text in the column

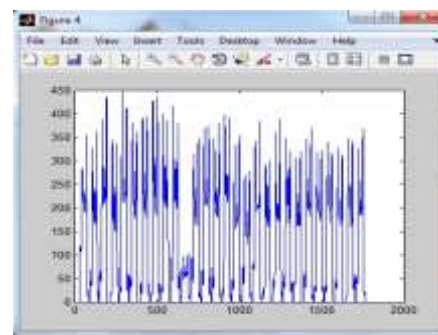


Fig 11: Horizontal projection profile

Separating words from the lines of the column: We use same method as mentioned in the first step. Using vertical projection profiles words from the lines of text are separated.

IV. RESULT AND DISCUSSION

To corroborate the efficiency and effectiveness of the proposed method, we have conducted extensive experimentation with large number of images. The images are obtained by scanning large number of English daily newspapers. Some of the sample outputs are shown below.



Fig.12: out of proposed method.

The proposed method also handles large number of columns and multifont documents also. The Table 1 shows our testing results for 20 magazine pages.

Table.I.: Result for layout analysis

No of Pages	No of Blocks	Wrongly Segmented blocks	Wrongly merged block
25	200	20	10

The Fig 12 shows that the algorithm can accurately identify textual regions on english news paper document. These segmented blocks can be passed on as input to an OCR system.

V. CONCLUSION

In this paper, we presented an efficient algorithm for segmenting unstructured document images. For the purpose of evaluating the proposed method, we have conducted experiments on the English newspaper documents. We tested this algorithm on variety of documents from different newspapers with different page layouts. From the results of the proposed method, it is evident that the proposed method handles the complex and most challenging cases. The result also shows that, the proposed method is efficient and works in hierarchal form.

REFERENCES

- [1] S. Khedekar, V. Ramanaprasad, S. Setlur, Text - Image Separation in Devanagari Documents. Proceedings of the Seventh International Conference on Document Analysis and Recognition (ICDAR'03), 2003.
- [2] K.Y. Wong, R.G. Casey and F.M. Wahl, Document analysis system. IBM Journal of Research and Development 1982; 26(6):647-656.
- [3] B. Kruatrachue, N. Moongfangklang and K. Siriboon, Fast Document Segmentation Using Contour and X-Y Cut Technique. International Journal of Computer, Information science and Engineering 2007; 1(5).
- [4] R. Garg, G. Harit and S. Chaudhury, A hierarchical analysis scheme for robust segmentation of Document Images using white-spaces. Proceedings of 1st National Conference on Computer Vision, Pattern Recognition, Image Processing and Graphics 2008. Document Image Segmentation Using Dynamic Thresholds and Identification 1875
- [5] K. Lee, Y. Choy, and S. Cho, Geometric Structure Analysis of Document Images: A Knowledge- Based Approach. IEEE transactions on Pattern Analysis and Machine Intelligence 2000; 22(11).
- [6] P. Mitchell, H. Yan, Newspaper document analysis featuring connected line segmentation. Proceedings of International Conference on Document Analysis and Recognition, ICDAR'01, 2001.
- [7] Q. Yuan, C.L. Tan, Text Extraction from Gray Scale Document Images Using Edge Information. Proceedings of the International Conference on Document Analysis and Recognition, ICDAR'01, 2001: 302-306.
- [8] A. Antona copoulos and R. T. Ritchings "Segmentation and Classification of Document Images", The Institution of Electrical Engineers 1995.
- [9] L. O'Gorman, The Document Spectrum for Page Layout Analysis. IEEE Transactions on Pattern Analysis and Machine Intelligence 1993; 15(11): 1162-1173.
- [10] S. S. G. Nagy and S. Stoddard, Document analysis with expert system. Proceedings of Pattern Recognition in Practice II, June 1985.
- [11] O. Okun, D. Doermann, and M. Pietikainen, Page segmentation and zone classification: The state of the art In UMD, 1999
- [12] A.Jain and B. Yu, Document representation and its application to page decomposition. IEEE trans. On Pattern Analysis and Machine Intelligence, 20(3):294 308, March 1998.
- [13] F. Wahl, K. Wong, and R. Casey, Block segmentation and text extraction in mixed text/image documents. CGIP, 20:375 390, 1982.
- [14] A. Jain, Fundamentals of digital image processing. Prentice Hall, 1990
- [15] C.Tan and Z. Zhang, Text block segmentation using pyramid structure. SPIE Document Recognition and Retrieval, San Jose, USA, 8:297306, January 24-25 2001.
- [16] D. Chetverikov, J. Liang, J. Komuves, and R. Haralick, Zone classification using texture features. In Proc. of Intl. Conf. on Pattern Recognition, volume 3, pages 676 680, 1996.
- [17] A. K. Jain and S. Bhattacharjee, Text segmentation using gabor filters for automatic document processing. Machine Vision and Applications, 5(3):169 184, 1992.
- [18] M. Sezgin & B. Sankur (2004). "Survey over image thresholding techniques and quantitative performance evaluation". Journal of Electronic Imaging. 13 (1): 146-165.

A Design of Crown Square Fractal Antenna Using Transmission Line Feed

Jyoti Dadwal¹, Arushi Bhardwaj², Dr.Yogesh Bhomia³

¹M.Tech Student, Department of Electronics & Communication, S.S.C.E.T, Badhani, Pathankot India

²Assistant Professor, Department of Electronics & Communication, S.S.C.E.T, Badhani, Pathankot, India

³Principal, Department of Electronics & Communication, S.S.C.E.T, Badhani, Pathankot, India

Abstract— The paper presents the designs of a crown square fractal antenna. The propounded antenna is designed on 1.6mm thick FR4 glass proxy substrate with dielectric constant ϵ_r of 4.4 and is fed by transmission line. The proposed antenna design helps in reducing the metal usage, save cost and provides good reflection coefficient and good VSWR. Performance of proposed antenna has been analyzed in terms of return loss, VSWR, input impedance, gain, and bandwidth in the 1 GHz to 7GHz frequency range. The proposed antenna provides an impedance bandwidth of 45 % around the resonant frequency of 0.5575 GHz and good return loss of -36.44.

Keywords— Feed, FR4, Micro strip patch antenna, Return loss, crown square shape, VSWR.

I. INTRODUCTION

In the electronics and communication system, variety of micro strip antennas are being utilized, the most general of which is microstrip patch antenna [12]. A patch antenna is a compact, narrow band, wide-beam, light-weight, conformal-shaped antenna which is fabricated by etching the antenna element pattern in metal trace conjoined to an insulating dielectric substrate [3]. It is incorporated with a flat rectangular sheet or “patch” of metal, mounted over a larger sheet of metal called the ground plane. A patch antenna is mainly built on a dielectric substrate employing the same materials & lithography techniques in order to make printed circuit boards. Microstrip or patch antennas [6] are becoming more and more useful because they can be printed directly onto a circuit board.

The word fractal is derived from the Latin word “fractals” meaning broken, uneven, any of various extremely irregular curves or shape that repeat themselves at any scale on which they are examined. Achieve wideband frequency band or multiband frequencies. Their efficiency is very less. It has different iterations (scale sizes).

In this paper, we have presented a design of microstrip Patch antenna using crown square shape fractal slot [13],

with rotated 45 angles and also with an aim to achieve a smaller size antenna [4]. In the present work, a combined crown and sierpinski fractal antenna has been designed to operate between 0-7GHz around the resonant frequency of 0.55 75GHz. Target of this work is to design a microstrip patch antenna and carrying out results using commercial simulation software like IE3D. IE3D, from Zealand software, Inc [17], is an electromagnetic simulation and optimization software useful for circuit and antenna design. IE3D has a menu driven graphic interfaces

II. ANTENNA PERFORMANCE MEASUREMENTS

To successfully design an antenna a number of measurements must be made to quantify the antenna performance. Below are the various antenna performance measurements.

A. Impedance and Antenna Bandwidth:

Antenna impedance is typically measured as return loss or VSWR [4]. The equipment used to measure this parameter is a Network Analyzer. The impedance measurement often requires special fixtures and assemblies to allow access to the antenna terminals.

B. Gain and Radiation Patterns:

Calibrated measurements of antenna gain and radiation patterns are made in an Anechoic Chamber. The anechoic environment eliminates all reflections and allows precise and repeatable measurements to be made. The device under test is typically rotated 360 degrees in multiple orientations to determine the shape of the radiation pattern from many different directions. Reference antennas are used as calibrated gain standards. As with impedance measurements, gain and radiation patterns should be measured using a complete product.

C. Efficiency Measurements:

As mentioned earlier, efficiency may be the single most important parameter to be measured, especially for an embedded antenna which can have degraded efficiency due to its tight integration with the device. Efficiency can be calculated from the calibrated gain and radiation pattern measurement but this can be a time-consuming effort.

III. DESIGN OF FRACTAL ANTENNA

The propounded antenna is designed on 1.6mm thick FR4 glass proxy substrate with dielectric constant ϵ_r of 4.4 and is fed by transmission line. The basic shape of proposed antenna consist of crown square patch of each side Length 20mm has been taken on the ground planesubstrate of length = 20mm and width =20mm.

Table.1: Design values of proposed micro antenna.

ANTENNA PARAMETERS	DESIGN VALUE
Dielectric constant	4.4
Substrate height(mm)	1.6
Loss tangent	0.001
Length of patch(mm)	20
Width of patch (mm)	20
Length of substrate (mm)	20

There are three essential parameters for design of a rectangular microstrip Patch Antenna. The dielectric constant of the substrate material is an important design parameter. Firstly, the dielectric material of the substrate is selected for the design.

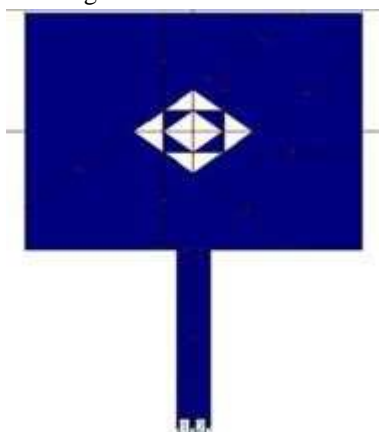


Fig.1(a): Model of 1st iteration,

The proposed antennas is designed using FR4 substrate with dielectric constant, $\epsilon_r = 4.4$, loss tangent equal to 0.001 and $h = 1.6\text{mm}$ which is the

height of the substrate. For feeding, transmission feeding method is used. For all iterations, the location of feed is same and the length of feed is 10mm .Same procedure is repeated and the result of simulation studies is presented up to third iteration. The frequency range is used from 2GHz to 7GHz.

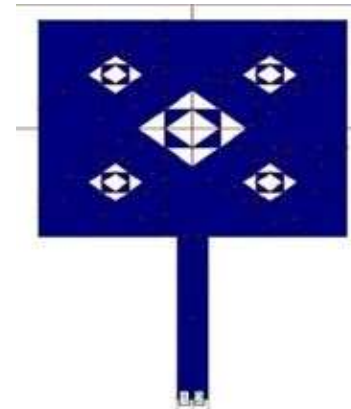


Fig.1.b) Model of 2nd iteration,

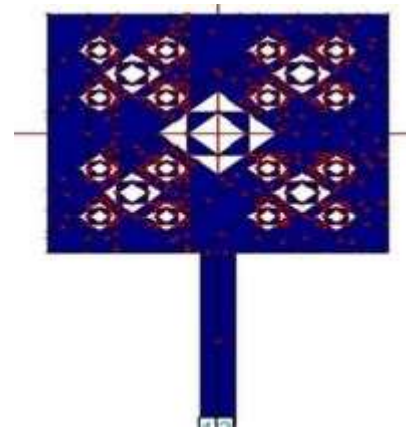


Fig.1.c) Model of 3rd iteration

Secondly, substrate thickness is another important design parameter. Thick substrate increases the fringing field at the patch periphery like low dielectric constant and thus increases the radiated power. The height of dielectric substrate employed in this design of antenna is $h = 1.6\text{mm}$.this design only. Lastly, the resonant frequency (f_r) of the antenna must be selected appropriately. The frequency range used is from 2GHz – 7GHz and the design of antenna must be operated within this frequency range. The resonant frequency selected for this design is 0.5575 GHz.

IV. FEED TECHNIQUE (MICROSTRIPLINE)

1) First iteration



Fig.2: The model for 1st iteration

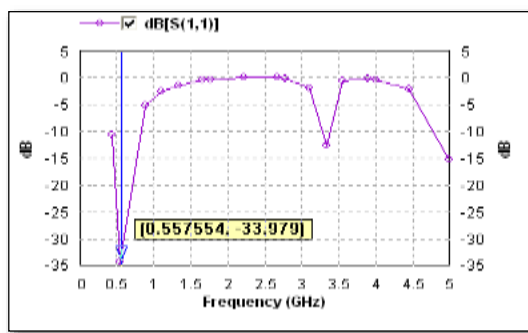


Fig.3: S11 Parameter

It is achieved by cutting crown square fractal slot is deploying crown geometry of each side length 4mm in the center of the square patch as shown in fig.2. Return loss of -33.97db and VSWR of 1.067

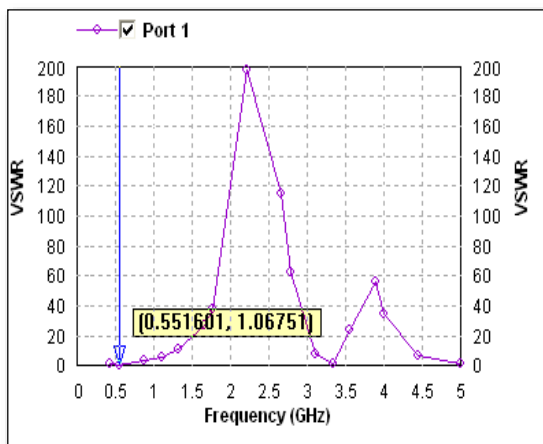


Fig.4: VSWR

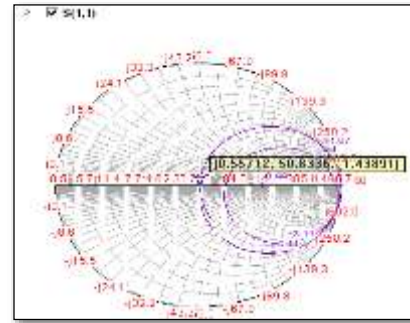


Fig. 5: Input impedance loci using smith chart

2) Second iteration

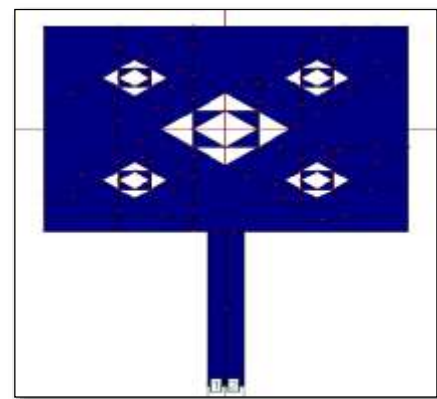


Fig.6: The model for 2nd iteration

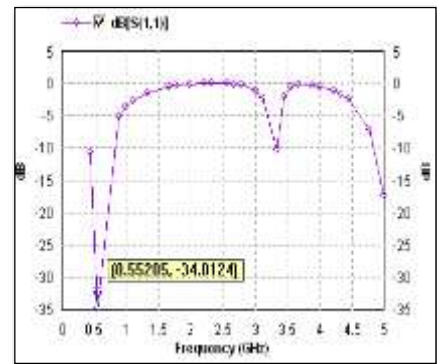


Fig.7: S11 parameter

Fig 6 shows the results of the second iteration of the proposed fractal antenna. In the centre one crown square fractal slot deploying crown square geometry each of side length 4mm is taken and similar four slots each of side length 2mm are taken on each corner of the central slot. A VSWR of 1.04 and return loss of -34.01 are available at the resonant frequency.

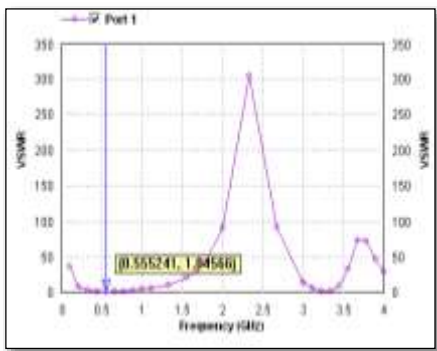


Fig.8: VSWR

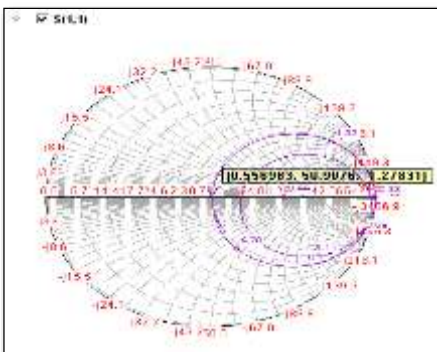


Fig.9: Input impedance loci using smith chart

3) Third iteration

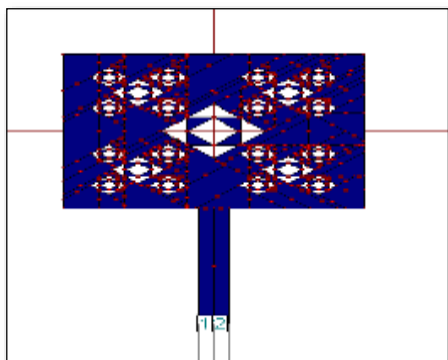


Fig.10: The model for 3rd iteration

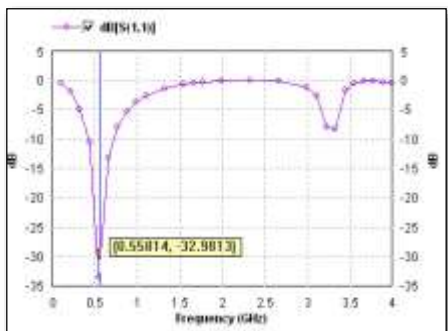


Fig.11: S11 parameter

In this one central crown square fractal slot deploying crown geometry is cut and twenty similar structured fractal slot are taken on each corner of the central slot with reduction in their sizes. These fractal slots have dimension of each side equals $L1=4\text{mm}$, $L2=2\text{mm}$, $L3=1\text{mm}$. shown in fig: 10

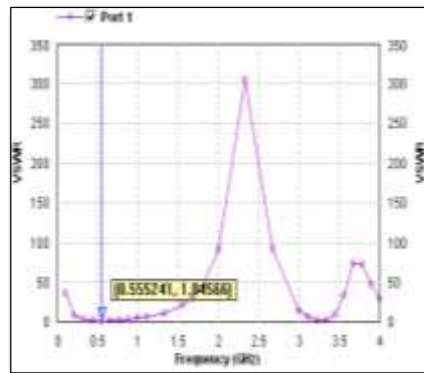


Fig.12: VSWR

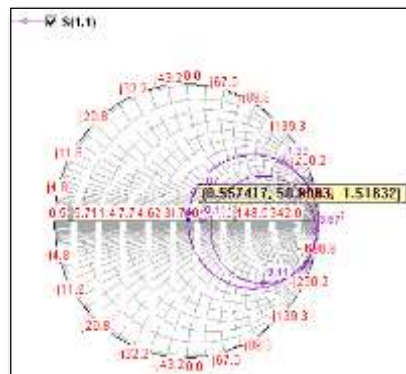


Fig.13: Input impedance loci using smith chart

The below table shows result in each iteration improves with respect to Bandwidth, VSWR

Table.2: Result comparison of Iteration 1, 2 & 3

Parameters	Iteration 1	Iteration 2	Iteration 3
Resonant Frequency	0.5576	0.5576	0.5576
Bandwidth	40.00%	45.20%	45.25%
VSWR	1.067	1.045	1.045
Return Loss	-33.979	-34.012	-32.981

V. CONCLUSION

The antenna is simulated by using IE3D by Zealand Software. The results demonstrated a maximum patch size reduction by the proposed any type fractal antennas, without degrading antenna's performance, such as the return loss

and radiation pattern, VSWR. The basis of the maintenance of the antenna radiation patterns is the self-similarity and Centro-symmetry properties of the fractal shapes [9]. The main advantages of the discussed method are: (i) miniaturization (ii) maintained radiation patterns (iii) wider and better operating frequency bandwidth, (iv) simple and easy to design. This paper presented a modified crown square shape antenna on a FR4 substrate of relative permittivity of 4.4 & thickness 1.6 mm.

Table 1 shows the variation of return loss with frequency, VSWR and Bandwidth for iteration I, II and III for transmission line feed this geometry shows high self-similarity and symmetry [14].

REFERENCES

- [1] James, J.R. and Hall, P.S.: 'Handbook of Microstrip Antennas'(Peter Peregrinus)
- [2] Constantine A. Balanis: 'Antenna Theory, Analysis and Design'(John Wiley & Sons)
- [3] Bhomia Y., Chaturvedi A., YadavD., "Truncated Tip Triangular Microstrip Patch Antenna", Proc. IEEE. IntSymp. Antenna Propag. vol. 2, pp. 212 -214, 2010.
- [4] Kai-Fong Lee, Kwai- Man Luk, Jashwant S. Dahele, 'Characteristics of the Equilateral Triangular Patch Antenna' IEEE Tran. Antennas Propag.1988; 36;1510.
- [5] C. L. Mak, K. M. Luk, K. F. Lee, 'Wideband Triangular Patch Antenna' IEE. Proc. Microwave Antennas Propag. 1999
- [6] I. J. Bahl and P. Bhartia, 'Microstrip Antennas, Artech House, Dedham, MA, 1980.
- [7] Jaswinder Kaur, Rajesh Khanna, M. V. Kartikeyan, "Optimization and Development of O-shaped Triple-band Microstrip Patch Antenna for Wireless Communication Applications", IETE Journal of Research, Vol. 60, Iss. 2, 2014
- [8] VahidSharbati, PejmanRezaei, Mohammad M. Fakharian&EhsanBeiranvand, "A Switchable Band-Notched UWB Antenna for Cognitive Radio Applications", IETE Journal of Research, Vol.61, Issue 4, 2015.
- [9] M. F. Barnsley, R. L. Devaney, B. B. Mandelbrot, H. O. Peitgen, D.Saupe, R. F. Voss, Y. Fisher, and M. McGuire, The Science of Fractal Images. New York: Springer-Verlag, 1988.
- [10] Yogesh Bhomia et.al., "V-Slotted Triangular Microstrip Patch Antenna", Int. Journal of Electronics Engineering, vol. 2,no.1, pp. 21-23,2010
- [11] K. J. Vinoy, J. K. Abraham, and V. K. Varadan, "On the Relationship Between Fractal Dimension and the Performance of Multi-Resonant Dipole Antennas using Koch Curves," IEEE Transactions on Antennas and Propagation, AP-5 1, 9,2003,pp.2296-2303.
- [12] Bhomia, Y., A. Kajla, and D. Yadav, "Slotted right angle triangular microstrip patch antenna," International Journal of Electronic Engineering Research, Vol. 2, No. 3, 393-398, 2010.
- [13] Bhomia Y.,Chaturvedi A., Yadav D., " Microstrip Patch Antenna Combining Crown and Sierpinski Fractal-Shapes ", Proc. IEEE. IntSymp. Antenna Propag.,vol. 2, pp. 212 -214, 2010
- [14] Ankur Aggarwal, M.V.Kartikeyan,"Design of Sierpinski Carpet Antenna using two different feeding mechanism for WLAN applications", IEEE,2010.
- [15] Yogesh Bhomia, AshviniChaturvedi, Yogesh Kumar Sharma," Microstrip Patch Antenna combining crown & Sierpinski Fractal Shapes, ACM, ICACCI'12.
- [16] H. O. Peitgen, H. Jurgens, and D. Saupe, Chaos and Fractals. NewYork: Springer-Verlag, 1990.
- [17] IE3D by Zeland software Inc.
- [18] Mahdi NaghshvarianJahromi, AbolfazlFalahti and Rob.M.Edward, "Bandwidth and Impedance-Matching Enhancement of Fractal Monopole Antenna Using Compact Grounded Coplanar Waveguide", IEEE Transaction on Antenna and Propagation, Vol.59, No.7, July 2011.
- [19] Sarita Bajaj, Ajaykaushik,"Analysis of Patch Antenna Based on the Sierpinski Fractal", International Journal of Engineering Research and Applications, Vol.2, Sep-Oct 2012, pp.023-026.
- [20] Neetu ,Savina Bansal, R.K.Bansal,"Design and Analysis of Fractal Antennas Based on Koch and Sierpinski Geometries,"International Journal of Advanced Research in Electrical,Electronics and Instrumentation Engineering ,Vol.2,June2013.

Heat Transfer Enhancement for Tube in Tube Heat Exchanger Using Twisted Tape Inserts

A. H. Dhumal , G. M. Kerkal , K.T. Pawale

Asst. Professor, Department of Mechanical Engineering , DYPIEMR, Akurdi, Pune-44, Maharashtra, India

Abstract— Heat transfer augmentation techniques refer to different methods like Swirl-flow devices include a number of geometric arrangements or tube inserts for forced flow that create rotating and/or secondary flow. Coiled tubes, inlet vortex generators, twisted-tape inserts, and axial core inserts with a screw-type winding used to increase rate of heat transfer without affecting much the overall performance of the system. These techniques are used in heat exchangers which are used in process industries, , air-conditioning equipments, refrigerators thermal Power plants, radiators for space vehicles and automobiles etc. This work mainly focuses on the twisted tape inserts with different pitch and twist ratio and its effect on friction factor.

Keywords— heat exchanger, swirl flow devices, twisted tapes, twist ratio, pitch, friction factor.

I. INTRODUCTION

Heat exchangers are used in different processes ranging from conversion, utilization & recovery of thermal energy in various industrial, commercial & domestic applications. Some common examples include steam generation, condensation in power & cogeneration plants, sensible heating & cooling in thermal processing of chemical, pharmaceutical & agricultural products, fluid heating in manufacturing & waste heat recovery etc. Increase in heat exchanger's performance can lead to more economical design of heat exchanger which can help to make energy, material & cost savings related to a heat exchange process. The need to increase the thermal performance of heat exchangers, thereby effecting energy, material & cost savings have led to development & use of many techniques termed as heat transfer augmentation. These techniques are also referred as heat transfer enhancement or intensification. Augmentation techniques increase convective heat transfer by reducing the thermal resistance in a heat exchanger. Use of Heat transfer enhancement techniques lead to increase in heat transfer coefficient but at the cost of increase in pressure drop. So, while designing a heat exchanger using any of these techniques, analysis of heat transfer rate & pressure drop has to be done.

Apart from this, issues like long term performance & detailed economic analysis of heat exchanger has to be studied. To achieve high heat transfer rate in an existing or

new heat exchanger while taking care of the increased pumping power, several techniques have been proposed in recent years. Twisted tapes a type of passive heat transfer augmentation techniques have shown significantly good results in past studies. For experimental work, different designs of twisted tapes used are typical twisted tape (TT). All these tapes have been studied with three different twist ratios ($\gamma = 4.213, 5.337, 6.4606$) and depth of cut ($d = 6$ mm) for notched twisted tapes.

II. LITERATURE REVIEW

Bodius Salam et.al. [1] have investigated the heat transfer enhancement in a tube using rectangular cut twisted tape insert. An experiment was carried for measuring tube side heat transfer coefficient, friction factor, heat transfer enhancement efficiency of water for turbulent flow in a circular tube fitted with rectangular cut twisted tape insert. A copper tube of 26.6 mm ID and 30 mm OD with 900 mm test length was used. A stainless steel rectangular cut twisted tape insert of 5.25 twist ratio was used. The rectangular cut had 8 mm depth and 14 mm width. The Re was varied in the range of 10000 to 19000 with heat flux variation of 14 to 22 kW/m² for smooth tube and 23 to 40 kW/m² for tube with insert. At comparable Re, Nu in tube with inserts were enhanced by 2.3 to 2.9 times at the cost of increase in the friction factor by 1.4 to 1.8 times compared to that of smooth tube. Heat transfer enhancement efficiencies were found to be in the range of 1.9 to 2.3 and increased with the increase of Re.

S. Naga Sarada et.al [2] have investigated the heat transfer augmentation using twisted tape inserts having different cut sections in a circular tube. It is observed that twisted tape generates swirling flow which causes higher turbulence and greater mixing in the tube. It is proved that as Re increases, Nu increases and friction factor decreases. For all tapes irrespective of their geometry and shape as the twist ratio of the tape increases both Nu and friction factor increases. Heat transfer rate is higher when cuts are provided on the twisted tape insert compared to the plain twisted tape insert and plain tube without insert.

Dnyaneshwar S. Nakate et.al. [3] investigated the performance of heat exchanger using different types of turbulators. It was derived that use of turbulators proved more appreciable in double pipe heat exchangers. A double pipe U bend heat exchanger with water as the cooling fluid

having a flow rate of 15lit/min was used to cool oil which had a flow rate of 2lit/min. Then a twisted tape of pitch=15cm and length 4m was added to the heat exchanger and the effectiveness was compared. It is computed that twisted tape inserts give 36-48% more heat transfer for full width and 33-39% for reduced width. The enhancement is mainly due to centrifugal forces resulting from the spiral motion of the fluid. The maximum friction factor rise was about 18% for 26mm width and only 17.3% for reduced width inserts. Reduction in the tape width causes reduction in Nusselt number as well as friction factor.

Mukesh P Mangtani et.al.[4] worked on modifications on geometry of twisted tapes in a double pipe heat exchanger. The heat transfer coefficient is found to increase by 40% with half-length twisted tape inserts when compared with plain heat exchangers. The value of heat transfer and friction factor of double pipe heat exchanger can be improved with the help of reduced width twisted tape (RWTT) with three types of different twist ratio ($\gamma=3.69, 4.39, 5.525$) based on constant flow rate. The heat transfer coefficient was found to be 1.18, 2.61, and 3.58 respectively times the smooth tube values. The heat transfer coefficient and friction factor increases with decrease in twist ratio compared with plain tube. It was derived that the values of Nusselt number, Reynolds number, Prandtl number, pressure drop and friction factor are dependent on the geometries of the twisted tape with different twist ratio, pitch ratio, tape width etc.

Prashant Tikhe et.al [5] have investigated the heat transfer enhancement using twisted tape inserts of different width ratio and under constant wall heat flux condition. The experiments were carried out to determine heat transfer, friction factor and thermal performance characteristics in turbulent flow ($7500 \leq Re \leq 13000$). The tapes of five different width ratios (W/D) of 0.35, 0.44, 0.53, 0.62, and 0.71 at constant twist ratio (H/D) of 2.5. The experimental results show that Nusselt number increases with increasing Reynolds number and increasing width ratio (W/D) of the swirl generators. Also the friction factor decreases with increasing Reynolds number and decreasing width ratio. Nusselt number increased in the ranges of 6.04% to 17.26% compared to the results of the tube without twisted tape depending on the operating conditions. At the same pumping power, the use of twisted tape inserts results in thermal performance factor up to 1.17 times of those of the plain tube.

K. Abdul Hamid et.al. [6] introduced the advance heat transfer fluid called nanofluid which is prepared by dilution technique of Titanium Oxide (TiO₂) in based fluid of mixture water and ethylene glycol (EG).

S. Eiamsa-ard et.al. [7] investigated the performance of a heat exchanger using TiO₂-H₂O nanofluid and overlapped dual twisted tapes. The study was carried out using TiO₂ with volume concentrations (ϕ) of 0.07%, 0.14% and 0.21% and (O-DT) with twist ratios (γ_o/γ) of 1.5, 2.0 and 2.5. The

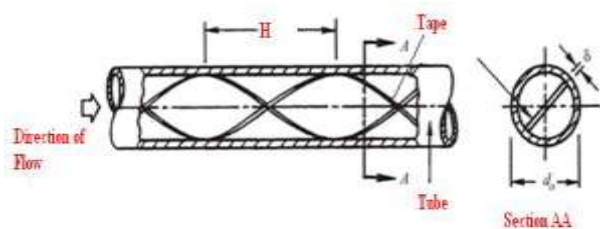
experimental and numerical results indicated that turbulators with small twist ratio delivered strong swirl intensity and high turbulent kinetic energy. The use of overlapped dual twisted tapes (O-DT) at twist ratio 1.5 enhanced heat transfer rate by 89%, friction factor by 5.43 times and thermal performance up to 1.13 times as compared to plain tube. Using $\phi=0.21\%$ and $\gamma_o/\gamma=1.5$ gave a heat transfer enhancement of about 9.9-11.2% and thermal performance improvement up to 4.5%.

Hafiz Muhammad Ali et.al. [8] focused on the use of water based MgO nanofluid for thermal management of a car radiator. Nanofluid of different volumetric concentrations (i.e. 0.06%, 0.09%, and 0.12%) showed enhancement in heat transfer compared to the pure base fluid. A peak heat transfer enhancement of 31% was obtained at 0.12% volumetric concentration of MgO in base fluid. The fluid flow rate was maintained in a range of 8-16 litre per minute. Lower flow rates resulted in greater heat transfer rates as compared to heat transfer rates at higher flow rates for the same volumetric concentration. Heat transfer rates are weakly dependant on the inlet fluid temperature. An increase in inlet temperature from 56° C to 64° C only showed a maximum 6% increase in heat transfer rate.

A Dewan et.al.[9] have shown that heat transfer passive augmentation are advantageous compared with active techniques, because the insert manufacturing process is simple and these techniques can be easily employed in an existing heat exchanger. In design of compact heat exchangers, passive techniques of heat transfer augmentation can play an important role if a proper passive insert configuration can be selected according to the heat exchanger working condition (both flow and heat transfer conditions). In the past decade, several studies on the passive techniques of heat transfer augmentation have been reported. He has taken review on progress with the passive augmentation techniques in the recent past and will be useful to designers implementing passive augmentation techniques in heat exchange. Twisted tapes, wire coils, ribs, fins, dimples, etc., are the most commonly used passive heat transfer augmentation tools. He emphasized to works dealing with twisted tapes and wire coils because, according to recent studies, these are known to be economic heat transfer augmentation tools. The former insert is found to be suitable in a laminar flow regime and the latter is suitable for turbulent flow. The thermo-hydraulic behaviour of an insert mainly depends on the flow conditions (laminar or turbulent) apart from the insert configurations.

III. TWISTED TAPE INSERTS

The insert used for the experiment are low carbon steel ANSI AS-177 helical twisted tapes. The present work deals with finding the heat transfer coefficient and the friction factor for the twisted tape with twist ratios ($p/w=4.213, p/w=5.337, p/w=6.4606$).



H or p = Pitch of the tape;
 d_o = Outer diameter of tube;
 δ = Thickness of tape; w = width of tape

IV. EXPERIMENTAL SETUP

A tube in tube heat exchanger consisting of a test section, rotameters, and a tank for supplying hot fluid and a heater for heating water is used for experimentation. The test section is a Plain copper tube with dimensions of 1400 mm length, inner tube-20.4 mm ID, and 25.4 mm OD, wall thickness- 2.5 mm; Outer MS pipe- 45.8 mm ID, 50.8 mm OD and wall thickness- 2.5 mm. Two calibrated rotameters, with the flow range 400 to 1600 LPH, are used to measure the flow of cooling water and hot water. The hot water at operating temperature is drawn from tank by using pump. Similarly a rotameter is provided to control the flow rate of hot water from the pump discharge. Cold water flow rate is varied and hot water is flowed at constant rate. Four RTD sensors measure the inlet & outlet temperature of hot water & cold water (T1, T2, and T3& T4) through a multipoint digital temperature indicator.

The twisted tapes are inserted from one end of the tube and by varying the pitches, the thermal performance of the heat exchanger is analyzed.

V. RESULTS

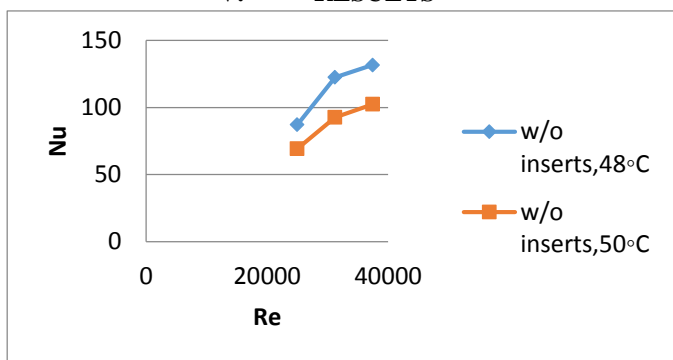


Chart-1: Plot of Nusselt Number Vs Reynolds Number for bulk mean fluid temperatures 48°C & 50°C.

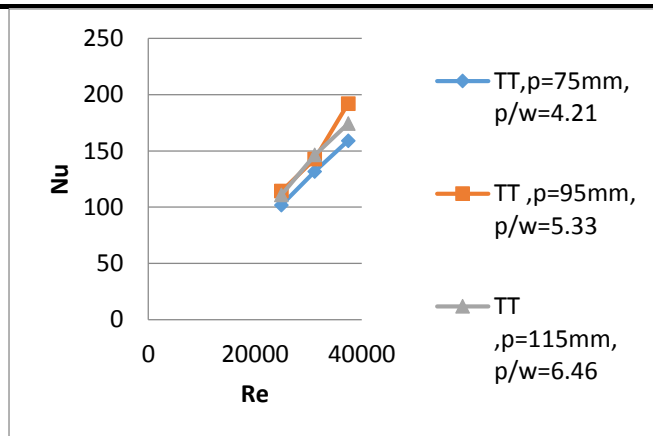


Chart-2: Plot of Nusselt Number Vs Reynolds Number for plain twisted tapes of pitches 75, 95, 115 mm for bulk mean fluid temperature 50°C.

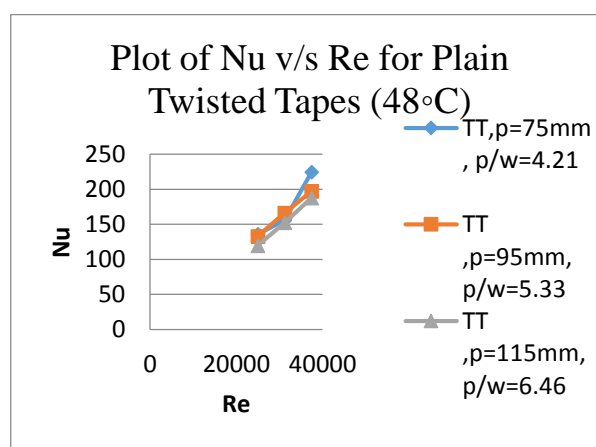


Chart-3: Plot of Nusselt Number Vs Reynolds Number for plain twisted tapes of pitches 75, 95, 115 mm for bulk mean fluid temperature 48°C.

Chart 1,2,3 show variation of Nusselt Number with Reynolds Number for plain tube as well as tube with typical twisted tapes. These variations are plotted for various twist ratios ($y = p/w$). The twist ratios 4.213, 5.337 and 6.4606 are considered. It is observed that Nusselt number is 30 - 45% larger with PTT than that of plain tube arrangement. While the PTT with twist ratio's 4.213 and 5.337 are responsible for the higher Nusselt Number. At the given Reynolds number, the Nusselt number consistently increases with the decrease in twist ratio. This is due to the fact that the tape with smaller twist ratio (y) induces stronger turbulent intensity. In addition, it gives longer flowing path which leads to longer residence time and thus more efficient heat transfer compared to that with larger twist ratio (y).

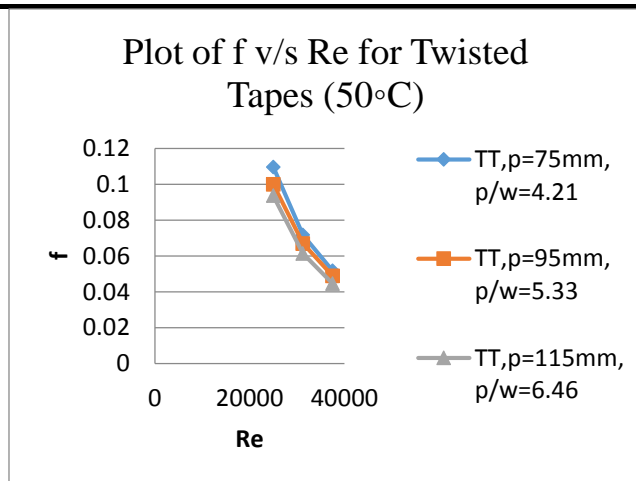


Chart-4: Plot of friction factor (f) Vs Reynolds Number for plain twisted tapes of pitches 75, 95, 115 mm for bulk mean fluid temperature 50 °C.

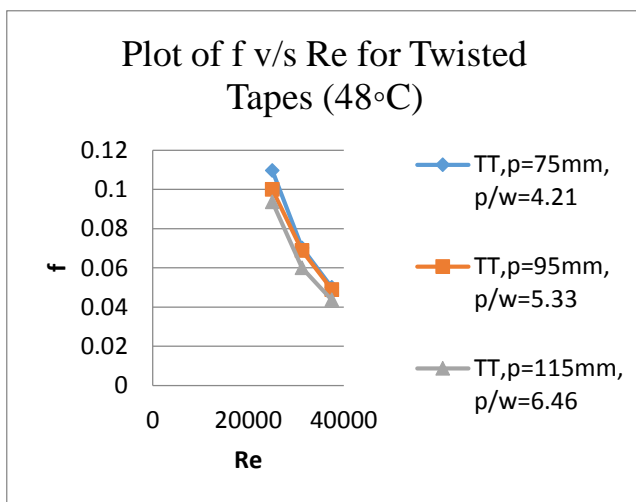


Chart-5: Plot of friction factor (f) Vs Reynolds Number for plain twisted tapes of pitches 75, 95, 115 mm for bulk mean fluid temperature 48 °C.

Chart 5 and 6 show variation of friction factor with Reynolds number for plain tube, plain and notched helical twisted tapes at various twist ratios ($p/w = 4.213, 5.337$ and 6.4606). As found, the friction factor decreases with increasing twist ratio (p/w). Because twisted tape with shorter twist length provides longer flowing path, resulting in larger tangential contact between the flowing stream and tube surface. Therefore loss due to the friction increases. Same time the formation of vertex due to twists and notches causes for the large variation in velocity which is also contribute to pressure drop. The larger pressure drop is not desirable. Hence to select the proper insert for heat transfer enhancement, one has to determine the enhancement efficiency which is ratio of Nusselt's number to Friction factor.

VI. CONCLUSIONS

The convective heat transfer performance a flow characteristics of fluids flowing in a double pipe heat exchanger has been theoretically investigated. The effect of Reynolds number on the heat transfer performance and flow behaviour of the fluid has been theoretically determined. Important conclusions are summarized as follows:

1. With increase in twist ratio, Nusselt's Number decreases but at the same time pressure drop also decreases.

2. For same twist ratio, plain twisted tape (TT or PTT) shows greater Nusselt's Number, heat transfer coefficient and friction factor than the value we get for Plain Twisted Tape (PTT).

3. In a heat exchanger, while the inserts can be used to enhance the heat transfer rate, they also bring in an increase in the pressure drop. When the pressure drop increases, the pumping power cost also increases, thereby increasing the operating cost. So depending on the requirement, one of the above mentioned inserts can be used for heat transfer augmentation.

REFERENCES

- [1] Bodius Salam, Sumana Biswas, Heat Transfer enhancement in a tube using rectangular cut twisted tape insert, Research Gate, October 2016.
- [2] S. Naga Sarada, JayaKrishna P, A review on heat transfer augmentation using twisted tape inserts having different cut sections in a circular tube, TROI ISSN 2394-0697, Volume 3, December 2016.
- [3] Dnyaneshwar S Nakate, S V Channapattana, Ravi H, Experimental investigation in the enhancement of heat transfer rate using twisted tape turbulators in heat exchangers, IJSET ISSN 2348-7968, March 2015.
- [4] Mukesh Mangatani, K M Watt, Effect of twisted tape inserts on heat transfer in a tube: A review, International Journal of Mechanical Engineering and Robotics Research, ISSN 2278-0149, April 2015.
- [5] Prashant Tikhe, Prof. A. M. Andhare, Heat transfer enhancement in circular tube using twisted tape inserts of different width ratio under constant wall heat flux conditions, IJERT ISSN 2278-0181, June 2015.
- [6] K Abdul Hamid, W. H. Azmi, N. A. Usri, Effect of Titanium Oxide nanofluid on pressure drop, ARPN Journal of Engineering and Applied Sciences ISSN 1819-6608, September 2015.
- [7] S.Eiamsa-ard, K.Kiakittipong, W.Jedsadaratanachai, Heat transfer enhancement of TiO_2 / water nanofluid in a heat exchanger tube equipped with overlapped dual twisted tapes, ELSEVIER 336-350, 2015.
- [8] Hafiz Muhammad Ali, Muhammad Danish Azhar, Musab Saleem, Qazi Saeed, Heat transfer enhancement of car radiator using Aqua based Magnesium Oxide nanofluids, THERMAL SCIENCE: Vol No. 19, No.6, 2039-2048, 2015.
- [9] A. Dewan, P. Mahanta, K. Sumithra Raju, P. Suresh Kumar, Review of passive heat transfer augmentation techniques, 2014.

Assessment of Heavy Metals in Fodder Crops Leaves Being Raised with Hudiara Drain Water (Punjab-Pakistan)

Arif Malik¹, Saima Jadoon², Mawish Arooj³, Muhammad Imran Latif⁴,

^{1,2}Institute of Molecular Biology and Biotechnology (IMBB), The University of Lahore-Pakistan.

³University College of Medicine and Dentistry (UCMD), The University of Lahore-Pakistan.

⁴Soil and Water Testing Laboratory, Lahore-Pakistan.

Abstract— The present study was designed with the objectives to assess heavy metals' concentration in Hudiara drain water and investigation of the concentration of heavy metals in different fodder crops grown with this drain water and the determination of heavy metals in milk of cattles grazing these contaminated fodder crops. A survey was conducted and ten different sites were selected along Hudiara drain after entering Lahore. Five water samples and three samples of crops from a each site. The samples were processed, stored and then analyzed for heavy metals like Lead, Cadmium, Chromium, Nickel, Zinc, Iron, Copper and manganese. Lead pollution was not found, whereas, Cadmium, Chromium and Nickel contamination was shown in Hudiara drain water. Similarly, Zinc pollution was not found in Hudiara drain water regarding irrigation and Iron, Copper and Manganese contamination was present in Water samples. Most of the fodder crops samples were contaminated with all heavy metals having levels of heavy metals above the Recommended Concentrations. It is noted that Pb^{+2} of Hudiara drain and irrigated Pb^{+2} of fodder crop were in positive correlation and negative correlation between Pb^{+2} and Cr^{+2} , Ni^{+2} , Cu^{+2} . There is positive correlation between Cd^{+2} and Cr^{+2} , Fe^{+2} and also negative correlation between Cd^{+2} and Pb^{+2} , Cd^{+2} , Ni^{+2} , Zn^{+2} , Cu^{+2} , Mn^{+2} of fodder crop irrigated with Hudiara drain.

Keywords—Heavy Metals, Hudiara Drain, Fodder crops, Water samples.

I. INTRODUCTION

Industrial effluents are the most potential water pollutants [1]. The effluents discharged by different industries have higher values of physico-chemical parameters like temperature, pH, conductivity, hardness, alkalinity, chemical oxygen demand, total soluble salts, nitrates, nitrites and cations (Na, K, Ca and Mg) [2]. This water also contains significant amount of heavy metals such as zinc, iron, copper, manganese, lead, cadmium, chromium, nickel, cobalt, arsenic etc. [3]. Some of the heavy metals are essential and some are even not essential for plant growth but after accumulating in the soil could be transferred to food chain [4]. Generally, farmers are not aware of the metal ion toxicity being introduced into food chain by vegetables grown with such polluted waters [5]. If these heavy metals leach out through the soil, they may also contaminate ground-water [6].

Hudiara Drain, which is a long natural storm water channel, originates from Batala in Gurdaspur District, India and after flowing nearly 55 km on Indian side at village Laloo enters Pakistan at Hudiara village on Pakistan side. After flowing for nearly 63 km inside Pakistan, it joins the river Ravi. The river Ravi has serious pollution problems. There are around hundreds of industries of different types located adjacent to the Hudiara drain on the 55 kilometers Indian side, so it is already quite polluted when it enters Pakistan [7].

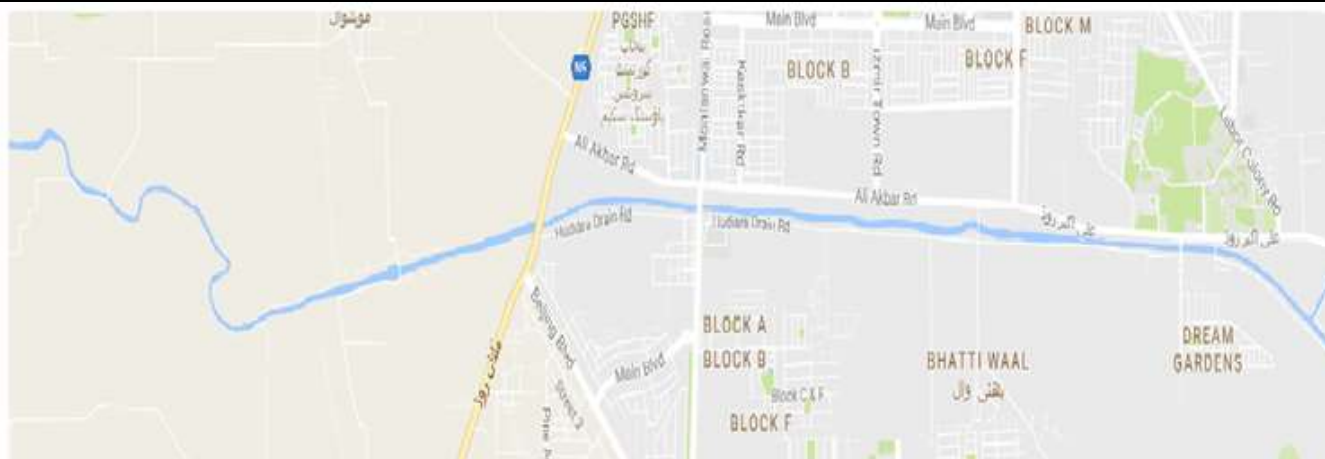


Fig.1: Hudiyara Drain in Map.

There are 112 small industries located next to the drain on Pakistani side as it travels 63 kilometers before entering into the Ravi. This water is also being used for irrigation along the length of the drain by using different methods. The villagers even use water from wells dug close to the drain, which are exposed to the pollution through seepage. With increasing water shortage for agriculture and increasing waste water volume in drains, farmers around these drains find it convenient to irrigate the fields with easily accessible and free of cost drain water. Untreated water, when used for irrigation, seeps into the soil and facilitates the entry of a number of pathogens and heavy metals into the food chain. Vegetables and other crops grown with polluted water may also have exceeded levels of heavy metals which may cause diseases when consumed by people or by animals.

Therefore, the present study has been undertaken with following objectives.

- 1- Assessment of heavy metals concentration in Hudiyara Drain water.
- 2- Investigation of the concentration of heavy metals in different fodder crops grown with this drain water.

II. MATERIALS AND METHODS

A survey was conducted along the Hudiyara drain inside Lahore city and ten different sites were selected along Hudiyara drain at a distance of three kilometers from each other. The sites were selected where Hudiyara drain water is being used for irrigating fodder crops and these fodder crops are being grazed by the cattles.

Water samples were collected directly from the Hudiyara drain and also from the tube wells installed at the banks of Hudiyara drain and the tube wells directly pumping the water of Hudiyara drain and using it for irrigating of fodder crops. Water samples were collected from different points within the distance of 3 kilometers. Five water samples were collected from each site. Water samples were collected in Polythene bottles washed with distilled water

and dried. The water samples were filtered through Whatman filter paper no 42 and acidified with few drops of 1 N Nitric Acid and stored for further analyses in clean polythene bottles washed with distilled water. These samples were properly labeled, for storage and further analyses. Leaves samples of Fodder crops, Berseem, Bajra, Maize and Oat were collected from the fields irrigated with the tube wells directly pumping the water of Hudiyara drain and also from the tube wells installed near the banks of Hudiyara drain. Fodder crops samples were collected from three different points of a site within the distance of 3 kilometers. Leaves samples were washed with distilled water, dried with blotting paper. Then the samples were air dried and then dried in oven till constant weight. The fodder crops samples were digested with double acid mixture in fume hood and were stored for analyses after making required volume.

The stored water and plant samples were subjected to heavy metals analyses including Lead, Cadmium, Chromium, Nickel, Zinc, Iron, Copper and Manganese on Atomic Absorption Spectrophotometer [8] and were compared with Maximum Recommended Concentrations. The data was also subjected to mean and percentage.

III. RESULTS AND DISCUSSION

HEAVY METALS CONTAMINATION IN HUDIARA DRAIN WATER

Heavy metals including Lead, Cadmium, Chromium, Nickel, Zinc, Iron, Copper and Manganese contamination showed quite a large variation in Hudiyara drain water (Table 1 and 2) and data was classified into safe and unsafe samples for irrigation considering the MRCs (Maximum Recommended Concentrations) provided by Food and Agriculture Organization (1985).

Lead contents in Hudiyara drain water ranged from 0.01 mg L⁻¹ to 0.15 mg L⁻¹ and all the water samples were below the Maximum Recommended Concentrations recommended by Food and Agriculture Organization

(1985). Hence, Lead pollution was not found in Hudiara drain water regarding irrigation. Whereas, Cadmium contamination was shown in Hudiara drain water. Cadmium contents in Hudiara drain ranged from 0.03 mg L⁻¹ to 0.18 mg L⁻¹ and all the samples were above the Maximum Recommended Concentrations given by FAO [9]. Chromium contents in Hudiara drain water showed a large variation and contents ranged from 0.02 mg L⁻¹ to 0.17 mg L⁻¹. The data was classified into safe and unsafe considering the Maximum Recommended Concentrations given by FAO (1985) and data showed that 37 samples being 74% were safe and remaining 13 (26%) samples were unsafe for irrigation according to the guidelines of FAO. Similarly, Nickel contamination in Hudiara drain water also showed huge variation and contents ranged from 0.07 mg L⁻¹ to 0.93 mg L⁻¹. The data was classified into safe and unsafe regarding Nickel contamination considering the Maximum Recommended Concentrations given by FAO (1985) and data showed that 5 samples being 10% were safe and remaining 45 (90%) samples were unsafe considering the guidelines of FAO. Zinc contents in Hudiara drain water ranged from 0.03 mg L⁻¹ to 0.19 mg L⁻¹ and all the water samples were below the Maximum Recommended Concentrations recommended by Food and Agriculture Organization (1985). Hence, Zinc pollution was not found in Hudiara drain water regarding irrigation. Whereas, Iron contamination was shown in Hudiara drain water. Iron contents in Hudiara drain ranged from 2.1 mg L⁻¹ to 8.7 mg L⁻¹ and 54% samples were below the Maximum Recommended Concentrations given by FAO (1985) and

46% were above. Copper contents in Hudiara drain water showed a large variation and contents ranged from 0.03 mg L⁻¹ to 0.42 mg L⁻¹. The data was classified into safe and unsafe considering the Maximum Recommended Concentrations given by FAO (1985) and data showed that 50% samples were safe and remaining 50% samples were unsafe for irrigation according to the guidelines of FAO. Manganese contamination in Hudiara drain water also showed huge variation and contents ranged from 0.11 mg L⁻¹ to 0.90 mg L⁻¹. The data was classified into safe and unsafe regarding Nickel contamination considering the Maximum Recommended Concentrations given by FAO (1985) and data showed that 41 samples being 82% were safe and remaining 18% samples were unsafe considering the guidelines of FAO.

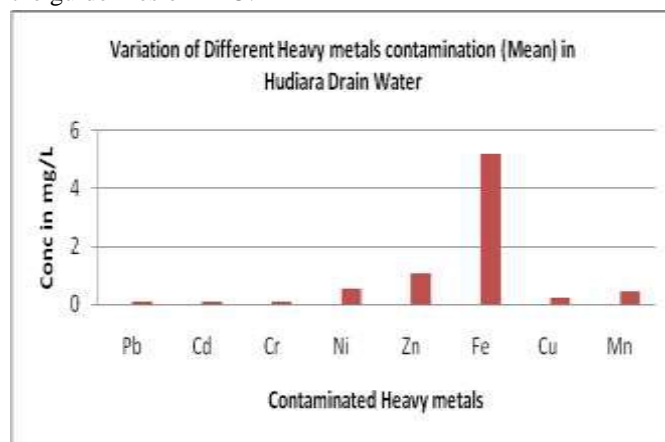


Fig.2: Variation of Different Heavy metals contamination (Mean) in Hudiara Drain Water.

Table.1: Heavy Metals Contamination (Mg/L) In Hudiara Drain Water

S. No	Site	Pb	Cd	Cr	Ni	Zn	Fe	Cu	Mn
1.	Site 1	0.03	0.13	0.07	0.60	1.1	2.1	0.12	0.31
2.		0.09	0.06	0.03	0.76	1.9	4.9	0.21	0.35
3.		0.15	0.07	0.05	0.52	0.03	4.4	0.32	0.71
4.		0.13	0.03	0.10	0.93	1.5	2.2	0.14	0.11
5.		0.07	0.04	0.15	0.21	0.04	7.2	0.01	0.27
6.	Site 2	0.09	0.12	0.12	0.75	1.4	5.4	0.06	0.76
7.		0.05	0.18	0.07	0.87	1.8	4.3	0.23	0.62
8.		0.07	0.10	0.05	0.62	0.09	6.3	0.15	0.37
9.		0.13	0.11	0.06	0.73	1.3	7.2	0.03	0.13
10.		0.12	0.09	0.02	0.86	1.7	5.4	0.34	0.26
11.	Site 3	0.11	0.03	0.08	0.22	0.06	6.4	0.45	0.79
12.		0.09	0.04	0.09	0.82	1.3	5.2	0.17	0.62
13.		0.04	0.09	0.06	0.31	1.2	6.0	0.07	0.82
14.		0.03	0.12	0.07	0.29	0.09	7.2	0.04	0.30
15.		0.09	0.15	0.09	0.71	1.8	8.7	0.24	0.15
16.	Site 4	0.12	0.03	0.12	0.82	0.07	7.4	0.37	0.23
17.		0.10	0.05	0.13	0.64	1.5	5.2	0.42	0.52
18.		0.14	0.12	0.03	0.53	1.1	4.0	0.18	0.61

19.	Site 5	0.13	0.11	0.09	0.72	0.08	6.5	0.05	0.42
20.		0.15	0.09	0.15	0.81	1.3	4.2	0.25	0.19
21.		0.01	0.12	0.07	0.60	1.2	4.3	0.32	0.29
22.		0.04	0.16	0.06	0.41	0.03	2.6	0.08	0.90
23.		0.12	0.10	0.09	0.52	1.4	6.2	0.02	0.67
24.		0.10	0.02	0.17	0.79	1.9	7.5	0.19	0.17
25.	0.15	0.03	0.08	0.80	0.05	5.2	0.41	0.19	
26.	Site 6	0.09	0.05	0.03	0.43	1.5	4.1	0.09	0.62
27.		0.06	0.07	0.13	0.74	1.4	6.8	0.24	0.25
28.		0.07	0.07	0.15	0.32	1.6	3.2	0.42	0.71
29.		0.12	0.12	0.06	0.42	1.7	5.0	0.10	0.62
30.		0.05	0.03	0.09	0.12	1.4	7.2	0.21	0.82
31.	Site 7	0.10	0.04	0.13	0.21	0.06	3.6	0.06	0.21
32.		0.13	0.05	0.05	0.83	1.4	5.1	0.19	0.13
33.		0.01	0.09	0.06	0.07	1.8	7.8	0.25	0.23
34.		0.03	0.12	0.09	0.41	0.07	3.5	0.30	0.65
35.		0.05	0.13	0.05	0.23	1.5	4.2	0.43	0.32
36.	Site 8	0.09	0.15	0.12	0.84	1.9	5.1	0.07	0.15
37.		0.12	0.09	0.04	0.73	1.6	7.2	0.15	0.90
38.		0.13	0.06	0.14	0.62	0.09	3.9	0.42	0.76
39.		0.15	0.03	0.03	0.08	1.9	4.5	0.27	0.62
40.		0.13	0.03	0.06	0.51	1.6	6.7	0.37	0.21
41.	Site 9	0.14	0.07	0.11	0.85	0.08	4.0	0.08	0.17
42.		0.06	0.03	0.07	0.79	1.2	5.2	0.13	0.82
43.		0.03	0.04	0.04	0.08	1.7	6.8	0.39	0.43
44.		0.11	0.05	0.02	0.09	1.6	3.8	0.41	0.22
45.		0.09	0.06	0.03	0.87	0.03	6.2	0.09	0.75
46.	Site 10	0.06	0.07	0.10	0.69	1.3	3.7	0.12	0.50
47.		0.01	0.10	0.03	0.15	1.8	4.2	0.32	0.20
48.		0.07	0.12	0.09	0.46	0.04	4.3	0.29	0.41
49.		0.06	0.09	0.06	0.55	1.4	3.9	0.12	0.55
50.		0.06	0.08	0.08	0.39	1.7	4.2	0.27	0.26
Average		0.087	0.0806	0.0792	0.5464	1.0862	5.204	0.2132	0.4454
MRCs*		5.0	0.01	0.10	0.20	2.0	5.0	0.20	0.20
No. of samples Safe		50 (100%)	0 (0%)	37 (74%)	5 (10%)	0/50 (0%)	27/50 (54%)	25/50 (50%)	41/50 (82%)
No. of samples Unsafe		0 (0%)	50 (100%)	13 (26%)	45 (90%)	50/50 (100%)	23/50 (46%)	25/50 (50%)	9/50 (18%)

*Maximum Recommended Concentrations in Irrigation water (FAO, 1985)

Table.2: Site Wise Comparisons of Heavy Metals in Hudiara Drain Water.

	Pb	Cd	Cr	Ni	Zn	Fe	Cu	Mn
Site 1	0.094	0.066	0.08	0.604	0.9	4.16	0.16	0.35
Site 2	0.092	0.12	0.064	0.766	1.26	5.72	0.17	0.43
Site 3	0.072	0.086	0.078	0.47	0.89	6.7	0.19	0.54
Site 4	0.128	0.080	0.104	0.704	0.81	5.46	0.25	0.39
Site 5	0.084	0.086	0.094	0.624	0.92	5.16	0.20	0.44
Site 6	0.078	0.068	0.092	0.406	1.52	5.26	0.21	0.60

Site 7	0.064	0.086	0.076	0.35	0.97	4.84	0.25	0.31
Site 8	0.124	0.072	0.078	0.556	1.42	5.48	0.26	0.53
Site 9	0.086	0.086	0.054	0.536	0.92	5.2	0.22	0.48
Site 10	0.052	0.052	0.072	0.448	1.25	4.06	0.22	0.38

Table.3: Descriptive Statistics of Different Elements in Hudiara Drain

	Mean	Std. Deviation	N
Pb	.0874	.04135	50
Cd	.0836	.03963	50
Cr	.0792	.03870	50
Ni	.5464	.26059	50
Zn	1.0862	.70755	50
Fe	5.2040	1.55037	50
Cu	.2132	.13168	50
Mn	.4162	.24025	50

In table 3 a low standard deviation indicates that the points are close to the mean and the expected value of the set close to the actual value.

Table.4: Correlation between the Heavy Metals of Hudiara Drain

		Pb	Cd	Cr	Ni	Zn	Fe	Cu	Mn
Pb	Pearson Correlation	1	.341*	.085	.396**	-.111	.022	.033	-.029
	Sig. (2-tailed)		.015	.555	.004	.444	.879	.822	.841
Cd	Pearson Correlation	.341*	1	.092	.354*	.054	.035	-.053	-.096
	Sig. (2-tailed)	.015		.523	.012	.710	.808	.716	.508
Cr	Pearson Correlation	.085	.092	1	.217	-.178	.057	-.045	-.163
	Sig. (2-tailed)	.555	.523		.129	.216	.695	.756	.258
Ni	Pearson Correlation	.396**	.354*	.217	1	-.014	-.011	-.215	-.079
	Sig. (2-tailed)	.004	.012	.129		.925	.942	.134	.587
Zn	Pearson Correlation	-.111	.054	-.178	-.014	1	.048	.090	-.064
	Sig. (2-tailed)	.444	.710	.216	.925		.742	.535	.657
Fe	Pearson Correlation	.022	.035	.057	-.011	.048	1	-.074	-.148
	Sig. (2-tailed)	.879	.808	.695	.942	.742		.612	.304
Cu	Pearson Correlation	.033	-.053	-.045	-.215	.090	-.074	1	-.107
	Sig. (2-tailed)	.822	.716	.756	.134	.535	.612		.458
Mn	Pearson Correlation	-.029	-.096	-.163	-.079	-.064	-.148	-.107	1
	Sig. (2-tailed)	.841	.508	.258	.587	.657	.304	.458	
		*. Correlation is significant at the 0.05 level (2-tailed).							
		**. Correlation is significant at the 0.01 level (2-tailed).							

In table 4 there is positive correlation between lead (Pb⁺²) with cadmium (Cd⁺²), chromium Cr⁺³, Nickel (Ni⁺²). There is negative correlation between lead (Pb⁺²) with Zinc (Zn⁺²), manganese (Mn⁺²). There is weak positive correlation between Cd⁺² with Pb⁺², Ni⁺², Zn⁺², Fe⁺², Cr⁺³ where there is negative correlation among copper (Cu⁺²) and (Cd⁺²). There is positive correlation between

Cr⁺³ with Pb⁺², Cd⁺², Ni⁺², Fe⁺², Cu⁺² where there is negative correlation between Cr⁺³ between with Mn⁺² and Zn⁺². There is positive correlation between Ni⁺² with Pb⁺², Cd⁺², Cr⁺³, Zn⁺². Where there is negative correlation between Ni⁺² with Fe⁺², Cu⁺², Mn⁺². There is positive correlation between Zn⁺² with Cd⁺², Ni⁺², Fe⁺², Cu⁺² and Mn⁺². There is positive correlation between Fe⁺² with

Pb⁺², Cd⁺², Cr⁺², Zn⁺² and negative correlation between Fe⁺² and Ni⁺², Cu⁺² and Mn⁺². There is positive correlation between Cu⁺² with Pb⁺², Zn⁺². There is negative correlation between Mn⁺² and Pb⁺², Cd⁺², Cr⁺³, Ni⁺², Fe⁺², Cu⁺².

HEAVY METALS CONTAMINATION IN FODDER CROPS SAMPLES IRRIGATED WITH HUDIARA DRAIN WATER

Heavy metals including Lead, Cadmium, Chromium, Nickel, Zinc, Iron, Copper and manganese contamination in fodder crops irrigated with Hudiara drain water given in Table 3 & 4 showed quite a large variation and data was classified into safe and unsafe samples considering the Critical levels described by Asaolu [10] and WHO [11]. Lead contents in fodder crops irrigated with Hudiara drain water ranged from 0.2 mg kg⁻¹ to 4.2 mg kg⁻¹ and 50% (15 No.) samples were below the Critical levels recommended by Asaolu. Hence, Lead pollution was found in fodder crops irrigated with Hudiara drain water. Cadmium contamination was shown in fodder crops irrigated with Hudiara drain water as the Hudiara drain water was contaminated with Cadmium and that depicted in fodder crops irrigated with Hudiara drain.

Cadmium contents in Hudiara drain irrigated fodder crops ranged from 0.7 mg kg⁻¹ to 3.1 mg kg⁻¹ and all the samples were above the Critical levels described by WHO (1996). Chromium contents in fodder crops irrigated with Hudiara drain water showed contamination and contents ranged from 4.0 mg kg⁻¹ to 32.0 mg kg⁻¹. The data was classified into safe and unsafe considering the Critical levels described by Asaolu (1995) and data showed that all samples were unsafe according to the guidelines given by Asaolu (1995). Nickel contamination in Hudiara drain water irrigated fodder crops also showed variation and contents ranged from 4.0 mg kg⁻¹ to 16.2 mg kg⁻¹. The data was classified into safe and unsafe regarding Nickel contamination considering the critical levels given by WHO (1996) and data showed that 19 (63.4%) samples were safe and remaining 11 (36.7%) samples were unsafe.

Zinc contents in fodder crops irrigated with Hudiara drain water ranged from 4.0 mg kg⁻¹ to 64.0 mg kg⁻¹ and 17% samples were below the Critical levels recommended by Soltanpur (1985). Hence, Zinc pollution was found in fodder crops irrigated with Hudiara drain water. Iron contamination was shown in fodder crops irrigated with Hudiara drain water ranged from 1000 mg kg⁻¹ to 3801 mg kg⁻¹ and all the samples were above the critical levels described by Soltanpur (1985). Copper contents in fodder crops irrigated with Hudiara drain water showed contamination and contents ranged from 50 mg kg⁻¹ to 319 mg kg⁻¹. The data was classified into safe and unsafe considering the critical levels described by Soltanpur (1985) and data showed that all samples were unsafe

according to the guidelines given by Soltanpur (1985). Manganese contamination in Hudiara drain water irrigated fodder crops also showed variation and contents ranged from 25 mg kg⁻¹ to 140 mg kg⁻¹. The data was classified into safe and unsafe regarding Nickel contamination considering the critical levels given by Soltanpur (1985) and data showed that all samples were unsafe.

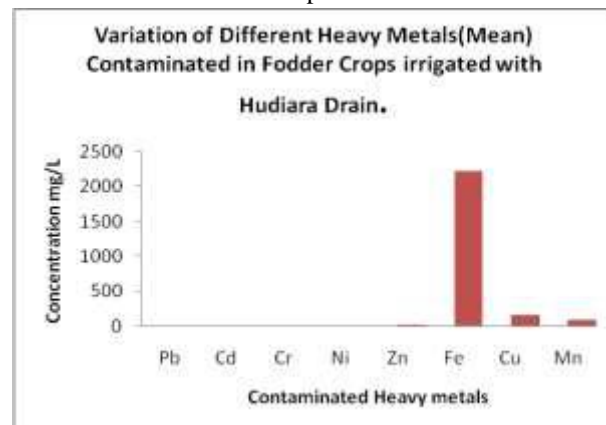


Fig.3: Variation of Different Heavy Metals (Mean) Contaminated in Fodder Crops irrigated with Hudiara Drain.

Cadmium contents in Hudiara drain irrigated fodder crops ranged from 0.7 mg kg⁻¹ to 3.1 mg kg⁻¹ and all the samples were above the Critical levels described by WHO (1996). Chromium contents in fodder crops irrigated with Hudiara drain water showed contamination and contents ranged from 4.0 mg kg⁻¹ to 32.0 mg kg⁻¹. The data was classified into safe and unsafe considering the Critical levels described by Asaolu (1995) and data showed that all samples were unsafe according to the guidelines given by Asaolu (1995). Nickel contamination in Hudiara drain water irrigated fodder crops also showed variation and contents ranged from 4.0 mg kg⁻¹ to 16.2 mg kg⁻¹. The data was classified into safe and unsafe regarding Nickel contamination considering the critical levels given by WHO (1996) and data showed that 19 (63.4%) samples were safe and remaining 11 (36.7%) samples were unsafe. Zinc contents in fodder crops irrigated with Hudiara drain water ranged from 4.0 mg kg⁻¹ to 64.0 mg kg⁻¹ and 17% samples were below the Critical levels recommended by Soltanpur (1985). Hence, Zinc pollution was found in fodder crops irrigated with Hudiara drain water. Iron contamination was shown in fodder crops irrigated with Hudiara drain water ranged from 1000 mg kg⁻¹ to 3801 mg kg⁻¹ and all the samples were above the Critical levels described by Soltanpur (1985). Copper contents in fodder crops irrigated with Hudiara drain water showed contamination and contents ranged from 50 mg kg⁻¹ to 319 mg kg⁻¹. The data was classified into safe and unsafe considering the Critical levels described by Soltanpur (1985) and data showed that all samples were unsafe

according to the guidelines given by Soltanpur (1985). Manganese contamination in Hudiarra drain water irrigated fodder crops also showed variation and contents ranged from 25 mg kg⁻¹ to 140 mg kg⁻¹. The data was classified

into safe and unsafe regarding Nickel contamination considering the critical levels given by Soltanpur (1985) and data showed that all samples were unsafe.

Table.5: Heavy Metals Contamination in Fodder Crops Irrigated with Hudiarra Drain

S. No	Site	Pb	Cd	Cr	Ni	Zn	Fe	Cu	Mn
1	Site 1	2.4	0.8	4.2	10.2	15.2	2502	131	71
2		3.7	1.8	12.0	5.9	20.1	2851	202	121
3		1.9	2.6	21.5	4.5	25.4	1215	217	109
4	Site 2	1.8	1.2	25.4	12.4	45.2	1527	117	127
5		0.2	2.7	27.3	4.9	59.5	2215	319	85
6		2.6	2.9	4.9	5.2	4.0	1000	145	121
7	Site 3	2.0	3.1	14.4	4.9	16.4	2973	50	37
8		1.7	1.9	23.2	11.7	27.8	1259	151	82
9		0.6	0.9	27.0	5.3	47.0	1571	209	121
10	Site 4	2.7	1.6	29.2	8.1	60.2	1210	201	125
11		3.9	3.0	9.2	5.6	4.6	2413	52	25
12		1.6	2.8	25.7	12.9	17.2	2581	177	90
13	Site 5	0.7	3.0	28.5	7.6	29.0	1107	301	119
14		2.9	0.8	25.4	6.2	49.5	1505	215	127
15		2.5	2.0	16.2	13.2	64.0	2619	91	42
16	Site 6	0.5	1.5	5.2	7.2	4.9	3801	181	77
17		1.4	2.1	27.8	6.7	19.4	2504	231	137
18		3.0	0.7	29.5	14.5	31.5	1709	99	131
19	Site 7	4.1	2.2	30.2	9.1	50.4	2425	192	41
20		0.9	2.1	6.7	7.1	61.5	2725	245	92
21		1.2	2.8	17.5	15.6	4.5	3235	201	139
22	Site 8	3.3	1.2	29.5	8.9	20.5	3445	257	57
23		3.9	2.3	32.0	8.5	33.3	1959	137	103
24		0.8	1.9	7.2	16.2	54.2	2231	125	140
25	Site 9	1.9	2.5	9.7	12.8	25.4	1905	110	59
26		4.2	1.5	18.2	9.6	4.7	2125	212	109
27		2.1	2.5	31.5	15.7	21.2	2702	258	140
28	Site 10	1.0	1.6	20.5	10.5	39.4	1702	129	63
29		3.5	2.3	10.1	9.5	32.5	3199	102	117
30		3.7	1.7	16.1	12.5	4.8	2506	125	51
Average		2.23	2.0	19.53	9.43	29.77667	2224.033	172.7333	95.26667
Critical Levels		2.0*	0.02**	1.30*	10.00**	5.0	150.0	10.00	6.61
No. of samples Safe		15 (50%)	0 (0%)	0 (0%)	19 (63.4%)	6/30 (20%)	0/30 (0%)	0/30 (0%)	0/30 (0%)
No. of samples Unsafe		15 (50%)	30 (100%)	30 (100%)	11 (36.7%)	24/30 (80%)	30/30 (100%)	30/30 (100%)	30/30 (100%)

Source: * Asaolu, 1995; ** WHO, 1996.

Table.6: Site Wise Comparison of Heavy Metals in Hudiarra Drain Irrigated Fodder Crops

	Pb	Cd	Cr	Ni	Zn	Fe	Cu	Mn
Site 1	2.67	1.73	12.56	6.87	20.23	2189.33	183.33	100.33
Site 2	1.53	2.27	19.2	7.5	36.23	1580.66	193.36	111.0
Site 3	1.43	1.97	21.53	7.3	30.4	1934.3	136.66	80.0
Site 4	2.73	2.47	21.36	8.87	27.33	2068.0	143.33	80.0

Site 5	2.03	1.93	23.36	9.0	47.5	1743.66	202.33	96.0
Site 6	1.63	1.43	20.83	9.47	18.6	2671.33	170.33	115.0
Site 7	2.07	2.37	18.13	10.6	38.8	2795.0	212.66	90.6
Site 8	2.67	1.8	22.9	11.2	36.0	2545.0	173.00	100.0
Site 9	2.73	2.17	19.8	12.7	17.1	2244.0	193.33	102.66
Site 10	2.73	1.87	15.56	10.83	25.57	2469.0	118.66	77.0

Table.7: Descriptive Statistics of Heavy Metals in Hudiaara Drain Irrigated Fodder Crops.

Metals in Fodder Crop	Mean	Std. Deviation	N
Pb	2.3733	1.25861	30
Cd	2.2400	1.28321	30
Cr	19.5267	9.22945	30
Ni	9.4333	3.59015	30
Zn	29.7633	19.29190	30
Fe	2.2240	739.31718	30
Cu	1.7273	68.19897	30
Mn	95.2667	35.44197	30

In table 7 a low standard deviation of Pb²⁺, Cd²⁺, Cr³⁺, Ni²⁺ and Zn²⁺ indicates that the points are close to the mean and the expected value of the set close to the actual value. Where high standard deviation of Cu²⁺ and Mn²⁺ indicates that the points are not close to the mean and the expected values are not to the actual value. In table 8 there is positive correlation between Pb²⁺ and Fe²⁺ where there is negative correlation between Pb²⁺ and Cr²⁺, Cd²⁺, Ni²⁺, Zn²⁺, Cu²⁺, Mn²⁺. There is positive correlation between

Cr²⁺ and Cd²⁺, Ni²⁺, Zn²⁺, Cu²⁺, Mn²⁺. In case of Ni²⁺ there is negative correlation between Ni²⁺ and Cu²⁺, Pb²⁺, Cd²⁺ where there is positive correlation between Ni²⁺ and Zn²⁺, Cr²⁺, Fe²⁺, Mn²⁺. In case of Zn²⁺ there is positive correlation between Zn²⁺ and Cd²⁺, Cr²⁺, Ni²⁺, Cu²⁺, Mn²⁺ where there is negative correlation between Pb²⁺ and Cu²⁺. There is positive correlation between Fe²⁺ and Pb²⁺, Ni²⁺ where there is negative correlation Fe²⁺ and Cd²⁺, Cr²⁺, Zn²⁺, Cu²⁺, Mn²⁺.

Table.8: Correlation of Heavy Metals in Hudiaara Drain Irrigated Fodder Crops.

		Pb	Cd	Cr	Ni	Zn	Fe	Cu	Mn
Pb	Pearson Correlation	1	-.031	-.143	-.092	-.398*	.331	-.303	-.280
	Sig. (2-tailed)		.870	.452	.629	.030	.074	.104	.135
Cd	Pearson Correlation	-.031	1	.059	-.248	.072	-.154	.131	.082
	Sig. (2-tailed)	.870		.758	.186	.706	.417	.489	.665
Cr	Pearson Correlation	-.143	.059	1	.057	.288	-.299	.436*	.235
	Sig. (2-tailed)	.452	.758		.764	.122	.108	.016	.212
Ni	Pearson Correlation	-.092	-.248	.057	1	.006	.143	-.240	.151
	Sig. (2-tailed)	.629	.186	.764		.973	.451	.202	.425
Zn	Pearson Correlation	-.398*	.072	.288	.006	1	-.277	.171	.095
	Sig. (2-tailed)	.030	.706	.122	.973		.138	.367	.619
Fe	Pearson Correlation	.331	-.154	-.299	.143	-.277	1	-.049	-.285
	Sig. (2-tailed)	.074	.417	.108	.451	.138		.797	.127
Cu	Pearson Correlation	-.303	.131	.436*	-.240	.171	-.049	1	.391*
	Sig. (2-tailed)	.104	.489	.016	.202	.367	.797		.033
Mn	Pearson Correlation	-.280	.082	.235	.151	.095	-.285	.391*	1
	Sig. (2-tailed)	.135	.665	.212	.425	.619	.127	.033	

In table 8 there is positive correlation between Pb²⁺ and Fe²⁺ where there is negative correlation between Pb²⁺ and Cr²⁺, Cd²⁺, Ni²⁺, Zn²⁺, Cu²⁺, Mn²⁺. There is positive

correlation between Cr²⁺ and Cd²⁺, Ni²⁺, Zn²⁺, Cu²⁺, Mn²⁺. In the case of Ni²⁺ there is negative correlation between Ni²⁺ and Cu²⁺, Pb²⁺, Cd²⁺ where there is positive

correlation between Ni^{+2} and Zn^{+2} , Cr^{+2} , Fe^{+2} , Mn^{+2} . In the case of Zn^{+2} there is positive correlation between Zn^{+2} and Cd^{+2} , Cr^{+2} , Ni^{+2} , Cu^{+2} , Mn^{+2} where there is negative

correlation between Pb^{+2} and Cu^{+2} . There is correlation between Fe^{+2} and Pb^{+2} , Ni^{+2} where there is negative correlation Fe^{+2} and Cd^{+2} , Cr^{+2} , Zn^{+2} , Cu^{+2} , Mn^{+2} .

Table.9: Correlation between the Heavy Metals of Hudiaara Drain and Fodder Copper Irrigated with Heavy Metals.

		Pb	Cd	Cr	Ni	Zn	Fe	Cu	Mn
Pb Fodder Crop	Pearson Correlation	.128	.172	-.378*	-.101	-.155	.056	-.011	.314
	Sig. (2-tailed)	.499	.364	.039	.595	.414	.767	.954	.091
Cd Fodder Crop	Pearson Correlation	-.318	-.257	.050	-.257	-.273	.320	-.118	-.137
	Sig. (2-tailed)	.086	.170	.792	.170	.144	.084	.535	.471
Cr Fodder Crop	Pearson Correlation	-.052	-.344	-.204	-.151	-.103	.046	-.296	.132
	Sig. (2-tailed)	.783	.062	.279	.425	.590	.810	.113	.487
Ni Fodder Crop	Pearson Correlation	-.131	-.189	.116	.160	.247	-.013	.118	-.259
	Sig. (2-tailed)	.492	.318	.540	.398	.188	.945	.533	.167
Zn Fodder Crop	Pearson Correlation	.306	.045	.219	.157	.083	.243	-.223	-.298
	Sig. (2-tailed)	.100	.815	.246	.408	.665	.196	.236	.110
Fe Fodder Crop	Pearson Correlation	-.189	.064	.169	.077	.028	-.016	.188	-.040
	Sig. (2-tailed)	.317	.738	.373	.687	.881	.932	.319	.835
Cu Fodder Crop	Pearson Correlation	-.192	-.464**	.090	-.151	-.225	.069	-.279	-.048
	Sig. (2-tailed)	.309	.010	.637	.427	.231	.716	.135	.801
Mn Fodder Crop	Pearson Correlation	.042	-.278	-.038	.196	.355	-.057	-.177	-.068
	Sig. (2-tailed)	.827	.137	.841	.299	.055	.763	.348	.720

In the above table the Pb^{+2} of Hudiaara drain and irrigated Pb^{+2} of fodder crop there positive correlation where there is also correlation Pb^{+2} of Hudiaara drain water and fodder crop irrigated with Hudiaara drain water and negative correlation between Pb^{+2} and Cr^{+2} , Ni^{+2} , Cu^{+2} . There is positive correlation between Cd^{+2} and Cr^{+2} , Fe^{+2} and also negative correlation between Cd^{+2} and Pb^{+2} , Cd^{+2} , Ni^{+2} , Zn^{+2} , Cu^{+2} , Mn^{+2} of fodder crop irrigated with Hudiaara drain.

Some of the heavy metals are essential and some are even not essential for plant growth but after accumulating in the soil are transferred to food chain [4]. These metal ions are either themselves toxic to biological organisms or induce deficiency of others [13]. These metals have their permissible limits quite low and show toxicity on plants, animals and human beings above their permissible limits [14]. Generally, our farmers are not aware of the metal ion toxicity being introduced into food chain by vegetables/crops grown with these polluted waters [15]. These heavy metals reduce the activity of hydrolysis viz., α amylase, phosphatase, RNase and proteins. They interfere in the enzyme action by replacing metal ions from the metalloenzymes. Among heavy metals cadmium shows severe effect on seedling length, dry weight, causes structural change in chloroplast, reduces photosystem-II activity, reduces process of photosynthesis, availability of carbon dioxide, reduce glycolipids, neutral lipids and total

lipids, lowers stomatal conductance, interfere membrane permeability and reduce respiration in leaves [12]. Toxic level of lead inhibits seed germination, reduces transpiration, reduce rate of photosynthesis, alters relative proportion of chlorophyll a and chlorophyll b, causes reduction in total chlorophyll production, and reduce gaseous exchange in leaves. Similarly toxicity of nickel and chromium showed drastic effect on dry matter production and crop yield [12].

IV. CONCLUSION

Sewage and Industrial wastes are big source of Heavy metals in drains, almost above the Maximum Recommended Concentrations and this water is used for irrigating fodder crops that causes exceeded amounts of Heavy metals, dangerous for animals and human's health. These heavy metals contaminated crops are grazed by cattles and cattle milk also have high quantities of these metals, which is also carcinogenic to human's health. Hence, it's the need of time to treat the contaminated water before throwing into drains or not to use this contaminated water for irrigation/drinking purpose, also the Government should emphasize and made regulations for this purpose.

REFERENCES

- [1] MB Aslam," Pollution abatement through effluent management. Proceedings of International

- Symposium on Agro-environmental issues and future Strategies towards 21st century". May, 25-30, Faisalabad, Pakistan 18-25, 1998.
- [2] A Ghafoor , A Rauf , W Muzaffar . "Trace Elements", J Drainage and Reclamation, 77:155, 1995.
- [3] K Ali, MA Javid , M Javid, "Pollution and industrial waste. 6th National Congress of Soil Science, Lahore", 122-131, 1996.
- [4] R Malla , Y Tanaka , K Mori , K L Totawat , " Short term effect of sewage irrigation on chemical buildup in soil and vegetables", The Agricultural Engineering. International CIGR Journal Manuscript 9:14 , 2007
- [5] S R Kashif , M Akram , M Yaseen ,S Ali "Studies on heavy metals status and their uptake by vegetables in adjoining areas of Hudiara drain in Lahore". Soil & Environ 28:7-12, 2009.
- [6] MI Latif , MI Lone , KS Khan , "Heavy metals contamination of different water sources, soil and vegetables in Rawalpindi area", Soil & Environ 27:29-35,2008.
- [7] W W F (2007) Report on National Surface Water Classification Criteria, Irrigation water Quality Guidelines for Pakistan.,Waste Water Forum Pakistan (2007).
- [8] AOAC Methods of Analysis by Association of Official Analytical Chemists. Washington DC, USA, 2000.
- [9] FAO, "Water quality for agriculture". UNESCO Publication, Rome 96, 1985
- [10] Asaolu , " Lead contents of vegetables and tomato at Erekesan Market, Ado-Ekiti", Pak J Sci Ind Res ,38:399-401, 1995
- [11] WHO Guidelines for drinking water quality, Health criteria and supporting information. 94/9960-Mastercom/ Wiener Verlag-800, Australia 1996.
- [12] SK Agarwal Pollution Management, Vol. IV, Heavy metal pollution. APH Publishing Company, New Delhi,2002
- [13] S Farid ,Toxic Elements concentration in vegetables irrigated with untreated city effluents. Science, Technol & Develop 22: 58-60, 2003.
- [14] A Rashid," Mapping zinc fertility of soils using indicator plants and soils analysis". PhD Dissertation, University of Hawaii, HI, USA 1986.
- [15] M Qadir , A Ghafoor , SI Hssain , G Murtaza , T Mahmood , " Copper concentration in city effluents irrigated soils and vegetables". Pak J Soil Sci 97-102, 1999.
- [16] AOAC Official methods of analysis.15th Edition, Arlington, Virginia, 22201, USA, 1984.

Design of a Pipeline Leakage Detection System

Maidala. A Y, Odujoko A.O., Sadjere E.G., Ariavie G.O

Department of Mechanical Engineering, University of Benin, Nigeria

Abstract— Pipeline leakage has both economical and environmental effect. This research work is aimed at the design of a pipeline leakage detection system. In this research work, pressure analysis and K-epsilon turbulence model is one of the common turbulence models used by star CCM+ in resolving fluid flow and is used in this simulation. The parameters used were velocity of fluid (crude oil and gas) and pressure. Different velocities (5m/s, 20m/s, etc.) were used to determined increase or drop pressure. The results from the research work show that excessive drop in pressure is as a result of pipeline leakage and this is mostly likely to occur at the highest bent in the pipeline.

Keywords—Pipeline leakage, Star CCM+, Pressure and Simulation.

I. INTRODUCTION

Hydrocarbons (CH), is a very important sources of energy and it is produced from oil or gas reservoirs. It comprises of carbon and it compound and it is main sources of crude oil. Even in intermediate processing of these hydrocarbons until they are present in useable form, there is requirement for at least one or two unit operations. The operations will require connections with one another through the aids of pipelines. Pipelines are media required for the transportation of crude oil from reservoir, wellbore and other stations to be delivered to destination point such as separator, storage tanks etc. Over time in operation, these pipelines due to ageing, corrosion and wear, design faults, operation outside design limit or deliberate damage in act of vandalism etc. are caused to leak (Teal, 2003). Considering the vast mileage of pipelines throughout the nation, it is vital that dependable leak detection systems are used to

promptly identify when a leak has occurred so that appropriate response actions are initiated quickly. The swiftness of these actions can help reduce the consequences of accidents or incidents to the public, environment, and facilities.

Leak detection systems capable of locating the position of the leak are obviously of an environmental kind. Considering the environment of oil spillage, the hazard of gas leakage, pipeline detection system design cannot be neglected. But the economical aspect of it is also important. In fact, pipeline leaks are also frequent problems to the producers and transporters of these hydrocarbons and failure to detect it can result in loss of life and facilities, direct cost of loss product and lie downtime, environmental cleanup cost and possible fines and legal suits from habitants. Various leak detection systems including both the hardware- and software- based methods are being employed by pipeline operators are in existence (Zhang, 1997; Wang et al., 2001; Theakston and Larnaes 2002; Liu et al. 2005; Batzias et al., 2011) and also biological based detection method. Of the hardware-based methods is the use of acoustics, fiber optics, ultrasonics, infrared radiometrics, vapour or liquid sensing tubes, and cable sensors, while mass/volume balance, transient modeling, statistical/hypothetical analysis, and pressure analysis are examples of software-based methods. By software-based detection methods, the leak is identified as a result of several detectable effects in terms of fluctuations in the monitoring pressures and/or flow rates (Mastandrea et al. 1990; Bonn 1998). Figure 1.1 shows classification of oil/gas Leak detection systems based on their technical nature.

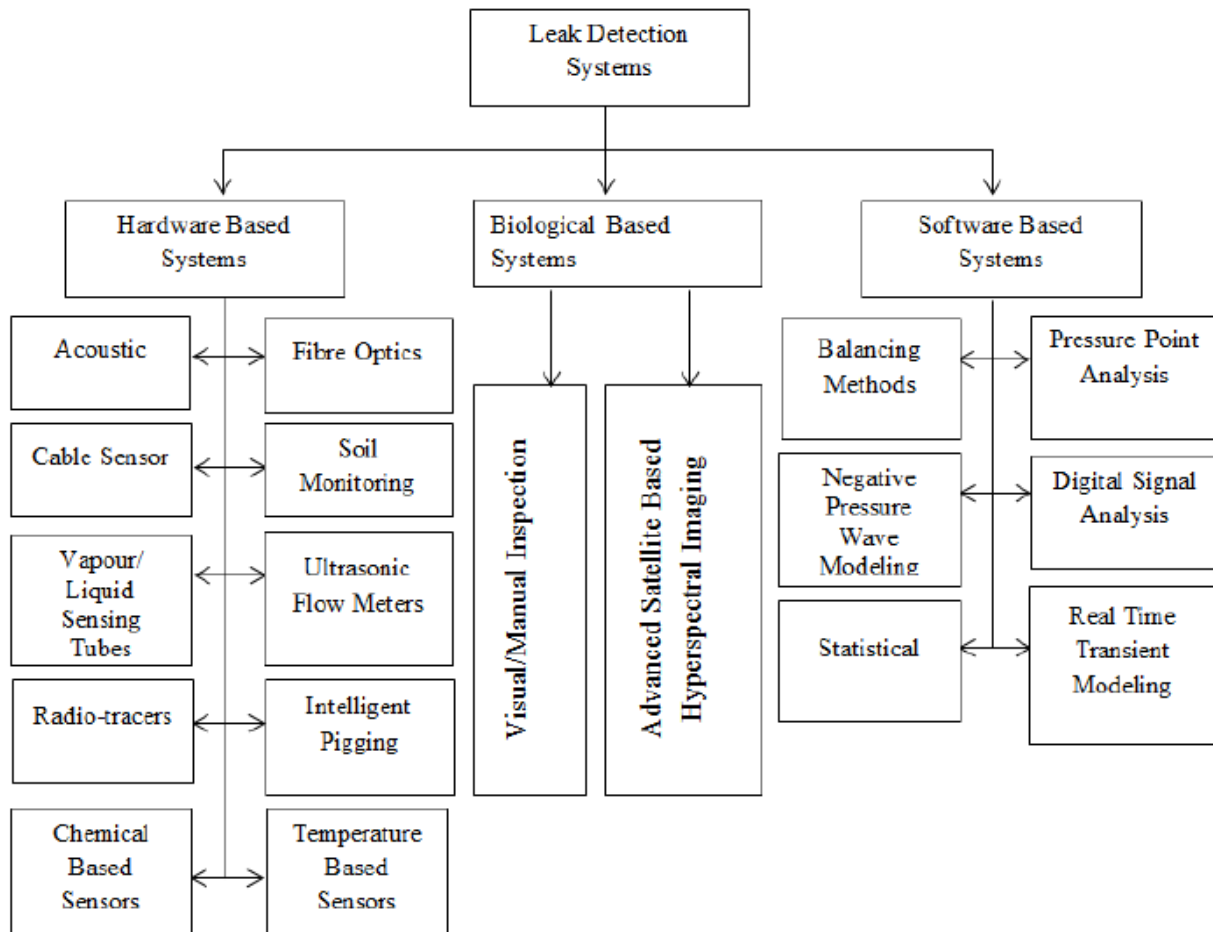


Fig.1.1: Classification of oil/gas Leak detection systems based on their technical nature

In this research work, pressure point analysis and K-epsilon turbulence model software will be used to model pipeline leakage detection system. The K-epsilon turbulence model is one of the common turbulence models used by Star CCM+ in resolving turbulent flow and is used in this simulation. The model is recommended for use for flows that assume net zero heat transfer but variation in pressure

(Cenjel, et al., 2012; Adapco, 2013). The letter “k” is the turbulent kinetic energy while ϵ is the rate of dispersion of the turbulent energy. K- Epsilon model resolves turbulence by finding the amount of kinetic energy per unit mass present in the turbulent fluctuations (Barati 2012; Scott-Pomerantz 2004). Table 1.1 shows the Star CCM+ Parameters used for the analysis.

II. RESEARCH METHODOLOGY

Table 2.1 shows the Star CCM+ Parameters used for the analysis.

Table.2.1: Star CCM+ Parameters used for the analysis (Janna 1993; Scott-Pomerantz 2004; Barati 2012)

	Parameter/Menu choice	Selection/ Value Inputted
Mesh Selection	Mesh type	Trimmer (for Volume Mesh); Surface Remesher (Surface mesh); Prism Layer Mesh (For the prism layer)
	Base size	15 mm
	Prism Layer thickness	Equal to the Boundary layer thickness for the given velocity
	Number of layers	20
	Prism layer stretching	1
Physics	Space	2D flow

Selection	Time	Steady
	Material	Gas
	Flow	Segregated flow
	Equation of State	Constant density
	Viscous Regime	Turbulent
	Reynolds-Averaged Turbulence	K-epsilon
Boundary condition selection	Inlet	Inlet Velocity
	Outlet	Outlet Pressure
	Wall	Wall
	Turbulent Intensity	10%
	Turbulence Specification	Intensity + Length scale
	Turbulent length scale	7% of the Hydraulic diameter
	Turbulent velocity scale	5% of the free steam velocity
	Temperature	293K
	Wall condition	No-slip

The pipeline was analyzed with fluid flow in a given duct to determine flow parameters and characteristics. The analysis was done in 2D using CFD package-Star CCM+ software. In general, flow in a two dimensional plane is considered as a special case of a 3D if the geometry is symmetrical in one coordinate (Jiyuan et al 2005). Experiments have shown that 2D models give a very close approximation to 3D

model for symmetrical model (Ekambara et al 2005).It has the following steps:

- i. Creation of the model in 3D (Figure 2.1). This could be done in star CCM+ or with CAE software and then imported to Star CCM+. Since the given model has a simple geometry, it was drawn in Star CCM+
- ii. The 3D model was then converted to part; follow by assigning of regions to parts (Figure 2.2).

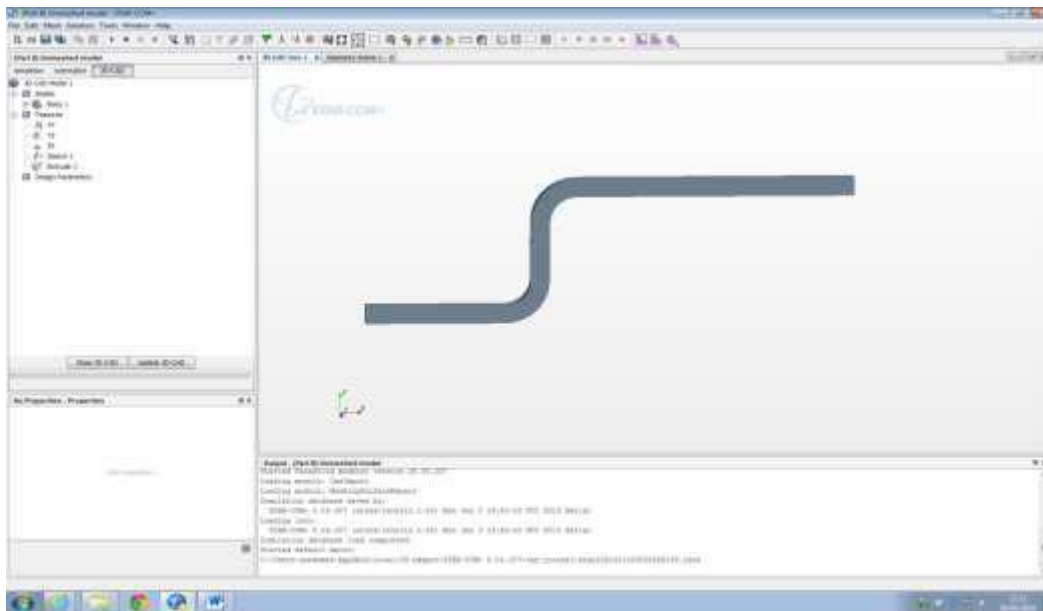


Fig.2.1: Creating the geometry in 3D

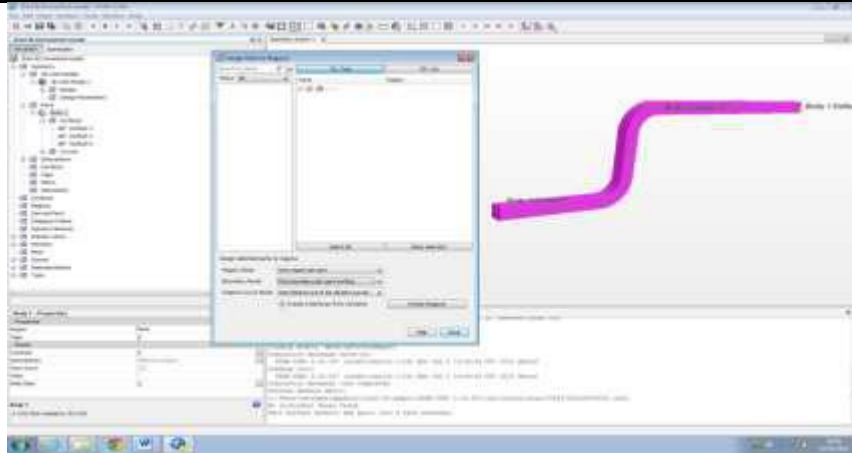


Fig.2.2: Creating the geometry in 3D

iii. The model was then meshed and converted to 2D.

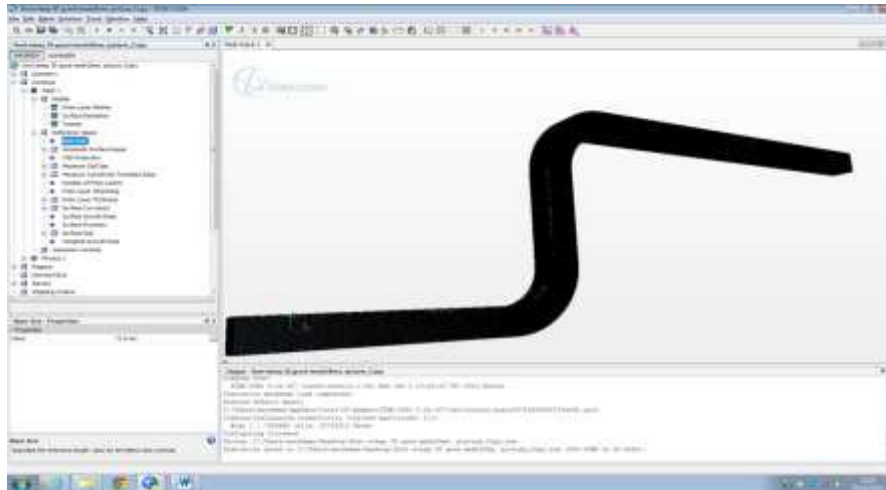


Fig.2.3: Creation of 3D mesh

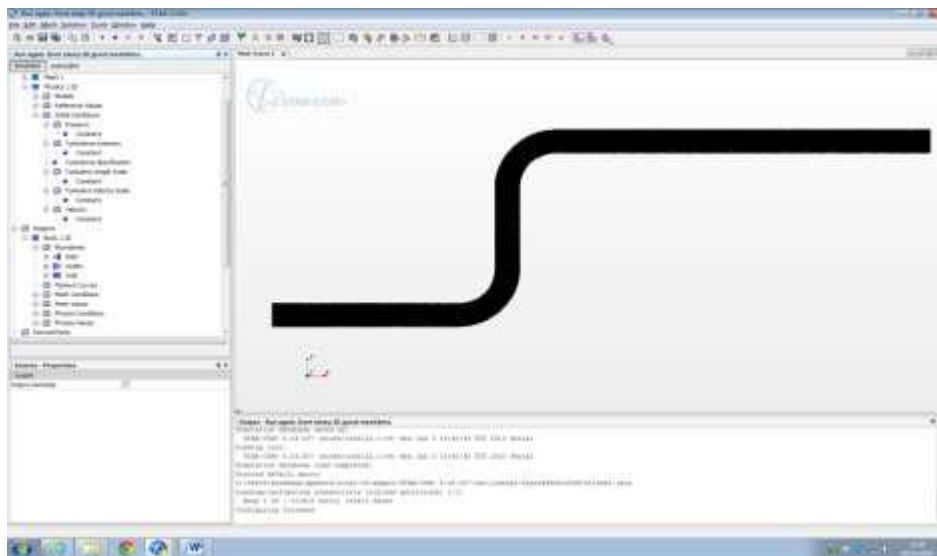


Fig.2.4: Converting 3D mesh to 2D mesh

- iv. The next step was setup the physics for the simulation after which the boundary conditions were specified.
- v. Running of simulation and post –processing in which the result obtained was analyze

solution of the computation. Due to the length of time required to obtain solutions using fine mesh, initial analyses were done using coarse mesh. The mesh size was gradually refined until convergence was achieved. Another important parameter which affects the result obtained from the simulation is the number of iteration to convergence. The iteration steps were increased until the results obtained are stabilized(i.e.when the results no longer change with time).

A number of iterations were done until convergence was achieved. Analysis in CFD is affected by the number of grid points (cells) generated to solve the computation. The number of cell generated is a function of the mesh size. Generally, as the number of cells is increased, the results obtained become more accurate while the computational time increases also. However as the mesh size is made finer and the number of cells increased, a point is reached when the results obtained is not or is marginally affected by the mesh size. At the point the mesh is said to have converged. The results obtained at this point are usually taken as the

III. RESULTS AND DISCUSSION

Table 3.1 shows the result of mesh convergence study at 20m/s. With a velocity of 20m/s, the solution was found to convergence at a mesh size of 15mm. At that speed of movement of fluid inside the pipeline, pressure drop is taken note of. A drop in pressure is as result of leakage along the pipeline.

Table.3.1: Mesh convergence study at 20m/s

Mesh Size (mm)	Number of Cells (2D)	Total inlet Pressure (Pa)	Inlet Static pressure (Pa)	Max. Mass flow rate at the inlet (Kg/s)	Number of steps taken to stabilize
50	69633	1797.693	143.6292	9.6	2600
40	85628	371.0221	131.0221	9.6	2800
20	105498	399.6862	159.6862	9.6	3000
15	105646	389.2385	149.2442	9.6	2200
10	105646	389.2442	149.2385	9.6	2800

This mesh size was therefore used to run the analysis for other velocity (5m/s, 10m/s, and 40m/s,) cases, and the following boundary conditions were obtained (Table 3.2).

Table.3.2: Boundary conditions obtained after the analysis for the respective velocities.

Inlet Velocity (m/s)	Outlet Velocity (m/s)	Mass Flow rate(Inlet) (kg/s)	Mass Flow rate Inlet) (kg/s)	Static Inlet Pressure (Pa)	Static Outlet Pressure (Pa)	Total Inlet pressure (pa)	Total Outlet Pressure (pa)
5	5.32	2.4	2.4	5.93	0	20.94	17.03
10	10.54	4.8	4.8	21.90	0	81.91	66.67
20	20.91	9.6	9.6	81.58	0	321.58	263.87
40	41.40	1.92	1.92	285.66	0	1245.66	1041.12

Figure 3.1 and 3.2 show the plot of total pressure for 20m/s velocity and 40m/s velocity.

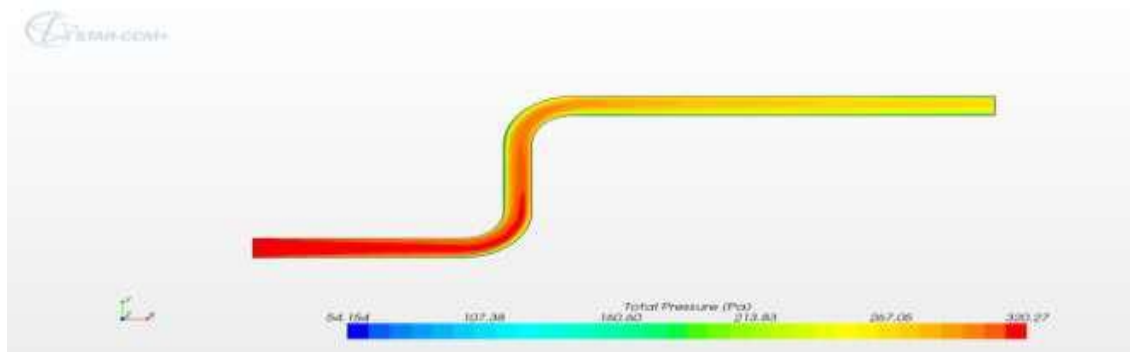


Fig.3.1: plot of total pressure for 20mls

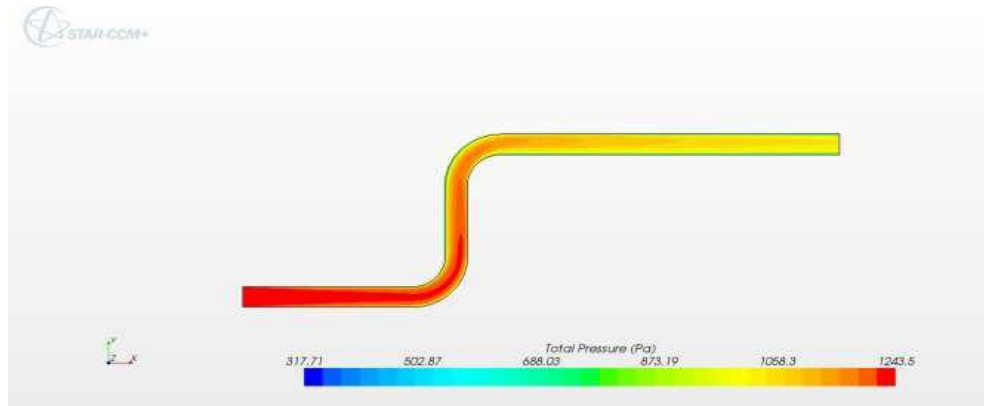


Fig.3.2: Plot of total pressure for 40m/s

Figure 3.3 shows the magnified velocity vector and streamline plots for 40m/s. It can be seen that there was no separation at the bends. The same was observed for other velocities (5m/s, 10m/s, and 20m/s).

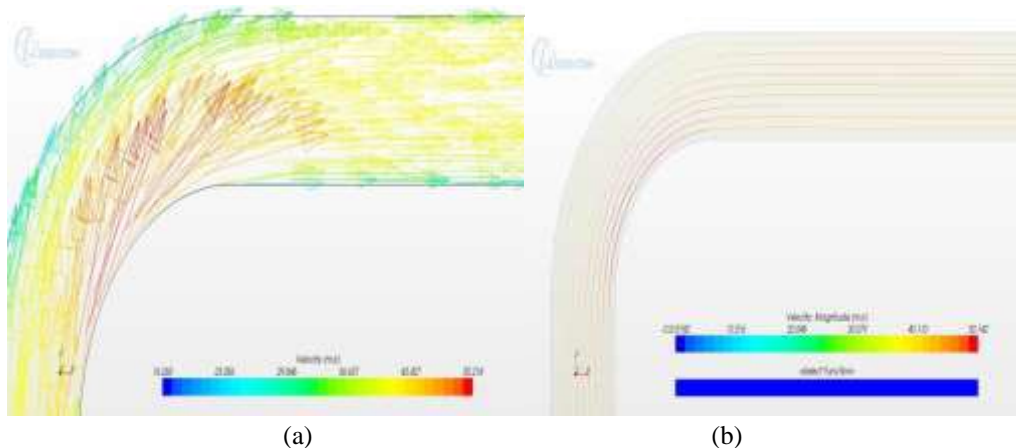


Fig.3.3: Magnified vector plot scene (a) and streamline plot (b) at one of the bends showing that no separation occurred at 40m/s

Figure 3.4 shows that the velocities around the bends are the greatest, and this can be explained by the law of conservation of mass. The bend restricts the movement of the fluid coming from the inlet. As the mass of fluid hit the restriction (i.e. the wall of the bend), the area available for the fluid to flow is reduced. Since the mass flow rate must be maintained, the velocity of the fluid passing through the bend is increased, hence maintaining continuity.

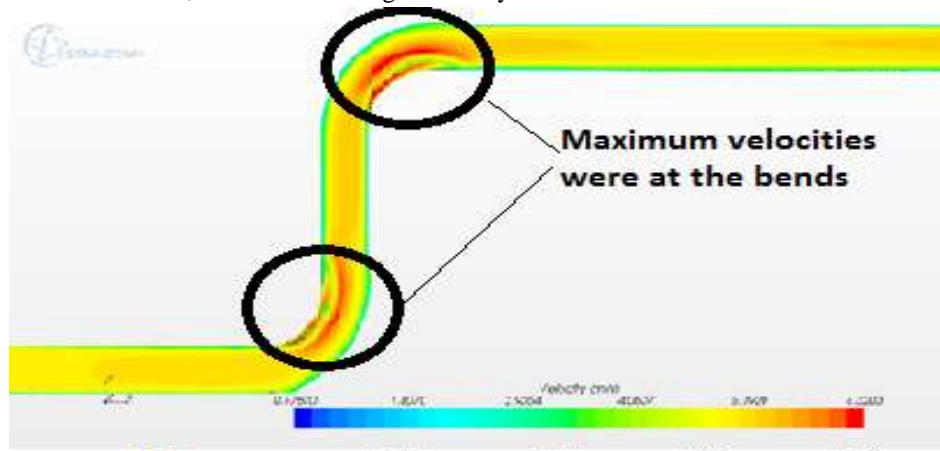


Fig. 3.4: Velocities at the bends at 5m/s

The velocity at the wall is zero due to the non-slip condition. Due to viscous effect too, the fluids closest to the layers in direct contact with the wall have velocities which are far much less than the velocity of the fluid (their velocity are nearer to the zero velocity at the wall). Because of this less velocity, a laminar sub-layer is created near the wall as shown in Figure 4.5. The flow in the remainder of the duct is turbulent.

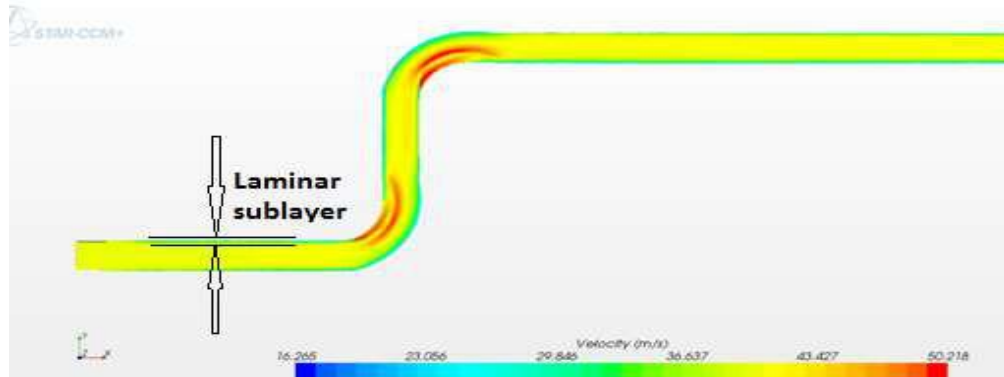


Fig.3.5: Laminar sub-layer at 40m/s

The pressure loss between the inlet and outlet is the difference in pressure between the inlet pressure and the outlet pressure and it can be used to predict leakage in a pipeline. A large drop in values of pressure is as results of pipeline leakage. The static values of pressure have been used in finding the loss (Table 3.3).

Table.3.3: Pressure Loss between the Inlet and Outlet

Case	Velocity (m/s)	Inlet Pressure (P ₁) (Pa)	Outlet Pressure (P ₂) (Pa)	Pressure Loss (P ₂ -P ₁) (Pa)
1	5	5.94	0	5.94
2	10	21.91	0	21.91
3	20	81.58	0	81.58
4	40	285.66	0	285.66

It can be seen that pressures increases as velocity increase. Therefore, high variation in velocity of the fluid in the pipeline might results to leakage. Also, it can be seen that the error decreases as velocity is increased from 5m/s to 40m/s.

IV. CONCLUSION

To avoid pipeline leakage, automated leak detection systems must be installed for new and upgraded pipelines. To design a cost effective system, it is necessary to improve the performance of existing techniques. Intensive research and development at oil facilities must be carried out to model leak detection system. In this research work, a commercial CFD package-Star CCM+ software was used to analyze possible leakage in a pipeline. The results obtained from the simulation shown that the software was able to simulate fluid flow in the pipeline. The outcome of the results obtained can be used to predict the velocity, pressure, mass flow rate, mesh size, etc. An indication of large drop in pressure is as a result of pipeline leakage.

REFERENCES

[1] Adapco C.D. (2013): User guide: STAR-CCM+ Version 8.04 [online] available from

<http://cumoodle.coventry.ac.uk/course/view.php?id=15595> [4th December, 2016]

[2] Barati, R.(2012): Numerical Investigation of Turbulent Flows Using k-epsilon [online] available From <https://www.google.co.uk/url?sa=t&rct=j&q=&esrc=s&source=web&cd=10&cad=rja&u=ct=8&ved=0CHwQFjAJ&url=http%3A%2F%2Fwww.researchgate.net%2Fprofile%2FReza_Barati%2Fpublication%2F235407247_Numerical_simulation_of_turbulent_flows_using_kepsilon%2Ffile%2F9fcfd5114c8f0aad54.ppt&ei=wt1WU4KiAsiv7AbK2YCoDA&usg=AFQjCNHoUARNQkAvUIjUIGkDtZ1g8-2cg&bvm=bv.65177938,d.ZGU> [4th December, 2016]

[3] Bose J. R., Olson M. K., (1993): “TAPS’s leak detection seeks greater precision”, Oil and Gas Journal, April 5, p43-47.

- [4] Cengel, Y., Cimbala, J., Turner, R., and Kanoglu, M. (2012): *Thermo-FluidSciences*. Newyork: MgGraw-Hill
- [5] Carlson B. N., "Selection and use of pipeline leak detection methods for liability management into the 21st century", Pipeline Infrastructure II, Proceedings of the International Conference, ASCE, 1993
- [6] Ekambara L. (2005): CFD simulations of bubble column reactors: 1D, 2D and 3D approach [online] available from <<http://www.sciencedirect.com/science/article/pii/S009250905004963>> [4th December, 2016]
- [7] Farmer E., Kohlrust R., Myers G., Verduzco G., (1998): "Leak detection tool undergoes field tests", Oil and Gas Journal,
- [8] Graf F.L., (1990): "Using ground-penetrating radar to pinpoint pipeline leaks", *Materials Performance*, Vol. 29, No. 4, p27-29 Griebenow G., Mears M., "Leak detection implementation: modelling and tuning methods", American Society of Mechanical Engineers, Petroleum Division, 1988, Vol.19, p9-18
- [9] Hamande A., Cie S. et, Sambre J. sur, (1995): "New system pinpoints leaks in ethylene pipeline", Pipeline & Gas Journal, Vol. 222, No. 4, p38-41
- [10] Hennigar G. W., (1993): "Leak detection: new technology that works", *Gas Industries*, Vol. 37, pp.16-18
- [11] Hough J.E., (1998): "Leak testing of pipelines uses pressure and acoustic velocity", *Oil and Gas Journal*, Vol. 86, No. 47, pp.35-41.
- [12] Klein W. R., (1993): "Acoustic leak detection", American Society of Mechanical Engineers, Petroleum Division, Vol.55, p57-61
- [13] Kurmer J. P., Kingsley S. A., Laudo J. S., Krak S. J., (1993): "Applicability of a novel distributed fibre optic acoustic sensor for leak detection", *Proceedings SPIE* Vol. 1797, 1993, pp. 63-71
- [14] Liou C. P., (1993): "Pipeline leak detection based on mass balance", Pipeline Infrastructure II, Proceedings of the International Conference, ASCE, 1993
- [15] Liou J. C. P., Tian J., (1994): "Leak detection: a transient flow simulation approach", American Society of Mechanical Engineers, Petroleum Division, Vol.60, p51-58
- [16] Mears M. N., (1993): "Real world applications of pipeline leak detection", Pipeline Infrastructure II, Proceedings of the International Conference, ASCE
- [17] Parry B., Mactaggart R., Toerper C., (1992): "Compensated volume balance leak detection on a batched LPG pipeline", Proceedings of Offshore Mechanics & Arctic Engineering conference (OMAE)
- [18] Sperl J. L., (1991): "System pinpoints leaks on Point Arguello offshore line", *Oil & Gas Journal*, pp.47-52
- [19] Turner N. C., (1991): "Hardware and software techniques for pipeline integrity and leak detection monitoring", *Proceedings of Offshore Europe 91*, Aberdeen, Scotland
- [20] Weil G.J., (1993): "Non contact, remote sensing of buried water pipeline leaks using infrared thermography", *Water Resources Planning and Management and Urban Water Resources*, p404-407
- [21] Zhang X. J., (1993): "Statistical leak detection in gas and liquid pipelines", *Pipes & Pipelines International*, p26-29

Numerical and Experimental Study of Natural Convection Air Flow in a Solar Tower Dryer

Germain W. P. Ouedraogo¹, Sié Kam¹, Moussa Sougoti¹, Ousmane Moctar^{1,2}, Dieudonné Joseph Bathiebo¹

¹Physic Department, Ouaga 1 University Professor Joseph Ki-Zerbo, Ouagadougou, Burkina Faso

²University of Agadez PO BOX 199 Niger

Abstract— This work focuses on the study of the flow of air in natural convection in a solar tower of small size. The behavior of air in the tower, considered as a solar dryer, provides information on the amount of heat absorbed by the air upon entry into the collector. A theoretical approach allows us to theoretically simulate the flow by using a mathematical model characterizing the physical parameters of the system during a daily sunshine. An analysis of this phenomenon is made and results are obtained.

Keywords— Flow of air, natural convection, solar tower, dryer.

I. INTRODUCTION

The concept of solar tower or solar power chimney was proposed first by Cabanyes [1]. Solar towers consist of a collector, a chimney and a turbine. They allow the production of electricity. A Solar tower without its turbine can have a use other than that of power generation: the drying of food products, thanks to the drying air coming out of its collector; hence its name of solar tower dryer.

The drying of food products is an appropriate means to curb losses of food after harvest and expand the consumption of these products during periods of non-production. This is an operation which is much practiced in West Africa by farmers. Several studies have shown the difficulty of getting indisputable elements of validation and comparison between different solar dryer models due to its technological diversity.

In our work, we study the operation of a solar tower dryer, running empty. The objective is the use of the energy gain received by the air through the collector for the drying of food products. To do so, it is essential to carry out a study of fluid flow in the system in order to know the amount of energy that the air must absorb with an average humidity of 40% in the cases of BURKINA FASO.

II. DESCRIPTION OF THE SOLAR TOWER DRYER

The solar tower dryer is a natural thermal power generator, which uses solar radiation to increase the internal energy of the air flowing in its collector. The useful gain of the solar collector is converted into kinetic energy flow circulating in the chimney where trays or racks are arranged.

2.1. Description of the solar tower

As part of our work, the solar tower has a function other than to produce electricity. Used as solar dryer, it is small compared to that producing electricity and consists mainly of a collector and a chimney.

- The collector has a radius of 1.2 meters. This is the part where the air circulates. It is heated by absorption of solar flux and subjected to phenomena of convection. The collector consists of a cover of four square shaped glass windows of a square meter and an absorber in alu-zinc painted matte black, between which the air flows.

- The chimney has a diameter of 0.4 meters and a height of 3 meters; it is the drying chamber and has racks for display of products to dry.

The chimney has two roles: that of drying-chamber and that of drawing of drying air. The greater its height, the more important its pull effect and it promotes the renewal of air in the [2-3] system.

2.2. Functioning of the solar dryer

The products to be dried are not directly exposed to solar radiation and that makes of the tower an indirect solar dryer. The air entering the collector is heated by natural convection from the sensor and moves through the chimney effect towards the drying chamber where the drying air takes away the water molecules from the products to be dried (Fig.1).

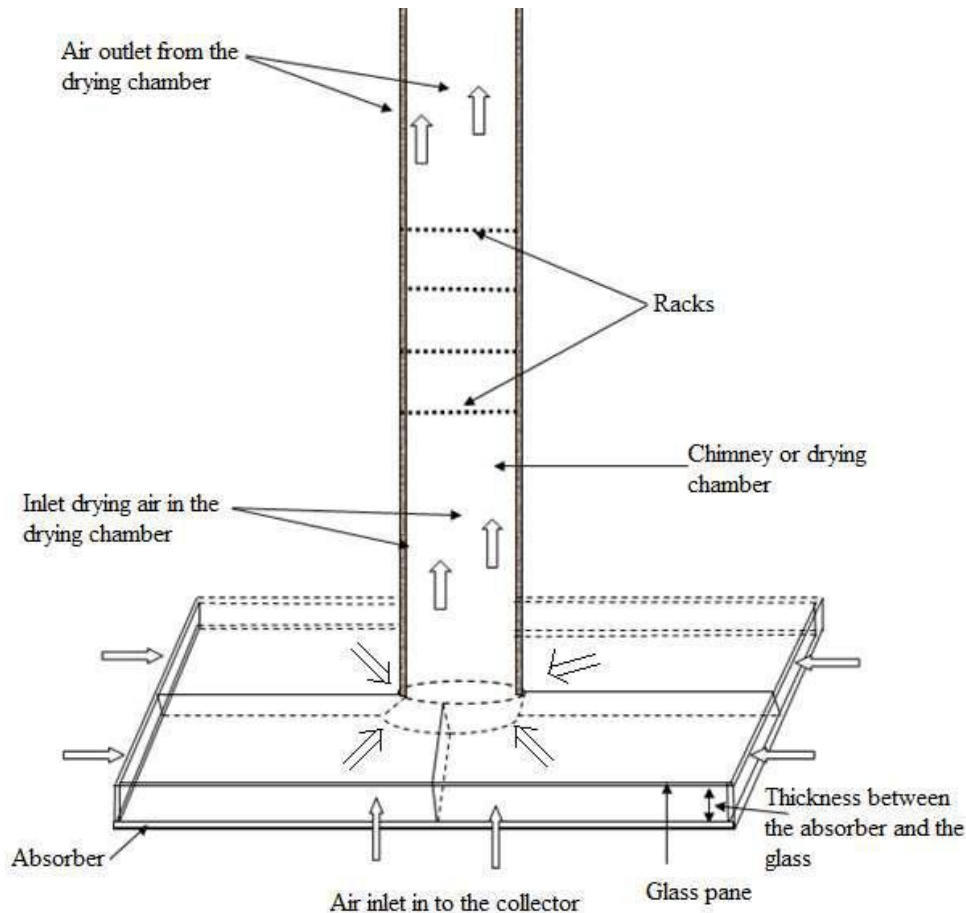


Fig.1: Diagram of the experimental solar tower dryer

III. MATHEMATICAL MODELING OF THE AIR FLOW IN THE SOLAR TOWER DRYER

The solar dryer is said to be empty when the drying chamber does not contain any products. The modeling consists in transcribing physical phenomena that can be observed and equations that can arise at different levels of the system.

3.1. Simplifying assumptions

The study of heat transfer in the system can be simplified by assuming:

- A uni-dimensional flow depending on an average radius in the chimney and the height in the chimney.
- Properties of the air such as dynamic viscosity, thermal conductivity, density and heat capacity that are considered constant.
- The air follows the Boussinesq approximation rules, which results in the expression:
 $\rho = \rho_0 [1 - \beta(T - T_0)]$
 with $\beta = \frac{1}{T_0}$
- Transfer by conduction of the sensor (absorber) is negligible as it is a thin metal and its conductivity

coefficient is very high; the temperatures of these two faces are therefore uniform.

- The heat transfer by conduction through the glass pane is negligible because it has a small thickness; the two sides have substantially the same temperature when the glass is exposed to sunlight.
- The radiative exchanges of air are negligible.

3.2. Equation governing the flow of air in the system

The rectangular collector is considered circular for its modeling in the system of polar coordinates. The equations of the air flow are a function of the radial axis r . In the chimney, the equations are a function of the axial axis z .

3.2.1. Continuity equation

In natural convection, air velocity is 'a priori' unknown. So we assume that the air flow is constant in the system.

$$V.S = cte \quad (1)$$

3.2.2. Flow equation

$$\frac{\partial V}{\partial t} = -\frac{1}{\rho_0} \frac{\partial P}{\partial r} - J.g - \frac{\rho}{\rho_0} g \sin \alpha \quad (4)$$

Where

$$J = \frac{f \cdot V^2}{2D \cdot g}$$

J is the pressure drop per unit length and f the factor of friction.

3.2.3. Heat equation

A heat balance of the collector and the chimney is required.

➤ Heat balance for the collector

Considering the above assumptions for an elementary control volume of the collector, the following Figure (Fig.2) illustrates the mechanism of heat exchange.

(5)

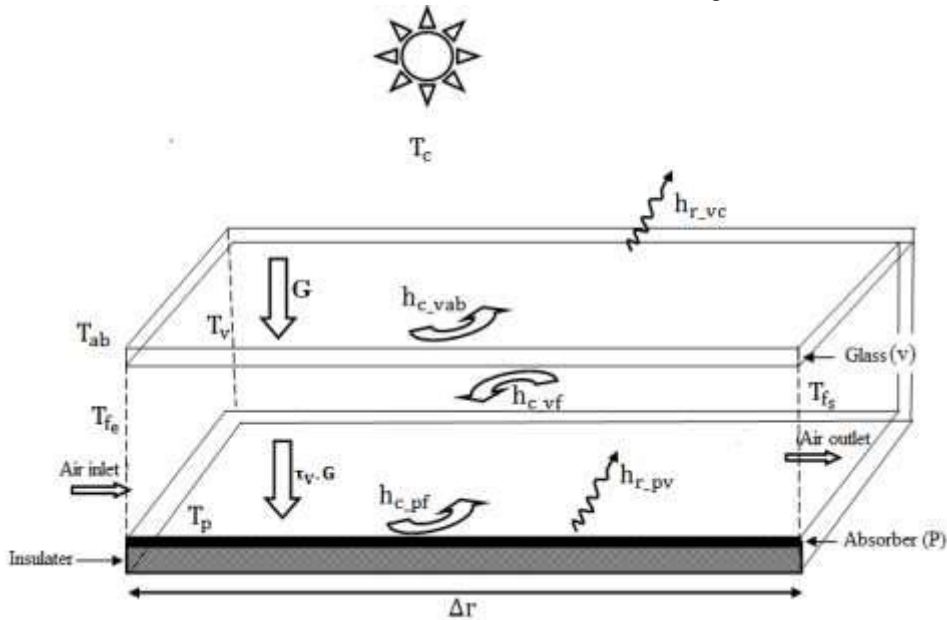


Fig.2: Illustration diagram of the different heat exchanges in the collector

- ✓ Thermal balance of the glass
 For an elementary surface and space Δr directed towards the center of the chimney, we get the following equation (6):

$$m_v C_{pv} \frac{\partial T_v}{\partial t} = -S_v h_{c,vab} (T_v - T_{ab}) - S_v h_{r,vc} (T_v - T_c) - S_v U_{av} (T_v - T_{ab}) + S_v h_{c,vf} (T_f - T_v) + S_p h_{r,pv} (T_p - T_v) + S_v \alpha_p \tau_v G$$
- ✓ Thermal balance of the absorber
 The solar energy received by the absorber is the difference between that transmitted by the surface of
- Heat balance of the drying chamber or chimney
 The various modes of heat exchange for a section of the fireplace are show in (Fig. 3).

the glass and that transferred to the fluid, including losses.

$$m_p C_{pp} \frac{\partial T_p}{\partial t} = -S_p h_{c,pf} (T_p - T_f) - S_p h_{r,pv} (T_p - T_v) - S_p U_{ar} (T_p - T_{ab}) + S_p \alpha_p \tau_v G$$

✓ Thermal balance of the fluid (air)

The heat balance of the fluid inside the chimney is given by the following equation:

$$m_f C_{pf} \frac{\partial T_f}{\partial t} = -S_v h_{c,vf} (T_f - T_v) + S_p h_{c,pf} (T_p - T_f) - \dot{m}_f S_f (T_{fe} - T_{fs}) \tag{6}$$

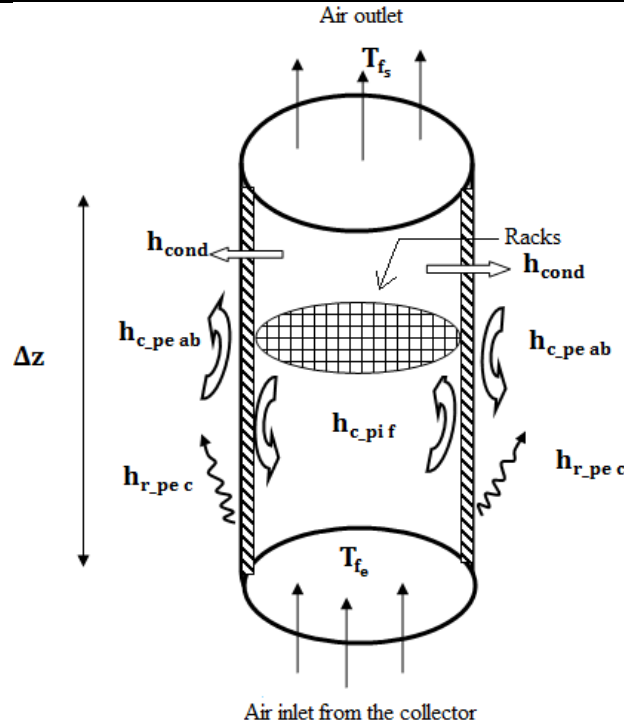


Fig.3: Illustration diagram of the different thermal exchanges in the drying chamber

- ✓ Thermal balance of the outer wall (pe)

$$m_{pe} C_{ppe} \frac{\partial T_{pe}}{\partial t} = -S_{pe} h_{c_{pe ab}} (T_{pe} - T_{ab}) - S_{pe} h_{r_{pe c}} (T_{pe} - T_c) + S_{pe} h_{cond} (T_{pi} - T_{pe}) \quad (9)$$
- ✓ Thermal balance of the inner wall (pi)

$$m_{pi} C_{ppi} \frac{\partial T_{pi}}{\partial t} = S_{pi} h_{c_{pi f}} (T_f - T_{pi}) - S_{pi} h_{cond} (T_{pi} - T_{pe})$$

- ✓ Thermal balance of the air in the drying chamber
 Heat exchanges related to the air are described by the following equation:

$$m_f C_{pf} \frac{\partial T_f}{\partial t} = -S_{pi} h_{c_{pi f}} (T_f - T_{pi}) - \dot{m}_f S_f (T_{fe} - T_{fs})$$

3.3 Coefficients of thermal exchanges

3.3.1. Coefficients of exchanges by convection

- The coefficient of convective heat exchange between the environment air and the upper wall of the glass is given by Mc Adams equation (1954) [4]:

$$h_{c_{vab}} = 5.67 + 3.86 V_{vent}$$

- For that between the fluid and the bottom wall of the glass, we have the expression:

$$h_{c_{vf}} = \frac{Nu \lambda_f}{L_c}$$

- For that between the absorber and the fluid, we have the same expression as the previous one:

$$h_{c_{pf}} = \frac{Nu \lambda_f}{L_c}$$

3.3.2. Coefficients of exchange by radiation

- Coefficient of radiative exchange between the glass and the sky:

$$h_{r_{vc}} = \sigma \epsilon_v (T_v + T_c) (T_v^2 + T_c^2)$$

With Swinbank relationship [5]

$$T_c = 0,0552 T_{ab}^{1.5}$$

- Coefficient of radiative exchange between the glass and the absorber:

$$h_{r_{pv}} = \frac{\sigma (T_v + T_p) (T_v^2 + T_p^2)}{\frac{1}{\epsilon_v} + \frac{1}{\epsilon_p} - 1}$$

- Coefficient of radiative exchange between the chimney and the sky:

$$h_{r_{pe c}} = \sigma \epsilon_{pe} (T_{pe} + T_c) (T_{pe}^2 + T_c^2) \quad (18)$$

3.3.3. Coefficients of loss

- Loss ratio before the collector

$$U_{av} = h_{c_{vab}} + h_{r_{vc}}$$

- Coefficient of rear losses of the collector

$$U_{av} = \frac{1}{\frac{\epsilon_p}{\lambda_p} + \frac{\epsilon_{isolant}}{\lambda_{isolant}} + \frac{\epsilon_{plaque}}{\lambda_{plaque}} + \frac{1}{h_{c_{vab}}}} \quad (20)$$

3.4. Correlations for calculating the Nusselt Number (12)

Nusselt number depends on the Prandtl number and Grashof number or Rayleigh number (R_a) in natural convection.

$$\text{The absorber and the glass being horizontal plates heated from above, the Nusselt number of equations (11) and (12) is determined through the following correlations [6].} \quad (13)$$

The absorber and the glass being horizontal plates heated from above, the Nusselt number of equations (11) and (12) is determined through the following correlations [6].

$$Nu = 0.54 \cdot R_a^{0,25} \quad (21) \quad (14)$$

$$\text{With } 2 \cdot 10^4 < R_a < 8 \cdot 10^6$$

$$Nu = 0.15 R_a^{0,33} \quad (23)$$

$$\text{With } 8 \cdot 10^6 < R_a < 8 \cdot 10^{11} \quad (24)$$

3.5. Choice of the method of resolution

To solve the equations of the system, we made the choice of the method of numerical solution with explicit finite differences. Using the method by slice, the system is divided into several dummy slices in the direction of the air flow.

IV. RESULTS AND DISCUSSION

4.1. Materials and methods

The experiment took place on June 30, 2016 from 9 to 17 o'clock. We used a temperature logger named midi-logger with ten lanes equipped with Type K thermocouples for measuring the temperatures of the glass, absorber, drying air in the collector and the chimney. A radiometer and an anemometer allowed us to measure respectively the solar radiation of the day and the air speed at the exit of the chimney. The figure (Fig.4) below shows a photo of the experimental device.

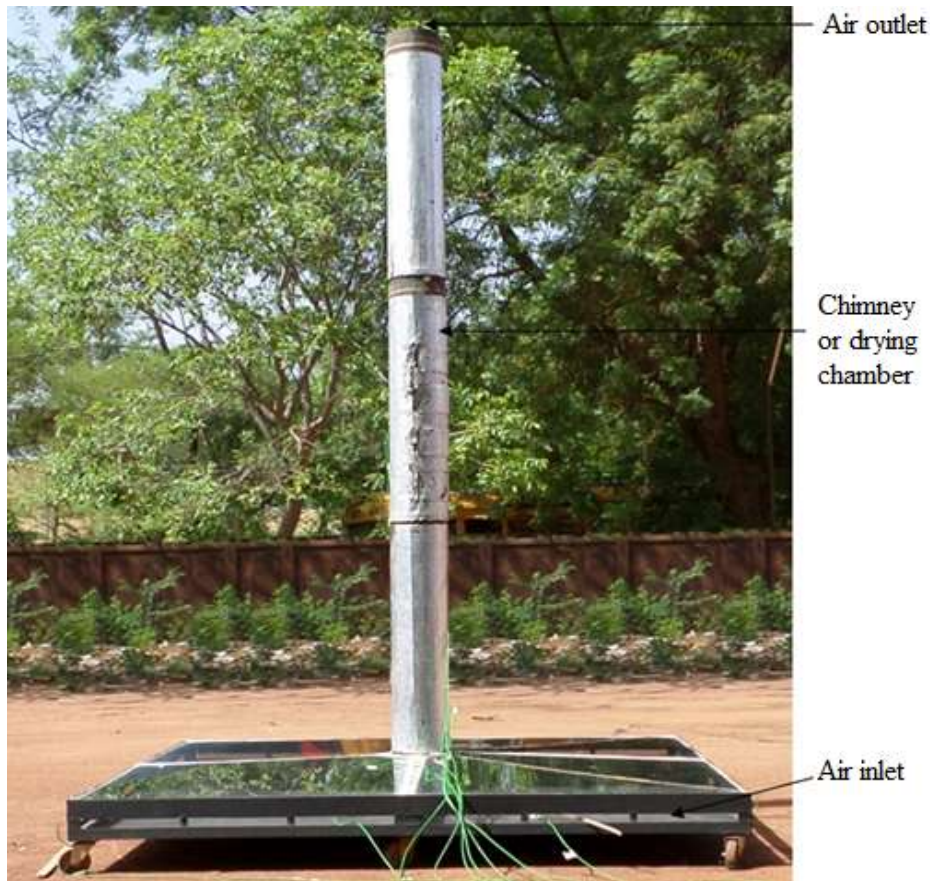


Fig.4: Photo of the experimental device

4.2. Comparison of theoretical and experimental global solar radiation

The following figures (Fig.5) and (Fig.6) respectively show the variation of the theoretical and experimental global solar radiation depending on the time of day on 30 June 2016 in Ouagadougou.

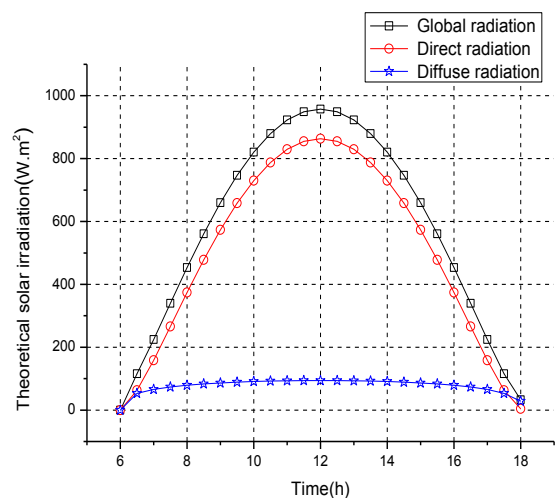


Fig.5: Theoretical variation in solar radiation

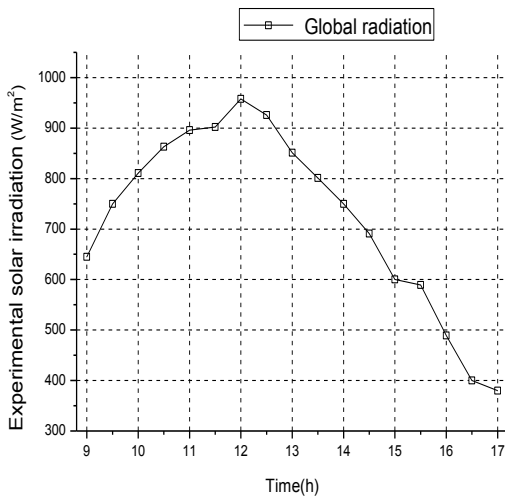


Fig.6: Experimental Variation of solar radiation

The manipulation began around 09 o'clock and we already saw a flux of 650W/m² slightly lower than that theoretically expected to be 700W/m² at the same time. Then this flow increases to reach its peak of 950W/m² at noon. We observe a sinusoidal growth in theory but the peak at 12o'clock is 967W/m². Some cloud passages were observed in the said day. The average systematic error (RMSE) between the theoretical and experimental values is about 56 W/m².

4.3. Experimental and simulation results of the collector

4.3.1. Results presentations

Figures (Fig.7) and (Fig.8) show the variation of the average temperatures of the glass, air and absorber as a function of time.

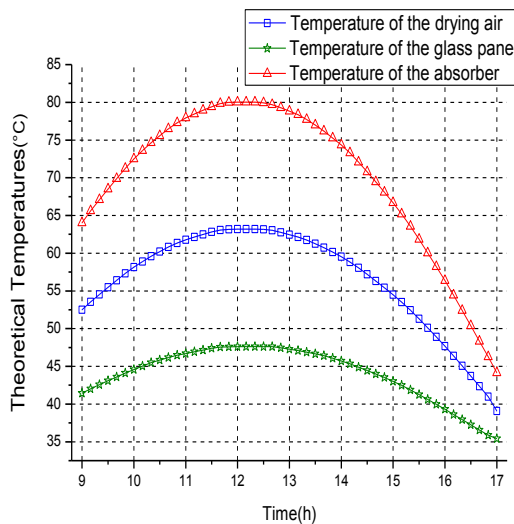


Fig.7: Theoretical temperature of the air, the glass and the absorber in the collector

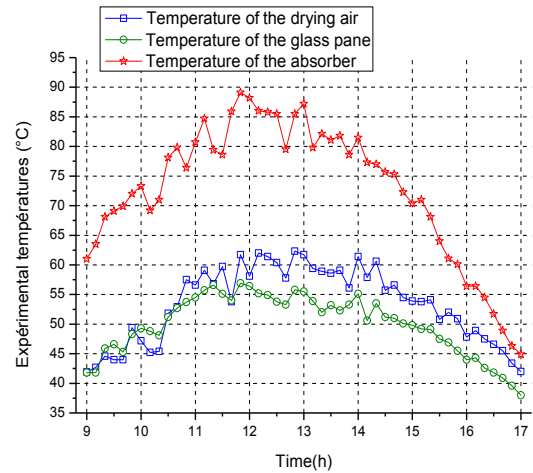


Fig.8: Experimental temperatures of air, glass and absorber in the collector

The various average temperatures of the absorber are superior to those of the air and glass respectively. We find that the temperatures rise gradually as solar radiation increases to maximum values between 12o'clock and 13o'clock. The theoretical maximum temperature of the absorber is 81° C against 88° C in practice. That of the glass is 49° C against 55 ° C and that of the air 63 ° C against 62° C.

4.3.2) Comparison between the various temperatures of the air at the outlet of the collector

To validate our results, a comparative study was carried out with experimental and theoretical results. The figure (Fig.9) below shows us that comparison.

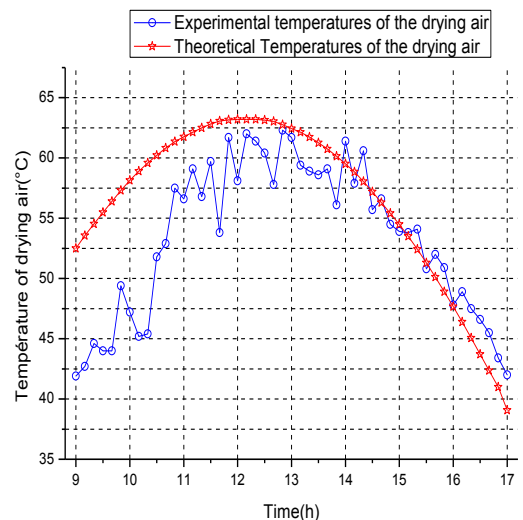


Fig.9: Comparison of experimental and theoretical temperature of the drying air

From 9 o'clock to 13.50, we see that the predicted temperatures are higher than the experimental temperatures while from 17o'clock to 14o'clock, experimental temperatures are slightly higher than those of the simulation. They increase or decrease according to the sunlight of that day and reach a maximum value of

about 62 ° C for the experimental temperature, and about 63 ° C for the simulated one with RMSE = 5.85 ° C. This same observation was made by al Hakim and sowed in 2013, when he simulated a solar tower with and without storage system. [7]

The temperature of drying air obtained at the outlet of the chimney enables the drying of certain food products whose drying temperatures do not exceed 62 ° C.

4.4. Temperature Fields at the level of the racks

The average temperatures of the drying air at the racks are given in Figures (Fig.10) and (Fig.11). They respectively show theoretical and experimental temperatures at the four racks in function of time.

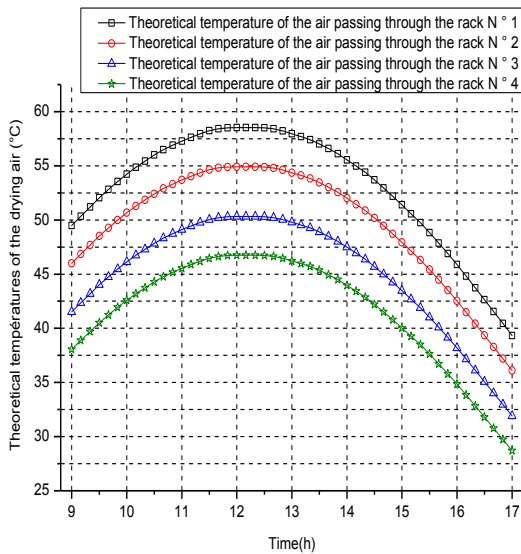


Fig.10: Theoretical average temperature of hot air in racks

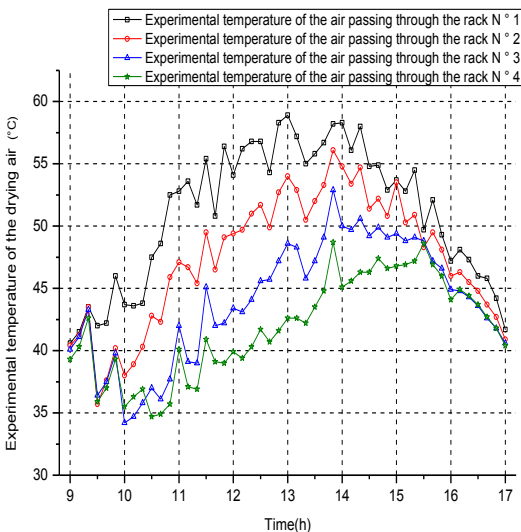


Fig.11: Experimental mean temperature of hot air at the racks

The temperature of the drying air at the racks also depends on sunshine. Rack N° 1 is traversed by a flow of hot air of higher temperature compared to the others. We

notice a decrease in the temperature of the hot air at the level of the racks (from rack N° 1 to N° 4). Respectively it shows theoretical and experimental maximum temperature of:

- 58 ° C and 59 ° C for rack N° 1,
- 55 ° C and 56 ° C for rack N° 2,
- 51 ° C and 52 ° C for rack N° 3
- 47 ° C and 48 ° C for rack N° 4.

This decrease in air temperature was noted by O.

MOCTAR et al in 2015, when he stated that the air temperature in the chimney decreases gradually as the air is ascending.

This range of air temperature at the location of the racks will allow us to dry products such as okra, medicinal or flavor leaves, green peas etc. [5]

4.5. Velocity field outlet of the chimney

In the design of solar dryer dimensions, the temperature of the drying air and humidity are certainly important, but so does the velocity of the air; hence the need to compare the simulated velocity to the experimental ones. Figure (Fig.12) shows us the comparison of theoretical and experimental speeds out of the chimney as a function of time.

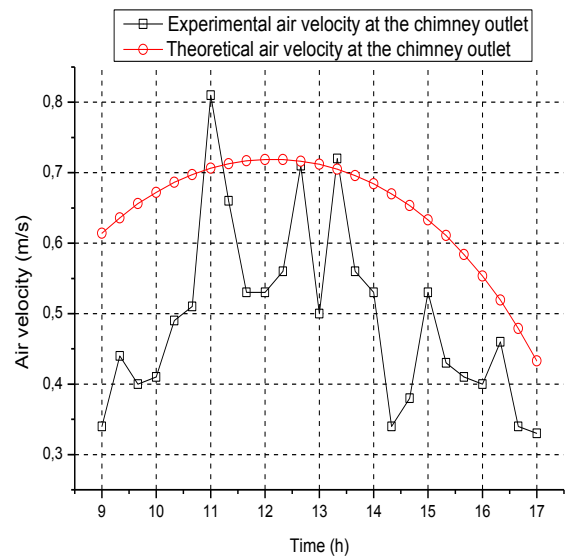


Fig.12: Comparison of experimental and theoretical speeds at the exit of the chimney.

The fluctuations of experimental velocity are due to the observed passages of cloud because these velocity also depend on sunlight. With a mean bias of 0.18 m / s, the maximum value of velocity measured at the outlet of the chimney or the drying chamber is 0.81 m / s while that of the theoretical is in the range of 0.72m /s.

V. CONCLUSION

Knowledge of the behavior of the airflow in the solar tower dryer is very important for the drying process. The range of theoretical and experimental temperatures at

different racks, tells us about the type of products to dry. Experimental velocity (0.81m / s) and theoretical (0.72m / s) out of the room to dry are low because our system works by natural convection. They have an impact on the drying time because they do not promote quick drying but can prevent the crusting of the product. These results will test the solar tower dryer by performing the drying of some agricultural products and improve our IT program to reduce average systematic errors.

Nomenclature

S: Surface (m^2)

Cp: Specific heat at constant pressure ($kJ \cdot kg^{-1}K^{-1}$)

g: Acceleration of gravity ($m \cdot s^{-1}$)

G: Golar radiation ($m \cdot s^{-1}$)

m: Mass (kg)

h: Heat transfer coefficient $W \cdot m^{-2}$

\dot{m} : Mass flow ($kg \cdot s^{-1}$)

R: radius of collector m

P: pressure (Pa)

Nu: Nusselt Number

T: Temperature (K)

V: velocity ($m \cdot s^{-1}$)

dr: Variable Radius

dz: Variable height

e: Thickness (m)

U: Loss Factor $W \cdot m^{-2}$

J: losses

f: friction factor

Greek symbols

λ : Thermal conductivity ($W \cdot m^{-1}K^{-1}$)

τ : Transmissivity

ε : Emissivity

ρ : Density of the air mass ($kg \cdot m^{-3}$)

σ : Stefan-Boltzmann constant $W \cdot m^{-2}k^{-4}$)

β : Coefficient of thermal expansion (K^{-1})

Indices

ab: Ambient

p: Absorber

f: fluid (air)

v: Glass window

av: Front window

RMSE: average bias

REFERENCES

- [1] I. Cabanyes, "Proyecto de motor solar, la energia eléctrica", Revista general de electricidad y sus aplicaciones, Vol 8,pp. 61-65, 1903.
- [2] S. Roozbeh, A. Majid, H. Behzad, " Modeling and numerical simulation of solar chimney power plants", Solar Energy, Vol. 85, pp. 829–838 , May 2011.
- [3] M. Ousmane, B. Dianda, S. Kam, "Experimental study in natural convection", Global journal of pure and applied sciences, Vol 21,pp. 155-169, 2015
- [4] M. Daguinet, Les séchoirs solaires : théorie et pratique. Unesco, 1985.
- [5] K. Swinbank. "Thermal performance of solar air heater: Mathematical model and solution procedure solar energy", vol 55, 1995.
- [6] A. Yunus Cengel, J.Afshin Ghajar, "Heat and Mass Transfer: Fundamentals & Applications." McGraw-Hill, 2011, p. 567.
- [7] H. Semai and A. Bouhdjar , " Modélisation d'une centrale à cheminée solaire en régime turbulent et avec stockage thermique ", 16^{ème} journée internationale de thermique.

A Queuing Model to Optimize the Performance of Surgical Units

M.G.R.U.K. Ferdinandes¹, G.H.J. Lanel², M.A.S.C. Samrarakoon³

¹Faculty of graduate studies (Financial Mathematics), University of Colombo.

²Department of Mathematics, University of Sri Jayewardenepura, Sri Lanka

²Accidents and Orthopedic Service Unit, National Hospital, Sri Lanka

Abstract— In any country healthcare service takes a major place which provides care for persons who are not well. When considering the Healthcare service in Sri Lanka, National Hospital of Sri Lanka plays a major role. The hospital faces the problem of overcrowding the patients and long waiting queues of patients for different healthcare needs specially on surgical purposes. The objective of the study is to introduce a queuing model for optimizing the performance of surgical units in National Hospital of Sri Lanka. In the study, the operation theaters of Accident and Emergency unit were only considered. According to the queuing model M/M/3 the existing system is not utilized well due to arrival rate is higher than the service rate. Hence it is needed to increase the service rate. According to the current system the theaters function in 4 equal work shifts in 24 hours. Some operation theaters do not function on all the shifts. It was identify that the average maximum service rate of one shift is 4.25 patients. By making all theaters functioning in that rate in all shifts the system can make efficient with the service rate of 51 patients per day. This task will be achieved by increasing the capacity of live resources.

Keywords— M/M/3 model, Operation Theater, Queuing theory, Surgical units

I. INTRODUCTION

Overcrowding in healthcare systems such as hospitals is a problem worldwide and affects the ability to provide emergency medical care within a reasonable period of time. Surgical units represent one of the most critical and expensive hospital resources since a high percentage of the hospital admissions is due to surgical interventions. Surgical units can be regarded as a network of queues and different types of servers where patients arrive, some patients wait for the list, get admitted to the hospital, wait for a service, undergo the surgery, get recover and then go home. Long waiting time in any hospital is considered as an indicator of poor service performance and needs improvement. If the waiting time and service time is high patients may leave the queue prematurely and this in turn results in patients dissatisfaction. Hence it is very important to manage the queues in surgical units. In the

other words find the balancing point where patients and the service providers may get satisfied.

Sri Lanka is a developing country and the National Hospital is the heartiest free healthcare service provider in the country. Hence the hospital faces the problem of overcrowding the patients and long waiting queues of patients for different healthcare needs specially on surgical purposes. In the study, the operation theaters of Accident and Emergency unit were only considered. In the current system of the Accident and Emergency unit consists with three operation theaters. Patients of ward 72 and 73 who come for surgical purposes arrive to theater in one queue and distributed among the three.

1.1 MOTIVATION

The National Hospital of Sri Lanka consists of eight surgical units. In Sri Lanka Most of the patients keep their trust on the National Hospital for their surgical purposes. Therefore there is a critical congestion and long waiting queues in surgical units. Overcrowding in surgical units and long waiting lists are a problem and affects the ability to provide emergency medical care within a reasonable period of time. For each surgical unit it is a challenge for the management to manage the congestions and long waiting queues to reduce the patients' waiting time for their surgery, and to improve the patient's satisfaction. Hence the study is based on the Accident and Emergency unit of National Hospital of Sri Lanka.

1.2 OBJECTIVES

The main objective of the study is to investigate how queuing models can be used to reduce the patients' waiting time in the list of patients and waiting time in the hospitals for their surgeries at Colombo National Hospital. The initial objective of the study is studying the situation gathering rich data. This study always evaluate the surgical unit service system such as patients' arrival rates, the average time that a patient has to wait in the queue for each operation theatre and the service rate. The study will also examine whether the resources of the surgical units are adequate to provide an effective and

efficient service to patients and how the utilization of the resources can be optimized.

II. PROBLEM DESCRIPTION

All the patients who get admitted to the Accident and Emergency unit in the hospital should give the same priority. But in present situation patients have to wait in queues to fulfill their surgical purposes. The arrows of the following figure illustrate the waiting queues of the surgical units that patients have to wait.

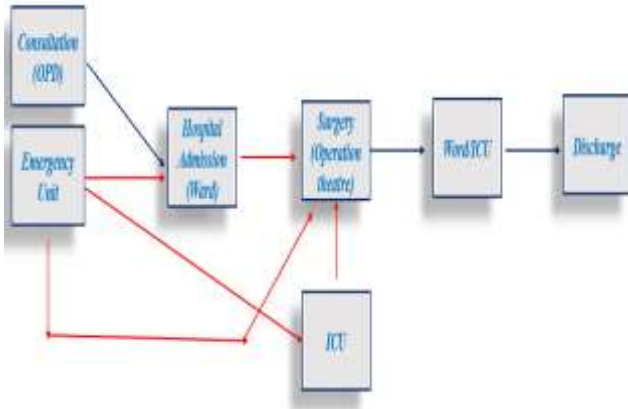


Fig. 1: The queuing network of the system

The study is based on the waiting queues which are indicated in red arrows.

III. LITERATURE REVIEW

Many of the researchers have applied queuing models to analysis the patient flow and optimize the patient flow in health care service systems in many other countries. Unfortunately in Sri Lanka there are no many research findings regarding the patients flow optimization in healthcare service systems. There is one study has base on National Hospital of Sri Lanka. In 2016 Dilrukshi, Nirmanamali, Lanel and Samarakoon have conducted a study, "A Strategy to Reduce the Waiting Time at the Outpatient Department of the National Hospital in Sri Lanka". This study has analyzed the patients flow in OPD. There is no more any clear evidence that the researchers have worked on analyzing the patients flow in National Hospital of Sri Lanka. Similarly there is no any significant study based on the surgical units of National Hospital. There are critical congestions in these units since many patients registered and get admitted to the hospital due to surgical purposes. Hence it is important to introduce an improved approach for optimizing the performance of the surgical units in National Hospital in Sri Lanka in order to increase the qualitative index of the healthcare service in Sri Lanka. This study will conduct to fulfill the above purposes. This project will identify the existing situation of the surgical units and measures the existing performance of the units by using queuing

models. Then the study will carry out for the necessary implementations.

IV. METHODOLOGY

There are two surgical wards (Ward 72 and 73) for Accident and Emergency department and three operation theaters. Considering one month daily data records of the wards and the operation theaters and the data of resources of above theaters and wards the analysis has carried.

Initially the existing conditions and the current practices were observed to identify the present situation. Then using the simple Descriptive Statistics techniques arrival rate of the patients' service rates of the operation theatres was calculated. Then the average functioning pattern of operation theaters and the average arrival pattern of the patients were identified.

Queuing theory has its origins in research by Agner Krarup Erlang when he created models to describe the Copenhagen telephone exchange. Queuing theory is the mathematical study of waiting lines, or queues. In queuing theory, a model is constructed so that queue lengths and waiting time can be predicted.

In queuing theory the arrivals can be either constant or random. If arrivals are random, it assumed that it follows poisson's distribution. Service patterns are like arrival patterns in that they may be either constant or random. If service time is constant, it takes the same amount of time to take care of each customer. More often, service times are randomly distributed. In many cases, it can be assumed that random service times are described by the negative exponential probability distribution.

Here the following queuing model has applied to the problem to reduce waiting time of a patient. Since the population is unlimited, the queue is infinite, and the queuing system is multichannel, hence the multichannel with single phase model (M/M/C) was selected for the further analysis.

The following queuing parameters and formulas were used for calculations.

Table.1: Queuing parameters and their formulas

λ – Average arrival rate	$a = \frac{\lambda}{\mu}$
μ – Average service rate at each server	$\rho = \frac{\lambda}{\mu C}$
L_q – The average number of patients waiting	$P_0 = \left(\sum_{K=0}^{C-1} \left(\frac{a^K}{K!} \right) + \left(\frac{a^C}{C!} * \frac{1}{1-\rho} \right) \right)^{-1}$
L – The average number of patients in the system	$L_q = P_0 * \frac{a^C}{C!} * \frac{\rho}{(1-\rho)^2}$
ρ – The system utilization	$W_q = \frac{L_q}{\lambda}$
W_q – The average time a patient spends waiting	$W_s = \frac{1}{\mu}$
W – The total time a patient spends in the system	$W = W_s + W_q$
W_s – Service time	$L = W\lambda$
P_0 – The probability of zero patients in the system	
C – The number of servers (channels)	

V. RESULTS

5.1 BASIC RESULTS

As the initial step the current situation is observed and the arrival and service rates were calculated in both wards and the operation theatres. The following table illustrates the summary records.

Table.2: Average no. of patients arrivals per day

Ward	Admission	Discharge	Total	Surgery
72	68	63	76	41
73	27	19	45	7

According to the existing system patients arrival rates in hourly time period for the operation theater has the following distribution.

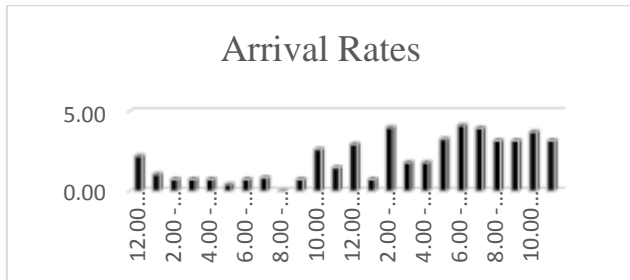


Fig. 2: Arrival rates of the patients (Arrival rates within time)

There are three operation theatres. The arrival and service rates of the operation theaters (OT) were calculated. The following table illustrates the summary records.

Table.3: Arrival rates and Service rates of the Theaters

	Arrival Rate	Service Rate
OT I	14	13
OT II	14	12
OT III	20	17
Theater	48	42

The service rates of the each theater were analyzed. The following figures described the service rate distribution of the each theater in hourly time period.

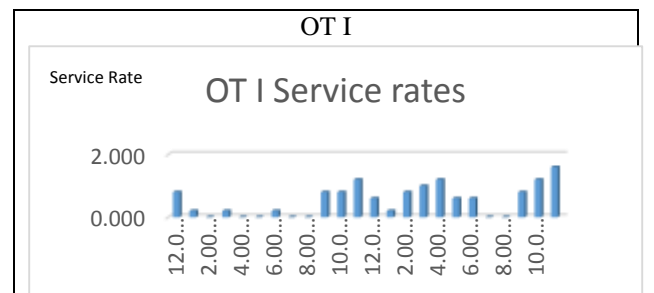


Fig. 3: Service rate pattern of OT I

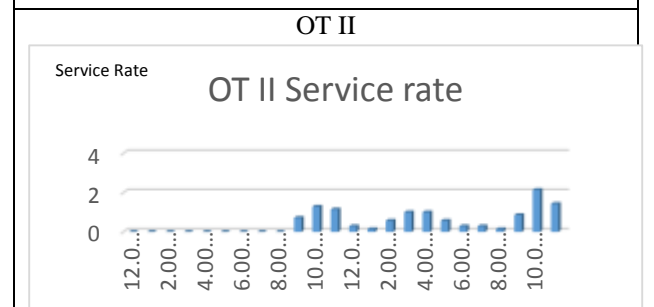


Fig. 4: Service rate pattern of OT II

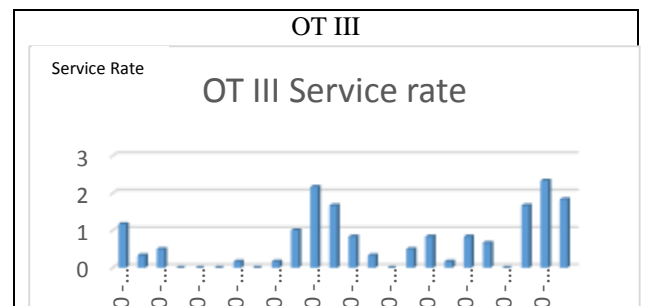


Fig. 5: Service rate pattern of OT III

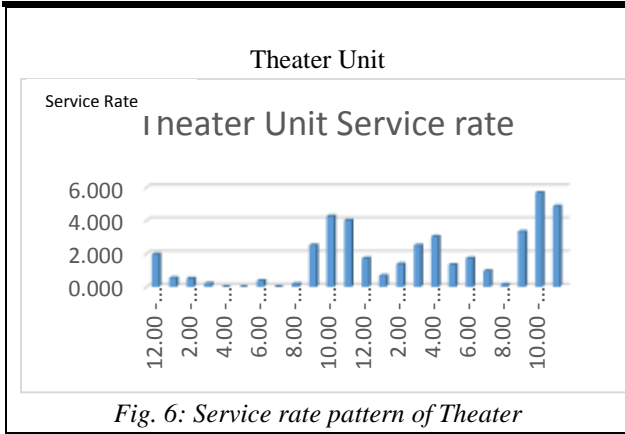


Fig. 6: Service rate pattern of Theater

By using M/M/3 queuing model the system utilization (ρ) was calculated.

$\rho = 1.142 > 1.00 \rightarrow$ The system is not utilized well.

Hence the other parameters cannot be calculated.

5.2 SUGGESTIONS AN IMPLEMENTATIONS

According to the existing system the theaters are functioning in four shifts. 8.00am - 2.00pm, 2.00pm - 8.00pm, 8.00pm - 2.00am, and 2.00am-8.00am, but OT II does not function on the 2.00am-8.00am shift. The physical capacities of all three theaters are equal. Hence the suggestions will be made with minor affect to the current practice. Due to the physical capacities of all theaters are equal, it is assumed that all theaters can perform in same level in each shift. By considering the current performance the average rate of service of the operation theaters in a shift are illustrated in the following table.

Table.4: Existing Average service rates for 6 hours shift

Operation Theater	Service Rate (patients)
OT I	3.25
OT II	4
OT III	4.25

The highest average rate is 4.25 patients per shift. Then it was assumed that the theaters can perform with the average service rate of 4.25 for a shift. There are three theaters and four shifts for each theater. Then the service rate of the Operation Theater of the day will be 51 patients. The arrival rate is 48 which is less than service rate.

By using M/M/3 queuing model the system utilization (ρ) was calculated.

Table.5: Queuing model parameters

Paramerts	Values (per day)
a	2.82353
ρ	0.94118 < 1 The system is efficient
P_0	0.01417
L_q	14.45647
W_q	0.30118 (7.228 hours)
W_s	0.05882 (1.411 hours)
W	0.36 (8.64 hours)
L	17.28

By making all three shifts to perform in same capacity the system can be made efficient with the existing physical resources. Using this model OT I and OT II function on that shift in the average service rate of 4.25 the system can be made efficient. Then the task is how make OT I and OT II to achieve the average service rate of 4.25 patients during the shift 2.00am – 8.00am. OT I still function on that shift. But OT II is not. Then the live resources should be allocated to the theater on the shift. The existing live resources capacities of the system are given below.

Table.6: Existing live capacities of the operation theater

	OT II & OT III			
	No. of Surgeons	Doctors	Nurses	Minor Staff
OT Capacity	6	9	33	30
One shift	1	2	2	2

	OT I			
	No. of Surgeons	Doctors	Nurses	Minor Staff
OT Capacity	4	6	28	23
One shift	1	2	2	2

Considering OT I and OT II combination, for a day there are 5 work shifts are functioning in the current. In the proposed system it increased up to 6. The staff roster is made for a one month period. By considering one month period (30 days) there are 150 shifts in a month. The average numbers of shifts for the staff are shown below.

Table.7: No. of working shifts for a month

	OT II & OT III			
	Surgeons	Doctors	Nurses	Minor Staff
No. of Shits	25	16.67	4.55	5

In the proposed system there are 6 work shifts, in other words there are 180 work shifts for a month. Without disturbing the current average number of shifts that an operation theater service provider has to work, the no. of

employees need to perform the proposed system is shown below.

Table.8: Proposed work capacity

	OT II & OT III			
	No. of Surgeons	Doctors	Nurses	Minor Staff
proposed capacity	7.2	10.80	39.60	36
	8	11	40	36

Then OT II and OT III will be able to achieve the proposed service target.

Then attention moved towards the OT I. The arrival rate of the OT I is comparatively low to other two theaters. By making patients distributing among the theatres equal and by increasing the service rate the target can be achieved. Furthermore OT I is not function as a practices in 2.00-3.00 am, 4.00-6.00am, 7.00-9.00 am, 7.00-9.00 pm. By making those time slots to functions the service rate can be increased.

VI. CONCLUSION

In the study, the operation theaters of Accident and Emergency unit were only considered, because the priorities of the all patients are equal.

It was found out that the queuing model of the existing system is M/M/3 model because the system has 3 theaters. By using M/M/3 queuing model the system utilization (ρ) was calculated. The ρ value is 1.142 which is greater than 1.00. it implies that The system is not utilized well.

The system can be made utilized well by increasing the service rate. It was found that the each theater should perform in the rate of 4.25 for 6 hour time period.

To achieve this service rate the operation theater staff carder should be enhanced. It was identified the staff carder of OT II and OT III same. Due to OT II is not functioning in 2.00am-8.00 am work shift; in order to make it function the work carder should be maximized.

Then by making above mention changes the system can be made efficient.

REFERENCES

- [1] M.G.R.U.K. Ferdinandes, H.K. Pallage, G.H.J. Lanel, and A.N.K. Angulgamuwa, 2015, "An improved strategy to reduce the passenger traffic at coastal and suburban area division of Sri Lanka fort railway station ticketing counters", International Journal of Information Research and Review, Volume 2, Issue 7, 909-913
- [2] P. A. D. Dilrukshi, H. D. I. M. Nirmanamali, G. H. J. Lanel and M. A. S. C. Samarakoon, 2016, "A Strategy to Reduce the Waiting Time at the Outpatient Department of the National Hospital in Sri Lanka", International Journal of Scientific and Research Publications, Volume 6, Issue 2

- [3] Hajnal Vassa, Zsuzsanna K. Szabob, 2015, "Application of Queuing Model to Patient Flow in Emergency Department.", Emerging Markets Queries in Finance and Business, Procedia Economics and Finance 32, 479-487
- [4] Sajeesh Kesavan, 2012, "Maximizing patient flow in the provision of cardiac surgery care", Trinity College, Dublin.
- [5] Reetu Mehandiratta, 2011, "Applications of Queuing theory in health care", International Journal of Computing and Business Research, Vol 2, Issue 2.

A Genetic Algorithm Based Feature Selection for Classification of Brain MRI Scan Images Using Random Forest Classifier

Dr. S. Mary Joans¹, J. Sandhiya²

¹Professor and Head, Department of ECE, Velammal Engineering College, Chennai, Tamil Nadu, India

²M.E applied Electronics, Department of ECE, Velammal Engineering College, Chennai, Tamil Nadu, India

Abstract— A brain tumour is a mass of tissue that is formed by a gradual addition of anomalous cells and it is important to classify brain tumours from the magnetic resonance imaging (MRI) for treatment. Magnetic Resonance Imaging is a useful imaging technique that is widely used by physicians to investigate different pathologies. After a long clinical research, it is proved to be harmless. Improvement in computing power has introduced Computer Aided Diagnosis (CAD) which can efficiently work in an automated environment. Diagnosis or classification accuracy of such a CAD system is associated with the selection of features. This paper proposes an enhanced brain MRI image classifier targeting two main objectives, the first is to achieve maximum classification accuracy and second is to minimize the number of features for classification. Feature selection is performed using Genetic Algorithm (GA) while classifiers used are Random forest Classifier.

Keywords— Feature selection, Brain MRI, Genetic algorithm, Classifier.

I. INTRODUCTION

A brain tumour is an intracranial solid neoplasm which is characterised as an abnormal growth of cells within the brain or the central spinal canal. It is important to find out tumour from MRI images but it is somewhat time-consuming and difficult task sometimes when performed manually by medical experts. Huge amount of time was spent by radiologist and doctors for detection of tumour and classifying it from other brain tissues. However, exact labelling of brain tumours is a time-consuming task, and considerable variation is observed between doctors. Subsequently, over the recent decade, from various research results it is being observed that it is very time consuming method but it will get faster if we use image processing techniques. Primary brain tumours do not multiply to other body parts and can be malignant or benign and secondary brain tumours are all the time malignant. Malignant tumour is more risky and life threatening than benign tumour. The benign tumour is

easier to identify than the malignant tumour. Also the first stage tumour may be malignant or benign but after first stage it will change to dangerous malignant tumour which is life frightening.

Different brain tumour detection algorithms have been developed over the last few years. Normally, the automatic classification problem is very tough and it is yet to be fully and satisfactorily solved. The main aim of this system is to make an automated system for detecting and identifying the tumour from normal MRI.

Magnetic resonance is at present one of the basic and most widely used techniques in medicine. The method commonly finds application in identifying suspected pathologies of the brain; in this case, the different signal intensities characteristic of the healthy and pathological tissues enable us to localize probable tumours.

The MRI brain tumour image classification is becoming increasingly essential in the medical arena. Physical classification of magnetic resonance (MR) brain tumour images is a difficult and time-consuming task. Medical Image Processing has developed to detect as well as analyse various disorders. The medical images facts are acquired from Bio-medical imaging procedures like Computed Tomography scan, Magnetic Resonance Imaging scan and Mammogram scan, which indicates the presence or absence of the lesion. The most vital challenge in brain MRI analysis has problems such as noise, intensity non-uniformity (INU), partial volume effect, shape complexity and natural tissue intensity variations. Inclusion of a priori medical knowledge is necessary for robust and exact analysis under such conditions.

The classification of MRI brain image data as normal and abnormal are vital to analysis for the normal patient and to consider only those who have the chance of having abnormalities. Diagnosis of abnormalities can be done automatic with more accuracy in feature selection and classification of disease. The supervised learning technique such as Random forest classifier is used for classification as it gives better accuracy and performance than other classifiers.

II. RELATED WORK

The MR human brain images are classified into its explicit category using supervised techniques like artificial neural networks, support vector machine, and unsupervised techniques like self-organization map (SOM), fuzzy c-means, via the feature set as discrimination function. Other supervised classification techniques, such as k-nearest neighbours (k-NN) also cluster pixels based on their similarities in every feature [3]. Classification of MR images both as normal or abnormal can be done using both supervised and unsupervised techniques [2].

Komal et al., [2] proposed an automation system, that performs binary classification to detect the presence of brain tumour. The dataset constitutes 212 brain MR images. It takes MR scan brain images as input, performs pre-processing, extracts texture features from processed image and classification is performed using machine learning algorithms such as Multi-Layer Perceptron (MLP) and Naive Bayes. It has been concluded with an accuracy of 93.6% and 91.6% respectively.

Namitha Agarwal et al., [4] proposed a technique where first and second order statistical features are used for classification of images. In this paper, investigations have been performed to evaluate texture based features and wavelet-based features with commonly used classifiers for the classification of Alzheimer's disease based on T2-weighted MRI brain image. It has been concluded that the first and second order statistical features are considerably better than wavelet based features in terms of all performance measures such as sensitivity, specificity, accuracy, training and testing time of classifiers.

Joshi et al., [17] proposed the brain tumour recognition and its type classification system using MR images. From the images, the lesion region is segmented and then texture features of that section are extracted using Gray Level Co-occurrence Matrix (GLCM) like energy, contrast, correlation and homogeneity [4]. For classification, neuro-fuzzy classifier is used. Gladis Pushpa et al., [19] proposed a technique that combines the intensity, texture and shape based features and classifies the lesion region as white matter, CSF, Gray matter, normal and abnormal area using SVM. Linear Discriminant Analysis (LDA) and Principle Component Analysis (PCA) are used to ease the number of features in classification.

Evangelia et al., [13] performed a binary classification to explore the use of pattern classification methods for distinguishing primary gliomas from metastases, and high grade tumour (type3 and type4) from low grade (type2). This scheme has a series of steps including ROI definition, feature extraction, feature selection and classification. The extracted features consist of tumour shape and intensity characteristics as well as rotation invariant texture features.

Feature subset selection is performed using Support Vector Machines (SVMs) with recursive feature elimination.

In our research work, the classification method has been used to classify brain tumour using different levels of statistical feature extraction methods. For classification, the supervised machine learning algorithm–Random forest classifier has been employed. From the analysis, the suitable feature set that discriminates a tumour with improved performance has been identified. Accuracy, specificity and sensitivity measures have been used to analyze the result of tumour region.

Classification is an automated process that intends to order every information/ data/instance in specific class, in light of the data portrayed by its features. However, without previous knowledge, useful features cannot be determined for classification. So initially it requires an introduction of large number of features for classification of a particular dataset. Introducing a large number of features may include irrelevant and redundant features which are not helpful for classification and this can even lessen the performance of a classifier due to large search space known as “the curse of dimensionality” [2]. This problem can be subsided by selecting just relevant features for grouping. By omitting irrelevant and unnecessary features, feature selection reduces the training time and minimizing the feature set, thus improving the performance of classifier [3, 4]. During the analysis of tissue in MRI by radiologists, image texture plays a pre-dominant role. In fact texture (in) homogeneity is one of the most common individual MRI features used for tumour diagnosis [5]. Studies have shown that texture information can improve accuracy of classification and produce comparable/preferable results to radiologists when used for machine classification of MRI tissue [6]. Different families of texture calculation methods are being used for MRI analysis and it has been shown that combination of texture features from different families can lead to better classification performance [7].

III. METHODS AND METHODOLOGY

The main purpose of this paper is to identify the tumour and to do the detailed diagnosis of that tumour which will be used in treating the cancer patient. The detailed description about the proposed system is given below.

A. Pre-processing

In the image processing the gray scale image is processed by using different methods like brightness, Filtering and thresholding. Brightness makes the image by which white objects are distinguished from gray and light items from dark objects. Hence by changing the brightness of the image the tumour recognition in the MRI image is easier.

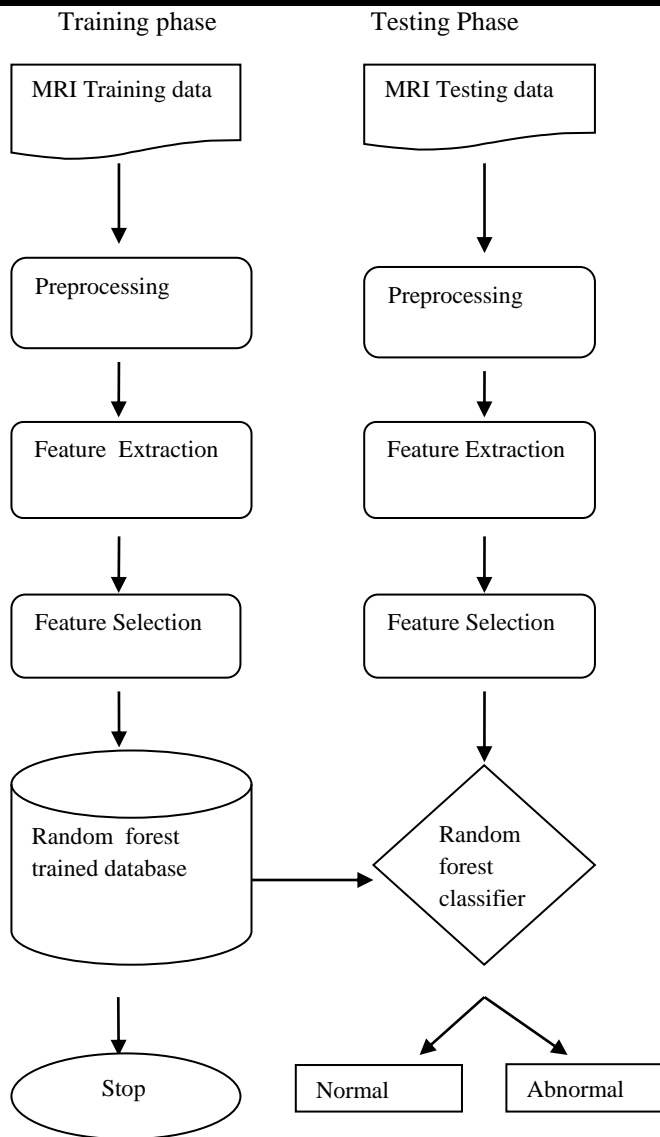


Fig.1: Flow diagram of proposed method

Filters can smooth, sharpen, transform, and remove unwanted noise from an image so that we can pull out the information needed to sharpen edges, counting the edges of any holes inside a particle, and create contrast between the elements and the background.

Preprocessing of MR brain image is the first step in our projected technique. Preprocessing includes image filtering for further processing. Our goal behind performing preprocessing is improvement of the image quality to get more surety and ease in spotting the lesion. Steps involved for preprocessing are as follows:

- 1) Input Image is converted to gray scale.
- 2) A 3x3 median filter is applied on MR brain image in order to eliminate the noise.

Median filter must only change the intensity of corrupted pixels on the damaged image in order to protect the local details of the image it has to be done. However, for fixed-valued impulse noise (i.e. salt-and-pepper noise) it is very

difficult to detect the tainted pixels from the image correctly.

B. Feature Extraction Using GLCM

The Gray Level Cooccurrence Matrix (GLCM) method is a way of extracting second order statistical texture features. A GLCM is a matrix in which the number of rows and columns is equal to the number of gray levels, G, in the image. The matrix element $P(i, j | \Delta x, \Delta y)$ is the relative frequency with the two pixels, separated by a pixel distance $(\Delta x, \Delta y)$, occur within the given neighborhood, one with intensity 'i' and the other with intensity 'j'. The matrix element $P(i, j | d, \theta)$ contains the second order statistical probability values for changes between gray levels 'i' and 'j' at a specific displacement distance d and at a particular angle (θ) . Using a huge number of intensity levels G implies storing a lot of impermanent data, i.e. a $G \times G$ matrix for every combination of $(\Delta x, \Delta y)$ or (d, θ) . Because to the high dimensionality, the GLCM matrix are extremely sensitive to the size of the texture samples on which they are approximate. Therefore, the number of gray levels is often reduced.

Gray Level Co-Occurrence Matrix (GLCM) has proved to be an accepted statistical method of extracting texture features from images. According to the gray level co-occurrence matrix, Haralick contains thirteen texture features measured from the probability matrix to extract the quality of texture statistics of brain MR images. Some of the important features are, Angular Second Moment or energy, Entropy, Correlation, and the Inverse Difference Moment.

1. Angular Second Moment

Angular Second Moment is also called as Uniformity or Energy. It is the sum of the squares of values in the GLCM. Angular Second Moment measures the image homogeneity. Angular Second Moment has high value when image has very good homogeneity / when pixels are very similar.

$$ASM = \sum_{i=0}^{Ng-1} \sum_{j=0}^{Ng-1} P_{ij}^2$$

Where i, j are the spatial coordinates of the function p (i, j), Ng is the gray tone.

2. Entropy

Entropy is the amount of information of the image that is needed for the image compression. Entropy process the loss of information or message in a transmitted signal and also measures the image information.

$$ENTROPY = \sum_{i=0}^{Ng-1} \sum_{j=0}^{Ng-1} -P_{ij} * \log P_{ij}$$

3. Correlation

Correlation measures the linear dependency of grey levels of neighbourhood pixels. This is often used to calculate strain, deformation, strain, displacement and optical flow,

but it is widely applied in many areas of science and engineering. One of the very common application is for measuring the activity of an optical mouse.

$$\text{Correlation} = \frac{\sum_{i=0}^{Ng-1} \sum_{j=0}^{Ng-1} (i,j)P(i,j) - \mu_x \mu_y}{\sigma_x \sigma_y}$$

4. Inverse Difference Moment

Inverse Difference Moment (IDM) is called as the local homogeneity. It is high when local gray level value is uniform and inverse of GLCM is high.

$$\text{IDM} = \frac{\sum_{i=0}^{Ng-1} \sum_{j=0}^{Ng-1} P_{ij}}{1+(i-j)^2}$$

IDM weight value is the inverse of the Contrast weight.

Co occurrence matrix is often formed by using two offsets i-e distance ($d = 1, 2, 3, \dots$) and angle ($h = 0, 45, 90, \text{ and } 135$).

To avoid direction dependency, Haralik also suggested using the angular mean $M_T(d)$, variance $V_T^2(d)$ and range $R_T(d)$ of GLCM.

$$M_T(d) = \frac{1}{N_\theta} \sum_{\theta} T(d, \theta)$$

$$R_T(d) = \text{Max}[T(d, \theta)] - \text{Min}[T(d, \theta)]$$

$$V_T^2(d) = \frac{1}{N_\theta} \sum_{\theta} [T(d, \theta) - M_T(d)]^2$$

Where N_θ represents the number of angular measurements and $T(d, \theta)$ are scalar texture measures.

C. Feature Selection:

The main assumption when using feature selection is that there are a lot of redundant or irrelevant features which sometimes reduces the classification accuracy [13]. Features are evaluated using a fitness function, thus selecting the best rated features among the feature set. A feature selection is an operator f_s which maps from the m dimensional (input) space to n dimensional (output) space given in mapping.

$$f_s : R^{*m} \rightarrow R^{*n}$$

Where $m \geq n$ and $m, n \in Z^+$, R^{*m} matrix containing original feature set having r instances; R^{*n} is a reduced feature set containing r instances in subset selection.

1. Discrete Binary Genetic Algorithm:

Genetic algorithms (GA) is the general adaptive optimization search methodology based on the direct correspondence to Darwinian's natural selection and genetics in biological systems. It has been proved to be a promising alternative to conventional heuristic techniques. It is based on the Darwinian standard of 'survival of the fittest', Genetic Algorithm works with a set of candidate solutions called a population and obtains the optimal solution after a series of iterative computations.

GA evaluates each individual's fitness, i.e. quality of the solution, through a fitness function. The fitter chromosomes have higher probability to be kept in the

next generation or to be selected into the recombination pool using the tournament selection techniques. If the the chromosome or the fittest individual in a population cannot meet the requirement, successive populations will be reproduced to provide more alternating solutions. The crossover and mutation functions are the main operators that randomly convert the chromosomes and finally impact their fitness value. The evolution will not stop until acceptable results are obtained. Associated with the characteristics of exploitation and exploration search, Genetic Algorithm can deal with large search spaces efficiently, and hence has fewer chance to get local optimal solution than other algorithms.

GA is a heuristic process of natural selection which is inspired from the procedures of evolution in nature. This algorithm uses the Darwin's theory "Survival of fittest" motivated by inheritance, mutation, selection, and crossover. In comparative terminology to human genetics, gene represent feature, chromosome are bit strings and allele is the feature value [14]. From algorithm perspective, population of individuals represented by chromosomes are the arrangement of binary strings in which each bit (gene) represents a specific feature within a Chromosome (bit strings). Chromosomes are evaluated using Objective function (fitness function) which ranks individual chrome by its numerical value (fitness) within a population.

2. Process of GA:

Step 1 (Generation begins): A random population ($a_{11} a_{12} \dots a_{mn}$) matrix p of size $n \times m$ is generated using population size n and number of features m .

Step 2 (Tournament): This phase selects the best-fit individuals for reproduction. Two chromosomes (parent chromes) with the highest fitness will take part in cross over.

Step 3 (Cross Over): Analogous to biological crossover, it is the exchange of bits within the selected parents to produce offspring. Number of bits b selected from parent P_n computed using $b = K * P_n$, where parameter: $0 < k < 1$ is a crossover probability.

$$b = K * P_n$$

Step 4 (Mutation): Mutation refers to the change (growth) in the genome of chromosome, flipping of bit strings (genes) of chromosome.

Step 5 (Fitness Evaluation): Analogous to "survival of fittest", chromosomes with a certain level of fitness will survive for next generation while the others whose fitness is less than the threshold value will be discarded.

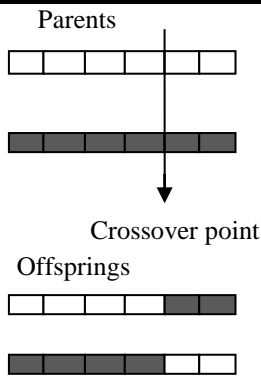


Fig.2: Illustration of crossover

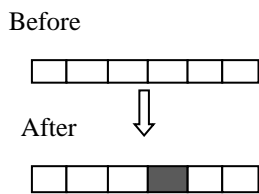


Fig.3: Illustration of Mutation.

D. Classification

Classification is the method of identification, discrimination of objects or patterns on the basis of their attributes. It is done using supervised learning. In this type of machine learning, machine classifies objects on the basis of previous knowledge. The system is trained using some attributes (features) along with their label, these attributes are used by classifier to guess the unknown objects.

1. Random Forest Classifier:

The random forest classification is an ensemble method that can be thought of as a form of nearest neighbour predictor.

The random forest starts with a standard machine learning technique called a “decision tree” which, in ensemble terms, corresponds to a weak learner. In a decision tree, an input is given at the top and as it traverses down the tree the data gets bucketed into smaller and smaller sets.

For some number of trees T , the system is trained as,

1. Sample N cases at random with replacement to generate a subset of the data . The subset must be about 66% of the total set.
2. At each node, For a few number m , predictor variables are selected at random from all the predictor variables. The predictor variable that gives the best split, according to some objective function, is used to do a binary split on that node.
3. At the subsequent or next node, choose other m variables at random from all predictor variables and repeat the same.

When a new input is entered into the system, it runs down all of the trees. The result may either be an average or the

weighted average of all of the terminal nodes that are reached, or, in the case of categorical variables, a voting majority.

IV. EXPERIMENTAL RESULTS

A. Dataset:

Project is carried out on Intel(R), Core(TM) i5-4530 s CPU @ 2.30 GHz, with 4.00 GB of RAM. MATLAB 8.1.0 (R2013a) is used for simulation. A set of 20 images of size (256 _ 256) with a format of Portable Network Graphics are taken from Harvard Medical school website <http://www.med.harvard.edu/AANLIB/> among which 10 are normal and remaining 10 are abnormal scans. The abnormal scans consist of three diseases viz. glioma, visual agnosia and meningioma.

The dataset of axial Magnetic Resonance Imaging (MRI), are collected from the subjects of various brain tumour types.

The brain tumour types considered in our system are Normal and Abnormal as shown in figure.

The images collected from different patients are grouped into two sets for using it during training and testing stages of the system.

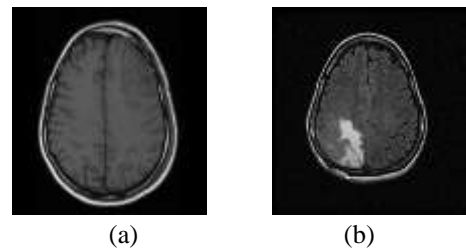
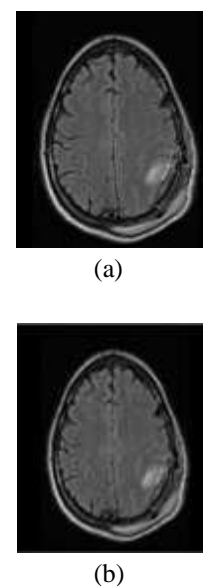
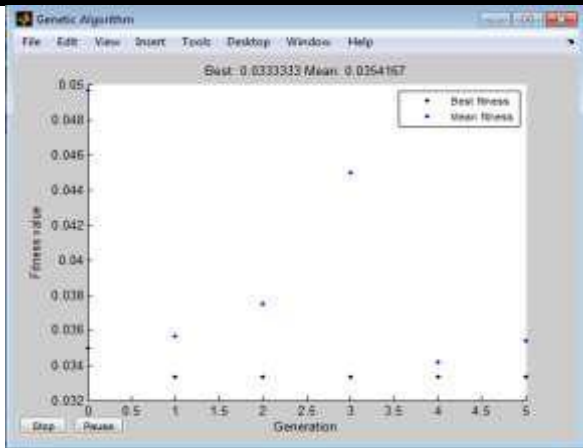


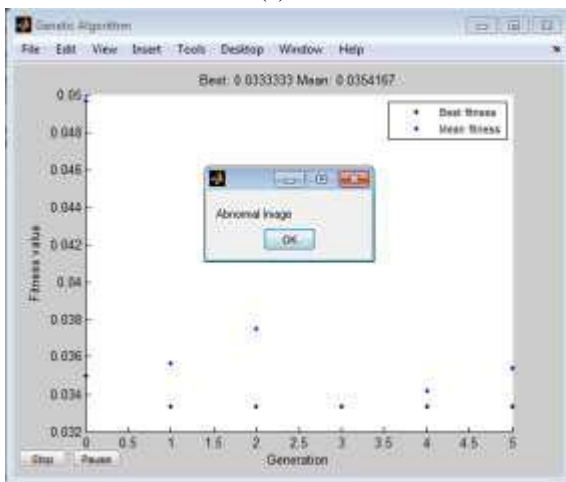
Fig.4. (a) Normal image (b) Abnormal image

B. Performance and Analysis of Proposed System





(c)



(d)

Fig.5(a): Input Image (b). Noise Removal (c).Feature Selection by Genetic Algorithm (d). Classifier Output

V. CONCLUSION AND DISCUSSION

Image processing has become a very important task in today's world. Today applications of image processing can be initiated in number of areas like medical, remote sensing, electronics and so on. If we focus on medical applications, image classification is widely used for diagnosis purpose.

Combining feature extraction and feature selection for classification has enhanced the accuracy of the classifier. Thus feature selection process has also enhanced the classification results. It is clearly seen, that without feature selection the classifier performance is weak, when compared with classification after feature selection.

Random Forest classifier has improved classification accuracy using least number of features.

The proposed work can be extended to classify different abnormalities in brain, such as, Alzheimer's disease, visual agnosia, Glioma with tumour, Herpes encephalitis with a tumour, bronchogenic carcinoma and Multiple scleris with a tumour by reducing computational cost and further

increase in mean-accuracy for the classification of Human Brain MRI scans.

Table.2: Performance of KNN classification

KNN Classification			
Image	Accuracy	Specificity	Sensitivity
Normal and Abnormal	93.34	90	95

Table.2: Performance of proposed system.

Random Forest Classification			
Image	Accuracy	Specificity	Sensitivity
Normal image	99	90	98
Abnormal image	90	95	98
Total	95	92	98

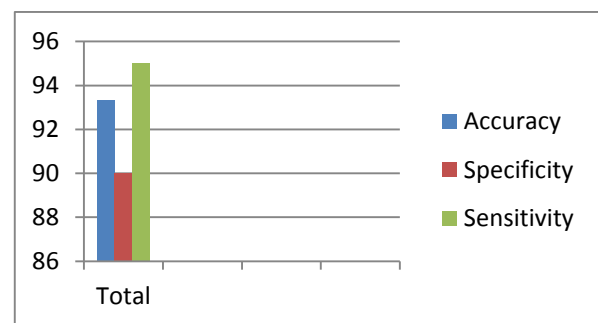


Fig.6: Performance of KNN classifier

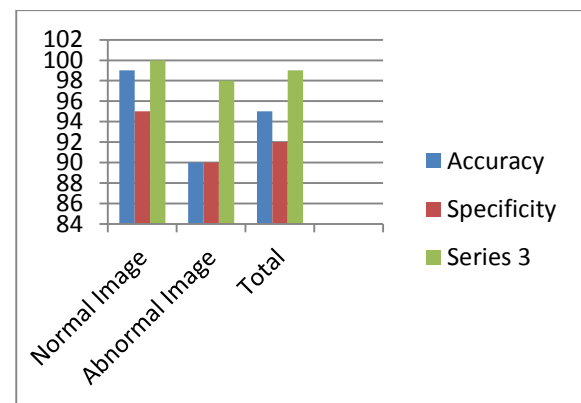


Fig.7: Performance of proposed system

REFERENCES

- [1] Atiq ur, R. et al.: Hybrid feature selection and tumor identification in brain MRI using swarm intelligence. In: 11th International Conference on Frontiers of Information Technology (2013).
- [2] Komal Sharma, Akwinder Kaura and Shruti Gujral, 2014, "Brain Tumor Detection based on Machine Learning Algorithms", International Journal of Computer Applications, vol. 103, no.1, pp. 7-11.

- [3] Walaa Hussein Ibrahim, Ahmed Abdel Rhman Ahmed Osman and Yusra Ibrahim Mohamed, 2013, "MRI Brain Image Classification using Neural Networks", IEEE International Conference On Computing, Electrical and Electronics Engineering, ICCEEE, pp. 253-258.
- [4] Namita Aggarwal and Agrawal R K, 2012, "First and Second Order Statistics Features for Classification of Magnetic Resonance Brain Images", Journal of Signal and Information Processing, vol. 3, no. 2, pp. 146-153.
- [5] Unler, A., Murat, A.: A discrete particle swarm optimization method for feature selection in binary classification problems. Eur. J. Oper. Res. 206(3), 528–539 (2010).
- [6] De Schepper, A., Vanhoenacker, F., Parizel, P., Gielen, J. (eds.): Imaging of Soft Tissue Tumors, 3rd edn. Springer, Berlin (2005).
- [7] Atiq ur, R. et al.: Hybrid feature selection and tumor identification in brain MRI using swarm intelligence. In: 11th International Conference on Frontiers of Information Technology (2013).
- [8] García, M.A., Puig, D.: Improving Texture Pattern Recognition by Integration of Multiple Texture Feature Extraction Methods, pp. 7–10 (2002).
- [9] Sidra et al.: Improved tissue segmentation algorithm using modified Gustafson-kessel Clustering for brain MRI (2014).
- [10] Sivanandam, S.N., Deepa, S.N.: Introduction to Genetic Algorithms. Springer, Heidelberg (2008).
- [11] Yao, M.: Research on learning evidence improvement for KNN based classification algorithm. Int. J. Database Theory Appl. 7(1), 103–110 (2014).
- [12] Juntu, J., De Schepper, A.M., Van Dyck, P., VanDyck, D., Gielen, J., Parizel, P.M., Sijbers, J.: Classification of Soft Tissue Tumors By Machine Learning Algorithms (2011).
- [13] Evangelia I. Zacharaki, Sumei Wang, Sanjeev Chawla, Dong Soo Yoo, Ronald Wolf, Elias R. Melhem and Christos Davatzikos, 2009, "Classification of Brain Tumor Type and Grade using MRI Texture and Shape in a Machine Learning Scheme", Magnetic Resonance in Medicine, vol. 62, no. 6, pp. 1609–1618.
- [14] Fritz et al.: Statistical Texture Measures Computed from Gray Level Concurrence Matrices, 5 November 2008.
- [15] Prasad, B.: Speech, Audio, Image and Biomedical Signal Processing Using Neural Networks. Springer, Berlin (2008). 356 p.
- [16] Fernández-Delgado, M., et al.: Do we need hundreds of classifiers to solve real world classification problems? J. Mach. Learn. Res. 15, 3133–3181 (2014).
- [17] Dipali M Joshi, Rana N K and Misra V M, 2010, "Classification of Brain Cancer Using Artificial Neural Network", IEEE International Conference on Electronic Computer Technology, ICECT, pp. 112-116.
- [18] Sidra et al.: Improved tissue segmentation algorithm using modified Gustafson-kessel Clustering for brain MRI (2014).
- [19] Gladis Pushpa Rathi V P and Palani S, 2012, "Brain Tumor MRI Image Classification with Feature Selection and Extraction using Linear Discriminant Analysis", International Journal of Information Sciences and Techniques, vol.2, no.4, pp. 131-146.
- [20] Quora: <https://www.quora.com/What-are-the-advantages-of-different-classification-algorithms>.

Six Sigma Methodology for Improving Manufacturing Process in a Foundry Industry

Sachin S.¹, Dileepal J.²

¹PG Scholar, Department of Mechanical Engineering, College of Engineering and Management, Punnappara, Alappuzha, Kerala, India

²Associate Professor, Department of Mechanical Engineering, College of Engineering and Management, Punnappara, Alappuzha, Kerala, India

Abstract — Six sigma is a project-driven management approach that is relevant to all the fields starting from manufacturing to service industries. The main goals of six sigma are improving efficiency, profitability, and process capability. In this paper, six sigma methodology based on DMAIC approach is applied to a foundry industry. The scope of the study is limited to automated high-pressure green sand moulding line. The root causes of different casting defects are identified and various actions are recommended to improve the production process. As a result, the overall sigma level of the industry is improved at an acceptable level.

Keywords— Casting Defects, DMAIC, FMEA, RPN, Six Sigma.

I. INTRODUCTION

In the present scenario, quality has become one of the most important competitive strategic tools which many organizations have realized it as a key to develop products and services in supporting continuing success [1]. The use of quality tools and technique provides long-term dividends through lower costs and productivity improvements. The companies have recognized the importance of quality system implementation in a volatile business environment in maintaining effectiveness [3]. Specifically meeting the needs of the customers is critical and must be done much better and efficiently than it has done in the past. TQM incorporates the concepts of product quality, process control, quality assurance, and quality improvement. Besides TQM there is other quality system used to improve quality such as six sigma [2]. Six sigma focuses on the reduction and removal of variation by the application of an extensive set of statistical tools and techniques. This would lead to improved productivity, improved customer satisfaction, enhanced quality of service, reduced cost of operations or costs of poor quality, and so on. This paper mainly focused on the implementation of six sigma quality methodology through DMAIC approach to rectify the casting defects in a foundry industry. The defect data of six months is collected to evaluate the performance of the company.

FMEA is used to analyze the various casting defects and their significance to make the casting defective. The root causes of defects are identified and improvement actions are suggested to eliminate defects. The adoption of six sigma has improved both the efficiency of the line and the production capability.

II. METHODOLOGY

Six sigma provides a customer focused, well-defined methodology supported by a clear set of comprehensive tools for process improvement [6]. In this study, six sigma is exercised through a classified project-oriented approach through DMAIC cycle. The DMAIC cycle is a more detailed version of the Deming PDCA (Plan, Do, Check, Act) cycle with continuous improvement. The different phases (Define, Measure, Analyze, Improve, and Control) provide a problem-solving process in which specific tools has employed to turn a practical problem into a statistical problem, generate a statistical solution, and then convert that back into a practical solution [4].

III. COMPANY BACKGROUND

The company has started with aim of production of all types of ferrous castings. It is a modern industrial casting unit with ISO 9002 certification. The unit has an optimum capacity of 18000 tons per annum and covers an area of 21500 sq. meters. The plant comprises of two distinct production lines, they are the conventional moulding line and high pressure moulding line. The company can manufacture ferrous castings of all grades and sizes ranging from 5kg to 8000kg. The high pressure moulding line is a semi-automatic system, which has used for mass production of small castings. The plant manufactures complex high precision items of mass production like cylinder block and cylinder heads for the entire range of automotive engines. The company has separate lines for the production of entire automotive castings from the smallest to the largest, such as housings, flywheels, pulleys, manifolds, brake drums etc. Apart from serving the diversified needs of the automobile industry, the company also manufactures pump castings, windmill hub,

machine tools etc. Currently, the company faces many quality problems in their production unit. The rejection is occurring mostly in the production of engine cylinder frame. Therefore, the company implements six sigma methodology to identify the cause of defects and to improve the sigma level of the company.

IV. SIX SIGMA IMPLEMENTATION

The rejection rate of engine cylinder frame was analyzed statistically using DMAIC methodology and suggestions for quality improvement are made to the company.

4.1 DEFINE PHASE

The purpose of this phase is to define the scope and goal of the improvement project in terms of customer requirements and to develop a process that provides these requirements. For defining the project, a project charter has made with all the necessary details of the project. The project charter is shown in Table 1. A good charter creates a roadmap for the team to achieve the changes as required by the management [7].

Table.1: Project Charter

Project title	To reduce rejection rate of engine cylinder frame
Project objective	Targeting to bring down the present defective rate
Critical to quality	Percentage of casting rejections is high due to casting defects
Project scope	Green sand casting process and high pressure production line
Expected benefits	Quality and defect free products Customer satisfaction Cost saving due to defects
Schedule	Define – one week Measure – two week Analyze – three week Improve – three week Control – three week

Before the process to be investigated, all circumstances have to be defined. The process mapping of the company that helps the team to understand entire casting process to reduce the variation in the production is shown in Fig.1.

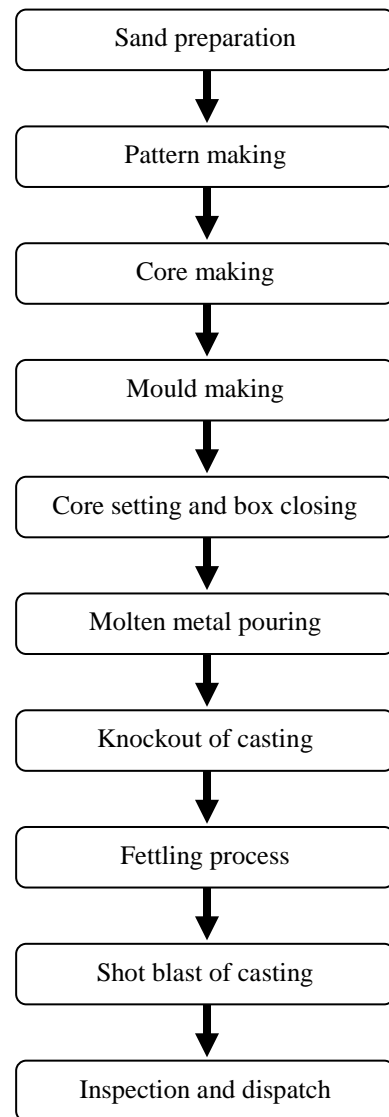


Fig.1: Process Mapping of the Company

4.2 MEASURE PHASE

The data was collected for six months continuously from July 2016 to December 2016 in the high pressure production line on the production of engine cylinder frame to track down the problem faced by this particular component. Table 2 shows the total production – rejection statement of the engine cylinder.

A Pareto chart was constructed as in Fig. 2, regarding the casting defects. It shows the various casting defects and their significance to make the casting defective.

Table.2 Production– Rejection statement

Month	Quantity produced	Quantity defective	Defective percentage
July	175	42	24.00
August	856	158	18.45

September	823	170	20.65
October	590	50	8.47
November	960	93	9.68
December	983	172	17.49
Total	4387	685	15.61

The sigma level of the casting process is calculated using sigma calculator, which is found to be 3.7 sigma level.

4.3 ANALYZE PHASE

In this phase, the collected data is verified, analyzed, and ranked in order to discover the possible root causes and their impact on output. FMEA is used to identify the significance of casting defects. The potential failure modes and potential causes for each of the casting defects are identified, followed by the effects of failures on the product. The intensity of the defects caused on the casting is measured using risk priority number (RPN). It (from 1 to 1000) is an index obtained from the multiplication of three risk parameters, which are severity, detection, and occurrence. The evaluation of the three risk parameters is prepared on the numerical scale based on the reference manual developed by AIAG [8]. 1 to 10 ranking is adopted in this study due to ease of interpretation, and at the same time, accuracy, and precision, which is adapted to the particular risk situation of the process. The result of FMEA is shown in Table 3. They are based on the requirements of the high pressure moulding line of the company or final product.

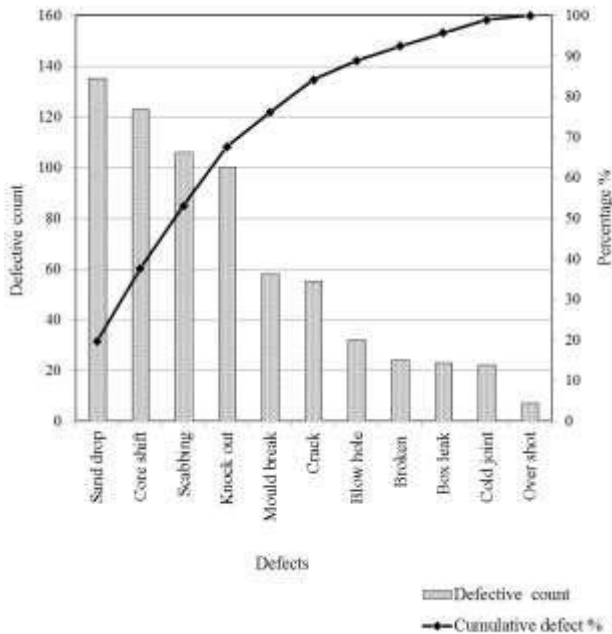


Fig. 2: Pareto Chart for the Casting Defects

It can be concluded by analyzing the Pareto chart that sand drop, core shift, scabbing, knockout defect and mould break are blow up as the prime reasons for 76% of the defective castings.

The calculation of sigma level is based on the number of defects per million opportunities (DPMO) [5]. In order to calculate the DPMO, three individual pieces of information are required as given below.

- The number of units produced = 4387
- The number of defect opportunities per unit = 11
- The number of defects = 685

DPMO =

$$= \left(\frac{\text{No. of defective units}}{\text{No. of opportunities for defect} \times \text{No. of units}} \right) \times 1000000$$

$$\text{DPMO} = \left(\frac{685}{11 \times 4387} \right) \times 1000000$$

$$\text{DPMO} = 14194.83$$

The defect having higher RPN is given priority. The monetary loss due to casting rejection is considered as a measure of risk. The results help to concentrate on the defects that having higher RPN in the rejection of casting. The most significant defects are core shift and scabbing having the highest RPN of 576 for both of it. The RPN number of crack is 512 and of sand drop is 504 are the following priority defects. Later cold joint and mould break are the important defect to consider having RPN value of 392 and 336 respectively. The remaining defects are to be considered, but least priority.

Table.3: FMEA Analysis

Failure	Failure mode	Failure effect	Failure cause	S	O	D	RPN
Sand drop	Sand mould drops and cause similar shaped sand holes on the casting	Change in required shape and affect surface finish	Fast metal pouring	7	9	8	504
Core shift	Displacement of core from its seat	Undesirable variation in wall thickness and final shape	Fast metal pouring	8	9	8	576

Scab	A portion of face of a mould lifts or breaks and the recess thus made is filled by metal	Sand is washed away and cavity is filled with metal. Change in required shape	High moisture content.	8	9	8	576
Knock out	Breakage of casting corners when it stuck on vibrator mesh plate	Affect surface finish	Damage d mesh plate	5	9	7	315
Mould break	Breakage of pattern print in the sand mould	Change in required shape	Jerking of the machine	6	8	7	336
Crack	Very thin parting lines on casting surface	Affect the mechanical properties of casting	Due to shrinkage of casting	8	8	8	512
Blow hole	Smooth round holes on casting surface	Change in required shape	High moisture content	3	7	7	147
Broken casting	Fractured sections of casting	Casting is separated into pieces	Operator fault	2	7	7	98
Box leak	Molten metal leaks in between mould box	Failed to obtain a casting	Mould box damage	3	7	7	147
Cold joint	Two metallic streams are not fused together	Change in required shape	Slow metal pouring	7	7	8	392
Over shot	Excess removal of metal from the surface	Change in required dimension	Operator fault	2	6	6	72

The details of casting rejection and subsequent monetary loss for six months are shown in Table 4. In this study, only castings rejected as scrap is considered in the estimation of the cost of rejection, the cost involved in reworking is not considered due to lack of significance because most of the defects in castings can be rectified through fettling and final finishing operations.

Table.4: Casting Rejection & Subsequent Monetary Loss

Defect	Reworked quantity	Rejected quantity	Cost of rejection Rs.3000/unit
Core shift	0	123	369,000
Scabbing	0	106	318,000
Crack	0	55	165,000
Sand drop	90	45	135,000
Mould break	15	43	129,000

Broken	0	24	72,000
Box leak	0	23	69,000
Cold joint	14	8	24,000
Blow hole	24	8	24,000
Over shot	0	7	21,000
Knock out	98	2	6000
Total	241	444	1,332,000
Average		74	222,000

The issue of core shift, scabbing, crack, sand drop, mould break, and cold joint of casting must be addressed first, eliminating these problems will result in a savings of Rs.1,140,000 more than for any other problem listed. The root cause for these casting defects is identified and listed as follows.

4.3.1 Scabbing, blow hole

The industry was using the reused sand for the mould making. Any variation from the specified limit of moisture content and total clay content may cause scabbing and blow hole in the casting. Therefore, three samples are tested to detect moisture content and total clay content and the results are shown in Table 5.

Table.5: Percentage of moisture content and total clay content

Sample no	Moisture content (%)	Total clay content (%)
1	5.1	7.4
2	4.8	6.9
3	5.4	7.9

The results revealed that the silica sand used for moulding has an average clay content of 7.4%, instead of company specification of 5-7%. The average moisture content of moulding sand is 5.1%, instead of company specification of 3-4%. Hence, the moisture content should be reduced in the sand by adding new silica sand.

4.3.2 Core shift, sand drop, cold joint

The pouring time should be maintained as per specified limit of 15-17 seconds. The pouring time tests for twenty random castings are performed to evaluate the casting defects such as core shift, sand drop, and cold joint. The test results are given in Table 6. It was found that castings with fast pouring have a chance for core shift and sand drop and the castings with slow pouring have chance for cold joint.

Table 6: Estimation of Pouring Time

Sample no	Pouring time	Condition of the casting	Remarks
1	10	Rejected	Core shift
2	15	Good	
3	16	Good	
4	12	Defective/Rework	Sand drop
5	15	Good	
6	17	Good	
7	19	Good	
8	21	Defective/Rework	Cold joint
9	14	Good	
10	13	Defective/Rework	Sand drop
11	11	Rejected	Core shift
12	16	Good	
13	11	Defective/Rework	Core shift
14	15	Good	
15	17	Good	
16	20	Defective/Rework	Cold joint
17	19	Good	
18	12	Defective/Rework	Sand drop
19	14	Good	
20	14	Defective/Rework	Sand drop

4.3.3 Crack

The reason for crack is due to shrinkage of casting. It is evident that the prominent reason is the shortage of molten metal in the casting process.

4.3.4 Mould break, box leak, knock out

In the company, the preventive maintenance is performed once in a week. Due to poor inventory management, preventive maintenance cannot be done efficiently. In the case of mould break, the main obstacle is the lack of materials or parts required for the maintenance at the right time. Also, in the maintenance schedule, there no provision for regular maintenance of the mould box. The mould box maintenance is performed only after the defect has occurred. This issue may cause the damage of box clamp. During knock out defect, it is noticed that the castings get defective during shake out process. The reason for this defect is low service life of vibrator mesh plate. The improper replacement and preventive maintenance schedule and poor inventory management are identified as the vital cause for knockout defect.

Table 7: Improvement Actions

	Defect	Cause	Improvement action
1	Scabbing	High moisture content	New silica sand is added to reduce moisture content in the reused mould sand.
2	Core shift	High metal pouring rate	Maintain the pouring time from 15sec to 17sec
3	Sand drop		
4	Crack	Shrinkage	Provide sufficient molten metal into mould.
5	Cold joint	Low pouring rate	Maintain the pouring time from 15sec to 17sec
6	Mould break	Jerking of machine	Revised the preventive maintenance schedule
7	Box leak	Damage to box clamp	Revised the preventive maintenance schedule and perform regular condition monitoring for mould box
8	Blow hole	Gas entrapped in metal	Decrease moisture content in sand and increase air ventilation
9	Knock out	Damage mesh sheet	Revised the preventive maintenance schedule and replacement schedule, and perform regular condition monitoring
10	Broken casting	Operator's fault	Give necessary instructions and training. Provide safety measures to operators.
11	Over shot		

4.3.5 Broken casting, overshot

The root cause of these defects is related to human factors such as operator's fault, lack of training, uncomfortable working environment, lack of safety measures and the working mentality of the worker. Considerably these defects have low risk priority compared to other defects. Overshot defect occurs when operator performs excess machining on the castings.

4.4 IMPROVEMENT PHASE

A number of solutions for the problem are suggested in this phase. The improvement actions recommended removing the defects in castings are shown in Table 7.

4.5 CONTROL PHASE

In this phase, the various actions to control and maintain the improvements efforts in the process is initiated. In addition, the current sigma value is calculated with respect to new improvements. The data is collected after improvement for the month of March 2017 and is shown in Table 8.

Table.8: Current Production - Rejection Statement

Month	Quantity produced	Quantity defective	Quantity rejected
March	851	63	28

$$DPMO = \left(\frac{63}{851 \times 11} \right) \times 1,000,000$$

$$DPMO = 6730.05$$

The current sigma level is calculated as 4.0

$$\begin{aligned} \text{Cost of rejection after improvement} \\ (\text{Rs.3000/unit}) &= 28 \times 3000 \\ &= \text{Rs.84,000} \end{aligned}$$

Table.9: Result after Improvement

	Before improvement	After improvement
Sigma level	3.7	4.0
Cost of rejection	222, 000 (July 2016 – December 2016; Six months average)	84, 000 (March 2017)

Table 9 shows the result after improvement. It reveals that the performance of the company had improved and the loss of company had decreased with compared to previous months. The standardization of the process is required for having the optimum results sustained in long run. The proper documentation of the process and appropriate training of the people related with the process should be conducted so that they can able to run the process effectively.

V. CONCLUSION

Global competitiveness is making the manufacturing industries going through a tough challenge to produce high quality and customized products at low cost to meet the rocketing market demand. Six sigma was progressed as one of the powerful methodology in order to challenge these situations. It enhances the process efficiency by identifying and eliminating the defects. This paper executes the systematic application of the six sigma DMAIC methodology for reducing the rejection rate of casting in a foundry industry. The research findings show

that the rejection rate of casting had reduced from 15.61% to 7.40%. As a result, the cost associated with rejection or scrap had reduced. In addition, complete organizational involvement and training of the employees and the encouragement of the people for participating in the six sigma improvement are initiated.

REFERENCES

- [1] Kwak Y. H. and Anbari F. T., “Benefits, obstacles, and future of six sigma approach”, *Technovation*, vol. 26, pp. 708-715, 2006.
- [2] Desai T. N. and Shrivastava R. L., “Six sigma - a new direction to quality and productivity management”, *World Congress on Engineering and Computer Science*, 2008.
- [3] Mandal P., “Improving process improvement: executing the analyze and improve phase of DMAIC better”, *International Journal of Lean Six Sigma*, vol. 3 (3), pp. 231-250, 2012.
- [4] Ismyrlis V. and Moschidis O., “Six sigma’s critical success factors and toolbox”, *International Journal of Lean Six Sigma*, vol. 4 (2), pp. 108-117, 2013.
- [5] Kabir M. E., Boby S. M. M. I., Lutfi M., “Productivity improvement by using six sigma”, *International Journal of Engineering and Technology*, vol. 3 (12), 2013
- [6] Ahirwar N. and Verma D., “A review of six sigma approach : methodology, implementation and future research”, *International Journal of Science and Research*, vol. 3 (6), 2014.
- [7] Thomas Pyzdek, “The Six Sigma Handbook”, McGraw-Hill, 2003.
- [8] Chrysler/Ford/General Motors Task Force, “FMEA Reference Manual”, Automobile Industry Action Group, 3rd Edition, 1995.

Modeling an Academic Test by Practicing Google Drive Cloud Computing

Waseem Saad Nsaif, Laith Rtalib Rasheed, Saja Salim Mohammed, Mohamed Hakem Mohamed

College of Physical Education and Sport Science, Diyala University, IRAQ.

Abstract— In Considering of technological development Awarded in all aspects of life, especially in education and university education in particular, and starting from the principle of modernity and innovation in the educational process, the idea of this research generated to use the cloud computing applications in the preparation of tests for university students, advanced, accessible and relevant newness in devising the scientific of students to determine their scientific level in accuracy, without being bound by traditional tests, Where we'll prepare tests using a cloud computing applications which prepare ready models tests using Google drive ready test models, in several ways including selections or writing census paragraphs or short answers or complete vacuum or Pauline. Then after arranged and prepared the models test sent online to the students at various means of communication via the Internet, such as different kinds of email, Facebook, Twitter or Google Plus, and then the students answer and respond to the mail sender. The cloud computing technology is very useful for tests, especially as the availability of new services in testing, but nevertheless, we find that the number of tests that take advantage of cloud computing technology is still a few, perhaps this is because of submit to the tests through techniques will lead to a significant change in the test method, in addition to that it is not easy to move to the use of new technology with no able people to deal with those techniques , but perhaps in the near future, we will find many of the tests carried out by cloud computing techniques, This service can give you the free storage space of up to 5 GB is (Google Drive), so featuring that you can share files with your friends or make them public watched all the people, it is suitable service for a lot work because you can edit the MS Office files, and create files such as Word and PowerPoint and Excel, it supports multiple files and formats, to access this service must have a Gmail account, the service is available on the Mac or Windows devices and also you can reach them by phone. Also features by submit a form questionnaire or question by email, and participation the result of tests or questionnaire in an Excel paper, with

the possibility of filtering, mathematical operations and other without the need for a program on your computer. And get a graphical summary of the result of questionnaire or test. Also can apply a theme to give a nice seen for the tests or questionnaire form. These tests constitute a clear difference from traditional tests in terms of the accuracy of assessing students, and their level of knowledge to be accurate, in addition to overcome all the problematic and cons of traditional tests. It is also developing the student's personality, spirit, minds, bodies and affection. Also develop the student talent tendencies, and provide a flexible learning environment, and prepare qualified and skilled teaching staff in the use of modern teaching strategies and methods.

Keywords— Google Drive, Cloud Computing, Academic Test.

I. INTRODUCTION

Cloud computing is a type of Internet-based computing that provides shared computer processing resources and data to computers and other devices on demand. It is a model for enabling ubiquitous, on-demand access to a shared pool of configurable computing resources (e.g., computer networks, servers, storage, applications and services),[1][2] which can be rapidly provisioned and released with minimal management effort. Cloud computing and storage solutions provide users and enterprises with various capabilities to store and process their data in either privately owned, or third-party data centers[3] that may be located far from the user—ranging in distance from across a city to across the world. Cloud computing relies on sharing of resources to achieve coherence and economy of scale, similar to a utility (like the electricity grid) over an electricity network. Advocates claim that cloud computing allows companies to avoid up-front infrastructure costs (e.g., purchasing servers). As well, it enables organizations to focus on their core businesses instead of spending time and money on computer infrastructure.[4] Proponents also claim that cloud computing allows enterprises to get their applications up and running faster, with improved manageability and less

maintenance, and enables Information technology (IT) teams to more rapidly adjust resources to meet fluctuating and unpredictable business demand.[4][5][6] Cloud providers typically use a "pay as you go" model. This will lead to unexpectedly high charges if administrators do not adapt to the cloud pricing model.[7]In 2009, the availability of high-capacity networks, low-cost computers and storage devices as well as the widespread adoption of hardware virtualization, service-oriented architecture, and autonomic and utility computing led to a growth in cloud computing.[8][9][10]Companies can scale up as computing needs increase and then scale down again as demands decrease.[11] In 2013, it was reported that cloud computing had become a highly demanded service or utility due to the advantages of high computing power, cheap cost of services, high performance, scalability, accessibility as well as availability. Some cloud vendors are experiencing growth rates of 50% per year,[12] but being still in a stage of infancy, it has pitfalls that need to be addressed to make cloud computing services more reliable and user friendly.[13][14]

II. GOOGLE DRIVE

is a file storage and synchronization service operated by Google.[15] It allows users to store files in the cloud, synchronize files across devices, and share files. Google Drive encompasses Google Docs, Sheets and Slides, an office suite that permits collaborative editing of documents, spreadsheets, presentations, drawings, forms, and more. Google Drive offers users 15 GB of free storage,[26] with optional paid plans, between 100 GB and 30 TB, offering more storage.[17]Google Drive was launched on April 24, 2012,[18] and had 240 million monthly active users in October 2014.[4] Google said in September 2015 that they had over one million organizational paying users of Google Drive.[19]Google Drive for Education was announced on September 30, 2014. It was made available for free to all Google Apps for Education users. It includes unlimited storage and support for individual files up to 5TB in size, in addition to full encryption.[20]

2.1 Computer apps

Google Drive is available for PCs running Windows Vista or later, and Macs running OS X Lion or later.[21]In October 2016, Google announced that versions 1.27 and lower of the Drive computer software will be discontinued and sync will stop on February 1, 2017. Going forward after that date, Google will drop support for versions of the software older

than 1 year.[22]Later in October 2016, Google announced that starting January 1, 2017, the computer software would end support for Windows versions XP and Vista. The software will continue to work on those platforms, but will not be actively tested and maintained.[23]Google indicated in April 2012 that work on Linux software was underway,[24] but there was no news on this as of November 2013.[25]In April 2012, Google's then-Senior Vice President "SundarPichai" said that Google Drive would be tightly integrated with Chrome OS version 20.[26]

2.2 Mobile apps
Google Drive is available for Android smartphones and tablets running Android 4.1 "Jelly Bean" or later,[27] and iPhones and iPads running iOS 8 or later.[28]In August 2016, Google Drive ended support for Android devices running Android 4.0 "Ice Cream Sandwich" or older versions,[29] citing Google's mobile app update policy, which states: "For Android devices, we provide updates for the current and 2 previous Android versions." According to the policy, the app will continue to work for devices running older Android versions, but any app updates are provided on a best-efforts basis. The policy also states a notice will be given for any planned end of service.[30]In January 2017, Google announced that certain legacy versions of the Google Drive mobile apps would be shut down on April 3, 2017, delivering a prompt that requires users to update their app to a newer version. App versions being shut down include Android versions earlier than 2.4.311 and iOS versions earlier than 4.16.[31]

2.3 Website interface

Google Drive has a website that allows users to see their files from any Internet-connected computer, without the need to download an app. The website received a visual overhaul in 2014, that gave it a completely new look and improved performance. It also simplified some of the most common tasks, such as clicking only once on a file to see recent activity or share the file, and added drag-and-drop functionality, where users can simply drag selected files to folders, for improved organization.[32][33]A new update in August 2016 changed several visual elements of the website; the logo was updated, search box design was refreshed, and the primary color was changed from red to blue. It also improved the functionality to download files locally from the website; users can now compress and download large Drive items into multiple 2 GB .zip files with an improved naming structure, better Google Forms handling, and empty folders will now be included in the .zip, thereby preserving the user's folder hierarchy.[34][35]An unlimited amount of photos at maximum 16 megapixels and videos at

maximum 1080p resolutions are stored for free using the "High quality" setting in Google Photos. Using the "Original quality" setting uses Google Drive quota.[36]As of 2016, these are the storage plans offered by Google:[37][38]

Storage	Price
15 GB	Free
100 GB	\$1.99 per month (\$19.99 per year with 16% discount)
1 TB	\$9.99 per month (\$99.99 per year with 17% discount)
10 TB	\$99.99 per month
20 TB	\$199.99 per month
30 TB	\$299.99 per month

Storage purchases renew automatically at the end of the subscription period. Users can upgrade their storage plan anytime, with the new storage tier taking effect immediately. If the auto-renewal fails, a 7-day grace period is offered for users to update their payment information. When the storage subscription expires or is cancelled, storage limit is set back to the 15 GB free level at the end of the subscription period. Users can still access all their content, but will not be able to add anything beyond the storage limit, which means:[39]

III. WRITTEN TESTS

Indonesian Students taking a written testWritten tests are tests that are administered on paper or on a computer (as an eExam). A test taker who takes a written test could respond to specific items by writing or typing within a given space of the test or on a separate form or document.In some tests; where knowledge of many constants or technical terms is required to effectively answer questions, like Chemistry or Biology - the test developer may allow every test taker to bring with them a cheat sheet.A test developer's choice of which style or format to use when developing a written test is usually arbitrary given that there is no single invariant standard for testing. Be that as it may, certain test styles and format have become more widely used than others. Below is a list of those formats of test items that are widely used by educators and test developers to construct paper or computer-based tests. As a result, these tests may consist of only one type of test item format (e.g., multiple choice test, essay test) or may have a combination of different test item formats (e.g., a test that has multiple choice and essay items).

3.1 Multiple choice

In a test that has items formatted as multiple choice questions, a candidate would be given a number of set answers for each question, and the candidate must choose which answer or group of answers is correct. There are two families of multiple choice questions. The first family is known as the True/False question and it requires a test taker to choose all answers that are appropriate. The second family is known as One-Best-Answer question and it requires a test taker to answer only one from a list of answers. There are several reasons to using multiple choice questions in tests. In terms of administration, multiple choice questions usually requires less time for test takers to answer, are easy to score and grade, provide greater coverage of material, allows for a wide range of difficulty, and can easily diagnose a test taker's difficulty with certain concepts. As an educational tool, multiple choice items test many levels of learning as well as a test taker's ability to integrate information, and it provides feedback to the test taker about why distractors were wrong and why correct answers were right. Nevertheless, there are difficulties associated with the use of multiple choice questions. In administrative terms, multiple choice items that are effective usually take a great time to construct. As an educational tool, multiple choice items do not allow test takers to demonstrate knowledge beyond the choices provided and may even encourage guessing or approximation due to the presence of at least one correct answer. For instance, test taker might not work out explicitly that $6.14 \cdot 7.95 = 48.813$ but knowing that $6 \cdot 8 = 48$ they would choose an answer close to 48. Moreover, test takers may misinterpret these items and in the process, perceive these items to be tricky or picky. Finally, multiple choice items do not test a test taker's attitudes towards learning because correct responses can be easily faked.

3.2 Alternative response

True/False questions present candidates with a binary choice - a statement are either true or false. This method presents problems, as depending on the number of questions, a significant number of candidates could get 100% just by guesswork, and should on average get 50%.

3.3 Matching type

A matching item is an item that provides a defined term and requires a test taker to match identifying characteristics to the correct term.

3.4 Completion type

A fill-in-the-blank item provides a test taker with identifying characteristics and requires the test taker to recall the correct term. There are two types of fill-in-the-blank tests. The easier version provides a word bank of possible words that will fill in the blanks. For some exams all words in the World Bank are used exactly once. If a teacher wanted to create a test of medium difficulty, they would provide a test with a word bank, but some words may be used more than once and others not at all. The hardest variety of such a test is a fill-in-the-blank test in which no word bank is provided at all. This generally requires a higher level of understanding and memory than a multiple choice test. Because of this, fill-in-the-blank tests[with no word bank] are often feared by students.

3.5 Essay

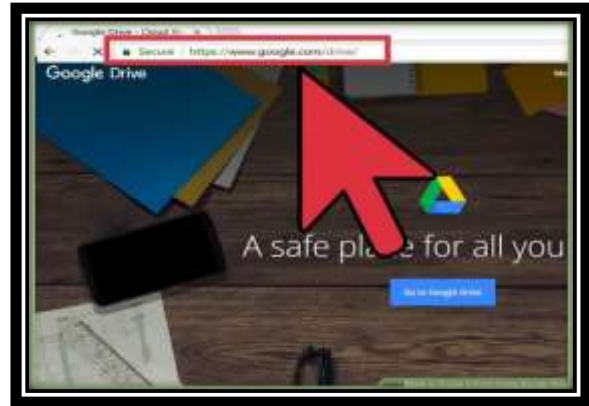
Items such as short answer or essay typically require a test taker to write a response to fulfill the requirements of the item. In administrative terms, essay items take less time to construct. As an assessment tool, essay items can test complex learning objectives as well as processes used to answer the question. The items can also provide a more realistic and generalizable task for test. Finally, these items make it difficult for test takers to guess the correct answers and require test takers to demonstrate their writing skills as well as correct spelling and grammar. The difficulties with essay items are primarily administrative. For one, these items take more time for test takers to answer. When these questions are answered, the answers themselves are usually poorly written because test takers may not have time to organize and proofread their answers. In turn, it takes more time to score or grade these items. When these items are being scored or graded, the grading process itself becomes subjective as non-test related information may influence the process. Thus, considerable effort is required to minimize the subjectivity of the grading process. Finally, as an assessment tool, essay questions may potentially be unreliable in assessing the entire content of a subject matter

IV. HOW TO CREATE A FORM USING GOOGLE DRIVE

Three Parts: Accessing Google Forms
Designing Your Form
Sending Your Google Form
Community Q&A. Thanks to Google Drive's "Forms" feature and the relative intuition with which one can use it, you can easily create a Google Form, Google Forms can be useful for a wide variety of applications, from data-gathering to event planning.

Part 1 Accessing Google Forms

Open your preferred browser. Google Forms are accessible through Google Drive; any created Google Forms will stay in Google Drive.



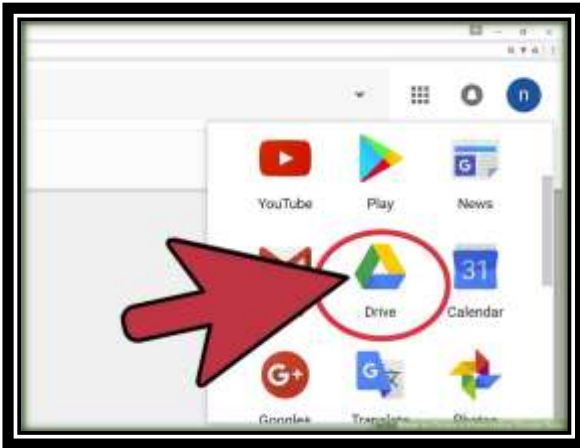
2- Navigate to your Gmail account. For best results, do this on a computer. You will need to enter your email address and password if you aren't already logged in.



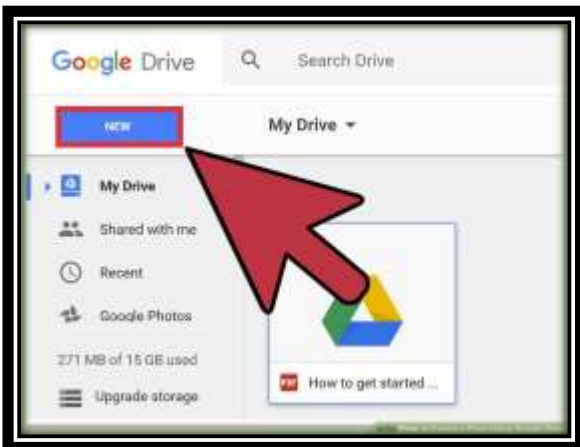
3- Click the Google apps menu. This is the nine-dot grid in the top right corner of your screen, to the left of your Gmail account picture.



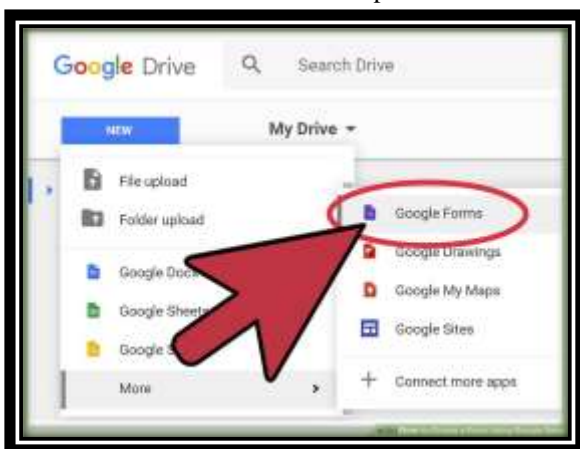
4- Click the "Drive" option. This will open your Google Drive account. Depending on your frequently-used apps, you may see the "Forms" option here. If so, click it to open Google Forms.



5- Click the "New" button. This is on the top left side of your Drive page, right above the "My Drive" option.

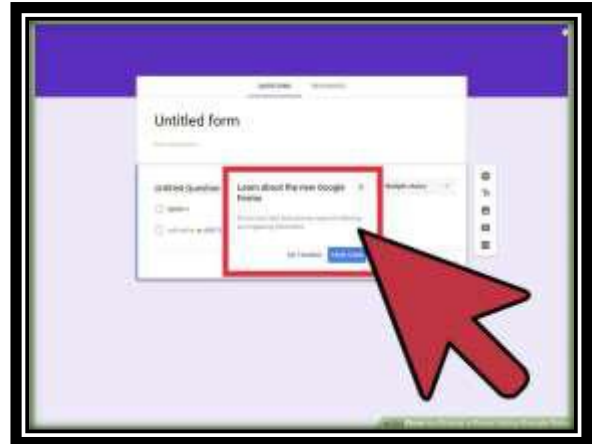


6- Hover over "More", then click "Google Forms". This will open a new, untitled Google Form. If you need to open a new form from the Google Forms home page, click the "+" button on the left side of the form templates.

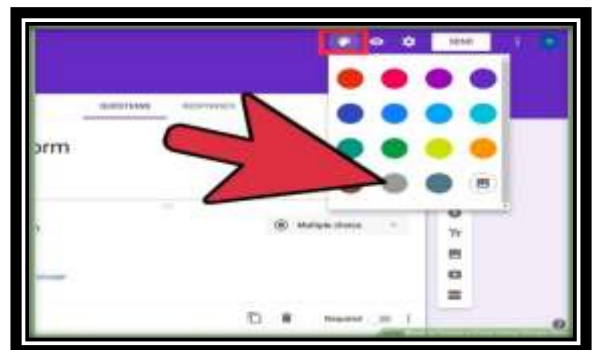


Part 2 Designing Form

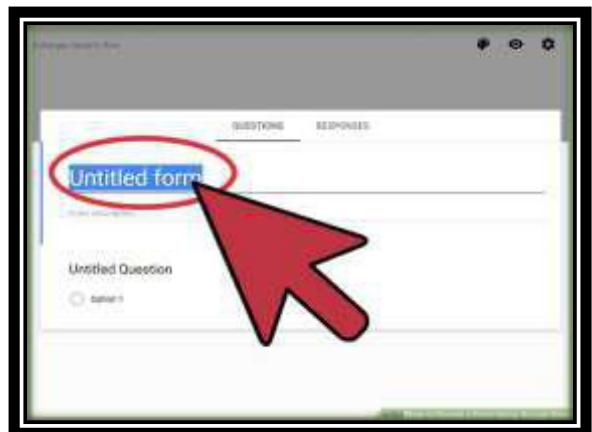
1- Decide on a purpose for your Google Form. Knowing what information you need to gather and the purpose it will serve will help you when deciding on formatting, step style, and so on.[1]



2- Change your form's color. You can do this by clicking the paintbrush palette icon to the left of the "Send" button, then selecting a color from the drop-down menu. Or, click the image icon next to the colors for a nice theme to use instead of a color.



3- Give your form a title. This option is at the top of the screen; you'll need to click the "Untitled Form" or "Form Title" text to type in this field.



4- Add a description to your form. Your respondents will be able to see this below the form title. Enter this information directly below the title field.



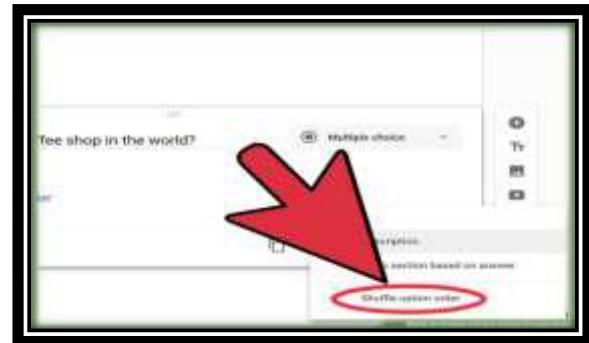
5- Add a question to your form. Questions are the basis of your data-gathering; users will answer these in whichever style you present the questions. To add a question: Click the "+" icon in the right-hand menu. Type your question text into the "Question" field. Replace the "Option 1" text with an answer. Tap the "Required" switch in the bottom-right corner for mandatory questions.



6- Select your questions type. You have several ways in which you can display your questions. To change your type of question: Click anywhere on a question card. Click the drop-down menu to the right of the question text. Select "Multiple Choice", "Checkboxes", or "Drop-Down". You can also choose longer answers like "Short answer" or "Paragraph".



7- Re-order your question cards if need be. You can do this by clicking the grid of six dots at the top of a card, then dragging it up or down and releasing it in its new location.

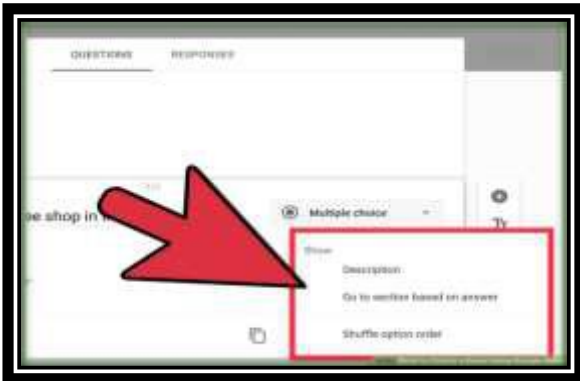


8- Review your other question card options. You can perform a couple of different actions on your question cards: Click the "Duplicate" button (two overlapping cards) to duplicate your current question card. Click the trash can icon to delete your current question card. Click the portrait icon next to an answer. This will allow you to add a photo; you'll need to hover over the question for this option to appear.



9- Review the additional options menu. You can do this by clicking the three vertical dots in the bottom right corner of your current question card: "Description" - Add a clarifying description to your question card. "Go to section based on answer" - Link different question cards to different answers. You'll do this from drop-down menus next to each answer

on a card."Shuffle option order" - Shuffle the answers for your current card.

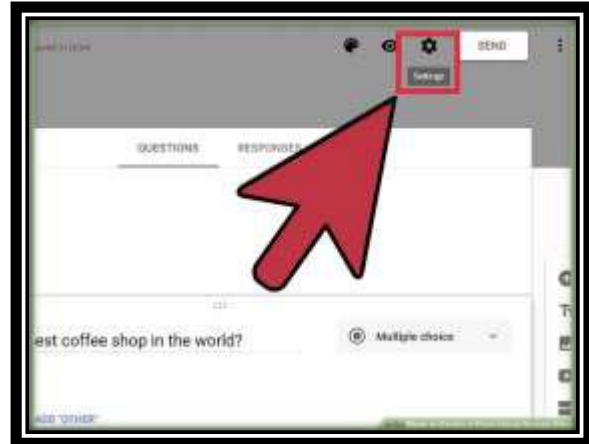


10- Click the "Preview" option to proofread your Form. This is the eye-shaped icon in the top right screen toolbar. When you're done reading through your Form and making sure all of the formatting is correct, you'll be ready to distribute your Form.

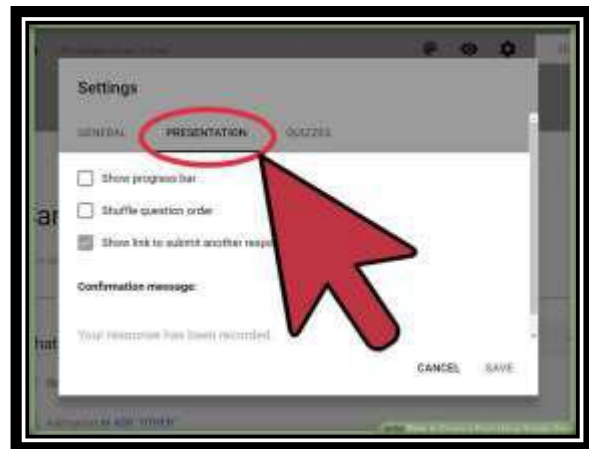


Part 3 Sending Your Google Form

1- Review your basic form settings. You can do this by clicking on the gear icon in the top right corner of the screen. Your form settings menu includes the following criteria:"Requires Sign-In" - Require respondents to sign into Google rather than being anonymous. Click the "Limit to 1 response" to enable this feature. Respondents can. Edit after submit" and "see summary charts and text responses" are your options here. These let respondents change their answers and view form results after submitting.



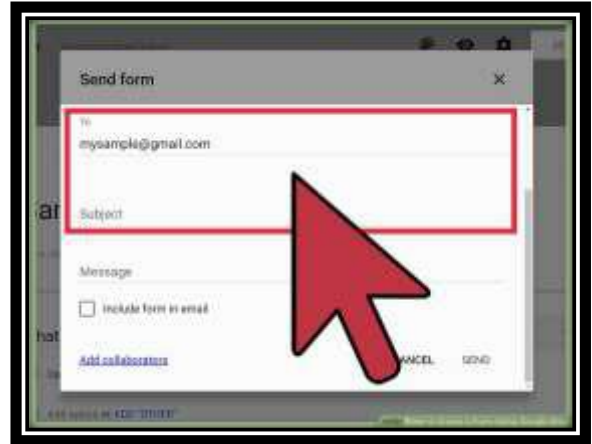
2- Review your presentation settings. These are also in the settings menu; switch from "General" to "Presentation" by clicking the pertinent option at the top of the settings window."Show progress bar" - Displays a metric that tells respondents how close they are to completing the form. "Shuffle question order" - Varies the question order from user to user."Show link to submit another response" - Creates a link to re-complete the form. This is ideal for invoicing forms."Confirmation message" - Customize your form's completion message by typing your preferred message into the field below this text.



3- Click the "Send" button. This is in the top right corner of your screen; clicking "Send" will bring up a "Send form" menu with several different sharing options through which you can cycle from the top of the window.



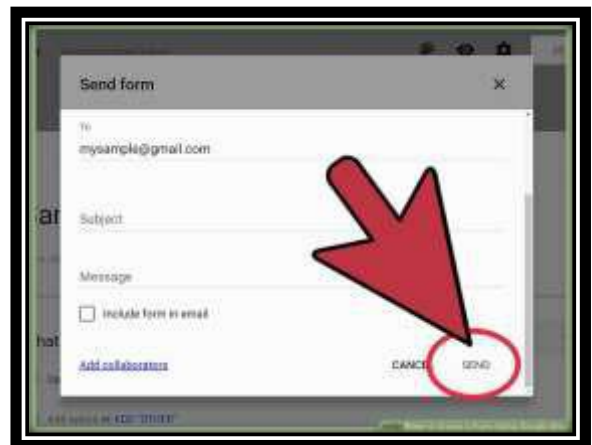
4- Review your sharing options. Depending on your form's purpose, your preferred option will vary: Email - Choose this option to send an email to your contacts directly from the Forms site. Link - Choose this option to get a link to copy-and-paste. Embed HTML - Only use this option if you're placing this form directly on your website. Google+, Facebook, or Twitter - These are quick-share options in the top right corner of your "Send form" menu.



6- Click "Send" if you're using email. This will distribute your form to everyone in the form contact list! To distribute the form via link, you'll need to manually post the link on a social media site or into an email.



5- Send your form using your selected service. Since you have a few different options for doing so, your process will vary: Email - Add a contact to the "To" field, a subject to the "Subject" field, and a brief message to the "Message" field. Click the "Include form in email" option to embed your form directly into the email. Link Right-click (or two-finger click) the link field and select "Copy". You can then paste this link in an email or on your preferred social media site. Embed - Right-click (or two-finger click) the HTML field and select "Copy". You can then paste this text into your website's HTML processor. Note that you can edit the width and height values of the form from here.



REFERENCES

- [1] Hassan, Qusay (2011). "Demystifying Cloud Computing" (PDF). The Journal of Defense Software Engineering. CrossTalk. 2011 (Jan/Feb): 16–21. Retrieved 11 December 2014.
- [2] Peter Mell and Timothy Grance (September 2011). The NIST Definition of Cloud Computing (Technical report). National Institute of Standards and Technology: U.S. Department of Commerce. doi:10.6028/NIST.SP.800-145. Special publication 800-145.
- [3] M. Haghghat, S. Zonouz, & M. Abdel-Mottaleb (2015). CloudID: Trustworthy Cloud-based and Cross-Enterprise Biometric Identification. Expert Systems with Applications, 42(21), 7905–7916.
- [4] "What is Cloud Computing?". Amazon Web Services. 2013-03-19. Retrieved 2013-03-20.

- [5] Baburajan, Rajani (2011-08-24). "The Rising Cloud Storage Market Opportunity Strengthens Vendors". It.tmcnet.com. Retrieved 2011-12-02.
- [6] Oestreich, Ken, (2010-11-15). "Converged Infrastructure". CTO Forum. Thectoforum.com. Retrieved 2011-12-02.
- [7] "Where's The Rub: Cloud Computing's Hidden Costs". 2014-02-27. Retrieved 2014-07-14.
- [8] "Cloud Computing: Clash of the clouds". The Economist. 2009-10-15. Retrieved 2009-11-03.
- [9] "Gartner Says Cloud Computing Will Be As Influential As E-business". Gartner. Retrieved 2010-08-22.
- [10] Gruman, Galen (2008-04-07). "What cloud computing really means". InfoWorld. Retrieved 2009-06-02.
- [11] Dealey, C. "Cloud Computing Working Group", Network Centric Operations Industry Consortium - NCOIC, 2013
- [12] "The economy is flat so why are financials Cloud vendors growing at more than 90 percent per annum?". FSN. March 5, 2013.
- [13] "Realization of Interoperability & Portability Among Open Clouds by Using Agent's Mobility & Intelligence - TechRepublic". TechRepublic. Retrieved 2015-10-24.
- [14] "Interoperability and Portability among Open Clouds Using FIPA Agent / 978-3-659-24863-4 / 9783659248634 / 3659248630". www.lap-publishing.com. Retrieved 2015-10-24.
- [15] Pichai, Sundar (April 24, 2012). "Introducing Google Drive... yes, really". Official Google Blog. Google. Retrieved January 16, 2017.
- [16] Bavor, Clay (May 13, 2013). "Bringing it all together: 15 GB now shared between Drive, Gmail, and Google+ Photos". Google Drive Blog. Google. Retrieved January 16, 2017.
- [17] "Google Drive storage plans & pricing". Drive Help. Google. Retrieved January 16, 2017.
- [18] Protalinski, Emil (October 1, 2014). "Google announces 10% price cut for all Compute Engine instances, Google Drive has passed 240M active users". The Next Web. Retrieved October 30, 2016.
- [19] Johnston, Scott (September 21, 2015). "Making Google Drive the safest place for all your work". Medium. Retrieved October 28, 2016.
- [20] Summers, Nick (September 30, 2014). "Google unveils Drive for Education with free, unlimited storage and 'Classroom' integration". The Next Web. Retrieved October 23, 2016.
- [21] "System requirements and browsers". Drive Help. Google. Retrieved January 16, 2017.
- [22] "Service for Google Drive for Mac/PC versions 1.27 and older ending after February 1, 2017". G Suite Updates. Google. October 18, 2016. Retrieved January 16, 2017.
- [23] "Google Drive desktop app ending support for Windows XP and Vista". G Suite Updates. Google. October 27, 2016. Retrieved January 16, 2017.
- [24] Noyes, Katherine (April 25, 2012). "Google Drive for Linux Is on the Way". PC World. International Data Group. Retrieved January 16, 2017.
- [25] Shankland, Stephen (November 28, 2013). "Google Drive for Linux? Patience, patience...". CNET. CBS Interactive. Retrieved January 16, 2017.
- [26] Metz, Cade (April 25, 2012). "Google Set to Meld GDriveWith Chrome OS". Wired. Condé Nast. Retrieved January 16, 2017.
- [27] "System requirements and browsers". Drive Help. Google. Retrieved January 16, 2017.
- [28] "System requirements and browsers". Drive Help. Google. Retrieved January 16, 2017.
- [29] Whitwam, Ryan (August 23, 2016). "Drive app update ends support for ICS, adds in-app storage upgrades, and more". Android Police. Retrieved January 16, 2017.
- [30] "Updates to G Suite mobile apps". G Suite Administrator Help. Google. Retrieved January 16, 2017.
- [31] "Legacy versions of Google Drive, Docs, Sheets, and Slides mobile apps shutting down on April 3, 2017". G Suite Updates. Google. January 19, 2017. Retrieved January 20, 2017.
- [32] "Meet the new Google Drive". Google Drive Blog. Google. June 25, 2014. Retrieved January 16, 2017.
- [33] Crider, Michael (July 8, 2014). "Google Drive Gets A Shiny New Interface On The Web, Rolling Out To Users Starting Now". Android Police. Retrieved January 16, 2017.
- [34] "Improvements to downloading files and folders in Google Drive on the web". G Suite Updates. Google. August 18, 2016. Retrieved January 16, 2017.
- [35] Whitwam, Ryan (August 18, 2016). "Google Drive on the web gets UI tweaks, better file downloads, and more". Android Police. Retrieved January 16, 2017.
- [36] Ruddock, David (December 21, 2016). "Nice: Google Drive adds annual billing - with discounts - for 100GB and 1TB plans". Android Police. Retrieved January 16, 2017.

- [37] "Drive storage". Google. Retrieved January 16, 2017. (registration required)
- [38] "Choose a storage size". Google Photos Help. Google. Retrieved January 16, 2017.
- [39] "Purchase, cancellation, & refund policies". Drive Help. Google. Retrieved January 16, 2017.

Greener One-pot Synthesis of Chromeno Oxazin and Oxazin Quinoline Derivatives and their Antibacterial Activity

V.Sruthi¹, M.Visalakshi¹, T.Rambabu¹, Ch.V.V.Srinivas^{1,2}, Y. Vamsi Kumar^{1,3},
M.Sunitha^{1,2}, S. Paul Douglas^{1*}

¹Department of Engineering Chemistry, Andhra University, Visakhapatnam, AP, India

²SRK College for Women, Rajamahendravaram, AP, India

³MR College (A), Vizianagaram, AP, India

Abstract— An efficient green method for the synthesis of oxazino quinoline-2-amine derivatives, oxazino quinoline derivatives and chromeno oxazin-5-one derivatives have been synthesized through cyclization of aromatic aldehyde, ammonium acetate, substituted amides and 8-hydroxy-quinoline or 4-hydroxy coumarin by one-pot condensation method is described. The synthesized compounds are characterized by FT-IR, ¹H NMR and MASS spectral techniques and are screened further for biological activities against *Escherichia coli*, *Pseudomonas aeruginosa*, *Staphylococcus aureus* and *Bacillus subtilis* using cup plate method and disc diffusion method.

Keywords — One-pot Synthesis, Biological activity, Chromeno oxazin-5-one derivatives, Oxazino quinoline-2-amine derivatives and Oxazino quinoline derivative.

I. INTRODUCTION

One pot synthesis through multi-component reactions [MCRs] has a great role in organic synthesis. These are one step reactions, where the reactants are subjected into a single reactor to form a desired product with high yields without any intermediate formation. Its importance lies mainly in the synthesis of medicinally potent compounds and its convenient preparation than the conventional methods, thereby having great advantage over convergent and conventional synthesis [1-3].

The compounds consisting of quinoline moiety have broad range of applications with biological activity such as anti-malarial, anti-asthmatic, anti-inflammatory and anti-bacterial properties [4,5]. On the other hand, oxazinone derivatives have a considerable property as a non-nucleoside reverse transcriptase inhibitor to fight against HIV virus which is approved by FDA [6]. Heterocyclic compounds having coumarin nuclei have aroused wide range of biological activities [7, 8] such as antibacterial, anticoagulant, antiviral, antifungal, anticancer and anti-inflammatory properties [9].

Coumarins acts as urease inhibitors [10], corrosion inhibitors [11], optical brighteners [12], dispersed fluorescent and laser dyes [13] used in Dye Sensitized Solar Cells (DSSCs)[14-21]. The main importance lies in the functionally substituted chromenes in the field of medicinal chemistry [22-23] as natural fruit and plant extract in Ammi Visnaga as visnadine [25] and in *Phlojodicarpus sibiricus* as Khellactone [26]. These have perfect vasodilatory properties.

Chromene is the privileged structural component for various natural products consisting of photochemical properties. It is the backbone of many polyphenols found mostly in alkaloids, flavanoids, tocopherols and anthocyanins [27]. The chromene derivatives are potential anticancer agents [28]. Earlier several methods are reported for the synthesis of oxazino quinolines, from aromatic aldehydes, 6-quinolinol and urea under solvent-free conditions using *p*-toluene sulfonic acid at 150 °C [6], 6-quinolinol, benzaldehyde and methylcarbamate using H₂O/ Triethylbenzylammonium- chloride using water as solvent [29] and quinoline, dimethyl acetylenedicarboxylate zwitterions and aldehydes using toluene as solvent [30], 8-hydroxyquinoline, thiourea and formaldehyde by condensation method using *N, N*-Dimethylformamide medium as solvent [31].

In this a novel preparation of oxazino quinolines using different reactants is reported. The main objective of our research is synthesis of active heterocyclic compounds, which involves greener procedures, shorter reaction times, lower temperature conditions, higher yields, and economically desirable processes.

Now we report an efficient greener synthesis of oxazino quinoline-2-amine derivatives, oxazino quinoline derivatives and chromeno oxazin-5-one derivatives through cyclization of aromatic aldehyde, ammonium acetate, amide and 8-hydroxy quinoline ("Fig.1") or 4-hydroxy coumarin ("Fig.2") through one pot condensation method without catalyst.

II. EXPERIMENTAL

2.1. Chemicals and Apparatus:

All chemicals used in this process are of AR grade fine chemicals, without any further purification. The synthesized oxazino quinoline-2-amine, oxazino quinoline derivatives and chromeno oxazin-5-one derivatives were characterized by FT-IR, ¹H NMR and MASS spectral techniques. FT-IR spectra recorded on a (Perkin Elmer Spectra-880) spectrophotometer by using KBr pellets in the region 400 - 4500 cm⁻¹ and ¹H NMR spectra was characterized by 400 MHz-(Bruker Avance) in CDCl₃ solvent and MASS spectra was recorded at 70 eV (MASPEC low resolution mass spectrometer).

2.2. General Procedure for the synthesis of oxazino quinoline-2-amine and oxazino quinoline derivatives and chromeno oxazin-5-one derivatives:

The one pot synthesis of oxazino quinoline-2-amine and oxazino quinoline derivatives and chromeno oxazin-5-one derivatives was carried out in 250 mL round bottomed flask by taking equimolar quantities of aromatic aldehydes (10 mmol), ammonium acetate(10 mmol), substituted amides (10 mmol), 8-hydroxyquinoline or 4-hydroxy coumarin (10 mmol) and 15 mL of ethanol were mixed together in a round bottomed flask and the flask was placed in an oil bath over a hotplate consisting of magnetic stirrer and kept for reflux at 80 °C for one hour. The progress of the reaction was monitored by TLC using mobile phase (n-Hexane:ethyl acetate 3:1). The excel solvent from product mixture was removed under rotatory evaporator to obtain the solid product, which was then recrystallized from hot ethanol, to get the pure products and they are characterized and compared by FT-IR, ¹H NMR and MASS spectral techniques which are presented in 3.2 spectral data.

III. RESULTS AND DISCUSSION

The procedure involves the cyclization of aromatic aldehyde, ammonium acetate, 8-hydroxy-quinoline and substituted amides to form oxazino quinoline-2-amine and oxazino quinoline derivatives is described as model reaction shown in "Fig.1" and cyclization of aromatic aldehyde, ammonium acetate, 4-hydroxy coumarin and substituted amides to form chromeno oxazin-5-one derivatives is described as model reaction shown in "Fig.2". The attainability of formation of these derivatives and the reaction conditions are tabulated in "Table 1".

3.1 Plausible Mechanism for the synthesis of oxazino quinoline-2-amine and oxazino quinoline derivatives and chromeno oxazin-5-one derivatives:

In this reaction 8-hydroxy quinoline or 4-hydroxy coumarin, benzaldehyde, ammonium acetate and substituted amides are taken as reactants to run the

process. Initially aromatic aldehydes undergo nucleophilic addition with 8-hydroxy quinoline or 4-hydroxy coumarin through Knoevenagel condensation reaction to form the intermediate Knoevenagel product (1). In the second step, ammonium acetate and substituted amides undergo enolisation. The formed enol product reacts with Knoevenagel product to form the highly stabilized product smoothly shown in "Fig.3". In this mechanism 8-hydroxy quinoline or 4-hydroxy coumarin consists of same OH groups and the reaction mechanism is same.

3.2. Spectral and physical data for the synthesized compounds:

2-methyl-4-phenyl-4a,10b-dihydro-4H-[1,3]oxazino[5,6-h]quinoline(4a):

IR (KBr, ν_{\max} cm⁻¹): 3056(CH str), 1515(-C=C str), 1274(-C=N str), 1104(-C-O-C str); ¹H NMR (400 MHz, CDCl₃ δ / ppm): 7.914 - 7.898 (m, Ar-H), 7.894 - 7.838 (m, Ar-H), 7.830 - 7.818 (m, Ar-H), 7.813-7.869 (m, Ar-H), 7.564-7.556 (m, Ar-H), 7.559 - 7.549(m, Ar-H), 7.543 - 7.532 (m, Ar-H), 7.529-7.519 (m, Ar-H), 7.516 - 7.470 (m, Ar-H), 7.320 - 7.260 (m, Ar-H), 4.04 (s,1H), 1.9 (s, methyl proton); ESMS:275.1 [M+1].

2,4-diphenyl-4a,10b-dihydro-4H-[1,3]oxazino[5,6-h]quinoline(4b):

IR (KBr, ν_{\max} cm⁻¹): 3172(CH str), 1624(-C=Cstr), 1250(-C=N str), 1150(-C-O-C str); ¹H NMR (400 MHz, CDCl₃ δ / ppm): 8.898 (m, Ar-H), 7.835 - 7.829 (m, Ar-H), 7.827 - 7.823 (m, Ar-H), 7.814-7.809 (m, Ar-H), 7.805-7.559 (m, Ar-H), 7.556 - 7.553(m, Ar-H), 7.543 - 7.537(m, Ar-H), 7.532-7.522 (m, Ar-H), 7.519 - 7.516 (m, Ar-H), 7.473 (m, Ar-H), 7.453 (m, Ar-H), 7.439 (m, Ar-H), 7.435 (m, Ar-H), 7.260 (m, Ar-H), 6.11 (m, Ar-H), 5.897 (s,1H); ESMS: 337.2 [M+1].

4-phenyl-4a,10b-dihydro-4H-[1,3]oxazino[5,6-h]quinolin-2-amine(4c):

IR (KBr, ν_{\max} cm⁻¹): 3072(CH str), 1508 (-C=C str), 1275 (-C=N str), 1103(-C-O-C str); ¹H NMR (400 MHz, CDCl₃ δ / ppm): 7.91 - 7.897 (m, Ar-H), 7.651 - 7.568 (m, Ar-H), 7.549-7.531 (m, Ar-H), 7.506-7.487 (m, Ar-H), 7.357-7.329 (m, Ar-H), 7.311 - 7.290(m, Ar-H), 7.260 - 7.126 (m, Ar-H), 7.107 (m, Ar-H), 7.089 (m, Ar-H), 5.862 (m, Ar-H), 4.01 (s,1H), 2.191(s, NH₂ proton); ESMS: 276.2 [M+1].

2,4-diphenylchromeno[3,4-e] [1,3]oxazin-5(4H)-one(4d):

IR (KBr, ν_{\max} cm⁻¹): 3090(CH str), 1590(-C=C str), 1200(-C=N str), 1050(-C-O-C str); ¹H NMR (400 MHz, CDCl₃ δ / ppm): 8.184(m, Ar-H), 8.163 (m, Ar-H), 7.487(m, Ar-H), 7.466(m, Ar-H), 7.454 (m, Ar-H),

7.447(m, Ar-H), 7.434(m, Ar-H), 7.532-7.522 (m, Ar-H), 7.355 (m, Ar-H), 7.353 (m, Ar-H), 7.334 (m, Ar-H), 7.332(m, Ar-H), 7.260 (m, Ar-H), 7.260 (m, Ar-H), 206(m, Ar-H), 7.187 (m, Ar-H) 5.01 (s,1H); ESMS: 354.2 [M+1].

2-methyl-4-phenylchromeno[3,4-e][1,3]oxazin-5(4H)-one(4e):

IR (KBr, ν_{\max} cm^{-1}): 3100(CH str), 1650(-C=C str), 1350(-C=N str), 1050(-C-O-C str); $^1\text{H NMR}$ (400 MHz, CDCl_3 δ / ppm): 7.504 (m, Ar-H), 7.485 (m, Ar-H), 7.334 (m, Ar-H), 7.315 (m, Ar-H), 7.295 (m, Ar-H), 7.260(m, Ar-H), 7.122 (m, Ar-H), 7.104 (m, Ar-H), 7.085 (m, Ar-H), 3.35 (s,1H), 1.5 (s, methyl proton); ESMS: 291.1 [M+1]

IV. BIOLOGICAL ACTIVITY

The antibiotic potency can be determined using the microbial assays. The basic principle of microbial assay lies in comparison of the inhibition of growth of bacteria by measuring concentration of the product to be investigated with that produced by known concentration of the antibiotic having a known activity.

The methods used for assay are cup plate method and disc diffusion method. The cup plate method is based on the diffusion of an antibiotic from a cavity through the solidified agar layer of a Petri-dish. Growth of inoculated microbe is inhibited entirely in a circular zone around a cavity containing a solution of the antibiotics. Antimicrobial activity of synthesized compounds was screened against 4 human pathogenic bacteria, two gram positive and two gram negative bacteria. Their respective MTCCNO numbers are, *Escherichia coli* (Gram-negativeve_(2692), *Pseudomonas aeruginosa* (Gram-negative)_ (2453), *Staphylococcus aureus* (Gram-positive)_ (902), *Bacillus subtilis* (Gram-positive)_ (441). The activities of the drug samples against 4 human pathogenic bacteria are tabulated in "Table 2". The antibacterial activity of the samples is assessed using the different concentration of the sample i.e., low, intermediate, high. The present investigation reveals that the zone of inhibition increased as the concentration of the sample increased. This is seen in case of the compounds 4a and 4c. Hence the MIC (Minimum Inhibitory Concentration) of these samples that can inhibit bacterial growth is 10 μl , 20 μl and 30 μl respectively. Thus the above samples are able to show antibacterial activity on *Escherichia coli*, *Pseudomonas aeruginosa*, *Staphylococcus aureus* and *Bacillus subtilis*. The standard drug streptomycin is found to be very effective anti-microbial agent. Here it is found that the standard drug show antibacterial activity on both gram-positive and gram-negative bacteria and it is found that

the zone of inhibition increased as the concentration of the sample increased.

V. FIGURES AND TABLES

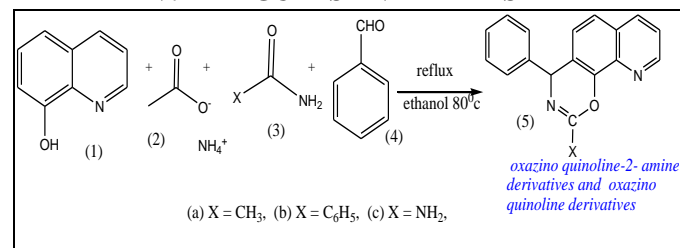


Fig.1: Synthesis of oxazino quinoline-2-amine and oxazino quinoline derivatives

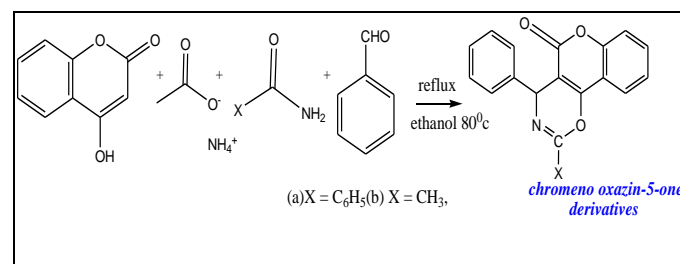


Fig.2: Synthesis of chromeno oxazin-5-one derivatives.

Table.1: Synthesis of oxazino quinoline-2-amine and oxazino quinoline derivatives and chromeno oxazin-5-one derivatives:

S. No	Quinoline/ Coumarin	Amide	Time (min)	Yield %	Product
1	8-hydroxy-quinoline	acetamide	55	96	4a
2	8-hydroxy-quinoline	benzamide	60	92	4b
3	8-hydroxy-quinoline	urea	75	89	4c
4	4- hydroxy coumarin	benzamide	75	85	4d
5	4- hydroxy coumarin	acetamide	70	89	4e

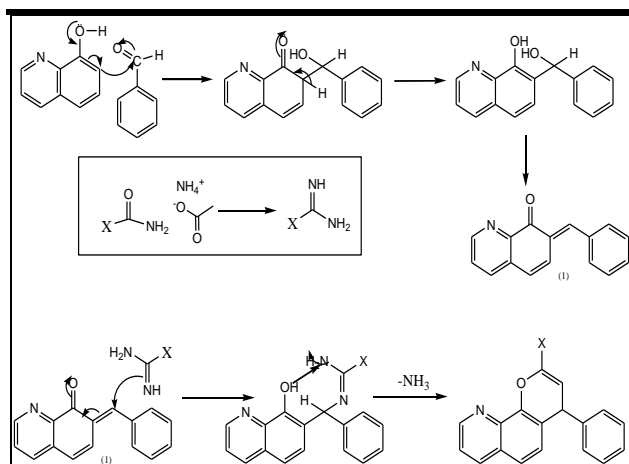


Fig.3: Plausible mechanism for the synthesis of oxazino quinoline-2- amine and oxazino quinoline derivatives

Table.2: Anti-Bacterial activity of drug sample

S.NO	Microorganism	Concentration of the Sample		
		10µl	20µl	30µl
4a	<i>Escherichia coli</i>	V3.7	V4.0	V4.7
	<i>Pseudomonas aeruginosa</i>	V3.0	V3.5	V4.0
	<i>Staphylococcus aureus</i>	V2.3	V2.5	V2.7
	<i>Bacillus subtilis</i>	V3.2	V3.5	V3.7
4b	<i>Escherichia coli</i>	V1.1	V1.2	V1.4
	<i>Pseudomonas aeruginosa</i>	V	V1.7	V1.9
	<i>Staphylococcus aureus</i>	V2.4	V2.7	V3.2
	<i>Bacillus subtilis</i>	-	-	-
4c	<i>Escherichia coli</i>	V3.0	V3.2	V3.5
	<i>Pseudomonas aeruginosa</i>	V2.2	V2.7	V3.5
	<i>Staphylococcus aureus</i>	V2.5	V3.0	V3.5
	<i>Bacillus subtilis</i>	V2.5	V3.6	V4.0
4d	<i>Escherichia coli</i>	V1.5	V2.0	V2.5
	<i>Pseudomonas aeruginosa</i>	V1.2	V1.7	V1.9
	<i>Staphylococcus aureus</i>	V1.4	V1.8	V2.0
	<i>Bacillus subtilis</i>	V1.5	V1.7	V2.1
4e	<i>Escherichia coli</i>	V2.4	V2.5	V2.9
	<i>Pseudomonas aeruginosa</i>	V1.8	V2.2	V2.5
	<i>Staphylococcus aureus</i>	-	V2.0	V2.3
	<i>Bacillus subtilis</i>	-	-	-

VI. CONCLUSION

In this present study, we report an efficient method for the synthesis of oxazino quinoline-2-amine derivatives, oxazino quinoline derivatives and chromeno oxazin-5-one derivative. This method has advantages like improved yield of products and less reaction times.

ACKNOWLEDGEMENTS

The authors wish to thank UGC for the facilities provided through UGC-MRP No. F.41-371/2012 to SPD, UGC-FIP to YVK and MS and DST-Advanced Analytical Laboratory, Andhra University, Visakhapatnam for the characterization facilities provided for the work.

REFERENCES

- [1] D. J. Ramon and Y.miguel, "Asymmetric Multicomponent Reactions (amcrs): The New Frontier." *Angew chem int ed*, vol. 44, pp. 1602 - 1634, March 2005.
- [2] A .Domling, "Recent Developments in Isocyanide Based Multicomponent Reactions in Applied Chemistry". *Chem Rev.*, vol. 106 (1), pp. 17-89 , December 2006.
- [3] S.Tu, B.Jiang, Y. Zhang, R. Jia, J. Zhang, C. Yao and S. Feng, "An Efficient and Chemoselective Synthesis of N-substituted 2-aminopyridines via a Micro-wave Assisted Multicomponent Reaction". *Org Biomol Chem*, vol. 5, pp. 355-359, 2007.
- [4] R. D. Larsen, G.Corley, A. O. King, J. D.Carrol, P.Davis, T. R.Verhoeven, P. J.Reider, M. Labelle, J. Y.Gauthier, Y. B. Xiang, R. J. Zamboni," Practical Route to A New Class of ltd4 Receptor Antagonists" *J. Org. Chem.*, vol. 61, pp. 3398, 1996.
- [5] Y.L.Chen, K. C. Fang, J. Y. Shen, S. L. Hsu, C. C.Tzeng, "Synthesis and Bacterial Evaluation certain Quinoline derivatives", *J. Med. Chem.*, Vol. 44, pp. 2374-2377, June 2001.
- [6] G.I.Shakibaei, H.R.Khavasi, P.Mirzaei, A.Bazgir, "A Three-Component, One-Pot Synthesis of Oxazino quinolin-3-oneDerivatives" *J.HeterocyclicChem.* Vol. 45, pp. 1481-1484, October 2008.
- [7] M.A. Musa, J.S. Cooperwood, and M.O.F. Khan. "A review of coumarin derivatives in pharmacotherapy of breast cancer". *Curr Med Chem.* Vol. 15, pp. 2664-79, 2008.
- [8] J. Neyts, E.D. Clercq and R .Singha, et al. *J Med Chem.* Vol. 52, pp. 1486, 2009.
- [9] K.N. Venugopala, V. Rashmi and B. Odhav, "Review on Natural Coumarin Lead Compounds for Their Pharmacological Activity", *BiomedRes Int.* vol. 96, pp. 3248, Febraury 2013.

- [10] K. M. Khan, S. Iqbal, M. A. Lodhi et al. *Bioorganic and Medicinal Chemistry*, vol. 12 (81), pp. 963, 2004.
- [11] A. A. Al-Amiry, Y. K. Al-Majedy, A. A. H. Kadhum, and A.B. Mohamad, "New Coumarin Derivative as an Eco-Friendly Inhibitor of Corrosion of Mild Steel in Acid Medium". *Molecules*, vol. 20 (1), pp. 366, September 2015.
- [12] M. Zabradnik, "The Production and Application of Fluorescent Brightening Agents". John Wiley and Sons: New York 1992.
- [13] R.D.Murray, J. Mendez and S.A. Brown, "The natural coumarins: Occurrence, Chemistry and Biochemistry". John Wiley and Sons: New York 1982.
- [14] X. Liu, J.M. Cole, P.G. Waddell, T-C. Lin, J. Radia and A.Zeidler. "Molecular origins of optoelectronic properties in coumarin dyes: toward designer solar cell and laser applications" *J Phys Chem*, vol. 116, pp. 727–737, January 2012.
- [15] Y. Hu, Y. Zhong, J. Li, L. Cai, H. Li "synthesis and characterisation of microencapsulated 7-alkoxy-4-trifluoromethylcoumarin dyes". *Color Technol*, vol. 127, pp. 335-339, October 2011.
- [16] S. Takizawa, C. Pérez-Bolívar, P. Anzenbacher and S. Murata. "cationic iridium complexes coordinated with coumarin dyes – sensitizers for visible-light-driven hydrogen generation". *Eur J Inorg Chem*, pp. 3975, June 2012.
- [17] N. Barooah, J. Mohanty, H. Pal, A.C Bhasikuttan, "Non-Covalent Interactions of Coumarin Dyes with Cucurbit Uril Macrocycle: Modulation of Ict to Tict State Conversion". *Org Biomol Chem*, vol. 10 pp. 5055-62, May 2012.
- [18] C. Ghatak, V.G. Rao, S. Mandal and N. Sarkar, "Photoinduced electron transfer between various coumarin analogues and N,N-dimethylaniline inside niosome, a nonionic innocuous polyethylene glycol-based surfactant assembly". *Phys Chem*, vol. 14, pp. 8925-35, March 2012.
- [19] B. Liu, R. Wang, W.Mi, X.Li and H. Yu. "Novel branched coumarin dyes for dye-sensitized solar cells: significant improvement in photovoltaic performance by simple structure modification". *J Mater Chem*, vol. 22, pp.15379-15387, June 2012.
- [20] S.S. Anufrik, V.V. Tarkovsky, G.G. Sazonko, M.M. Asimov, "New laser dyes based on 3-imidazopyridylcoumarin derivatives". *J Appl Spectrosc*. Vol. 79, pp.46- 52, March 2012.
- [21] L. Chen, T-S Hu and Z-J Yao, "Development of new pyrrolocoumarin derivatives with satisfactory fluorescent properties and notably large stokes shifts". *Eur J Org Chem*, pp. 6175-6182, 2008.
- [22] M.N. Elinson, A.S. Dorofeev and S.K. Feducovich, et al. "Electrochemically induced chain transformation of salicylaldehydes and alkyl cyanoacetates into substituted 4H-chromenes". *Tetrahedron Lett*. Vol. 47, pp.7629-7633, October 2006.
- [23] W. Sun, L.D. Cama, E.T. Birzin, et al. "6h-benzo[c]chromen-6-one derivatives as selective $\epsilon\delta$ agonists". *Bioorg Med Chem Lett*. Vol. 16, pp.1468-72, March 2006.
- [24] A.V. Stachulski, N.G. Berry and A.C. Lilian Low et al. "Identification of isoflavone derivatives as effective anticryptosporidial agents in vitro and in vivo". *J Med Chem*. Vol.49 pp.1450 – 1454, 2006
- [25] M. Iranshahi, M. Askari, A. Sahebkar, Hadjipavlou-Litina D. DARU, "Evaluation of antioxidant, anti-inflammatory and lipooxygenase inhibitory activities of the prenylated coumarin umbelliprenin". *J Pharm Sci*, vol.17, pp. 99, June 2009.
- [26] D. Gantimur, A.I. Syrchina and A.A Semenov. "Review on Natural Coumarin Lead Compounds for Their Pharmacological Activity". *Chem Nat Compd*. Vol. 22 ,pp.103-104, 1986.
- [27] R. Qiao, Y.S. Woon, D. Zhiyun, Z. Kun, W. Jian, "Expedient Assembly of a 2-Amino-4H-Chromene Skeleton by Using an Enantioselective Mannich Intramolecular Ring Cyclization–Tautomerization Cascade Sequence". *Chem Eur J*, vol. 17, pp.7781–7785, 2011.
- [28] M. Vosooghi, S. Rajabalian, M.Sorkhi, M. Badinloo, M. Nakhjiri, and A.S. Negahbani, "Synthesis and Cytotoxic Activity of Some 2-amino-4-aryl-3-Cyano-7-(dimethylamino)-4H-Chromenes". *Res Pharm Sci*, vol. 5(1), pp. 9–14, 2010.
- [29] M.H. Mosslemin, M.R. Nateghi, R. Mohebat, "A clean synthesis of oxazino[5,6-f]quinolinone and naphtho[1,2-e]oxazinone derivatives" *Monatsh Chem*, vol.139, pp. 1247- 1250, April 2008.
- [30] V. Nair, S. Devipriya, S.Eringathodi, " efficient synthesis of [1,3]oxazino[2,3-a]quinoline derivatives by a novel 1,4-dipolar cycloaddition involving a quinoline-dmad zwitterion and carbonyl compounds" *Tetrahedron Letters*, vol. 48, pp. 3667-3670, February 2007.
- [31] S.S.S. Abuthahiri, A.J.A. Nasser, S. Rajendran, G. Brindha, "Synthesis, spectral Studies and antibacterial activities of 8-hydroxquinoline Derivatives and its metal complexes " *Chemical Science Transactions*, vol. 3(1), pp.303-313, 2014.

An Experimental Investigation and Modal Analysis of an Engine Supporting Bracket

A.S. Adkine¹, Prof.G.P.Overikar², Prof. S .S. Surwase³

¹PG Student Department of Mechanical Engineering, Shree Tuljabhavani College of Engineering, Tuljapur, India

²Assistant Prof. Department of Mechanical Engineering, Shree Tuljabhavani College of Engineering, Tuljapur, India

³Associate Prof. Department of Mechanical Engineering, Shree Tuljabhavani College of Engineering, Tuljapur, India

Abstract— Engine supporting bracket plays a vital role in improving the ride comfort and work environments of the vehicle. It is anticipated that improvement in vibration control can be achieved by the determination of natural frequency of engine supporting bracket system and must be less than self-excitation frequency range. This paper describes higher stresses induced and its critical region on the component. In static structural analysis design is suggested against deformation, equivalent stress and strain energy using finite element analysis concept. Existing design is modified and provided with the isolation effects and on stress distribution from critical region which concentrates on strengthened body part was suggested. Further scope of this work involves in carrying out vibration study using fast Fourier transform (FFT) analyzer.

Keywords—Engine bracket, FEA, Static Analysis, Natural Frequency.

I. INTRODUCTION

An engine supporting bracket is a very important component of an automotive transmission system. An engine is generated undesirable vibration to develop power & transmitted to the skeleton of the vehicle through the supporting members. Engine is rest on the supporting member and it's attached to vehicle body. In the automotive engine bracket is very important in different aspect of vehicle performance. It is significant study of which have depth investigated to understand failure of engine supporting bracket is mainly due to generated crack at high level stress region. It has designed frame work to support the engine. The goal to achieving to minimize stress level on targeted area it means that provided strength on this region or increases negligible thickness. Thus, the process to develop design produce the best structural characteristic and optimum natural frequency performance of engine supporting bracket.

II. METHODOLOGY

Firstly, theoretical study of engine supporting members is done. The main purpose of engine supporting bracket is to support the main body of vehicle skeleton. An engine which is rest in balanced condition undergoes undesirable vibration induced by engine and tires from uneven road surface. Many possible causes are identified of failure supporting system using Fishbone diagram and modification are identified. The works focused in this study to find optimum frequency of the bracket of two different design models. Best design selected with suited material and same boundary condition.

III. ROOT CAUSE FAILURE ANALYSIS

There is not a single defined methodology Root cause failure analysis; however, there are various ways, tools, processes & philosophies of Root cause failure analysis. In its broader sense it is used to identify, rectify and eliminate component failures & it is most effective when subjected to breakdowns. Even though the failure appears to be contributed by various factors initially, there is always one root cause of the failure. We adopted fishbone diagram methodology to arrive at the logical conclusion at root cause of failure. The diagram presented here is the fishbone diagram constructed, for the component being studied. Following points are considered:

Man: Human being is the factor which would result in weld related defects like incomplete penetration between joints, incomplete fusion, less CO₂ penetration undercutting and bad weld design.

Material: Here materials being used for production of component are decided. The criterion for selection of material is the yield strength. In that sense low yield strength of material will lead to insufficient strength and poor weldability.

Methods: This factor summarizes the setup and different production processes used for manufacturing the component. Process like hydroforming & welding are

performed to contribute for manufacturing. Any wrong sequence in Procedure can lead to defects described above.

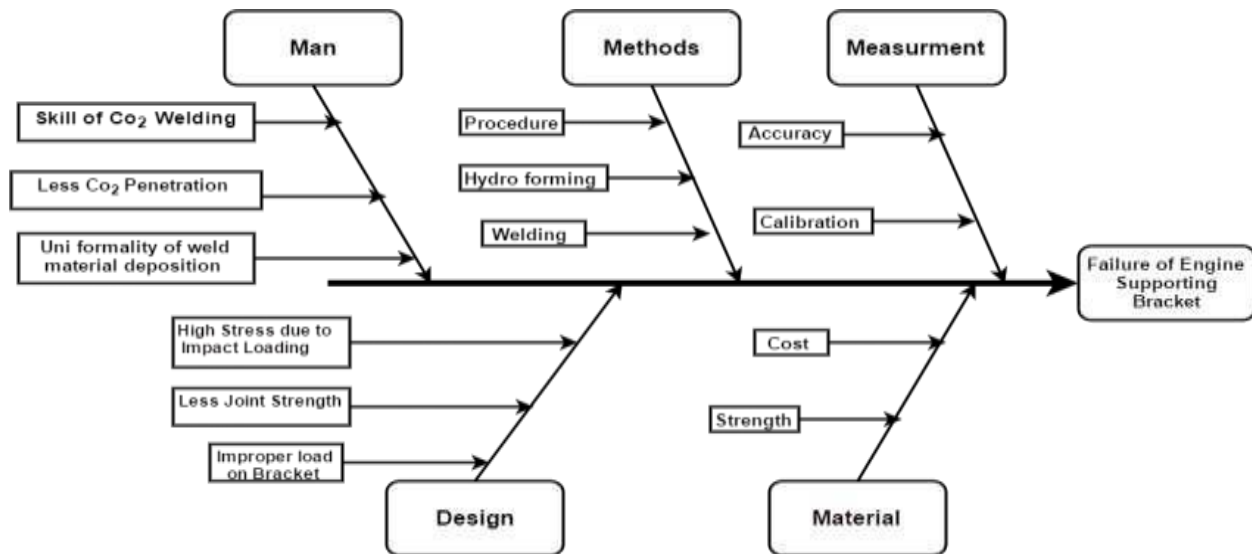


Fig.1: Schematic view of Fishbone diagram

Measurement: this factor deal with various measuring system used for calibration of instrument. Tolerances and allowances are to be studied. Any misfortune in inspection would definitely affect the accuracy and ultimately the final quality of the component.

Design: The major problems associated with factor design are bracket acting as cantilever beam, high thermal stress due to radiation effect, ergonomic consideration; improper load on bracket has strong influences on weld failure. Meanwhile the above factors will govern the range of dimensions of component.

- **Static & Modal Analysis of Engine supporting bracket:**

Finite element analysis is most important software tool with the capability to find a wide range of different problem and gives approximate solution for any complex shape design. The engine supporting bracket is prepared 3-D Part

modeling using CATIA V5 software & imports this CAD Geometry in ANSYS workbench R 15.0. Select their material properties from engineering material data (like young modulus, density, poissons ratio, yield strength of materials). At that time only one material is selected. The process for dividing the complex shape into small pieces is called as discretization or mesh generation. The pre-processing of the engine supporting bracket is the purpose of the dividing the problem into node, elements and to developing the equation for an element matrices. Further apply the boundary conditions & select area for fixed supports. In static structural analysis is analyzed deformation, equivalent stress & Strain energy of the components. In modal analysis to determine natural frequency of the component. Generating results and save the file.

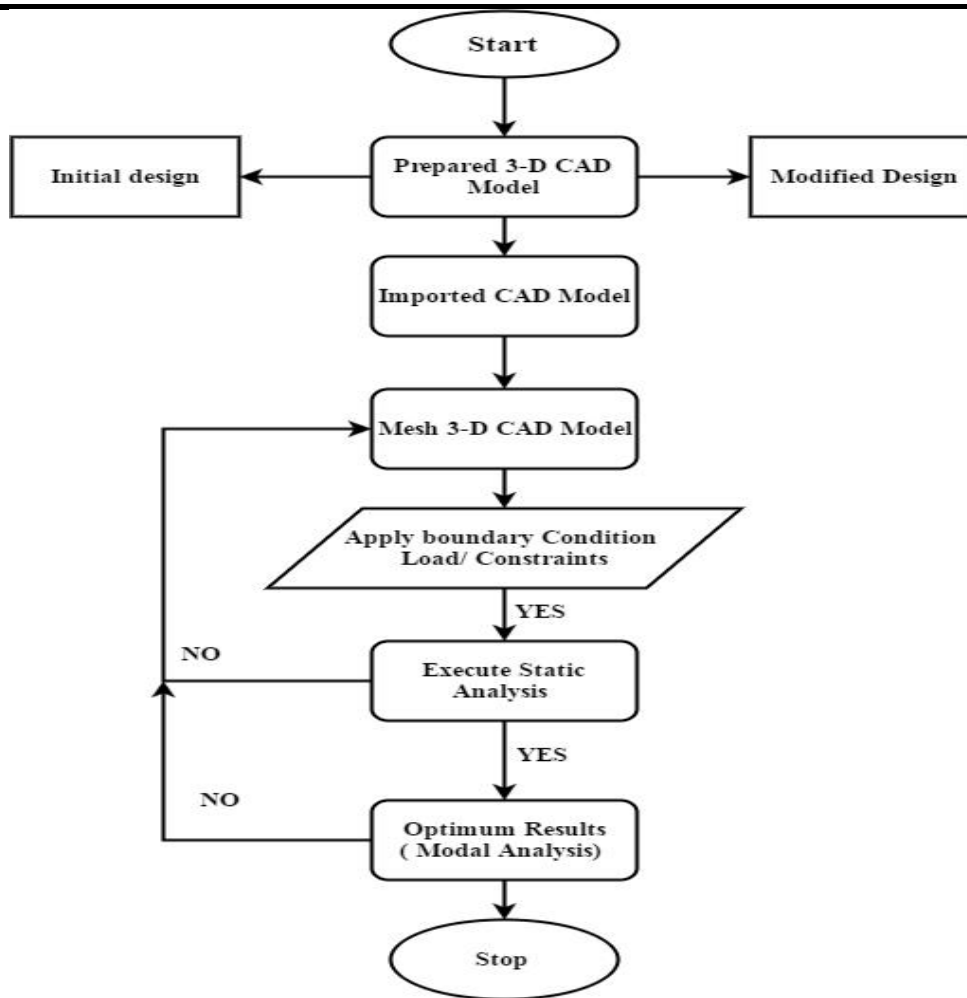


Fig.2: Typical Design process flow

IV. MATERIAL & MATERIAL PROPERTIES

ERW-1: Electrical resistance welded steel tube & seamless tube are often used in application with automobiles ERW to their convention properties should also innovation which reduces cost, weight & to their high strength. Mechanical Properties of ERW-1 are

IS 3074 ERW-1	
Young’s modulus N/m ²	2.1 e+10 N/m ²
Poisson’s ratio	0.29
Density Kg/m ³	7800 Kg/m ³
Yield strength N/m ²	2.4e+8 N/m ²

V. BOUNDARY CONDITION

Basic model of engine supporting bracket is prepared by using CAD Software modelling CATIA V5. CAD Model geometry is imported in Ansys workbench and next step are part, coordinate system, Contact & contact region. Engine

is rest on the engine supporting structural link is known as Engine supporting bracket. Weight of Baja Mega Max diesel Engine is 800N is acted on four mounting position on the structure bracket in equilibrium condition and Silencer weight is 20N is applied on end section. This force is acted vertically download on the bracket and the force that acted upon externally when the system is not under motion in static structural analysis. Weight of engine is equally distributed on the bracket component and upper end is connected to the main skeleton of the vehicle. In finite element analysis is very important for deciding boundary condition.

Meshing: Engine supporting bracket component is dividing into small pieces is known as meshing or discretization. Meshing is done using FEA package Ansys Workbench and meshing are dividing three group are coarse, medium and fine option are available. Meanwhile node is 112312 and element 37782.

VI. RESULTS AND DISCUSSION

6.1 Static Structural and Modal Analysis of Initial Design

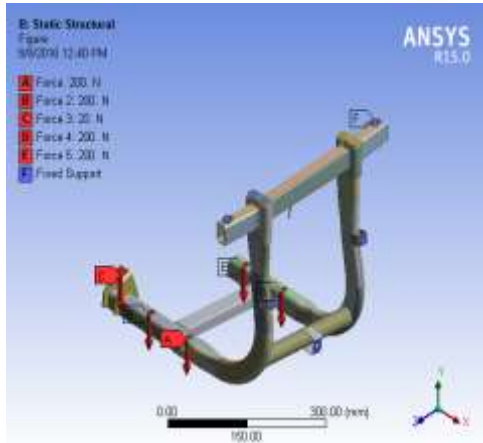


Fig.3: Boundary condition of initial design

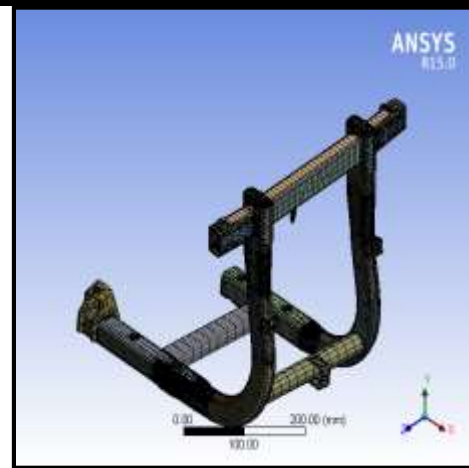
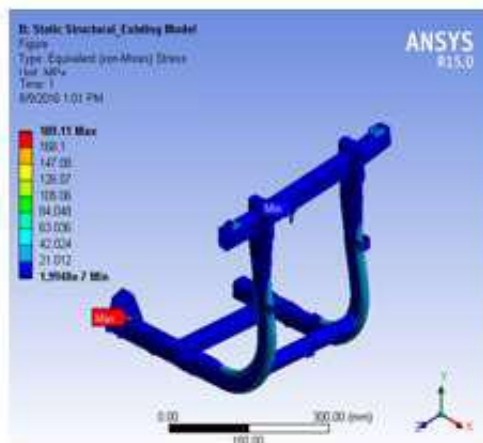
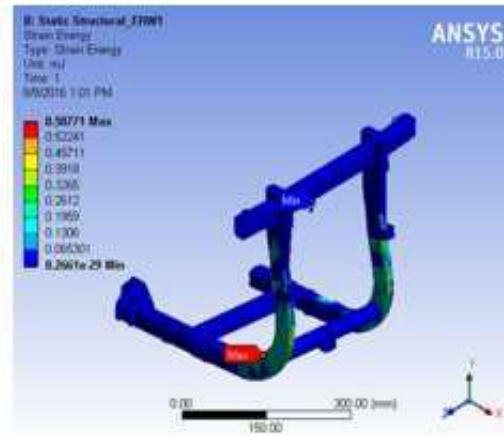
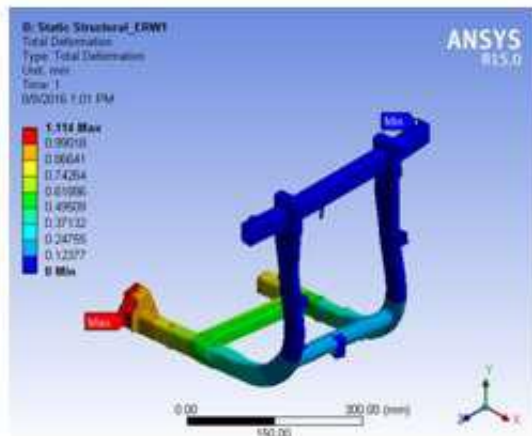


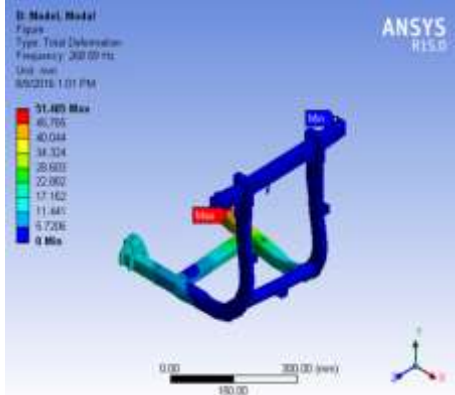
Fig.4: Meshed Model of ESB



Static structural Analysis of Engine Supporting Bracket ERW-1. (Initial Design)	
Total Deformation mm	1.114
Von-Mises Stress Mpa	189.11
Strain Energy mJ	0.58771

Fig.5: Total deformation, Equivalent (Von- Mises) Stress & Strain Energy for Initial design of ESB of Initial Model

6.2 Modal Analysis of Initial Engine supporting Bracket.



Mode	Frequency [Hz]
1	148.12
2	167.32
3	268.59
4	500.92
5	630.92
6	700.3

Fig.6: Modal Analysis of Initial Engine supporting Bracket.

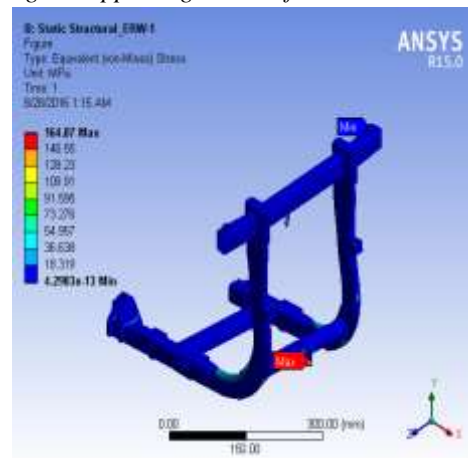
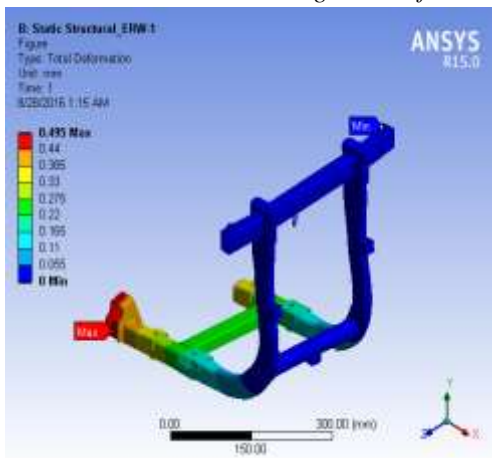
Static structural of Engine supporting frame using ERW-1 material for initial design analysis by ANSYS Workbench R15.0 and getting results of total deformation is 1.114 mm, Equivalent (Von- Mises) Stress is 189.11 MPa& Strain Energy is 0.58771 mJ.

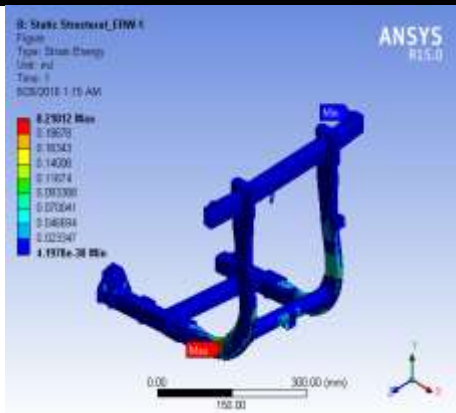
6.3 Static Structural and Modal Analysis of Modified Design

Static Analysis deals with the conditions of the equilibrium of the bodies acted upon by forces .A Static analysis is used to determine the total deformation in mm with Same material i.eERW-1.



Fig.7: Modified design of engine supporting bracket for 3-D Model

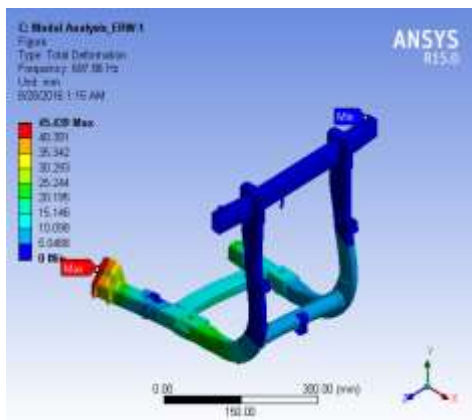




Static structural Analysis of Engine Supporting Bracket ERW-1. (Modified Design)	
Total Deformation mm	0.495
Von-Mises Stress Mpa	164.87
Strain Energy mJ	0.21012

Fig. 8: Total deformations, Equivalent (Von- Mises) Stress & Strain Energy for Modified design of ESB.

6.4 Modal Analysis of Modified design Engine supporting Bracket.



Mode	Frequency [Hz]
1	145.86
2	164.62
3	257.83
4	489.68
5	607.07
6	145.86

Fig. 9: Modal Analysis of Engine Supporting bracket Modified Design.

Parameter	Initial Design	Modified Design
Total deformation mm	1.114	0.495
Von Mises stress Mpa	189.11	164.87
Strain energy mJ	0.58771	0.21012

Comparative study of initial and modified design for ERW-1 (Static Structural Analysis). It can be anticipated from the above analysis that the modified Engine Supporting bracket is safe and suitable for further operation.

VII. VIBRATION STUDY USING FAST FOURIER TRANSFORM

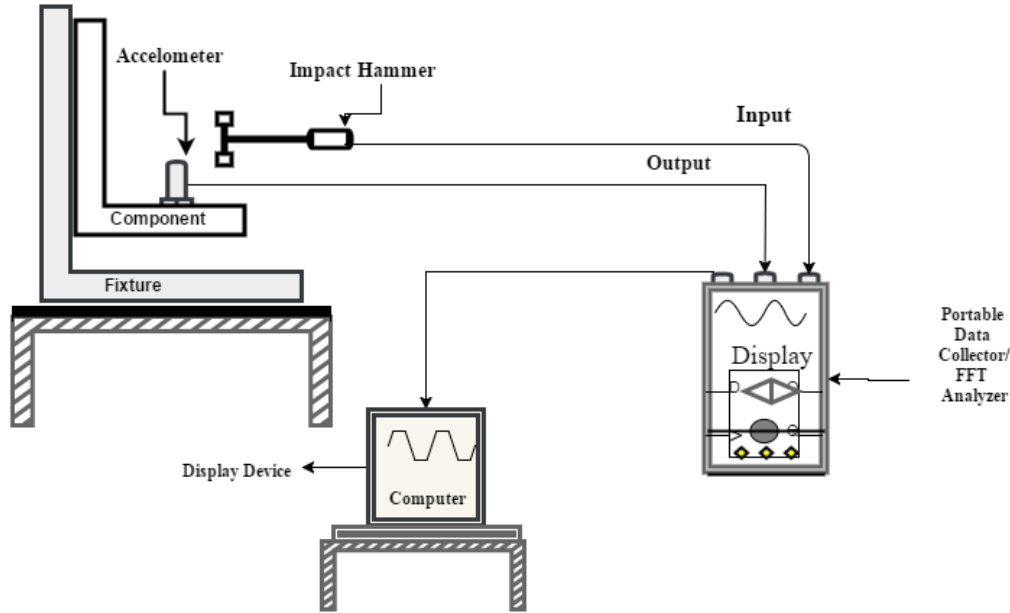


Fig.10: Experimental set up connections

- Engine Supporting bracket placed over the rubber pad as isolation on the table
- An accelerometer (with magnetic base) was placed at one end of the bracket & is connected to FFT Analyzer.
- The Impact Hammer and Accelerometer is connected to FFT, the output of FFT is given to PC.
- Applied the load by using Impact Hammer as excitation at Different points & the Power is supplied to FFT and PC.
- The Result is displayed on PC.
 - Vibration analysis of Initial Model by using FFT Analyzer the result are shows in graphical representation are as below:-

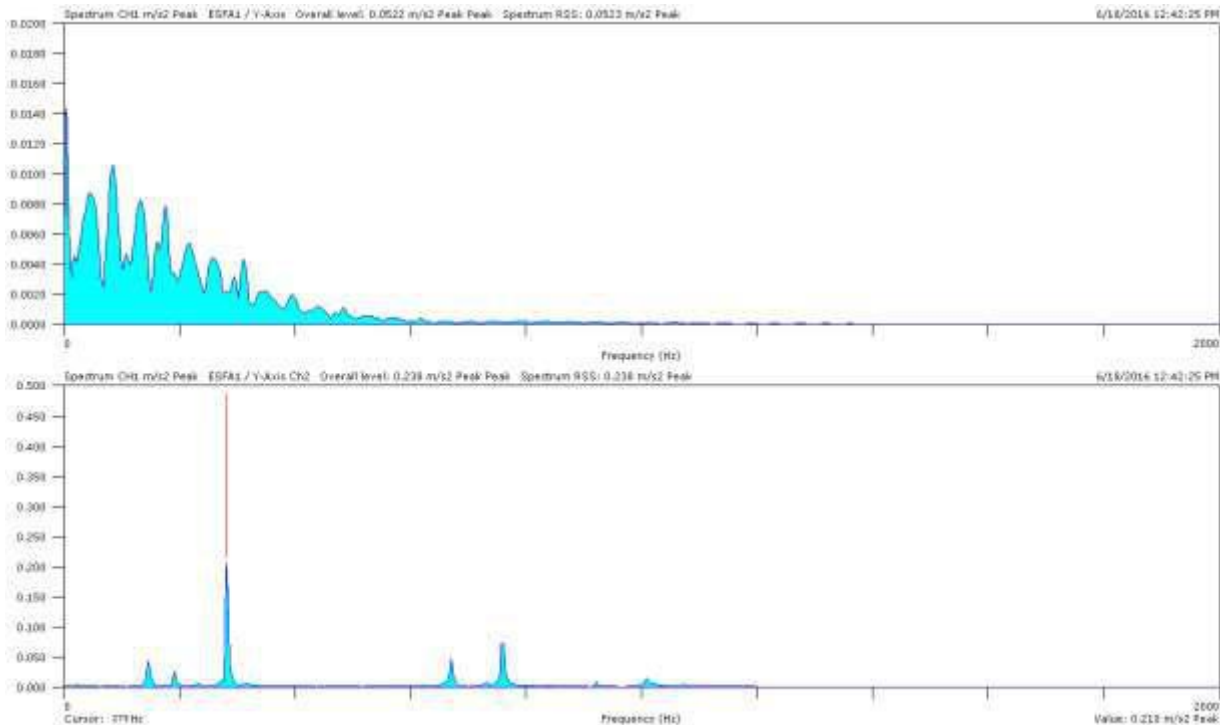


Fig. 11: Vibration study under the consideration of acceleration vs. frequency.

The vibration study for investigating whether the self-excitation frequency of the Engine Supporting bracket is greater than or equal to the natural frequency of the Engine Supporting bracket.

- Vibration analysis of Modified Model by using FFT Analyzer the result are shows in graphical representation are as below:-

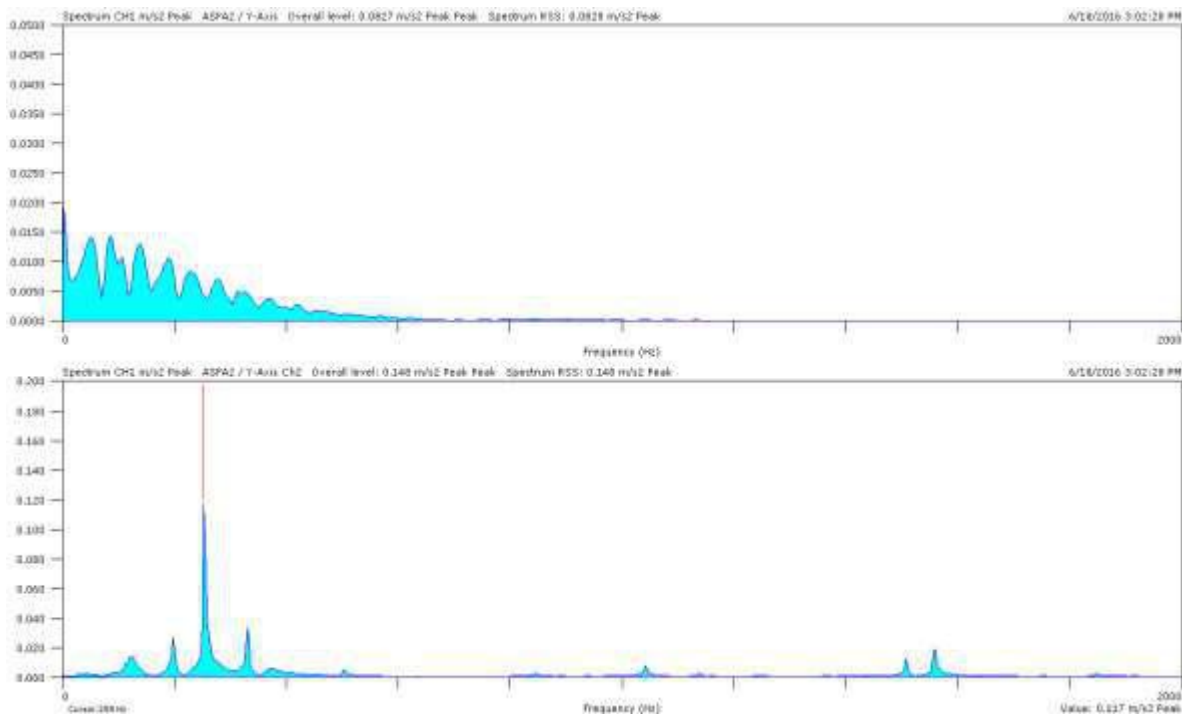


Fig. 12: Vibration study under the consideration of acceleration vs. frequency

It was found that for the initial design of Engine Supporting bracket the frequency mode 273 Hz the acceleration was 0.209729 m/s^2 . But for modifies design it was found that at 259 Hz frequency the acceleration 0.116604 m/s^2 which was much less than the earlier one.

VIII. CONCLUSIONS

Evaluation of modified engine Supporting bracket was done using static structural, modal and fast Fourier transform analysis. Use of Finite Element method was found out to be very significant in this work as experimental work and time reduced by huge margin. It was found that, for the modified design deformation was 0.4950 mm with equivalent von-Mises stress 164.87 MPa which was very less than initial design with 1.14 mm displacement and equivalent von-Mises stress 189.11 MPa. Further natural frequency of modified design was found to be 257.83 Hz which well within the range below self-excitation frequency and less than the natural frequency 268.59 Hz of initial design. From the results obtained for initial design and modified design, it can be anticipated that ERW-1 material best suit the requirement of the desired application.

REFERENCES

- [1] Walunje Prasant .S.V. N. chougule, AnibanC.Mitra "Investigation on modal parameter of rectangular cantilever beam using Experimental Modal analysis" 4th international conference on material processing and characterization Science Direct Material Today: Proceeding 2 (2015) 2121-2130, doi:10.1016
- [2] Mohammad Vaziri, Ali Vazari, Prof. S.S. Kadam "Vibration Analysis of Cantilever Beam By Using F.F.T Analyser" International Journal of Advanced Engineering Technology (IJAET) ISSN: 0976-3945/ Volume-IV/ Issue-II/ April-June, 2013.
- [3] Senthilnathan Subbian, O.P. Singh, Srikanth K. Mohan, Arockia P, Jeyaraj, "Effect of muffler mounting bracket design on durability" ELSEVIER at Science Direct Engineering Failure Analysis 18 (2011) 1094-1107 doi: 10.1016
- [4] Chetan D. Gaonkar "Modal Analysis of Exhaust System to Optimize Mounting Hanger Location" International Journal of Engineering Research & Technology (IJERT) ISSN: 2278-0181 Vol. 4 Issue 03, March-2015.

- [5] Umesh S. Ghorpade, Prof. D. S. Chavan, Prof..M.V.Kavade, “ *Static Structural and modal analysis of engine bracket using Finite Element analysis*” International journal of engineering research & technology (IJERT) ISSN:2278-0181, Vol.I, Issue 10, December-2012, pp1-6.
- [6] Pavan B. Chaudhari, Dr.D. R. Panchagad “*Comparison of Magnesium, Aluminium and Cast Iron to obtain Optimum Frequency for Engine Bracket using Finite Element Analysis*” International Journal of Engineering Research and Applications (IJERA) ISSN: 2248-9622 Vol. 2, Issue 5, September- October 2012, pp.1016-1020).
- [7] Jasvir Singh Dhillon, PriyankaRao, V.P. Sawant, “*Design of Engine Mount Bracket for a FSAE Car Using Finite Element Analysis*” Int. Journal of Engineering Research and Applications, (2014), vol. 4, Issue 9, pp 74-81.

Crack Calculation of Beams from Self-Compacted Concrete

Hajdar E. Sadiku, Esat Gashi, Misin Misini

Civil Engineering and Architectural Faculty, Pristina, Kosovo

Abstract— *The latest developments of construction of high rise buildings like skyscrapers and different towers indicate that building such constructions with conventional concrete of low consistency is impossible due to the hard concreting process, mounting/demounting of scaffolding and the duration of concrete curing. Lately the most widely used material for construction of special buildings is self-compacting concrete because of the ability to fill entire section of formworks without compaction and vibration and better homogeneity between concrete and reinforcement. With massive usage of Self Compacted Concrete (SCC) in special buildings, series of researches are conducted all over the world analyzing cracks, mechanical characteristics and deformations of SCC.*

These researches shows that calculation of concrete elements with normal concrete do not give adequate results according to EC2 because of the concrete class consistency and amount of reinforcement in the cross section. The SCC as raw material provides better results in term of concrete consistency gives better cross section homogeneity and it is vibration free. However SCC concrete cracks, deformations, creep, deflections are different than normal concrete and as such must be calculated and analyzed before application. In this paperwork we have presented calculation of cracks on long term process of SCC beam element after period of $t=400$ days from concreting and comparison of results with the theoretical ones in line with Eurocode 2 (EC2) requirements.

Keywords— *Conventional concrete, compression, cracks, modulus of elasticity, self-compacting concrete.*

I. INTRODUCTION

With appearance of new generate of admixtures (Super-plasticizers) the researcher Hajime Okamura presents for first time concrete which in regard to the content is different from the conventional concrete named this concrete as Self Compacted Concrete. Self-compacting concrete (SCC), also referred to as self-consolidating concrete, is a relatively new concrete technology that is used in the construction industry. It differs from normal compacting concrete

(conventional mix design) in one key material property, it is able to flow under its own weight. Because of this material property, it is able to compact into every corner of the formwork, purely by means of its own weight and without the need for vibrating equipment (Ouchi, 2000:29).

SCC was first developed in 1988, in Japan. The material has since been applied for a multitude of reasons, as is the normal course of a new technology, but the high flowability is still the main advantage.

Self-compacting concrete (SCC) is defined as a concrete which is capable of self-consolidating without any external efforts like vibration, floating, poking etc. The mix is therefore required to have ability of passing, ability of filling and ability of being stable. Concrete is heterogeneous material and the ingredients having various specific gravity values and hence it is difficult to keep them in cohesive form. This is principally true when the consistency is too high. Super-plasticizers reduce water demand and at the same time increase fluidity. However, there is a probability of bleeding and mix may become adhesive. To overcome this problem viscosity-modifying agent (VMA) is required to be added. VMA is a pseudo plastic agent, which thickens the water and keeps the mixture under suspension, providing segregation resistance. The principle of sedimentation velocity is inversely proportional to the viscosity of the floating medium is applied in the system. The intrinsic insufficiency of SCC as any other type of concrete is to defend against tension.

The term Self-Compacting Concrete (SCC) refers to a special type of concrete mixture, characterized by high resistance to segregation that can be cast without compaction or vibration. The material has been described as one of the most important developments in the building industry. It has also been noted that it (SCC) has the potential to dramatically alter and improve the future of concrete placement and construction processes.

The objective of this study is to compare cracks of SCC beam and make comparison with cracks from similar concrete conventional beam.

For analyzing cracks of two types of concrete, trial of 6 concrete beams with SCC and another 6 conventional concrete beam was prepared. Instrumentation was installed on the beams before the transfer of stress to measure cracks. Camber monitoring started immediately after the transfer of stress and continued for 400 days from casting when the full collapse of concrete beam was done.

The intrinsic insufficiency of SCC as any other type of concrete is to defend against tension. In basic concrete the crack appears as soon as principal stresses increases the tensile strength of concrete and after the first crack immediately the collapse occurs. The inherent weakness of concrete to resist tension can be overcome to some extent by mixing the steel fibers in concrete or steel reinforcement. In our case steel reinforcement of beam was provided to carry the tensile stresses in a member due to applied loads. It is expected that cracks will develop in a reinforced concrete member under service loads (the expected loads during the lifetime of the structure).

The laboratory conditions in term of relative humidity and temperature during the research period of long term process were: $T_m=17.7^{\circ}C$ $R_m=75.5\%$ [3].

Rather, SCC test was performed As per EN 206-9, 2010 instructions with : [2], [3].

- J ring h=7.5cm, d=57cm
- V funnel $t_1=8.1s, t_2=9.48s$
- U box h=40mm

II. SELF-COMPACTED CONCRETE BEAM

The static scheme is assumed as simple supported beam with size 15x28 cm in cross section, and length of beam $l=3m$, prestress with two concentrated forces and supports in distance $l=2.8m$, the flexural reinforcement in cross section of the beam is 2 $\Phi 12$ mm rather in compressing zone with 2 $\Phi 8$ mm. Long-term loading was performed by gravitational concrete elements weight. Recording was done from the first crack appearance in the concrete beam rather width was measured with microscope with a accuracy 0.02mm see, figure 1.

Process of cracks measurement and the measurement instrument is presented in figure 2. In figure 3 is presented measurement of crack width with microscope.

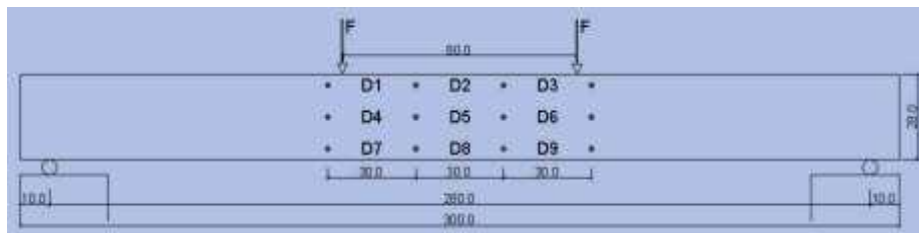


Fig. 1. Static scheme of the beam [3]



Fig.2: Measurement of the crack with and gravitationally load from concrete cerbs [3].

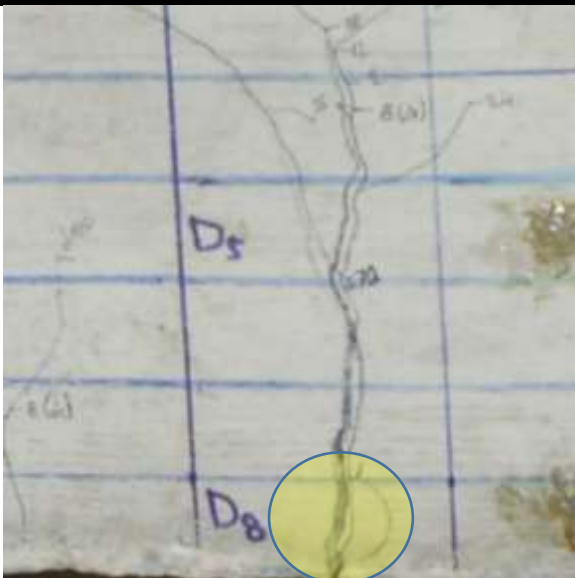


Fig. 3a.: Measurement point of crack for long term proces[3]

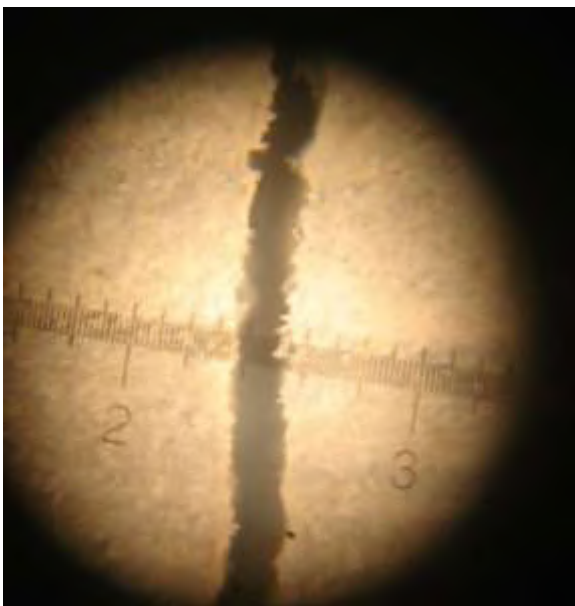


Fig. 3b: Crack width[3]

III. FORMATION OF CRACKS

Cracking as phenomena in the concrete beams is typical and cannot be avoided. Usually occurs in such parts of a concrete where tension stress reaches tensile strength. As it is known tensile stresses may be developed due to, external loading, imposed deformations or chemical reactions.

The cracks may be classified on the basis of their activeness, time of occurrence, their width and the components of building on which they are developed. According to EC 2 the surface width of crack should not

exceed 0.3mm in members where cracking is not harmful and does not have any serious adverse effects upon the preservation of reinforcing steel, nor upon the durability of the structures. In the members where cracking in tensile zone is harmful either because they are exposed to moisture or in contact of soil or ground water, an upper limit of 0.2mm is suggested for maximum width of crack. For particularly aggressive environment such as the 'severe' category, the assessed surface width of crack should not in generally exceed 0.1mm.

However, cracking is not always detrimental to concrete. Crack spacing and crack width must be kept small enough by a proper design and construction of a structure. Therefore, the statically behavior, stability in use and appearance of the concrete structure is ensured. [6]

IV. TYPES OF CRACKS

Loading cracks-Types of loading cracks vary depending on the type of loading.

It is normally that some cracks will appear at points of maximum tensile stress of load level. If direct tension is applied to a concrete member, cracks are developing through the entire cross-section. Spacing of cracks in such cases is approximately 0,75 to 2 times the minimum thickness of the member. [6]

V. CRACKS UNDER BENDING MOMENT

This so called cracking moment (M_r) can be calculated as follows:

$$M_r = W_{cp} * f_{ctk}(1)$$

Where, W_{cp} is the plastic flexural resistance for a rectangular cross-section when the effect of the reinforcement is not taken into account [6].

Creep and shrinkage

Creep is defined as deformation of structure under sustained load. Basically, long term pressure or stress on concrete can make it change shape, while shrinkage means decrease in volume of concrete with time. In steel-concrete composite structures, creep and shrinkage are highly associated with concrete, and these two inelastic and time-varying strains cause increase in deformation and redistribution of internal stresses [3][8].

Creep and shrinkage of concrete are too complicated to capture in any detail, many researchers have instead chosen to propose procedures that approximate the real phenomena but utilize more convenient methods to facilitate the design process. In this section, four existing models to predict creep and shrinkage that are in widespread use will be introduced, and the characteristics of each will be briefly described. [7]

Drying shrinkage– is defined as the contracting of a hardened concrete mixture due to the loss of capillary water. This shrinkage causes an increase in tensile stress, which may lead to cracking, internal warping, and external deflection, before the concrete is subjected to any kind of loading. [2].

Shrinkage from drying is a part of the total strains in the concrete elements.

There are two types of factors where affecting drying shrinkage:

Internal factors: mix design of concrete, aggregate (granulometry, forms, type of stones, with low absorption, etc), water content (more water on the concrete mix higher shrinkage strains), type of admixtures. [9]

External factors: environmental conditions (temperature, relative humidity), compactions, placing, dimensions of the cross section of concrete elements, curing, etc. [9]



Fig. 3c: Beams treated on shrinkage [3]



Fig. 3d: Strain measurement with mechanical strain gauge [3]

VI. FACTORS AFFECTING THE LONG-TERM CRACKS

Under sustained service loads, flexural cracks frequently form with time between the most widely spaced cracks in a cracked tensile region, thereby reducing the average crack spacing with time. In addition, flexural cracks frequently form with time in previously un-cracked regions thereby increasing extent of cracking [4].

VII. EXPERIMENTAL RESULTS

For determination mechanical characteristics of concrete, several trials and samples were prepared, the concrete samples were cubic, cylindrical and prismatic in accordance with EC 2, Some trials were tested at period of concrete $t=40$ days and the rest at period of concrete $t = \infty$.

Results are presented as following: in diagram 1 are presented results of splitting tensile strength f_{ct} for $t = \infty$, while in diagram 2, results of the Modulus of elasticity E_c for $t = \infty$.

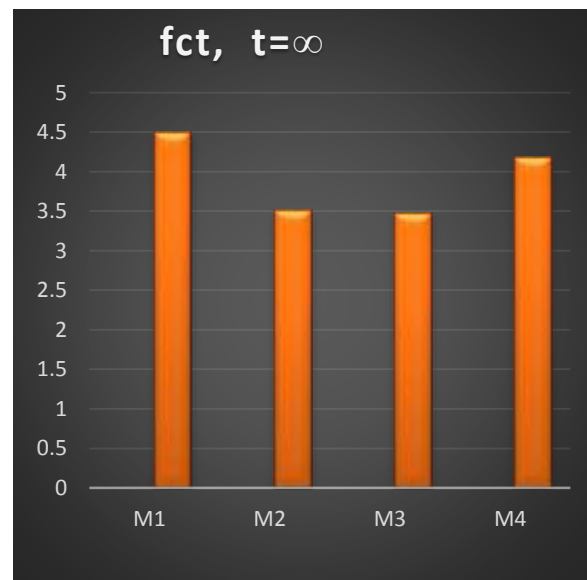


Diagram 2. Results of splitting tensile strength

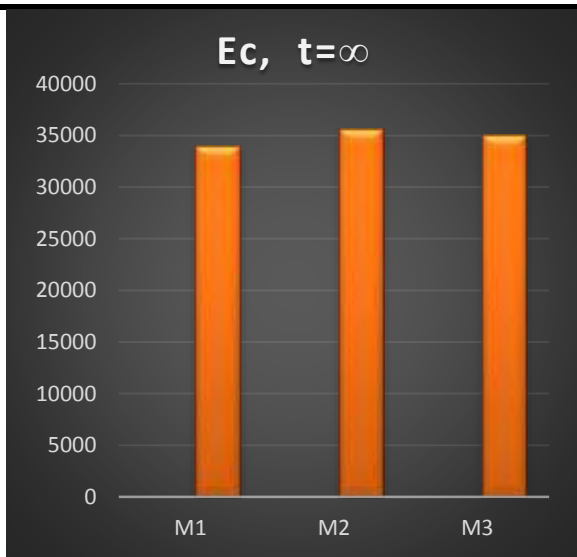
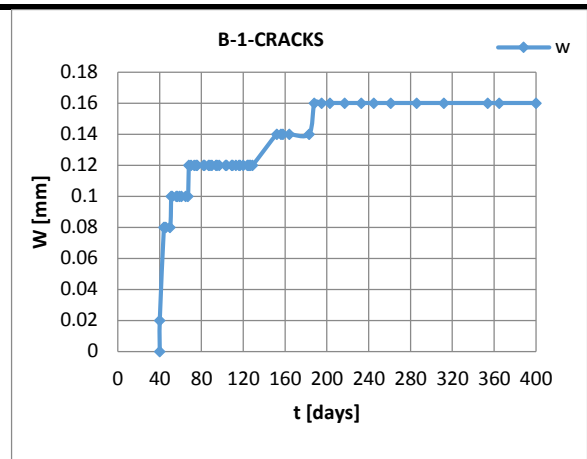


Diagram 3. Results Elasticity Module[3]

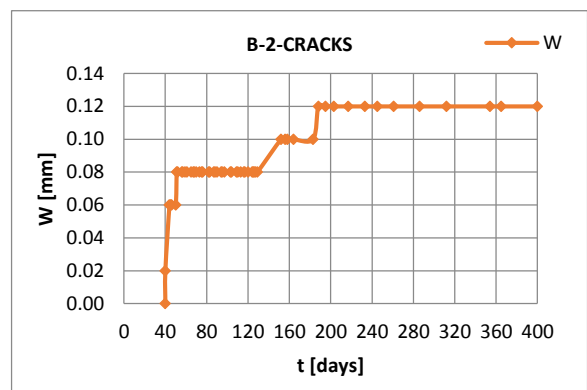
Table 1 presents the numerical values of the cracking width whereas diagram 4 shows its corresponding graphical results. The initial crack on beam B-1 occurs when we acting upon it with force of $F=8kN$ thus causing the cracks width of $w=0.08mm$ whereas the crack on beam B-2 occurs after acting upon it with $F=7kN$ in which case, the cracks width will be $w=0.06mm$.

Table.1: Results for Cracks with the beams of self-compacted concrete [3]

t	W-B		
	B 1	B 2	B
40	0	0	0.000
40	0.07	0.06	0.065
100	0.12	0.08	0.100
200	0.16	0.12	0.140
300	0.16	0.12	0.140
400	0.16	0.12	0.140



a)



b)

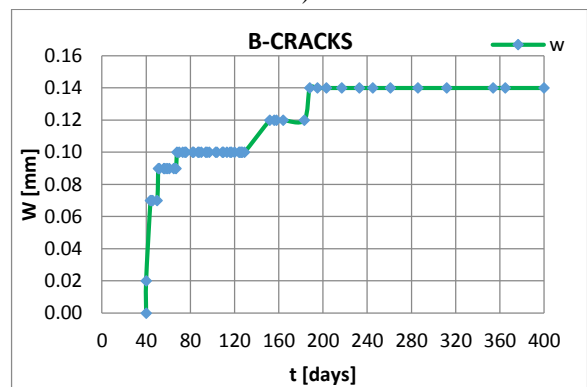


Diagram 4. Crack width for SCC beams[3]

VIII. THEORITICAL RESULTS

Middle beam cracks analysis was done according to EC 2 model for comparing theoretical and experimental results. It has been noticed that EC 2 gives lower values of cracks than thus obtained by trial. This difference is mainly due to the reason that SCC contains more percentage of fine particles than conventional concrete. Tensile solidity and the module of elasticity have lower values as well. [5].

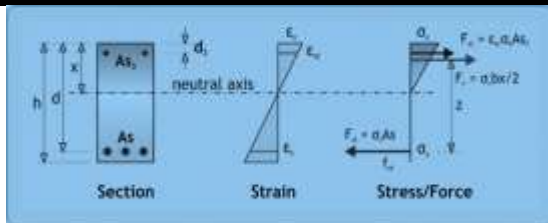


Fig.4: Strains in beam

INPUT DATA

fck =	30	MPa	As1 =	226	mm ²
fyk =	500	MPa	d =	128	mm
b =	150	mm	As2 =	100	mm ²
h =	280	mm	d2 =	32	mm
M =	9.2	KNm	S =	76	mm
Age =	28	days	∅eq =	12	mm
Cement =	R			L	L
φ =	0.7		As, c =	25	mm

OUTPUT DATA

Mcr =	6.41	kNm
→ section is CRACKED		
sr,max =	178.2	mm
εsm-εcm =	619.4	μstrain
Wk =	0.110	mm

IX. CONCLUSIONS

Based on the experimental findings it can be concluded that the contents of the grained aggregates reduces the tensile solidity and self-compacting concrete Modulus of Elasticity. First cracks under ultimate loading appears early in SCC than in conventional concrete beams. Final results of crack width for period t=400 with trial were slightly higher than the results calculated with EC 2.

Difference between trial and theoretical results differed in range of approximately 30%.

International standards for calculation of crack width gives different results and as such are not unified. The Designer must consider this difference.

REFERENCES:

- [1] EN 1992, Euro code 2: 2010,
- [2] EN 206-9:2010, Concrete, Part 9: Additional Rules for Self-compacting Concrete (SCC), 2010,
- [3] Sadiku Hajdar, (2010) Determination of impact load of self-compacting concrete elements in long-term process, Ph. D. Thesis, Skopje, Macedonia,
- [4] Seunghwan Kim - Creep and Shrinkage Effects on Steel-Concrete Composite Beams May 1st, 2014 Blacksburg, Virginia,
- [5] R.I. Gilbert Calculation of Long-Term Deflection The University of New South Wales 2008
- [6] Park CK, Noh MH, Park TH (2005). Rheological properties of cementitious materials containing mineral admixtures. J. Cem. Concr. 35:842–849. pastes containing or not mineral additives. J. Cem. Concr. 30:1477–1483.
- [7] Perssoiv B (1998). Technical Report, Japan Society for the Promotion of Science
- [8] Philippe T (2004). Formulation influence on the withdrawal and cracking of self-compactingconcrete. Doctoral thesis, Nantes Central School, pp. 20-32. Kennouche 169 ,
- [9] Baolu Li, Koichi MAEKAWA and Hajime OKAMURA, Contact Density Model for Stress Transfer across Cracks in Concrete Journal of the Faculty of Engineering, The University of Tokyo(B), Vol.40, No.1, 1989, pp.9-52

Literature Review on Design and Working of 3 Way Pilot Operated Diaphragm Controlled Hydraulic Control Valve

Kunal Mehra

Department of R&D, Automat Industries Private Limited, New Delhi, India

Abstract—Most flow applications require regulating the flow of liquid and usually the parameter of flow is pressure. This paper focuses on the design assembly and working of a 3 way pilot operated diaphragm controlled hydraulic control valve. A 3 way pilot operated hydraulic control valve is used in this study for reducing the pressure on the main line, sustaining the pressure on the main line and quick pressure relief for a by-pass line. This study has been carried out on a 2" line with a bronze 2" diaphragm operated hydraulic control valve a brass pilot with pressure adjustment range of 0.7 bars to 6.5 bars. Through the study, I also found about the chaotic behaviour of the pilot with the sudden variation in the upstream pressure of the main line.

Keywords— 3 way pilot, upstream pressure, diaphragm operated hydraulic control valve.

I. INTRODUCTION

A hydraulic valve is a device which properly directs the flow of a liquid medium through a hydraulic system.

Hydraulic valve are available in a variety of sizes and according to multiple international standards. They are available in different mounting styles such as the threaded connections and flanged connections. Hydraulic valves are sub divided into three main categories- directional control valves, pressure control valves and flow control valves. All valves operate a different function in the hydraulic system. Check valves permit free flow in one direction and block flow in the opposite direction. The directional control valve is used to pass on the pressure medium or flow in an orderly manner to a particular direction. Pressure control valves switch (or control) at a certain pressure while the switching pressure may be adjusted on the valve. Flow control valves regulate the flow and this is done by adjusting the size of the bores or orifices.

Hydraulic Flow Control Valve

Our study was carried on a diaphragm operated hydraulic flow control valve. Diaphragm valves get their name from a flexible disc which comes into contact at the top of the valve body to form a seal. A diaphragm is a flexible,

pressure responsive element that transmits force to open, close or limit the flow through a valve.

The valve that I chose for testing uses a moulded diaphragm. It has an aluminium insert to which EPDM rubber is moulded. This bronze hydraulic control valve with brass pilot is used for general water supply system, filtration network and systems subjected to sudden demand changes with medium pressure rating. The 3 way brass pilot with unique diaphragm enables precise pressure control.

II. MATERIALS

Table.1: Brass Pilot Parts List

Part No	Part Name
1	Pilot Base
2	Pilot Base Cap
3	Stem Cylinder
4	Stem Cylinder O-ring
5	Stem
6	Stem O-ring
7	Diaphragm Seat
8	Diaphragm
9	Actuator
10	Spring
11	Spring Button
12	Nut
13	Adjusting Screw

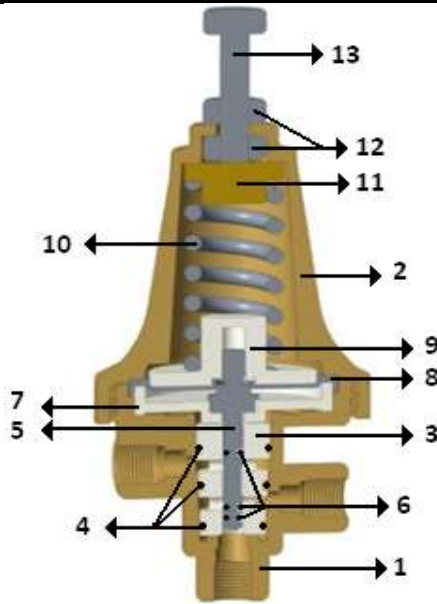


Fig.1: Pilot Sectional View

Table.2: HCV Parts List

Part No	Part Name
1	Body
2	Cover Plate
3	Valve Lid
4	Spring
5	Bolt

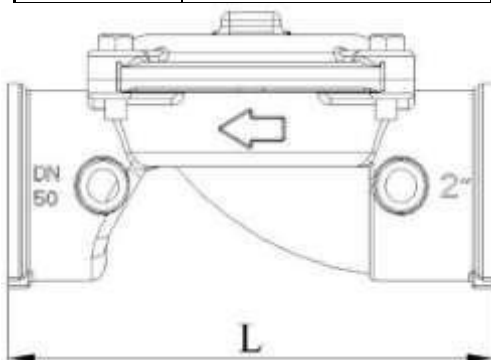


Fig.2: HCV Direction of flow

Operating Conditions

The pilot and hydraulic flow control valve selected have been made to work for below mentioned conditions:

- 1). Pressure Reducing Valve
- 2). Pressure Sustaining Valve
- 3). Quick Pressure Relief Valve

In this edition, the working of pilot with control valve has been studied to make the valve work as a pressure reducing valve.

The connections between the hydraulic valve and the pilot are done as shown in figure 3. The pilot is marked with numbers 0-1-2-3 at the ports. The following is the description:

- 0- Upstream

- 1- Downstream
- 2- Atmosphere
- 3- Control Chamber

The valve maintains a constant pre-set downstream pressure regardless of upstream pressure or flow fluctuations. The hydraulic valve is controlled by the pilot. The pilot has a spring loaded diaphragm as shown figure 1, which is sensitive to downstream pressure. The pilot spring is pre-set to downstream pressure which is explained in the working section below. The pilot maintains a constant downstream pressure by gradually opening and closing the hydraulic valve at any flow rate. When no flow exists in the system, it closes itself automatically. The diagram shown below shows the connection of different ports of the hydraulic control valve with the pilot.

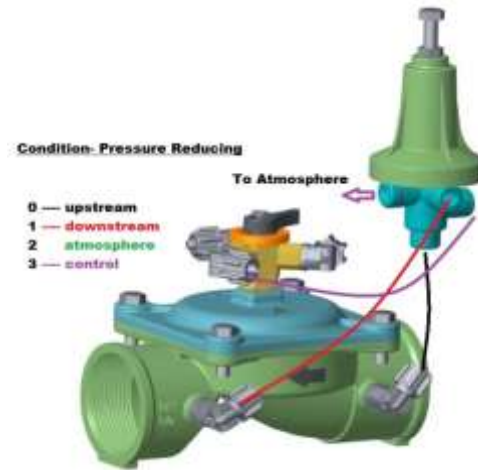


Fig.3: Valve Connection Diagram

III. WORKING

Initially, the adjusting screw of the pilot is set free which means there is no force on the spring. When the line is opened, the water flows through the valve. Since the upstream, downstream and control chamber of hydraulic valve are connected to the pilot, it comes into action because of flow of water. The water from the upstream and downstream enters the pilot from port '0' and '1'. The downstream water forces the spring to move back which in turn moves the shaft of pilot due to which the ports '0' and '3' come into contact. The water then flows towards the upper section of the diaphragm called the control chamber. This flowing water maintains pressure on the HCV diaphragm and shuts the valve.

Now we gradually adjust the downstream pressure using the pressure adjusting screw on the pilot. When we screw in clockwise direction, it compresses the spring. Now the water flowing through the port '1', coming from downstream side has to work against the spring force. When the downstream pressure becomes greater than the

spring force, the spring and assembly moves which in turns connect the port '0' and '3' again. The amount of water flowing through port '3' depends on the pressure difference of the downstream and the spring force. When the required water gets accumulated and generates pressure on diaphragm of HCV in the control chamber, the diaphragm lowers and closes the valve partially maintaining the set downstream pressure equivalent to that of the spring force. At this stage, equilibrium is achieved and the downstream pressure remains constant. This happens at every set pressure and with the fluctuations in the inlet pressure i.e. increases of decrease in the pressure. Figure 4 shows the different working positions of the diaphragm of the hydraulic valve i.e. the control chamber.

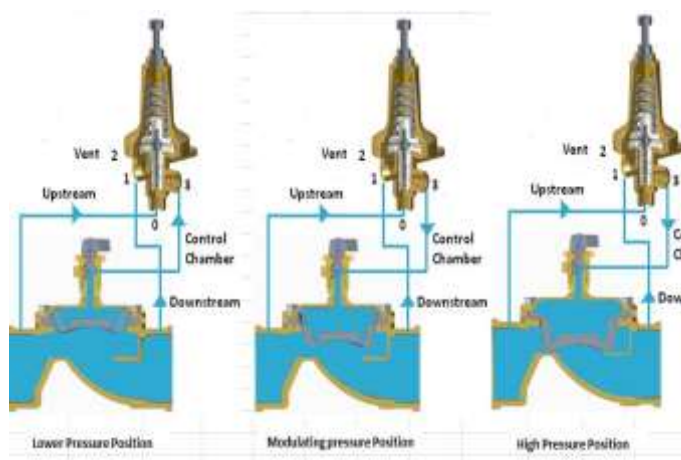


Fig.4

IV. RESULTS AND DISCUSSION

With the working of hydraulic valve with pilot, we can maintain a particular downstream pressure which is as per requirement of the end user whether it is in the field of agriculture, landscaping and piping systems for storing or discharge of water. The user just needs to adjust the pressure adjustment screw to get the required downstream pressure in the case where the upstream pressure gets more than the required downstream pressure.

During the working, we encountered certain issues related to the pilot which in turn is about the accuracy of the valve. A pilot is considered good when it is working at the set downstream pressure with a tolerance of ± 0.1 bars.

During the study and performing the practical, another way of improving the accuracy of the valve is to select a downstream port at about a meters length of the downstream section. The reason to do this is that the flow gets linear and is apparently **more** uniform.

REFERENCES

- [1] <https://dta.eu/hydraulics/hydraulic-valves/flow-controls/pressure-compensated-flow-control-valve/>

- [2] <http://www.bermad.com.au/products/2pb-pressure-reducing-pilot/>
- [3] <http://www.hydraulicspneumatics.com/other-technologies/book-2-chapter-8-directional-control-valves.>
- [4] http://www.etc.ipfw.edu/~dupenb/MET_330/Fluid%20Power%20Notes%204%20Hydraulic%20valves.pdf
- [5] http://www.controlglobal.com/assets/Media/MediaManager/RefBook_Cashco_ControlValves.pdf
- [6] Hydraulic Control Systems - Herbert E. Merritt.

Segmentation of Optic Disc in Fundus Images using Convolutional Neural Networks for Detection of Glaucoma

R. Priyanka¹, Prof. S. J. Grace Shoba², Dr. A. Brintha Therese³

¹M.E Applied Electronics, Velammal Engineering College Chennai, India

²Professor Velammal Engineering College, Chennai, India

³Professor /SENSE, VIT University, Chennai, India

Abstract— The condition of the vascular network of human eye is an important diagnostic factor in ophthalmology. Its segmentation in fundus imaging is a difficult task due to various anatomical structures like blood vessel, optic cup, optic disc, macula and fovea. Blood vessel segmentation can assist in the detection of pathological changes which are possible indicators for arteriosclerosis, retinopathy, microaneurysms and macular degeneration. The segmentation of optic disc and optic cup from retinal images is used to calculate an important indicator, cup-to-disc ratio (CDR) accurately to help the professionals in the detection of Glaucoma in fundus images. In this proposed work, an automated segmentation of anatomical structures in fundus images such as blood vessel and optic disc is done using Convolutional Neural Networks (CNN). A Convolutional Neural Network is a composite of multiple elementary processing units, each featuring several weighted inputs and one output, performing convolution of input signals with weights and transforming the outcome with some form of nonlinearity. The units are arranged in rectangular layers (grids), and their locations in a layer correspond to pixels in an input image. The spatial arrangement of units is the primary characteristics that makes CNNs suitable for processing visual information; the other features are local connectivity, parameter sharing and pooling of hidden units. The advantage of CNN is that it can be trained repeatedly so more features can be found. An average accuracy of 95.64% is determined in the classification of blood vessel or not. Optic cup is also segmented from the optic disc by Fuzzy C Means Clustering (FCM). This proposed algorithm is tested on a sample of hospital images and CDR value is determined. The obtained values of CDR is compared with the given values of the sample images and hence the performance of proposed system in which Convolutional Neural Networks

for segmentation is employed, is excellent in automated detection of healthy and Glaucoma images.

Keywords— Fundus images ,blood vessel segmentation ,global contrast normalization ,zero phase component analysis, convolutional neural networks, Optic cup and disc, FCM.

I. INTRODUCTION

Glaucoma is a typical eye illness that is irreversible and the second driving reason for visual impairment. Because of absence of a powerful early screening framework it end up noticeably mindful just in the last phases of glaucoma. The quantity of individuals with glaucoma was 64.3 million, and is expected to ascend to 76.0 million in 2020. Early analysis and treatment are essential to avoid loss of vision in glaucoma patients. Glaucoma can be recognized right on time by checking retinal fundus images condition. The fundus image of the eye incorporates the retina, optic circle, fovea, macula and back post. Retinal fundus images have remained the top standard for assessing the adjustments in retina. Out of the few techniques utilized for clinical determination of glaucoma, fundus image examination is the one most appropriate for recognizing. A programmed framework for glaucoma location is proposed here, which makes utilization of fundus image utilizing CDR. The optic disc (OD) or optic nerve head in the retina where cell axons leave the eye to shape the optic nerve. Optic disc division utilizing CNN is the initial phases in the proposed approach. The optic disc has a focal wretchedness, denied of sensory tissue. Glaucoma, described by loss of nerve tissue causes extending of this disc area, happening in the prevalent and substandard localities in the early stages. Optic cup is segmented by Fuzzy C means utilizing ROI and morphological operation. The parameter Cup-to-Disc Ratio is figured to check for glaucoma. The retina is the

inward most essential layer of the eye where the fastest obsessive changes can be seen. It is made out of a few vital anatomical structures, for example, optic disc, fovea, macula and veins which can show numerous sicknesses that cause visual loss. The optic disc is the brightest part in the typical fundus image that can be viewed as a pale, round or vertically marginally oval plate. It is the opening of veins and optic nerves to the retina and it regularly fills in as a point of interest and reference for alternate elements in fundus images. Figure 1 represents a fundus images. The optic cup is a two-walled gloom that can be found in the focal point of the eye's optic disc. This zone is named for its area and cup like shape. The optic cup is one of the segments of the visual system. The fovea is the inside most part of the macula. The modest region is in charge of our focal, most keen vision. A solid fovea is key perusing, sitting in front of the driving, and different exercises that require the capacity to see detail. The macula is found generally in the focal point of the retina, transient to the optic nerve. It is exceptionally touchy piece of retina is capable of point by point focal vision. The fovea is the exceptionally focus of the macula. In the focal point of retina is the optic nerve, a round to oval white territory that measures around 2 x 1.5 mm over. From the focal point of the optic nerve transmits the real blood two and half plate distances across to one side of the disc, can be seen the somewhat oval molded. The retina is a layered tissue coating the inside surface of the eye. It changes over approaching light to the activity potential which is further prepared in the visual focuses of the cerebrum. Retina is one of a veins that can be specifically identified non-invasively. It is of incredible reason in prescription to picture the retina and create calculations for investigating those pictures. Late innovation in most recent a quarter century to the improvement of advanced retinal imaging frameworks. The retinal vessels are associated and make a parallel treelike structure, however some foundation elements may likewise have comparable ascribes to vessels.

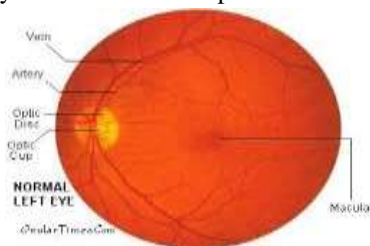


Fig.1: Retinal fundus image

A few morphological components of retinal veins and courses have symptomatic importance so can be utilized as

a part of checking the infection, treatment, and assessment of different cardiovascular and ophthalmologic diseases due to the manual vein division is a tedious and dreary undertaking which requires preparing, programmed division of retinal vessels is the underlying stride in the advancement of a PC helped demonstrative framework for ophthalmic issue . Programmed division of the veins in retinal pictures is vital in recognizing the number of eye infections in light of the fact that now and again they influence vessel tree itself. In different cases (e.g. obsessive injuries) the execution of programmed discovery might be enhanced if vein tree is prohibited from the examination. Thus the programmed vessel division shapes a pivotal segment of any robotized screening framework. Manufactured Neural Systems (NNs) have an amazing record of uses in image examination and understanding, including medicinal imaging.

II. RELATED WORK

Segmentation methods can be divided into unsupervised and supervised. In the former ones, the properties of structures to be detected are manually hard-coded into algorithm's structure, and learning is limited or altogether absent. In the unsupervised methods category, algorithms that apply matched filtering, vessel tracking, morphological transformations and model-based algorithms are predominant. In the matched filtering-based method [1], a 2-D linear structuring element is used to extract a Gaussian intensity profile of the retinal blood vessels, using Gaussian derivatives, for vessel enhancement. The structuring element is rotated 8-12 times to fit the vessels in different configurations to extract the boundary of the vessels. This method has high time complexity since a stopping criterion is evaluated for each end pixel. In another vessel tracking method [2], Gabor filters are designed to detect and extract the blood vessels. This method suffers from over-detection of blood vessel pixels due to the introduction of a large number of false edges. A morphology based method in [3] combines morphological transformations with curvature information and matched-filtering for centerline detection. This method has high time complexity due to the vessel center-line detection followed by vessel filling operation, and it is sensitive to false edges introduced by bright region edges such as optic disc and exudates. Another morphology based method [4] in uses multiple structuring elements to extract vessel ridges followed by connected component analysis. In another model-based method [5], blood vessel structures are extracted by convolving with a Laplacian kernel followed by thresholding and connecting broken line

components. An improvement of this methodology was presented in [6], where the blood vessels are extracted by the Laplacian operator and noisy objects are pruned according to center lines. This method focuses on vessel extraction from images with bright abnormalities, but it does not perform very effectively on retinal images with hemorrhages or microaneurysms. In [10] a new hybrid approach called genetic algorithm for blood vessel detection which uses geometrical parameters. There are two methods proposed in [12] that uses the line detectors to detect the presence of blood vessel in image pixel. In [13] co-occurrence matrix is calculated and thresholding decision is made from the matrix. Automatic segmentation of vessel using B-Cosfire filter by collinear aligned difference of Gaussian [14]. In [15] a new infinite contour model for the detection of blood vessel that uses hybrid information. All such unsupervised methods are either computationally intensive or sensitive to retinal abnormalities. In supervised methods, segmentation algorithms acquire the necessary knowledge by learning from image patches annotated by ground truth. For instance in [9], ridge features (zero-crossings of brightness derivative) are detected, grouped, and fed into a nearest-neighbor classifier. In [16], a multiscale Gabor transform (wavelets) is used to extract features from a patch, and train Bayesian classifiers on them. In [17], a morphology-based method detects the evident vessels and background areas, while a Gaussian mixture model classifies the more difficult pixels. These methods use training data to train a classifier using SVM [18]. to train a classifier However these method are not purely supervised in the strict meaning of this term, as the network learns from features defined by a human expert. According to, the only purely neural and thus fully supervised approach (i.e., with a network directly applied to image patches) was presented in, which however contained only visual inspection of the resulting segmentations and did not report objective quality measures. In the context of the past work, the method proposed in this paper should be classified as supervised: no prior domain knowledge on vessel structure was used for its design. Glaucoma is the common cause of blindness with about 79 million in the world likely to be afflicted with glaucoma by the year 2020 [19].

Glaucoma is asymptomatic in the early stages and its early detection and subsequent treatment is essential to prevent visual damage [20]. There have been efforts to automatically detect glaucoma from 3-D images [21], [22]. However, due to their high cost they are generally unavailable at primary care centers Gopal and Jayanthi

proposed an automated OD Parameterization techniques for segmenting optic disc and cup from retinal images [23]. In 2011, another researcher Rajendra et al. proposed a texture feature based technique for identifying Glaucoma retinal images [24]. Another automated system for the detection of Glaucoma from the fundus image as proposed by Chalinee et al. [25]. They extracted disc through edge detection method and level set method then cup was segmented using color component analysis method. Gopal Dat joshi proposed another technique for intensity changes in vessels minimization using active contour in specific region, though deformation of cup will not be constant due to changes in vessels [26]. S Chandrika and K. Nirmala detected Glaucoma by k-mean clustering and Gabor wavelet transform technique from which they have computed CDR [27]. Cup-to-disc ratio (CDR) is the most famous indicator. Cup to disc ratio is calculated by using a optic cup diameter divided by a optic disc diameter [28]. Optic disc margin, neuroretinal rim, cup-to-disc ratio and optic disc hemorrhages are some examples of clinical indicators that use to evaluate glaucoma [29]. Optic disc margin, neuroretinal rim, cup-to-disc ratio and optic disc hemorrhages are some examples of clinical indicators that use to evaluate glaucoma [30].

III. DEEP LEARNING

Many models intended to work with image information, specifically convolutional systems (CNNs), were routinely manufactured as of now in 1970's and figured out how to discover business applications and outperform different methodologies on testing errands like manually written character acknowledgment. In any case, the break of centuries saw recognizable stagnation in spite of exceptional research endeavors, NNs neglected to scale well with errand unpredictability. The beginning of option ML procedures, similar to support vector machines and Bayesian systems, incidentally downgraded the NNs, and it was just the generally late entry of profound learning (DL) that brought them once more into the spotlight. Today, expansive scale DL-prepared NNs effectively handle bland protest acknowledgment undertakings with a huge number of question classes, an accomplishment that many considered unbelievable before ten years. The capacities of profound NNs came from a few improvements. Transfer elements of units in traditional NNs are normally crushing capacities (sigmoid or hyperbolic digression), with subordinates near zero all over the place. This prompts lessening the angle for preparing the backpropagated mistakes rapidly diminish with each system layer, rendering

inadequate or agonizingly moderate. Interestingly, these capacities utilized as a part of profound CNNs, most outstandingly correcting straight units don't vanish in extremes, thus permit powerful preparing of systems with many layers . Also, DL carried with it new strategies for boosting system heartiness like dropout where haphazardly chose units that are incidentally crippled. This powers a system to shape weight setup, that give adjust yields regardless of the possibility that some picture elements are missing, thus enhances speculation.. In this paper, we propose a DL-based technique for the issue of distinguishing blood vessels and optical cup and disc in fundus symbolism, a medicinal imaging undertaking that has huge analytic pertinence and was liable to many reviews in the past . The proposed approach beats past techniques on two noteworthy execution markers, i.e., precision of characterization and territory under the ROC bend. We consider a few system models and image preprocessing strategies, confirm the outcomes on three picture databases, perform cross-check between the databases, analyse the outcomes against the past techniques, and investigate the divisions outwardly.

IV. METHODS AND METHODOLOGY

The first step is to segment the blood vessels in retinal fundus images with convolutional neural networks, involves following steps

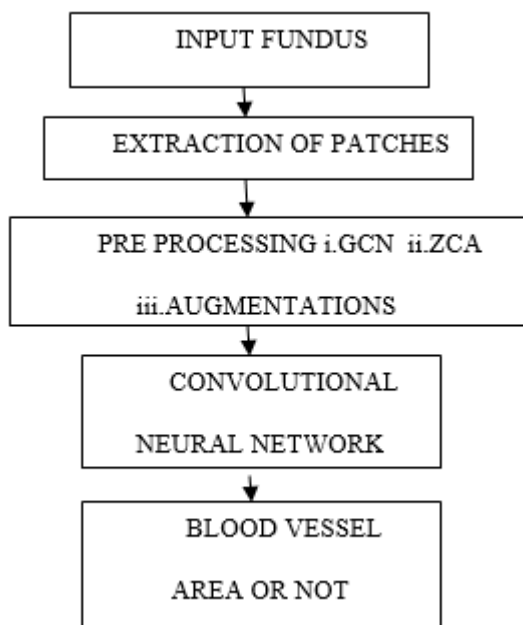


Fig.2: block diagram of the blood vessel segmentation

A) Extraction Of Patches

The ground-truth data provided in the handbook segmentations frames the blood vessel detection as a binary classification problem. As in many other studies, in our approach the decision on the class of a particular pixel is based on an $m * m$ patch centered at that pixel. A triple of such patches, each reflecting image content at the same location for the RGB channels, forms the input fed into a neural network. Together with the associated class label of the central pixel, it forms an example. In this study, we use $m = 27$, so an example is a vector of length $3 * 27 * 27 = 2187$.

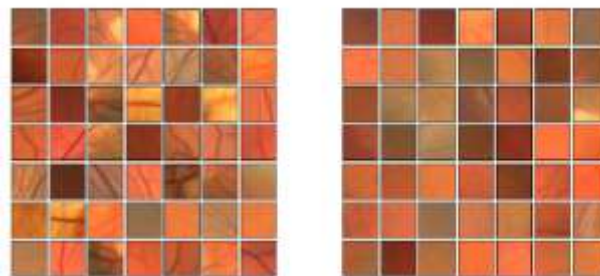


Fig.3: Patches of the input image

B) Global Contrast Normalization

The images is clearly specify that brightness may vary across the FOV. In order to help the learning process to abstract from these fluctuations and focus on vessel detection, we perform local (per-patch) brightness and contrast normalization. Every patch is standardized by subtracting the mean and dividing by the standard deviation of its elements (independently in the R, G, and B channel), which also maps the originally byte-encoded brightness to signed reals.

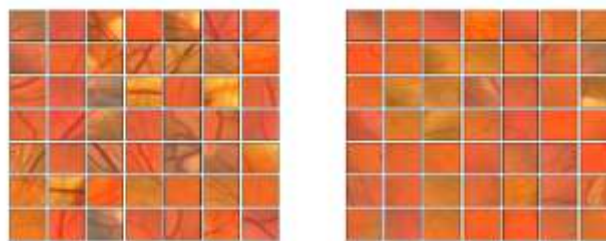


Fig.4: Global contrast normalization

C) Zero-Phase Component Analysis

In natural images, neighboring pixels are strongly connected as they are likely to represent the same structure in a scene. When learning a algebraic model of images (which is what a neural network is essentially doing), it is thus desirable to abstract from these universal

characteristics and focus on the higher-order correlations, i.e., capture the relevant regularities rather than the quite obvious fact that nearby pixels are likely to be similar. Removal of universal correlations can be achieved by multiplying the data matrix by a whitening matrix. After this common in DL transformation, it becomes unfeasible to expect the value of one pixel given the value of only one other pixel.

Formally, let the centered (zero mean) data be stored in matrix X with features in columns and data points in rows. In our case, X has $3 \times 27 \times 27 = 2187$ columns and the number of rows equal to the number of examples (patches). Let the covariance matrix have eigenvectors in columns of U and eigen values on the diagonal, so that $\text{SIGMA} = U \cdot U^T$. Then, U is an orthogonal rotation matrix, and U^T gives a rotation needed to decorrelate the data (i.e., it maps the original features onto the principal components). The classical PCA whitening transformation is given by:

$$W = \Lambda^{1/2} \cdot U^T$$

Each component of WPCA has variance given by the related eigenvalue. However, whitening is not unique; the whitened data remains whitened under rotation, which means that any $W = RWPCA$ with an orthogonal matrix R will also be a whitening transformation. In what is called zero-phase component analysis (ZCA) whitening, we take U as this orthogonal matrix, i.e.:

$$W = U \cdot \Lambda^{1/2} \cdot U^T$$

In experiments, we first apply GCN to individual patches in the training set, then learn the ZCA transformation from these patches, and finally apply it to convolutional neural networks.

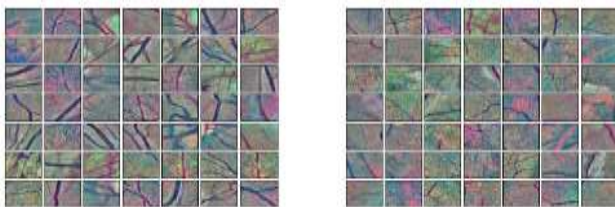


Fig.5: Zero phase component analysis

D) Augmentations

Despite using large numbers of relatively small (27X 27) patches for training, the CNNs may overfit. Other works on deep learning show that the reason for that is the still relatively small number of examples compared to the number of model (CNN's) parameters, which for the network is in the order of 48 millions. The remedy commonly used in deep learning is augmentation, meant as generation of additional examples by (typically

randomized) transformations of existing training examples. The data was enlarged offline, prior to learning. Each patch, normalized and whitened and was subject to 10 independent transformations, each composed of four randomized actions from the following list:

- _ Scaling by a factor between 0.7 and 1.2,
- _ Rotation by an angle from $[-90; 90]$,
- _ Flipping horizontally or vertically,
- _ Gamma correction of Saturation and Value (of the HSV colorspace) by raising pixels to a power in $[0.25; 4]$.

E) Convolutional Neural Networks

A convolutional neural network (CNNs) is a composite of multiple elementary processing units, each featuring several weighted inputs and one output, performing convolution of input signals with weights and transforming the outcome with some form of nonlinearity. The units are arranged in rectangular grids, and their locations in a layer correspond to pixels in an input image. The spatial arrangement of units is the primary characteristics that makes CNNs suitable for processing visual information; the other features are local connectivity, parameter sharing and pooling of hidden units.

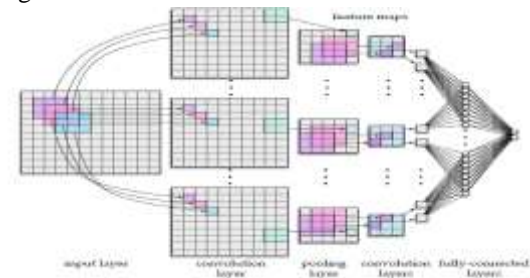


Fig.6: Convolutional neural network

Local connectivity means that a given unit receives data only from its receptive field (RF), a small rectangle of image pixels (for the units in the first layer) or units in the previous layer (for the subsequent layers). The RFs of neighboring units in a layer typically offset by stride. Image size, RF size and stride together determine the dimensions of a layer. For instance, a layer of units with 3×3 RFs with one pixel stride needs only 9 units when applied to a 5×5 monochromatic image, because three RFs of width 3 each, overlapping by two pixels, span the entire image. Larger stride and larger RFs lead to smaller layers. Local connectivity significantly reduces the number of weights in contrast to the fully-connected conventional networks. It is also consistent with the spatial nature of visual information and mimics certain aspects of natural visual systems.

Parameter sharing consists in sharing weights across units in the same layer. When the units in a given layer share the same vector of weights, they form a feature map, with each of them calculating the same local feature, even though from a different part of the image. This reduces the number of parameters even further and makes the extracted features equivariant. For instance, a layer of units with 3×3 RFs connected to a single channel image has only 10 parameters (nine per channel for the pixels in the RF and one for neuron threshold), regardless the number of units.

Pooling consists in aggregating outputs of multiple units by other means than convolution. In the most popular aggregation scheme, max-pooling, each aggregating unit returns the maximum value in its RF. Like local connectivity, pooling reduces the resolution w.r.t. previous layer and provides for translational invariance.

A typical CNN architecture consists of several convolutional feature maps entwined with max-pooling layers, finalized with at least one fully-connected layer that 'funnels' the excitations into output neurons, each corresponding to one decision class. Sliding RFs by the number of pixels defined in stride across the input image causes successive layers to be smaller, so that the final grid fed into the fully connected is usually much smaller than the input image. There are often several feature maps working in parallel, each of them responsible for extracting one feature. Large networks may involve even several dozens of feature maps. In case of multi-channel images, separate feature maps are connected to all channels. The consequent layers fetch data from multiple maps in the previous layer and so combine the information from particular channels. In such a case, each unit has multiple RFs with separate weight vectors, and the weighted signals coming from all input maps together form its excitation.

F) Optic Disc and Cup Segmentation

The next step is to segment cup and disc in fundus images and to calculate the CDR ratio to detect presence of Glaucoma. The block diagram is

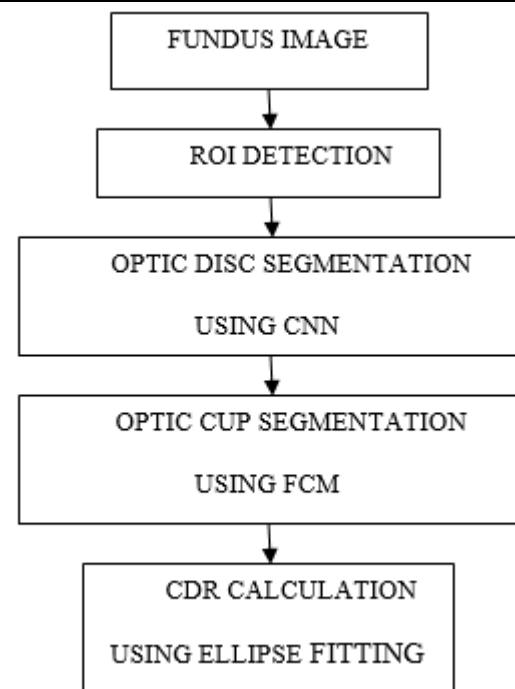


Fig.7: Block diagram of cup and disc segmentation

G) Region Of Interest Detection (ROI)

For the calculation of cup to disc ratio first step is optic cup and optic disc segmentation. Figure 8 is showing framework for the calculation of CDR. In order to detect optic cup or disc, Fundus images are taken by the high resolution retinal fundus camera. Firstly the region of interest which is around optic disc is depicted as shown in the Figure 8. If ROI is detected accurately it will generate small image which will fasten the speed of CDR calculation. Normally its size ranges less than 11% of fundus image. ROI can be found in large number of retinal images without human interruption and it is effective for mass screening. It is found that optic disc area is having higher intensity as compare to the surrounding area of the retinal fundus image. Optic disc center is selected as the point having highest intensity. An approximate high intensity region is calculated via intensity weighted centroid method that would be called as optic disc center. A rectangle twice the diameter of the optic disc is drawn around the ROI known as ROI Boundary which is used for optic disc and cup segmentation.

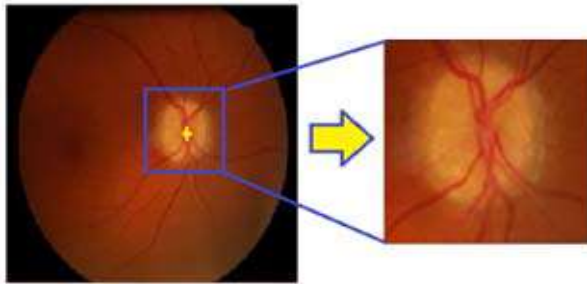


Fig.8: ROI Extration

H) Optic Disc Segmentation

Detection of the OD is a fundamental task for automated diagnosis of various ophthalmic diseases like glaucoma, diabetic retinopathy and pathological myopia. Hence, there is a huge literature available on segmentation of the OD. The OD segmentation estimate the OD boundary using convolutional neural networks in section E.

I) Optic Cup Segmentation

After OD segmentation, the next stage is optic cup segmentation. Optic cup segmentation using Fuzzy C Means.

Fuzzy c-means is a method of clustering which allows one piece of data to belong to two or more clusters.It is based on minimization of the objective function:

$$J_m = \sum_{i=1}^N \sum_{j=1}^C u_{ij}^m \|x_i - c_j\|^2 \quad 1 \leq m < \infty$$

Where $\|*\|$ is any norm expressing similarity between any measured data and the center. m is real number greater than 1, the degree of membership is u_{ij} of x_i in the cluster j , the i th of d -dimensional measured data is x_i , the d -dimension center of the cluster is c_j , Fuzzy partitioning is carried out through an minimization of the objective function shown above, with the update of u_{ij} and the cluster c_j by:

$$u_{ij} = \frac{1}{\sum_{k=1}^C \left(\frac{\|x_i - c_j\|}{\|x_i - c_k\|} \right)^{\frac{2}{m-1}}}, \quad c_j = \frac{\sum_{i=1}^N u_{ij}^m \cdot x_i}{\sum_{i=1}^N u_{ij}^m}$$

This iteration will stop when $\max_{ij} \left\{ \left| u_{ij}^{(k+1)} - u_{ij}^{(k)} \right| \right\} < \epsilon$, where ϵ is a termination criterion between 0 and 1, where k are the number of iteration steps. This procedure converges to a saddle point of J_m .

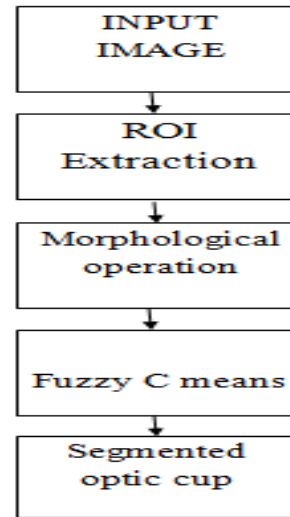


Fig.9: Block diagram for cup segmentation

J) Ellipse Fitting

The ellipse fitting algorithm can be used to smooth the disc and cup boundary. Ellipse fitting is usually based on least square fitting algorithm which assumes that the best-fit curve of a given type is the curve that minimizes the algebraic distance over the set of N data points in the least square. By minimizing the algebraic distance subject to the constraint $4ac^2 + b^2 = 1$, the new method incorporates the ellipticity constraint. It is the best to fit the optic disc and cup since it minimizes the algebraic distance subject to a constraint, and incorporates the elliptic constraint into the normalization factor. It is ellipse-specific, so that effect of noise (ocular blood vessel, hemorrhage, etc.) around the cup area can be minimized while forming the ellipse. It can also be easily solved naturally by a generalized Eigenvalue system. An approximate round estimation of cup boundary is applied as the best fitting least square ellipse. The area enclosed within the ellipse can be considered as the cup and disc surfaces when CDR is calculated by this method

K) Glaucoma Detection

Several parameters used for glaucoma detection such as cup-to disc ratio (CDR), cup-to-disc area ratio, neuro-retinal rim thickness etc. can be found out using this approach.

Cup-to-Disc Ratio: Cup-to-disc ratio is a Significant parameter indicating the expansion of the cup region. Glaucoma tends to affect the superior and inferior regions of the opticnerve first, thereby producing visual field defects. Therefore, CDR, a measure of elongation of the

cup vertically can be used to detect glaucoma in early stages. CDR value of 0.5 and above is a sign of glaucoma

$$\text{CDR} = \frac{\text{DIAMETER OF CUP}}{\text{DIAMETER OF DISC}}$$

V EXPERIMENTAL RESULTS

I) Blood Vessel Segmentation

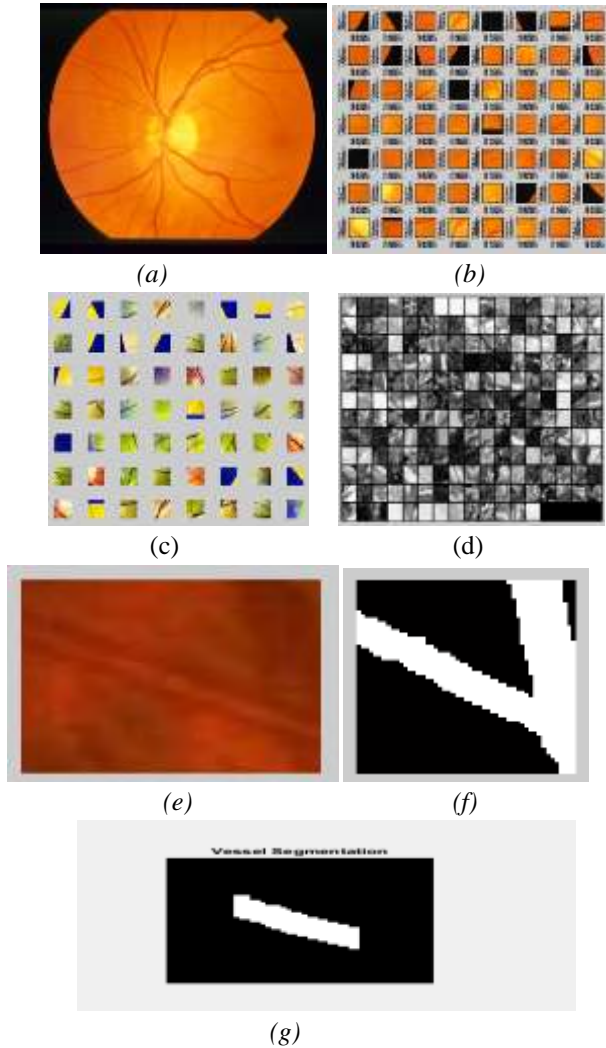


Fig.10: (a) Fundus image (b) Patches of the image (c) GCN (d) ZCA (e) Particular patch of the image (f) Ground truth image (g) segmented blood vessel.

This algorithm is tested on hospital images for calculating the accuracy. The accuracy of a test is its ability to differentiate the blood vessel and non blood vessel correctly. To estimate the accuracy of a test, we should calculate the proportion of true positive and true negative in all evaluated cases. Mathematically, this can be stated as:

$$\text{Accuracy} = \frac{TP + TN}{TN + TP + FP + FN}$$

TP-Blood vessel area FP-Non blood vessel area

The average accuracy for the classification of blood vessel is 95.64%.

II) Optic Cup And Disc Segmentation

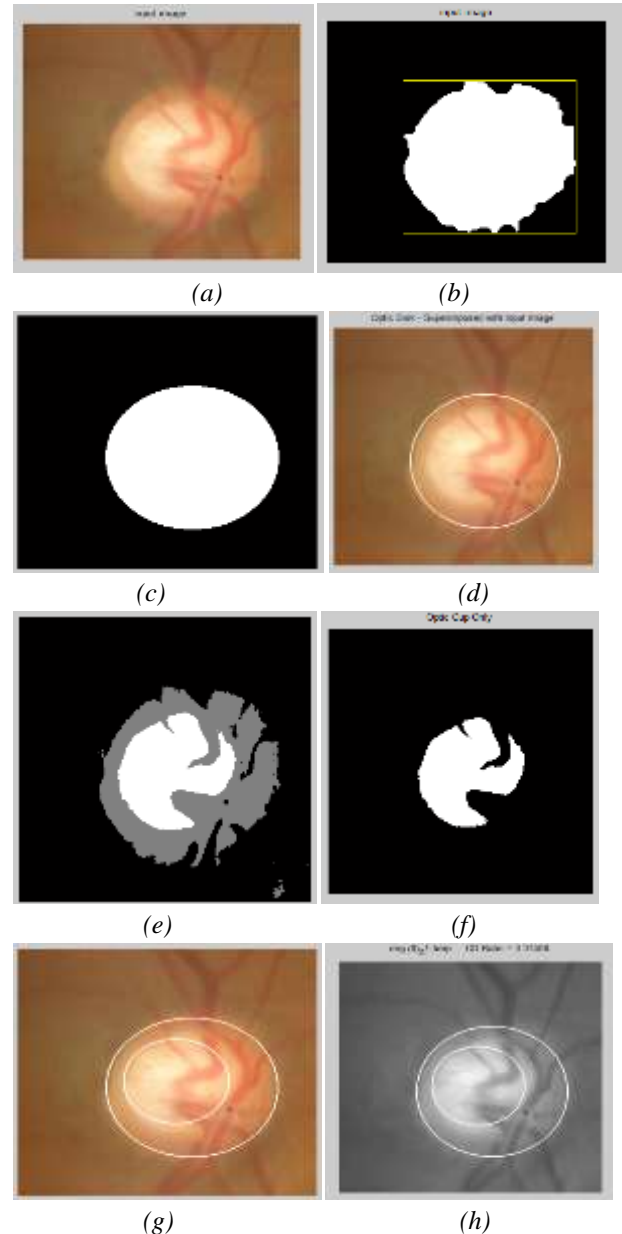


Fig.11: (a)ROI detection ,(b)Ground truth image,(c)Bounding ellipse,(d)Segmented optic disc,(e) Cup and disc (f) segmented cup(g) Ellipsefitting,(h) CDR calculation

TABULAR FORM II

IMAGE	CDR VALUE	CONDITION OF THE IMAGE
1	0.51	GLAUCOMA
2	0.37	HEALTHY
3	0.26	HEALTHY
4	0.51	GLAUCOMA
5	0.43	HEALTHY

V. DISCUSSION AND CONCLUSION

This study brings evidence that deep neural networks are a viable methodology for medical imaging, even though they solve the task in question in a different way than virtually all well-documented past work. We find this encouraging, in particular given the entirely supervised character of the neural approach, which learns from raw pixel data and does not rely on any prior domain knowledge on vessel structure. While learning, a network autonomously extracts low-level features that are invariant to small geometric variations, then gradually transforms and combines them into higher-order features. In this way, the raw raster image is transformed into a more abstract and a priori unknown representation that fosters effective vessel segmentation. The features learned at multiple levels of abstraction are then automatically composed into a complex function that maps an input patch to its label.

An average accuracy of 95.64% is determined in the classification of blood vessel or not. Optic cup is also segmented from the optic disc by Fuzzy C Means Clustering (FCM). This proposed algorithm is tested on a sample of hospital images and CDR value is determined. The obtained values of CDR is compared with the given values of the sample images and hence the performance of proposed system in which Convolutional Neural Networks for segmentation is employed, is excellent in automated detection of healthy and Glaucoma images.

REFERENCES

- [1] A. Hoover, V. Kouznetsova, and M. Goldbaum, "Locating blood vessels in retinal images by piecewise threshold probing of a matched filter response," *IEEE Transactions on Medical Imaging*, vol. 19, pp. 203–210, 2000.
- [2] R. Rangayyan, F. Oloumi, F. Oloumi, P. Eshghzadeh-Zanjani, and F. Ayres, "Detection of blood vessels in the retina using gabor filters," in *Canadian Conference*

on Electrical and Computer Engineering, 2007, pp. 717–720.

- [3] A. Mendonca and A. Campilho, "Segmentation of retinal blood vessels by combining the detection of centerlines and morphological reconstruction," *IEEE Transactions on Medical Imaging*, vol. 25, no. 9, pp. 1200–1213, 2006.
- [4] M. Miri and A. Mahloojifar, "Retinal image analysis using curvelet transform and multistructure elements morphology by reconstruction," *IEEE Transactions on Biomedical Engineering*, vol. 58, no. 5, pp. 1183–1192, 2011.
- [5] K. A. Vermeer, F. M. Vos, H. G. Lemij, and A. M. Vossepoel, "A model based method for retinal blood vessel detection," *Computers in Biology and Medicine*, vol. 34, no. 3, pp. 209–219, 2004.
- [6] B. Lam and H. Yan, "A novel vessel segmentation algorithm for pathological retina images based on the divergence of vector fields," *IEEE Transactions on Medical Imaging*, vol. 27, no. 2, pp. 237–246, 2008.
- [7] Y. Bengio, P. Lamblin, D. Popovici, H. Larochelle et al., "Greedy layer-wise training of deep networks," *Advances in neural information processing systems*, vol. 19, p. 153, 2007.
- [8] M. Fraz, P. Remagnino, A. Hoppe, B. Uyyanonvara, A. Rudnicka, C. Owen, and S. Barman, "Blood vessel segmentation methodologies in retinal images - a survey," *Comput. Methods Prog. Biomed.*, vol. 108, no. 1, pp. 407–433, Oct. 2012. [Online].
- [9] J. Staal, M. D. Abràmoff, M. Niemeijer, M. A. Viergever, and B. van Ginneken, "Ridge-based vessel segmentation in color images of the retina," *Medical Imaging, IEEE Transactions on*, vol. 23, no. 4, pp. 501–509, 2004.
- [10] A. Hoover, V. Kouznetsova, and M. Goldbaum, "Locating blood vessels in retinal images by piecewise threshold probing of a matched filter response," *Medical Imaging, IEEE Transactions on*, vol. 19, no. 3, pp. 203–210, 2000.
- [11] C. G. Owen, A. R. Rudnicka, R. Mullen, S. A. Barman, D. Monekosso, P. H. Whincup, J. Ng, and C. Paterson, "Measuring retinal vessel tortuosity in 10-year-old children: validation of the computer-assisted image analysis of the retina (caiar) program," *Investigative ophthalmology & visual science*, vol. 50, no. 5, pp. 2004–2010, 2009.
- [12] E. Ricci and R. Perfetti, "Retinal blood vessel segmentation using line operators and support vector

- classification,” *Medical Imaging, IEEE Transactions on*, vol. 26, no. 10, pp. 1357–1365, 2007.
- [13] F. M. Villalobos-Castaldi, E. M. Felipe-Riverón, and L. P. Sánchez-Fernández, “A fast, efficient and automated method to extract vessels from fundus images,” *J. Vis.*, vol. 13, no. 3, pp. 263–270, Aug. 2010.
- [14] G. Azzopardi, N. Strisciuglio, M. Vento, and N. Petkov, “Trainable cosfire filters for vessel delineation with application to retinal images,” *Medical image analysis*, vol. 19, no. 1, pp. 46–57, 2015.
- [15] Y. Zhao, L. Rada, K. Chen, S. P. Harding, and Y. Zheng, “Automated vessel segmentation using infinite perimeter active contour model with hybrid region information with application to retinal images,” *Medical Imaging, IEEE Transactions on*, vol. 34, no. 9, pp. 1797–1807, 2015.
- [16] J. V. Soares, J. J. Leandro, R. M. Cesar Jr, H. F. Jelinek, and M. J. Cree, “Retinal vessel segmentation using the 2-d gabor wavelet and supervised classification,” *Medical Imaging, IEEE Transactions on*, vol. 25, no. 9, pp. 1214–1222, 2006.
- [17] S. Roychowdhury, D. D. Koozekanani, and K. K. Parhi, “Blood vessel segmentation of fundus images by major vessel extraction and subimage classification,” *Biomedical and Health Informatics, IEEE Journal of*, vol. 19, no. 3, pp. 1118–1128, 2015.
- [18] X. You, Q. Peng, Y. Yuan, Y. Cheung, and J. Lei, “Segmentation of retinal blood vessels using the radial projection and semi-supervised approach,” *Pattern Recogn.*, vol. 44, pp. 2314–2324, 2011.
- [19] World health organization programme for the prevention of blindness and deafness- global initiative for the elimination of avoidable blindness World health organization, Geneva, Switzerland, WHO/PBL/97.61 Rev.1, 1997.
- [20] G. Michelson, S. Wrtges, J. Hornegger, and B. Lausen, “The papilla as screening parameter for early diagnosis of glaucoma,” *Deutsches Aerzteblatt Int.*, vol. 105, pp. 34–35, 2008.
- [21] P. L. Rosin, D. Marshall, and J. E. Morgan, “Multimodal retinal imaging: New strategies for the detection of glaucoma,” in *Proc. ICIP*, 2002.
- [22] M.-L. Huang, H.-Y. Chen, and J.-J. Huang, “Glaucoma detection using adaptive neuro-fuzzy inference system,” *Expert Syst. Appl.*, vol. 32, no. 2, pp. 458–468, 2007.
- [23] G. D. Joshi, J. Sivaswamy, K. Karan, and S. Krishnadas, “Optic disk and cup boundary detection using regional information,” in *Biomedical Imaging: From Nano to Macro, 2010 IEEE International Symposium on*, 2010, pp. 948–951.
- [24] U. R. Acharya, S. Dua, X. Du, S. Vinitha Sree, and C. K. Chua, “Automated diagnosis of glaucoma using texture and higher order spectra features,” *Information Technology in Biomedicine, IEEE Transactions on*, vol. 15, pp. 449–455, 2011.
- [25] C. Burana-Anusorn, W. Kongprawechnon, T. Kondo, S. Sintuwong, and K. Tungpimolrut, “Image Processing Techniques for Glaucoma Detection Using the Cup-to-Disc Ratio,” *Thammasat International Journal of Science and Technology*, vol. 18, p. 22, 2013.
- [26] G. D. Joshi, J. Sivaswamy, and S. Krishnadas, “Optic disk and cup segmentation from monocular color retinal images for glaucoma assessment,” *Medical Imaging, IEEE Transactions on*, vol. 30, pp. 1192–1205, 2011.
- [27] S. Chandrika and K. Nirmala, “Analysis of CDR Detection for Glaucoma Diagnosis,” *International Journal of engineering research and application (IJERA) ISSN*, pp. 2248-9622.
- [28] C. Burana-Anusorn, W. Kongprawechnon, T. Kondo, S. Sintuwong and K. Tungpimolrut, *Image processing techniques for glaucoma detection using the cup-to-disc ratio*, in *Thammasat International Journal of Science and Technology*, January Mar 2013, vol. 19, No. 1, pp. 22-34.
- [29] Hrynchak P., Hutchings N, Jones D. and Simpson T., *A comparison of cup-to-disc ratio measurement in normal subjects using optical coherence tomography image analysis of the optic nerve head and stereo fundusbiomicroscopy.*, in *Touch Briefings 2012*. pp. 92-97.
- [30] A. SC Reis, A. Toren and M. T. Nicolela, *Clinical optic disc evaluation in glaucoma.*, in *Ophthalmic Physiol Opt.* vol.6 Nov 24, 2004 pp. 543-550

A Review on Advancements in Optical Communication System

Aparna Tomar, Dr. Vandana Vikas Thakare

Department of ECE, MITS, Gwalior, India

Abstract--- *Communication systems are revolutionized by the tremendous research being done in this direction. The need is the mother of the invention. The need of data transfer is increasing every day. There is the big demand for the fast optical communication systems. The optical fibers have the big potential of carrying the different channels which can transmit the data at amazing speed. In this work we have studied the research done in the field of technological development taking place in fiber communication system. The focus is on the use of fiber link as a modern medium of communication in the optical range.*
Keywords--- *Communication system, Optical data transfer, Channel, Fiber link, Optical range.*

I. INTRODUCTION

There are certain inherent flaws with the optical transmission system like intersymbol interference and noise. This distortion is introduced by the narrow bandwidth and some distortions due to the media through the optical signals travel. The linear transversal filter is used to reduce symbol interference. The system designed to remove unknown distortion is called an adaptive equalizer. The corrective measure is to identify the distortion and adjust accordingly with the objective to remove it. The equalizer can be the supervised or unsupervised type. In the TV or radio Transmission, blind equalizers are used.

Xuen He and et.al have employed step size controller method to achieve an efficient solution in fiber communication system is to the communication system. This work makes the use of PSD directed adaptive FD-LMS algorithm. This algorithm nullifies the posterior derivation of each frequency being in the FMI system with AWGN channels. The proposed algorithm has been verified by simulation results. The three algorithms namely conventional adaptive FD-LMS, signal PSD dependent noise PSD directed FD-LMS is found to be minimum. The convergence speed is improved by 48-39%.

It has also been established that the convergence is faster in longer transmission distance or larger differential mode group delay. The proposed algorithms are evaluated at

different system MDL. The complexity comparison for three algorithms is done in terms of needed complex multiplication. The check is formed over long distance thus simulating transmission length varying between 1000 and 3000 km. The power spectral density methodology requires in complex and needs of higher order. The hardware complexity of noise PSD directed method slowly decreases with the increase in the transmission distance. It has been found practically when the step size increased from 0.001 to 0.002 frequency domain least mean square algorithm needs simple hardware and this tends to converge efficiently. The equalizer converges to higher MSE. The noise PSD directed method iterated over 3000 km transmission on all six modes and it tends to convergence at same MSE to get the standard -10 dB normalized MSE (NMSE). The noise PSD directed algorithms require 47 blocks and the conventional algorithm needs 48 blocks [1]. Sean O'Arık and et.al have proposed Long-haul mode-division multiplexing (MDM) for adaptive multi-input-multi-output (MIMO) equalization to reduce for modal crosstalk and modal dispersion. To minimize computational complexity, use MIMO frequency-domain equalization (FDE). Polarization division multiplexing (PDM) system use single mode fiber but its transmission effected by noise, fiber nonlinearity and dispersion. In multi-mode fiber (MMF) with multi-input-multi-output (MIMO) transmission Increasing per-fiber capacity can be achieved more readily by increasing spatial dimensionality the total number of dimensions available for multiplexing, including spatial and polarization degrees of freedom denoted by D . In first case two polarization modes of single mode fiber using $D=2$. This is made possible by equalization techniques goes on going up with the upward drift of D and higher group delay. In second case systems using mode-division multiplexing (MDM) in MMFs ($D>2$) receiver, computational complexity increases because of an increase in D and because of the large group delay (GD) spread from the modal dispersion (MD). Two approaches for minimizing GD spread and controlling receiver complexity are optimization of the fiber index profile and

the introduction of strong mode coupling. High group delay has been obtained in step index fiber and low group delay obtained in graded index fibers with large cores (D). LMS algorithm and recursive version are used for MIMO FDE. It has been observed that RLS achieves faster convergence, higher throughput efficiency, lower output SER, and greater tolerance to mode-dependent loss, but gives higher complexity per FFT block. Therefore, RLS preferable for adapting to an unknown channel but LMS continuously might be preferable, depending on channel dynamics and system requirements [2].

Md. Saifuddin Faruk and et.al have been proposed a novel adaptive frequency-domain equalization (FDE) scheme in digital coherent optical receivers, which can work with rationally-oversampled input sequences using the constant modulus algorithm (CMA). Adaptive filters play an important role in digital coherent optical receivers because they can perform signal-processing functions such as equalization, polarization demultiplexing, and clock recovery all at once. the frequency-domain based equalization algorithm needs simple logic and computational expression. This requires lesser time the logic is to apply the processing in the blocks and fast implementation of the discrete Fourier transform (DFT) with the FFT algorithm. The proposed scheme is based on frequency-domain up sampling and down sampling the symbol-spaced error signal is obtained by the constant modulus algorithm (CMA). It has been obtained that comparison of previous scheme and proposed scheme. The equalization is done without dividing into groups. Thus, the required number of adaptive filters for dual-polarization (DP) systems is reduced from eight to four. The filter designed for the purpose is to initialize in such a way that the problem of singularity does not come on the way. The effectiveness of the proposed scheme is verified with 10-Gbaud dual-polarization QPSK transmission experiments [3].

Neng and et.al have propounded the normalized FDE over a thousand km. distance experiment. This work makes the use of master-slave phase estimation (MS-PE) which can be used to reduce the complexity of carrier recovery with minimal Q2-penalty. To provide multiplicative capacity growth on a single fiber mode-division multiplexing (MDM) has been proposed. MDM transmission using few-mode fiber (FMF) in a long haul because of mode coupling it is difficult to reduce multimode interferences multiple-input-multiple-output (MIMO) equalization is required. Differential mode group delay (DMGD) is responsible for increase the algorithmic complexity of MIMO equalization. The collected DMGD grows the TDE becomes more

complex, while FDE may be more feasible. The channel out consist of sharp spikes between the LP01 and LP11 modes. The MDM transmission for the first time based on NA-FDE to increase the speed of convergence. The step size μ is responsible for the convergence speed for the specified frequency range. Different frequencies have different rates of convergence. In NA-FDE, a normalized step size $\mu(k) = \alpha / P(k)$ is used for FDE. In both cases, an equalizer length of 1024 taps was used and same step size was used for fair Comparison. It has been observed that NA-FDE converges six times faster compared with CA-FDE at a mean square error (MSE) of 10^{-5} . The application of NA-FDE for FMI transmission has been checked over loop over 1000 cm. In master-slave phase estimation (MS-PS) the LP01, X mode selected as master mode and LP01, X selected as phase noise. NA-FDE was found to give similar performance as a TDE but has 16.2 times reduced complexity [4].

An Li and et.al have demonstrated the use of mechanical grating based mode converters to achieve two forms of dual-spatial-mode transmission LP01 and LP11 and dual LP11 modes. It has demonstrated mode-division multiplexing (MDM) of LP01 and LP11 modes to generate LP11 modes (LP11a+LP11b) and even all three modes (LP01+LP11a+LP11b) over few-mode fiber (FMF). The transmission system with mode multiplexing are a very crucial problem. The mode selective devices proposed in divided into two major categories: free-space based (FSB) and fiber based (FB). Free space components are bulky in size ex liquid-crystal-on-silicon (Lcos) spatial light modulator (SLM). But fiber based mode selective device have compact and easiness of integration. Firstly proposed 107-Gb/s coherent optical OFDM (CO-OFDM) transmission over a 4.5-km two-mode fiber using LP01 and LP11 modes. Secondly proposed 58.8-Gb/s CO-OFDM transmission using dual modes where the mode separation is achieved via 4×4 electronic MIMO processing [5].

Sebastian Randel and et.al have been demonstrated the impulse response matrix of few-mode fiber links that support the propagation of LP01 and LP11 modes over up to 1,200-km. Results are obtained by by multiple-input multiple-output (MIMO) digital signal processing (DSP) in combination with differential group delay (DGD) compensated fiber spans. Equalizer is used to remove complexity in long haul transmission so two scheme must be remembered. first optical means to minimize the modal delay spread (MDS), i.e. the width of the impulse response, must be analyzed. second In a second step, the performance-complexity of efficient equalizer structures such as the frequency-domain equalizer (FDE) must be studied. it has been observed that MDS can be reduced to

about 10 ns using a DGD compensated fiber span. Also observed that the system MDL is below 5 dB after 1,200 km. characterize the channel's model delay spread and mode-dependent loss [6].

Joseph M. Kahn and et.al have proposed a mode coupling scheme for overcoming major challenges incoherent mode-division-multiplexed systems. SMC (strong mode coupling) helps to bring down the delay done to the group and helps to optimize the complexity of MI (multiple inputs) multi-output signal processing. Strong mode coupling is responsible for creating frequency diversity dramatically reducing out stage probability. Transfer of energy from one ideal mode to another during propagation only due to mode coupling. It has been observed that practically strong couple modes having equal or nearly equal propagation constant but weakly coupled modes having a highly unequal propagation constant. The separation between two modes results in modal dispersion increasing capacity through mode division multiplexing (MDM). SMF (single-mode fiber) helps in the wave movement in two polarization conditions. Polarization-mode dispersion (PMD) and polarization-dependent loss (PDL) have long been described by field coupling models. It has been observed that strongly coupled modal group delay or gain depend only on no. of modes and variance of accumulated delay or gain and can be derived from the eigenvalue distributions of certain random variables [7].

SDM (space division multiplexing) has been put forth by Savory. SDM is extremely challenging technology, of requiring developments in all areas of Photonics Technology. The optical communication systems are being upgraded every day. There is a rapid development taking place in this field at the global level in the space division multiplexing. Space Division Multiplexing (SDM) is conceptually simple, SDM is extremely challenging technologically, requiring the development of new fibers, amplifiers, multiplexers, digital signal processing circuits, and other components. The multiplexing means the utilization of channel by the division of the space. It is suggested that the SDM technology would be adopted by the operators provided the cost of the technical operation reduces, 1) lowers the cost per bit (i.e., SDM-based systems must be less costly than multiple independent systems), 2) provides there is a larger requirement of flexible photonic network. It must allow flexibility to an extent. 3) allows a reasonable transitional strategy from systems based on standard single-mode fibers [8].

Omid Zia-Chalabi and et.al have proposed a computationally efficient frequency-domain implementation of a fractionally spaced block-least-mean-square (LMS)

equalization. Polarization division multiplexing (PDM) and digital signal processing have helped to a paradigm shift in optical communication systems, by providing greater spectral efficiency than Intensity-Modulated. Digital equalization of chromatic dispersion (CD) and linear polarization-dependent effects usually preferred the dual-stage receiver architecture. A fractionally spaced equalizer (FSE) is mostly preferred for increase robustness of the receiver. Where the input signal is sampled at twice or more the symbol rate $1/T$. It has been proving more efficient for real-time processing to implement filtering in the frequency-domain (FD) as compared in the time-domain (TD). FD equalizers (FDE) could bring significant computational savings in the second stage, compared to TD equalizers (TDE). But requires the insertion of the block of the transmitter with a circular prefix. Another attractive solution is FD adaptive filtering based on the overlap-save technique (OS-FDE). Thus, the proposed equalizer architecture appears as a promising solution for 100 Gb/s and beyond real-time digital coherent receivers, which impose stringent constraints on algorithm complexity. Finally, the proposed FDE may be extended to weight update criteria other than LMS or CMA, by modify accordingly [9].

Kun Shi and et.al have proposed frequency domain adaptive filters require very simple circulations hence simple circuitry to implement by using the overlap-and-save implementation method. FD algorithms may improve the convergence speed in comparison to the Time-domain algorithms. To optimize the convergence behavior of the adaptive filter a step size control scheme proposed for each frequency bin. A step-size control method is also proposed in to improve convergence behavior for systems working in a non-stationary environment. Discrete Fourier transform is proposed to improve the convergence rate. Step sizes that are inversely proportional to the signal power levels in the frequency bins of the discrete Fourier transform (DFT). A variable step-size algorithm is proposed for obtaining the low residual error. Therefore, overcome the compromise between fast convergence and low steady-state error in the existing method the proposed method achieves faster convergence rate as well as smaller MSD and MSE [10].

Multiple input multiple outputs (MIMO) has been performed using Stokes algorithm in a frequency domain (SSA). The unique work is the analysis of the convergence speed and frequency offset of the SSA. It is not compulsory to go for pre-compensation of frequency offset. There is tremendous growth in the transmission capacity of the optical fiber link. The hardware has improved which allows lower losses and longer distances of optical cable. The less

line consuming algorithms can further increase the channel width. The research is going on in SDM [11].

II. CONCLUSION

We have carefully examined all the technological advancements in the use of fiber communication link as a smart channel with larger capacity to carry the digital data. The modern era is marked by the smart hardware better picture and sound quality means more data. All these requirements can only be met by the smart communication link i.e. the fiber communication system. The revolution in this field is need generated. The industry and researchers have joined hands to meet out this global demand.

REFERENCES

- [1] Xuan He ,Yi Weng, “A Step-Size Controlled Method for Fast Convergent Adaptive FD-LMS Algorithm in a Few-Mode fiber communication system”, journal of lightwave technology, vol. 32, no. 22, november 15, 2014.
- [2] Sercan O. Arik, Daulet Askarov, and Joseph M. Kahn, “ Adaptive Frequency-Domain Equalization in Mode-Division Multiplexing Systems ”, journal of lightwave technology, vol. 32, no. 10, may 15, 2014.
- [3] Md. Saifuddin Faruk and Kazuro Kikuchi, “Frequency-Domain Adaptive Equalizer with Rational Oversampling Rates in Coherent Optical Receive”, ECOC 2014, Cannes – France P.3.22
- [4] Neng Bai, Ezra Ip, Ming-Jun Li, Ting Wang and Guifang li, “ Long-Distance Mode-Division Multiplexed Transmission using Normalized Adaptive Frequency-Domain Equalization”, 978-1-4673-50600/\$31.00 ©2013 IEEE.
- [5] An Li, Abdullah Al Amin, “Reception of Dual-Spatial-Mode CO-OFDM in optical fiber”, journal of lightwave technology, vol. 30, no. 4, february 15, 2012.
- [6] Sebastian Randel, Miquel A. Mestre, Roland Ryf, and Peter J. Winze “Digital Signal Processing in Spatially Multiplexed Coherent Communications”, ECOC Technical Digest © 2012 OSA
- [7] Joseph M. Kahn and Keang-Po H02, “Mode Coupling in Coherent Mode-Division Multiplexed Systems Impact on Capacity and Signal Processing Complexity”, 978-1-4673-5051-8/12/\$31.00 © 20 12 iee.
- [8] SEB J. SAVORY, “Editorial Special Issue on Photonics Technology for Space Division Multiplexing”, iee photonics technology letters, vol. 24, no. 21, november 1, 2012.
- [9] Omid Zia-Chah “Efficient Frequency-Domain Implementation of Block-LMS/CMA Fractionally Spaced Equalization for Coherent Optical Communication”, iee photonics technology letters, vol. 23, no. 22, november 15, 2011.
- [10] Kun Shi, “A Frequency Domain Step-Size Control A method for LMS Algorithms”, iee signal processing letters, vol. 17, no. 2, february 2010
- [11] D. J. Richardson¹, J. M. Fini² and L E. Nelson³ “Space Division Multiplexing in Optical Fibres” ,Optoelectronics Research Centre, University of Southampton, Highfield, Southampton, SO17 1BJ, UK. 2OFS Laboratories,19 Schoolhouse Road, Somerset, New Jersey 08873, USA.3AT&T Labs - Research, 200 S. Laurel Avenue, Middletown, New Jersey 07747, USA

Problem Solving Approach

Arkeya Pal¹, Er. Faruk Bin Poyen²

¹Army Institute of Management, Kolkata, India

²Dept. of AEIE, UIT, BU, India

Abstract—Problem is something that we can never get rid of, how much we try and howmany anticipatory actions we take. Therefore, to deal with problems in our everyday life, every project implementation is to solve the problem as and when required. In this article we will try and study about problems and the techniques and methods by which we can solve it or mitigate the situation. Again it is worthy to mention as a prelude and also to conclude that problem solving is an individual skill and it therefore varies from person to person and from situation to situation and there exist no thumb rule to redress ay problem as a generalized rule. By the end of this article, we will try and develop certain tools by which we may approach a problematic situation before redressing the problem.

Keywords— Problem, situation, operational research, decision making, DMAIC, PDCA.

I. INTRODUCTION

Before we talk about problem solving, it is mandatory to define problem. A problem is defined as any event or situation, unforeseen, unwanted and therefore unwanted in any project or job which needs to be addressed and resolved before it becomes too complexing. In our personal life, business events or for any other matter, always something or the other happens that was not foreseen and therefore was not planned to address to. Problem may originate from family, work, health issues, social agendas, or it may even arise from within an individual. Under such circumstances, we need to come up with certain contingency plans which is defined as, problem solving. Problem can also be defined in other terms as the deviation from what is expected to happen and what is actually happening. Thus, arises the issue of solving a problem in order to achieve ones particular objective. Problem solving is defined as the area of cognitive psychology which deals with the processes involved in solving problems.

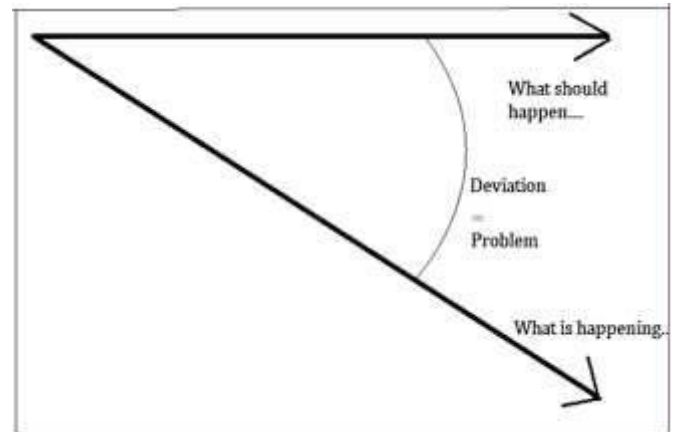


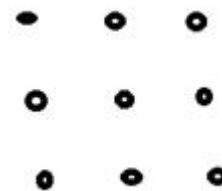
Fig. 1: Deviation is Problem

Problem solving depends on individual skill and capacity. The prerequisite of problem solving is that one has to be the owner of the situation. Unless and until one owns the problem, one cannot possibly solve the problem.

In order to establish the point, let us discuss two cases

Case I: Certain arithmetic and interpretational operations

- Putting of arithmetic operators in between four 4s to obtain 20.
 - i.e. $4 \ 4 \ 4 \ 4 = 20$
- Finding the sum of 1 to 100 without applying Arithmetic Progression formula.
- Express $613 = A^B + B^A$
- Draw four straight lines without lifting the pen and cutting across all the nine points as shown in figure below.



- Hens lay eggs, crows lay eggs, certainly all birds lay eggs, but peacocks do not. Why?
- With three match sticks, form a number which is greater than 3 but less than 4, without breaking the match sticks.

Solutions:

- $(4 \div 4 + 4) \times 4 = 20$

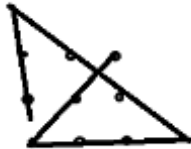
b. $X = 1 + 2 + \dots + 100$

$$X = 100 + 99 + 98 + \dots + 2 + 1$$

$$2X = 101 + 101 + \dots + 101 \text{ (100 times)}$$

$$X = (101) * \frac{100}{2} = 5050$$

c. $613 = 612 + 1; A = 612; B = 1; 612^1 + 1^{612} = 613$



e. It is because peacocks do not lay eggs, peahens do.

f. π

The point of submission here is that different set of people will take different amount of time to solve the given problems; even there will be a group of people who will be totally unable to solve these problems. And hence we come to the inference that problem solving depends on individual skill and capacity.

Case II: Two incidents with equal conditions but with little differences.

- A. A boat with four passengers viz. you, your parent, your spouse and your ward, caught up in turmoil and one needs to be abandoned to save the others. Nobody knows swimming which means imminent death of being abandoned. Whom will you abandon from boat?
- B. Same situation as above and here instead of four passengers there are now five passengers, the fifth being your boss.

From rigorous surveys, it was found that in situation B, people without hesitation chose their boss but in situation A, people got confused, perplexed and came up different answers.

So the inference may be drawn as in situation A, people were actually not bothered about the boss, they were just concerned. But in situation, people got confused because

it was their situation i.e. they were the owner of the situation and hence it is a problem to them.

II. PROBLEM SOLVING TOOLS

There exists variety of problem solving methods, among them the two very popular ones are DMAIC (Define, Measure, Analyse, Improve, Control) and PDCA (Plan, Do, Check, Act) [4]. In the PDCA model, P does a huge part of the job as it emphasizes on what, why, how and when. In DMAIC model, all the steps are equally important, starting from defining the problem to controlling it. All these methods rely on different tools of Problem solving. Here we will speak about a few on them. These tools find application when one sets goals to determine the root causes of the problem. Multi-Disciplinary Teamwork (MDT), Brainstorming, Pareto analysis (80/20 rule), Fishbone Diagram (cause – effect analysis), 5W tool, Check sheet and Control Chart (CC) are very popular tools in this domain.

MDT finds its success through thinking “out of the box”, as a heterogenic cluster of individuals look upon the problem from different vantage points. Brainstorming tool is somewhat ubiquitous in its application domain. Check sheet and Control Chart are more of an objective approach when judgment is based on pure numbers and their representations. Pareto’s principle, very popularly known as “vital few and trivial many” believes in the doctrine that 20 % of something is always responsible for 80 % of the outcome. In the 5 W tool, it is assumed that the 5th Why is the root cause of the problem and hence it is the one that should be improvised upon. The 5 whys also form parts of the fishbone structure. The fishbone model, by far and large the most preferred and popular tool operates on the basis of cause – effect analysis. The head of the fish structure denotes the outcome whereas the skeleton bone analyses the cause – effect relationships. The fishbone can be constructed with 6 Ms or 6 Ps as the vertices where the 6 Ms denote Man, Machine, Method, Material, Mother-nature and Measurement and 6 Ps denote Procedure, Policy, Plant, Person, Planet and Programs respectively.

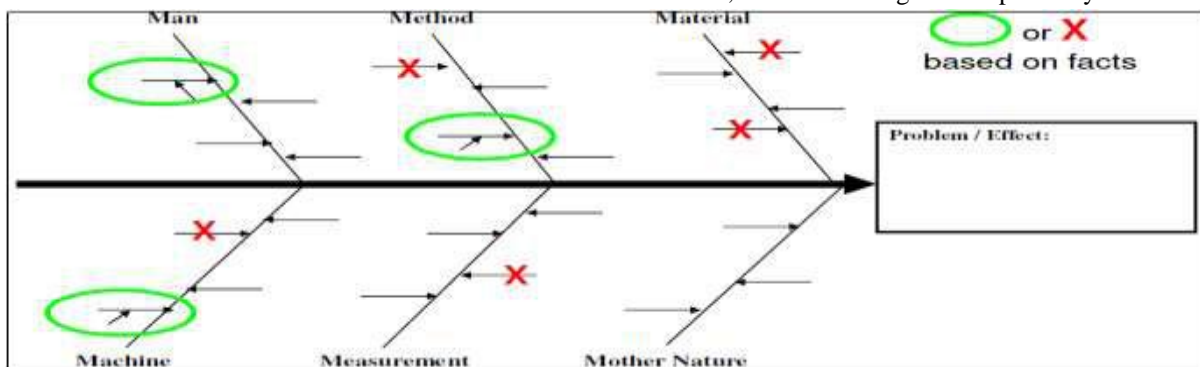


Fig 2: Fishbone Diagram

Preliminary steps towards attending a problem:

Whenever a problematic situation arises, we should proceed towards the situation as shown in the under given flowchart. [1] (R B Shivagunde et. al.). We select our tool of choice for preference in analysing these steps. Here we can look at the situation in two ways, firstly in the Deductive Analysis Approach where huge data is collected, followed by analysis and eventually we come to conclusions drawing recommendations. The second approach is Inductive Analysis Approach where we start with a hypothesis, analyze its subsistence and thereby draw a result to validate the conclusion with some recommendations. A point to mention here is that there is no such best tool dedicated for any particular problematic environment. It depends and suits one’s individual intuition and capability.

Step I: What should happen !!!

Step II: What is happening !!!

Step III: Why is it happening !!!

Step IV: Prioritizing the causes of problem.

Step V: What should be done!!! Finding solution to the causes.

Step VI: What has been done!!! Applying the solution to solve the problem.

Again in step I, when we are expecting what should happen, it has certain aspects towards its determination.

We expect things to happen based on

- What plans we have made,
- Expectation
- Experience
- Intuition
- Social norms

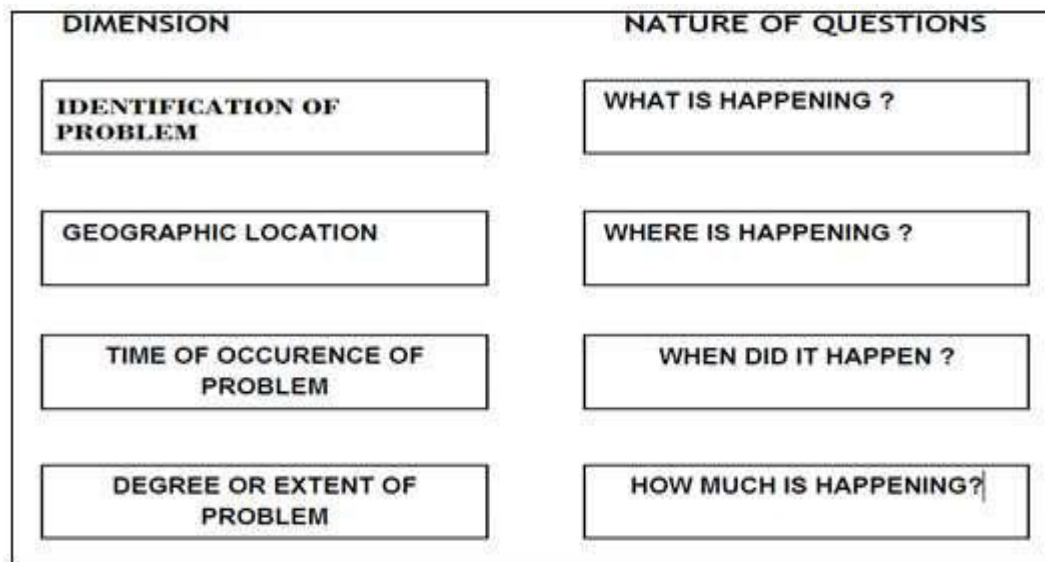


Fig 3: Problem Analysis

Step II has two sub steps for determining what is happening and they monitoring and feedback with time limiting to zero i.e.

$$\lim_{t \rightarrow 0} \text{Feedback}$$



Fig 4: The flowchart of problem solving

Operations Research in Problem Solving:

Operations research was developed keeping in mind of problem solving area where the nature of problem is complex and also there exists no clear cut or in fact no solution. It is a mathematical based analysis method to

provide a quantitative basis for tough managerial decisions. (Hillier and Lieberman et. al.)

As elaborated in “Introduction to Mathematical Programming” by Hillier and Lieberman, it prescribes seven element analysis towards problem solving. The seven elements are enumerated as defining the problem,

value system design, synthesis of alternatives, system modelling and analysis, optimization of alternatives, decision making, and finally planning for action. As these are mathematical based analysis they rely on a lot of mathematical and statistical tools as validation methodology.

Problem defining step is marked by research, data analysis and knowledge application. Needs analysis, input – output analysis and objective trees clarify and organize the goals and boundary conditions. Value system design organizes objectives into a hierarchy tree with the help of tools like weighted criteria tree, flow charts and causal loop diagrams. Quality Function Deployment (QFD) matrix helps generate alternatives based on these tools. Different alternatives are prognosticated in synthesis of alternatives to satisfy the demands. Methods like nominal group technique, computer simulation, Zwicky's morphological box are exercised in the step.

Systems modelling and analysis step develops models for analysing and comparing the alternatives. Techniques that find application here are data analysis, probability theory, econometric modelling, regression, forecasting, queuing, networks, reliability analysis and mathematical programming. To make substantial comparison, numerical iteration, derivative calculus, calculus of variations and graphical methods and used in the optimization of alternatives and effect of changes is measured through parametric sensitivity analysis.

In the decision making step, evaluation of alternatives gives the operator the end result to choose from options. Tools used are multi – attribute utility (MAU) theory, game theory, risk analysis, influence diagram, decision analysis, data analysis and statistical methods. Effect of changes in judgment is measured by value system sensitivity analysis. Final step is planning for action where the implementation is carried out and documented by resource planning scheduling.

III. ANALYSING THE PROBLEM AND SOLUTION

This section speaks about analysing the domain and depth of problem before proceeding to solve it. Any set of problem can be represented in a set of four quadrants, the axes being problem and solution extending from simple problem to complex and solution available to solution unavailable respectively.[7][8] The following diagrams depicts the quadrants involved in solving problems. Firstly we have to locate in which quadrant, a particular problem rests and then based on that, we need to proceed

towards solving it. So we start from first quadrant and finish at fourth quadrant. [9]

Quadrant I: Problem is of simple nature and also the solution to it available. Here we apply the solution immediately before the problem can shift from simple to complex.

Quadrant II: Here problem has complex nature but still the solutions are available. In this case, we start applying solutions one after another, if there exists more than one solution. We actually are searching for the best possible solution through trial and error method.

Quadrant III: In this region, the nature of problem is complex and also no solutions are available. This particular quadrant gives rise to a very important statistical tool viz. operations research to address and redress these kind of situations. It has three sub components and they are formulation, analysis and interpretation. Here in this quadrant, we sectionalize the problem into small pockets and try and fit them in the three other quadrants. This way we can reduce the effect of the problem. After this is done, there may still remain certain sections which remain in third quadrant. We again repeat the process until we can minimize the problem to the least.

Quadrant IV: In this quadrant, the nature of problem is simple but no solutions are available to redress. Here, one needs to be creative thorough innovation either at individual scale or in groups. In order to illustrate the situation, we will do a very popular case study.

A person has 17 gold coins and he has three heirs A, B and C. On his death bed, he declares that A will receive half of the coins while B will receive one-third of the coins and C will get one-ninth of the coins. Here the problem is known and simple but the solution is not available as 17 is not divisible by 3.

Solution to the above case: I add one gold coin to 17 gold coins and then carry out the calculations as declared by the person. Now we have 18 gold coins. So A will receive 9 gold coins i.e. half the property. B will receive 6 gold coins, one-third of the property and C will get 2 gold coins, one-ninth of the share. Therefore total gold coins distributed are $(9+6+2) = 17$ and then take back the extra gold coin. Thus the solution is creative through innovation.



Fig 5: Solution Analysis based on problem criticality.

Thus we can solve problems by addressing them through the above methods. Hence it can be rightly said that finding the cause through analysis and then by applying the required remedies, we can minimize the deviation and therefore can solve the problem or minimize it.

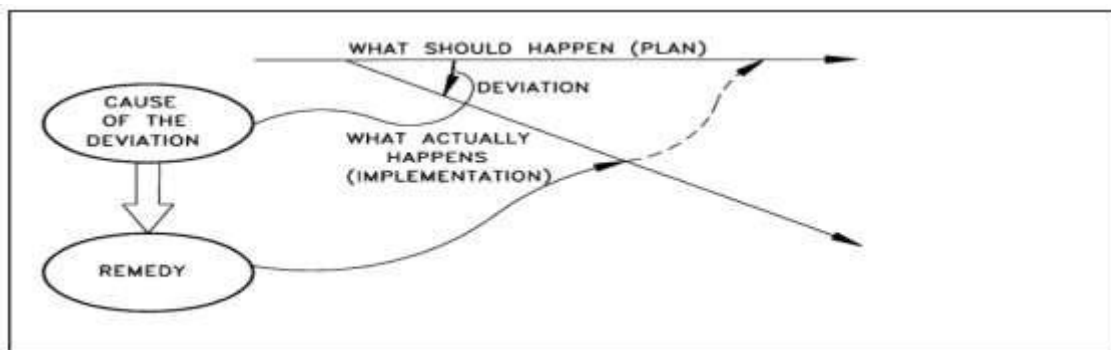


Fig 6: Post Problem Solving Technique Application

IV. DECISION MAKING

One very vital entity of solving problems is making the right decisions. Decision making is a very important skill one should possess to effectively and efficiently guide a team or run a project. Decision making is defined as the way of inspecting potentials, equating them and thereafter selecting a course of action. The back bone of a good decision making is gathering plethora of data regarding the situation in hand. And then analysing and scrutinizing them very minutely to have a very clear understanding of the situation. Factors that influence decision making are vision, mission, perception, priority, acceptability, risk, resources, goals, values, demands, styles and judgment. [5]

The DECIDE model is a very effective technique for making a more logical decision. The acronym DECIDE [2] stands for

D = Detect change

E = Estimate significance of change

C = Choose outcome

I = Identify options

D = Do best options

E = Evaluate results.

Rule of 6 C's of Decision Making.

1. Construct: a clear picture of what needs to be done.
2. Compile: A list of requirements.
3. Collect: Information on alternatives.
4. Compare: Alternatives.
5. Consider: What might go wrong.
6. Commit: The action.

V. CONCLUSION

Things can go wrong & they will. Problems will occur while implementing a project or job in spite of all possible preventive measures taken, be it personal domain

or professional, “object” problem or “people” problem. So the best and only way to cope with the situation is to face the problem and try and minimize the effects if it cannot be solved in totality. We therefore prescribe certain remedial steps by which things can be dealt with. If activity is not properly defined, problem solving is impeded. It is therefore mandatory to define the situation in its totality. One must also know where an event starts and where it ends. The event must be constantly monitored to keep the problem within check before it gets too complicated or messy. To put all aspects in a nut shell, to solve a problem, one must identify it and then focus on one aspect to address at one time and while doing so, must gather information on potential causes to come to a solution. [3] Applying the solution in the desired area, one must reassess the issue and redress the situation with a revised plan. All the steps mentioned must be recursive until one completes the job. Quick action to any and all problems ensured lesser and controllable deviations. However the potential lacuna of problem solving is jumping to conclusions without thorough analysis. And always it is easier to solve object problems over problems related to people. As the concluding statement, we may point here that there exist so many techniques viz. TPS 8 steps, PDCA, Six Sigma DMAIC, MDF and 8 D model and they all approach the solution in their own ways which maintain congruency among each other. And it is totally the onus of the individual to use these tools and methods efficiently with good efficacy to achieve the best possible results.

REFERENCES

- [1] R. B. Shivagunde, “Project Implementation Strategies, Monitoring And Problem Solving Mechanisms”, pp 4 – 10, TTTI, Bhopal, August, 2000.
- [2] Chapter 6, Decision – Making, page 5, TCT, U.S Department of Homeland Security.
- [3] UM HS 2003, Dr. D. A. Williams and Dr. M. Carey, Pages 1 – 10.
- [4] Dirk Denut, “Problem Solving”, Brady, 2011, pages 8 – 74.
- [5] The 6’C’s of —Decision Making, Full Gospel Businessmen’s Training.
- [6] Managing Organisational Behaviour by Tassi, Ruzzi, Rizz and Carmal, Pitman Publishing Inc., Masschusetts U.S.A.
- [7] Management handbook for Public Administrator by J. Sutherlnd, Van Nosstrand Reinhold Inc, New York.
- [8] Project Management: A learning package by R.K. Mani, and others, Commonwealth Youth Programme Asia Centre, Chandigarh, India.
- [9] Problem Solving Grand Slam: 7 Steps to Master, Summer 2013, ASHESI.
- [10] Hillier and Lieberman, “Introduction to Mathematical Programming”, McGraw Hill, 1990

Study of Broadside Linear Array Antenna with Different Spacing and Number of Elements

Kailash Pati Dutta

Asst. Professor, Department of ECE, Cambridge Institute of Technology, Ranchi, India

Abstract— A uniform linear antenna array has all its elements placed along a straight line with same spacing between them. This paper presents the comparative study of the consequences of different spacing and number of elements in terms of array factor, antenna directivity and half power beam-width (HPBW) for Broadside array. The results were obtained through the antenna parameters algorithm and simulations were done with MATLAB. The algorithm has been designed to operate with random number of elements with specific spacing. Output was studied with 2, 10, 40, 70 and 100 numbers of elements having specific spacing. The particular spacings are 0.1λ , 0.25λ , 0.5λ and 0.75λ . With the increase of number of elements and spacing between them, the directivity and array factor increases.

Keywords— Algorithm, Array factor, linear antenna array, Directivity, Half power beamwidth

I. INTRODUCTION

Among the large variety of arrays of radiating elements, the simplest, type is the uniform linear array. An array is said to be Broadside array if the main beam is perpendicular to the axis of the array. This array is completely specified by the spacing and the phase progression constants [1]. Antenna exhibits a specific radiation pattern. Whenever the several antenna arrays are combined in an array, the overall radiation pattern changes. This is due to the array factor which quantifies the effect of combining the radiating elements. The overall radiation pattern of an array is determined by this array factor combined with the array factor of the antenna element [2].

A uniformly spaced antenna array [3] consisting of number of elements with non-uniform amplitude distribution [4] spaced at a distance d from each other spaced along the x -axis in a horizontal manner. The elements in both cases are placed symmetrically along the x -axis about the origin and the amplitude excitation is also symmetrical about the origin. The topology for linear array is shown in Figure 1.

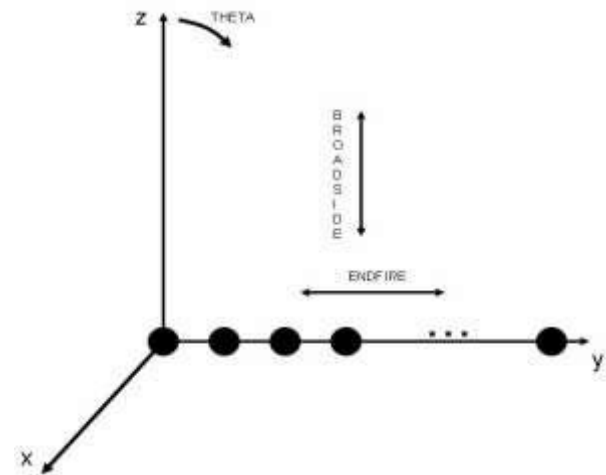


Fig.1. Topology of Linear Array

In a uniform array, the antennas are equi-spaced and are excited with uniform current with constant progressive phase shift (phase shift between adjacent antenna elements) as shown in Figure 2.

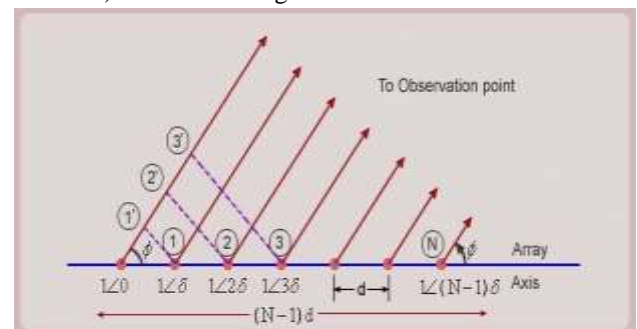


Fig.2. Uniform Antenna Array

II. ARRAY FACTOR AND DIRECTIVITY OF UNIFORM BROADSIDE ANTENNA ARRAY

The ability of an antenna to increase the quality of the performance depends on their parameters such as number of elements, spacing between elements, phase and amplitude excitation [5]. This accordingly changes the HPBW which in turn result in change in other parameters.

Array Factor

The Array Factor (AF) of the uniform array [5, 6] can be obtained by considering the individual elements as point (isotropic) sources. Then, the total field pattern can be obtained by simply multiplying the AF by the normalized

field pattern of the individual element (provided the elements are not coupled). The AF of an N-element linear array of isotropic sources is given by:

$$AF = 1 + e^{j(kd \cos\theta + \beta)} + e^{j2(kd \cos\theta + \beta)} + \dots + e^{j(N-1)(kd \cos\theta + \beta)} \quad (1)$$

The above equation (1) may be written as

$$AF = \sum_{n=1}^N e^{j(n-1)(kd \cos\theta + \beta)},$$

$$AF = \sum_{n=1}^N e^{j(n-1)\Psi}, \quad (2)$$

Where β is the progressive phase lead and $\Psi = kd \cos\theta + \beta$. From above equation, it is obvious that the AFs of uniform linear arrays can be controlled by the relative phase β between the elements. The AF in equation (2) may be expressed in a closed form, which is more convenient for pattern analysis:

$$AF \cdot e^{j\Psi} = \sum_{n=1}^N e^{jn\Psi},$$

$$AF \cdot e^{j\Psi} - AF = e^{jN\Psi} - 1,$$

$$AF = \frac{e^{jN\Psi} - 1}{e^{j\Psi} - 1} = \frac{e^{j\frac{N}{2}\Psi} \left(e^{j\frac{N}{2}\Psi} - e^{-j\frac{N}{2}\Psi} \right)}{e^{j\frac{\Psi}{2}} \left(e^{j\frac{\Psi}{2}} - e^{-j\frac{\Psi}{2}} \right)},$$

$$AF = e^{j\left(\frac{N-1}{2}\right)\Psi} \cdot \frac{\sin(N\Psi/2)}{\sin(\Psi/2)}. \quad (3)$$

Here, N shows the location of the last element with respect to the reference point in steps of the length d. The phase factor, $\exp.[(N-1)\Psi/2]$, is not important unless the array output signal is further combined with the output signal of another antenna. It represents the phase shift of the array's phase centre relative to the origin, and it would be equal to one if the origin were to coincide with the array centre.

B. Directivity

The directivity in case of broadside array [5,6,7] is defined as

$$G_{Dmax} = \frac{\text{Maximum radiation intensity}}{\text{Average radiation intensity}} = \frac{U_{max}}{U_{avg}} = \frac{U_{max}}{U_0}$$

where, U_0 is average radiation intensity which is given by,

$$U_0 = \frac{P_{rad}}{4\pi} = \frac{1}{4\pi} \int_{\phi=0}^{2\pi} \int_{\theta=0}^{\pi} |E(\theta, \phi)|^2 \sin\theta \, d\theta \, d\phi \quad (4)$$

From the expression of ratio of magnitudes we can write,

$$\left| \frac{E_T}{E_0} \right| = n$$

$$|E_T| = n |E_0|$$

or

For the normalized condition let us assume $E_0 = 1$, then

$$|E_T| = n$$

The normalized field pattern is given by

$$E_{Normalized} = \left| \frac{E_T}{E_{Tmax}} \right| = \frac{|E_0|}{n|E_0|} = \frac{1}{n}$$

Hence the field is given by,

$$\therefore E_{Normalized} = \frac{\sin n \frac{\Psi}{2}}{n \left(\sin \frac{\Psi}{2} \right)}$$

On further derivations, we deduce the following

$$U_0 = \frac{1}{2} \int_{-\frac{n}{2}\beta d}^{\frac{n}{2}\beta d} \left[\frac{\sin z}{z} \right]^2 \cdot \frac{dz}{-\frac{n}{2}\beta d}$$

$$\therefore U_0 = -\frac{1}{n\beta d} \int_{\frac{n}{2}\beta d}^{-\frac{n}{2}\beta d} \left[\frac{\sin z}{z} \right]^2 dz \quad (5)$$

For large array, n is large hence $n\beta d$ is also very large.

C. The Half Power Beam Width

For a given array, the HPBW is a function of the direction of the main beam. The HPBW is minimum for a broadside direction [8]. For large arrays, the HPBW is approximately taken as half of the BWFN.

$$\varphi_{BS} = \frac{\lambda}{dN} = \frac{\lambda}{\text{Length of the array}}$$

III. SIMULATION OF N-ELEMENT FOR DIFFERENT SPACING ELEMENTS OF BROADSIDE LINEAR ARRAY ANTENNA

In this section, the simulation method using MATLAB tool has been described where the HPBW and directivity was compared with the increasing number of elements and their spacing. The MATLAB Codes were run in MATLAB version R2015b and presented in tabular form as shown in Table 1.

The simulations started with 2, 10, 40, 70 and 100 elements in linear array with a spacing of $.01\lambda$, 0.25λ , and 0.5λ . The graphical results obtained for the later four are illustrated in Figure 1(a)-4(f).

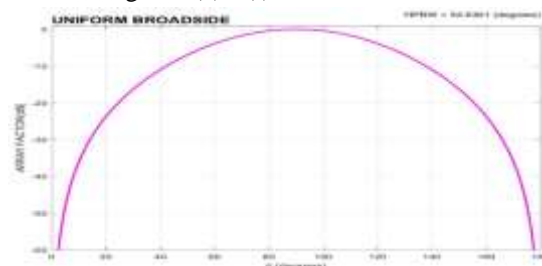


Fig. 1(a): HPBW with 10 elements, 0.1λ spacing

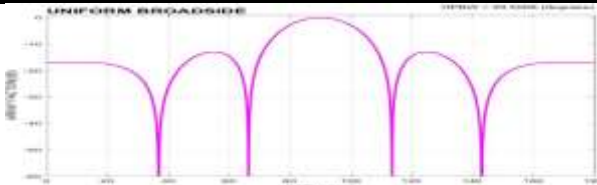


Fig. 1(b): HPBW with 10 elements, 0.25λ spacing

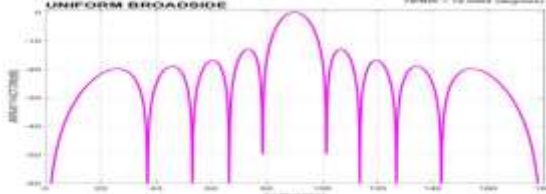


Fig. 1(c): HPBW with 10 elements, 0.5λ spacing

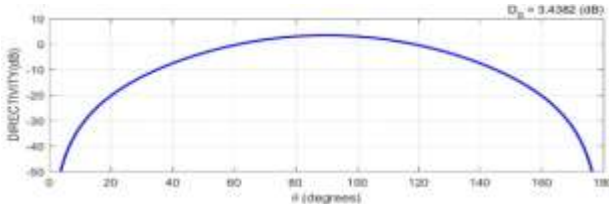


Fig. 1(d): Directivity(dB) with 10 elements, 0.1λ spacing

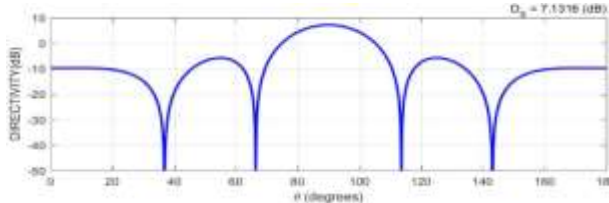


Fig. 1(e): Directivity(dB) with 10 elements, 0.25λ spacing

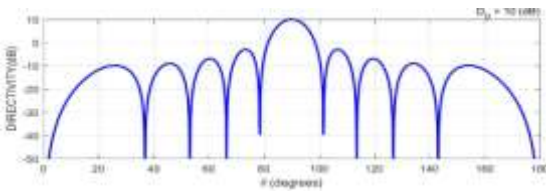


Fig. 1(f): Directivity (dB) with 10 elements, 0.5λ spacing

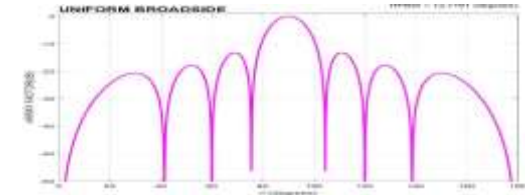


Fig. 2(a): HPBW with 40 elements, 0.1λ spacing

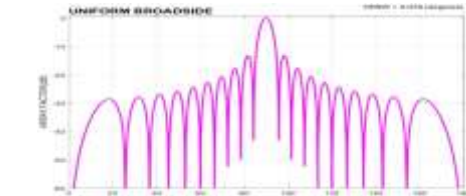


Fig. 2(b): HPBW with 40 elements, 0.25λ spacing

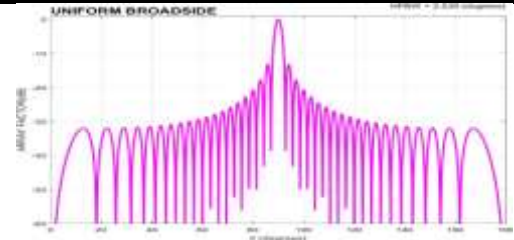


Fig. 2(c): HPBW with 40 elements, 0.5λ spacing

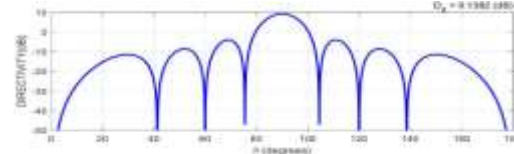


Fig. 2(d): Directivity (dB) with 40 elements, 0.1λ spacing

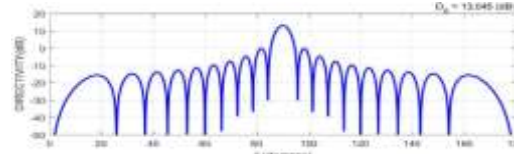


Fig. 2(e): Directivity (dB) with 40 elements, 0.25λ spacing

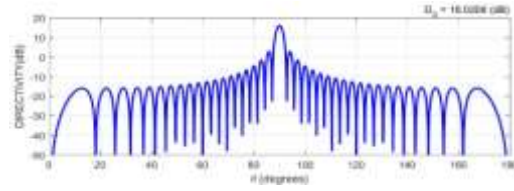


Fig. 2(f): Directivity (dB) with 40 elements, 0.5λ spacing

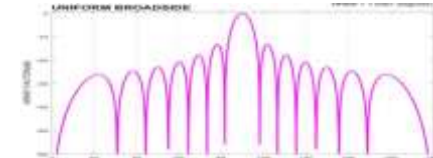


Fig. 3(a): HPBW with 70 elements, 0.1λ spacing

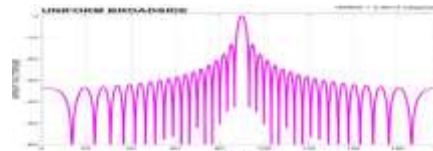


Fig. 3(b): HPBW with 70 elements, 0.25λ spacing

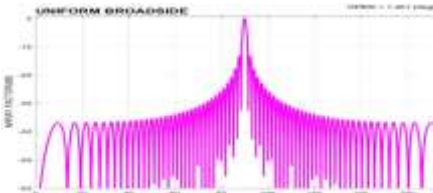


Fig. 3(c): HPBW with 70 elements, 0.5λ spacing

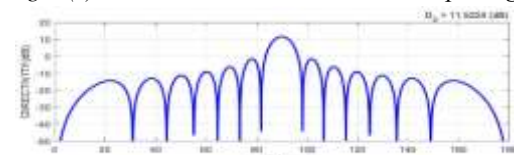


Fig. 3(d): Directivity (dB) with 70 elements, 0.1λ spacing

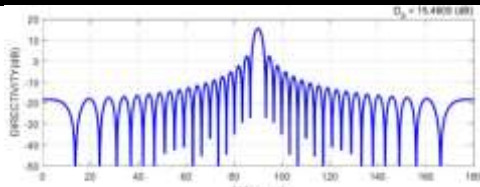


Fig. 3(e): Directivity (dB) with 70 elements, 0.25λ spacing

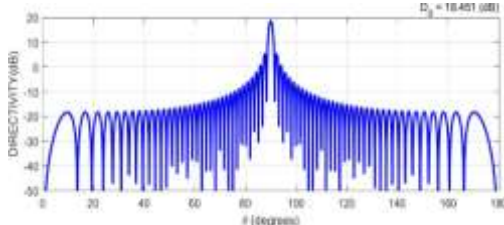


Fig. 3(f): Directivity (dB) with 70 elements, 0.5λ spacing

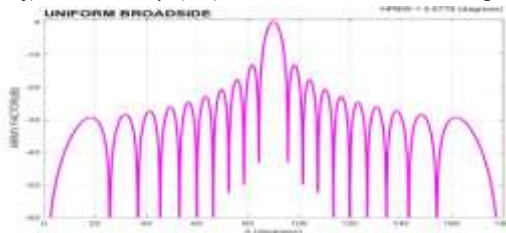


Fig. 4(a): HPBW with 100 elements, 0.1λ spacing

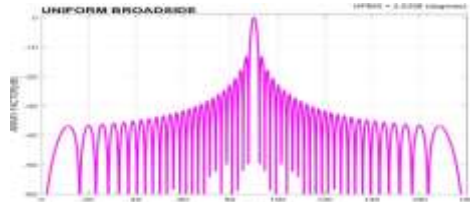


Fig. 4(b): HPBW with 100 elements, 0.25λ spacing

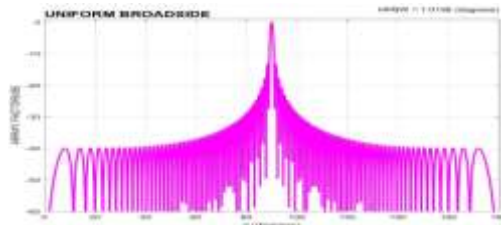


Fig. 4(c): HPBW with 100 elements, 0.5λ spacing

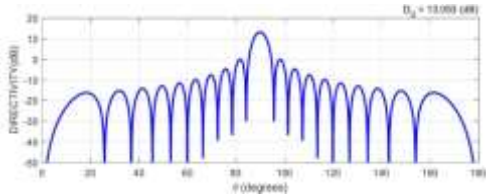


Fig. 4(d): Directivity (dB) with 100 elements, 0.1λ spacing

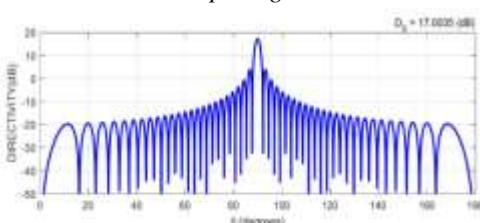


Fig. 4(e): Directivity (dB) with 100 elements, 0.25λ spacing

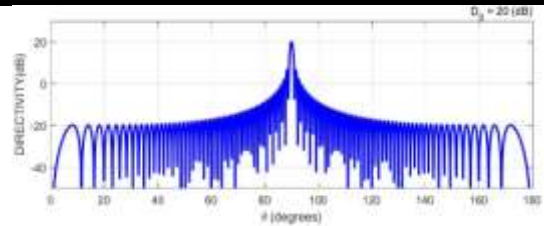


Fig. 4(f): Directivity (dB) with 100 elements, 0.5λ spacing

The above simulations is presented in tabular form in table 1

Table 1: HPBW and Directivity (D, dB) for elements $N = 2, 10, 40, 70$ and 100 at $0.1\lambda, 0.25\lambda$ and 0.5λ spacing elements.

N	0.1λ		0.25λ		0.5λ	
	HPBW	D(dB)	HPBW	D(dB)	HPBW	D(dB)
2	91.83°	0.1424	75.09°	0.878	60.000°	3.010
10	52.83°	3.438	20.50°	7.132	10.209°	10.000
40	12.72°	9.138	5.079°	13.045	2.539°	16.021
70	7.25°	11.522	2.901°	15.460	1.451°	18.451
100	5.008°	13.198	2.031°	17.003	1.015°	20.000

The HPBW is decreasing with the increasing of number of elements with specific Spacing in between them. However, if we carry out the study according to the same number of elements with varying spacing, the HPBW decreases and the Directivity increases with the increment in element spacing. For example When $N=10$ with element spacing of 0.1λ to 0.5λ , the half power beam width goes on decreasing from 52.8° for 0.1λ , 20.50° for 0.25λ and 10.209° for 0.5λ . In this condition, the directivity goes on increasing from 3.4383 dB for 0.1λ to 10 dB for 0.5λ .

IV. FUTURE SCOPE

Better results may be obtained in terms of directivity and HPBW with the application of Evolutionary Algorithms like Genetic Algorithm, Particle Swarm Optimization technique, QPSO technique etc. The performance of the antenna due to larger number of array elements may cause formation of grating and unwanted lobes which may be improved further.

V. CONCLUSION

This paper focuses on the investigations that are carried out with respect to the number of antenna elements used in a broadside linear antenna array for different spacing and number of elements. A thorough examination has

been made with respect to the array factor, HPBW and directivity of the arrays. It has been observed that more the number of elements, better is the directivity. Also, lesser the spacing between antenna elements, more is the HPBW. This paper presents the practical consequences of the number of elements present in the array and their spacing on Directivity and HPBW. These results are directly applicable for planar array of the Broadside Uniform Planar Linear Array.

REFERENCES

- [1] H Bach, "Directivity of Basic Linear Arrays" IEEE Transactions on Antennas And Propagation, pp 108-110, January 1970
- [2] G.J.K. Moernaut and D.Orban, "The Basics of Antenna Arrays", Orban Microwave Products.
- [3] Paul B, Thomas B, Werner Renhart, "Limitations of the pattern multiplication technique for uniformly spaced linear antenna arrays", International Conference on Broadband Communications for Next Generation Networks and Multimedia Applications (CoBCom), Graz, Austria ISBN: 978-1-5090-2270-0, September 14-16, 2016
- [4] Nesteruk S. V. , Protsenko M. B., "Non-uniform amplitude excitation of elements in an antenna array", International Conference on Antenna Theory and Techniques, , Sevastopol, Ukraine pp. 429-431, 21 September, 2007
- [5] C.A. Balanis, Antenna Theory, 3th ed., Canada, A John Wiley & Sons, Inc, 2005
- [6] Nikolova, "Linear Array Theory, Part I-", McMaster University, Hamilton
- [7] Bach, Henning, "Directivity of basic linear arrays", I E E E Transactions on Antennas and Propagation, 1970.
- [8] G. Ram, D. Mandal, R. Kar, and S. P. Ghoshal, "CRPSOWM for linear antenna arrays with improved SLL and directivity," IETE J. Res., Vol. 61, no. 2, pp. 109-20, Mar.-Apr. 2015.

A Review of Aggregate and Asphalt mixture Specific Gravity measurements and their Impacts on Asphalt Mix Design Properties and Mix Acceptance

Esat Gashi, Hajdar Sadiku, Misin Misini

Faculty of Civil Engineering and Architecture, University of Prishtina, Kosovo

Abstract— Stone Mastic Asphalt (SMA) mixtures rely on stone-to-stone contacts among particles to resist applied forces, and permanent deformation. Aggregates in SMA should resist degradation (fracture and abrasion) under high stresses at the contact points. Current practices for asphalt mix design and acceptance testing rely on volumetric properties. Vital to the calculation of mix volumetric properties are specific gravity measurements of the mixture and the aggregate in the mixture. For the Motorways wearing course, SMA stone grid must fulfil the mineralogical-petrographic condition to be on rock of igneous and/or metamorphic origin but of silicate composition, specific weight and LA method on resistance to fragmentation. During the construction of the Kosovo motorway for wearing course was used the SMA as asphalt layer for providing longer lifetime to the road construction. The super-pave mix design for SMA wearing course has been composed considering the available stone with high mineralogical and petrographic composition. The stone used for the wearing course on this motorway has resistance to crushing of LA =18 which is below the standard criteria for heavy traffic roads and motorways wearing courses. The specific weight of used stone was 3100 kg/m³ which is about 15% heavier than standard weight. For this specific stone were prepared special super-pave design mix with binder content 4.5% which was well below than typical SMA composition of 6.0–7.0% binder rather of mixture was 3100 kg/m³.

In this paperwork it is described the design mix of SMA composed with relatively high specific weight and their impacts on asphalt mix design properties used in Kosovo Motorway.

Key words— SMA design mix, stone grid, structural design, bitumen content, quality assurance, quality control.

I. INTRODUCTION

Current practices for asphalt mix design and acceptance testing rely on volumetric properties. Vital to the calculation of mix volumetric properties are specific gravity measurements of the mixture and the aggregate in the mixture. In essence, the specific gravity measurements are conversion factors which allow conversion of mass percentages to volume proportions/percentages. The accuracy and reliability of the specific gravity measurements are therefore fundamental to the business of building quality hot-mix asphalt (HMA) pavements.

By the nature of the materials used for construction, it is impossible to design a road pavement which does not deteriorate in some way with time and traffic, hence the aim of structural design is to limit the level of pavement distress, measured primarily in terms of riding quality, rut depth and cracking, to pre-determined values. Generally these values are set so that a suitable remedial treatment at the end of the design period is a strengthening overlay of some kind but this is not necessarily so and roads can in principle be designed to reach a terminal condition at which major rehabilitation or even complete reconstruction is necessary.

Variability in material properties and construction control is always much greater than desired by the design engineer and must be taken into account explicitly in the design process. Only a very small percentage of the area of the surface of a road needs to show distress for the road to be considered unacceptable by road users.

The purpose of structural design is to limit the stresses induced in the sub grade by traffic to a safe level at which sub grade deformation is insignificant whilst at the same time ensuring that the road pavement layers themselves do not deteriorate to any serious extent within specified period of time. Each new structure initially need to be design and calculated, road structure as well,

There are three main steps to be followed in designing a new road pavement:

1. Estimating the amount of traffic and the cumulative number of equivalent standard axles that will use the road over the selected design life
2. Assessing the strength of the sub-grade soil over which the road to be build
3. Selecting the most economical combination type of pavement, together with the pavement materials and layer thickness that will provide satisfactory service over the design life of the pavement

For Kosovo motorway the Mechanistic-Empirical design method for determination of the layer thicknesses and

pavement structure was used. This method takes in consideration, traffic load analysis, climatic and hydrological conditions and materials. Pavement structure is designed for the predicted traffic load for 20 year period of use, starting from year 2014 until year 2033.

Traffic load analysis

Because this is totally new motorway connecting corridor X with Adriatic Sea the detail traffic studies were carried out prior to start designing the road structure. The highest AADT (Annual average daily traffic) was around the Capitol Prishtina with the following structure table 1:

Table.1: Distribution of vehicles for traffic calculation

Type of vehicles	Car	Minibus	Pick up	Bus	2-Ax Truck	3-Ax Truck	>3-Ax Truck
percentage	74.7%	3.4%	8.5%	1,1%	6.2%	0.8%	5,3%

Traffic load for pavement calculation is expressed in the total number of equivalent 82 kN axleload passage. The average utilization of vehicle bearing capacity of 85% was applied. The calculation of the equivalent traffic load on both directions during the design period (from year 2014 till year 2033) on main route presented, shows the average number of crossings ESOO relevant for pavement structure dimensioning amount to: $2.81 \times 10^7 \times 0,45 = 1.27 \times 10^7$ which bring this motorway to the heavy traffic load facility.

Climatic and hydrological conditions

Kosovo have continental climate condition with warm summers up to 40 Celsius degree and cold winters up to -25 Celsius degree. Hot and cold periods lasts up to 1 month during the July August respectively cold during January February. The freezing depth is taken 50-70 cm.

Material Quality

The third factor considered in defining the thickness of pavement structure are materials selected for the construction of each individual pavement structure layer. This is particularly important in designing of roads characterized by heavy and very heavy traffic loads and successful selection depends on the knowledge of deterioration mechanisms of each individual material type. The quality of materials for construction of the selected pavement structure layers has to comply with the applicable factors of equivalent resistance to material deterioration under dynamic impact of traffic.

Applicable values of basic materials equivalency selected for this structural designing are presented in table 2.

Table.2: Material equivalency factor

Material type	Equivalency factor a_i
Asphalt concrete AC and Stone Mastic Asphalt SMA – wearing layers	$a_1=0.42$
Binder layer + bituminized bearing layer	$a_2=0.35$
Cement Stabilized mixture of stone grains	$a_3=0.20$
Unbound stone material	$a_4=0.14$

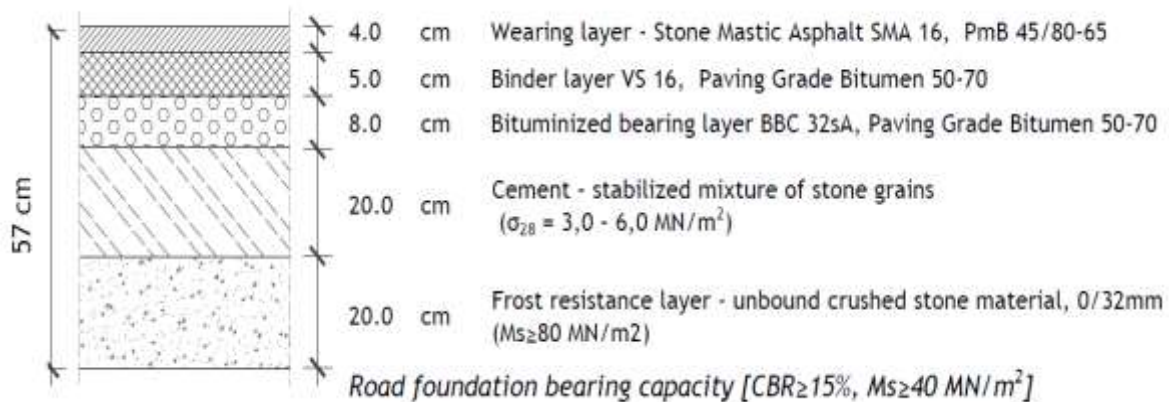
Selected pavement structure

The adequate thickness of pavement structure was calculated based on the above-mentioned input data and taking in consideration the traffic load. From the calculated traffic load, climatic and hydrological conditions, material in disposal and soil bearing capacity pavement structure type 3 was selected.

Pavement structure 3 is composed by wearing course from Stone Mastic Asphalt (SMA 16)- thickness 40 mm,

binderlayer from of VS 16 - thickness 50 mm, bearing layer from bituminized bearing layer (BBC 32s A) -thickness 80 mm, base layers from cement stabilized layer (CS) - thickness 200 mm and loose crushed stone material (LCSM) -thickness 200 mm. This structure is adequate for the traffic stated above taking considering the average annual traffic grow 4% and for design period 2014 – 2033. The pavement structure is presented at figure 1.

Fig.1: Pavement structure layers



Stone Mastic Asphalt Mixes

Stone Mastic Asphalt is a high stiffness, high macro texture bituminous mixture suitable for use in high demand and/or high speed areas. The high macrotexture compared with asphaltic concrete allows good surface drainage hence reducing the risk of aquaplaning, and also reduces traffic noise compared with chip seals or asphaltic concrete. International evidence has shown that Stone Mastic Asphalt resists the reflection of cracks in underlying layers as well. The process of designing a SMA mixture involves adjusting the grading to accommodate the required binder and void content rather than the more familiar process of adjusting the binder content to suit the aggregate grading.

Commonly used additives are fibres, such as cellulose fibres. Mastic is the mortar comprised of fines, filler, binder and stabilising additive, and may be modified with polymers to improve its rheological properties. The composition of the mastic mortar is a crucial factor contributing to the performance of Stone Mastic Asphalt. Bituminous binder shall be 60/70 penetration grade bitumen. Sufficient stabilising additives shall be added to the Stone Mastic Asphalt to ensure binder drainage does not occur during storage, transportation and construction. The

design process for Stone Mastic Asphalt involves adjusting the grading to accommodate the required binder content (minimum of 6% to 7% depending on maximum aggregate particle size) and voids content rather than the traditional design process for other asphalt mixes, of adjusting the binder content to suit an aggregate gradation. Only crushed aggregates are specified for the Stone Mastic Asphalt to ensure suitable aggregate interlock. The use of natural aggregates containing polished or rounded particles, such as sand, is not permitted.

Stone

The use of certain types of stone in the pavement structure asphalt courses depends on the mineralogical and petrographic composition, the physical and mechanical properties and the granular stone materials production technology.

Quality requirements

Stone quality as raw material for production of granular stone material must fulfill the conditions in order to be used for the asphalt pavements, some of the criterias are shown at the Table 3.

Table.3: Criteria for stone grid

Property	Quality of physical and mechanical properties of crushed stone grid		
	K- I	K- II	K- III
Mineralogical –petrographic division	Igneous group	Igneous and carbonate group	Carbonate group
Compressive strength in dry state, minimum Mpa	160	140	120
Resistance to wear by sanding, maximum $\text{cm}^3/50 \text{ cm}^2$	12	18	22
Water absorption, maximum, % (m/m)	0.75	0.75	1.0
Resistance to frost	Resistant	Resistant	Resistant
Resistance to crushing (Los Angeles) maximum % (m/m)	16	18	22

II. ASPHALT MIX DESIGN PROPERTIES

Due to the fact that close to the Motorway site it was not available stone quarry with stone resistance to crushing LA < 16 as it is requested by the EN standard for stones, it was taken in consideration to design a new asphalt mix using the stone granular from the quarry close to the Motorway (MIM Golesh quarry) with following to major characteristics:

Stone resistance factor to crushing $LA = 18$ Density of stone material mix $\rho_{\text{smm}} = 3100 \text{ kg/m}^3$

The new super pave asphalt design mix was prepared for wearing course from stone mastic asphalt with this stone with maximum (nominal) particle size of 16 mm (SMA 16 mm). For new asphalt design mix were prepared 6 samples for initial job mix formula according to standard procedures.

Table.4: Composition of designed mixtures of stone material fractions.

	AM1	AM2	AM3	AM4	AM5	AM6
Relation P(KB)/P(FKM)	2,4	2,4	2,4	2,9	3,7	5
Percentage of filler in KM [%m/m]	6,5	6,5	6,5	7,0	8,4	10,0
Extracted filler from SKM [%m/m]	0,3	0,3	0,3	5,9	4,7	9,3
Coefficient for RF	5,05	5,05	5,05	5,73	7,27	9,17
Coefficient for 0/4	21,90	21,90	21,90	21,68	21,34	20,85
Coefficient for 4/8	16,11	16,11	16,11	16,01	15,74	15,43
Coefficient for 8/11	15,53	15,53	15,53	15,43	15,17	14,87
Coefficient for 11/16	41,41	41,41	41,41	41,16	40,47	39,68

Table.5: Composition and properties of designed asphalt mixtures.

	AM1	AM2	AM3	AM4	AM5	AM6
Density of mixture FKM [t/m^3]	3,070	3,070	3,070	3,067	3,061	3,054
Density AM [t/m^3]	2,829	2,863	2,881	2,816	2,818	2,820
Percentage of bitumen content in AM [% (m/m)]	4,12	3,49	3,18	4,33	4,20	4,04

Bitumen density: The density of bitumen used for preparation of asphalt mixtures and test specimen made according to Marshall Method (EN 15326), Pycnometer Method $\rho_B = 100,1 \text{ kg/m}^3$. Bitumen type is PmB 45/80 – 65 (Ex – Fis), and the bitumen content in asphalt mix design is 4.5 %.

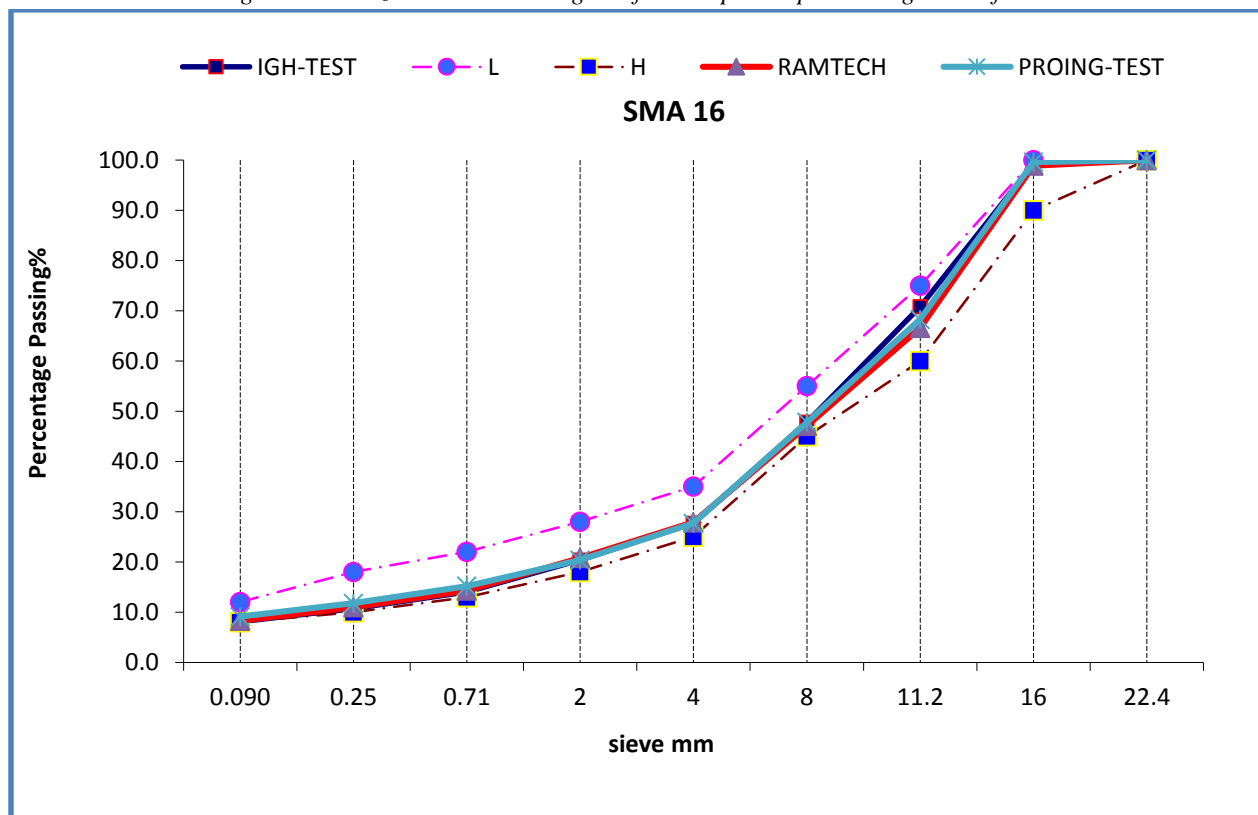
Additives: used at the design mix were: Fibres ,, Arbocel ZZ 8/1 with share in design mix 0.4 % and ,,Interflow – T’’ as chemical additive with share id design mix 0.6%.

The final mix design for wearing course of highway with stone mastic asphalt of stone material with maximum (nominal) particle size of 16 mm (SMA 16 mm) was accepted with following distribution See table 6.

Table.6: New asphalt mix design for wearing course type: split mastic asphalt

ASPHALT MIX DESIGN			
Stone material	Aggregate fraction	Share in mix [% (m/m)]	Density [kg/m ³]
Cement	Filler	6.7	3000
MimGolesh	0-4	21.6	3108
MimGolesh	4-8	16.7	3107
MimGolesh	8-11	18.5	3096
MimGolesh	11-16	36.5	3120
Density of stone material [t/m ³]			3105
Type of bitumen			PmB 45/80-65
Density of bitumen [t/m ³]			1,012
Bitumen content in AM design			4.5%
Additive ; Fibres ,, Arbocel ZZ 8/1			0.4%
,,Interflow – T''			0.6%

Fig.2: Grain size distribution diagram for accepted asphalt design mix of SMA



III. TESTING OF ASPHALT MIX DESIGN AND RESULTS OBTAINED

A trial section was prepared in order to test the new asphalt mix design in order to check workability of new mix design with length of 300 m. The following tests were performed during the trial test:

- ✓ Asphalt mixture temperature during loading into the finisher from every delivery,
- ✓ Composition and the physical and mechanical properties of asphalt mixture on at least three samples
- ✓ Change in the rate of compaction of the asphalt layer by non-destructive method during placing and on cooled asphalt layer at six points minimum,

- ✓ Rate of compaction, percentage of voids, thickness of executed layer and the adhesive binder strength with the base, on at least three original samples,
- ✓ Evenness of each traffic lane in the full trial section length,
- ✓ Skid resistance (for wearing layers) on at least three points, and Results are presented at the table 7

Table.7: Physical-mechanical properties an laboratory testing results for asphalt mixture Stone Mastic asphalt SMA

No.	Technical characteristics		Test standard	Laboratory Results	Quality conditions	Category EN 13108
1(a)	Void content, Vmax	[%]	EN 12697-8	4.5	3 - 6	Vmax6 Vmin3
2(a)	Voids filled with bitumen, VFB max	[%]		73.8	71 - 83	VFBmax83
3(a)	Voids filled with bitumen, VFB min	[%]				VFBmin71
4(b)	Drained material, D	[%]	EN 12697-18	0.11	≤0,6	D0,6
5(c)	Indirect tensile strength ratio, ITSR [%]		EN 12697-12 EN 12697-23	86.93	≥ 80	ITSR80
6(d)	Wheel tracking slope, WTSAIR	[%]	EN 12697-22	0.038	≤ 0.07	WTSAIR 0.07
7(d)	Proportional rut depth, PRDAIR	[%]		4.63	≤ 5.0 [%]	PRDAIR5.0
8(e)	Stiffness	[MPa]	EN 12697-26	4022	3600 - 7000	Smin3600
9	Bulk Density	[kg/m ³]	EN 12697-6	2702	-	-
10	Maximum Bulk Density	[kg/m ³]	EN 12697-5	2828	-	-
11	Degree of compaction, min.	[%]	EN	98	98	Min 98
12	Stability	[kN]	EN 12697-34	8.8	-	-
13	Deformation	[mm]		3.9	-	-
14	S/D	[kN/mm]		2.3	-	-
15	Bitumen cont. in AM	[%]	EN 15326	4.5	6-7%	-

Results from trial section proofed that the super pave asphalt design mix for the wearing course from stone mastic asphalt full fill conditions for using stone from MiMGolesh quarry for producing the SMA.

So far 60 km of dual motorway carriageway are paved with this stone and the results followed up by QC satisfy conditions set up by EN standards for this material.

IV. CONCLUSION

- Stone quality as raw material for production of granular stone material must fullfill the conditions standards or general technical requirements –GTR in order to be used for the asphalt pavements.

- Sometimes can be considered stone for producing the granular material with the higher resistance on fragmentation and higher specific weight than standard or GTR specify.
- Superpave design mix with stone granular material with higher spetic weight than optimum stones requires less bitumen in the design mix.
- Designer who prepare the super pave design mix need to consider parallel testing of the new design mix with the design mix which was used on previous project as reference and proofed that it was adequate design mix.
- In our case by parallel testing of reference aggregate it was found that this aggregate has similar resistance to degradation which is measured by compaction of

marshal sample, despite the fact LA coefficient was found to be $La=13\%$.

- SMA design mix used in Kosovo motorway requires less energy for the compaction than reference design mix,
- Higher specific weight of stone increase the total volumetric weight.
- With increase of weight with specific percentage the contractor must decrease the unit price for that percentage because the asphalt wearing course mass is same for two different stone materials even the specific weights change.

REFERENCES

- [1] AASHTO *Guide for Design of Pavement Structures* 1993,
- [2] *Hot – Mix Asphalt paving Handbook 2000*, US Army Corps of Engineers,
- [3] Druschner, L; Schafer, V; „*Stone Mastic Asphalt*” German Asphalt Associations – English Version 2005,
- [4] Ramljak, Z;Pejnovic,V; „*Possibilities for using the carbonate stone material for binder courses on asphalt pavement of all traffic loading categories*”, Construction Almanac, Union of Construction Engineers and technicians of Yugoslavia, Belgrade (1983), pages 337-340.
- [5] Test Report No MD (BEGP – KMP) -08-03/2011, (WC – SMA 16), Ramtech October 2011, Zagreb,
- [6] Test Report No 61054-20-2739/11 Resistance to degradation of crushed rock aggregate from MiMGolesh by compaction of Marshall Sample, Zagreb October 2011,
- [7] General Technical requirement for Motorway Construction , Zagreb 2011,
- [8] EN 12697-1;2005 Bituminous mixtures – Test method for hot mix asphalt, Binder content
- [9] EN 12697-2;2002 Bituminous mixtures – Test method for hot mix asphalt, Determination of particle size distribution ,
- [10] EN 12697-30;2004 +A1;2007 Bituminous mixtures – Test method for hot mix asphalt, Specimen preparation by impact factor.

Super complete-antimagicness of Amalgamation of any Graph

R.M Prihandini^{1,3}, Ika Hesti Agustin^{1,4}, Dafik^{1,2}, Ridho Alfarisi^{1,3}

¹ CGANT-University of Jember, Jember, Indonesia

² Department of Mathematics Education, University of Jember, Jember, Indonesia

³ Department of Elementary School Teacher Education, University of Jember, Jember, Indonesia

⁴ Department of Mathematics, University of Jember, Jember, Indonesia

Abstract—Let H_i be a finite collection of simple, nontrivial and undirected graphs and let each H_i have a fixed vertex v_j called a terminal. The amalgamation H_i as v_j as a terminal is formed by taking all the H_i 's and identifying their terminal. When H_i are all isomorphic graphs, for any positive integer n we denote such amalgamation by $G = Amal(H, v, n)$, where n denotes the number of copies of H . The graph G is said to be an $(a, d) - H$ -antimagic total graph if there exist a bijective function $f: V(G) \cup E(G) \rightarrow \{1, 2, \dots, |V(G)| + |E(G)|\}$ such that for all subgraphs isomorphic to H , the total H -weights $W(H) = \sum_{v \in V(H)} f(v) + \sum_{e \in E(H)} f(e)$ form an arithmetic sequence $\{a, a + d, a + 2d, \dots, a + (n - 1)d\}$, where a and d are positive integers and n is the number of all subgraphs isomorphic to H . An $(a, d) - H$ -antimagic total labeling f is called super if the smallest labels appear in the vertices. In this paper, we study a super $(a, d) - H$ antimagic total labeling of $G = Amal(H, v, n)$ and its disjoint union.

Keywords—Super H -antimagic total graph, Amalgamation of graph, arithmetic sequence.

I. INTRODUCTION

A graph G is said to be an $(a, d) - H$ -antimagic total graph if there exist a bijective function $f: V(G) \cup E(G) \rightarrow \{1, 2, \dots, |V(G)| + |E(G)|\}$ such that for all subgraphs of G isomorphic to H , the total H -weights $w(H) = \sum_{v \in V(H)} f(v) + \sum_{e \in E(H)} f(e)$ form an arithmetic sequence $\{a, a + d, a + 2d, \dots, a + (n - 1)d\}$, where a and d are positive integers and n is the number of all subgraphs of G isomorphic to H . If such a function exist then f is called an $(a, d) - H$ -antimagic total labeling of G . An $(a, d) - H$ -antimagic total labeling f is called super if $f: V(G) \rightarrow \{1, 2, \dots, |V(G)|\}$.

There many articles have been published in many journals, some of them can be cited in [2, 3, 7, 8] and [9, 10, 11, 12, 13]. For connected graph, Inayah *et al.* in [7] proved that, for H is a non-trivial connected graph and $k \geq 2$ is an integer, $shack(H, v, k)$ which contains exactly k subgraphs isomorphic to H is H -super antimagic. They

only covered a connected version of shackle of graph when a vertex as a connector, and their paper did not cover all feasible d . Our paper attempt to solve a super $(a, d) - H$ antimagic total labeling of $G = Amal(H, v, n)$ and its disjoint union when H is a complete graph for feasible d . To show those existence, we will use a special technique, namely an integer set partition technique. We consider the partition $P_{m,d}^{n,s}(i, j)$ of the set $\{1, 2, \dots, mn\}$ into n columns with $n \geq 2$, m -rows such that the difference between the sum of the numbers in the $(j + 1)$ th m -rows and the sum of the numbers in the j th m -rows is always equal to the constant d , where $j = 1, 2, \dots, n - 1$. The partition $P_{m,d}^{n,s}(i, j, k)$ of the set $\{1, 2, \dots, mns\}$ into ns columns with $n, s \geq 2$, m -rows such that the difference between the sum of the numbers in the $(k + 1)$ th m -rows and the sum of the numbers in the k th m -rows is always equal to the constant d for $j = 1, 2, \dots, n$, where $k = 1, 2, \dots, k - 1$. Thus these sums form an arithmetic sequence with the difference d . We need to establish some lemmas related to the partition $P_{m,d}^n(i, j)$ and $P_{m,d}^{n,s}(i, j, k)$. These lemmas are useful to develop the super $(a, d) - H$ antimagic total labeling of $G = Amal(H, v, n)$ and $G = sAmal(H, v, n)$.

II. SOME USEFUL LEMMAS

Let G be an amalgamation of any graph H , denoted by $G = Amal(H, v, n)$. The graph G is a connected graph with $|V(G)| = p_G$, $|E(G)| = q_G$, $|V(H)| = p_H$, and $|E(H)| = q_H$. The vertex set and edge set of the graph $G = Amal(H, v, n)$ can be split into following sets: $V(G) = \{A\} \cup \{x_{ij}; 1 \leq i \leq p_H - 1, 1 \leq j \leq n\}$ and $E(G) = \{e_{lj}; 1 \leq l \leq q_H, 1 \leq j \leq n\}$. Let n, m be positive integers with $n \geq 2$ and $m \geq 3$. Thus $|V(G)| = p_G = n(p_H - 1) + 1$ and $|E(G)| = q_G = nq_H$. Furthermore, let G be a disjoint union of amalgamation of graph H , denoted by $G = sAmal(H, v, n)$ and s be an odd positive integer. The graph G is a disconnected graph with $|V(G)| = p_G$, $|E(G)| = q_G$, $|V(H)| = p_H$, and $|E(H)| = q_H$. The vertex set and edge set of the graph $G =$

$sAmal(H, v, n)$ can be split into following sets: $V(G) = \{A^k; 1 \leq k \leq s\} \cup \{x_{ij}^k; 1 \leq i \leq p_H - 1, 1 \leq j \leq n, 1 \leq k \leq s\}$ and $E(G) = \{e_{ij}^k; 1 \leq j \leq n, 1 \leq l \leq q_H, 1 \leq k \leq s\}$. Let n, m , and odd s be positive integers with $n \geq 2$ and $m, s \geq 3$. Thus $|V(G)| = p_G = s(n(p_H - 1) + 1)$ and $|E(G)| = q_G = snq_H$.

The upper bound of feasible d for $G = Amal(H, v, n)$ and $G = sAmal(H, v, n)$ to be a super $(a, d) - H$ -antimagic total labeling follows the following lemma [2].

Lemma 2.1 [2]

Let G be a simple graph of order p and size q . If G is super $(a, d) - H$ -antimagic total labeling then $d \leq \frac{\{(p(G)-p(H))p(H)+(q(G)-q(H))q(H)\}}{n-1}$, for $p_{\{G\}} = |V(G)|, q_{\{G\}} = |E(G)|, p_{\{H\}} = |V(H)|, q_{\{H\}} = |E(H)|$, and $n = |H_j|$.

Corollary 2.1

For $n \geq 2$, if the graph $G = Amal(H, v, n)$ admits super $(a, d) - H$ -antimagic total labeling then $d \leq p_H^2 + q_H^2 - p_H$

Corollary 2.2

For $n \geq 2$ and odd $s \geq 3$, if the disconnected graph $G = sAmal(H, v, n)$ admits super $(a, d) - H$ -antimagic total labeling then $d \leq p_H^2 + q_H^2 - p_H + \frac{\{(s-1)p_H\}}{sn-1}$

We recall a partition $P_{\{m,d\}}^n(i, j)$ introduced in [4]. We will use the partition for a linear combination in developing a bijection of vertex and edge label of the main theorem.

Lemma 2.2[4]

Let n and m be positive integers. The sum of $P_{\{m,d\}}^n(i, j) = \{(i-1)n + j, 1 \leq i \leq m\}$ and $P_{\{m,d\}}^n(i, j) = \{(j-1)m + i; 1 \leq i \leq m\}$ form an arithmetic sequence of difference $d \in \{m, m^2\}$, respectively.

III. THE RESULTS

The Connected Graph

The following four lemmas are useful for the existence of super $(a, d) - H$ antimagic total labeling $G = Amal(H, v, n)$.

Lemma 3.1

Let n and m be positive integers. For $1 \leq j \leq n$, the sum of $P_{\{m,d_1\}}^n(i, j) = \{1 + ni - j; 1 \leq i \leq m\}$ and $P_{\{m,d_2\}}^n(i, j) = \{mn + i - mj; 1 \leq i \leq m\}$ form an arithmetic sequence of differences $d_1 = -m, d_2 = -m^2$.

Proof.

By simple calculation, for $j = 1, 2, \dots, n$, it gives $\sum_{i=1}^m P_{\{m,d_1\}}^n(i, j) = P_{\{m,d_1\}}^n(j) \leftrightarrow P_{\{m,d_1\}}^n(j) = \{\frac{n}{2}(m^2 + m) + m - mj\} \leftrightarrow P_{\{m,d_1\}}^n(j) = \{\frac{n}{2}(m^2 + m), \frac{n}{2}(m^2 + m) - m, \frac{n}{2}(m^2 + m) - 2m, \dots, \frac{n}{2}(m^2 + m)m - mn\}$ and $\sum_{i=1}^m P_{\{m,d_2\}}^n(i, j) \leftrightarrow P_{\{m,d_2\}}^n(j) \leftrightarrow P_{\{m,d_2\}}^n(j) = \{\frac{m}{2}(2mn + m + 1) - m^2j\} \leftrightarrow$

$P_{\{m,d_2\}}^n(j) = \{\frac{m}{2}(2mn + m + 1) - m^2, \frac{m}{2}(2mn + m + 1) - 2m^2, \dots, \frac{m}{2}(2mn + m + 1) - m^2n\}$. It is easy to see that the differences of those sequences are $d_1 = -m, d_2 = -m^2$. It concludes the proof. ■

Lemma 3.2

Let n and m be positive integers. For $1 \leq j \leq n$, the sum of

$$P_{\{m,d_3\}}^n(i, j) = \begin{cases} i + (j-1)m; & 1 \leq i \leq m; i \text{ odd} \\ n(i-2) + 2j; & 1 \leq i \leq m; i \text{ even} \end{cases}$$

form an arithmetic sequence of difference $d_3 = \frac{1}{2}m^2 + m$.

Proof.

By simple calculation, it gives $\sum_{i=1}^m P_{\{m,d_3\}}^n(i, j) = P_{\{m,d_3\}}^n(j) \leftrightarrow P_{\{m,d_3\}}^n(j) = \{(\frac{m^2}{2} + m)j + \frac{m}{4}(mn - 2n - m)\} \leftrightarrow P_{\{m,d_3\}}^n(j) = \{(\frac{m^2}{2} + m) + \frac{m}{4}(mn - 2n - m), (\frac{m^2}{2} + m) + \frac{m}{4}(mn - 2n - m), \dots, (\frac{m^2}{2} + m)n + \frac{m}{4}(mn - 2n - m)\}$. It concludes the proof. ■

Lemma 3.3

Let n and m be positive integers. For $1 \leq j \leq n$, the sum of

$$P_{\{m,d_4\}}^n(i, j) = \begin{cases} mn - mj + i; & 1 \leq i \leq m; i \text{ odd} \\ ni + 2 - 2j; & 1 \leq i \leq m; i \text{ even} \end{cases}$$

form an arithmetic sequence of difference $d_4 = -(\frac{1}{2}m^2 + m)$.

Proof.

By simple calculation, it gives $\sum_{i=1}^m P_{\{m,d_4\}}^n(i, j) = P_{\{m,d_4\}}^n(j) \leftrightarrow P_{\{m,d_4\}}^n(j) = \{\frac{m}{4}(3mn + m + 2n + 4) - (\frac{m^2}{2} + m)\} \leftrightarrow P_{\{m,d_4\}}^n(j) = \{\frac{m}{4}(3mn + m + 2n + 4) - \frac{m^2}{2} - m, (\frac{m}{4}(3mn + m + 2n + 4) - m^2 - 2m), \dots, \frac{m}{4}(3mn + m + 2n + 4) - \frac{3m^2}{2} - 3m\}$. We have the desired difference. ■

Now we are ready to present the main theorem related to the existence of super $(a, d) - H$ antimagicness of the connected graph $G = Amal(H, v, n)$, in the following theorem.

Theorem 3.1

For $n \geq 2$, the graph $G = Amal(H, v, n)$ admits a super $(a, d) - H$ antimagic total labeling with feasible $d = m_1 - m_2 + m_3^2 - m_4^2 + \frac{1}{2}m_5^2 + m_5 - (\frac{1}{2}m_6^2 + m_6) + r_1 - r_2 + r_3^2 - r_4^2 + (\frac{1}{2}r_5^2 + r_5) - (\frac{1}{2}r_6^2 + r_6)$

Proof.

Let m and r be positive integers, with $m = p_H - 1$ and $r = q_H$. For $i = 1, 2, \dots, m$ and $j = 1, 2, \dots, n$, by Lemma 2.2, 3.1, 3.2 and 3.3 we define the vertex and the edge labels as a linear combination of $P_{\{m_1, m_1\}}^n(i, j); P_{\{m_2, -m_2\}}^n(i, j); P_{\{m_2, -m_2\}}^n(i, j); P_{\{m_3, m_3^2\}}^n(i, j);$

$$P_{\{m_4, -m_4\}}^n(i, j); P_{\{m_5, \frac{1}{2}m_5 + m_5\}}^n(i, j);$$

and $P_{\{m_6, -(\frac{1}{2}m_6 + m_6)\}}^n(i, j)$ as follows:

$$f_{-1}(A) = 1, \text{ and}$$

$$f_1(x_{\{i,j\}}) = \{P_{\{m_1, m_1\}}^n \oplus 1\} \cup \{P_{\{m_2, -m_2\}}^n \oplus [n(m_1) + 1]\} \\ \cup \{P_{\{m_3, m_3\}}^n \oplus [n(m_1 + m_2) + 1]\} \\ \cup \{P_{\{m_4, -m_4\}}^n \oplus [n(m_1 + m_2 + m_3) + 1]\} \\ \cup \{P_{\{m_5, \frac{1}{2}m_5 + m_5\}}^n \oplus [n \sum_{t=1}^4 m_t + 1]\} \\ \cup \{P_{\{m_6, -(\frac{1}{2}m_6 + m_6)\}}^n \oplus [n \sum_{t=1}^5 m_t + 1]\}$$

$$f_1(e_{\{l,j\}}) = \{P_{\{r_1, r_1\}}^n \oplus [mn + 1]\} \\ \cup \{P_{\{r_2, -r_2\}}^n \oplus [n(r_1) + mn + 1]\} \\ \cup \{P_{\{r_3, r_3\}}^n \oplus [n(r_1 + r_2) + mn + 1]\} \\ \cup \{P_{\{r_4, -r_4\}}^n \oplus [n(r_1 + r_2 + r_3) + mn + 1]\} \\ \cup \{P_{\{r_5, \frac{1}{2}r_5 + r_5\}}^n \oplus [n \sum_{t=1}^4 r_t + mn + 1]\} \\ \cup \{P_{\{r_6, -(\frac{1}{2}r_6 + r_6)\}}^n \oplus [n \sum_{t=1}^5 r_t + mn + 1]\}$$

The vertex labeling f is a bijective function: $V(G) \cup E(G) \rightarrow \{1, 2, \dots, p_G + q_G\}$. The total edge-weights of $G = Amal(H, v, n)$ under the labeling f , for $j = 1, 2, \dots, n$, constitute the following sets:

$$W_{\{f_1\}} = \sum f_1(A) + \sum f_1(x_{\{i,j\}}) + \sum f_1(e_{\{l,j\}}) \\ = C_{\{m,d\}}^n + [m_1 - m_2 + m_3^2 - m_4^2 + \frac{1}{2}m_5^2 + m_5 \\ - (\frac{1}{2}m_6^2 + m_6) + r_1 - r_2 + r_3^2 - r_4^2 + (\frac{1}{2}r_5^2 + r_5)]$$

It is easy that the set of total edge-weights $W_{\{f_1\}}$ consists of an arithmetic sequence of the smallest value a and the difference $d = m_1 - m_2 + m_3^2 - m_4^2 + \frac{1}{2}m_5^2 + m_5 - (\frac{1}{2}m_6^2 + m_6) + r_1 - r_2 + r_3^2 - r_4^2 + (\frac{1}{2}r_5^2 + r_5) - (\frac{1}{2}r_6^2 + r_6)$. Since the biggest d is attained when $d = m^2 + r^2$ then, for $m = p_H - 1$ and $r = q_H$, it gives $0 \leq d \leq p_H^2 + q_H^2 - p_H \leftrightarrow 0 \leq (p_H - 1)^2 + q_H^2 \leq p_H^2 + q_H^2 - p_H \leftrightarrow 0 \leq p_H^2 + q_H^2 - p_H - (p_H - 1) \leq p_H^2 + q_H^2 - p_H$. It concludes the proof. ■

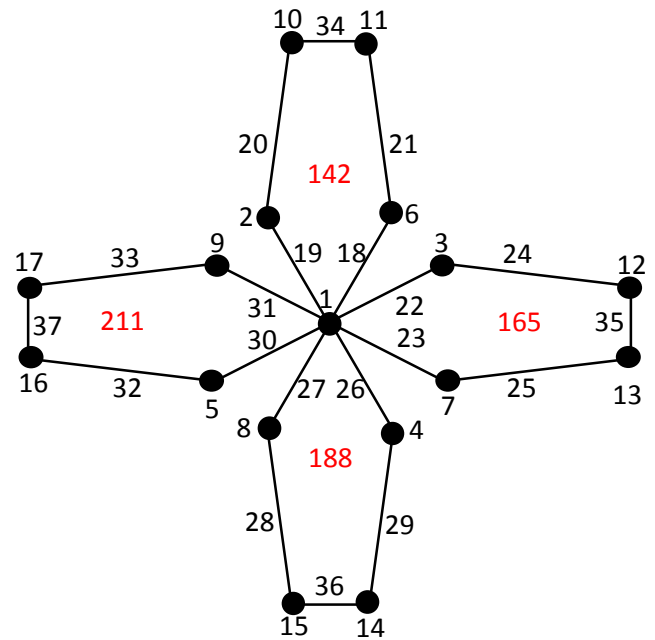


Fig.1: Super (142,23)-H- antimagic total covering of graph $G=Amal(C_5, v, 4)$

The Disjoint Union Graph

The following lemmas are useful for the existence of super $(a, d) - H$ antimagic total labeling disjoint union of the graph G , denoted by $G = sAmal(H, v, n)$.

Lemma 3.5

Let n, m and s be positive integers $1 \leq j \leq n; 1 \leq k \leq s$, the sum of $P_{\{m, d_7\}}^{\{n, s\}}(i, j, k) = \{(k - 1)m + i + (j - 1)ms; 1 \leq i \leq m; 1 \leq j \leq n; 3 \leq k \leq s\}$ and the sum of $P_{\{m, d_8\}}^{\{n, s\}}(i, j, k) = \{(j - 1)s + i + k + (i - 1)ns; 1 \leq i \leq m\}$ form an arithmetic sequence of differences $d_5 = m^2$ and $d_6 = m$.

Proof.

By simple calculation, for $j = 1, 2, \dots, n$,

$$\text{it gives } \sum_{i=1}^m P_{\{m, d_5\}}^{\{n, s\}}(j, k) = P_{\{m, d_5\}}^{\{n, s\}}(k) \leftrightarrow P_{\{m, d_5\}}^{\{n, s\}}(j, k) = \left\{ \frac{1}{2}(m - m^2) + m^2k + m^2s(j - 1) \right\} \leftrightarrow P_{\{m, d_5\}}^{\{n, s\}}(j, k) = \left\{ \frac{1}{2}(m - m^2) + m^2, \frac{1}{2}(m - m^2) + 2m^2, \dots, \frac{1}{2}(m - m^2) + sm^2, \frac{1}{2}(m - m^2) + (s + 1)m^2, \frac{1}{2}(m - m^2) + (s + 2)m^2, \dots, \frac{1}{2}(m - m^2) + snm^2 \right\}.$$

$$\text{Furthermore } \sum_{i=1}^m P_{\{m, d_6\}}^{\{n, s\}}(j, k) = P_{\{m, d_6\}}^{\{n, s\}}(k) \leftrightarrow P_{\{m, d_6\}}^{\{n, s\}}(j, k) = \left\{ \frac{ns}{2}(m^2 - m) + m((j - 1)s + k) \right\} \leftrightarrow P_{\{m, d_6\}}^{\{n, s\}}(j, k) = \left\{ \frac{ns}{2}(m^2 - m) + m, \frac{ns}{2}(m^2 - m) + 2m, \dots, \frac{ns}{2}(m^2 - m) + sm, \frac{ns}{2}(m^2 - m) + (s + 1)m, \frac{ns}{2}(m^2 - m) + (s + 2)m, \dots, \frac{ns}{2}(m^2 - m) + snm \right\}.$$

It concludes the proof. ■

Lemma 3.6

Let m and s be positive integers $1 \leq j \leq n$; $1 \leq k \leq s$, the sum of $P_{\{m,d_7\}}^{\{n,s\}}(i, j, k) = \{ms + i - mk + (n - j)ms$; $1 \leq i \leq m\}$ and the sum of $P_{\{m,d_8\}}^{\{n,s\}}(i, j, k) = \{i - k - s(j - 1) + (ns)i$; $1 \leq i \leq m$; $1 \leq j \leq n$; $3 \leq k \leq s\}$ form an arithmetic sequences of difference $d_7 = -m^2$ and $d_8 = -m$.

Proof.

By simple calculation, for $j = 1, 2, \dots, n$,

it gives $\sum_{i=1}^m P_{\{m,d_7\}}^{\{n,s\}}(j, k) = P_{\{m,d_7\}}^{\{n,s\}}(k) \leftrightarrow P_{\{m,d_7\}}^{\{n,s\}}(j, k) = \left\{ \frac{m}{2}(2ms + m + 1) + m^2sn - m^2(js + k) \right\} \leftrightarrow$

$P_{\{m,d_7\}}^{\{n,s\}}(j, k) = \left\{ \frac{m}{2}(2ms + m + 1) + m^2sn - m^2(s + 1), \frac{m}{2}(2ms + m + 1) + m^2sn - m^2(s + 2), \dots, \frac{m}{2}(2ms + m + 1) + m^2sn - m^2(2s), \frac{m}{2}(2ms + m + 1) + m^2sn - m^2(2s + 1), \dots, \frac{m}{2}(2ms + m + 1) + m^2sn - m^2(ns + s) \right\}$. Furthermore

$\sum_{i=1}^m P_{\{m,d_8\}}^{\{n,s\}}(j, k) = P_{\{m,d_8\}}^{\{n,s\}}(k) \leftrightarrow P_{\{m,d_8\}}^{\{n,s\}}(j, k) =$

$\left\{ \frac{1}{2}(m^2 + m)(ns + 1) + ms - m(js + k) \right\} \leftrightarrow P_{\{m,d_8\}}^{\{n,s\}}(j, k) = \left\{ \frac{1}{2}(m^2 + m)(ns + 1) + ms - m(s + 1), \frac{1}{2}(m^2 + m)(ns + 1) + ms - m(s + 2), \dots, \frac{1}{2}(m^2 + m)(ns + 1) + ms - m(2s), \frac{1}{2}(m^2 + m)(ns + 1) + ms - m(2s + 1), \dots, \frac{1}{2}(m^2 + m)(ns + 1) + ms - m(ns + s) \right\}$. It concludes the proof. ■

Now we are ready to present the main theorem related to the existence of super $(a, d) - H$ antimagicness of the disconnected graph $G = sAmal(H, v, n)$, in the following theorem.

Theorem 3.2

For $n \geq 2$ and odd $s \geq 3$, the graph $G = sAmal(H, v, n)$ admits a super $(a, d) - H$ antimagic total labeling with feasible $d = m_1 - m_2 + m_3^2 - m_4^2 + r_1 - r_2 + r_3^2 - r_4^2$.

Proof.

For $i = 1, 2, \dots, m$ and $j = 1, 2, \dots, n$, by Lemma 3.5 and 3.6 we define the vertex and the edge labels as a linear combination of

$P_{\{m_1, m_1\}}^{\{n, s\}}(i, j, k), P_{\{m_2, -m_2\}}^{\{n, s\}}(i, j, k), P_{\{m_3, m_3^2\}}^{\{n, s\}}(i, j, k)$, and

$P_{\{m_4, -m_4^2\}}^{\{n, s\}}(i, j, k)$ as follows:

$f_1(A^k) = k$, and for $i = 1, 2, \dots, m - 2$

$f_2(x_{\{i,j\}}^k) = \left\{ P_{\{m_1, m_1\}}^{\{n, s\}} \oplus s \right\} \cup \left\{ P_{\{m_2, -m_2\}}^{\{n, s\}} \oplus s(nm_1 + 1) \right\} \cup \left\{ P_{\{m_3, m_3^2\}}^{\{n, s\}} \oplus s(n(m_1 + m_2) + 1) \right\} \cup \left\{ P_{\{m_4, -m_4^2\}}^{\{n, s\}} \oplus s(n(m_1 + m_2 + m_3) + 1) \right\}$

$$f_2(x_{\{i,j\}}^k) = \begin{cases} s(n+1) + 1 - js - 2k + s[n(m-2) + 1], \\ \text{for } 1 \leq k \leq \frac{\{s-1\}}{2}, i = m-1 \\ s(n+2) + 1 - js - 2k + s[n(m-2) + 1], \\ \text{for } \frac{s+1}{2} \leq i \leq s, i = m-1 \\ \frac{1}{2}(1-s) + js + k + ns + s[n(m-2) + 1], \\ \text{for } \frac{s+1}{2} \leq k \leq s, i = m \\ \frac{1}{2}(1-3s) + js + k + ns + s[n(m-2) + 1], \\ \text{for } \frac{s+1}{2} \leq k \leq s, i = m \end{cases}$$

$$f_2(e_{\{i,j\}}^k) = \left\{ P_{\{r_1, r_1\}}^{\{n, s\}} \oplus s[(mn+1)] \right\} \cup \left\{ P_{\{r_2, -r_2\}}^{\{n, s\}} \oplus s[(n(r_1) + mn + 1)] \right\} \cup \left\{ P_{\{r_3, r_3^2\}}^{\{n, s\}} \oplus s[(n(r_1) + n(r_2) + mn + 1)] \right\} \cup \left\{ P_{\{r_4, -r_4^2\}}^{\{n, s\}} \oplus s[(n(r_1) + n(r_2) + n(r_3) + mn + 1)] \right\}$$

The vertex labeling f_2 is a bijective function $f_2: V(G) \cup E(G) \rightarrow \{1, 2, \dots, p_G + q_G\}$. The total edge-weights of $G = sAmal(H, v, n)$ under the labeling f , for $j = 1, 2, \dots, n$ and $k = 1, 2, \dots, s$, constitute the following sets:

$$W_{\{f_2\}} = \sum f_2(A^k) + \sum f_2(x_{\{i,j\}}^k)_{1 \leq i \leq m-2} + \sum f_2(x_{\{i,j\}}^k)_{m-1 \leq i \leq m} + \sum f_1(e_{\{i,j\}}^k)$$

$$W_{\{f_2\}} = \left\{ C_{\{m,d\}}^{\{n,s\}} + [m_1 - m_2 + m_3^2 - m_4^2 + r_1 - r_2 + r_3^2 - r_4^2] \right\} (js + k)$$

It is easy that the set of total edge-weights $W_{\{f_2\}}$ consists of an arithmetic sequence of the smallest value a and the difference $d = m_1 - m_2 + m_3^2 - m_4^2 + r_1 - r_2 + r_3^2 - r_4^2$. Since the biggest d is attained when $d = m^2 + r^2$ then, for $m = p_H - 3$ and $r = q_H$, it gives $0 \leq d \leq p_H^2 + q_H^2 - p_H + \frac{(s-1)p_H}{sn-1} \leftrightarrow 0 \leq (p_H - 3)^2 + q_H^2 \leq p_H^2 + q_H^2 - p_H + \frac{(s-1)p_H}{sn-1}$ It concludes the proof. ■

IV. CONCLUSION

We have shown the existence of super antimagicness of amalgamation of complete graph H , denoted by $G = Amal(H, v, n)$ for connected one and $G = sAmal(H, v, n)$ for disconnected one, where H is any graph. By using a partition technique we can prove that $Amal(H, v, n)$ admits a super $(a, d) - H$ antimagic total labeling with $d = m_1 - m_2 + m_3^2 - m_4^2 + \frac{1}{2}m_5^2 + m_5 - \left(\frac{1}{2}m_6^2 + m_6\right) + r_1 - r_2 + r_3^2 - r_4^2 + \left(\frac{1}{2}r_5^2 + r_5\right) - \left(\frac{1}{2}r_6^2 + r_6\right)$, but for $G = sAmal(H, v, n)$, the existence of its super antimagicness only holds for s odd with $d = m_1 - m_2 + m_3^2 - m_4^2 + r_1 - r_2 + r_3^2 - r_4^2$. We also note that if the amalgamation of complete graph H contains a subgraph as a connector then finding the labels for feasible d remains

widely open. Thus, we propose the following open problem.

Open Problem

Let H be a subgraph of G and $G = sAmal(H, v, n)$. For s even, does G admit a super $(a, d) - H$ antimagic total labeling for $n \geq 2$ and feasible d ?

ACKNOWLEDGEMENTS

We gratefully acknowledge the support from DP2M research grant HIKOM-DIKTI and CGANT University of Jember of year 2016.

REFERENCES

- [1] M. Ba-ca, L. Brankovic, M. Lascsakova, O., Phanalasy, A. Semani-cova-Fe-nov-c³kova, On d-antimagic labelings of plane graphs, *Electr. J. Graph Theory Appl.*, 1(1), 28-39, (2013)
- [2] Dafik, A.K. Purnapraja, R Hidayat, Cycle-Super Antimagicness of Connected and Disconnected TensorProduct of Graphs, *Procedia Computer Science*, 74, (2015), 9399
- [3] Dafik, Slamir, Dushyant Tanna, Andrea Semani-cova-Fe-nov-c³kova, Martin Ba-ca, Constructions of Hantimagicgraphs using smaller edge-antimagic graphs, *Ars Combinatoria*, 100 (2017), In Press
- [4] Dafik, Moh. Hasan, Y.N. Azizah, Ika Hesti Agustin, A Generalized Shackle of Any Graph H Admits a Super H-Antimagic Total Labeling, *Mathematics in Computer Science Journal*, (2016). Submitted
- [5] J.L. Gross, J. Yellen and P. Zhang, *Handbook of Graph Theory*, Second Edition, CRC Press, Taylor and Francis Group, 2014
- [6] N. Inayah, A.N.M. Salman and R. Simanjuntak, On $(a; d) \downarrow H$ -antimagic coverings of graphs, *J. Combin.Math. Combin. Comput.* 71 (2009), 273281.
- [7] N. Inayah, R. Simanjuntak, A. N. M. Salman, Super $(a; d)$ -H-antimagic total labelings for shackles of a connected graph H, *The Australasian Journal of Combinatorics*, 57 (2013), 127138.
- [8] P. Jeyanthi, P. Selvagopal, More classes of H-supermagic Graphs, *Intern. J. of Algorithms, Computing and Mathematics* 3(1) (2010), 93-108.
- [9] A. Llado and J. Moragas, Cycle-magic graphs, *Discrete Math.* 307 (2007), 2925 2933.
- [10] T.K. Maryati, A. N. M. Salman, E.T. Baskoro, J. Ryan, M. Miller, On H- supermagic labelings for certain shackles and amalgamations of a connected graph, *Utilitas Mathematica*, 83 (2010), 333-342.
- [11] A. A. G. Ngurah, A. N. M. Salman, L. Susilowati, H-supermagic labeling of graphs, *Discrete Math.*, 310 (2010), 1293-1300.
- [12] S.T.R. Rizvi, K. Ali, M. Hussain, Cycle-supermagic labelings of the disjoint union of graphs, *Utilitas Mathematica*, (2014), in press.
- [13] Roswitha, M. and Baskoro, E. T., H-magic covering on some classes of graphs, *American Institute of Physics Conference Proceedings* 1450 (2012), 135-138.
- [14] R. Simanjuntak, M. Miller and F. Bertault, Two new $(a; d)$ -antimagic graph labelings, *Proc. Eleventh Australas. Workshop Combin. Alg. (AWOCA)* (2000), 179189.

Charge Discreteness as Model in Charge Migration in a Chain of DNA Molecules under Radiation

Hector Torres-Silva, Erik Santos

Universidad de Tarapacá, EIEE, Arica, Chile

Abstract— Charge migration through DNA is a problem to be solved. A numerical wavefront solution for quantum transmission lines with charge discreteness is obtained as a model for the charge migration of a chain of DNA molecules induced by electromagnetic radiation. The nonlinearity of the system becomes deeply related to charge discreteness. The wavefront velocity depends on the normalized (pseudo) flux variable. Finding the dispersion relation for the normalized flux ϕ / ϕ_0 we show that the condition $v^2 \geq 0$ on the wave-front velocity gives the band-gap conditions for the charge propagation on the system.

Keywords— Charge migration, DNA, wavefront, quantum transmission line, discreteness.

I. INTRODUCTION

Currently nanostructures are embedded in countless devices and systems [1-5]. Naturally, at this scale and for low temperature, quantum mechanics plays a key role. Lately, much effort has been dedicated to study nanostructures, using as a model of quantum circuits with charge discreteness [6-12]. On the other hand, the discovery of charge migration in deoxyribonucleic acid (DNA) stimulated intensive investigations of the electronic properties of DNA due to their significance in biosynthesis and radiation-induced damage and repair processes [1-3]. Furthermore, considerable interest in nanodimensional structures of DNA possessing unique self-assembling and self-recognition properties has increased the last decade in connection with the possibility of the development of molecular nanoelectronic devices which are expected to provide high storage of information and high-speed signal processing within a wide temperature range [4-6]. In fact, DNA molecules can be well combined with silicon technology transcending the potential of the present quantum wires and are supposed to be used in modern computer technology as a binary data structure by applying a programmable linear self-assembly of the sequence of complementary nucleic base pairs of DNA. It

is in this context that we are interested in spatially transmission lines with charge discreteness [13]. In this work we will consider a wavefront solution for a quantum circuit (transmission line) simulating the DNA molecule in a cell sample. A numerical solution is founded and characterized for this specific system with charge discreteness, which can be extended for the description of more complex extended systems. In section 2 we will introduce a generalization of classical transmission lines with charge discreteness and we present the quantum transmission lines with charge discreteness, the Hamiltonian for coupled circuits, and the equations of motion for the spatially continuous system. In Sec. 3, the wavefront solution is considered. Finally, we give our conclusions.

II. GENERALIZATION OF TRANSMISSION LINE AND QUANTUM DISCRETENESS

For a chain of molecules of DNA, we consider a homogeneous classical transmission line, assumed infinite, where every cell is constituted of a LC circuit with inductance L and capacitance C per unit length. Assume that the interaction between neighbor cells is through the capacitors (direct line), the classical evolution equations for the electrical current and charge, become in this case

$$L \frac{d}{dt} i_m = \frac{1}{C} (2q_m - q_{m+1} - q_{m-1}) \quad (1)$$

Where the integer m designates the cell at position in the chain and, as usual, $i_m = \frac{d}{dt} q_m$ is the electrical current.

The above linear equation of evolution becomes directly from the classical Lagrangian L_{ag} given by

$$L_{ag} = \sum_m \left(\frac{L}{2} \dot{i}_m^2 - \frac{1}{2C} (q_m - q_{m-1})^2 \right) \quad (2)$$

Using the Lagrange equations one obtains (1).

Supporting solutions like a plane wave. Explicitly we have,

$$q_m = q_0 \exp(i\omega t - ikm) \quad (3)$$

Where, as usual in this case, the frequency ω and the wavenumber k become related through the dispersion relation. The variable q_0 is a constant parameter describing the amplitude of the wave. Note that we have considered by sake of simplicity the lattice-size a as one, ($a=1$). That is the adimensional number k in the equation (6) is really ka .

After some algebra, one obtains from (3) the dispersion relation. The infrared limit ($ka \rightarrow 0$) related to the continuous x -space structure becomes direct and corresponds to the dispersion relation $\omega = k / \sqrt{LC}$, namely a non dispersive medium.

From $\omega = k / \sqrt{LC}$, we get the phase velocity and group velocity

$$v_p = \frac{\omega}{k} = 1 / \sqrt{LC}, \quad v_g = \frac{\partial \omega}{\partial k} = 1 / \sqrt{LC} \quad (4)$$

From a general point of view, for arbitrary composition of a cell in the line, the Hamiltonian of this generalized electrical transmission line becomes quadratic, namely,

$$H = \sum_{m,s} \left(\frac{1}{2} \left(\frac{1}{L} \right)_{m,s} \phi_m \phi_s + \frac{1}{2} \left(\frac{1}{C} \right)_{m,s} q_m q_s \right) \quad (5)$$

As illustration and following [6-12, 14], and from the Hamiltonian (5), the usual quantization procedure for flux and charge, and the prescription (2) for charge discreteness, we could construct the quantum Hamiltonian for the direct transmission line with charge discreteness (q_e), which may be written as:

$$H = \sum_{m=-\infty}^{\infty} \left\{ \frac{2\hbar^2}{Lq_e^2} \sin^2 \frac{q_e}{2\hbar} \phi_m + \frac{1}{2C} (q_m - q_{m-1})^2 \right\} \quad (6)$$

where the index m describes the cell (circuit) at position m , containing an inductance L and capacitance C . The conjugate operators, charge q and pseudoflux ϕ , satisfy the usual commutation rule

$$\left[q_m, \phi_m \right] = i\hbar \delta_{m,m}, \quad \text{and} \quad \left[q_m, q_s \right] = \left[\phi_m, \phi_s \right] = 0. \quad (7)$$

A spatially extended solution of Eq. (6) corresponds to the quantization of the classical electric transmission line with discrete charge (i.e. elementary charge q_e). Note that in the formal limit $q_e \rightarrow 0$ the above Hamiltonian gives the well-known dynamics related to the one-band quantum transmission line, similar to the phonon case. The system described by Eq. (10) is very cumbersome

since the equations of motion for the operators are highly nonlinear due to charge discreteness. However, this system is invariant under transformation $q_k \rightarrow q_k + q$, that is, the total pseudo flux operator $\phi = \sum \phi_m$ commutes with the Hamiltonian; simplifying the study of this system.

$$H_m = \frac{2\hbar^2}{Lq_e^2} \sin^2 \frac{q_e}{2\hbar} \phi_m - \frac{1}{2C} (q_{m+1} - \phi_m)^2 \quad (8)$$

where H_m represents the Hamiltonian density operator for the fields. From the above Hamiltonian we find the equations of motion (Heisenberg equations) for the field operators:

$$\frac{\partial}{\partial t} \phi_m = \frac{1}{C} (q_{m+1} + q_{m-1} - 2q_m) \quad (9)$$

$$\frac{\partial}{\partial t} q = \frac{\hbar}{Lq_e} \sin \left(\frac{q_e}{\hbar} \phi \right) \quad (10)$$

and from eq. (6), the dispersion relation is given by

$$\omega = 2 \frac{|\sin k / 2|}{\sqrt{LC}} \quad (11)$$

If $k \ll 1$, $\omega = k / \sqrt{LC}$, from here we can obtain

$$v_p = \frac{\omega}{k} = 1 / \sqrt{LC}, \quad v_g = \frac{\partial \omega}{\partial k} = 1 / \sqrt{LC} \quad (12)$$

III. WAVEFRONT SOLUTION

In real seismic applications there is always the presence of damping. We shall consider the effect of its simplest form, small viscous damping. Eq. (3) is extended by adding a linear damping term λ :

Now we consider a homogeneous classical transmission line, assumed infinite, where the every cell is constituted of a LC circuit with series inductance L and shunt capacitance C per unit length. The approach is based on the mapping of field components (i.e., E and H) in the medium to the voltages and currents of the equivalent distributed L-C network [15, 17]. It is well known that dielectric properties like permittivity and permeability can be modeled using distributed L-C networks. To illustrate how these material parameters relate the distributed series impedances and shunt admittances of the network, 1-D distributed L-C network is depicted in Fig. 1. The network consists of a series per-unit-length impedance Z' in z direction and a shunt per-unit-length admittance Y' in y direction.

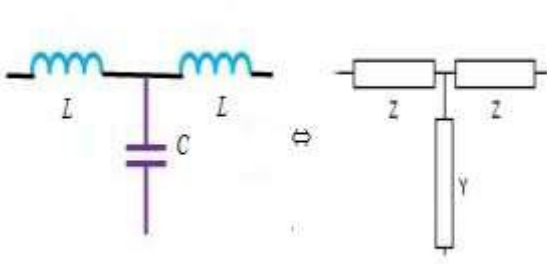


Fig.1: Transmission line model with L, C per unit length.

For the conventional homogeneous isotropic RHM with positive permittivity ϵ and permeability μ , Eqs.(1, 2) implies a network of a low-pass topology with series inductor $L' = \mu$ (H/m) and shunt capacitor $C' = \epsilon$ (F/m), or $Z = j\omega L'$ and $Y = j\omega C'$, both of which are positive quantities. The negative permittivity and permeability [16, 17] in LHM leads to the question whether the parameters Z' and Y' in the network representation can also be made negative. From the impedance perspective, a negative L' and C' can be realized by exchanging their inductive and capacitive roles, which means the series inductor becomes a series capacitor, and the shunt capacitor becomes a shunt inductor. In this paper we are interested in the normal RHM transmission line which in the limit $q_e \rightarrow 0$ becomes the usual one band transmission wave equation.

$v^2 = \omega^2 / k^2 = 1 / LC$. In general the dispersion relation from Eqs. (9) and (10) is

$$\frac{\omega^2 LC}{k^2} = \cos(q_e \phi / \hbar) \left(\frac{\sin(k/2)}{k/2} \right)^2 \quad (13)$$

where v is the phase velocity given by

$$v = \sqrt{\frac{\omega^2 LC}{k^2}} = \sqrt{\cos(q_e \phi / \hbar) \left(\frac{\sin(k/2)}{k/2} \right)^2} \quad (14)$$

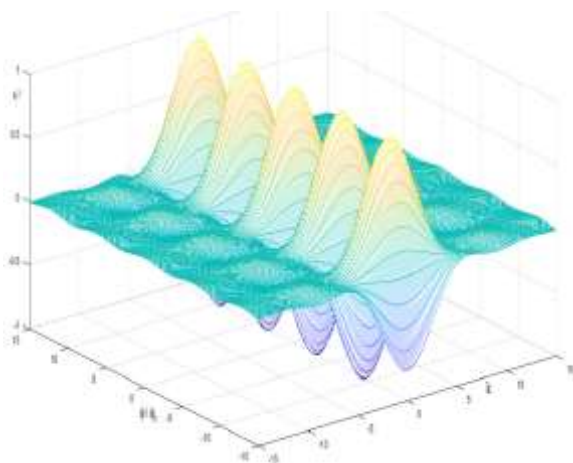


Fig.2: The normalized expression (17) v^2 is shown as a function of ϕ / ϕ_0 and k

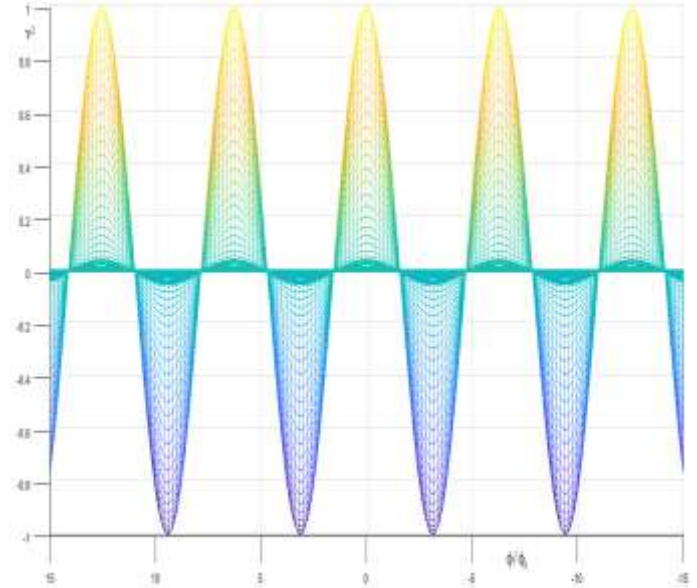


Fig.3: Profile of v^2 as a function of ϕ / ϕ_0 with $k = cte$

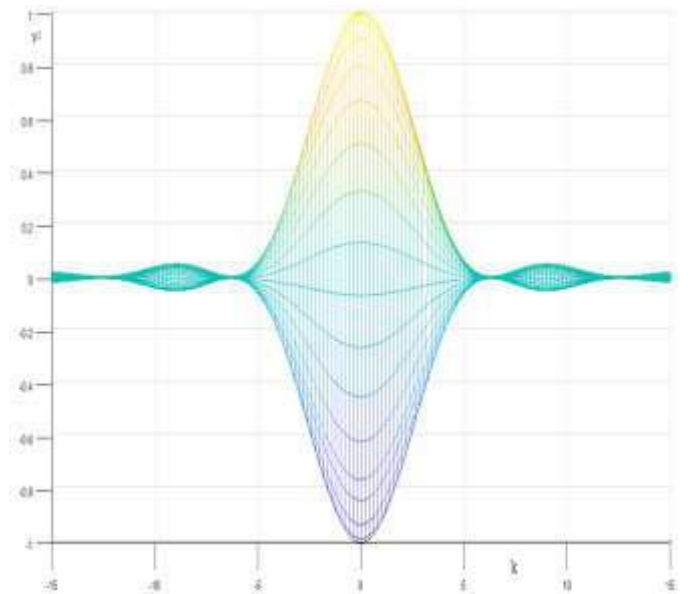


Fig.4: Profile of v^2 as a function of k with $\phi / \phi_0 = cte$

Figures 2-4 show the normalized v^2 of the charge migration in a transmission line where we can see that the velocity of wavefront which has bands and gaps. To see this in a clearer way we know that always v^2 must be positive ($v^2 LC > 0$), so the two equations (13), (14), are satisfied simultaneously when $\phi / \phi_0 = 2n\pi$, $n = \pm 1, \pm 2, \dots$ that means that $\phi = 2n\pi\phi_0 = nh / q_e$. Let

$$f(k) = v^2 LC = \frac{\omega^2 LC}{k^2} = \cos(pk) \left(\frac{\sin(k/2)}{k/2} \right)^2 \quad (15)$$

Where we define $pk = q_e \phi / \hbar = \phi / \phi_0$, so we have the factor p as a free parameter to analyze the quantum circuit.

In figure 5 we present the case with $\phi / \phi_0 = 0$ where $f(k) \geq 0$ and there is not a structure of bands and gaps because $q_e \rightarrow 0$. In figure 6 we have a structure of bands and gaps because $pk = q_e \phi / \hbar = \phi / \phi_0 \neq 0$

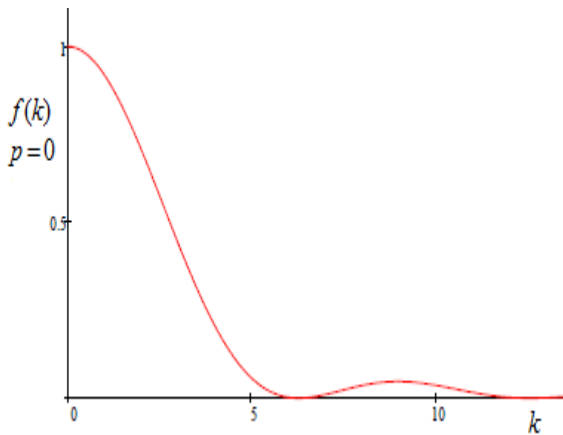


Fig.5: Plot of the velocity of the wavefront, as a function of k with the magnetic flux as the parameter p . As specified by Eq. (18), if $p=0$, there is only a structure of bands because $pk = q_e \phi / \hbar = \phi / \phi_0 = 0$, that is $q_e \rightarrow 0$.

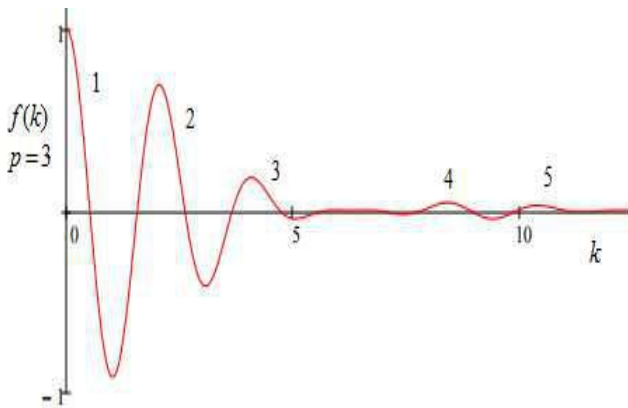


Fig. 6. Plot of the velocity of the wavefront, as a function of k with the magnetic flux as the parameter p . As specified by Eq. (18) there is a structure of bands and gaps because $pk = q_e \phi / \hbar = \phi / \phi_0 \neq 0$ with $p=3$, so that have five bands where there is wave propagation and charge migration as are shown in Figure 7.

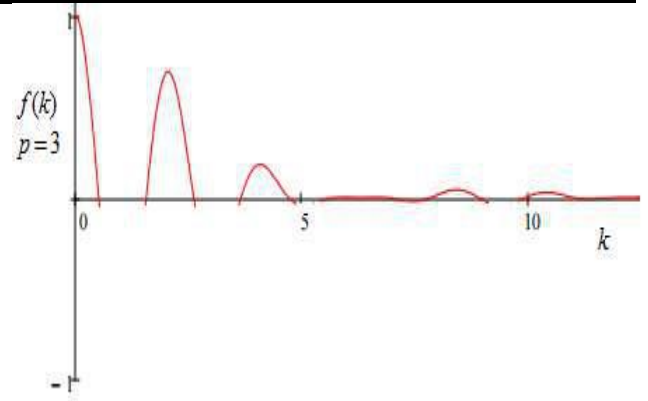


Fig. 7. $v^2 LC \geq 0$ where there are wave propagation. As we have seen from these graphs, the condition $v^2 \geq 0$ on the wave-front velocity gives the band-gap conditions on the system. In fact, from (16) the restriction $v^2 = \frac{1}{LC} \cos(q_e \phi / \hbar) \left(\frac{\sin(k/2)}{k/2} \right)^2 \geq 0$ means that there exists a sequence of bands and gaps. The nonlinearity of the system becomes be deeply related to charge discreteness or in terms Of discrete values of quantum flux $\phi_0 = \hbar / q_e$. The wavefront velocity is found to depend on a step discontinuity on the (pseudo) flux variable, p , displaying allowed and forbidden regions (gaps), as a function of p .

Defining, $\phi / \phi_0 = pk$, any complex function Ψ can be written as $\psi = \psi_0 \exp(ipk)$ where ψ_0 is the amplitude and θ is the phase. It is obvious that changing the phase pk by $2n\pi$ will not change ψ and, correspondingly, will not change any physical properties in this quantum transmission line. However, in the superconductor of non-trivial topology, e.g. superconductor with the hole or superconducting loop/cylinder, the phase pk may continuously change from some value pk_0 to the value $pk_0 + 2\pi n$ as one goes around the hole/loop and comes to the same starting point. If this is so, then one has n magnetic flux quanta trapped in the hole/loop, [18, 19], In the case of charge migration in DNA, charge discreteness is the statement that charge comes in packets which are of size 1 electron charge. These results enable the investigation of charge migration as quantum charge in both longitudinal and transverse configurations and stimulate theoretical interpretations [20-24]. Some of these studies are concerned with the issues of the charge migration induced by environmental factors, among which ionizing radiation or RF fields are of great interest.

Charge migration through DNA has been the focus of considerable interest in recent years because DNA is the

molecule that contains all of the information required to build and maintain the cell . A deeper understanding of the nature of charge transfer and transport along the double helix is important in fields as diverse as physics, chemistry and nanotechnology. It has also important implications in biology, in particular in DNA damage and repair. In this context this paper can be a contribution in the study of this topic.

IV. CONCLUSIONS

A charge migration in a chain of DNA molecules is simulated with the quantum electric transmission line with charge discreteness described by the Hamiltonian (12), and equations of motion (13-14), Wavefront solution was found.. One condition on the velocity generates a band-gap structure dependent on the pseudo flux parameter, namely, there exist regions for which a solitary wavefront propagates with constant speed according the value of ϕ/ϕ_0 . The main results of this work are the existence of the band-gap structures for $0 < \phi/\phi_0 < 1$. Charge migration under radiation is possible when $v^2 \geq 0$.

REFERENCES

- [1] S. Datta, Lessons from Nanoelectronics, a Lecture Notes Series (Volume 1, Publication, Singapore :World Scientific Press, 2012).
- [2] S. Lyshevski, Nano and Molecular Electronics Handbook, CRC Press. Taylor & Francis Group, 2016.
- [3] H. J. de Los Santos, Principles and Applications of Nano MEMS Physics. Springer, Berlin, 2005.
- [4] David K. Ferry and Stephen M. Goodnick, Transport in Nanostructures. (Cambridge University Press, 2009).
- [5] W. D. Heiss (Ed.), Quantum Dots: Doorway to Nanoscales Physics. (Springer, Berlin 2005).
- [6] Y. Q. Li and B. Chen, Phys. Rev. B 53, 4027 (1996).
- [7] B. Chen et al, Phys. Lett. A 335, 103 (2005), and references therein.
- [8] J. C. Flores, Phys. Rev. B 6 , 235309 (2001).
- [9] J. C. Flores, Europhys. Lett. 69, 116 (2005).
- [10] T. Lu and Y. Q. Li, Mod. Phys. Lett. B, 16, 975 (2002).
- [11] S. A. Gurvitz, Phys.Rev.Lett.85, 812 (2000).
- [12] C. A. Contreras and D. Laroze, Physica B, 476, 77-81, (2015).
- [13] N. V. Grib et al, Distance-dependent coherent charge transport in DNA: crossover from tunneling to free propagation, Journal of Biophysical Chemistry, Vol.1, No.2, 77-85 (2010).
- [14] J. C. Flores et al, Phys. Rev. B 74, 193319, (2006), and references therein.
- [15] H. Torres-Silva, "A Transmission Line Model with Metamaterial Effects in Gamma Ray Bursts", Journal of Electronics and Communication Engineering Research, Volume 3, Issue 5, P 12-17, (2016).
- [16] H. Torres-Silva, D. Torres-Cabezas and J. López-Bonilla, Charge discreteness in LC quantum circuit, Open Journal of Technology & Engineering Disciplines (OJTED), Vol. 2, No. 3, September 2016, pp. 01-06.
- [17] H. Torres-Silva, Metamateriales, Actualidad y Desarrollo, Dyna, vol 92, nº 3, Cod 8244, 2017, and references therein.
- [18] S. Frankel, National Mathematics Magazine, Vol. 11, No. 4, pp. 177-182 (1937)
- [19] D. Bascom; F. William , Review Letters. 7 (2): 43–46, (1961)
- [20] R. Doll, N. Näbauer, (July 1961).. Physical Review Letters. 7 (2): 51–52, (1961).
- [21] B. Giese B, S. Wessely, M. Spormann, U. Lindemann, E. Meggers and M.E. Michel-Beyerle, On the mechanism of long-range electron transfer through DNA, Angewandte Chemie International Edition 38 (1999), 996-998.
- [22] V.D. Lakhno, Soliton-like solutions and electron transfer in DNA, Journal of Biological Physics 26 (2000), 133-147.
- [23] S. Eh. Shirmovsky and D.L. Boyda, Study of DNA conducting properties: Reversible and irreversible evolution, Biophysical Chemistry 180-181 (2013), 95-101.
- [24] C.T. Shih, Sequence and energy dependence of electric transport properties of DNA –A tight-binding model study, Chinese Journal of Physics 45 (2007), 703-707.

Employees' Emotional Intelligence Determinants in Handling Dengue Fever (*Case Study: Jember Regency, East Java Province, Indonesia*)

A.T. Hendrawijaya, T.A. Gumanti, Sasongko, Dan Z.Puspitaningtyas

FKIP – The University of Jember, Indonesia

Abstract— *Dengue fever is one of endemic diseases in Jember regency. The research observes and analyzes the effect of working motivation, compensation, working satisfaction, and working climate towards emotional intelligence of employees. The research samples are 96 operational employees of civil servants in handling dengue fever (DBD) in Jember regency. The research data was analyzed using double linier regression analysis. The research result indicated that working motivation, compensation, working satisfaction and working climate showed significantly positive effect towards emotional intelligence. The variable of working satisfaction showed the most dominant effect towards emotional intelligence.*

Keywords— *Working Motivation, Compensation, Working Satisfaction, Working Climate, Emotional Intelligence.*

I. INTRODUCTION

The effort of handling dengue fever (DBD) in Jember regency has been regulated in the Regent Regulation of Jember regency no. 188.45 / 222/012/2015. However, in the execution prevention and handling of dengue fever (DBD) the local government frequently encountered various problems. The problems were generally posed by policy factors released by the local government including people and other medical institutions and other external factors Such as factor of social environment. This arises because of a mismatch between what was expected and what was conducted by the field officer. Dengue fever (DBD) is one of endemic diseases growing each year in Jember regency. The number of victim of dengue fever (DBD) in Jember regency by the end of 2015 is approximately 905 people. Yet, as a matter of fact, the Department of Health of Jember regency confirmed that It was due to lack of human resources especially field staff in terms of both quantity and quality (Department of Health of Jember regency 2016). Limited capacity of human resources of local civil servants in fulfilling the need for public services such as DBD counter measures leads to the

use of democratic public administration concept / paradigm / new public service (NPS) in practice. This particular paradigm suggested that people or citizens are assumed to possess sufficient human resources to meet the need through synergy and collaboration with human resources of other agents.

Emotional intelligence works as intra as well as extra-personal skill in which one can motivate and have self-control in dealt with social relationship (Goleman, 1997). Thus, emotional intelligence refers to ability of identifying own and others' feeling, ability to motivate our own selves, and ability to control own emotion well in social relationship.

Dann (2002) suggested that emotional intelligence is one's ability to cope with their emotions to solve problems in getting through the life well and effectively. Abraham (1997) also stated the same thing that someone with great emotional intelligence can eventually achieve something best and work well. The research aims at observing and analyzing the effect of working motivation, compensation, working satisfaction and working climate towards employees' emotional intelligence.

According to Dann (2002), working motivation and emotional intelligence is desperately needed in an organization for the sake of dynamics as expected. When an employee is in charge of performing the task of always keeping the working spirit, the positive emotional intelligence will eventually (Shapiro, 2003). Working motivation works as a driving force in working and is closely related to as well as proof of the employees' emotional intelligence in an organization (Sala, 2004). Cooper dan Sawaf (2001) even confirmed that working motivation is closely related to emotional intelligence. Furthermore, the previous researches showed that working motivation had significantly positive effect towards emotional intelligence (Rizal, 2012). Whereas, another research conducted by Diab and Ajlouni (2012) suggested that working motivation also showed effect towards

emotional intelligence. In short, working motivation is closely related to emotional intelligence.

H₁ : working motivation showed positive effect towards emotional intelligence.

Compensation is the reward of services obtained by employees in the form of material or non-material, direct or indirect, extrinsic or intrinsic to create healthy emotional conditions that work productivity increases (Carruso, 1999). Compensation comprises financial changes, services and allowances in the form of non-financial such as testimonials, promotions, rewards among individuals, achievement, autonomy and growth achieved by someone changing their contribution to the organization where they work and dedicate themselves. Thus, the organization will grow and develop stronger due to the employees' emotional intelligence (Chakraborty, 2004).

Nawawi (2005) stated that compensation is anything instituted and assumed as compensation or equivalent to create healthy balance emotion. Function of compensation handover in an organization declared by Handoko, while Day (2004) states: a) efficient allocation for human resources, b) effective and efficient use of human resources, c) to encourage economic growth. This means that sufficient compensation will be encouraged by the achievement of productive performance.

Whereas, previous research carried out by Rizal (2012) and Saeed, et al (2011) found that working motivation had significantly positive effect towards emotional intelligence. From the above-mentioned description, it can be concluded that the higher the compensation is obtained, the better is the employees' emotional intelligence. In other words, compensation and emotional intelligence show a positive correlation.

H₂ : Compensation has a positive impact towards emotional intelligence.

Working satisfaction is a pleasant emotional condition resulted in working assessment as expected working values are achieved so that positive and healthy emotional conditions are created to support the development of the organization (Anoraga, 2005). People will experience reduced satisfaction when their needs are well-fulfilled, and they will also experience less working satisfaction when their needs are not well-fulfilled. In other words, the level of working satisfaction is the function of need fulfillment (Porter, 1962; Locke, 1968; Shaffer, 1987). Locke (1968), in Firmansyah (2006) considered that working satisfaction might be more closely related to values than needs. Values are defined as passion or wish to achieve certain result as expected (content) or how many contents as expected (intensity).

How big the satisfaction is achieved by people is the result of a comparison between perceptions of what should be achieved and what has been achieved (Lawler, 1973). The perception achieved is shown in three aspects: perception of working input-output such as education, expertise seniority, input-input and other results perceived and perceptions, working characteristics such as level of jobs, level of difficulties and responsibilities. Whereas, perceptions of quantity perceived is the real results achieved and other perceived results. Thus, each individual achieves good emotional intelligence in the organization. Muhamad Idrus (2002) stated that the dominant determinant of working satisfaction is physical simulation located in central network, not in the process of comparison. According to Muhamad Idrus, though job remains the same, everybody's satisfaction varies over the time depending on working environment and each person's emotional intelligence.

The previous research has found that working satisfaction indicated significantly positive correlation with emotional intelligence (Munawaroh dkk, 2011; Saeed, dkk, 2011), while another research by Diab and Ajlouni (2012) found different result that working satisfaction do not significantly affect emotional intelligence. Thus, the higher the working satisfaction is, one has better emotional intelligence. It means that there is a positif correlation between working satisfaction and emotional intelligence.

H₃ : Working Satisfaction showed positive impact towards Emotional Intelligence.

According to Joseph (1997) in Sergiovanni (2005) working climate is working condition and situation in an organization. It will absolutely influence the members' emotional condition that can be described through the characteristic values of the organization. Miner (1998) in Firmansyah (2006) stated that working climate are as follows: 1) working climate is closely related to big organizations with specific characteristic, 2) Working climate refers to the organization not the value, 3) working climate comes from organizational practice, and 4) working climate influences the members' behavior and emotional intelligence.

The previous researches found various results. The research conducted by Munawaroh, et al (2011) found that working climate do not significantly influence emotional intelligence, while the research by Saeed, et al (2011) found that there is a significantly positive correlation of variables of working climate towards emotional intelligence. Further research by Sekar (2012) found that working climate plays a pivotal role in encouraging employees to do the jobs which will likely affect the

employees' emotional intelligence. Thus, working climate indeed affects the emotional intelligence.

H₄ : Working climate shows positif impact towards Emotional Intelligence.

Based on theoretical and empirical analysis, the research hypothetical frame is illustrated as follows:

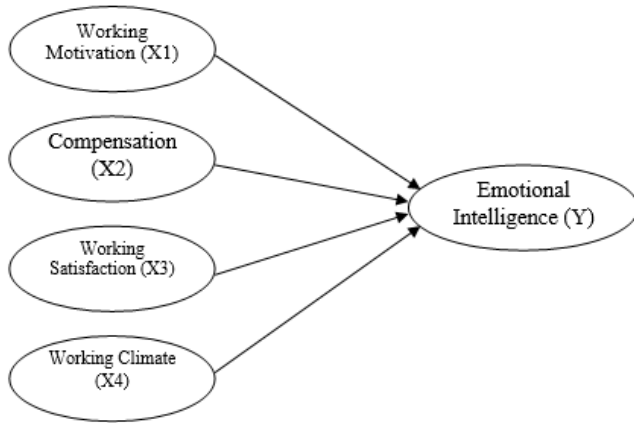


Image.1: Conceptual Frame

II. RESEARCH METHOD

The research deployed quantitative approach. The data was shown in numbers and the research aims at testing certain hypothesis (Arikunto, 1989; Tuckman, 1999). The research works in correlational design, in the work of survey with the use of cross sectional survey (Borg dan Gall, 1993; Ardhana, 1987).

The research population was taken from all field officers in handling dengue fever (DBD) in the filed under the Department of Health of Jember regency. The research samples were taken by using the total sampling method. In other words, 96 field staff in handling of dengue fever (DBD) in the area of the Department of Health of Jember regency works as the research respondents.

The research focuses on the efforts of identifying the effect of working motivation, compensation, working satisfaction and working climate towards the emotional intelligence of field staff in handling dengue fever (DBD) in Jember regency.

The primary data was collected through questionnaire as the main method. Technique of data collection was conducted through respondents' cooperation by filling out the questionnaire and interview by the researcher. The

questionnaire and data collection was conducted in December 2016 to February 2017 whereas the secondary data was collected from the Department of Health of Jember regency and related references.

The questionnaire used 5 point Likert scale adapted from reference related to the research. The measurement of working motivation variables adopted the questionnaire developed by Borich (1977), Lerry (1984), Robbins (1996), Sulton (2005), Daresh (1989), Rudi (2007) and Arikunto (1996). The measurement of compensation variables adopted the questionnaire developed by Opshal and Dunnette (1996), David (1981), Rudi (2007), Handoko (1998), Henry (1997) dan Martoyo (1998). Rudy (2007) and Smith (1975 The measurement of working satisfaction variables adopted questionnaire developed by). The measurement of working climate variables adopted questionnaire developed by Halphin (1971), Soetopo (2001), Rudi (2007), Owen (1991), Salabi (2006), Meter (1993), Julie (2005) and Gaspar (2006). The measurement of emotional intelligence variables adopted questionnaire developed by Shapiro (2003), Mulyani (2008), Abraham (1997), Carison (2004) dan Gowell (2003).

Data analysis method used double linier regression to identify the impact of working motivation, compensation, working satisfaction and working climate towards emotional intelligence.

III. RESULT AND DISCUSSION

The test result of instrument validity of variables such as working motivation, compensation, working satisfaction, working climate and emotional intelligence has correlation ranging 0,366 to 0,731 with significant value ranging 0,000 to 0,047 that it shows significant value less than α (0,05). Thus, it concludes that all items in the research are valid. The test of instrument reliability obtained coefficient value of Cronbach's Alpha ranging 0,873 to 0,955 and higher than 0,70 that instrument of working motivation variables is absolutely reliable.

The research result tried out to the field officer with the status of civil servant in handling dengue fever (DBD) in Jember regency with 96 respondents which is the description of various results. Whereas, respondents' general data lies as follows: sex, age, education and workplace illustrated in the following table.

Table.1: General Description of Respondents

Characteristic	Description	Distribution	
		Frequency	Percentage (%)
Sex	Male	64	66,7
	Female	32	33,3
Age	15-24 years	0	0,0
	25-34 years	8	8,4
	35-44 years	63	65,6
	45-54 years	25	26,0
	Over 55 years	0	0,0
Education	SLTA	75	78,1
	D3	11	11,5
	S1	10	10,4
	S2	0	0,0
Years of Service	< 6 years	0	0,0
	6-12 years	8	8,4
	13-18 years	27	28,1
	19-24 years	51	62,5
	> 24 years	1	1,0
Total		96	100

The research respondents are mostly males; 64 people (66, 7%) and females (33,3%). The respondents are mostly at 35 to 44 years of age around 63 people (65, 6%), then respondents of 45-54 years of age around 25 people (26, 0%). Most respondents have educational background of secondary schools / senior high schools (SMA/SMK) around 75 people (78,1%), then respondents with educational background of diploma and undergraduate study consecutively 11 people or 11,5% (Diploma) and 10

people or 10,4% (Undergraduate). Most respondents around 60 people (62,5%) have years of service between 19 to 24 years then 27 respondents (28,1%) with years of service between 13 to 18 years. Only 1 (1,0%) respondent with years of service more than 24 years.

The result of double linier regression analysis of the impact of working motivation, compensation, working satisfaction and working climate towards emotional intelligence is illustrated in the table 2.

Table.2: The Recapitulation of result of double linier regression analysis

No.	Free Variables	Koefisien regresi	Hypothesis		Sign.
			t-count	t-table	
1.	Working motivation (X ₁)	0,271	3,324	1,986	0,001
2.	Compensation (X ₂)	0,287	3,273		0,002
3.	Working Satisfaction (X ₃)	0,307	3,660		0,000
4.	Working Climate (X ₄)	0,186	2,006		0,048
Konstanta		= -0,161			
R ²		= 0,614			
Adjusted R ²		= 0,597			
F-count		= 36,242			
F-table (5%;4;91)		= 2,472			
Significance		= 0,000			

The result of data analysis of working motivation impact towards emotional intelligence showed regression

coefficient as 0,271 indicating the increase of working motivation and at the same time will likely lead to the

increase of emotional intelligence with the assumption of other free variables are constant. The test for the impact of working motivation towards emotional intelligence. Emotional intelligence shows value t-count as 3,324 (p-value = 0,001). Significant value is 0,001 less than α (0, 01) which means that working motivation variables show significant impact towards emotional intelligence. Thus, it is proven that hypothesis 1 (H₁) stating that working motivation shows significant impact towards emotional intelligence.

The result of data analysis on the impact of compensation towards emotional intelligence shows regression coefficient as 0,287 which indicates the increase of compensation will likely cause increase of emotional intelligence with the assumption that other free variables are constant. Test of the impact of compensation towards emotional intelligence shows value t-count as 3,273 (p-value = 0,002). Significant value is 0,002 less than α (0, 01) indicating that compensation variables show significant impact towards emotional intelligence. Thus, it is proven that hypothesis 2 (H₂) stating that compensation shows significant impact towards emotional intelligence.

The result of data analysis on the impact of working satisfaction towards emotional intelligence shows regression coefficient as 0,307 which indicates the increase of working satisfaction will likely cause the increase of emotional intelligence with the assumption that other free variables are constant. Test of the impact of working satisfaction towards emotional intelligence shows value t-count as 3,660 (p-value = 0,000). Significant value is 0,000 less than α (0, 01) indicating that working satisfaction variables show significant impact towards emotional

intelligence. Thus, it is proven that hypothesis 3 (H₃) stating that working satisfaction shows significant impact towards emotional intelligence.

The result of data analysis on the impact of working climate towards emotional intelligence shows regression coefficient as 0,186 which indicates the increase of working climate will likely cause the increase of emotional intelligence with the assumption that other free variables are constant. Test of the impact of working climate towards emotional intelligence shows value t-count as 2,006 (p-value = 0,048). Significant value 0,048 less than α (0, 05) indicating that working climate variables show significant impact towards emotional intelligence. Thus, it is proven that hypothesis 4 (H₄) stating that working climate shows significant impact towards emotional intelligence.

Determination coefficient (R²) mainly measures to what extent the ability of model in describing dependent variables. The value of determination coefficient is between zero and one. The small value of R² means the ability of independent variables in describing the variety of dependent variables is fairly limited. The value closed to one means the independent variables offer almost all information needed to predict the variety of dependent variables (Ghozali, 2006). Effective support is used to identify which variables own big support towards the income of street vendors or which is the most dominant factor among the independent variables. The identification of effective support is through standardized coefficient multiplication with correlation zero order to each independent variable. The result of effective support is illustrated in Table 3.

Table.3: Effective Support of Free Variables

Free Variables	Standardized Coefficient	Correlation of Zero Order	Effective Support
Working Motivation (X ₁)	0,254	0,575	0,146
Compensation (X ₂)	0,276	0,636	0,176
Working Satisfaction (X ₃)	0,303	0,647	0,196
Working Climate (X ₄)	0,167	0,580	0,097
Determination Coefficient (R ²)			0,614

Based on the above table value of coefficient of determination (R²) of 0.614 means that the independent variables (Working motivation, compensation, working satisfaction and working climate) affect the dependent variable (emotional intelligence) as 61.4%, while the rest of 38.6% is influenced by other factors beyond the model. The effective contribution of each independent

variable is working motivation of 0.146 (14.6%), compensation of 0.176 (17.6%), job satisfaction of 0.196 (19.6%) and work climate of 0.097 (9.7 %). From the results it can be concluded that the most dominant variable that affects emotional intelligence is the variable of job satisfaction with a contribution of 19.6%.

Discussion

Hypothesis 1 (H₁) suggested that working motivation shows significant impact towards emotional intelligence. The research confirmed that working motivation shows significantly positive impact towards emotional intelligence. This indicates that the indicators in the working motivation such as discipline in carrying out tasks, responsibilities of completion of tasks, seriousness in solving problems, increasing the business in work, developing tools to work, the innovation and creativity, seriousness in evaluating the work, working on target as well as working motivation and attendance which enable to improve emotional intelligence.

The world of work has a variety of problems and challenges, such as tight competition, task demands, uncomfortable working climate and social problems with other colleagues. Such problems in the world of work do not only require intellectual ability, but also require ability of solving problems, emotional ability or emotional intelligence is even needed more desperately. If someone can solve problems in the workplace dealing with his / her emotions then he will produce better work (Agustian, 2001). The results of this study support research conducted by Rizal (2012) and Diab and Ajlouni (2012) found that morale has a positive and significant effect on emotional intelligence.

Hypothesis 2 (H₂) states that compensation has a significant effect on emotional intelligence. This study found that compensation has a significant positive effect on emotional intelligence. This indicates that indicators in compensation such as financial rewards, interpersonal rewards and sense of settlement, recognition and autonomy and promotion, achievement and growth are sufficient to improve emotional intelligence.

The function of compensation in an organization is an efficient allocation of human resources, the use of human resources more effectively and efficiently and the driver of economic growth. According to Handoko (2004), the intent of providing such compensation will encourage better employees' emotional intelligence that will likely lead to more productive works. These results support a research conducted by Rizal (2012) and Saeed, et al (2011) who found that working motivation positively and significantly influences emotional intelligence.

Hypothesis 3 (H₃) states that working satisfaction has a significant effect on emotional intelligence. This study found that working satisfaction has a significant positive effect on emotional intelligence. It concludes that indicators in working satisfaction such as working with current employment, current salary, opportunity for promotion, supervision on the current job, supportive

colleagues and jobs in general are sufficient to improve emotional intelligence.

Working satisfaction is a physical simulation that exists in the central network organs, not the comparative process, although the work remains the same, each person's working satisfaction varies over time depending on the work environment and each individual's emotional intelligence (Idrus, 2002). The results of this study are in line with the research conducted by Munawaroh et al (2011); Saeed et al. (2011) suggesting that working satisfaction has a positive and significant relationship to emotional intelligence, while another study conducted by Diab and Ajlouni (2012) found different results that is working satisfaction has no significant effect on emotional intelligence.

Hypothesis 4 (H₄) states that the working climate has a significant effect on emotional intelligence. This study found that working climate has a significant positive effect on emotional intelligence. This way, indicators in the working climate such as non-participation, obstacles, spirit, intimacy, joy, emphasis on results, confidence and attention / humanity are sufficient to improve emotional intelligence.

Working climate is an climate of work within an organization that greatly affects the emotional state of the members and this problem can be described with the organization's characteristic values. According Firmansyah (2006), working climate affects the behavior and its members' emotional intelligence. The results of this study are not relevant to the results of Munawaroh's research, et al. (2011) which found that the working climate do not significantly affect the emotional intelligence, while Saeed, et al. (2011) found that there was a significant and positive correlation between the atmosphere variables of Emotional Intelligence. Further research by Sekar (2012) found that the working climate becomes an important role in motivating employees to carry out their duties which will likely be able to affect the employees' emotional intelligence.

Implication

These findings may contribute to the testing and clarification of the theories developed in this study and the consistency of the findings resulted from previous studies. The assessment of working motivation variables, compensation, working satisfaction, working climate and emotional intelligence in this research are included in the scope of human resource management.

Working motivation consists of discipline in carrying out tasks, responsibilities of completion of tasks, seriousness

in solving problems, increasing business in work, developing tools to work, innovation and creativity, seriousness in evaluating the work, working on target and working motivation And presence can enhance employees' emotional intelligence. Compensation consists of financial rewards, interpersonal rewards and a sense of settlement, recognition and autonomy and promotion, achievement and growth which will likely be able to enhance emotional intelligence. Working satisfaction consists of working with current employment, current salary, opportunity for promotion, supervision on current work, supportive colleagues and employment in general which will likely be able to improve emotional intelligence. Working climate consists of non-participation, obstruction, enthusiasm, intimacy, joy, emphasis on results, confidence and attention / humanity which will likely be able to enhance emotional intelligence.

This study found that working motivation, compensation, working satisfaction and working climate have significantly positive effect on emotional intelligence. This contributes to the government, especially the District Health Office of Jember to emphasize on improving working motivation, compensation, working satisfaction and working climate in an effort to improve employees' emotional intelligence in response to dengue fever more effectively and based on target.

Constraints

This research was conducted specifically in Jember District Health Office especially in the prevention of dengue fever, so that generalization cannot be carried out on a wider scale. The research sample was only taken from the field officers carrying out the tasks. Thus, it was conducted through the level of decision makers. The field officer is in direct contact with the dengue fever victims (DBD), but with no recommendation released by the superior (the decision maker), the field officer will not be able to take actions.

IV. CONCLUSION

Working motivation, compensation, working satisfaction and working climate have a significant effect on emotional intelligence. In other words, these four combinations are sufficient to improve emotional intelligence. However, working satisfaction is the most dominant variable which influences emotional intelligence.

REFERENCES

- [1] Abraham, C. dan Shanley E. 1997. Social Psychology for Nurse. Jakarta: Buku Kedokteran EGC.
- [2] Agustian, A.G. 2001. Rahasia Sukses Membangun Kecerdasan Emosi dan Spiritual : ESQ. Jakarta: Arga.
- [3] Anoraga, P. 2005. Psikologi Kepemimpinan, Cetakan Ketiga, Jakarta: Penerbit Rineka Cipta.
- [4] Ardana. 2003. "Pengaruh Beberapa Variabel Terhadap Kepuasan Kerja Pegawai Negeri Sipil Dinas Pariwisata Kota Denpasar". Tesis. Denpasar: Program Studi Magister Manajemen Universitas Udayana.
- [5] Arikunto, S. 1996. Prosedur Penelitian, Suatu Pendekatan Praktek. Jakarta: Pt. Rineka Cipta.
- [6] Borich, G.D. 2007. Effective Teaching Methods Research Based Practice. New Jersey : Pearson Education, Inc.
- [7] Carlson, N.R. 2004. Psychology : The Science of Behavior. Boston : Allyn & Bacon.
- [8] Carruso, D.R. 1999. Applying The Ability Model Of Emotional Intelligence To The World Of Work. <http://cjwolfe.com/article.doc>, 15 Oktober 2016.
- [9] Chakraborty, S.K. dan Chakraborty, D. 2004. The Transformed Leader and Spiritual Psychology : A Few Insight, Journal of Organizational Change Management, Vol.17 No.2: 184-210.
- [10] Cooper, RK dan A. Sawaf. 2001. Executive EQ : Emotional intelligencedalam Kepemimpinan dan Organisasi. Jakarta: PT Gramedia Pustaka Utama.
- [11] Dann, J. 2002. Memahami Emotional intelligencedalam Seminggu. Jakarta: Prestasi Pustaka.
- [12] Daresh, J.C. 1989. Supervision as a Proactive Process. New York & London: Longman.
- [13] David, F.R. 1981. Manajemen Strategis: Konsep, Edisi Bahasa Indonesia. Diterjemahkan oleh Alexander Sindoro. Jakarta: Prenhallindo.
- [14] Firmansyah. 2006. Pengaruh Iklim Organisasi terhadap Kepuasan Kerja Guru di Mojokerto. Disertasi. Malang: Program Pascasarjana Universitas Brawijaya.
- [15] Gasperz, V. 2006. Kualitas dalam Industri Jasa. Jakarta: PT Gramedia Pustaka Utama.
- [16] Ghozali, I. 2004. Aplikasi Analisis Multivariate dengan program SPSS, Edisi Ketiga, Semarang: Badan Penerbit Universitas Diponegoro.

- [17] Goleman, D. 1997. Emotional Intelligence : Mengapa EI lebih penting dari pada IQ. Jakarta: PT Gramedia Pustaka Utama.
- [18] Gordon, E. 2004. EQ dan Kesuksesan Kerja, Focus-online, <http://www.epsikologi.com>. 12 Desember 2016.
- [19] Halphin, A.W. 1971. Manual for Leader Behavior Description Questionnaire. Columbus, OH: Bureau of Educational Research, Ohio State University.
- [20] Handoko, T.H. 2004. Manajemen Personalia dan Sumber Daya Manusia. Yogyakarta: BPFE.
- [21] Henry, N. 2004. Public Administration & Public Affairs. 6th Edition. USA: Pearson Prentice-Hall.
- [22] Idrus, M. 2002. Kecerdasan Spiritual Mahasiswa Yogyakarta, Psikologi Phronesis, Jurnal Ilmiah dan Terapan, Vol.4 No.8, Desember 2002.
- [23] Lawler III, E.E. 1973. Motivation in Work Organization Monetary, CA: Brooks/Cole.
- [24] Locke, E.A. 1968. The Natural and Causes of Job Satisfaction, Handbook of Industrial and Organizational Psychology. Chicago: Rand Mc Nally.
- [25] Martoyo, S. 1998. Manajemen Sumberdaya Manusia. Edisi 5. Yogyakarta: BPFE.
- [26] Meter, D.V. dan C.E. Van Horn, 1975, The Policy Implementatiton Proses: A Conceptual Framework. Journal Administration and Society, Vol 6. No. 4.
- [27] Mulyani, S. 2008. Analisis Pengaruh Faktor-faktor Kecerdasan Emosi terhadap Komunikasi Interpersonal Perawat dengan Pasien di Unit Rawat Inap RSJD Dr. Amino Gondohutomo Semarang Tahun 2008. Thesis. Semarang: Program Pascasarjana Program Ilmu Kesehatan Masyarakat Universitas Diponegoro.
- [28] Nawawi, H. 2000. Manajemen Sumber Daya Manusia. Yogyakarta: Gajah Mada University Press.
- [29] Opshal, R.L. dan Dunnette, M.A. 1996. The Role of Financial Compensation in Industrial Motivation. Psychological Bulletin. Agustus 1966.
- [30] Owens, R.G. 1991. Organizational Behavior in Education. Bonston: Allyn and Bacon.
- [31] Porter, M.E. 1962. Competitive Advantage, Creating and Sustaining Superior Performance, With a New Introduction, New York: The Free Press.
- [32] Robbins, S.P. 1996. Organizational Behavior: Concept, Controversies and Application. New Jersey: Prentice Hall.
- [33] Sala, F. 2004. Do Programs Designed to Increase Emotional Intelligence at Work, Emotional Intelligence Consortium Research Journal. Boston.
- [34] Salabi, A. 2006. Hubungan Keterampilan Manajerial Kepala Sekolah, Komunikasi Organisasi, Pengendalian Konflik dan Iklim Organisasi dengan Keefektifan Organisasi Madrasah Aliyah Negeri di Propinsi Kalimantan Selatan. Disertasi. Malang: PPS Universitas Negeri Malang.
- [35] Sergiovanny, T.J. 1987. Educational Governance and Administration. New Jersey: Prentice Hall Inc.
- [36] Shaffer, D.R. 1987. Social and Personality Development. Belmont, California: Thomson Wadsworth.
- [37] Shapiro, L.E. 2003. Mengajarkan Emotional Intelligence Pada Anak. Jakarta: PT Gramedia Pustaka Utama.
- [38] Smith, H.W. 1975. Kepuasan Kerja. New Jersey USA: Prentice-Hall, Inc. Englewood Cliffs.
- [39] Soetopo, H. dan W. Sumanto. 2001. Pengantar Operasional Administrasi Pendidikan. Surabaya: Usaha Nasional.
- [40] Sumarsono, R. 2007. Hubungan Tunjangan Kinerja, Keikutsertaan dalam Pengambilan Keputusan, Suasana Kerja dengan Semangat Kerja Guru di Kabupaten Jember. Thesis. Jember: Universitas Jember.
- [41] Tuckman, B.W. 1999. A Tripartite Model of Motivation for Achievement: Attitude / Drive / Strategy. New York: John Wiley & Sons Inc.

Cloud Computing Security with Identity-Based Authentication Using Heritage-Based Technique

Rishi Kumar Sharma¹, Dr. R.K.Kapoor²

¹Computer Science, AISECT University, Bhopal, India

²Computer Science, NITTTR, Bhopal, India

Abstract— More organizations start to give various types of distributed computing administrations for Internet clients in the meantime these administrations additionally bring some security issues. Presently the many of cloud computing systems endow digital identity for clients to access their services, this will bring some drawback for a hybrid cloud that includes multiple private clouds and/or public clouds. Today most cloud computing framework use asymmetric and traditional public key cryptography to give information security and common authentication. Identity-based cryptography has some attraction attributes that appear to fit well the necessities of cloud computing. In this paper, by receiving federated identity management together with hierarchical identity-based cryptography (HIBC) with cloud heritage technique, not only the key distribution but also the mutual validation can be rearranged in the cloud.

Keywords— cloud computing, cloud heritage, security, authentication.

I. INTRODUCTION

Cloud computing is a technique of computing in which dynamically scalable and often virtualized resources are provided as a service over the Internet. It is the result of improvement of infrastructure as a service (IAAS), platform as a service (PAAS), and software as a service (SAAS). With broadband Internet access, Internet clients are able to occupy computing resource, storage space and different kinds of software services according to their necessities. In the cloud heritage, with a lot of different computing resources, client can easily tackle their issues with the resources gave by a cloud. This brings incredible adaptability for the clients. Using cloud computing service, clients can store their basic data in servers and can get their data anyplace they can with the Internet and do not have to stress about system breakdown or disk faults, etc. Also, distinctive clients in one system can share their data and work. Numerous important organizations, for example Amazon, Google, IBM,

Microsoft, and Yahoo are the forerunners that give cloud computing services.

Cloud heritage is a concept of object oriented .The capability of one cloud to inherit services from another cloud is called cloud heritage. This is the property of client oriented network.

As of now, as appeared in Figure 1, there are essentially three sorts of clouds: private clouds, public clouds and hybrid clouds [15]. Private clouds, likewise called internal clouds, are the private networks that offer cloud computing services for a very restrictive set of clients within internal network. Public clouds or external clouds refer to clouds in the conventional sense [13] Hybrid clouds are the clouds that incorporate different private and/or public clouds [14]. Giving security in a private cloud and a public cloud is easier, comparing with a hybrid cloud since commonly a private cloud or a public cloud only has one service provider in the cloud. Giving security in a hybrid cloud that consisting multiple service providers is much more difficult especially for key distribution and mutual authentication, so we are use cloud heritage technique. Also for client to access the services in a cloud, a client digital identity is needed for the servers of the cloud to manage the access control. While in the entire cloud, there are numerous different types of clouds and each of them has its own identity management system. Thus client who needs to get services from various clouds needs numerous digital identities from various clouds, which will bring disservice for clients. Using federated identity management, every client will have his unique digital identity and with this identity, he can get various services from various clouds. Identity-based cryptography [10] could be a public key technology that permits the shopper of a public symbol of as hopper because the client's public key. Hierarchy identity-based cryptography is that the improvement from it so asto resolve the measurability drawback. Recently identity-based cryptography and hierarchy identity-based cryptography are projected to supply security for a few web applications.

This paper proposes to use united identity management within the heritage cloud specified each shopper and each server can have its own distinctive identity. With this distinctive identity and graded identity-based cryptography (HIBC), the key distribution and mutual authentication will be greatly simplified.

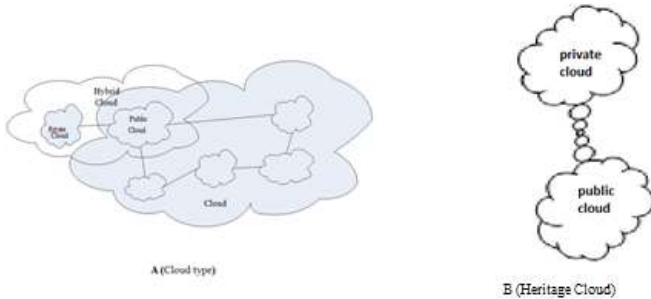


Fig. 1:

II. SECURITY IN CLOUD COMPUTING

Cloud computing have numerous advantages in cost diminishment, resource sharing, time saving for new service deployment. While in a cloud computing system, major part data and software that clients use reside on the Internet, which bring some new difficulties for the system, particularly security and privacy. Since every application may use resource from various servers. The servers are possibly based at multiple locations and the services provided by the cloud may use various infrastructures across organizations. All these attributes of cloud computing make it complicated to give security in cloud computing. To ensure adequate security in cloud computing, different security issues, for example, authentication, data confidentiality and integrity, and non-repudiation, all need to be contracted into account.

As such that before, there square measure 3 varieties of clouds in general: non-public cloud, public cloud and hybrid cloud. during a public cloud, resources square measure dynamically provisioned on a fine-grained, self-service basis over the net. Services within the cloud square measure provided by associate degree off-site third-party supplier WHO shares resources and bills on a fine-grained utility computing basis. whereas in most non-public clouds, with restricted computing resources, it's troublesome for a personal cloud to supply all services for his or her consumer, as some services could additional resources than internal cloud will offer. Cloud heritage technique could be a potential answer for this issue since they will get the computing resources from external cloud computing suppliers. non-public clouds have their blessings in corporation governance and provide reliable services, furthermore as they permit additional management than public clouds do. For the protection issues, once a cloud surroundings is formed within a firewall, it will offer its shoppers with less exposure to net

security risks. conjointly within the non-public cloud, all the services may be accessed through internal connections instead of public net connections, that build it easier to use existing security measures and standards. this could build non-public clouds additional acceptable for services with sensitive information that has got to be protected. whereas during a hybrid cloud, it includes quite one domain, which can increase the issue of security provision, particularly key management and mutual authentication. The domains during a hybrid cloud may be heterogeneous networks, thus there could also be gaps between these networks and between the various services suppliers. Even security may be well secure in every of private/public cloud, whereas during a hybrid cloud with quite one reasonably clouds that have completely different| completely different} styles of network conditions and different security policies, the way to offer economical security protection is way harder.

In a cloud, the cloud ADPS must offer a robust and client-friendly method for purchasers to access every kind of services within the system. Once a consumer desires to run AN application within the cloud, the consumer is needed to produce a digital identity. Normally, this identity may be a set of bytes that associated with the consumer. Supported the digital identity, a cloud system will apprehend what right this consumer has and what the consumer is allowed to try and do within the system. Most of cloud platforms embrace AN identity service since identity data is needed for many distributed applications [3]. These cloud computing systems can offer a digital identity for each consumer.

To solve these problems in the cloud, we offer to use federated identity management in clouds with HIBC and CHT. The proposed scheme does not only allow clients from a cloud to access services from other clouds with a single digital identity, it also over-simplify the key distribution and mutual authentication in a heritage cloud.

III. IDENTITY-BASED CRYPTOGRAPHY AND SIGNATURE

Identity-based cryptography and signature schemes were foremost projected by Shamir [10] in 1984. however solely in 2001, a economical approach of identity-based encoding schemes was developed by Dan Boneh and Matthew K. Franklin [2] and Clifford Cocks [4]. These schemes ar supported additive pairings on elliptic curves and have obvious security. Recently stratified identity-based cryptography (HIBC) has been projected in [6, 7] to enhance the measurability of ancient identity-based cryptography theme.

Identity-based scientific discipline theme could be a reasonably public-key based mostly approach which will be used for 2 parties to exchange messages and

effectively verify every other's signatures. in contrast to in ancient public-key systems that employing a random string because the public key, with identity-based cryptography shopper's identity which will unambiguously determine that client is employed because the public key for secret writing and signature verification. Identity-based cryptography will ease the key management quality as public keys don't seem to be needed to be distributed firmly to others. Another advantage of identity-based secret writing is that secret writing and coding are often conducted offline while not the key generation center.

In the identity-based cryptography approach, the PKG ought to creates a "master" public key and a corresponding "master" non-public key first off, then it'll create this "master" public key public for all the interested shoppers. Any shopper will use this "master" public key and also the identity of a shopper to make the general public key of this shopper. every shopper desires to urge his non-public key must contact the PKG together with his identity. PKG can use the identity and also the "master" non-public key to get the non-public key for this shopper. In Dan Boneh and Matthew K. Franklin's approach, they outlined four algorithms for a whole identity-based cryptography system. It includes setup, extract, secret writing and decipherment.

1. **Setup:** PKG create a master key K_m and the system parameters P . K_m is kept secret and used to generate private key for clients. System parameters P are made public for all the clients and can be used to generate clients' public key with their identities.
2. **Extract:** When a client requests his private key from the PKG, PKG will use the identity of this client, system parameters P and master key K_m to generate a private key for this client.
3. **Encryption:** When a client wants to encrypt a message and send to another client, he can use the system parameters P , receiver's identity and the message as input to generate the cipher text.
4. **Decryption:** Receiving a cipher text, receiver can use the system parameters P and his private key got from the PKG to decrypt the cipher text.

In a network mistreatment identity-based cryptography, the PKG wants not solely to come up with personal keys for all the shoppers, however additionally to verify the shopper identities and establish secure channels to transmit personal keys. during a giant network with only 1 PKG, the PKG can have a onerous job. during this case, HIBC [6] will be a far better alternative. during a HIBC network, a root PKG can generate and distribute personal keys for domain-level PKGs and therefore the domain-level PKGs can generate and distribute personal keys to

the shoppers in their own domain. HIBC is appropriate for an oversized scale network since it will scale back the work of root PKG by distribute the work of shopper authentication, personal key generation and distribution to the various level of PKGs. It can even improve the safety of the network as a result of shopper authentication and personal key distribution will be done regionally. The HIBC secret writing and signature algorithms embrace root setup, lower-level setup, extraction, encryption, and decipherment.

1. **Root setup:** root PKG will generate the root PKG system parameters and a root secret. The root secret will be used for private key generation for the lower-level PKGs. The root system parameters are made publicly available and will be used to generate public keys for lower-level PKGs and clients.
2. **Lower-level setup:** Each lower-level PKG will get the root system parameters and generate its own lower-level secret. This lower-level secret will be used to generate private keys for the clients in its domain.
3. **Extract:** When a client or PKG at level t with its identity (ID_1, \dots, ID_t) re-requests his private key from its upper-level PKG, where (ID_1, \dots, ID_i) is the identity of its ancestor at level i ($1 \leq i \leq t$), the upper-level PKG will use this identity, system parameters and its own private key to generate a private key for this client.
4. **Encryption:** Client who wants to encrypt a message M can use the system parameters, receiver's identity and the message as input to generate the cipher text.
 $C = \text{Encryption}(\text{parameters}, \text{receiver ID}, M)$.
5. **Decryption:** Receiving a cipher text, receiver can use system parameters and his private key got from the PKG to decrypt the cipher text.
 $M = \text{Decryption}(\text{parameters}, k, C)$, k is the private key of the receiver
6. **Signing and verification:** A client can use parameters, its private key, and message M to generate a digital signature and sends to the receiver. Receiver and verify the signature using the parameters, message M , and the sender's ID.
 $\text{Signature} = \text{Signing}(\text{parameters}, k, M)$,
 k is the sender's private key.
 $\text{Verification} = (\text{parameters}, \text{sender ID}, M, \text{Signature})$.

There are some inherent limitations with the identity-based cryptography [1]. one amongst downsides is that the key written agreement problem. Since clients' non-public keys are generated by PKG, the PKG will rewrite a client's message and build any client's digital signature while not

authorization. This really implies that PKGs should be extremely trusty. that the identity-based theme is additional applicable for a closed cluster of shoppers like an enormous company or a university. Since solely beneath this example, PKGs will be established with clients' trust.

In a system exploitation HIBC, each PKG within the hierarchy is aware of the clients' non-public keys within the domain beneath the PKG. though key written agreement drawback cannot be avoided, this will limit the scope of key written agreement drawback. Another disadvantage of the identity-based cryptography is that the revocation drawback. as a result of all the purchasers within the system use some distinctive identifiers as their public keys, if one client's non-public key has been compromised, the shopper ought to modification its public key.

IV. USING FEDERATED IDENTITY MANAGEMENT IN CLOUD

4.1 Federated Identity Management in the Cloud

Compared with centralized identity, that is employed to take are of security issues among constant networks, federate identity is adopted to take care of the safety issues that a consumer might want to access external networks or associate degree external consumer might want to access internal networks. federate identity may be a standard-based mechanism totally different[for various] organization to share identity between them and it will change the movability of identity info to across different networks. One common use of federate identity is secure net single sign-on, wherever a consumer World Health Organization logs in with success at one organization will access all partner networks while not having to log in once more. mistreatment identity federation will increase the safety of network since it solely needs a consumer to spot and attest him to the system for just one occasion and this identity info are often utilized in totally different networks. Use of identity federation standards cannot solely facilitate the consumer to across multiple networks embrace external networks with just one time log in, however can also facilitate purchasers from totally different networks to trust one another.

Using identity federation within the cloud means that shoppers from totally different clouds will use a united identification to spot themselves, that naturally suit the necessity of identity based mostly cryptography in cloud computing. In our approach, server to server, shoppers and servers within the cloud have their own distinctive identities. These identities area unit class-conscious identities. To access services within the cloud, shoppers area unit needed to attest themselves for every service in their own clouds. In some cases, servers also are needed

to attest themselves to shoppers. in an exceedingly little and closed cloud, this demand will be happy simply. whereas in an exceedingly hybrid cloud, there area unit multiple non-public and/or public clouds and these clouds could have faith in totally different authentication mechanisms. Providing effective authentications for shoppers and servers from totally different cloud domains would be tough. during this paper, we have a tendency to propose to use united identity management and HIBC with cloud heritage technique within the cloud. within the cloud trustworthy authority PKGs area unit used and these PKGs won't solely act as PKGs in ancient identity-based cryptography system however conjointly apportion class-conscious identities to shoppers in their domains. there's a root PKG in overall domain of every cloud, and every sub-level domain (private or public cloud) inside the cloud heritage conjointly has its own PKG. the basis PKG can manage the full heritage cloud, every non-public cloud or public cloud is that the 1st level and shoppers and servers in these clouds area unit the second level. the basis PKG of the cloud can apportion and attest identities for all the non-public and public clouds.

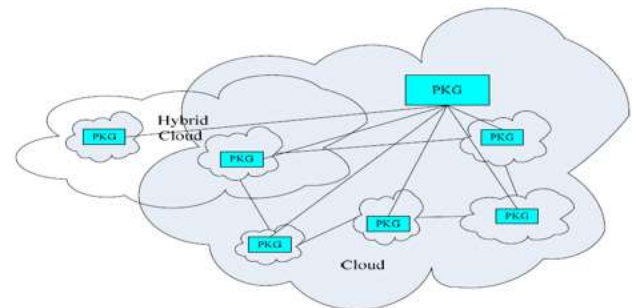


Fig.2: Federated identity management in cloud

4.2: Key Generation and in the Cloud

Using HIBC in the heritage cloud, an important part is key generation and distribution. As shown in [6], the security of HIBC scheme is based on the using of admissible pairing. Let G_1 and G_2 be two groups of some large prime order q and G_1 is an additive group and G_2 is a multiplicative group, we can call e an admissible pairing if e :

$G_1 \times G_2 \rightarrow G_2$ have the following properties.

1. **Billinear:** For all $1 P, Q \in G$ and $q a b \in Z^*$, $e(aP, bQ) = e(P, Q)ab$.
2. **Non-degenerate:** There exists $1 P, Q \in G$, such that $e(P, Q) \neq 1$.
3. **Computable:** For all $1 P, Q \in G$, there exists a efficient way to calculate

$$e(P, Q).$$

An admissible pairing can be generated by using a Weil pairing or a Tate pairing [2]. Here, in the cloud we use two levels PKG, the root PKG is 0 level PKG and the

PKGs in the private or public clouds are 1 level PKGs.

The root setup can be done as follow:

1. Root PKG generates G_1, G_2 and an admissible pairing $\hat{e}(aP, bQ) = \hat{e}(P, Q) \neq 1 (G_1, G_2, \hat{e}, P_0, Q_0, H_1, H_2)$ $\hat{e} : G_1 \times G_2 \rightarrow G_2$.
2. Root PKG chooses $P_0 \in G_1$ and $s_0 \in Z_p^*$ and set $Q_0 = s_0 P_0$.
3. Root PKG chooses hash function $H_1 : \{0,1\}^* \rightarrow G_1$ and $H_2 : G_1 \rightarrow \{0,1\}^*$.

Then the system parameters are $(G_1, G_2, \hat{e}, P_0, Q_0, H_1, H_2)$ and are public available, s_0 is the root PKG's secret and is known only by the root PKG.

For the lower level PKGs and users and servers in the cloud, they can use the system parameters and any user's identity to generate its public key. And every user or servers in the cloud can connect the PKGs in their cloud domain to get their private keys. For example, the PKG in private cloud of University with identity UIS, its public key can be generated as

$P_{uis} = H_1(UIS)$ and the root PKG can generate its private key as $s_{uis} = s_0 P_{uis}$. For a user with identity $UIS.Alice$ in the private cloud University of Stavanger, her public key can be generated as $P_{uis.alice} = H_1(UIS || Alice)$ and the PKG can generate her private key as $s_{uis.alice} = s_{uis} + s_{uis} P_{uis.alice}$.

4.3 Date Encryption and Digital Signature

In the cloud, one amongst the foremost necessary security issues are mutual authentication between shoppers and servers, protection of knowledge of knowledge of information confidentiality and integrity throughout data transmission by secret writing victimisation secret keys. In a very cloud victimisation united identity, any shopper and server has its distinctive identity and any shopper and server will get the identity of the other client/server by request with the PKGs. With HIBC, the general public key distribution are often greatly simplified within the cloud. shoppers and servers don't have to be compelled to raise a public key directory to induce the general public key of alternative shoppers and servers as in ancient public key schemes. If any shopper or server desires to encipher the info that transmitted within the cloud, the sender will acquire the identity of the receiver, then the sender will en-cript the info with receiver's identity.

4.4 Secret Session Key Exchange and Mutual Authentication

Identity-based cryptography is a public key cryptography scheme, it is much slower when it is compared with symmetric key cryptography. In practice, public key cryptography is not used for data encryption in most of the clouds. While in the cloud with HIBC, this secret symmetric key distribution can be avoided since identity-based cryptography can be used for secret session key exchange. According to [9], for every two parties in the

system using identity-based cryptography, it is easy for each one of the two parties to calculate a secret session key between them using its own private key and public key of other party, this is call identity-based non-interactive key distribution. For example, two parties Alice and Bob in a cloud with their public keys and private keys $P_{alice}, Q_{alice}, P_{bob}$ and Q_{bob} can calculate their shared secret session key by computing

$$K_s = \hat{e}(Q_{alice}, P_{bob}) = \hat{e}(Q_{bob}, P_{alice}) \quad (1)$$

This means in an exceedingly cloud victimization HIBC, every shopper or server will calculate a secret session key between it and therefore the different party it needs to speak with while not message exchange. This advantage of identity-based cryptography can't solely scale back message transmission however can also avoid session key revelation throughout transmission.

This secret session key can be used not only for data encryption, but also for mutual authentication [8]. We assume if a client with identity $Alice@UIS$ and a server with identity $Storage@google$ in the cloud want to authenticate each other. First, they can calculate a secret session key K_s between them. Then Alice can send a message to the server as:

$$Alice \rightarrow Server : Alice@UIS, M, f(K_s, Alice@UIS, Storage@google, M)$$

Here M is a randomly selected message and f is a one way hash function. Here, to compute the correct hash value, a correct secret session key K_s is needed. Since K_s computation requires Alice's private key and this private key can only be allocated from the PKG in the private cloud, thus Alice can be verified that she is a legal client of this cloud. Also the server can authenticate itself to Alice the same way. We can notice that this mutual authentication does not include any certification form a third party.

4.5 Key Escrow

For a system exploitation identity-based cryptography, key written agreement downside is inherent and may not be avoided since PKG is aware of the non-public keys of all the shoppers. whereas within the ranked identity-based cryptography system, solely the PKG within the same domain because the shoppers will is aware of their non-public keys. PKGs in different domains or at different levels cannot apprehend these non-public keys, such the key written agreement downside may be restricted in an exceedingly little vary.

V. CONCLUSION

The quick development of cloud computing bring some security issues similarly as several edges to net

purchasers. Current solutions have some disadvantages in key management and authentication particularly in a very hybrid cloud with many public/private clouds. during this paper, we have a tendency to portrayed the principles of identity-based cryptography heritage technique and gradable identity-based cryptography and notice the properties of HIBC match well with the protection demands of heritage cloud. we have a tendency to projected to use federate identity management and HIBC within the cloud and portrayed however will the system generate and distribute the general public and personal keys to purchasers and servers. Compared with the present Ws-Security approach, we will see our approach has its blessings in simplifying public key distribution and reducing SOAP header size. additionally we have a tendency to showed however the purchasers and servers within the cloud will generate secret session key while not message exchange and demonstrate one another with an easy manner mistreatment identity-based cryptography. additionally we will see the key written agreement downside of identity-based cryptography are often restricted with HIBC approach.

REFERENCES

- [1] Beak, J., Newmarch, J., Safavi-Naini, R., Susilo, W.: A Survey of Identity-Based Cryptography.
- [2] In: Proc. of the 10th Annual Conference for Australian Unix User's Group (AUUG2004), pp. 95–102 (2004)
- [3] Boneh, D., Franklin, M.: Identity-based Encryption from the Weil Pairing. In: Kilian, J. (ed.) CRYPTO 2001. LNCS, vol. 2139, pp. 433–439. Springer, Heidelberg (2001)
- [4] Chappell, D.: A Short Introduction to Cloud Platforms, <http://www.davidchappell.com/CloudPlatforms-Chappell.pdf>
- [5] Cocks, C.: An Identity-based Encryption Scheme Based on Quadratic Residues. In: Proceeding of 8th IMA International Conference on Cryptography and Coding (2001)
- [6] Crampton, J., Lim, H.W., Paterson, K.G.: What Can Identity-Based Cryptography Offer to Web Services? In: Proceedings of the 5th ACM Workshop on Secure Web Services (SWS 2007), Alexandria, Virginia, USA, pp. 26–36. ACM Press, New York (2007)
- [7] Gentry, C., Silverberg, A.: Hierarchical ID-Based cryptography. In: Zheng, Y. (ed.) ASIACRYPT 2002. LNCS, vol. 2501, pp. 548–566. Springer, Heidelberg (2002)
- [8] Horwitz, J., Lynn, B.: Toward Hierarchical Identity-Based Encryption. In: Knudsen, L.R. (ed.) EUROCRYPT 2002. LNCS, vol. 2332, pp. 466–481. Springer, Heidelberg (2002)
- [9] Mao, W.: An Identity-based Non-interactive Authentication Framework for Computational Grids. HP Lab, Technical Report HPL-2004-96 (June 2004)
- [10] Sakai, R., Ohgishi, K., Kasahara, M.: Cryptosystems based on pairing. In: Proceedings of the 2000 Symposium on Cryptography and Information Security, Okinawa, Japan (January 2000)
- [11] Shamir, A.: Identity-based cryptosystems and signature schemes. In: Blakely, G.R., Chaum, D. (eds.) CRYPTO 1984. LNCS, vol. 196, pp. 47–53. Springer, Heidelberg (1985)
- [12] Lim, H.W., Robshaw, M.J.B.: On identity-based cryptography and GRID computing. In: Bubak, M., van Albada, G.D., Sloot, P.M.A., Dongarra, J. (eds.) ICCS 2004. LNCS, vol. 3036, pp. 474–477. Springer, Heidelberg (2004)
- [13] Lim, H.W., Paterson, K.G.: Identity-Based Cryptography for Grid Security. In: Proceedings of the 1st IEEE International Conference on e-Science and Grid Computing (e- Science 2005). IEEE Computer Society Press, Los Alamitos (2005) Defining Cloud Services and Cloud Computing, <http://blogs.idc.com/ie/?p=190>
- [14] IBM Embraces Juniper For Its Smart Hybrid Cloud, Disses Cisco (IBM), <http://www.businessinsider.com/2009/2/ibm-embraces-juniper-for-its-smart-hybrid-cloud-disses-cisco-ibm>
- [15] http://en.wikipedia.org/wiki/Cloud_computing#cite_note-61
- [16] XML Signature Syntax and Processing (Second Edition) ,<http://www.w3.org/TR/xmlsig-core/#sec-KeyInfo>
- [17] Barreto, P.S.L.M., Kim, H.Y., Lynn, B., Scott, M.: Efficient algorithms for pairing-based cryptosystems. In: Yung, M. (ed.) CRYPTO 2002. LNCS, vol. 2442, pp. 354–368. Springer, Heidelberg (2002)
- [18] M. Turner, D. Budgen, and P. Brereton, “Turning software into a service,” *Computer*, vol. 36, no. 10, pp. 38–44, 2003.
- [19] T. O'Reilly, “What is Web 2.0: Design patterns and business models for the next generation of software,” O'Reilly Media, Tech. Rep., 2008. [Online]. Available: <http://www.oreillynet.com/pub/a/oreilly/tim/news/2005/09/30/what-is-web-20.html>
- [20] R. Buyya, C. Yeo, and S. Venugopal, “Market-oriented cloud computing: Vision, hype, and reality for delivering it services as computing utilities,” in

- Conference on High Performance Computing and Communications. IEEE, 2008.
- [21] A. Newman, A. Steinberg, and J. Thomas, Enterprise 2.0 Implementation. McGraw-Hill Osborne Media, 2008.
- [22] Amazon, "Amazon Elastic Compute Cloud (EC2)," Amazon Web Services LLC, Tech. Rep., 2009. [Online]. Available: <http://aws.amazon.com/ec2/>
- [23] Mosso, "Deploy and scale websites, servers and storage in minutes," Rackspace, Tech. Rep., 2009. [Online]. Available: <http://www.mosso.com/>
- [24] R. Buyya, C. Yeo, and S. Venugopal, "Market-oriented Cloud Computing: Vision, hype, and reality for delivering it services as computing utilities," in High Performance Computing and Communications. IEEE Press, 2008.
- [25] Google, "Google App Engine: Run your web apps on Google's infrastructure." Google, Tech. Rep., 2009. [Online]. Available: <http://code.google.com/appengine/>
- [26] T. Bain, "Is the relational database doomed?" ReadWriteWeb.com, 2008. [Online]. Available: http://www.readwriteweb.com/archives/is_the_relational_database_doomed.php
- [27] F. Chang, J. Dean, S. Ghemawat, W. Hsieh, D. Wallach, M. Burrows, T. Chandra, A. Fikes, and R. Gruber, "Bigtable: A distributed storage system for structured data," in USENIX Symposium on Operating Systems Design and Implementation, 2006.
- [28] G. DeCandia, D. Hastorun, M. Jampani, G. Kakulapati, A. Lakshman, Pilchin, S. Sivasubramanian, P. Voshall, and W. Vogels, "Dynamo: Amazon's highly available key-value store," in Symposium on Operating Systems Principles. ACM, 2007, pp. 205–220.
- [29] B. Johnson, "Cloud Computing is a trap, warns GNU founder Richard Stallman," The Guardian, Tech. Rep., 2008. [Online]. Available: <http://www.guardian.co.uk/technology/2008/sep/29/cloud.computing.richard.stallman>
- [30] J. McCabe, Network analysis, architecture, and design. Morgan Kaufmann, 2007. [Online]. Available: <http://books.google.co.uk/books?id=iddGPgR48MC>
- [31] A. Modine, "Web startups crumble under Amazon S3 outage," The Register, Tech. Rep., 2008. [Online]. Available: http://www.theregister.co.uk/2008/02/15/amazon_s3_outage_feb_2008/
- [32] J. Montgomery, "Google Apps sees 99.9reliability," Tech.Blorge, Tech. Rep., 2008. [Online]. Available: <http://tech.blorge.com/Structure:%20/2008/11/02/google-apps-sees-999-uptime-proves-cloud-reliability/>
- [33] J. Perez, "Google Apps customers miffed over downtime," IDG News Service, Tech. Rep., 2007. [Online]. Available: http://www.pcworld.com/businesscenter/article/130234/google_apps_customers_miffed_over_downtime.html
- [34] Kable, "Carter recommends 'g cloud' for gov it," The Register, 2009. [Online]. Available: http://www.channelregister.co.uk/2009/06/17/government_cloud_computing/
- [35] Environmental Protection Agency, "EPA report to congress on server and data center energy efficiency," US Congress, Tech. Rep., 2007.
- [36] R. Miller, "NSA maxes out Baltimore power grid," Data Center Knowledge, Tech. Rep., 2006. [Online]. Available: <http://www.datacenterknowledge.com/archives/2006/08/06/nsa-maxes-out-baltimore-power-grid/>
- [37] K. McIsaac, "The data centre goes green, the CFO saves money," Intelligent Business Research Services, Tech. Rep., 2007.
- [38] C. Wolf and E. Halter, Virtualization: from the desktop to the enterprise. Apress, 2005.
- [39] R. Talaber, T. Brey, and L. Lamers, "Using virtualization to improve data center efficiency," The Green Grid, Tech. Rep., 2009.
- [40] K. Brill, "The invisible crisis in the data center: The economic meltdown of Moore's law," Uptime Institute, Tech. Rep., 2007.
- [41] J. Brodtkin, "Gartner in 'green' data centre warning," Techworld, 2008. [Online]. Available: <http://www.techworld.com/green-it/news/index.cfm?newsid=106292>
- [42] Microsoft, "Azure services platform," Microsoft, Tech. Rep., 2009. [Online]. Available: <http://www.microsoft.com/azure/>
- [43] C. Metz, "The Meta Cloud - flying data centers enter fourth dimension," The Register, Tech. Rep., 2009. [Online]. Available: http://www.theregister.co.uk/2009/02/24/the_meta_cloud/
- [44] T. Kulmala, "The cloud's hidden lock-in: Latency," Archivd, 2009. [Online]. Available: <http://blog.archivd.com/1/post/2009/04/the-clouds-hidden-lock-in-latency.html>
- [45] D. Nurmi, R. Wolski, C. Grzegorzczak, G. Obertelli, S. Soman, L. Youseff, and D. Zagorodnov, "The Eucalyptus open-source cloud-computing system," in Cloud Computing and Its Applications, 2008.

- [46] J. Abbate, *Inventing the internet*. MIT press, 1999.
- [47] I. Foster and C. Kesselman, *The grid: blueprint for a new computing infrastructure*. Morgan Kaufmann, 2004.
- [48] G. Briscoe and P. De Wilde, "Digital Ecosystems: Evolving service-oriented architectures," in *Conference on Bio Inspired Models of Network, Information and Computing Systems*. IEEE Press, 2006. [Online]. Available: <http://arxiv.org/abs/0712.4102>
- [49] G. Briscoe, "Digital ecosystems," Ph.D. dissertation, Imperial College London, 2009.
- [50] L. Rivera Le´on. *Regions for Digital Ecosystems Network (REDEN)*. [Online]. Available: <http://reden.opaals.org>.

Effective Handover Technique in Cluster Based MANET Using Cooperative Communication

Suryakumar.V, Dr. V. Latha

Applied Electronics Department, Velammal Engineering College, Chennai, India
Electronics and Communication Department, Velammal Engineering College, Chennai, India

Abstract— Mobile ad hoc networks (MANETs) are becoming increasingly common now a days and typical network loads considered for MANETs are increasing as applications evolve. This increases the importance of bandwidth efficiency and requirements on energy consumption delay and jitter. Coordinated channel access protocols have been shown to be well suited for MANETs under uniform load distributions. However, these protocols are not well suited for non-uniform load distributions as uncoordinated channel access protocols due to the lack of on-demand dynamic channel allocation mechanisms that exist in infrastructure based coordinated protocols. We have considered a lightweight dynamic channel allocation algorithm and a cooperative load balancing strategy that are helpful for the cluster based MANETs and an effective handover technique to improve the increased packet transmission mechanism. This helps in reduce jitter, packet delay and packet transfer speed, we use a novel handover algorithm to address this problem We present protocols that utilize these mechanisms to improve performance in terms of throughput, energy consumption and inter-packet delay variation (IPDV).

Keywords— MANET, handover, dynamic channel allocation, cooperative communication.

I. INTRODUCTION

An ad hoc network is a decentralized form of wireless network. The network is ad hoc because it does not depend on a preexisting infrastructure, such as routers in wired networks or access points in managed wireless networks.

A mobile ad-hoc network [1],[3],[5] is a self-configuration, infrastructure less network connected wirelessly. Each system in a MANET is free to move independently in Omni direction and will change its link to various other devices frequently. MANET's are a kind of ad-hoc network that has a routable networking environment above a linked layer ad-hoc network. MANET's consist of peer to peer , self-forming and a self-healing network.

Cooperative wireless network [1] are the model allowing coordinated operation among two or more wireless network out fitted with two or more communication device. It helps in network utilization Cooperative load balancing [1] is used to increase the capacity combined with the reliability of application. It is used to balance traffic nodes across various WAN [8],[11] without any complex protocol. Cooperative Load balancing aims to optimize resource usage and maximize throughput with minimum response time and to avoid overload of any resource. If a wireless user travels from one area of coverage to another area within the call duration then that call has to be switched to new base station. This mobility is obtained by a handover mechanism [17].

Process of data transfer in wireless communication to maintain the continuity with its own signal strength direction and decision making. Below given are some of the handover techniques [17] that belong in wireless ad-hoc networks. Handover between one or more base stations of the similar network is called Horizontal Handover.

In handover the mobile node changes after one cell to extra of the same area to maintain the signal strength and quality. There are two types in horizontal handover, the horizontal handoff between two base stations under the equal base station is recognized as Intra system Handoff. In Intersystem, handover works with the different base station (BS). It takes within the intra system when a mobile terminal gets access to the single admittance router and makes path into the planned colony of further admission router within the present network.

Vertical Handover occurs in diverse of network technologies such that between various access points. A base place of a network handover is then again classified into ascendant, downhill, upright level transportable trick meticulous system assisted and web measured mobile assisted handover.

The existing system provided with the packet transfer from one cluster to another within a system that are dynamically allocated. We proposed a dynamic channel allocation algorithm for the dynamically arranged channel and a novel MAC protocol for a non-uniform cooperative

channels in MANET. This helps in increasing throughput, reduce packet delay and jitter in the system.

- Thus the proposed system works on Cooperative load balancing algorithm is used for non-uniform load distribution system.
- A novel MAC [1] protocols proposed with MH TRACE algorithm[1],[9].
- Applying DCA(Dynamic channel allocation) and Cooperative load balancing to TRACE [1],[6],[18].
- CDCA-TRACE(Coordinated Dynamic Channel Allocation) algorithm is proposed by combining DCA and CLB algorithm[1] .

The performance parameters are based on the throughput, energy efficiency, network connectivity and packet transfer functions. These parameters are responsible for the effective packet transfer.

The network throughput is the amount of data moved successfully from one place to another in a given time period. They are typically measured in bits per second (bps) and given by the equation

Throughput = Amount of data moved / Time period

With the fastest development in the wireless networks the energy efficiency of wireless networking protocols becomes a concern to many wireless networking stakeholders. Different wireless networking protocols have different energy efficiency measures to reduce the power consumption according to their payload, cover area Network is a group of two or more devices that can communicate.

Network connectivity describes the extensive process of connecting various network parts to one and other, for example, through the use of routers, switches and gateways, and how that process works.

The packet transfer is the process by which the number of packet received per the number of packets sent to the destination, this ratio is called packet delivery ratio given by the equation.

The existing system provided with the process of packet transfer from one cluster to another within a system that are dynamically allocated. Proposed a dynamic channel allocation algorithm for the dynamically arranged channel and a novel MAC protocol for a non uniform cooperative channels in MANET. This helps in increasing throughput, reduce packet delay and jitter in the system.

II. EFFICIENT DATA TRANSFER INCOOPERATIVE NETWORK

The existing system is explained using the flow diagram as shown below in figure 1 shows the flow chart explaining the complete process in existing system

- . Selection of nodes. The nodes that are to be included in a cluster are selected dynamically based on the energy level and based on the dynamic search distance vector routing protocol as shown in the figure 2.

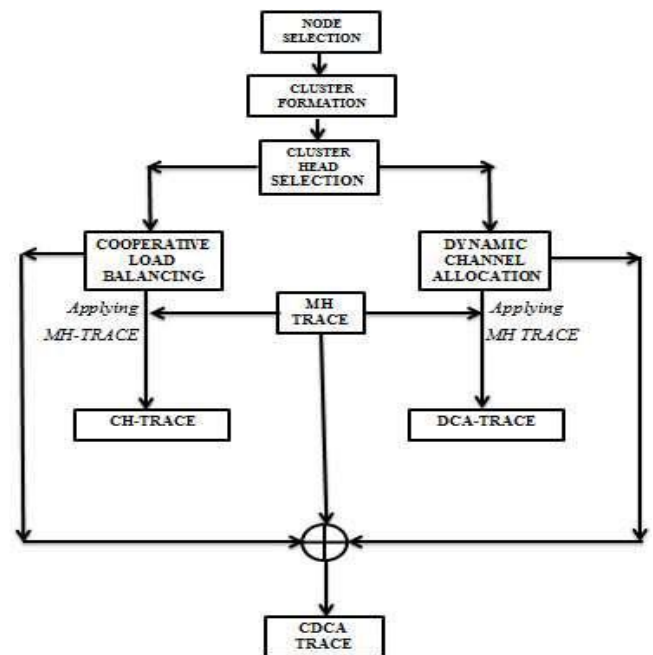


Fig.1: Flow Diagram of Existing Method

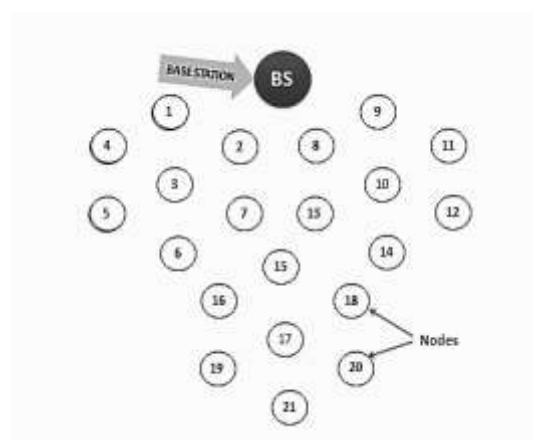


Fig.2: Selection Of Nodes

- Formation of clusters and CH. thus by the DSDV algorithm the clusters are formed and based on the energy level of the nodes choosing the best among them becomes the cluster head as shown in the figure 3. There are 3 different clusters that are shown below with different colors .the cluster heads are represented in hexagon shaped, figure 3 shows the formation of clusters and the CH's node 3,10,17.

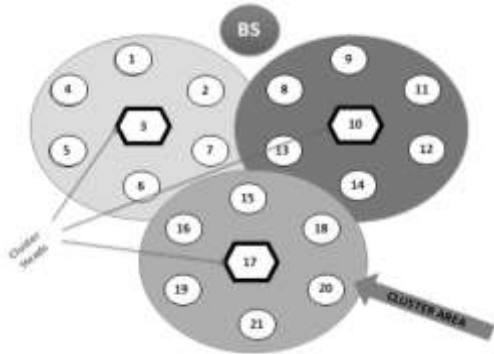


Fig.3: formation of clusters and cluster head

- **Function of cluster head.** The cluster head does the function of collecting the data of the cluster members and maintains the regular update of the cluster members, since it is a cooperative cluster communication the CH even collects the information from the neighboring nodes. This helps the cluster to automatically help or it can borrow the nodes if any of the path is dropped, below given figures show the function of cluster head.

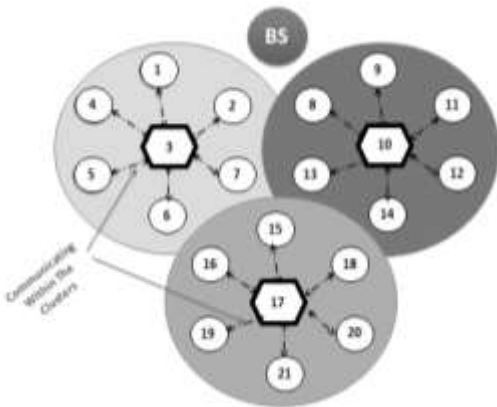


Fig.a.

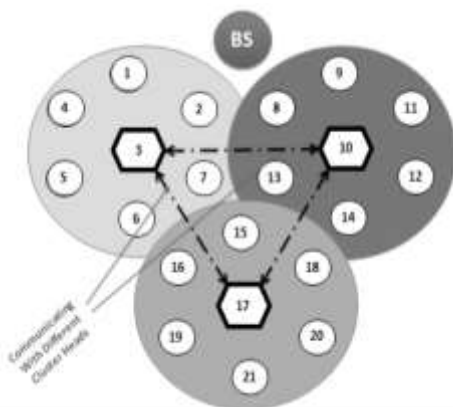


Fig.b.

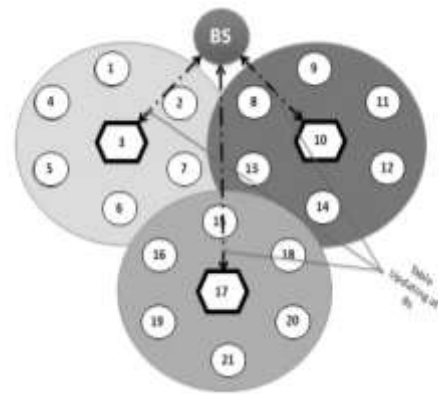


Figure c.

Fig.4: A) CH Collecting Cluster Members Details, B) CH Sharing The Cluster Details With Neighboring Clusters, C) Base Station Collecting And Updating The MAC Table

Thus the above function is processed by using the following algorithms that are explained in the following chapters.

A. **Dynamic Channel Allocation Algorithm**

The dynamic channel allocation algorithm is mainly functions in places of non-uniform loads. This algorithm helps the channel coordinator with the increasing local network load by increasing the sharing of bandwidth. By using DCA algorithm the channel controller continuously monitors the power level in all available channels in the network and will access the availability of the channels by comparing them by measuring the power level by threshold status.

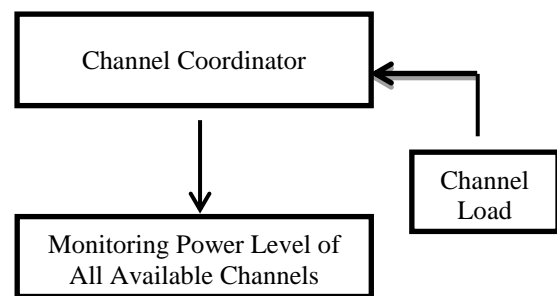


Fig.5: Flow diagram explaining the dynamic channel allocation algorithm

Considering if the load in channel controller is beyond capacity and measured power is minimum, the channel coordinator seeks and uses the additional channel with lowest power level measured. Once the channel coordinator starts to use another channels, the transmission level increases the power level measurement of that channel for nearby channel controllers this intern prevents them from accessing same channel that is been

used currently. Also the local network load decreases the controller which do not need some channel, will stop channel transmission in that particular channel and making it available for other channel controllers.

B. Cooperative Load Balancing Algorithm

The cooperative load balancing algorithm is also used to consider the issues of non-uniform load distribution but by the use of other nodes in the network. The aim of this algorithm is that , each active nodes in cooperative network continuously monitor the load of the channel coordinator and then switches from heavily loaded coordinator to the coordinators with available resources.

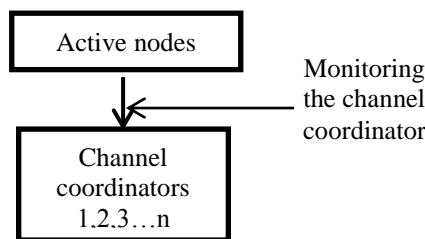


Fig.6: Flow Diagram Explaining Cooperative Load Balancing Algorithm

These active nodes detect the rise and fall of the channel by the coordinators and transfers load to other channel coordinators which has considerable resources. These resources vacated by the nodes are now available for other nodes which do not have any other channel coordinators. Thus increasing the total number of nodes that access the same channel hence increases the throughput.

C. MH Trace Algorithm

In MH-TRACE, some nodes take the role of channel coordinators called as cluster-heads. Each nodes are made up of super frames and these super frames are subdivided into different sub frames.

- **Control sub frame.** This control sub frame sends signal between the nodes and the cluster heads. This sub frame sends beacon packets by using the beacon slot this allows CH announcing its existence. The other part is the CA slot or canal access slot that helps in interference elimination. The contention slot takes care of the transmission scheduling. The IS slot sends short packets to notify the neighboring nodes to cluster head.

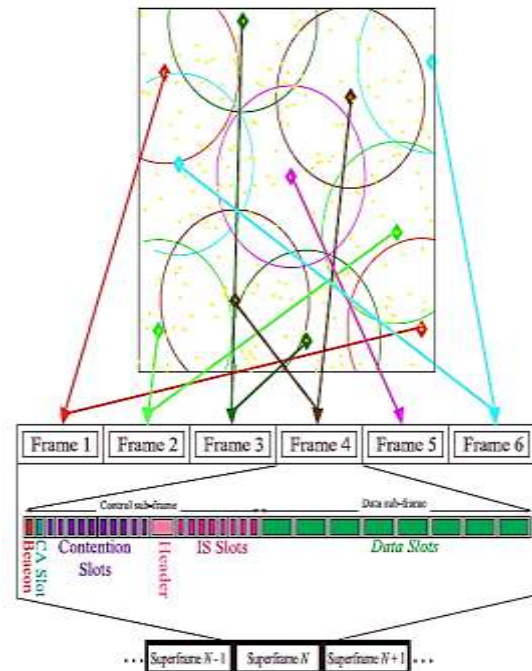


Fig.7: Snapshot of MH-TRACE Clustering and Medium Access , the Diamond Shaped are CHs.

- **Data sub frame.** this sub frame transmit data payload. In the data slot the CH receives as it has a reservation in super frame and the CH drops the reservation if the IS packets are lost.

In the beginning of the frame each CH calculates the available data slots and information of beacon. Thus this allows the data transfer from one cluster to another in a more streamline way in dynamic nodes mainly in cooperative networks. From the above figure 4 the data is to be transferred from a source node say node 2 to the destination node18, this data transfer takes place in different paths

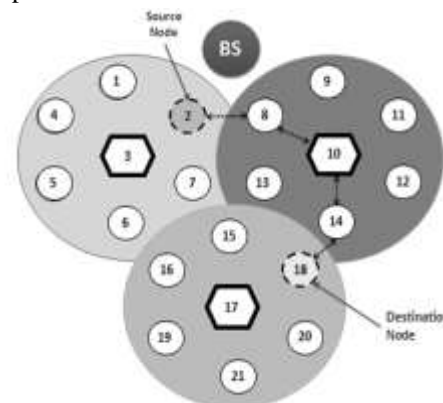


Fig.8: Data Packet Transfer From Node 2 To Node 18 but by choosing the best path with the help of the cluster head the routing path is found easily. Thus increases speed of the data transfer in the system.

D. *DCA TRACE, CH TRACE And CDCA TRACE*
 DCA-TRACE helps CHs to operate in more than one frame per super frame, if it is overloaded. Instead of selecting and operating in the less noisy frame as that in MH-TRACE, the DCA-TRACE is based on the level of the load, CHs decides the number of frames they can require and resourcefully chooses as many frames from the least noisy ones. DCA-TRACE includes additional mechanisms on top of MH-TRACE:

- a. a mechanism to keep track of the interference level in each frame from other CH;
- b. a mechanism to sense the interference level in each data slot in each frame from the transmitting nodes.

In MH-TRACE, cluster heads use this mechanism to choose the less interference frame for themselves. DCATRACE makes use of the such structure. However, in order to maintain temporary changes in the interference levels that may occur due to CH resignation or unexpected packet drops, an exponential moving average update mechanism is considered to determine the present interference levels in each frame. At the end of each frame, the interference level of the Beacon slots and CA slots are continuously updated with the measured values in that frame using.

$$I_{k,t} = \begin{cases} M_{k,t} & \text{if } I_{k,t-1} < M_{k,t}; \\ (1 - \alpha)I_{k,t-1} + \alpha M_{k,t} & \text{o. w. ,} \end{cases}$$

Where $I_{k,t}$ and $I_{k,t-1}$ are the interference levels of the k^{th} number slot in the current and the previous superframe, respectively. $M_{k,t}$ is the calculated interference level of the k^{th} slot in the current super frame, and as a smoothing factor, which is set to 0.2 in this simulations. The interference equal of the frame is taken as the maximum interference level among the interference levels of the Beacon and CA slots.

Another mechanism that DCA-TRACE computes with the MH-TRACE is the dynamically assigning the data slots. In MH-TRACE the data slots are assigned in a serialized order. On the other hand, since DCA-TRACE introduces channel borrowing the CH had to cease from reallocating a data slot instead must allocate another data slot that has a lower interference value from that had borrowed by another CH. In the TRACE protocols, nodes resist for channel access from one of the CHs that have available data slots around them.

After successfully obtaining the contention, CH do not monitor the available data slots of the CHs around them. Since the network load is dynamic in nature, a cluster having lots of free spaced or available data slots may become heavily loaded at the time of data stream. In order to overcome this issue, each nodes should consider the load of the CH not only when in the first contention for

channel access but also after obtaining a reserved data slot during the entire time of their data stream.

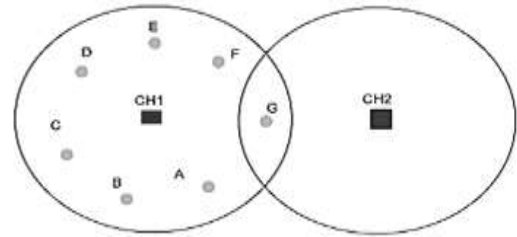


Fig.9: Demonstrating Scenario of Collaborative Load Balancing

In DCA-TRACE, once one of the CH allocates all of its available slots, it activates the algorithm to select an extra frame. However, accessing one additional frame might not always be possible, if the interference levels on all the other frames are comparatively very high. In case if accessing additional frames it increases the interference in the Beacon slots and Header slots of these frames and may cause Cluster Head to reassign and reselect in the rest of the network that provisionally affects the ongoing data streams on the resigned cluster heads. By using additional frames, the increases in interference in the IS slots and data slots of the new frame and decreases the potential extent of these packets that are able to reach finally.

In order to overcome such difficulties, we propose CMH-TRACE and CDCA-TRACE, which adds cooperative CH monitoring and reselection of MH-TRACE and DCA-TRACE, respectively. In CMH-TRACE and CDCATRACE, nodes continuously monitor the available data slots at the CHs around themselves broadcast by the Beacon messages. When all the available data slots for a CH are allocated, with a probability p , the active nodes attempt to trigger the cooperative load balancing algorithm. When the cooperative load balancing is activated, the node that is currently using a particular data slot from a heavily loaded cluster head contends for data slots from the nearby cluster heads while keeping and using its reserved data slot until it secures a new data slot from another CH.

III. HANDOVER TECHNIQUE WITH CLUSTERS

This existing system has to concentrate on handover function too, in order to prevent data loss within or outer networks. This makes the system more active, in any of the node drops from transmission the other takes in charge to pass the data to the next cluster.

In order to perform the effective way of handover mechanism two important algorithm has been proposed in

this system they are distance vector routing protocol and the tour planning algorithm

A. Distance Vector Routing Algorithm

A DSDV algorithm requires the routing information of the neighbor topology changes periodically. It manipulates with the distance of the nodes in a network. Calculates the direction and distance of any link in a network Updates are done periodically where the routing table are sent to all neighbor nodes

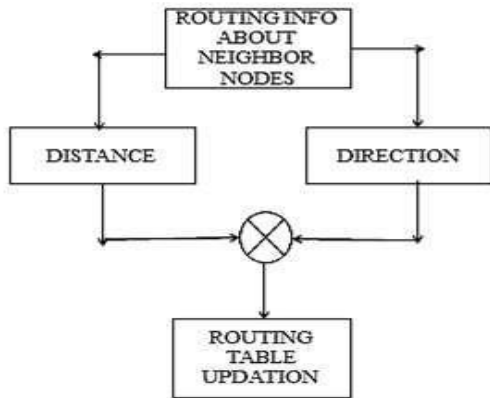


Fig.10: flow diagram explaining distance vector routing

B. Tour Planning Algorithm

By knowing the available number of the nodes in the network, route trace is been done. By this technique when a node is dropped or lost or less energy efficient then choosing of more effective node to transfer the packets to the network. Once the path is known the data is transferred automatically.

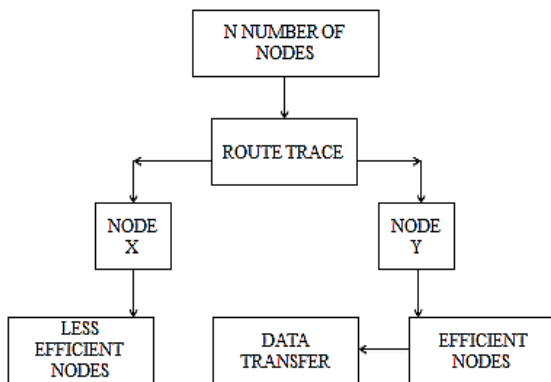


Fig.11: Flow Chart Explaining the Tour Planning Algorithm

The hand over technique is been introduced with the help of tour selection protocol is used so as to find the suitable path for the cluster node transfer. We have mainly concentrated in packet loss and delay less connectivity in cooperative communication. Below given is the process of performing the hand over in the system in a cooperative cluster communication.

- **Cluster Monitoring.** Since the function of CH is to monitor the cluster and its member activities it also looks for the neighbor in case of any emergency.

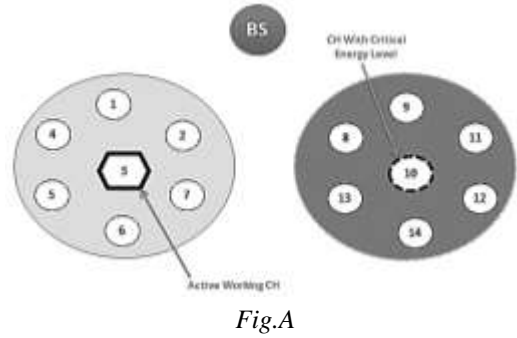


Fig.A

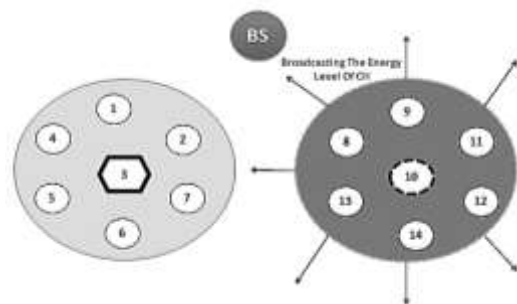


Fig.B

Fig.12: A-Ch 3 is Continuously Monitoring the Cluster and Member Nodes, B- the CH 10 Sends the Message to its Neighboring Nodes.

This makes an up to date information of the clusters. This is the function of the cooperative networks that includes the channel borrowing etc.

- **Energy Transfer.** Since the CH 10 has the critical energy the neighbor cluster tries to help the node thus the hand over function is done within the cluster networks. Below shown is the energy transfer from one system to another.

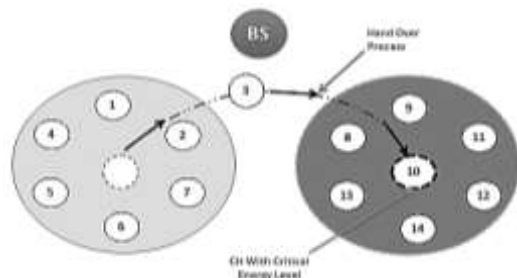


Fig.13: Energy Transfer Attempt From CH 3 to CH 10.

Above shown is one of the cluster head has the critical energy that is been indicated to the entire network, thus the nearest and the best node helps the cluster to gain control or share its energy in order to avoid the data loss.

- **Cluster Heads After Handover.** By effective handover technique the CH has been to the active stage and the node that delivered has its position within the cluster or any suitable clusters. This clusters formed are with new cluster heads and are been updated in the base station, this process continues from one cluster to another.

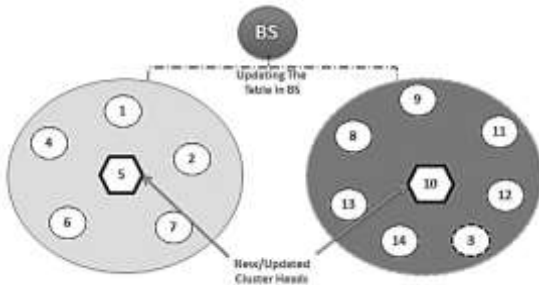


Fig.14: New and Updated Cluster Heads

IV. PERFORMANCE COMPARISON

The performance measure is done base on these important parameters such that comparing the performance with three different networks, the non-cooperative networks , cooperative networks and the cooperative network with hand over.

The parameters include the throughput, network connectivity, packet received, packet transfer and the energy efficiency of the proposed system .

A. Packet Received

The below given graph represents packet received during the transmission of packets from one cluster to other. The comparison shown between the two network is clear that the packet received in given time is gradually increasing in cooperative network compared with the non-cooperative network. Packets received are measured 0.2×10^3 per second. Packet delivery ratio = $\frac{\text{received packets}}{\text{sent packets}}$

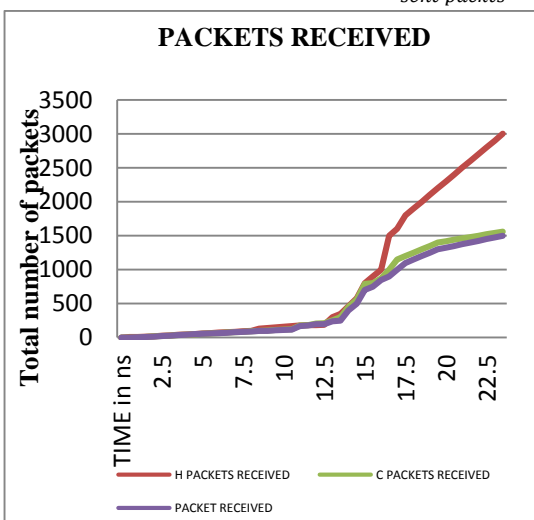


Fig.15: Graph Describing Packet Received.

B. Network Connectivity Delay

Below given graph shows the network connectivity delay

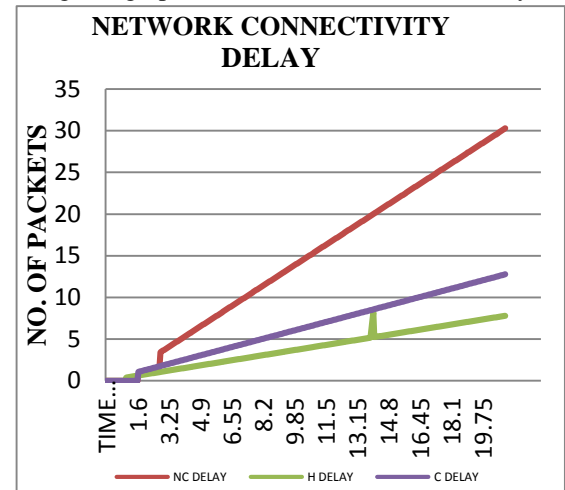


Fig.16: Graph Describing Network Delay comparing the cooperative network and non-cooperative network. Below shown Figure 4.10 is that the cooperative network has delay time less compared with the other network.

C. Energy Efficiency

Below given graph shown figure 4.11 the energy dissipation between cooperative network and non-cooperative network.

The graph given is gradual energy loss on both the networks comparatively cooperative networks has minimum dissipation of energy. The energy used during the transmission are given in joules. Energy (J) = coulomb(C) x voltage (V)

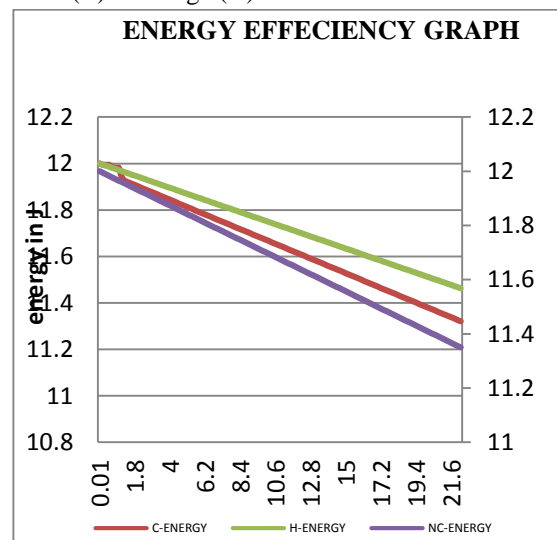


Fig.17: Graph Describing Energy Efficiency

V. DISCUSSION AND CONCLUSION

By the above simulation and execution of the proposed system it is clear that the performance level in case of delay, trough put, and packet loss is reduced in cooperative network using MANET compared with the

other ad-hoc networks. The above give simulated output shows the function of the cooperative network in packet data transferring using cluster based MANET.

The performance measure for packet delay, time delay, throughput and energy deception are represented graphically comparing cooperative network verses non-cooperative network. According to the result it is clear that the cooperative network has much more efficient way of data packets transfer compared to any other non-cooperative network

For the delay less packet transfer through the high traffic network, the future work will focus on the effective handover technique to improve the packet transfer. This helps in the improvement in throughput, reduced jitter and traffic management .a novel cluster management algorithm can be used and decision making algorithm for channel heads in order to make out in coordinated network.

REFERENCES

- [1] Bora Karaoglu&Wendi Heinzelman (2015), ‘Cooperative Load Balancing and Dynamic Channel Allocation for Cluster-Based Mobile Ad Hoc Networks’, IEEE Transactions on Mobile Computing, Volume: 14, Issue: 5 ,Pages: 951 – 963.
- [2] Brian Keegan & Mark Davis (2006), ‘An Experimental Analysis of the Call Capacity of IEEE 802.11b Wireless Local Area Networks for VoIP Telephony’, Irish Signals and Systems Conference, 2006. IET ,Pages: 283 – 287.
- [3] Celimuge Wu, Kazuya KumeKawa&Toshihiko Kato (2009), ‘A MANET protocol considering link stability and bandwidth efficiency’, International Conference on Ultra Modern Telecommunications & Workshops Pages: 1 – 8.
- [4] Guanlin Chen & Ying Wu (2016), ‘A wireless intrusion Alerts Clustering Method for mobile internet’, China Communications,Volume: 13, Issue: 4,Pages: 108 – 118.
- [5] Haiying Shen & Ze Li (2015), ‘A Hierarchical Account-Aided Reputation Management System for MANETs’, IEEE/ACM Transactions on Networking ,Volume: 23, Issue: 1, Pages: 70 – 84.
- [6] Jianping Jiang, Ten-Hwang Lai&N. Soundarajan(2002) ‘On distributed dynamic channel allocation in mobile cellular networks’ , IEEE Transactions on Parallel and Distributed Systems , Volume: 13, Issue: 10 ,Pages: 1024 – 1037.
- [7] Komali ,RS. &MacKenzie ,AB. (2009) , ‘Analyzing Selfish Topology Control in Multi-Radio Multi-Channel Multi-Hop Wireless Networks’,IEEE International conference on Communications Pages: 1 – 6.
- [8] Sarbani Roy, NatwarDarak&AsisNasipuri (2014), ‘A game theoretic approach for channel selection in multi-channel wireless sensor networks’ ,2014 11th Annual High Capacity Optical Networks and Emerging/Enabling Technologies (Photonics for Energy),Pages: 145 – 149.
- [9] Tavli ,B. &Heinzelman ,WB. (2004), ‘MH-TRACE: multihop time reservation using adaptive control for energy efficiency’, IEEE Journal on Selected Areas in Communications, Volume: 22, Issue: 5 Pages: 942 – 953.
- [10] Wei Song ,WeihuaZhuang&Yu Cheng (2007) , ‘Load balancing for cellular/WLAN integrated networks’ , IEEE Network , Volume: 21, Issue: 1 Pages: 27 – 33.
- [11] Xiaomin Ma&Xianbo Chen (2008), ‘Performance Analysis of IEEE 802.11 Broadcast Scheme in Ad Hoc Wireless LANs’,IEEE Transactions on Vehicular Technology, Volume: 57, Issue: 6 ,Pages: 3757 – 3768.
- [12] AndrGuerreiro J. R., Souza J. L. R., “Improving NS-2 network simulator for IEEE 802.15.4 standard operation,”in Proc. 5th Simpsio de Informtica, Sep. 2013, pp. 432–443.
- [13] A. Morton and B. Claise. (2009, Mar.). Packet delay variation applicability statement. RFC 5481 (Informational), Internet Eng. Task Force
- [14] Karaoglu B., and Heinzelman W.,(2010) “Multicasting vs. broadcasting:What are the trade-offs?” in Proc. IEEE Global Telecommun. Conf., pp. 1–5.
- [15] Patel Ahmed, QassimQais, Wills Christopher (2009),“A survey of intrusion detection and prevention systems”, Information Management and Computer Security, vol.18, no.4, pp 277-290.
- [16] Karaoglu B. and Heinzelman W.,(2012) “A dynamic channel allocation scheme using spectrum sensing for mobile ad hoc networks,” in Proc. IEEE Global Telecommun. Conf. ., vol. 59, no. 5, pp. 707–719.
- [17] Quang B., Prasad R., and Niemegeers I. (2012),“A Survey on Handoffs –Lessons for 60 GHz Based Wireless Systems,” IEEE Comm. Survey & Tutorial, Vol. 14, No.1, 1st Quarter, pp. 64-86
- [18] Refaei M. T., DaSilva L. A., Eltoweissy M., and Nadeem T. (2012), “Adaptationof reputation management systems to dynamic network conditions in ad hoc networks,” IEEE Trans. comput., vol. 59, no. 5, pp. 707–719.
- [19] Bettstetter C. (2002), “On the minimum node degree and connectivity of a wireless multihop network,” in

- In Proc. ACM Intern. Symp.on Mobile Ad Hoc Networking and Computing (MobiHoc), pp. 80–91.
- [20]Chen Y. (2009), “Analytical Performance of Collaborative Spectrum Sensing Using Censored Energy Detection,” IEEE Transactions on Wireless Communications, vol.9, no.12, pp.3856-3865.

Efficient Routing Scheme for Mobile Wireless Sensor Networks using Hybrid multi-hop LEACH

Mr Mallikarjun Mugli¹, Dr A. M. Bhavikatti²

¹Assistant Professor, CSE Dept, BKIT, Bhalki (Kar) , India

²Professor, CSE Dept, BKIT, Bhalki(Kar), India

Abstract— A Wireless Sensor Network (WSN) consists of spatially distributed autonomous sensors connected via a (wireless) communications infrastructure to cooperatively monitor, record and store physical or environmental conditions, such as temperature, sound, vibration, pressure, motion or pollutants. This makes it more popular in emerging technologies that are used in our daily life. While WSNs have many benefits, there are also a few drawbacks. A big area of research into WSNs has concentrated on creating routing protocols that are energy efficient. It is a tremendous challenge to design routing protocols for applications of WSNs, which are mobility centric and energy efficient; because of network topology is often being changed. The concept of clustering offers more benefit than the other flat based routing protocols. A common side-effect of the many-to-one traffic pattern is the hot spot issue, which characterizes the majority of wireless sensor networks: nodes having the optimal path to the sink become overloaded with traffic from all other areas of the network which cause it to lose energy at a faster rate than the other nodes. This research work is aimed at evaluating and validating the proposed Mobile Data Collector-based routing protocol (MDC maximum residual energy LEACH) with A Novel Application Specific Network Protocol for Wireless Sensor Networks routing protocol (Hybrid multi-hop LEACH). A computer simulation was employed to obtain the results that have indicated an improvement in the overall energy efficiency of the network.

Keywords—LEACH, Mobile Data Collector, Energy Efficient and Hierarchical routing protocol.

I. INTRODUCTION

Because of the advances recently made in wireless communications and micro-electronics, wireless sensor networks (WSNs) are expected to become ever-present in the daily life of mankind [1]. Further, WSNs have already surfaced as a hot area of research, which consist of many sensor nodes that are low cost and have the ability to process and communicate. WSNs must be able to operate autonomously for extended lengths of time in the majority of

their applications even though their sensors are tiny devices that possess power supplies which are limited. Appropriate solutions are necessary at each layer of the networking protocol stack so that the usage of energy can be better managed and the network lifetime as a whole can be increased. Most particularly, a tremendous amount of attention has been given to routing protocols that are energy aware at the network layer. This is because wireless communication has been well established to be the key cause of the consumption of power in WSNs.

The WSN's network layer has the responsibility of delivering packets and implementing an approach for addressing to take care of this task. It primarily creates routes for transmitting data throughout the network. Routing in WSNs is more challenging than in the common ad-hoc networks. This is because they possess resources that are limited in regards to the available power, processing ability and communication. These are considerable constraints to all applications in the sensor networks. Moreover, route maintenance is a difficult task because of frequent modifications to the topology resulting from these constraints [1, 2].

When considering the perspective of the network organization, there are roughly two main categories for the classification of routing protocols: hierarchical routing and flat routing. Hierarchical routing protocols have been seen as having greater scalability and being more energy-aware in the context of WSNs. Nodes play various roles in the network and are usually arranged into clusters in the hierarchical-based routing. The technique of sensor nodes in a network organizing themselves into groups in relation to particular prerequisites or metrics is known as clustering. Each cluster/group possesses a leader known as a cluster head (CH) and other member nodes (MNs) that are ordinary. The cluster heads can be arranged into further hierarchical levels. On the other hand, in a flat topology, all of the sensor nodes play the same role and have the same functionality as each other in the network. A flat routing protocol tries to locate a path to the sink, hop by hop, making some form of flooding whenever a node needs to transmit data. In

networks that are relatively small, flat routing protocols are quite effective. On the other hand, they do not scale to large and dense networks very well as, usually, all of the nodes are alive and create greater processing and bandwidth usage [3, 4 and 5].

Single-sink data collection naturally results in a many-to-one traffic pattern from the sensing nodes to the sink. This single-sink data collection is the normal use in WSNs. It is usual for routing protocols to stay away from lossy links at any cost, because WSNs are very resource limited. Clustering approach provides a hierarchical architecture that is more easily scaled and has less power usage; therefore, it provides the entire network with a longer lifetime. Most of the sensing, processing of data and activities involved in communication can be carried out within the clusters. However, flat and cluster based routing protocols have own benefits but both created communication holes within the network.

Energy and routing holes are the major types of communication holes. The energy hole problem is a key factor in WSNs which disturbs the lifetime of network because sensor nodes normally perform as originator and router of data. The communication obeys a many-to-one and converge-cast pattern, where nodes transmit heavy communication load near the base station, causing increased energy dissipation rate. The primary and utmost objective in communication network is efficient routing. The efficient routing protocol in WSNs is to increase the quality of network services and prolong the network lifetime. Two types of "routing holes" can exist in real time sensor networks such as redeployable and non-redeployable holes [6, 7 and 8].

The MDC maximum residual energy LEACH was proposed for the validation of communication holes arguments. It is a protocol for multi-hop cluster-based routing for environmental applications in WSNs. It makes use of a mobility model with a pre-defined trajectory and transmits a beacon message at 5 sec intervals to the cluster heads (CHs) and the base station (BS). This beacon message has MDC location and the residual energy level of MDC. When the CHs received the beacon message from MDC, they choose the maximum residual MDC for the routing of sensed aggregated data towards the BS or some central location. The general network parameters are as follows: firstly, they possess a fixed BS that is situated far away from the area of the sensors; secondly, they are homogenous; thirdly, they are controlled by energy and finally, the communication process does not use any high energy sensor node. Data fusion is the optimal way to avoid the duplicate and overloaded data that is typically used in various existing hierarchical protocols of cluster-based routing.

This paper has been arranged as follows. Related work of energy efficient routing protocol is presented in Section 2. A

description of the proposed MDC maximum residual energy LEACH protocol is given in Section 3. The performance evaluation of the proposed protocol is given in Section 4. Finally, the conclusions have been drawn in Section 5.

II. RELATED WORKS

The development of routing protocols in WSNs is experiencing a tremendous research effort presently. These protocols are being development on the basis of application specific needs and the particular architecture of the network. Nevertheless, when creating routing protocols for WSNs, several factors must be considered. As energy efficiency directly affects the network lifetime, it is the most important factor of all. In the literature, it has been found that there has been some effort to pursue WSNs energy efficiency.

A. A Modified SPIN for Wireless Sensor Network

When the data-centric method is used as the basis of the routing protocols it is appropriate to be used in applications performing in-network aggregation of data to produce data dissemination that saves energy. In [9], an altered SPIN protocol was proposed named M-SPIN, Its performance was compared with the commonly used SPIN protocol that makes use of broadcast communication.

The Modified-SPIN (M-SPIN) protocol sends data to a sink node only rather than throughout the entire network. A substantial amount of total energy can be saved as the total number of packets being transmitted is less in the proposed protocol. The proposed M-SPIN protocol makes use of the hop-count values of the sensor nodes for WSNs. In a typical SPIN protocol, negotiation is also performed before the actual data is transmitted; however, in M-SPIN, the nodes closer to the sink node transmit REQ packets as a reply to an ADV packet transmitted by the source node. As a result, the dissemination of the data is towards the sink or to the neighboring nodes on towards the sink node. The M-SPIN protocol gains energy savings by not transmitting packets to the direction that is opposite the sink node. The M-SPIN protocol is illustrated in Fig. 1.

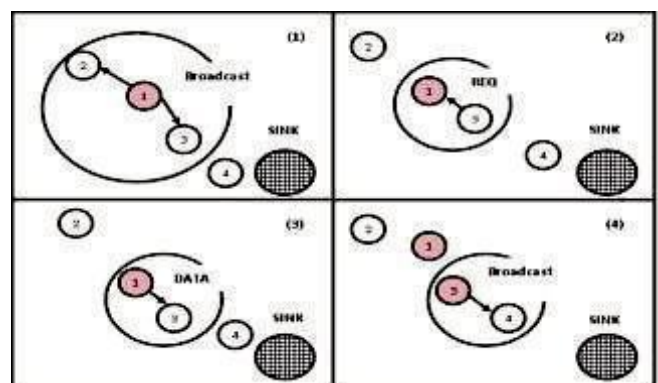


Fig.1: The M-SPIN Protocol

B Threshold Sensitive Energy Efficient Sensor Network Protocol (TEEN)

Threshold sensitive Energy Efficient sensor Network protocol (TEEN) [10] proposes a reactive routing protocol specifically applicable to time sensitive applications. TEEN adopts the principle of hierarchical clustering. Sensor nodes are grouped together that is geographically close to each other with one common cluster head. For the purposes of this section, these cluster heads are seen as first layer cluster heads. The first layer of cluster heads collect data messages from the sensor nodes within its cluster, aggregate the data messages and forward the aggregated messages to a higher layer. The main disadvantage of TEEN is that if the hard threshold is never reached, no data messages will be forwarded towards the base station.

C. A Novel Application Specific Network Protocol for Wireless Sensor Networks

The newly developed self-organizing Hybrid Network Protocol for WSNs has been created on the basis of a cluster-based hierarchical architecture and multi-hop routing. This basis has been used so that energy efficiency can be improved and the lifetime of the network is extended. Multi-hop routing is employed in the hybrid protocol for inter-cluster communication between CHs and the BS rather than direct transmission. In this way, the transmission energy can be minimized and the energy load can be distributed throughout the entire network in an even manner. In addition, the same suppositions as created in the LEACH protocol are created in this protocol; the Carrier Sense Multiple Access (CSMA) MAC protocol, similar to the network model, is employed to reduce the potential of a collision taking place during the set-up phase. The node in the network knows of its own location. This is important to provide the multi-hop routing between CHs and is accomplished by using the Global Positioning System (GPS) technology. It makes use of a rotation of the local base stations (CHs) that is randomized so that the load of the energy can be allocated consistently among the sensors in the network [11].

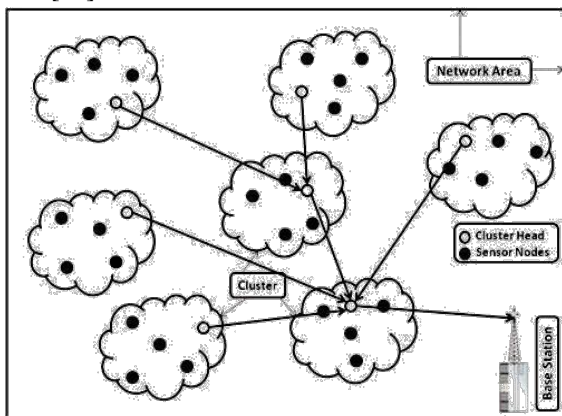


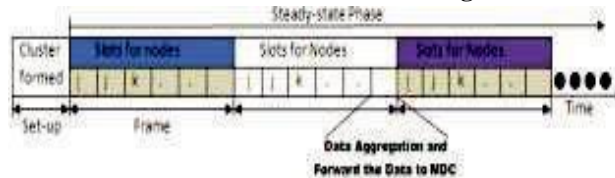
Fig.2: Architectural view of Hybrid multi-hop LEACH

Many frames make up the steady-state phase of the Hybrid multi-hop LEACH, same as LEACH routing protocol. Each member node stays in its own time slot to transmit its data to the CH. When a CH has any fused data to send to the BS, it attempts to locate a multi-hop route from among all of the CHs. Then it will send the data packet to the BS in accordance with the routing algorithm as illustrated in Fig. 2. This solution is one that is straightforward in the group of multi-hop routing algorithms. While a substantial advantage of this protocol is the decrease in the consumption of the transmission energy that directly enhances the overall network lifetime. The drawback of this Hybrid multi-hop LEACH routing protocol is facing energy and routing hole problems, since cluster head near the base station relaying heavy traffic load from another cluster heads in every round and relaying cluster head is died in current round because of energy depletion. According to energy hole concern in Hybrid multi-hop LEACH protocol which directly impacts in routing mechanism of the network. The routing path from cluster head to the base station is not available any more due to heavy traffic loads from another CH's and immediately drains the energy.

III. MOBILE DATA COLLECTOR MAXIMUM RESIDUAL ENERGY LEACH

In this section, a novel cluster based energy efficient routing protocol, named MDC maximum residual energy LEACH, is presented. This Protocol utilizes multi-hop communication and three-tier network architecture for data collection and communication from source to destination. It has been experiential that this type of architecture enhances the network scalability for large scale non-delay sensitive environmental applications; multi-hop communication is to reduce the channel disputation area and provide prospective energy savings by the help of long and multi-hop communication.

The MDC maximum residual energy LEACH protocol is divided into rounds and each round is followed by set-up phase for cluster formation and steady phase for data transmission from sensor nodes to the MDC and finally towards the base station as illustrated in Fig. 3.



A. Radio Model for Transmission of Data

There have been multiple studies carried out into low-energy propagation radio models over the last few years. The MDC maximum residual energy LEACH routing protocol possessing a maximum level of residual energy makes use of a basic First Order Radio Model. In this

model, the receiver and transmitter dissipate E_{elec} 50 nJ/bit and transmit the amplifier circuit ϵ_{amp} 100 pJ/bit/m² to obtain an adequate E_b/N_0 . The current state-of-the-art in radio design, the First Order Radio Model parameters are slightly better than the other models.

Consider that r^2 is the energy loss within the transmission of a channel when transmitting a k -bit message from a distance of d using a radio model; the calculations for the transmission end are seen in equations 1 and 2:

$$E_{Tx}(k, d) = E_{Tx-circ}(k) + E_{Tx-amp}(k, d)$$

$$E_{Tx}(k, d) = E_{circ} * k + \epsilon_{amp} * k * d^2 \quad (1)$$

And the calculations for the receiving end are:

$$E_{Rx}(k) = E_{Rx-circ}(k)$$

$$E_{Rx}(k) = E_{circ} * k \quad (2)$$

B. Setup Phase or Cluster Formation

In the period of cluster formation, each node is autonomous and self-organized, and formed into clusters through short messages using the Carrier Sense Multiple Access (CSMA). MDC maximum residual energy LEACH creates clusters by the help of distributed algorithm where each node in the network must individually choose to become a cluster head or not using the probability of P_i [12]. The P_i node is computed utilizing the LEACH algorithm:

$$P_i(t) = \begin{cases} \frac{k}{N-k+(r \bmod \frac{N}{k})} & \text{if } i \in S_{r-1} \\ 0 & \text{otherwise} \end{cases} \quad (3)$$

While the set-up phase is initiated, each node employs this formula to compute the probability of P_i . The expected number of cluster heads for each round is guaranteed to be k . Because of this, the entire network is grouped into k clusters, the total number of nodes in the network is N . Each node has been chosen to be a cluster head once after N/k rounds on average and r represents the number of the round. Where P is the desired percentage of the total amount of nodes to function as a cluster heads at any given moment, the current round is denoted as r and the set of nodes participating in the selection of the cluster head that has not acted as a cluster head in the last $\frac{1}{P}$ rounds is denoted as G . Each node chosen to act as a cluster head in the current interval cannot be chosen to act as a cluster head in the following interval. A CSMA protocol applies for an announcement by each of the cluster heads in the network for all of the nodes. This message contains data like the position of the cluster head and the kind of message that it is; for example, it is a short message. Each of the nodes receives several announcement messages from various cluster heads after t_1 time. After receiving these all messages, the neighboring node determines which cluster head is nearest to it based on the strength of the signal from the packet announcement. It will

then choose the cluster head that is the shortest distance away.

C. Steady Phase of MDC Maximum Residual Energy LEACH:

After the cluster formation, the cluster head sets up the TDMA schedule for every node to send data to the cluster head. This scheduling is to avoid collisions and reduce energy consumption between the data messages in the cluster and enables each member of the radio equipment to be off when not in use. To reduce inter cluster interference, every cluster uses a unique spreading code; when the node is selected as a cluster head, it selects that unique code and informs all of the member nodes within the cluster to transmit their data using this spreading code

Using Code Division Multiple Access (CDMA) codes, while not necessarily the most bandwidth efficient solution, does solve the problem of multiple-access in a distributed manner [13]. In data fusion mechanism towards the base station, all MDC's transmits a beacon message for all CH's which contained their current position and residual energy level. When CH received the beacon message from MDC, then CH selects the maximum residual energy MDC to route the data towards the base station (BS) in each round. Fig. 4 explains the detailed data fusion mechanism by the approach of maximum residual energy of MDC, in current round cluster head S_1 and S_2 received the residual energy level from MDC 1 and MDC 2 that is 25j and 23j respectively. Cluster head S_1 and S_2 select MDC 1 for transmitting the data because the RE level of MDC 1 is higher than MDC 2. In next round all cluster heads again received residual energy information along with MDC current location by beacon message from MDC's. At this round the RE level of MDC 2 is 23j and MDC 1 is 22j, all cluster heads selects MDC 2 as a relay node for data collection at the base station. Same procedure will follow for data collection within the network at the base station till the residual energy of sensor nodes and MDC's are accessible.

- *Route 1 at Round 1:* S_1 and S_2 – MDC 1 – BS
- *Route 2 at Round 2:* S_1 and S_2 – MDC 2 – BS
- *Route 3 at Round 3:* S_1 and S_2 – MDC 1 – BS

This approach clearly maintains the energy level of relay nodes that is MDC's throughout the network till the sensor nodes and MDC's are alive.

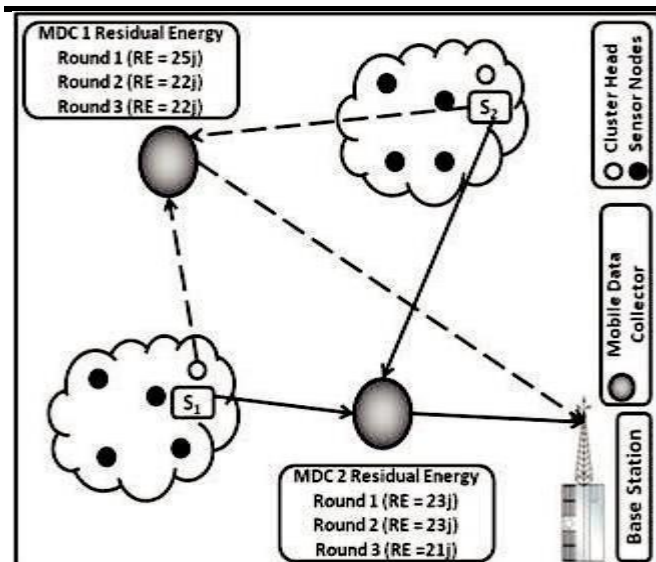


Fig. 4

Number of MDC's	2
-----------------	---

A computer simulation was used to measure the following performance metrics. Since sensor nodes have a limited battery power source, the consumption of energy is the greatest metric in both static and mobile WSNs. A sensor node's energy usage is the same as the sum of the dissipation of the energy during the states of receiving, transmitting, sensing, overhearing, sleeping and idling. This research work put emphasis on addressing the depletion of energy during communication for not only the process of transmitting but also receiving. Furthermore, the amount of energy dissipation from the sensor nodes directly impacts on network lifetime. More energy dissipation means less network lifetime and a smaller amount of energy dissipation means longer network lifetime

IV. RESULT AND DISCUSSION

The simulation parameters of the MDC maximum residual energy LEACH routing protocol are based on environmental applications of WSNs. The main simulation parameters are summarized in Table 1 Shows simulation set up for different parameter used for different areas different nodes and cluster heads etc also it represent battery life number of nodes used and data rate handling, number of MDC is used velocity of MDC etc

Table.1: Simulation Setup

PARAMETERS	VALUES
Number of Nodes	Forty (40)
Simulation Area	1000 * 1000 (m)
Sensor Node Deployment	Random Deployment
Number of Cluster Head	Five (5)
Transmitter Electronics ($E_{TX-elec}$)	50 nj/bit
Receiver Electronics ($E_{RX-elec}$)	
Transmission Amplifier (E_{amp})	100 pj/bit/m ²
Battery	Initial capacity is assumed to be constant
Data Rate	250 kbps
Packet size	288 bits/packet or 36 Bytes
MDC Beacon Message Rate	5 sec/message
MDC Velocity	0.054 m/sec

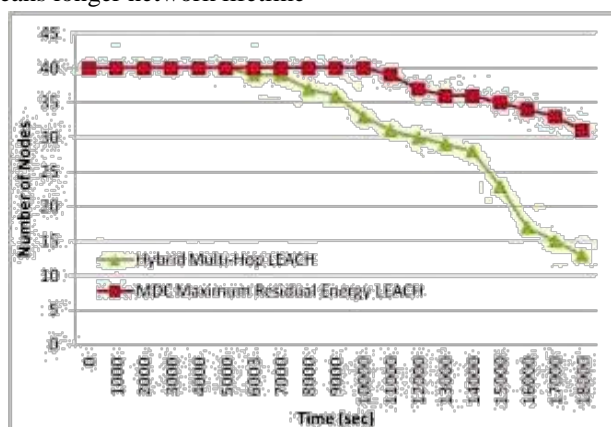


Fig.5: Energy Consumption of Node 14

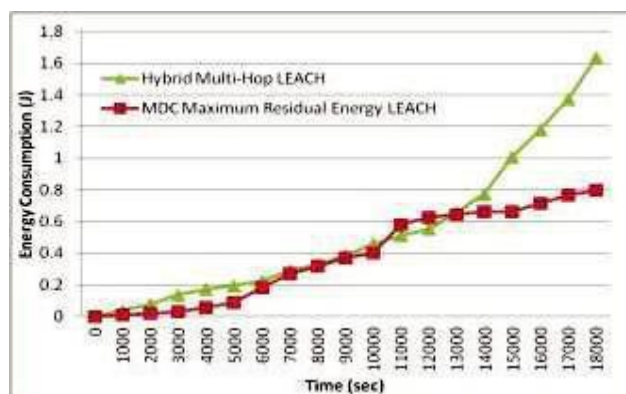


Fig.6: Energy Consumption of Node 21

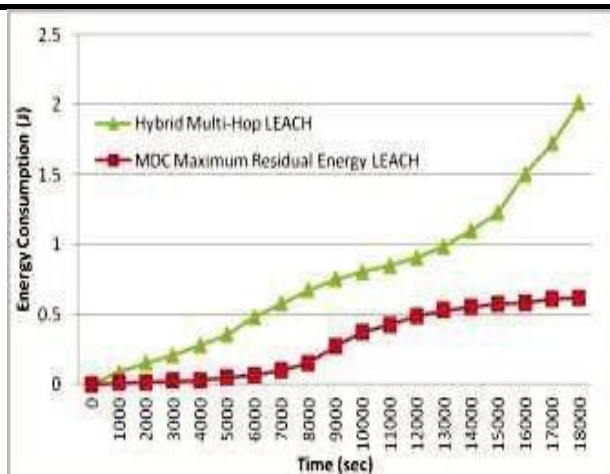
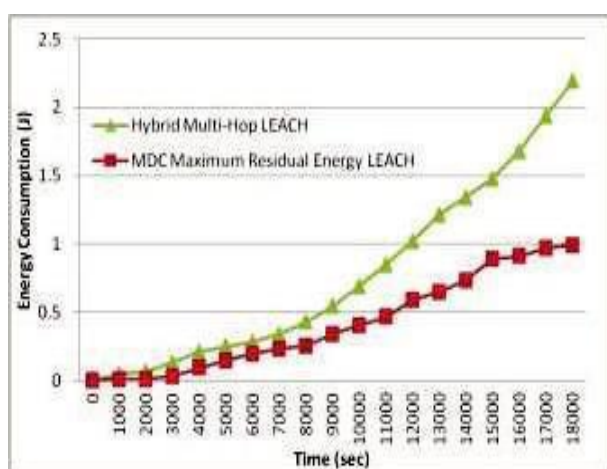


Fig.7: Energy Consumption of Node 37.



Energy Consumption of Sensor Nodes and Network Lifetime:

Fig.8: Network Lifetime

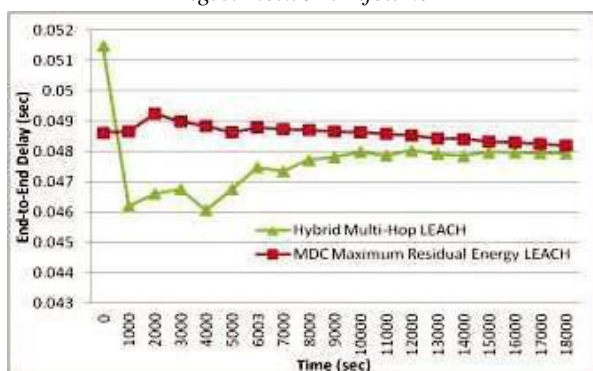
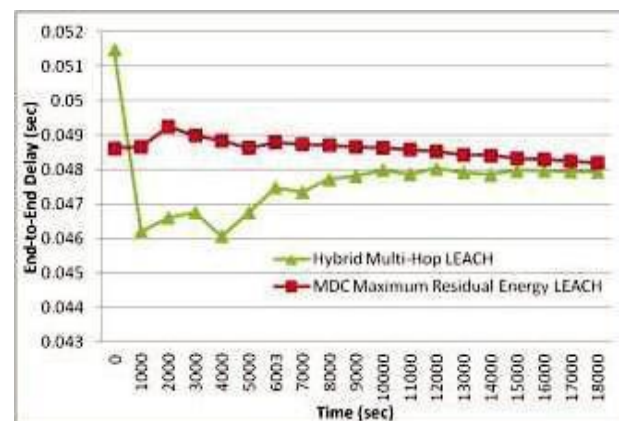


Fig.9: End-to-End Transmission Delay

The simulated result of Fig. 8 exposed the considerable variation in the network lifetime. Therefore, the MDC maximum residual energy LEACH routing protocol is better than the Hybrid multi-hop LEACH routing protocol in terms of network lifetime because it stayed active, on the whole, longer and falling slightly faster. Reached by the receiver. Normally this delay is determined by channel bandwidth, packet length and the coding scheme



Figures 5, 6 and 7 show the usage of power of the individual sensor nodes, 14, 21 and 37, respectively. These were the results obtained upon running the simulations several times using the MDC maximum residual energy LEACH and the Hybrid multi-hop LEACH routing protocols. There was a random distribution of the sensor nodes throughout the network with the farthest, average and nearest distances from the BS. In addition, the MDC (mobile agent) was employed to provide communication towards the BS. A substantial variation in the level of the energy consumption of the sensor nodes is shown in the graphs. This variation had a direct impact on the performance of the network lifetime.

The End-to-End delay is the primary metric of the network latency. It can be specified as the channel access delay, time latency of the data packet and other possible delays from the source to the destination. The graph illustrated in Fig. 9 is of the average End-to-End transmission delay over time when the MDC maximum residual energy LEACH routing protocol and the Hybrid multi-hop LEACH routing protocol were simulated. The End-to-End transmission delay of the MDC maximum residual energy LEACH routing protocol was found to be very similar to the Hybrid multi-hop LEACH routing protocol. This was because the aggregated data packets took multiple hops and used up a greater amount of processing time to get to the BS or control center.

V. CONCLUSION AND FUTURE WORK

The proposed algorithm is an improvement on the clustering

To provide communication towards the BS. A substantial variation in the level of the energy consumption of the sensor nodes is shown in the graphs. This variation had a direct impact on the performance of the network lifetime. Variation in the network lifetime. Therefore, the MDC maximum residual energy LEACH routing protocol is better than the Hybrid multi-hop LEACH routing protocol in terms of network lifetime because it stayed active, on the whole, longer and falling slightly faster. Reached by the receiver. Normally this delay is determined by channel bandwidth, packet length and the coding scheme adopted.

routing protocol. This improvement was brought about by utilizing the MDC maximum residual energy approach. A multi-hop communication between sensor nodes to MDC and then to the BS is provided by this mobile data collector. It reduces the consumption of the energy of all of the nodes in the network. Further, it can be employed in WSNs used in geographical areas that are large. The simulation studies that the proposed MDC maximum residual energy routing protocol is better than the Hybrid multi-hop LEACH routing protocol in terms of energy consumption of sensor nodes and the extensive improvement of network lifetime. In future work, the authors will enhance and validate the multi-hop MDC based clustering routing protocol by a multi-channel concept at the base station to directly allocate the channel for the MDCs instead of a single channel.

REFERENCES

- [1] Arshad, M.; Kamel, N.; Saad, N.M.; Armi, N.; , "Performance enhancement of wireless sensor nodes for environmental applications," Intelligent and Advanced Systems (ICIAS), 2010 International Conference on, vol., no., pp. 1-5, 15-17 June 2010.
- [2] Muhammad Arshad, Nasrullah Armi, Nidal Kamel, N.M. Saad, "Mobile data collector based routing protocol for wireless sensor networks," Scientific Research and Essays Vol. 6(29), pp. 6162-6175, 30 November, 2011, ISSN 1992-2248 ©2011 Academic Journals.
- [3] Arshad, M.; Saad, N.M.; Kamel, N.; Armi, N.; , "Routing strategies in hierarchical cluster based mobile wireless sensor networks," International Conference on Electrical, Control and Computer Engineering (INECCE), 2011, vol., no., pp.65-69, 21-22 June 2011.
- [4] Muhammad Arshad, Mohamad Alsalem, Farhan A. Siddqui, N. M. Saad, Nasrullah Armi, Nidal Kamel; , "Data Fusion in Mobile Wireless Sensor Networks," International MultiConference of Engineers and Computer Scientists, 14 -16 March 2012, Hong Kong.
- [5] Arshad, M.; Alsalem, M.; Siddqui, F.A.; Kamel, N.; Saad, N.M., "Efficient cluster head selection scheme in Mobile Data Collector based routing protocol," Intelligent and Advanced Systems (ICIAS), 2012 4th International Conference on, vol.1, no., pp.280,284, 12-14 June 2012
- [6] Arshad, M.; Aalsalem, M.Y.; Siddqui, F.A., "Multi-hop routing protocol for Mobile Wireless Sensor Networks," Computer and Information Technology (WCCIT), 2013 World Congress on, vol., no., pp.1,6, 22-24 June 2013
- [7] Akyildiz, I.F.; Weilian Su; Sankarasubramaniam, Y.; Cayirci, E.; , "A survey on sensor networks," Communications Magazine, IEEE, vol.40, no.8, pp. 102- 114, Aug 2002.
- [8] Rehena, Z., Roy, S., Mukherjee, N., "A modified SPIN for wireless sensor networks," Communication Systems and Networks (COMSNETS), 2011 Third International Conference on, vol., no., pp.1-4, 4-8 Jan. 2011.
- [9] Manjeshwar, A. and Agrawal, D.P., "TEEN: a routing protocol for enhanced efficiency in wireless sensor networks," Parallel and Distributed Processing Symposium., Proceedings 15th International, vol., no., pp.2009-2015, 23-27 April 2000.
- [10] Zhao, J.; Erdogan, A.T.; , "A Novel Self-Organizing Hybrid Network Protocol for Wireless Sensor Networks," Adaptive Hardware and Systems, 2006. AHS 2006. First NASA/ESA Conference on, vol., no., pp.412-419, 15-18 June 2006.
- [11] W. R. Heinzelman, A. Chandrakasan, and H. Balakrishnan, "Energy-Efficient Communication Protocol for WSNs," Proceedings of the 33th Hawaii International Conference on System Sciences, 2000.
- [12] Gianluca Dini, Marco Pelagatti, Ida Maria Savino, "An algorithm for reconnecting wireless sensor network partitions," in Proceedings of the 5th European conference on Wireless sensor networks (EWSN'08), Roberto Verdone (Ed.). Springer-Verlag, Berlin, Heidelberg, 253-267.
- [13] Gandham, S.R.; Dawande, M.; Prakash, R.; Venkatesan, S.; , "Energy efficient schemes for WSNs with multiple mobile base stations," Global Telecommunications Conference, 2003. GLOBECOM '03. IEEE, vol.1, no., pp. 377- 381.
- [14] Munir, S.A.; Biao Ren; Weiwei Jiao; Bin Wang; Dongliang Xie; Man Ma; , "Mobile Wireless Sensor Network: Architecture and Enabling Technologies for Ubiquitous Computing," Advanced Information Networking and Applications Workshops, 2007, AINAW '07. 21st International Conference on, vol.2, no., pp.113-120, 21-23 May 2007.
- [15] Jeong Hee-Jin; Nam Choon-Sung; Jeong Yi-Seok; Shin Dong-Ryeol; , "A Mobile Agent Based LEACH in Wireless Sensor Networks," Advanced Communication Technology, 2008. ICACT 2008. 10th International Conference on, vol.1, no., pp.75-78, 17-20 Feb. 2008
- [16] Lotf, J.; Bonab, M.; Khorsandi, S. A Novel Cluster-based Routing Protocol with Extending Lifetime for Wireless Sensor Networks. In Proceedings of the 5th International Conference on Wireless and Optical Communications Networks, Surabaya, India, 2008; pp. 1-5.
- [17] Allirani, A.; Suganthi, M. An Energy Efficient Cluster Formation Protocol with Low Latency In Wireless Sensor Networks. World Aca.